Pertanika Journal of

TROPICAL AGRICULTURAL SCIENCE

JTAS

VOL. 48 (6) NOV. 2025

PERTANIKA JOURNALS

A scientific journal published by Universiti Putra Malaysia Press

Pertanika Journal of Tropical Agricultural Science
Pertanika Journal of Tropical Agricultural Science

PERTANIKA JOURNAL OF TROPICAL AGRICULTURAL SCIENCE

About the Journal

Overview

Pertanika Journal of Tropical Agricultural Science is an official journal of Universiti Putra Malaysia. It is an open-access online scientific journal. It publishes the scientific outputs. It neither accepts nor commissions third party content.

Recognised internationally as the leading peer-reviewed interdisciplinary journal devoted to the publication of original papers, it serves as a forum for practical approaches in improving quality on issues pertaining to tropical agriculture and its related fields.

Pertanika Journal of Tropical Agricultural Science currently publishes 6 issues per year (*January, February*, *May*, *June, August*, and *November*). It is considered for publication of original articles as per its scope. The journal publishes in **English** and it is open for submission by authors from all over the world.

The journal is available world-wide.

Aims and Scope

Pertanika Journal of Tropical Agricultural Science aims to provide a forum for high quality research related to tropical agricultural research. Areas relevant to the scope of the journal include agricultural biotechnology, biochemistry, biology, ecology, fisheries, forestry, food sciences, genetics, microbiology, pathology and management, physiology, plant and animal sciences, production of plants and animals of economic importance, and veterinary medicine.

History

Pertanika was founded in 1978. Currently, as an interdisciplinary journal of agriculture, the revamped journal, *Pertanika* Journal of Tropical Agricultural Science now focusses on tropical agricultural research and its related fields.

Vision

To publish journals of international repute.

Mission

Our goal is to bring the highest quality research to the widest possible audience.

Quality

We aim for excellence, sustained by a responsible and professional approach to journal publishing. Submissions are guaranteed to receive a decision within 90 days. The elapsed time from submission to publication for the articles averages 180 days. We are working towards decreasing the processing time with the help of our editors and the reviewers.

Abstracting and Indexing of Pertanika

Pertanika Journal of Tropical Agricultural Science is now over 47 years old; this accumulated knowledge has resulted in *Pertanika* Journal of Tropical Agricultural Science being abstracted and indexed in Journal Citation Reports (JCR-Clarivate), SCOPUS (Elsevier), BIOSIS, National Agricultural Science (NAL), Google Scholar, MyCite, and ISC.

Citing Journal Articles

The abbreviation for *Pertanika* Journal of Tropical Agricultural Science is *Pertanika J. Trop. Agric. Sci*.

Publication Policy

Pertanika policy prohibits an author from submitting the same manuscript for concurrent consideration by two or more publications. It prohibits as well publication of any manuscript that has already been published either in whole or substantial part elsewhere. It also does not permit publication of manuscript that has been published in full in proceedings.

Code of Ethics

The *Pertanika* journals and Universiti Putra Malaysia take seriously the responsibility of all its journal publications to reflect the highest publication ethics. Thus, all journals and journal editors are expected to abide by the journal's codes of ethics. Refer to *Pertanika*'s **Code of Ethics** for full details, available on the official website of *Pertanika*.

Originality

The author must ensure that when a manuscript is submitted to *Pertanika*, the manuscript must be an original work. The author should check the manuscript for any possible plagiarism using any programme such as Turn-It-In or any other software before submitting the manuscripts to the *Pertanika* Editorial Office, Journal Division.

All submitted manuscripts must be in the journal's acceptable **similarity index range**:
≤ 20% – *PASS*; **> 20%** – *REJECT*.

International Standard Serial Number (ISSN)

An ISSN is an 8-digit code used to identify periodicals such as journals of all kinds and on all media–print and electronic. All *Pertanika* journals have an e-ISSN.

Pertanika Journal of Tropical Agricultural Science: e-ISSN 2231-8542 (Online).

Lag Time

A decision on acceptance or rejection of a manuscript is expected within 90 days (average). The elapsed time from submission to publication for the articles averages 180 days.

Authorship

Authors are not permitted to add or remove any names from the authorship provided at the time of initial submission without the consent of the journal's Chief Executive Editor.

Manuscript Preparation

For manuscript preparation, authors may refer to *Pertanika*'s **INSTRUCTION TO AUTHORS**, available on the official website of *Pertanika*.

Editorial Process

Authors who complete any submission are notified with an acknowledgement containing a manuscript ID on receipt of a manuscript, and upon the editorial decision regarding publication.

Pertanika follows a **double-blind peer review** process. Manuscripts deemed suitable for publication are sent to reviewers. Authors are encouraged to suggest names of at least 3 potential reviewers at the time of submission of their manuscripts to *Pertanika,* but the editors will make the final selection and are not, however, bound by these suggestions.

Notification of the editorial decision is usually provided within 90 days from the receipt of manuscript. Publication of solicited manuscripts is not guaranteed. In most cases, manuscripts are accepted conditionally, pending an author's revision of the material.

The Journal's Peer Review

In the peer review process, 2 or 3 referees independently evaluate the scientific quality of the submitted manuscripts. At least 2 referee reports are required to help make a decision.

Peer reviewers are experts chosen by journal editors to provide written assessment of the **strengths** and **weaknesses** of the written research, with the aim of improving the reporting of research and identifying the most appropriate and highest quality material for the journal.

Pertanika Journal of Tropical Agricultural Science
Pertanika Journal of Tropical Agricultural Science

Pertanika Journal of Tropical Agricultural Science
Pertanika Journal of Tropical Agricultural Science

Operating and Review Process

What happens to a manuscript once it is submitted to *Pertanika*? Typically, there are 7 steps to the editorial review process:

1. The journal's Chief Executive Editor and Editor-in-Chief examine the paper to determine whether it is relevance to the journal's needs in terms of novelty, impact, design, procedure, language as well as presentation and allow it to proceed to the reviewing process. If it is not appropriate, the manuscript is rejected outright and the author is informed.

2. The Chief Executive Editor sends the article-identifying information having been removed, to 2 or 3 reviewers. They are specialists in the subject matter of the article. The Chief Executive Editor requests that they complete the review within 3 weeks.

   Comments to authors are about the appropriateness and adequacy of the theoretical or conceptual framework, literature review, method, results and discussion, and conclusions. Reviewers often include suggestions to strengthen the manuscript. Comments to the editor are in the nature of the significance of the work and its potential contribution to the research field.

3. The Editor-in-Chief examines the review reports and decides whether to accept or reject the manuscript, invite the authors to revise and resubmit the manuscript, or seek additional review reports. In rare instances, the manuscript is accepted with almost no revision. Almost without exception, reviewers' comments (to the authors) are forwarded to the authors. If a revision is indicated, the editor provides guidelines to the authors to attend to the reviewers' suggestions and perhaps additional advice on how to revise the manuscript.

4. The authors decide whether and how to address the reviewers' comments and criticisms and the editor's concerns. The authors return a revised version of the paper to the Chief Executive Editor along with specific information describing how they have answered the concerns of the reviewers and editor, usually in a tabular form. The authors may also submit a rebuttal if there is a need especially when the authors disagree with certain comments provided by the reviewers.

5. The Chief Executive Editor sends the revised manuscript out for re-review. Typically, at least 1 of the original reviewers will be asked to examine the article.

6. When the reviewers have completed their work, the Editor-in-Chief examines their comments and decides whether the manuscript is ready to be published, needs another round of revisions, or should be rejected. If the decision is to accept, the Chief Executive Editor is notified.

7. The Chief Executive Editor reserves the final right to accept or reject any material for publication, if the processing of a particular manuscript is deemed not to be in compliance with the S.O.P. of *Pertanika.* An acceptance notification is sent to all the authors.

   The editorial office ensures that the manuscript adheres to the correct style (in-text citations, the reference list, and tables are typical areas of concern, clarity, and grammar). The authors are asked to respond to any minor queries by the editorial office. Following these corrections, page proofs are mailed to the corresponding authors for their final approval. At this point, **only essential changes are accepted**. Finally, the manuscript appears in the pages of the journal and is posted online.

Pertanika Journal of

TROPICAL AGRICULTURAL SCIENCE

Vol. 48 (6) Nov. 2025

PERTANIKA JOURNALS

A scientific journal published by Universiti Putra Malaysia Press

PJTAS

***Pertanika* Journal of Tropical Agricultural Science**

AN INTERNATIONAL PEER-REVIEWED JOURNAL

JOURNAL SECTION, UPM PRESS
Putra Science Park
1st Floor, IDEA Tower II
UPM-MTDC Technology Centre
Universiti Putra Malaysia
43400 Serdang, Selangor Malaysia

General Enquiry
Tel. No: +603 9769 1622
E-mail: executive_editor.pertanika@upm.edu.my
URL: http://www.pertanika.upm.edu.my

PUBLISHER
UPM PRESS
Universiti Putra Malaysia
43400 UPM, Serdang, Selangor, Malaysia
Tel: +603 9769 8855
E-mail: dir.penerbit@upm.edu.my
URL: http://penerbit.upm.edu.my

ABSTRACTING AND INDEXING OF PERTANIKA JOURNALS

The journal is indexed in the Journal Citation Reports (JCR-Clarivate), SCOPUS (Elsevier), BIOSIS, National Agricultural Science (NAL), Google Scholar, MyCite and ISC.

Pertanika Journal of Tropical Agricultural Science
Vol. 48 (6) Nov. 2025

Contents

Foreword

Welcome to the sixth issue of 2025 of the Pertanika Journal of Tropical Agricultural Science (PJTAS)!

PJTAS is an open-access journal for studies in Tropical Agricultural Science published by Universiti Putra Malaysia Press. It is independently owned and managed by the university for the benefit of the world-wide science community.

This issue contains 25 articles: three review articles; and the rest are regular articles. The authors of these articles come from different countries namely Bangladesh, China, Colombia, Czech Republic, Indonesia, Malaysia, Philippines, Sri Lanka, Tanzania, and Thailand.

A selected article Salmah Yaakop and team entitled "Species Composition of Bee and Non-bee Hymenoptera as Effective and Less Effective Pollinators in the Tengku Hassanal Wildlife Reserve Forest, Pahang, Malaysia, with New Insights from DNA Barcoding", investigated Hymenoptera diversity and pollination roles using a combined morphological and molecular approach. Specimens were collected, DNA from 56 specimens was successfully extracted, and COI gene sequences were analysed using a Neighbour-Joining tree to examine species relatedness. The study identified 34 species from 33 genera across 11 families. Eight families—including Apidae, Halictidae, and Vespidae—were recognised as effective floral visitors responsible for meaningful pollination activity, while three families—Braconidae, Evaniidae, and Ichneumonidae—were categorised as less effective or incidental pollinators, often functioning as parasitoids. The study not only establishes vital baseline data for pollinator conservation but also underscores the ecological significance of maintaining both bee and non-bee hymenopteran populations for forest ecosystem stability. Full information on this study is presented on page 2007.

A study entitled "Exploring Venom-derived Peptides from *Calloselasma rhodostoma* Snake as Promising Cholinesterase Inhibitors for Alzheimer's Disease Therapy" examined the therapeutic potential of venom proteins and peptides as natural cholinesterase inhibitors for neurodegenerative disease management. The study focussed on butyrylcholinesterase (BChE), an enzyme increasingly linked to the formation of neurotoxic amyloid plaques and disease progression in Alzheimer's patients. Venom from *C. rhodostoma* was extracted and fractionated, followed by biochemical and proteomic characterisation using ultrafiltration, SDS-PAGE, and LC-HRMS to identify peptide constituents. *In vitro* assays were conducted to evaluate inhibitory activity, while molecular docking analyses assessed peptide–enzyme binding behavior. Several peptides showed strong inhibitory potential and these promising bioactive peptides highlight the potential of Southeast Asian pit viper venom as a novel source of therapeutic lead compounds for Alzheimer's disease. The detailed information of this article is available on page 2087.

A regular article entitled "Antagonistic Potential and Plant Growth Enhancement by Endophytic *Bacillus* Isolated from Citrus Plants". This study aimed to isolate endophytic *Bacillus* from citrus plants as plant growth-promoting bacteria. Endophytic bacteria were initially isolated from citrus leaf tissue, followed by morphological characterisation and KOH tests and the detection of growth-encoding (*ipdC*, *acdS*, *pqqE*, and *nifH*), antibacterial (*aiiA* and *sfp*), and antifungal (*fenD*, *bamC*, and *ituA*) genes with specific primers. Thereafter, antagonistic tests against *Colletotrichum* sp. were performed, and the *Bacillus* isolates were applied to citrus seedlings. Detection of the plant-beneficial traits encoding genes showed that the isolate BYL-4 had all the genes encoding for growth, antibacterial, and antifungal properties. Antagonist testing revealed that the SH-1, SH-2, SH-3, BYL-1, BYL-2, BYL-3, B2B, M2, and P4 isolates were able to inhibit the growth of *Colletotrichum* sp. The detail of the study is presented on page 2153.

We anticipate that you will find the evidence presented in this issue to be intriguing, thought-provoking and useful in reaching new milestones in your own research. Please recommend the journal to your colleagues and students to make this endeavour meaningful.

All the papers published in this edition underwent Pertanika's stringent peer-review process involving a minimum of two reviewers comprising internal as well as external referees. This was to ensure that the quality of the papers justified the high ranking of the journal, which is renowned as a heavily-cited journal not only by authors and researchers in Malaysia but by those in other countries around the world as well.

We would also like to express our gratitude to all the contributors, namely the authors, reviewers, and Editorial Board Members of PJTAS, who have made this issue possible.

PJTAS is currently accepting manuscripts for upcoming issues based on original qualitative or quantitative research that opens new areas of inquiry and investigation.

Editor-in-Chief
Mohamed Thariq Hameed Sultan

Pertanika J. Trop. Agric. Sci. 48 (6): 1677 - 1689 (2025)

PERTANIKA JOURNALS

TROPICAL AGRICULTURAL SCIENCE

Journal homepage: http://www.pertanika.upm.edu.my/

Abscisic Acid Promotes Ripening in Sapodilla (*Manilkara zapota* L.) Fruit after Refrigerated Storage

Nafi Ananda Utama*, Ananda Elmanisa Ramadhani, Indira Prabasari, and Chandra Kurnia Setiawan

Department of Agrotechnology, Faculty of Agriculture, Universitas Muhammadiyah Yogyakarta, Indonesia

ABSTRACT

Sapodilla is a climacteric fruit with high marketing potential but limited export viability due to its short shelf life. During transport, the fruit is refrigerated in a semi-ripe state and is expected to be ready for consumption upon reaching consumers. This study aims to determine the physical and chemical characteristics of sapodilla fruit treated with abscisic acid after refrigerated storage. Half-ripe sapodilla fruits (n=66) were selected, washed, and stored at 10°C for 10 days. The fruits were then divided into control (n=33) and treatment (n=33) groups. Samples in the treatment group were sprayed with a 0.1% ABA solution before further storage at room temperature for 16 days. During this period, weight loss (%), firmness (N/mm²), total soluble solids (°Brix), titratable acidity (%), and reducing sugar levels (%) were observed. The Wilcoxon rank-sum test ($\alpha = 0.05$) was used to analyze mean differences between groups for each parameter. Significant differences between groups emerged on the 12th day of storage at room temperature. On day 12, ABA-treated samples exhibited significantly lower firmness (0.13 ± 0.01 N/mm²) and reduced sugar levels (0.207 ± 0.074%) compared to the control (0.26 ± 0.06 N/mm² and 0.427 ± 0.040%, respectively). The titratable acidity of ABA-treated samples (3.57 ± 0.26%) was also significantly lower than that of the control (5.96 ± 0.45%). However, ABA-treated sapodilla exhibited higher total soluble solids (17.6 ± 1.53 °Brix) than the control (14.1 ± 0.58 °Brix). Similarly, vitamin C content was higher in ABA-treated samples (0.032 ± 0.002%) compared to the control (0.006 ± 0.007%). These changes suggest a synergistic relationship between ABA and ethylene. Therefore, the application of ABA can accelerate ripening in sapodilla fruit after refrigeration.

Keywords: Abscisic acid, climacteric fruit, fruit ripening, post-harvest, sapodilla, shelf-life

ARTICLE INFO

Article history:
Received: 18 April 2024
Accepted: 17 April 2025
Published: 25 November 2025

DOI: https://doi.org/10.47836/pjtas.48.6.01

E-mail addresses:
nafi@umy.ac.id (Nafi Ananda Utama)
ananda.elmanisa.fp18@mail.umy.ac.id (Ananda Elmanisa Ramadhani)
i.prabasari@umy.ac.id (Indira Prabasari)
chandra_fp@umy.ac.id (Chandra Kurnia Setiawan)
*Corresponding author

e-ISSN: 2231-8542

INTRODUCTION

Sapodilla (*Manilkara zapota* L.) belongs to the Sapotaceae family and is known for its sweet taste and high nutritional value. It contains 69.46% moisture, 20.0 g of carbohydrates, 15.96% total sugars, and various vitamins (vitamin A, vitamin C, pantothenic acid, and niacin) and minerals (calcium, potassium, and iron) (Bangar et al., 2022; Shinwari & Rao, 2020). Sapodilla fruit also exhibits antioxidant activity and phytochemicals, such as phenols, flavonoids, and anthocyanins (Cortes et al., 2022). In Indonesia, sapodilla, commonly known as *sawo*, has gained economic significance. According to BPS-Statistics Indonesia (2020), sapodilla fruit production increased from 144,966 tons in 2019 to 186,706 tons in 2020. This rise in production indicates the potential expansion of sapodilla cultivation to meet growing market demand and even possible export opportunities.

However, as a climacteric fruit, sapodilla continues to ripen after harvest, posing challenges during transportation from orchards to consumers or distributors. During ripening, total soluble solids increase as starch is converted into soluble sugars, but these levels decline as the fruit progresses into senescence (Baidya et al., 2020). The firmness of fleshy fruits irreversibly decreases due to transpiration, respiration, and other postharvest metabolic processes. Physical weight loss (PWL) increases over time as moisture content decreases. Additionally, titratable acidity, which indicates organic acid content, declines as the fruit ripens, as these acids are either utilized in respiration or converted into sugar (Blissett et al., 2019). These physicochemical changes significantly influence the fruit's sensory properties, which are critical in shaping consumer purchasing decisions. Therefore, controlling ripening-related physicochemical properties is essential to maintaining fruit quality.

Temperature control is a widely used postharvest handling technique to preserve fruit quality. Cold storage slows the general metabolism of harvested fruits by reducing respiration rates and enzyme activity, thereby delaying ripening (Brizzolara et al., 2020). This method is particularly beneficial for exported fruits, which may take weeks or months to reach their destination. Typically, fruits are harvested in a semi-ripe condition and stored at low temperatures to extend shelf life during transit. However, once the fruits reach their destination, consumers and distributors expect them to be ready for immediate sale or consumption. Thus, the ripening process must be re-induced to develop desirable sensory properties.

Abscisic acid (ABA) is a growth-regulating substance involved in fruit development, maturation, and ripening. The effect of ABA application on fruit ripening is closely associated with its synergistic relationship with ethylene, a plant hormone crucial in climacteric fruit ripening. During climacteric fruit ripening, ABA levels peak earlier than ethylene levels, highlighting its role in regulating ethylene production (Bai et al., 2021). Previous research mentioned that the core signaling pathway between ABA and ethylene is

conserved in climacteric fruits, with key regulators (i.e., 9-cis epoxycarotenoid dioxygenase (NCED), abscisic acid-responsive elements (ABRE) binding proteins (AREB) or binding factors (ABFs), 1-aminocyclopropane-1-carboxylic (ACC) synthase (ACS) and ACC oxidase (ACO), and ethylene response factors (ERFs)) and ethylene-related transcription factors (i.e., Mcm1, Agamous, Deficiens and SRF or MADS-ripening inhibitor (MADS-RIN), Tomato AGAMOUS-LIKE1 (TAGL1), Colorless Non-ripening (CNR), and Non-ripening (NOR)) are highly likely mediating ABA-ethylene interactions (Bai et al., 2021). However, the precise mechanism of ABA-mediated ethylene regulation during climacteric fruit ripening remains unclear, requiring further research. This study investigates whether ABA can be applied to sapodilla fruit to induce ripening after refrigerated storage. To mimic the postharvest transportation condition, sapodilla fruits were stored at low temperatures before ABA application.

MATERIALS AND METHODS

Sample Preparation

The sapodilla fruits used in this study were handpicked by farmers in Wonosari, Gunungkidul, Indonesia (7° 58.0393' S, 110° 36.0668' E). Fruits at a half-ripe maturity stage were selected based on the physical characteristics described by (Brito & Narain, 2002). Each selected fruit weighed between 80–90 g, was fresh, free from disease, and had no physical damage. A total of sixty-six sapodilla fruits were obtained and arranged in groups of three on Styrofoam trays.

Refrigerated Storage Treatment

Before refrigeration, the fruits were washed with water containing 20 ppm chlorine and then air-dried. The cleaned fruits were subsequently stored in a refrigerator at 10 °C for ten days, with relative humidity maintained at 95%.

Application of Abscisic Acid Solution

To prepare a 0.1% abscisic acid (ABA) solution, 100 mg of ABA (HiMedia, Mumbai, India) was dissolved in 500 mL of distilled water and 500 mL of 96% ethanol. Subsequently, 0.05% (0.5 mL/L) Tween 20 was added as a surfactant. This solution was applied to the treatment group (n = 33) after ten days of refrigerated storage. Before application, the refrigerated fruits were placed on a metal drying tray and allowed to rest for ten minutes. The ABA solution was then sprayed onto the fruits to the point of run-off while slowly rotating them to ensure even coverage. The treated samples were subsequently air-dried in a dark place and stored at room temperature for 16 days.

Measured Parameters

The ripening process of ABA-treated sapodilla fruits was monitored over 16 days of storage at room temperature. Physicochemical parameters were assessed, including physical attributes such as weight loss and firmness, as well as chemical characteristics such as total soluble solids (TSS), titratable acidity (TTA), reducing sugar levels, and vitamin C content. Measurements were conducted every two days, except for weight loss, which was recorded daily. Each parameter was measured in triplicate to ensure reliability.

Physical Parameters Measurement

Weight loss was determined using an analytical scale (OHAUS Scout Pro, New Jersey, USA) by subtracting the weight at each measurement point from the initial weight and expressing the result as a percentage. Firmness was assessed using a fruit penetrometer (MRC Lab Equipment, Essex, United Kingdom) with a force specification of 13 kg and a penetration depth of 100 mm. Measurements were taken at three points on each fruit: tip, middle, and base.

Chemical Characteristics Measurement

Total soluble solids (TSS) were measured using an ATAGO Pal-3 hand refractometer (ATAGO, Tokyo, Japan). Sapodilla fruits were cut into sections and blended (Miyako, Jakarta, Indonesia) to extract juice. Three drops of the juice were placed on the refractometer prism, and the TSS value was recorded in °Brix. Titratable acidity (TTA) was determined following the method described by (Sadler & Murphy, 2010) and expressed as a percentage. Reducing sugar levels was quantified using the modified Nelson-Somogyi method (Romadhoni et al., 2017), while vitamin C content was analyzed according to (Satpathy et al., 2021).

Statistical Analysis

All statistical computations and graphical visualizations were performed using R in RStudio (version 2023.06.0). The observed parameter values between treatments on the same day were analyzed for significant differences using the non-parametric Wilcoxon rank-sum test with a significance level of 0.05. Line plots were generated using the ggplot2 package.

RESULTS

ABA Application and Weight Loss

Figure 1 illustrates the changes in weight loss and firmness of sapodilla fruit under different treatments following ten days of refrigerated storage. Both ABA-treated and untreated fruits exhibited increasing weight loss after being transferred to room

temperature (Figure 1A). No significant differences were observed between the treatments across all measured days.

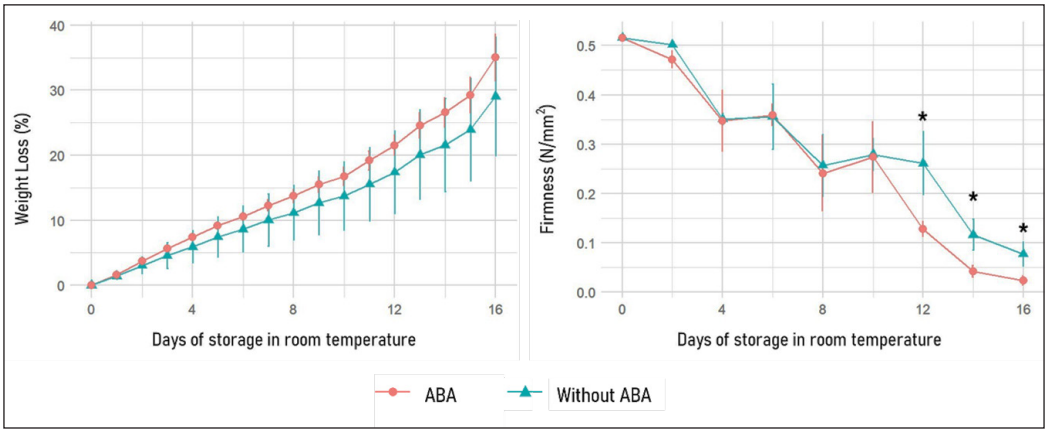

(A) (B)

Figure 1. Changes in physical observation of (A) weight loss and (B) firmness in 16 days of room temperature storage between sapodilla fruit treated with and without abscisic acid (ABA) after refrigerated storage (10 days at 10°C). Asterisks (*) represent significant differences between two treatments within the same day of storage (p = 0.05)

ABA Application Reduces Firmness After Refrigerated Storage

The firmness measurements are presented in Figure 1B. Regardless of treatment, the firmness of sapodilla fruit continuously declined throughout the observation period. However, fruits treated with ABA exhibited significantly lower firmness than the control group on days 12 (P = 0.023), 14 (P = 0.020), and 16 (P = 0.013) of room temperature storage. On day 12, ABA-treated fruits had a firmness of 0.13 ± 0.01 N/mm², compared to 0.26 ± 0.06 N/mm² in the control samples. By the final observation day, firmness values dropped to 0.02 ± 0.01 N/mm² and 0.08 ± 0.02 N/mm² for ABA-treated and untreated fruits, respectively.

ABA Application Enhances Total Soluble Solids and Reduces Sugar Levels

As shown in Figure 2A, the total soluble solids (TSS) content in untreated sapodilla fruit gradually declined after six days of room temperature storage, with a pronounced drop between days 10 and 12. In contrast, ABA-treated fruits exhibited an increase in TSS levels after day 10, continuing to rise throughout the remaining observation period. A significant difference (P = 0.008) was observed on day 12, where the TSS content in ABA-treated fruits (17.6 ± 1.53 °Brix) was notably higher than in the control group (14.1 ± 0.58 °Brix). By day 16, TSS levels reached 23.1 ± 1.53 °Brix in ABA-treated samples, whereas control samples measured 15.3 ± 0.58 °Brix.

A similar trend was observed in reducing sugar content (Figure 2B). Both treatments initially showed a decline after four days of room temperature storage, with a divergence occurring between days 10 and 12. On day 12, ABA-treated fruits exhibited a continuous increase in reducing sugar content (0.427 ± 0.040%), while untreated fruits continued to decline (0.207 ± 0.074%). A statistically significant difference emerged in the final three days of observation, with ABA-treated fruits reaching 0.475 ± 0.034% and untreated fruits at 0.261 ± 0.007% on day 16 (P = 0.048).

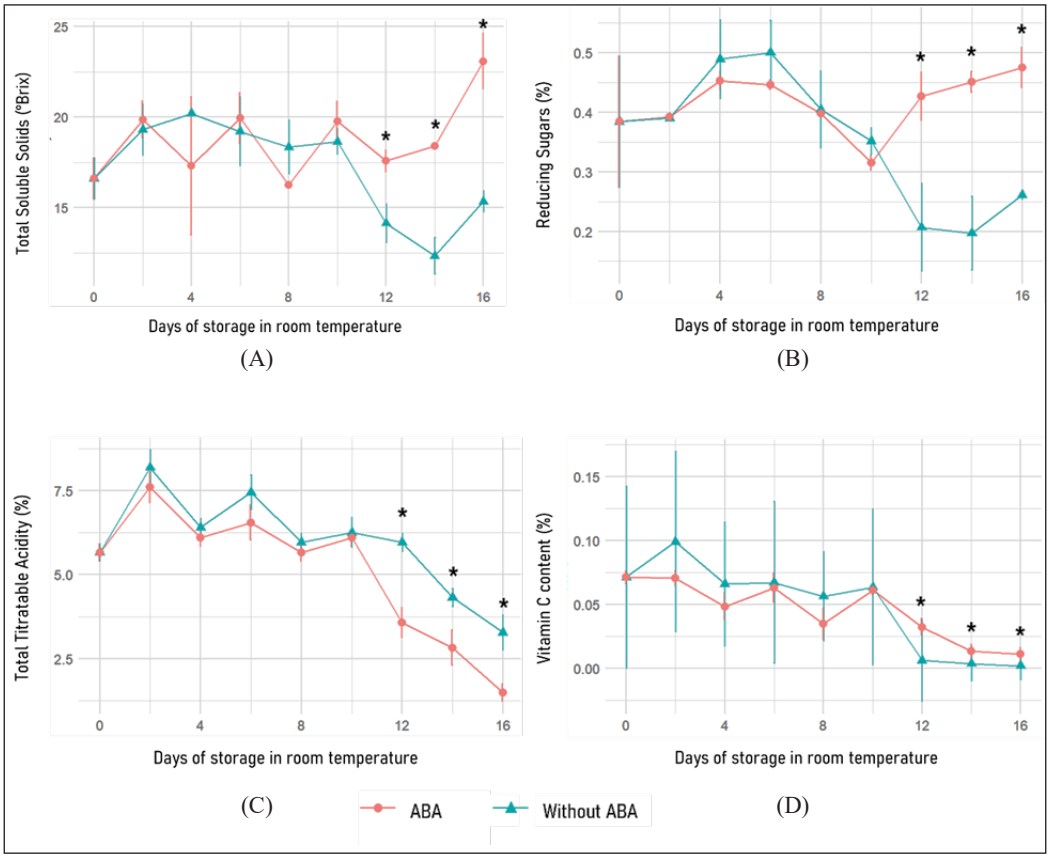

Figure 2. Changes in chemical observation of (A) total soluble solids, (B) reducing sugar level, (C) total titratable acidity, and (D) vitamin C level in 16 days of room temperature storage between sapodilla fruit treated with and without abscisic acid (ABA) after refrigerated storage (10 days at 10°C). Asterisks (*) represent significant differences between the two treatments within the same day of storage (p = 0.05)

ABA Treatment Reduces Total Titratable Acidity

Both ABA-treated and untreated fruits exhibited a progressive decline in total titratable acidity (TTA) throughout the 16-day room temperature storage period after ten days of refrigerated storage at 10 °C (Figure 2C). Similar to the TSS trends, significant differences in

TTA were observed on days 12, 14, and 16, with untreated fruits maintaining higher acidity than ABA-treated samples. On day 12, TTA values were 5.96 ± 0.45% for control samples and 3.57 ± 0.26% for ABA-treated fruits. The decline persisted until day 16, resulting in TTA values of 3.28 ± 0.52% (control) and 1.49 ± 0.26% (ABA-treated) ($P = 0.003$).

ABA Application Increases Vitamin C Content

Figure 2D presents the vitamin C content of sapodilla fruits under both treatments after ten days of refrigerated storage at 10 °C. While both groups showed a gradual decline over the 16-day room temperature storage, ABA-treated fruits consistently retained higher vitamin C levels than untreated fruits in the final three days. By day 16, vitamin C content reached its lowest values, with ABA-treated fruits maintaining 0.011 ± 0.002%, compared to just 0.002 ± 0.005% in untreated fruits ($P = 0.037$).

DISCUSSION

The production of sapodilla fruit in Indonesia is increasing annually, indicating its potential for global market distribution. However, extending shelf life by delaying ripening during transport while ensuring optimal ripening upon arrival is crucial for maintaining fruit quality. Low-temperature storage is a commonly used postharvest technique to slow the ripening process. In this study, abscisic acid (ABA) was investigated as a potential trigger for promoting sapodilla fruit ripening after refrigerated storage, mimicking the transportation process after harvest. While several studies (Kou et al., 2021; Wu et al., 2023; Zhang et al., 2021) have reported the ability of ABA to accelerate ripening, none have examined its application after refrigerated storage to enhance ripening and achieve the desired fruit quality for consumers.

The present study found that applying ABA after refrigerated storage significantly promoted the ripening of sapodilla fruit. Fruits in the treatment group exhibited significantly higher total soluble solids, reducing sugar content, and vitamin C levels (Figure 2), while titratable acidity (Figure 2) and firmness (Figure 1) were lower than those of the control samples. The differences in ripening parameters between treatment groups highlight the role of ABA as a ripening promoter in sapodilla fruit. However, physical weight loss showed no significant difference between treatments (Figure 1).

During storage, fruits inevitably undergo weight loss, which affects their quality. This weight loss results from water loss due to transpiration and respiration. In fresh produce such as fruits and vegetables, excessive water loss can reduce quality and cause damage. As shown in Figure 1A, although not statistically significant, the trendline of weight loss in sapodilla fruits treated with ABA was slightly higher than in untreated fruits. Similar results were observed in ABA-treated tomato and capsicum (Prajapati et al., 2019). Exogenous ABA treatment can activate enzymatic activities, including cell wall-degrading

enzymes such as polygalacturonase, through the upregulation of genes responsible for pectin degradation (*PcPG1*, *PcPG2*, *PcPL*, *PcPME2*, *PcPME3*, and *PcGAL1*) and ABA biosynthesis (*PcNCED1* and *PcNCED2*) (Xu et al., 2024).

Several mechanisms, including the loss of turgor pressure, pectin degradation, and damage to the fruit's cell walls, can cause texture changes such as softening in most fruits. After day 10, sapodilla fruit treated with ABA exhibited significantly lower firmness values (Figure 1). Similar firmness loss and softening effects have been reported in various fruit commodities treated with ABA. In non-climacteric strawberry fruits, both the control and ABA-treated samples showed no firmness loss after 48 hours; however, thermogravimetric analysis (TGA) revealed cell wall alterations (Castro et al., 2021). The breakdown of the xyloglucan-cellulose network and pectin solubilization were associated with cell wall deconstruction, a process mediated by ABA. Total degradation and a decrease in hemicellulose content were observed in ABA-treated samples due to ABA-induced breakdown of cell wall polymers, leading to their decomposition into low-molecular-weight compounds, primarily carbohydrates such as xylose and glucose, which are related to hemicellulose degradation (Castro et al., 2021; Castro & Morales-Quintana, 2019).

As shown in Figure 1, ABA-treated sapodilla fruit exhibited decreased firmness and slight weight loss. The relationship between ripening-related physical changes, ABA, and ethylene has also been explored in previous studies. Long-term kiwifruit storage at 0°C under varying humidity conditions showed that storage beyond eight weeks led to a rapid loss of fruit firmness (Huang et al., 2021). The fastest weight loss was observed in low-humidity conditions due to environmental factors and respiratory metabolism changes, which accelerated softening. Water loss also promoted ethylene biosynthesis and fruit softening during storage. However, these changes were not directly linked to an increase in ABA content. Instead, the strongest correlation was found between ABA concentration in fruit tissues and firmness reduction, regardless of weight loss. A higher ABA concentration was associated with decreased fruit firmness, but no correlation was observed between ABA content and weight loss. This suggests that while water loss may induce ethylene production and fruit softening, ABA concentration in tissues is more closely related to firmness than weight loss. The rapid softening of 'Hayward' kiwifruit due to dehydration may be mediated by ethylene, but ABA's specific role, whether direct or indirect, remains unclear (Huang et al., 2021).

The sapodilla samples treated with ABA have higher total soluble solids (Figure 2A) and reducing sugar content (Figure 2B) compared to control samples. Higher total soluble solids, indicative of sugar accumulation, were observed in this study and have also been reported in other fruits, including date, peach, papaya, cucumber, and tomato (Elbar et al., 2022; Utama et al., 2023). ABA plays a crucial role in various metabolic pathways, including sugar signaling. Sugar accumulation during fruit ripening can be attributed to the interaction between ABA and sugar signaling pathways, as well as the release of sugars

from storage carbohydrates or the import of sugars from distal organs via phloem transport (Gupta et al., 2022).

By stimulating enzymes involved in cell wall degradation, such as pectin methylesterase (PME) and polygalacturonase (PG), ABA promotes the conversion of complex insoluble sugars into simple soluble sugars. The respiration rate in ABA-treated fruits decreased, contributing to higher sugar accumulation (Prajapati et al., 2019). Increased sugar accumulation reflects a rise in sugar content, including reducing sugars such as fructose and glucose. Previous research indicated that ABA promotes soluble sugar accumulation in different climacteric fruits. Application of 600 μM and 800 μM ABA in blueberry conferred higher soluble sugar than the control samples after 14 and 21 days of treatment. The study explained that the increase of soluble solids in the initial period of storage was likely due to a higher rate of acid and sugar biosynthesis compared to degradation at the time of harvest when the fruit was not fully ripe. However, these levels subsequently declined in the later storage period, presumably due to respiratory metabolism (Qiao et al., 2024). A recent study found the relation between key ABA signal transducers (MdbZIP23 and MdbZIP46) with the expression of the MdSWEET9b gene transporter, which affected sugar accumulation in apple fruits (Zhang et al., 2023). The study further elucidates the regulatory impacts between the ABA-signalling network and fruit sugar accumulation.

As shown in Figure 2C, ABA-treated sapodilla fruit exhibited lower TTA levels than the control. A similar trend was observed in ABA-treated detached capsicum. Since various organic acids are catabolized in the later stages of fruit development and storage, titratable acidity naturally declines during ripening (Prajapati et al., 2019). The higher TTA content in ABA-treated fruits could be attributed to a reduced respiration rate, as organic acids serve as respiratory substrates. A lower respiration rate would slow the breakdown of organic acids, resulting in lower TTA levels.

A study investigating the effects of exogenous ABA on ripening-related genes in citrus fruit explored the potential relationship between ABA, sugar, and organic acid pathways (Wang et al., 2016). The study found that ABA significantly decreased organic acid content and regulated the expression of genes associated with sugar and acid metabolism in citrus fruits. ABA and sucrose signaling pathways played a key role in citrus fruit ripening, with transcript levels of *CsACO1* and *CsNADP-IDH* in ABA-treated fruits being higher than those in the control. When the ABA inhibitor nordihydroguaiaretic acid (NDGA) was applied, the opposite trend was observed, further supporting the role of ABA in promoting organic acid degradation. The study reported that ABA and NDGA influenced sugar accumulation and acid degradation during ripening. Sugar-related genes were upregulated, whereas acid-related genes either decreased or remained unchanged. These findings suggest that ABA and NDGA play a significant role in the degradation of organic acids such as malic acid, citric acid, and quinic acid.

The level of vitamin C was higher in fruits treated with ABA than in the control samples (Figure 2D). Similar results have been observed in other commodities. Abscisic acid potentially enhances ascorbic acid accumulation in drought-stressed tomatoes by inducing the expression of SIMAPK8 (Xu et al., 2022). Additionally, abscisic acid mitigates the inhibitory effect of auxin on ascorbic acid biosynthesis. In strawberries, the accumulation of ascorbic acid is driven by the upregulation of *FaGLDH*, *FaAPX*, and *FaMR* genes, suggesting that ABA-mediated regulatory mechanisms play a crucial role in ascorbic acid biosynthesis during fruit ripening (Zhang et al., 2023). Another study further explained that in salt-stress-induced strawberries, ABA exogenous application significantly enhances the accumulation of ascorbic acid compared to the samples in salt stress without ABA treatment (Crizel et al., 2020). Thus, the protective or acclimatory effect of ABA under stress conditions favors the ascorbic acid production.

The findings of this study suggest that ABA can be used to promote fruit ripening after refrigerated storage, presenting new research opportunities for both academia and industry. The results indicate that exogenous ABA application in sapodilla fruit after refrigeration storage can extend its shelf life by approximately two additional days compared to untreated samples. This extension could be commercially beneficial, particularly for long-distance transportation and export markets. However, it is important to note that different fruits may respond differently to refrigerated storage and ABA treatment. Future research could explore various aspects, such as optimizing ABA concentrations, determining the most effective application methods, and refining refrigerated storage processes in combination with ABA treatment.

CONCLUSION

Abscisic acid (ABA) treatment after refrigerated storage enhances the ripening qualities of sapodilla (*Manilkara zapota* L.) fruit. The application of ABA resulted in higher total soluble solids, reducing sugar content, and vitamin C levels compared to control samples. Additionally, ABA-treated sapodilla fruit exhibited lower firmness and total titratable acidity than untreated fruit. These findings indicate that ABA can effectively promote ripening in sapodilla fruit following low-temperature storage. This study highlights the potential of ABA in post-storage fruit ripening, offering insights for further research and industrial applications. Future studies could investigate the responses of different fruit types, optimal ABA concentrations, application methods, and the integration of ABA treatment with refrigerated storage optimization.

ACKNOWLEDGEMENT

The authors would like to thank Universitas Muhammadiyah Yogyakarta for giving financial aid (47/R-LRI/1/XI/2023) in the research activities of this study.

REFERENCES

Bai, Q., Huang, Y., & Shen, Y. (2021). The physiological and molecular mechanisms of abscisic acid in regulation of fleshy fruit ripening. *Frontiers in Plant Science*, *11*, Article 619953. https://doi.org/10.3389/fpls.2020.619953

Baidya, B. K., Mahato, A., Pattnaik, R. K., & Sethy, P. (2020). A review of physiological and biochemical changes related to ripening along with post-harvest handling and treatments of Sapota. *Journal of Pharmacognosy and Phytochemistry*, *9*(4), 2030–2035. https://doi.org/10.22271/phyto.2020.v9.i4ab.12054

Bangar, S. P., Sharma, N., Kaur, H., Kaur, M., Sandhu, K. S., Maqsood, S., & Ozogul, F. (2022). A review of Sapodilla (Manilkara zapota) in human nutrition, health, and industrial applications. *Trends in Food Science & Technology*, *127*, 319–334. https://doi.org/10.1016/J.TIFS.2022.05.016

Blissett, K. A., Emanuel, M., & Barnaby, A. G. (2019). Biochemical properties of tree ripened and post harvest ripened Mangifera indica (cv. East Indian). *International Journal of Fruit Science*, *19*(4), 452–463. https://doi.org/10.1080/15538362.2019.1596866

BPS-Statistics Indonesia. (2020). *Production of fruits in year 2020*. BPS-Statistics Indonesia. https://www.bps.go.id/indicator/55/62/1/produksitanaman-%0Abuah-buahan.html

Brito, E. S. D., & Narain, N. (2002). Physical and chemical characteristics of sapota fruit at different stages of maturation. *Pesquisa Agropecuaria Brasileira*, *37*(4), 567–572. https://doi.org/10.1590/s0100-204x2002000400020

Brizzolara, S., Manganaris, G. A., Fotopoulos, V., Watkins, C. B., & Tonutti, P. (2020). Primary metabolism in fresh fruits during storage. *Frontiers in Plant Science*, *11*, Article 80. https://doi.org/10.3389/fpls.2020.00080

Castro, R. I., Gonzalez-Feliu, A., Valenzuela-Riffo, F., Parra-Palma, C., & Morales-Quintana, L. (2021). Changes in the cell wall components produced by exogenous abscisic acid treatment in strawberry fruit. *Cellulose*, *28*(3), 1555–1570. https://doi.org/10.1007/s10570-020-03607-7

Castro, R. I., & Morales-Quintana, L. (2019). Study of the cell wall components produced during different ripening stages through thermogravimetric analysis. *Cellulose*, *26*(5), 3009–3020. https://doi.org/10.1007/S10570-019-02305-3/FIGURES/6

Cortes, N. R. R., Ortega, T. D. J. A., & Muñoz, R. C. (2022). Phytochemical content and antioxidant potential of tropical sapodilla fruit (Manilkara zapota). *Fruits*, *77*(3), 23–28. https://doi.org/10.17660/th2022/013

Crizel, R. L., Perin, E. C., Siebeneichler, T. J., Borowski, J. M., Messias, R. S., Rombaldi, C. V., & Galli, V. (2020). Abscisic acid and stress induced by salt: Effect on the phenylpropanoid, L-ascorbic acid and abscisic acid metabolism of strawberry fruits. *Plant Physiology and Biochemistry*, *152*, 211–220. https://doi.org/10.1016/j.plaphy.2020.05.003

Elbar, S., Maytal, Y., David, I., Carmeli-Weissberg, M., Shaya, F., Barnea-Danino, Y., Bustan, A., & Harpaz-Saad, S. (2022). Abscisic acid plays a key role in the regulation of date palm fruit ripening. *Frontiers in Plant Science*, *13*, Article 1066142. https://doi.org/10.3389/fpls.2022.1066142

Gupta, K., Wani, S. H., Razzaq, A., Skalicky, M., Samantara, K., Gupta, S., Pandita, D., Goel, S., Grewal, S., Hejnak, V., Shiv, A., El-Sabrout, A. M., Elansary, H. O., Alaklabi, A., & Brestic, M. (2022). Abscisic

acid: Role in fruit development and ripening. *Frontiers in Plant Science*, *13*, Article 817500. https://doi.org/10.3389/FPLS.2022.817500/BIBTEX

Huang, W., Billing, D., Cooney, J., Wang, R., & Burdon, J. (2021). The role of ethylene and abscisic acid in kiwifruit ripening during postharvest dehydration. *Postharvest Biology and Technology*, *178*, Article 111559. https://doi.org/10.1016/j.postharvbio.2021.111559

Kou, X., Yang, S., Chai, L., Wu, C., Zhou, J., Liu, Y., & Xue, Z. (2021). Abscisic acid and fruit ripening: Multifaceted analysis of the effect of abscisic acid on fleshy fruit ripening. *Scientia Horticulturae*, *281*, Article 109999. https://doi.org/10.1016/J.SCIENTA.2021.109999

Prajapati, U., Asrey, R., Arora, A., Singh, A. K., & Hasan, M. (2019). Differential effects of abscisic acid and fluridone on postharvest quality parameters of detached capsicum (Capsicum Annuum L.) fruits. *Journal of Scientific and Industrial Research*, *78*(4), 242–247.

Qiao, H., Wu, W., Zhang, Y., Kong, Q., Chen, H., Wang, L., Fang, X., & Gao, H. (2024). Impact of abscisic acid treatment on postharvest storage quality and volatile flavor substances in blueberries. *EFood*, *5*(3), Article e148. https://doi.org/10.1002/efd2.148

Romadhoni, R. P., Purbaningtias, T. E., Muhaimin, & Fauzi'ah, L. (2017, September 13-13). *Determination of reduction sugar form banana (Musa Acuminat a Balbisiana Colla) with different cooking process by UV-visible spectrophotometer*. [Paper presentation]. Proceeding The 2nd International Seminar on Chemical Education, Yogyakarta, Indonesia.

Sadler, G. D., & Murphy, P. A. (2010). pH and titratable acidity. In S. S. Nielsen (Ed.) *Food Analysis* (pp. 219–238). Springer. https://doi.org/10.1007/978-1-4419-1478-1_13

Satpathy, L., Pradhan, N., Dash, D., Baral, P. P., & Parida, S. P. (2021). Quantitative determination of vitamin C concentration of common edible food sources by redox titration using iodine solution. *Letters in Applied NanoBioScience*, *10*(3), 2361–2369. https://doi.org/10.33263/LIANBS103.23612369

Shinwari, K. J., & Rao, P. S. (2020). Development of a reduced-calorie high pressure processed sapodilla (Manilkara zapota L.) jam based on rheological, textural, and sensory properties. *Journal of Food Science*, *85*(9), 2699–2710. https://doi.org/10.1111/1750-3841.15364

Utama, N. A., Utami, P. T., Daryanto, M. G. A. Y., & Dewi, S. S. (2023). Effects of abscisic acid on bioactive compounds and postharvest quality of climacteric and non-climacteric fruit. *Planta Tropika*, *11*(1), 41–49. https://doi.org/10.18196/pt.v11i1.17615

Wang, X., Yin, W., Wu, J., Chai, L., & Yi, H. (2016). Effects of exogenous abscisic acid on the expression of citrus fruit ripening-related genes and fruit ripening. *Scientia Horticulturae*, *201*, 175–183. https://doi.org/10.1016/j.scienta.2015.12.024

Wu, W., Cao, S. F., Shi, L. Y., Chen, W., Yin, X. R., & Yang, Z. F. (2023). Abscisic acid biosynthesis, metabolism and signaling in ripening fruit. *Frontiers in Plant Science*, *14,* Article 1279031. https://doi.org/10.3389/FPLS.2023.1279031/FULL

Xu, X., Zhang, Q., Gao, X., Wu, G., Wu, M., Yuan, Y., Zheng, X., Gong, Z., Hu, X., Gong, M., Qi, T., Li, H., Luo, Z., Li, Z., & Deng, W. (2022). Auxin and abscisic acid antagonistically regulate ascorbic acid production via the SlMAPK8–SlARF4–SlMYB11 module in tomato. *The Plant Cell*, *34*(11), Article 4409. https://doi.org/10.1093/PLCELL/KOAC262

Xu, X., Zhu, X., Jiang, F., Li, Q., Zhang, A., Zhang, H., & Li, J. (2024). Mechanism of abscisic acid in promoting softening of postharvest 'Docteur Jules Guyot' pear (*Pyrus communis* L.). *Frontiers in Plant Science*, *15*, Article 1502623. https://doi.org/10.3389/FPLS.2024.1502623/FULL

Zhang, C., Wu, Y., Xiong, Z., Li, W., & Wu, W. (2021). ABA accelerates blackberry (*Rubus* spp.) fruit ripening by positively affecting ripening-related gene expression and metabolite profiles. *Journal of Berry Research*, *11*(4), 705–720. https://doi.org/10.3233/JBR-210725/SUPPL_FILE/SJ-XLS-4-BER-10.3233_JBR-210725.XLS

Zhang, S., Wang, H., Wang, T., Zhang, J., Liu, W., Fang, H., Zhang, Z., Peng, F., Chen, X., & Wang, N. (2023). Abscisic acid and regulation of the sugar transporter gene MdSWEET9b promote apple sugar accumulation. *Plant Physiology*, *192*(3), Article 2081. https://doi.org/10.1093/PLPHYS/KIAD119

Pertanika J. Trop. Agric. Sci. 48 (6): 1691 - 1709 (2025)

PERTANIKA JOURNALS

TROPICAL AGRICULTURAL SCIENCE

Journal homepage: http://www.pertanika.upm.edu.my/

Growth Performance Together with Analysis of Haematological and Biochemical Indices of Nile Tilapia Fed Citric Acid and Phytase-supplemented Peas

Jan Mareš, Lucie Všetičková*, Miroslava Palíková, Marija Radojičić, Ondřej Malý, and Eva Poštulková

Mendel University in Brno, Faculty of AgriSciences, Department of Zoology, Fisheries, Hydrobiology and Apiculture, Zemědělská 1665/1, 61300 Brno, Czech Republic

ABSTRACT

At present, fish farmers are searching for cheaper alternatives of fish feed. Here, we assess the suitability of pea meal (*Pisum sativum*), with and without enzyme (phytase)/citric acid supplementation, as a feed for Nile tilapia (*Oreochromis niloticus*). After 90 days, we recorded a significant increase in total length, weight, and weight gain in groups fed 60% pea meal, both with and without citric acid and/or phytase. The number of erythrocytes dropped significantly against controls in all 60% pea meal groups, while leucocytes were higher in all groups fed 30 and 60% pea meal. No significant changes were recorded in plasma biochemical parameters, except for aspartate aminotransferase, triacylglycerol, and chlorine which were significantly lower, and contrarily calcium, sodium and blood plasma iron were significantly higher, than in controls in all 60% groups. Consequently, feed with 30 and 60% pea meal is suitable for feeding farmed tilapia and enrichment with phytase and citric acid is recommended. The results of the study show that peas can be a new source of protein in intensive fish aquaculture nutrition. It therefore has the potential to partially replace soybeans in aqua feeds. Peas may also have the advantage of being a crop easy to grow, widespread throughout the world, and not genetically modified.

ARTICLE INFO

Article history:
Received: 28 January 2025
Accepted: 14 May 2025
Published: 25 November 2025

DOI: https://doi.org/10.47836/pjtas.48.6.02

E-mail addresses:
jan.mares@mendelu.cz (Jan Mareš)
lucie.vsetickova@mendelu.cz (Lucie Všetičková)
miroslava.palikova@mendelu.cz (Miroslava Palíková)
marija.radojicic@mendelu.cz (Marija Radojičić)
ondra.malous@gmail.com (Ondřej Malý)
eva.postulkova@mendelu.cz (Eva Poštulková)
*Corresponding author

Keywords: Acidulation, aquacultural feed, enzyme, *Oreochromis niloticus*, pea meal

INTRODUCTION

Current trends in human nutrition place an emphasis on the production of healthy, high quality raw materials, whether of plant or animal origin. As the world population grows, and individual countries' economies

improve, so the demand for quality plant, and especially animal, foodstuffs increases. Increasingly, therefore, the agricultural sector is focusing on those areas that can produce quality food in the shortest time. In livestock production, this is mainly fish and poultry farming (FAO, 2021).

Quality feed is one of the most important, if not the most important, factors influencing the growth rate of animals and the quality of the final product. At the same time, however, feed is one of the main costs in animal husbandry. Consequently, full knowledge of the impacts of a given nutritional strategy on the quality and marketability of animal products is essential for the profitability of livestock farming (Szollosi et al., 2021), including aquaculture (Watson et al., 2021).

Both animal and plant ingredients can be used as the main source of protein in fish feed; however, not only are these ingredients the most expensive component in the feed but the digestibility of different forms can vary greatly, with subsequent impacts on fish growth (Imsland et al., 2016). The digestion pattern of fish, as cold-blooded animals, differs somewhat to that of warm-blooded animals. From this point of view, ground fishmeal is a particularly suitable animal protein group in fish feed (Luthada-Raswiswi et al., 2021); however, it is both expensive and its use carries certain risks, e.g. contamination with heavy metals (Murthy et al., 2013). Insect meal is beginning to be used in aquaculture (Bullon et al., 2023) but the most commonly used substitute for fishmeal in animal feed is soybean (*Glycine max*) meal. However, soya is the most common genetically modified crop (GMC) (Sieradzki & Kwiatek, 2006), which restricts its use in Europe, and Europe itself is far from self-sufficient in non-GMC soybean production (FAO, 2021). Consequently, efforts are being made to find other high-quality protein sources for animal feed, such as peas (*Pisum sativum)* (Allan et al., 2000), peanuts (*Arachis hypogaea)* (Vo et al., 2020) or lupine (*Lupinus angustifolius)* (Glencross et al., 2011).

Peas are an important legume, grown mainly for their tasty fruits, which are high in vitamins (mainly B vitamins) and minerals, especially phosphorus (P) and potassium (K), but also calcium (C) and magnesium (Mg). Furthermore, Crépon (2007) reported that peas contain around 20 to 25% of protein substances and a high lysine content, though actual content varies depending on the soil quality and length of growing season. Not all the microelements in peas are available to fish in their natural form, however. Indeed, fish receive a significant proportion of their P intake from plant foods in a form that is difficult to utilise as fish do not produce the enzyme phytase, which breaks down the phytate bond to release P. Therefore, fish digest this form of P poorly and most is excreted in the faeces and passes into the aquatic environment without being used. Moreover, phytate readily forms complexes with divalent and trivalent cations of zinc (Zn), C or Mg, which also limits utilisation of these minerals. Some fish species produce low levels of acid in their digestive tract, which can negatively affect digestion and nutrient utilisation and increase the risk of pathogens developing in the digestive tract (Shah et al., 2015).

In this study, we determine the effect of adding i) pea protein, (ii) pea protein with added phytase and (iii) pea protein with added phytase and citric acid on a) haematological and biochemical plasma parameters, and b) production parameters, of Nile tilapia (*Oreochromis niloticus*), a fish commonly bred under intensive aquaculture. In doing so, we determine whether pea protein is a suitable feed additive for intensively reared tilapia, and whether one, or both, of the additives improve utilisation of the pea protein. The percentage of pea inclusion in the feed was determined on the basis of the previous pilot tests. Both doses are high for the reason that they were intended to ensure sufficient protein in the feed. The hypothesis was as follows: the addition of peas as a protein source in the diet will not adversely affect the growth and haematological parameters of tilapia.

MATERIAL AND METHODS

Fish

Three hundred and sixty clinically healthy (without injuries and symptoms of disease) Nile tilapia (originating from our own breeding ponds) were divided into nine groups comprising two replications, with 180 tilapia per replication. The number of tilapia in the experiment was determined taking into account the capacity of the recirculation system and the welfare of the fish. For each test run, 20 weight balanced tilapia (for mean weights, see Table 1) were placed into an 80 L tank fed by a Nexus Easy 210 recirculation system (Evolution Aqua s.r.o., Czech Republic). Prior to each replication, the fish were given a two-week acclimatization period, during which they were fed with a standard KP1 feed mixture.

Table 1
Mean weights (+ standard deviation [SD]) in each treatment tank (two replicates per treatment)

Treatment	Tank 1	Tank 2
C	85.25 ± 15.64 g	87.75 ± 15.52 g
CF	88.65 ± 10.61 g	87.15 ± 14.88 g
CF+	87.55 ± 11.63 g	91.00 ± 14.37 g
P30	85.25 ± 19.06 g	86.30 ± 11.84 g
P30F	78.35 ± 12.20 g	78.45 ± 15.73 g
P30F+	91.20 ± 12.36 g	91.95 ± 11.28 g
P60	88.65 ± 11.95 g	90.70 ± 14.59 g
P60F	77.10 ± 8.50 g	77.85 ± 14.28 g
P60F+	91.35 ± 11.65 g	88.50 ± 10.00 g

Note. Treatments: 30% (P30) and 60% (P60) pea meal, commercial carp feed as control (C) and feeds enriched with the enzyme phytase (CF, P30F, P60F) and phytase and citric acid (CF+, P30F+, P60F+)

Dietary Feed and Feeding During the Experiment

Three diet variants were used in the experiment. The control (C) group were fed a commercially prepared carp feed (KP1, FMP Silver Mountains, Czech republic) containing wheat, wheat flour, rapeseed cake, wheat bran, soybean meal, barley, corn and calcium carbonate ($CaCO_3$), sodium chloride (NaCL) and soybean oil (see Table 2). In addition, two test variants were prepared by the feed producer, where part of the KP1 was substituted with pea meal in the following proportions: 70:30 KP1/pea meal (group P30) and 40:60 KP1/pea meal (group P60). Each of these three diets was also prepared as a variant with 500 FTU of phytase (CF, P30F and P60F) and 500 FTU of phytase and 3% citric acid (CF+, P30F+ and P60F+). The pea meal was produced by a local agricultural farm ZD Kojcice using cultivar ESO pea seeds that had previously been analysed in our laboratory to determine protein content (confirmed at 20.30%). The phytase used was commercial Phyzyme XP 10.000 TPT in fine granular form, produced by Danisco Animal Nutrition (United Kingdom), and the citric acid was a commonly available food grade product suitable for human consumption.

Table 2
Analytical composition of the feed mixture (KP1) used in this study

Component	Content
Moisture (%)	11.53
Crude protein (%)	17.84
Crude fibre (%)	4.81
Crude oils and fats (%)	4.51
Crude ash (%)	5.84
Lysin (%)	0.73
Methionine (%)	0.29
Calcium (%)	0.96
Phosphorus (%)	0.57
Sodium (%)	0.18
Butylhydroxyanisol (mg)	1.25
Butylhydroxytoluene (mg)	5.48
Vitamin D3 (IU)	1,500.00
Vitamin A (IU)	8,100.00
Sulphate ferrous monohydrate (mg)	100.26
Iodine calcium (mg)	1.02
Sulphate cupric pentahydrate (mg)	4.95

All test fish were fed three times a day at 8 a.m., noon and 4 p.m. over the 10-week experiment, with the daily feeding ratio corresponding to 3% of tank stock weight. Control weighing took place every 14 days (i.e. five times per experiment), after which the daily feed ration was recalculated based on the actual weight of the fish. The control days also served for examination of fish health. Mortality caused by aggressive behaviour due to tilapia switching gender during the experiment was as follows: C = 2 ind., CF = 0 ind., CF+ = 2 ind., P30 = 4 ind., P30F = 4 ind., P30F+ = 0 ind., P60 = 2 ind., P60F = 3 ind. and P60F+ = 4 ind.

There were no significant differences in water quality parameters throughout the experiment (for details see Table 3).

Table 3
Mean water quality parameters for each test treatment over the course of the experiment

	Group									
Parameter	**Biofilter**	**C**	**F**	**CF+**	**P30**	**P30F**	**P30F+**	**P60**	**P60F**	**P60F+**
Water temperature (°C)	25.17 ± 0.67	25.10 ± 0.70	25.14 ± 0.68	25.16 ± 0.67	25.15 ± 0.70	25.16 ± 0.66	25.18 ± 0.68	25.17 ± 0.69	25.15 ± 0.70	25.17 ± 0.69
Dissolved oxygen content ($mg.L^{-1}$)	5.96 ± 0.66	6.84 ± 0.58	6.59 ± 0.62	6.58 ± 0.62	7.13 ± 0.50	6.54 ± 0.64	6.46 ± 0.67	6.61 ± 0.62	6.59 ± 0.71	6.49 ± 0.64
Oxygen saturation (%)	75.02 ± 7.75	85.48 ± 6.47	82.25 ± 7.21	82.19 ± 7.15	83.24 ± 7.07	81.60 ± 7.39	80.71 ± 7.79	82.40 ± 7.02	82.28 ± 8.00	80.88 ± 7.59
pH	7.81 ± 0.47	7.95 ± 0.51	7.94 ± 0.49	7.92 ± 0.49	7.92 ± 0.50	7.90 ± 0.48	7.90 ± 0.48	7.91 ± 0.49	7.92 ± 0.51	7.89 ± 0.49
$N\text{-}NH_4$ ($mg.L^{-1}$)[1]	0.21 ± 0.08									
$N\text{-}NO_2^-$ ($mg.L^{-1}$)[1]	0.36 ± 0.22									
Cl^- ($mg.L^{-1}$)[1]	123.85 ± 16.05									

Note. Treatments: 30% (P30) and 60% (P60) pea meal, commercial carp feed as control (C) and feeds enriched with the enzyme phytase (CF, P30F, P60F) and phytase plus citric acid (CF+, P30F+, P60F+). [1] parameters measured only on the biofilter not in each fish tank

Fish Body Parameters

At the end of the experiment, the fish were removed from the water, stunned by a blow to the head and, after collecting blood (see below), they were killed by cutting the branchial venae. The fish were treated in accordance with current legislative rules and approved by the Ethics Committee of the Central Commission for Animal Welfare at the Ministry of Education of the Czech Republic. Ethical approval number is MSMT-6675/2018-3. Each fish was measured for total length, standard length, body height, body width, body weight, liver weight, pancreas weight, gonad weight and eviscerated body weight. Three fish were randomly selected from each group and ground whole for analysis of ash, fat and protein content, while filleted muscle only was taken from another three randomly selected fish for the same analysis. All analyses were undertaken at the laboratory of the Department of Chemistry at Mendel University in Brno (Czech Republic). Fulton's condition factor, Clark's condition factor and the highbackedness and widebackedness index were then calculated from these basic data (Gela & Linhart, 2000), along with the feed conversion ratio, specific growth rate, weight gain, hepatosomatic index, viscerosomatic index, splenosomatic index and gonadosomatic index. (Note that not all parameters are listed in the tables as some were only used for the calculation of the indices.)

Blood Examination

Blood samples (2 ml) were taken from eight stunned fish in each tank at the end of the experiment by puncturing the *vena caudalis* and storing the sample in a heparinised syringe, rinsed out with heparin sodium salt to avoid coagulation. Each blood sample was divided into two parts, one being used for haematological examination (haemoglobin, number of erythrocytes, number of leukocytes, haematocrit), while the other part was centrifuged (1500 rpm, 5 minutes) using a MPW 140 350R cooling centrifuge (MPW Med. Instruments, Poland), the plasma obtained being stored in a freezer (Arctiko ULTF 80, Denmark) at -75°C until further analysis. Blood smears, haemoglobin and haematocrit determination (Svobodová et al., 2012) were undertaken immediately after blood collection. Blood smears were stained using the Hemacolor Rapid staining kit (Merck, Darmstadt, Germany). The blood plasma biochemical profile (alanine aminotransferase (ALT), aspartate aminotransferase (AST), lactate dehydrogenase (LDH), alkaline phosphatase (ALP), albumin (ALB), cholesterol (CHOL), creatine (CREA), glucose (GLUC), urea (UREA), total protein (TP), triacylglycerol (TAG), calcium (Ca) and inorganic phosphorous (PI), sodium (Na), potassium (K), chloride (Cl), iron (Fe) and magnesium (Mg)) was measured using the Konelab 20i kit and other commercially available kits (BioVendor, Czech Republic).

Statistical Analysis

Analysis of variance (ANOVA), with subsequent Tukey post-hoc tests, were used to determine significant differences between experimental variants, with all data being first log (x+1) transformed to meet the assumptions of the parametric test - normality of data and homogeneity of variances. In all cases, each fish was considered as an individual replicate and differences were considered significant at $P < 0.05$. All analyses were performed in Statistica 14 (TIBCO Software Inc., 2020).

RESULTS

Fish Body Parameters

Both tilapia body length and weight increased as the proportion of pea meal in the feed increased (i.e. P60 > P30), with the addition of both phytase and phytase with citric acid also having a positive impact. Tilapia in groups P60, P60F and P60F+ all had a significantly greater body length than those in group C (Table 4). While there was also a significant increase in body weight in group P60, a similar increase in body weight in groups P60F and P60F+ was not significant (Table 4). Similarly, while values for Fulton's condition factor were significantly higher than C in groups P30 and P60, the increase resulting from the addition of the two additives was non-significant. In comparison, Clark's condition factor tended to remain relatively static, with no discernible trend between groups. Hepatosomatic, viscerosomatic and gonadosomatic indices also showed no discernible trend in relation to pea meal content, except for group P30F, where the addition of phytase appeared to have a significant effect (Table 4). While the widebackedness index showed a significant increasing trend in groups P30, P30F and P60F+ compared to C and all P60 groups, the highbackedness index showed the opposite trend, with values in P60, P60F and P60F+ all being significantly higher than those in C and all P30 groups (Table 4).

Production Parameters

None of the fat, ash or protein parameters examined displayed statistically significant changes against C, whether in relation to pea meal concentration or addition of phytase or citric acid (Table 5). Overall trends were variable, with fat content in whole fish similar between P30 and P60, but showing a decreasing trend in groups P30F and P60F and P30F+ and P60F+. While fat in muscle tended to decrease with increasing proportion of pea meal, addition of both additives had little or no further effect. Only minor changes were noted in ash content, with no visible trend among groups. Protein levels in both whole fish and muscle showed little change, the only notable difference being between group P60F+ and CF+ (Table 5). Weight gain increased with increasing proportion of pea meal, with the addition of phytase having a significant positive effect. Feed conversion ratio was highest

Table 4
Fish body parameters at the end of the experiment (mean ± SD)

	Group										
Parameter	**C**	**CF**	**CF+**	**P30**	**P30F**	**P30F+**	**P60**	**P60F**	**P60F+**	**CA**	**F**
TL (mm)	184.15 ± 9.69^{a}	202.30 ± 10.97^{a}	205.00 ± 15.75^{a}	190.85 ± 9.30^{a,b}	198.25 ± 11.88^{a,b}	208.45 ± 11.95^{a,b}	195.25 ± 8.29^{b}	203.55 ± 11.19^{b}	207.70 ± 11.43^{b}	↑	↑
BW (g)	117.36 ± 18.77^{a}	153.80 ± 26.91^{a}	164.95 ± 37.42^{a}	131.16 ± 19.07^{a,b}	149.53 ± 29.70^{a,b}	172.79 ± 28.05^{a,b}	138.69 ± 13.95^{b}	158.07 ± 24.91^{b}	167.44 ± 26.24^{b}		
F_C	3.42 ± 0.19^{a}	3.28 ± 0.15^{a}	3.38 ± 0.24^{a}	3.42 ± 0.15^{b}	3.47 ± 0.15^{b}	3.45 ± 0.15^{b}	3.37 ± 0.20^{a,b}	3.40 ± 0.22^{a,b}	3.33 ± 0.20^{a,b}		
C_C	3.08 ± 0.17	2.97 ± 0.14	3.02 ± 0.19	3.07 ± 0.11	3.07 ± 0.13	3.08 ± 0.14	3.04 ± 0.17	3.03 ± 0.18	3.00 ± 0.17		
HBI (%)	2.58 ± 0.07^{a}	2.62 ± 0.09^{a}	2.57 ± 0.10^{a}	2.58 ± 0.07^{a}	2.59 ± 0.07^{a}	2.56 ± 0.06^{a}	2.65 ± 0.08^{b}	2.63 ± 0.08^{b}	2.63 ± 0.10^{b}		
WBI (%)	18.09 ± 0.56^{a}	17.70 ± 0.50^{a}	17.72 ± 0.59^{a}	18.09 ± 0.48^{b}	18.31 ± 0.57^{b}	18.29 ± 0.45^{b}	17.83 ± 0.64^{a}	18.14 ± 0.62^{a}	17.99 ± 0.47^{a}		
HSI (%)	2.68 ± 0.59	3.00 ± 0.58	2.99 ± 0.71	2.63 ± 0.58	3.40 ± 1.13	2.72 ± 0.64	2.84 ± 0.62	2.44 ± 0.58	2.63 ± 0.48		
VSI (%)	10.14 ± 1.56	9.67 ± 1.01	10.53 ± 2.20	9.96 ± 1.77	11.27 ± 1.93	10.60 ± 1.79	9.73 ± 1.59	10.9 ± 1.18	10.10 ± 1.53		↑
GSI (%)	1.77 ± 1.52	1.06 ± 1.02	2.13 ± 1.63	1.65 ± 1.69	1.56 ± 1.56	2.35 ± 2.27	1.40 ± 1.34	1.35 ± 1.29	1.27 ± 1.62		

Note. Treatments: 30% (P30) and 60% (P60) pea meal, commercial carp feed as control (C) and feeds enriched with the enzyme phytase (CF, P30F, P60F) and phytase plus citric acid (CF+, P30F+, P60F+). Significant effect of pea meal is shown by superscript letters (same letters represents no effect); significant effect of citric acid (CA) and F addition is indicated by arrows: ↑ = parameter higher, ↓ = parameter lower. CA = citric acid, F = phytase, TL = total length, BW = body weight, Fc = Fulton's condition factor, Cc = Clark's condition factor, HBI = highbackedness index, WBI = widebackedness index, HIS = hepatosomatic index, VSI = viscerosomatic index, GSI = gonadosomatic index

in group C, but fell sharply in groups CF and CF+. There was also a significant reduction in group P30F, and less so in P60F, following addition of phytase. On the other hand, specific growth rate increased significantly compared to C in all experimental groups following addition of phytase. Finally, the FCR:SGR ratio was significantly lower in the P60, P60F and P60F+ groups than the C, CF and CF+ groups, with a similar but non-significant decreasing trend for the P30, P30F and P30F+ groups (Table 5).

Haematological and Biochemical Parameters

The number of erythrocytes was significantly lower than C in groups P60, P60F and P60F+, and slightly lower in P30F and P30F+ (Table 6). In comparison, while the number of leucocytes showed an increasing trend in the P30, P30F+, P60 and P60F+ groups, there was a significant decrease in P30F and P60F, i.e. the groups with added phytase. Haemoglobin and haematocrit values in the P60, P60F and P60F+ groups were significantly lower than those in the other groups, with the highest contrast between groups CF+ and P60F+ (Table 6).

Values for AST, Cl and TAG decreased in all experimental groups compared to the controls, with the decrease being significant in P60, P60F and P60F+. Noticeably, TAG values for P60F and P60F+ were around half those of the CF, CF+, P30F and P30F+ groups, and those for P60 around two thirds. Likewise, Cl values differed significantly at P60, P60F and P60F+, with phytase and citric acid having a significant impact, while Ca levels differed significantly at P30 and P60, with addition of citric acid having a significant impact. Values for Fe values were increasing increased significantly in all six experimental groups, while Na values were significantly different in P30, P30F and P30F+ comparing to both the C and P60 groups, with addition of phytase having a significant impact which can be viewed in Table 6.

While all other parameters showed increasing or decreasing trends, none of the differences were significant (Table 6). Both ALP and CHOL in P60, P60F and P60F+, for example, tended to drop compared the C (ALP) and P30 groups (CHOL), while ALB values dropped in groups P30F+ and P60F+ compared with CF+, and GLUC and TP (phytase significant) showed decreasing values in groups P30F, P60F and P60F+, with values for the other groups tending to fluctuate at the same levels. While non-significant, there was a clear impact from the addition of phytase on TP, and LDH values were lower in all experimental groups compared with the controls. Values for Mg and K showed no significant change in any of the groups, despite the addition of phytase having a significant positive effect on Mg and addition of citric acid having a significant decreasing effect on Mg and K. Likewise, CREA, UREA and IP values fluctuated only slightly between groups, despite the significant positive impacts of phytase on IP and citric acid on UREA.

Table 5
Production parameters at the end of the experiment (mean ± SD)

Parameter	Group										
	C	CF	CF+	P30	P30F	P30F+	P60	P60F	P60F+	CA	F
FCR	6.56 ± 0.03	2.69 ± 0.10	2.59 ± 0.25	4.66 ± 0.51	3.16 ± 1.15	2.29 ± 0.07	3.87 ± 0.53	2.47 ± 0.02	2.93 ± 0.72		↓
SGR (%.d-1)	0.33 ± 0.00^{a}	0.69 ± 0.01^{a}	0.78 ± 0.07^{a}	0.52 ± 0.07^{b}	0.79 ± 0.00^{b}	0.81 ± 0.03^{b}	0.55 ± 0.05^{b}	0.84 ± 0.06^{b}	0.83 ± 0.06^{b}		↑
FCR:SGR	20.20 ± 0.20^{a}	3.90 ± 0.20^{a}	3.30 ± 0.00^{a}	9.00 ± 0.30^{a,b}	4.00 ± 1.50^{a,b}	2.80 ± 0.20^{a,b}	7.00 ± 0.40^{b}	2.90 ± 0.20^{b}	3.60 ± 1.10^{b}		↓
Weight gain (%)	119.30 ± 0.20	161.90 ± 1.20	164.10 ± 4.60	129.20 ± 3.60	156.30 ± 24.50	176.60 ± 3.60	139.90 ± 5.80	166.70 ± 0.30	160.90 ± 19.00		↑
Fat in whole fish (%)	34.89 ± 0.17	34.87 ± 0.14	36.61 ± 0.39	34.20 ± 0.11	32.69 ± 0.43	41.12 ± 5.14	36.05 ± 0.17	30.04 ± 5.18	37.52 ± 0.17		
Ash in whole fish (%)	12.93 ± 1.07	14.25 ± 0.09	14.25 ± 0.10	13.33 ± 0.27	13.28 ± 0.56	14.95 ± 0.06	14.59 ± 0.08	16.49 ± 1.08	13.40 ± 0.70		
Protein in whole fish (%)	52.21 ± 1.56	55.32 ± 0.50	53.38 ± 0.59	52.30 ± 0.48	53.98 ± 0.57	50.83 ± 4.45	53.73 ± 0.64	52.44 ± 0.62	55.44 ± 0.47		
Fat in muscle (%)	24.69 ± 0.59	25.71 ± 0.58	19.74 ± 4.71	14.25 ± 8.58	19.93 ± 4.13	18.34 ± 5.64	12.71 ± 10.62	22.28 ± 1.58	22.35 ± 1.48		
Ash in muscle (%)	5.54 ± 0.03	5.57 ± 0.10	5.47 ± 0.25	5.56 ± 0.51	5.95 ± 0.75	5.77 ± 0.07	5.69 ± 0.53	5.51 ± 0.02	5.83 ± 0.72		
Protein in muscle (%)	79.13 ± 2.00	83.84 ± 2.01	77.29 ± 4.07	79.85 ± 0.97	82.05± 0.50	82.89 ± 0.03	81.67 ± 0.25	82.24 ± 0.06	83.97 ± 0.86		

Note. Treatments: 30% (P30) and 60% (P60) pea meal, commercial carp feed as control (C) and feeds enriched with the enzyme phytase (CF, P30F, P60F) and phytase plus citric acid (CF+, P30F+, P60F+). Significant effect of pea meal is shown by superscript letters (same letters represents no effect); significant effect of citric acid (CA) and F addition is indicated by arrows: ↑ = parameter higher, ↓ = parameter lower. FCR = feed conversion ratio, SGR = specific growth rate

Table 6
Haematological and biochemical parameters at the end of the experiment (mean ± SD)

Parameter	Group										
	C	CF	CF+	P30	P30F	P30F+	P60	P60F	P60F+	CA	F
Haemoglobin ($g.l^{-1}$)	70.62 ± 7.98[a]	77.38 ± 7.76[a]	86.45 ± 12.25[a]	80.86 ± 6.63[a]	72.33 ± 5.37[a]	82.79 ± 6.04[a]	69.86 ± 16.46[b]	76.29 ± 4.31[b]	69.28 ± 5.89[b]		
Erythrocytes ($T.l^{-1}$)	1.82 ± 0.18[a]	2.05 ± 0.34[a]	2.00 ± 0.28[a]	2.08 ± 0.25[a]	1.84 ± 0.18[a]	1.94 ± 0.15[a]	1.76 ± 0.25[b]	1.83 ± 0.20[b]	1.70 ± 0.13[b]		
Leukocytes ($G.l^{-1}$)	83.10 ± 14.93	79.80 ± 28.24	65.50 ± 13.33	98.00 ± 12.92	70.60 ± 22.14	83.40 ± 20.00	93.50 ± 24.95	71.80 ± 19.72	88.40 ± 9.97		↓
Haematocrit ($g.l^{-1}$)	0.28 ± 0.03[a]	0.31 ± 0.04[a]	0.31 ± 0.04[a]	0.30 ± 0.02[a]	0.27 ± 0.03[a]	0.31 ± 0.02[a]	0.27 ± 0.05[b]	0.27 ± 0.02[b]	0.23 ± 0.02[b]		
ALB ($g.l^{-1}$)	8.20 ± 1.95	10.04 ± 2.52	12.15 ± 2.35	10.13 ± 1.13	10.38 ± 2.74	9.98 ± 1.72	9.59 ± 1.14	10.19 ± 1.64	10.74 ± 1.97		
ALP ($\mu kat.l^{-1}$)	0.53 ± 0.07	0.51 ± 0.09	0.56 ± 0.12	0.53 ± 0.09	0.63 ± 0.14	0.49 ± 0.07	0.49 ± 0.13	0.46 ± 0.13	0.47 ± 0.08		
ALT($\mu kat.l^{-1}$)	0.31 ± 0.14	0.32 ± 0.12	0.39 ± 0.32	0.31 ± 0.10	0.31 ± 0.16	0.29 ± 0.12	0.29 ± 0.12	0.23 ± 0.10	0.24 ± 0.11		
AST ($\mu kat.l^{-1}$)	2.19 ± 1.25[a]	1.96 ± 1.91[a]	2.06 ± 1.85[a]	1.27 ± 0.73[a,b]	1.88 ± 1.77[a,b]	1.36 ± 1.14[a,b]	1.11 ± 0.80[b]	1.06 ± 0.95[b]	1.20 ± 0.91[b]		
Ca ($mmol.l^{-1}$)	2.65 ± 0.37[a,b]	2.49 ± 0.19[a,b]	3.28 ± 0.46[a,b]	2.98 ± 0.50[a]	2.84 ± 0.40[a]	3.27 ± 0.71[a]	2.73 ± 0.27[b]	2.76 ± 0.45[b]	2.70 ± 0.12[b]	↑	
CHOL ($mmol.l^{-1}$)	4.57 ± 1.53	4.67 ± 2.38	5.13 ± 1.81	4.83 ± 1.58	4.81 ± 1.90	5.00 ± 1.78	3.83 ± 1.36	3.74 ± 1.15	4.14 ± 1.14		
CREA ($\mu mol.l^{-1}$)	15.64 ± 5.80	16.76 ± 12.39	12.81 ± 5.52	15.60 ± 3.83	11.72 ± 5.09	12.99 ± 4.71	16.16 ± 5.94	12.82 ± 5.23	15.29 ± 4.72		
GLU ($mmol.l^{-1}$)	3.09 ± 0.53	3.21 ± 0.55	3.06 ± 0.36	3.03 ± 0.53	3.20 ± 0.89	2.80 ± 0.28	3.07 ± 0.45	2.74 ± 0.42	2.86 ± 0.44		
Fe ($mmol.l^{-1}$)	17.72 ± 4.92[a]	15.04 ± 5.07[a]	19.40 ± 4.59[a]	17.57 ± 3.57[b]	21.22 ± 7.97[b]	24.29 ± 4.00[b]	19.92 ± 8.76[b]	25.19 ± 5.33[b]	24.01 ± 5.88[b]		

Table 6 *(continue)*

Parameter	Group										
	C	CF	CF+	P30	P30F	P30F+	P60	P60F	P60F+	CA	F
LDH (μkat.l^{-1})	15.67 ± 11.08	20.71 ± 20.76	14.46 ± 11.51	9.89 ± 5.18	14.14 ± 14.52	11.71 ± 12.63	10.90 ± 9.89	9.87 ± 10.15	12.53 ± 13.75		
Mg (mmol.l^{-1})	0.79 ± 0.13	0.91 ± 0.16	1.02 ± 0.16	0.86 ± 0.12	1.02 ± 0.21	1.07 ± 0.14	0.88 ± 0.08	0.94 ± 0.11	0.95 ± 0.07		↑
IP (mmol.l^{-1})	1.32 ± 0.28	1.48 ± 0.29	1.61 ± 0.21	1.41 ± 0.36	1.60 ± 0.24	1.98 ± 0.50	1.25 ± 0.24	1.82 ± 0.59	1.48 ± 0.15		↑
TP (g.l^{-1})	34.61 ± 4.18	38.01 ± 7.78	40.42 ± 4.24	34.95 ± 3.22	41.77 ± 11.82	38.89 ± 9.50	33.20 ± 4.42	36.65 ± 8.03	34.72 ± 3.80		↑
TAG (mmol.l^{-1})	6.88 ± 3.70^{a}	6.41 ± 3.30^{a}	8.65 ± 4.76^{a}	5.51 ± 2.57^{a}	7.48 ± 4.56^{a}	8.08 ± 3.45^{a}	5.90 ± 4.12^{b}	3.76 ± 2.04^{b}	4.31 ± 2.61^{b}		
UREA (mmol.l^{-1})	0.54 ± 0.52	0.30 ± 0.16	0.41 ± 0.28	0.36 ± 0.20	0.32 ± 0.28	0.61 ± 0.60	0.26 ± 0.17	0.25 ± 0.12	0.45 ± 0.16	↑	
Na (mmol.l^{-1})	156.27 ± 1.74^{a}	165.37 ± 2.10^{a}	161.44 ± 2.16^{a}	160.97 ± 3.09^{b}	166.62 ± 1.59^{b}	165.96 ± 4.76^{b}	156.61 ± 1.60^{a}	160.90 ± 2.31^{a}	163.32 ± 2.88^{a}		↑
K (mmol.l^{-1})	3.49 ± 0.62	3.74 ± 0.58	3.59 ± 0.82	2.92 ± 0.50	3.73 ± 0.34	3.39 ± 0.26	3.20 ± 0.33	4.00 ± 0.30	3.54 ± 0.38	↓	↑
Cl (mmol.l^{-1})	138.20 ± 2.20^{a}	135.19 ± 1.80^{a}	141.74 ± 2.03^{a}	142.37 ± 3.54^{a}	131.45 ± 2.39^{a}	141.56 ± 3.87^{a}	137.79 ± 2.35^{b}	129.95 ± 1.96^{b}	134.34 ± 2.13^{b}	↑	↓

Note. Treatments: 30% (P30) and 60% (P60) pea meal, commercial carp feed as control (C) and feeds enriched with the enzyme phytase (CF, P30F, P60F) and phytase plus citric acid (CF+, P30F+, P60F+). Significant effect of pea meal is shown by superscript letters (same letters represents no effect); significant effect of citric acid (CA) and F addition is indicated by arrows: ↑ = parameter higher, ↓ = parameter lower. ALB = albumin, ALP = alkaline phosphatase, ALT = alanine aminotransferase, AST = aspartate aminotransferase, Ca = calcium, CHOL = cholesterol, CREA = creatine, GLUC = glucose, LDH = lactate dehydrogenase, Na = sodium, K = potassium, Cl = chloride, Fe = iron, Mg = magnesium, IP = inorganic phosphorus, TP = total protein, TAG = triacylglycerol, UREA = urea

DISCUSSION

In this study, addition of pea meal to tilapia feed had a positive impact on fish growth, with fish in the P30 and P60 groups showing an increase in total length of 3.64% and 6.03%, and an increase in weight of 11.76% and 18.17%, respectively, compared to the control group. These figures were increased even further through the addition of phytase and phytase with citric acid. Interestingly, Schulz et al. (2007), working with tilapia fry (body weight 2.25 g), came to the opposite results when partially substituting fishmeal protein with pea meal at 30, 45 and 60%, finding a significant decrease in growth performance at higher inclusion levels. In one of the most recent studies about the use of new protein sources in fish feeds by Iheanacho et al. (2025) is pea protein considered as promising alternative to soy. The difference between this and Schulz´s et al. (2007) results is probably explained by the different age categories of fish examined as tilapia of such a small size are probably unable to effectively utilise the pea protein. Furthermore, Schulz et al. (2007) did not enrich the diet with citric acid or phytase. Citric acid has been extensively used as an additive in aquafeeds, both for acidification and to improve nutrient utilisation, the associated decrease in stomach pH being shown to have a positive effect on the efficiency of nutrient utilisation (Sarker et al., 2012). According to Daba and Morris (2021), peas already contain small amounts of citric acid, averaging around 1–4 g/kg, which would also aid digestion. Indeed, the addition of 3% citric acid to our feed had the effect of increasing weight gain in the CF+, P30F+ and P60F+ groups. The same positive results were also obtained by Shah et al. (2015) after adding citric acid to rainbow trout (*Oncorhynchus mykiss*), red seabream (*Pagrus major*) and rohu (*Labeo rohita*) feed. Peas are also a good source of phosphorus and phytase was added to the feed as it is known to improve phosphorous utilisation (Sajjadi & Carter, 2004). As in previous studies (Adeshina et al., 2023), we did indeed observe improved phosphorous utilisation after adding this enzyme. In line with the improved results for fish growth, we also observed improvements in other production parameters (i.e. highbackedness and widebackedness indices) and in Fulton's condition factor in the pea meal supplemented groups, although these parameters showed no additional improvements following addition of citric acid.

No changes were observed in the nutritional composition of the whole fish body or muscles in any of the groups studied, regardless of whether pea meal, citric acid or phytase were added. However, this improvement in muscle composition parameters was not conclusive, as also found in the study of Nascimento et al. (2021), who studied juvenile tambaqui (*Colossoma macropomum*). The tambaqui, a plant-eating piranha, were fed a plant protein-based diet supplemented with citric acid added and, while there was no negative effect on fish nutritional status, health or welfare, retention of nutrients and minerals in the muscle was not improved. Similarly, Hisano et al. (2017) found that acidification of the diet of pacu (*Piaractus mesopotamicus*) did not affect fish muscle composition. The fact that

fish of different species fed a plant protein-based diet with added citric acid did not show any improvement in muscle composition may be due to the length of the experiment, the ideal water temperature of the fish species or the different concentration of citric acid in the diet compared with our own study.

While increasing pea meal content and the addition of citric acid and/or phytase negatively affected FCR, growth parameters (SGR and weight gain) were affected positively by increasing the amount of pea meal in the diet and, more importantly, following the addition of phytase. Djeziri et al. (2020) added 15% of pea meal to tilapia and observed no positive effect on FCR and SGR of tilapia compared to a control group fed a fish meal based diet. In this study, these improved results were clearly influenced by the addition of phytase, which presumably helped to destroy the phosphorus bound in phytic acid. Phytic acid is classified as an anti-nutritional substance that binds minerals (calcium, iron, zinc and magnesium) and forms complexes that are difficult to absorb (Baruah et al., 2004). Ravindran (2000) reported that phytate acid also binds with proteins and amino acids and causes a decrease in digestibility. Conceicao et al. (2023) noted that digestibility and use of nutrients and minerals depend not only on the addition of digestive enzymes but also on breeding condition, the source of protein and the size and age of the fish. Rachmawati et al. (2018) studied tilapia fry (av. wt. 0.62 ± 0.01 g) fed diets with phytase at 500 FTU.kg^{-1} feed, 1000 FTU.kg^{-1} feed and 1500 FTU.kg^{-1} feed, and found that the optimum content of phytase positively affecting SGR, FCR and weight gain ranged from 1060 to 1100 FTU.kg^{-1}. In our study, we added phytase at a lower concentration (500 FTU.kg^{-1} feed); nevertheless, the positive effect on the SGR, FCR and weight gain was conclusive. Interestingly, if we look purely at the effect of adding pea meal, minus the additives, we find that SGR and weight gain increased with increasing pea protein content while FCR decreased. In terms of fattening economics, fish grew faster in both groups and were able to use the higher pea protein content with no problems. However, according to El-Saidy and Saad (2008), who examined tilapia fry fed a mixture with cow pea (*Vigna sinensis*) meal, the replacement should not exceed 50% otherwise the growth and feed conversion rates would deteriorate. In this case, it is possible that the use of cow pea was to blame for the difference in results. The cow pea is a non-cultivar pea variety, and therefore contains less nutrients and more anti-nutrients than cultivar varieties.

Tilapia are farmed worldwide under intensive aquaculture and, under such conditions, any stress caused by either poor water quality or inadequate nutrition will quickly become apparent. Haematological parameters, such as number of blood cells or changes in plasma mineral composition, are a commonly used method of monitoring for stress in fish (Seibel et al., 2021). In this study, we decided to evaluate whether the changes in diet would impact fish welfare in a way that could be monitored with the help of blood cell count and plasma biochemical parameters. Haemoglobin values decreased slightly in our P30F+ fish group

and significantly so in the P60F+ group, suggesting that the effect of phytase and citric acid was less significant than the increasing concentration of pea meal. According to Palikova et al. (2015), higher levels of haemoglobin and higher erythrocyte counts in fish are most often caused by increased stress. Kesbiç et al. (2024) added pea flour to rainbow trout feed at concentrations of 25, 50 , 75 and 100%. None of these concentrations had significantly changed the haematological values of fish, except those fed 100% pea flour diet, which displayed a reduction in erythrocyte counts, haemoglobin content and haematocrit. The slight decrease in haemoglobin and erythrocyte values following addition of phytase (erythrocytes down by 10.5%) and phytase and citric acid (down 9%) in our study, therefore, suggest that the fish were not subject to any further stress. Novák et al. added pea flour to trout feed at concentrations of 25, 50 and 75%. None of these concentrations had any effect. These findings agree with those of Bozorgnia et al. (2011), who recorded increased numbers of red blood cells, and thus an increase in haemoglobin level, in carp under stressful conditions. Leukocyte counts should follow the same trend as they have also been shown to increase in fish under stress (Roberts, 2012). In our study, leukocyte counts were highly variable with no statistically significant change; nevertheless, except for the P30F and P60F groups, levels were slightly higher in all groups compared to the control. While addition of phytase had lowering effect on the reduction in leukocyte count, there was no apparent positive effect from the addition of citric acid.

While studying mrigal carp (*Cirrhinus mrigala*) fingerlings, Hussain et al. (2022) recommended acidification of their seed meal-based diet with 3% citric acid due to its positive effect on mineral absorption, carcass composition and haematological indices. In our own study, however, we observed no significant changes in plasma LDH, ALB, CHOL, UREA, CREA, TP, PI, K or Mg concentrations. Vazirzadeh et al. (2022) suggested that the CHOL levels could be affected by feeding duration, and although this 60-day feeding test is standard in length, no changes in CHOL were observed which may be considered positive. UREA and CREA levels are indicative of feed quality, especially the amount of protein, and if these levels are within the fish's physiological limits, it will ensure healthy excretion by the kidneys and metabolic functioning of the liver (Schrama et al., 2018). Our results show that these values did indeed remain stable and, therefore, it can be assumed that pea meal is a suitable source of protein for tilapia. Blood serum Ca and Fe values increased significantly in our study, especially in the groups with 30% pea meal supplementation, and significantly so following acidification with citric acid. This improvement in Ca and Fe could be attributed to maximum liberation of Ca, P, Fe and Cu from the feed ingredients following acid supplementation (Khajepour & Hosseini, 2012). Levels of GLU in the blood serum remained stable in all study groups, indicating no significant glycemic response, even at higher pea-meal concentrations (60%). In agreement with our results, Affonso et al. (2007) described significantly lower plasma Na and Cl concentrations in matrinxa (*Brycon*

amazonicus) fed a diet acidified with vitamin C, suggesting that matrinxa displayed a lowered metabolism and mineral absorption on the new diet. Plasma ALT, AST and ALP are all cytosolic enzymes found in many tissues; consequently, they are used as blood plasma indicators of tissue health (Haschek et al., 2009). ALT and AST levels fluctuated only slightly in our study and, since these refer to the health of the liver, a highly important organ as regards digestion, we can assume that the addition of pea protein had no effect on digestion and nutrient utilisation by the fish. AST also plays a role in glucose production from amino acids (blood glycemic state is a stress marker; Tejpal et al., 2009) and, in our experiment, AST values decreased proportionally with increasing addition of pea meal (significantly in all three P60 groups). According to our results, therefore, a diet based on pea protein is suitable for tilapia and subsequent acidification with citric acid, together with the addition of phytase, has no adverse effect on the health status of the fish; on the contrary, in most cases these additives had a positive effect on production parameters.

CONCLUSION

This study showed that fish feed based solely on pea protein is suitable for tilapia, with the pea meal having a positive impact on fish production parameters. Furthermore, addition of phytase and citric acid helped decrease any potential negative effects of a plant-protein based diet, and increased utilisation of feed minerals. Consequently, we suggest that a feed containing 30 or 60% pea meal is suitable for feeding tilapia under intensive aquacultural conditions, and its enrichment with phytase and citric acid is recommended.

ACKNOWLEDGEMENT

The authors would like to thank Dr. Kevin Roche for proofreading the English text and Dr. Michal Šorf for help with the statistical evaluation of the results. This study was supported through the Project PROFISH, CZ.02.1.01/0.0/0.0/16_019/0000869.

REFERENCES

Adeshina, I., Akpoilih, B. U., Udom, B. F., Adeniyi, O. V., & Abdel-Tawwab, M. (2023). Interactive effects of dietary phosphorus and microbial phytase on growth performance, intestinal morphometry, and welfare of Nile tilapia (*Oreochromis niloticus*) fed on low-fishmeal diets. *Aquaculture, 563*(1), Article 738995. https://doi.org/10.1016/j.aquaculture.2022.738995

Affonso, E. G., Silva, E. D., Tavares-Dias, M., de Menezes, G. C., de Carvalho, C. S. M., Nunes, E. D. S., Ituassú, D. R., Roubach, R., Ono, E. A., Fim, J. D. I., & Marcon, J. L. (2007). Effect of high levels of dietary vitamin C on the blood responses of matrinxa (*Brycon amazonicus*). *Comparative Biochemistry and Physiology*, *147*(2), 383-388. https://doi.org/10.1016/j.cbpa.2007.01.004

Allan, G. L., Parkinson, S., Booth, M. A., Stone, D. A. J., Rowland, S. J., Frances, J., & Warner-Smith, R. (2000). Replacement of fish meal in diets for Australian silver perch, *Bidyanus bidyanus*: I. Digestibility of alternative ingredients. *Aquaculture, 186*(3-4), 293-310. https://doi.org/10.1016/S0044-8486(99)00380-4

Baruah, K., Sahu, N. P., Pal, A. K., & Debnath, D. (2004). Dietary phytase: An ideal approach for a cost effective and low-polluting aqua feed. *NAGA, World Fish Center Quarterly*, *27*(3), 15-19.

Bozorgnia, A., Hosseinifard, M., & Alimohammadi, R. (2011). Acute effects of different temperature in the blood parameters of common carp (*Cyprinus carpio*). In *2nd International Conference on Environmental Science and Technology* (pp. 52-55). IACSIT Press.

Bullon, N., Seyfoddin, A., Hamid, N., Manivannan, M., & Alfaro, A. C. (2023). Effects of insect meal and grape marc in the nutritional profile, growth, and digestibility of juvenile New Zealand farmed abalone. *Aquaculture International*, *32*(2), 1507-1536. https://doi.org/10.1007/s10499-023-01227-z

Conceicao, L. E. C., Morais, S., & Ronnestad, I. (2023). Tracers in fish larvae nutrition: A review of methods and applications. Aquaculture, 267(1-4), 62-75SI. https://doi.org/10.1016/j.aquaculture.2007.02.035

Crépon, K. (2007). Nutritional values of legumes (pea and faba bean) and economics of their use. *Recent Advances in Animal Nutrition, 2006*(1), 331-366. https://doi.org/10.5661/recadv-06-331

Daba, S. D., & Morris, C. F. (2021). Pea proteins: Variation, composition, genetics, and functional properties. *Cereal Chemistry*, *99*(1), 8-20. https://doi.org/10.1002/cche.10439

Djeziri, M., Nouri, L., & Kacher, M. (2020). An investigation on the effects of different diets on the growth performance of Nile tilapia, *Oreochromis niloticus* (Linne 1758). *Iranian Journal of Fisheries Science, 19*(1), 136-150. https://doi.org/10.22092/ijfs.2019.118813

El-Saidy, D. M. S. D., & Saad, A. S. (2008). Evaluation of cow pea seed meal, *Vigna sinensis*, as a dietary protein replacer for Nile tilapia, *Oreochromis niloticus* (L.), fingerlings. *Journal of World Aquaculture and Society*, *39*(5), 636-645. https://doi.org/10.1111/j.1749-7345.2008.00192.x

FAO. (2021). *Detailed data are publically accessible*. Food and Agriculture Organization of the United Nations. https://www.fao.org/faostat/en/#home.

Gela, D., & Linhart, O. (2000). Evaluation of slaughtering value of common carp from diallel crossing. *Czech Journal of Animal Science, 45*(2), 53-58.

Glencross, B., Rutherford, N., & Hawkins, W. (2011). A comparison of the growth performance of rainbow trout (*Oncorhynchus mykiss*) when fed soybean, narrow-leaf or yellow lupin meals in extruded diets. *Aquaculture Nutrition, 17*(3), E317-E325. https://doi.org/10.1111/j.1365-2095.2010.00765.x

Haschek, W. M., Rousseaux, C. G., & Wallig, M. A. (2009). *Fundamentals of toxicologic pathology.* Academic Press.

Hisano, H., Sanchez, M. S. S., & Nascimento, S. M. (2017). Acid citric as a feed additive in pacu *Piaractus mesopotamicus* (Holmberg, 1887) diets. *Journal of Applied Ichthyology, 33*(3), 478-448. https://doi.org/10.1111/jai.13289

Hussain, M., Hussain, S. M., Iqbal, R., Shahzad, M. M., Shah, S. Z. H., Akram, A. M., Ahmad, N., & Arsalan, M. Z. H. (2022). Effect of Citric acid acidified *moringa oleifera* seed meal based diet on minerals absorption,

carcass composition and hematological indices of *cirrhinus mrigala* fingerlings. *Pakistan Journal of Zoology, 54*(4), 1737-1745. https:// doi.org/10.17582/journal.pjz/20190531050527

Iheanacho, S., Hornburg, S. C., Schulz, C., & Kaiser, F. (2025). Toward resilient aquaculture in Africa: Innovative and sustainable aquafeeds through alternative protein sources. *Reviewes in Aquaculture 17*(2), Article e13009. https://doi.org/10.1111/raq.13009

Imsland, A. K. C., Helmvig, T., Kristjansson, G. O., & Arnason, J. (2016). Effect of fish protein replacement in diets for juvenile turbot *Scophthalmus maximus*. *Turkish Journal of Fisheries and Aquatic Sciences, 16*(2), 267-273. https://doi.org/10.4194/1303-2712-v16_2_06

Kesbiç, O. S., Acar, Ü., Kesbiç, F. I., & Yilmaz, S. (2024). Growth performance, health status, gut microbiome, and expression of immune and growth-related genes of rainbow trout (*Oncorhynchus mykiss*) fed diets with pea protein replacement of fish meal. *Comparative Biochemistry and Physiology B-Biochemistry & Molecular Biology, 273,* Article 110968. https://doi.org/10.1016/j.cbpb.2024.110968

Khajepour, F., & Hosseini, S. A. (2012). Citric acid improves growth performance and phosphorus digestibility in Beluga (*Huso huso*) fed diets where soybean meal partly replaced fish meal. *Animal Feed Science and Technology, 171*(1), Article 68e73. https://doi.org/10.1111/j.1365-2109.2011.02843.x

Luthada-Raswiswi, R., Mukaratirwa, S., & O´Brien, G. (2021). Animal protein sources as a substitute for fishmeal in aquaculture diets: a systematic review and meta-analysis. *Applied Sciences-Basel*, *11*(9), Article 3854. https://doi.org/10.3390/app11093854

Murthy, L. N., Mohan, C. O., Ravishankar, C. N., & Badonia, R. (2013). Biochemical quality and heavy metal content of fish meal and squid meal produced in Veraval, Gujarat. *Indian Journal of Fisheries, 60*(3), 113-117.

Nascimento, M. D., de Mattos, B. O., Bussons, M. R. F. M., de Oliveira, A. T., Liebl, A. R. D., & Carvalho, T. B. (2021). Supplementation of citric acid in plant protein-based diets for juvenile tambaqui, *Colossoma macropomum*. *Journal of the World Aquaculture Society*, *52*(1), 231-243. https://doi.org/10.1111/jwas.12735

Palikova, M., Papezikova, I., Kopp, R., Mares, J., Markova, Z., Navratil, S., Adamovsky, O., Kohoutek, J., Navratil, L., & Blaha, L. (2015). Effect of arsenic and cyanobacterial co-exposure on pathological, haematological and immunological parameters of rainbow trout (*Oncorhynchus mykiss*). *Neuroendocrinological Letters*, *36*(S1), 57–63.

Rachmawati, D., Samidjan, I., & Elfitasari, T. (2018, October 2-4). *Effect of the phytase enzyme addition in the artificial feed on digestibility of feed, feed conversion ratio and growth of gift tilapia saline fish (Oreochromis niloticus) nursery stadia*. [Paper presentation]. 3rd International Conference on Tropical and Coastal Region Eco Development, Earth and Environmental Science, Indonesia. https://doi.org/10.1088/1755-1315/116/1/012009

Ravindran, V. (2000). *Effect of natuphos phytase on the bioavailability of protein and amino acids – A review.* Massey University.

Roberts, R. J. (2012). *Fish pathology* (4th ed.) John Wiley and Sons.

Sajjadi, M., & Carter, C. G. (2004). Dietary phytase supplementation and the utilisation of phosphorus by Atlantic salmon (*Salmo salar* L.) fed a canola-meal-based diet. *Aquaculture*, *240*(1-4), 417-431. https://doi.org/10.1016/j.aquaculture.2004.07.003

Sarker, M., Satoh, S., Kamata, K., Haga, Y., & Yamamoto, Y. (2012). Partial replacement of fish meal with plant protein sources using organic acids to practical diets for juvenile yellowtail, *Seriola quinqueradiata*. *Aquacultural Nutrition*, *18*(1), 1-89. https://doi.org/10.1111/j.1365-2095.2011.00880.x

Schulz, C., Wickert, M., Kijora, C., Ogunji, J., & Rennert, B. (2007). Evaluation of pea protein isolate as alternative protein source in diets for juvenila tilapia (*Oreochromis niloticus*). *Aquaculture Research*, *38*(5), 537-545. https://doi.org/10.1111/j.1365-2109.2007.01699.x

Schrama, D., Cerqueira, M., Raposo, C. S., da Costa, A. M. R., Wulff, T., Goncalves, A., Camacho, C., Colen, R., Fonseca, F., & Rodrigues, P. M. (2018). Dietary creatine supplementation in gilthead seabream (*Sparus aurata*): Comparative proteomics analysis of fish allergens, muscle quality, and liver. *Frontiers in Physiology*, *9*, Article 1844. https://doi.org/10.3389/fphys.2018.01844

Seibel, H., Baßmann, B., & Rebl, A. (2021). Blood will tell: What haematological analyses can reveal about fish welfare. *Frontiers in Veterinary Science*, *8*, Article 616955. https://doi.org/10.3389/fvets.2021.616955

Shah, S. Z. H., Afzal, M., Khan, S. Y., Hussain, S. M., & Habib, R. Z. (2015). Prospects of using citric acid as fish feed. *International Journal of Agriculture and Biology, 17*(1), 1-8.

Sieradzki, Z., & Kwiatek, K. (2006). Wykrywanie w paszach kukurydzy i soi genetycznie zmodyfikowanych [Occurrence of genetically modified maize and soybean in feed]. *Medycyna Weterynarnyja, 62*(9), 1035-1037.

Svobodová, Z., Pravda, D., & Modrá, H. (2012). *Metody hematologického vyšetřování ryb. Edice metodik* [Methods of haematology examination of fish. Edition of methodologies]. FROV JU.

Szollosi, L., Beres, E., & Szucs, I. (2021). Effects of modern technology on broiler chicken performance and economic indicators - A Hungarian case study. *Italian Journal of Animal Science*, *20*(1), 188-194. https://doi.org/10.1080/1828051X.2021.1877575

Tejpal, C. S., Pal, A. K., Sahu, N. P., Kumar, J. A., Muthappa, N. A., Vidya, S., & Rajan, M. G. (2009). Dietary supplementation of l - Tryptophan mitigates crowding stress and augments the growth in *Cirrhinus mrigala* fingerlings. *Aquaculture, 293*(3-4), 272–277. https://doi.org/10.1016/j.aquaculture.2008.09.014

TIBCO Software Inc. (2020). *Data science workbench, version 14*. TIBCO. http://tibco.com.

Vazirzadeh, A., Marhamati, A., & Chisti, Y. (2022). Seaweed-based diets lead to normal growth, improved fillet color but a down-regulated expression of somatotropic axis genes in rainbow trout (Oncorhynchus mykiss). *Aquaculture 554,* Article 738183. https://doi.org/10.1016/j.aquaculture.2022.738183

Vo, B. V., Siddiki, M. A. B., Chaklader, M. R., Fotedar, R., Nahar, A., Foysal, M. J., Bui, D. P., & Nguyen, H. Q. (2020). Growth and health of juvenile barramundi (*Lates calcarifer*) challenged with DO hypoxia after feeding various inclusions of germinated, fermented and untreated peanut meals. *Plos One*, *15*(4), Article 0232278. https://doi.org/10.1371/journal.pone.0232278

Watson, B., Reimer, M. N., Guettabi, M., & Haynie, A. (2021). Commercial fisheries and local economies. *Journal of Environmental Economics and Management, 106*, Article 102419. https://doi.org/10.1016/j.jeem.2021.1024

Pertanika J. Trop. Agric. Sci. 48 (6): 1711 - 1732 (2025)

PERTANIKA JOURNALS

TROPICAL AGRICULTURAL SCIENCE

Journal homepage: http://www.pertanika.upm.edu.my/

Chemical Composition, Physicochemical Properties, and *In Vitro* Digestibility of Pretreated Corn Grain for Use as Animal Feed

Sukanya Poolthajit[1], Suriyanee Takaeh[1], Waraporn Hahor[1], Nutt Nuntapong[2], Wanwisa Ngampongsai[3], and Karun Thongprajukaew[1]*

[1]Division of Health and Applied Sciences, Faculty of Science, Prince of Songkla University, Songkhla 90110, Thailand
[2]Kidchakan Supamattaya Aquatic Animal Health Research Center, Aquatic Science and Innovative Management Division, Faculty of Natural Resources, Prince of Songkla University, Songkhla 90110, Thailand
[3]Animal Production Innovation and Management Division, Faculty of Natural Resources, Prince of Songkla University, Songkhla 90110, Thailand

ABSTRACT

Pretreatment techniques have been widely used to improve the quality of animal feed ingredients. In the current study, the chemical composition and the physicochemical properties of treated corn grain (extrusion, microwave irradiation, gamma irradiation, or NaOH hydrolysis) were investigated. The *in vitro* digestibility was evaluated using digestive enzyme extracts from Nile tilapia (*Oreochromis niloticus*) and broiler chicken (*Gallus gallus domesticus*), as well as the pepsin-cellulase technique of the ruminant model. There were notable changes in the chemical compositions ($p < 0.001$), as well as a nutritive profile assessment with Fourier transform infrared spectroscopy. The extrusion pretreatment significantly increased crude protein and ether extract contents, as well as gross energy. However, this method reduced ash and non-fiber carbohydrate contents while increasing the amount of neutral detergent fiber ($p < 0.001$). The determination of pH, water solubility, water absorption capacity, and thermal properties, and observation of diffraction patterns and microstructures indicated that the altered physicochemical properties of treated corn enhanced enzymatic hydrolysis. The results of carbohydrate digestibility testing suggested that microwave irradiation or extrusion were the best pretreatments for aquatic animals, while only extrusion was suitable for poultry. However, the pepsin-cellulase digestibility test revealed no differences in cellulase organic matter solubility, digestible organic matter, and metabolizable

ARTICLE INFO

Article history:
Received: 31 January 2025
Accepted: 12 June 2025
Published: 25 November 2025

DOI: https://doi.org/10.47836/pjtas.48.6.03

E-mail addresses:
spx_nu177@hotmail.com (Sukanya Poolthajit)
suriyanee.ta@gmail.com (Suriyanee Takaeh)
waraporn.hahor@gmail.com (Waraporn Hahor)
nutt.n@psu.ac.th (Nutt Nuntapong)
wanwisa.n@psu.ac.th (Wanwisa Ngampongsai)
karun.t@psu.ac.th (Karun Thongprajukaew)
*Corresponding author

e-ISSN: 2231-8542

energy. Therefore, the most suitable pretreatment method for corn grain used in animal feed is dependent on the target animal group.

Keywords: Alkali treatment, aquatic animal, corn grain processing, gamma radiation, microwave treatment, poultry, pretreatment, ruminant

INTRODUCTION

Animal feed uses between 70 and 80% of the world's corn crop (Dozier et al., 2011). Pigs, poultry, and aquatic animals consume between 50 and 70% corn grain in their diets (Numoto et al., 2019). It serves as the primary source of energy and carotene in animal feed. In most countries, corn grain is the raw material most used as an energy supplement in cattle feed (Freitas et al., 2020). The different starches contained in cattle feed grains are digested at different rates and corn is an excellent grain to offer cattle because of the slow rumen solubility of its starch content. Dietary fiber must be reduced while available carbohydrates rise to increase the percentage of energy feed elements in animal diets. Therefore, increasing the efficiency of ruminant production requires improving the usage of corn, especially the utilization of carbohydrates.

Many previous studies have found that distinct changes occur in the chemical structure of grain during processing. For example, when processing grain by heating or alkaline treatment, proportions of amylopectin to amylose may affect chemical structures and physical morphology. Amylopectin component readily spreads in water to create a gel that retrogrades. Starch with a high amylose content forms a gel that undergoes stronger retrogradation (Silva et al., 2016). The morphology of starch granules changed during processing, suggesting that heat and alkaline treatments can both have an impact on starch granular structure. The strong pericarp and cuticle protein of corn seed was also broken by high temperatures and alkaline treatments, which improved ruminal degradation and increased solubility (Berger et al., 1981). In feed production, microwave and gamma irradiation can improve the quality of feed by modifying physicochemical properties to enhance enzymatic digestion (Sansuwan et al., 2017; Thongprajukaew et al., 2013). Gelatinization has been shown to increase starch availability, and gelatinized starch has been extruded and pelletized successfully in feed manufacturing (Sansuwan et al., 2017). This hydrothermal pretreatment has improved the quality of feed in a number of studies (Han et al., 2022; Karami et al., 2018; Ma et al., 2023).

The structure of the starch granule and the grain are directly impacted by the physical pretreatment techniques listed above (extrusion, microwave irradiation, gamma irradiation, and alkaline treatment). The animal feed industry accepts these techniques, which can be used to alter animal feeds in bulk at once. In general, the desirable effects of pretreatments not only affect proximate chemical compositions, but also provide qualitative changes,

involving physicochemical properties such as pH, water solubility, water absorption capacity (WAC), thermal properties, X-ray diffraction behaviors, relative crystallinity (RC) and microstructures. These characteristics are related to *in vitro* enzyme digestion, indicating whether the pretreated raw material is suitable for use as animal feed (Hahor et al., 2022; Thongprajukaew et al., 2015; Zhou et al., 2018).

Before performing an *in vivo* feeding trial, feed utilization can be examined using an *in vitro* digestibility test (Hahor et al., 2022; Thongprajukaew et al., 2015; Zhou et al., 2018). As a result, the purpose of this study was to determine how four pretreatment strategies (extrusion, microwave irradiation, gamma irradiation, or NaOH hydrolysis) affected the physicochemical characteristics and approximate chemical composition of corn grain. *In vitro* digestibility was investigated using digestive enzymes from the Nile tilapia (*Oreochromis niloticus*) and the broiler chicken (*Gallus gallus domesticus*), which were representative of aquatic animal and poultry models, respectively. Commercially available pepsin and cellulase were also used in an *in vitro* ruminant model. The obtained results could be applied for improving corn grain quality for animal feeds.

MATERIALS AND METHODS

Corn Grain Pretreatments

The yellow corn grain (CP 801; ≤ 14.5% moisture, ≥ 8 % crude protein) was purchased from Mitrkasetphand Co., Ltd. in Nakhon Pathom, Thailand. They were packed in sacks and stored at room temperature during distribution. No more than 4% of cracked grains were found during the selection and production standards. Fifty-kilogram samples were downsized to accommodate fifteen experimental units (1 kg each), derived from five treatments and three replications. The pretreatment methods were applied as used in previous studies on feed or food. The control was untreated corn (a). A pellet mill (Model 1112-4; California Pellet Mill, Crawfordsville, IN, USA) was used to extrude the corn mash through a 4.0 mm diameter ring die after it had been conditioned at 82°C for 45 s. The extrudates were separated and dried at 50 °C for 2 h (b). In a round plastic container of 23 cm in diameter by 10.5 cm in height, 300 g of corn grain was combined with distilled water (2: 1 *w*/*v*) for the microwave irradiation treatment. The mixture was exposed to radiation for 11 min at 700 W in a microwave oven (MW71B; Samsung, Kuala Lumpur, Malaysia) (Sansuwan et al., 2017) (c). In the treatment with gamma radiation, corn grain was irradiated at a dose of 30 kGy (Shawrang et al., 2008) using Co from a carrier-type gamma irradiator (JS 8900 IR-155; MDS Nordion, Ottawa, ON, Canada) (d). The grain was treated with 3.5% of concentrated NaOH (35% *w*/*v*) for 15 min as part of the alkaline pretreatment, as detailed by Takaeh et al. (2024). Loosely packed in a jar, the treated samples were spread out over a carpet and dried for 48 h at 60 °C (e). All the triplicate samples of

untreated and treated corn were freeze-dried for 24 h, ground, and sieved. Before being used for chemical analysis, the samples were stored in a desiccator.

Proximate Chemical Compositions and Nutritive Profiles

The chemical compositions of samples were determined as described by the Association of Official Analytical Chemists (1990), including dry matter (DM), crude protein (CP), ether extract (EE), and ash contents. The quantities of neutral detergent fiber (NDF) and acid detergent fiber (ADF) in the samples were measured using the Van Soest et al. (1991) method. The formula for determining non-fiber carbohydrate (NFC, %) was 100 – (% CP + % EE + % NDF + % ash). Gross energy (GE) was measured using an adiabatic bomb calorimeter (AC500; Leco, St. Joseph, MI, USA).

Fourier transform infrared (FTIR8400s; Shimadzu, Kyoto, Japan) spectroscopy was applied to untreated and treated samples to evaluate qualitative variations in the treated samples' nutritional values. Using an infrared tablet press (FW-4; Thermo Fisher Scientific, Waltham, MA, USA), two hundred milligrams of KBr were combined with two milligrams of dried corn, ground evenly, and then formed into a tablet. The spectra were obtained at a resolution of 4 cm^{-1} and in the mid-IR range of 4000 to 400 cm^{-1}.

Physicochemical Properties

pH

Distilled water (6.25 mL) was used to suspend 0.25 g of untreated and treated corn samples, which were then shaken for 10 min (Sokhey & Chinnaswamy, 1993). A pH meter (Five Easy F20; Mettler-Toledo GmbH, Greifensee, Switzerland) was used to measure the pH.

Water Solubility

Corn samples that were both untreated and treated were tested for water solubility using the protocol described by Chung et al. (2010). To summarize, 1 g of the material was mixed with 10 mL of water, shaken at 200 rpm for 1 h at room temperature, and then centrifuged for 10 min at 1500 × *g*. Following collection, the supernatant was weighed and dried for 48 h at 60 °C. The solubility of the sample was calculated by dividing the weight of the dissolved particles in the supernatant by the weight of the dry solids in the original sample.

Water Absorption Capacity (WAC)

WAC analysis was performed as described by Jitngarmkusol et al. (2008). In summary, 2 g samples of both untreated and treated corn were suspended in 5 mL of distilled water and allowed to stand at room temperature for 30 min. The suspended samples were centrifuged

for 10 min at 2000 × *g*. Following the supernatant's decantation, the sample was weighed again, and the WAC was expressed as grams of water absorbed per gram of material and was computed on a dry basis.

Differential Scanning Calorimeter (DSC)

The thermal characteristics of untreated and treated corn samples, including onset (T_o), peak (T_p) and conclusion (T_c) temperatures of starch gelatinization, temperature range (T_c–T_o), and transition enthalpy (ΔH), were determined by DSC (DSC7; Perkin Elmer, Waltham, MA, USA). Three milligrams of the sample were placed in an aluminum pan, which was sealed, allowed to acclimate for 1 h at room temperature, and then heated at a rate of 10 °C/min from 40 to 400 °C.

Diffraction Pattern and RC

Using an X-ray diffractometer (XRD, X′ Pert MPD; Philips, Netherlands), the RC and diffraction patterns of both untreated and treated corn samples were ascertained at 40 kV and 30 mA. Only a range of 4 to 40 ° was given; however, the angles were scanned from 4 to 90 ° (2θ). The RC (%) was estimated from (Area under peaks/total area) × 100.

Microstructure

Scanning electron microscopy (SEM, Quanta 400; FEI, Brno, Czech Republic) was used to examine samples of both untreated and treated corn. For the dried samples, double-sided sticky tape was used first, and then gold plating. Surface microstructures were captured at 250× and 1 500×.

In Vitro Digestibility Screening

Aquatic Animal and Poultry Models

Three specimens of four-month-old Nile tilapia and three specimens of forty-two-day-old broilers were acquired from a farm located within Prince of Songkla University. The Institutional Animal Care and Use Committee granted approval for the animal protocols (Code 2022-Sci11-018). The intestinal specimens of the investigated species were obtained and subjected to extraction using a micro-homogenizer (THP-220; Omni International, Kennesaw GA, USA) and 0.2 M Na_2HPO_4-NaH_2PO_4 buffer at pH 8 (1:5 *w*/*v*). Following a 30-minute centrifugation of the homogenate at 4°C at 15000 × *g*, the recovered supernatant was dialyzed overnight against an extraction buffer. Until they were needed, the dialyzed enzymes were stored as tiny aliquots at –20 °C. The *in vitro* digestibility trial was carried out using Thongprajukaew et al. (2011)'s methodology. Five milligrams of dried corn, 10 mL of

50 mM Na_2HPO_4-NaH_2PO_4 buffer at pH 8, 50 µL of 0.5% chloramphenicol, and 125 µL of dialyzed crude enzyme extract were added to reaction mixtures, which were then incubated for 24 h at 25 °C. Protein digestibility *in vitro* was measured spectrophotometrically at 420 nm using the *DL*-alanine standard curve, and carbohydrate digestibility at 540 nm using the maltose standard curve.

Ruminant Model

The pepsin-cellulase method, as described by De Boever et al. (1986), was used to evaluate the digestibility of untreated and treated corn samples. A glass filter-crucible containing 300 mg of freeze-dried sample was filled with 30 mL of a pepsin-hydrochloric acid solution. Every five hours, the crucible was shaken during its 24-h incubation at 40 °C. After 45 minutes of immersion in a water bath at 80 °C, the crucible was rinsed with distilled water to remove any remaining residue, and the solution was aspirated. Cellulase buffer was added to 30 mL of solution at 40 °C, and the mixture was shaken every five hours for 24 h. The residue was washed with distilled water at 40 °C after the solution was aspirated. The cellulase organic matter solubility (COMS) was calculated by burning the residue at 550 °C after the digested fraction was dried at 103 °C to determine the dry matter value. The formula for COMS (%) is $(W_o–W_t/W_o) \times 100$, where W_o and W_t represent the weights of organic matter (OM) prior to and following incubation. According to De Boever et al. (1986), the metabolizable energy (ME) and digestible organic matter (DOM) of the untreated and treated corn samples were determined as follows: ME (MJ/kg DM) = (0.150 × COMS) + (0.214 × EE) – 0.99, and DOM (%) = (0.973 × COMS) – 2.49.

Statistical Analysis

There was a completely randomized design (CRD) for the studies. The presented data are the means ± standard error of mean (SEM). Significant differences between means were examined and ranked using One-Way Analysis of Variance and Duncan's Multiple Range Test (DMRT) at 95% confidence levels.

RESULTS

Chemical Compositions of Untreated and Treated Corn

Table 1 shows the proximate chemical contents of both untreated and treated corns. Relative to untreated corn, significantly decreased DM was observed in corn pretreated by extrusion and NaOH, while corn pretreated by microwave and gamma irradiation showed increased DM ($p < 0.05$). Decreased OM was observed only in the NaOH treatment. Extruded and gamma-irradiated corns showed higher CP contents, but the NaOH-treated group showed the opposite effect. The CP content of the untreated and microwave-irradiated groups did

not differ significantly. Improved EE contents were observed in all treatments, except for the NaOH treatment. Among the four treatments, large amounts of NDF and ADF were disrupted by gamma irradiation. The remaining treatments increased both indigestible components, with the exception of ADF in extruded corn. Ash content was significantly higher in the NaOH treatment relative to untreated corn, and lower in the extrusion, microwave irradiation, and gamma irradiation treatments. Increased NFC content was observed only in gamma-irradiated corn. The gross energy of the extruded sample increased, but the gamma-irradiated samples displayed the opposite pattern.

Although there were variations in peak heights and intensities, overall, the FTIR spectra were similar. At least eighteen bands (2924, 2852, 1743, 1652, 1542, 1462, 1373, 1240, 1157, 1059, 991, 927, 858, 765, 711, 574, 526, and 437 cm^{-1}) were observed in the range of 4000 to 400 cm^{-1} (Figure 1), showing qualitative alterations in nutritional profiles, particularly in the components of proteins, lipids, carbohydrates, and inorganic matter (Table S1).

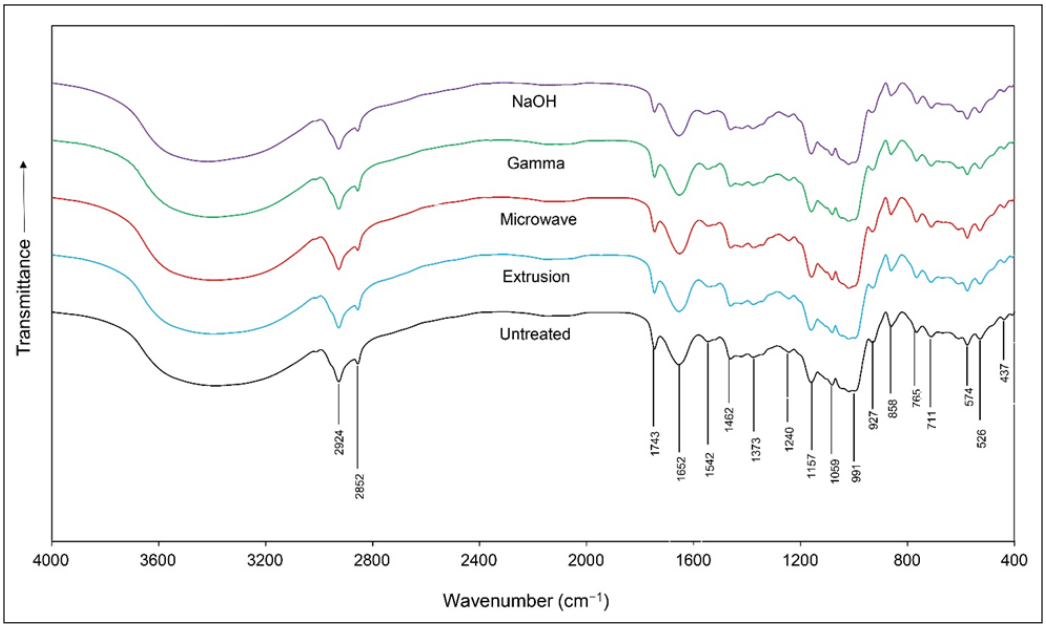

Figure 1. FTIR spectra of untreated, extruded, microwave-irradiated, gamma-irradiated, and NaOH-treated corn samples

Physicochemical Properties of Untreated and Treated Corn

pH

The pretreatment changed the pH of the corn samples ($p < 0.05$, Table 2). The corn that had been treated with NaOH had the highest pH, followed by the corn that had been microwave-

Table 1
The chemical compositions of dry matter of untreated and treated corn grains. Three separate samples were used to calculate the values

Chemical composition	Untreated	Extrusion	Microwave	Gamma	NaOH	*p*-value
Dry matter (%)	93.3 ± 0.6^{c}	82.4 ± 0.2^{e}	93.9 ± 0.1^{b}	94.4 ± 1.9^{a}	92.1 ± 0.5^{d}	<0.001
Organic matter (%)	98.5 ± 0.1^{b}	98.8 ± 0.1^{a}	98.8 ± 0.1^{a}	98.7 ± 0.1^{a}	94.7 ± 0.1^{c}	<0.001
Crude protein (%)	9.7 ± 0.1^{b}	12.3 ± 0.1^{a}	10.0 ± 0.1^{b}	12.1 ± 0.2^{a}	8.1 ± 0.1^{c}	<0.001
Ether extract (%)	4.16 ± 0.05^{c}	4.29 ± 0.01^{b}	4.52 ± 0.04^{a}	4.15 ± 0.02^{c}	2.75 ± 0.01^{d}	<0.001
Neutral detergent fiber (%)	21.3 ± 0.4^{d}	24.6 ± 0.5^{c}	28.2 ± 0.3^{b}	11.5 ± 0.3^{e}	31.9 ± 0.3^{a}	<0.001
Acid detergent fiber (%)	3.51 ± 0.03^{c}	3.49 ± 0.04^{c}	4.79 ± 0.03^{a}	2.98 ± 0.04^{d}	4.43 ± 0.02^{b}	<0.001
Ash (%)	1.66 ± 0.03^{b}	1.47 ± 0.01^{c}	1.33 ± 0.01^{c}	1.36 ± 0.01^{c}	5.74 ± 0.09^{a}	<0.001
Non-fiber carbohydrate (%)	63.1 ± 0.4^{b}	57.3 ± 0.5^{c}	55.9 ± 0.3^{d}	71.0 ± 0.3^{a}	51.5 ± 0.3^{e}	<0.001
Gross energy (kJ/g)	18.3 ± 0.1^{b}	19.0 ± 0.1^{a}	18.1 ± 0.1^{b}	18.2 ± 0.1^{c}	17.2 ± 0.1^{b}	<0.001

$^{a-e}$ Significant differences are indicated by means in the same row with different superscripts ($p < 0.05$)

Table 2
pH, water solubility, and water absorption capacity (WAC) of untreated and treated corn grains. Three separate samples were used to calculate the values

Item	Untreated	Extrusion	Microwave	Gamma	NaOH	*p*-value
pH	6.6 ± 0.1^{c}	6.3 ± 0.1^{d}	6.8 ± 0.1^{b}	6.3 ± 0.1^{d}	10.9 ± 0.1^{a}	<0.001
Water solubility (%)	6.9 ± 0.6^{c}	19.3 ± 0.24^{a}	5.8 ± 0.1^{c}	8.5 ± 1.9^{c}	12.8 ± 0.5^{b}	<0.001
WAC (g water/g feed)	0.26 ± 0.01^{bc}	0.23 ± 0.01^{c}	0.29 ± 0.01^{b}	0.27 ± 0.03^{bc}	0.37 ± 0.01^{a}	0.001

$^{a-d}$ Significant differences are indicated by means in the same row with different superscripts ($p < 0.05$)

irradiated. The pH values of extruded and gamma-irradiated corn were significantly reduced relative to untreated corn.

Water solubility and WAC

Pretreatment techniques had a substantial impact on water solubility and WAC ($p < 0.05$, Table 2). The corn that was extruded showed a maximum solubility, followed by NaOH-treated corn. Corn treated with NaOH showed the highest WAC, while the other treatments did not differ significantly compared to untreated corn.

Thermal Transition Properties

Starch gelatinization and phase change were quantified by DSC. Within the studied temperature range, all samples produced two transition peaks, except NaOH-treated corn, which produced only one peak (Table 3). Peaks I and II designated available nutrients and available nutrients in complex with other compartments. These peaks spanned temperature ranges from 45.4 to 159 °C and 264 to 286 °C, respectively. Overall, significant shifts in transition temperatures (T_o, T_p, and T_c) were observed in all pretreatments. In peak I, broader T_c–T_o ranges were observed in extruded, gamma-irradiated, and NaOH-treated corn, while ΔH did not differ significantly compared to untreated corn. For peak II, the T_c–T_o ranges in the gamma and extrusion pretreatments were wider and narrower, respectively. Corn pretreated by microwave irradiation exhibited the highest ΔH value. ΣΔH values were unaffected by pretreatment.

Diffraction Patterns

The main peaks in the diffraction patterns of the untreated and treated corn samples were similar (16.5, 18.3, and 24.6 º) (Figure 2). Nonetheless, minor variations were noted at the angles of 14.5 to 19.0 º and 22.0 to 23.5 º. Pretreatment had little effect on RC, which ranged from 21.2 to 22.7%.

Microstructure

Across the four corn grain treatments, there were a few minor variations in microstructure architectures. All of the samples had agglomerated irregular particles as their general morphology at low magnification. Smooth surfaces and swelling were observed at higher magnification. Untreated (Figures 3a and 3b), extruded (Figures 3c and 3d), and gamma-irradiated (Figures 3g and 3h) samples had similar general features. Fusion and aggregation of starch granules were seen in corn pretreated by microwave irradiation (Figures 3e and 3f). Rough, laminated, and abraded surfaces with shallow grooves were observed in corn pretreated by NaOH (Figures 3i and 3j).

Table 3
Thermal transition properties of untreated and treated corn grains. Three separate samples were used to calculate the values

Thermal parameter	Untreated	Extrusion	Microwave	Gamma	NaOH	*p*-value
Peak I						
T_o (°C)	46.8 ± 1.6	45.4 ± 1.3	46.3 ± 0.9	48.6 ± 0.6	46.1 ± 0.7	0.380
T_p (°C)	88.6 ± 0.9^{b}	90.3 ± 1.2^{ab}	88.7 ± 1.2^{b}	91.9 ± 0.5^{a}	92.5 ± 0.4^{a}	0.030
T_c (°C)	147 ± 1^{c}	157 ± 1^{ab}	149 ± 1^{c}	155 ± 1^{b}	159 ± 1^{a}	<0.001
T_c–T_o (°C)	100 ± 2^{c}	111 ± 1^{a}	103 ± 1^{c}	107 ± 1^{b}	113 ± 1^{a}	<0.001
ΔH (J/g)	207 ± 3^{ab}	180 ± 7^{b}	194 ± 1^{b}	198 ± 10^{ab}	224 ± 6^{a}	0.030
Peak II						
T_o (°C)	270 ± 1^{a}	270 ± 1^{a}	270 ± 1^{a}	264 ± 1^{b}	–	<0.001
T_p (°C)	277 ± 1^{b}	275 ± 1^{c}	278 ± 1^{a}	274 ± 1^{d}	–	<0.001
T_c (°C)	285 ± 1^{b}	280 ± 1^{d}	286 ± 1^{a}	281 ± 1^{c}	–	<0.001
T_c–T_o (°C)	15.1 ± 0.5^{b}	10.0 ± 0.2^{c}	15.9 ± 0.8^{ab}	16.8 ± 0.3^{a}	–	<0.001
ΔH (J/g)	6.13 ± 0.10^{b}	4.74 ± 0.21^{b}	7.57 ± 0.93^{a}	5.65 ± 0.26^{b}	–	<0.001
ΣΔH (J/g)	213 ± 3	185 ± 7	202 ± 12	204 ± 10	224 ± 6	0.060

T_o, onset temperature; T_p, peak temperature; T_c, conclusion temperature; T_c–T_o, melting temperature range, ΔH, enthalpy
$^{a–d}$ Significant differences are indicated by means in the same row with different superscripts ($p < 0.05$)

Table 4
The dry matter digestibility of untreated and treated corn grains using pepsin-cellulase for a ruminant model. Three separate samples were used to calculate the values

Digestibility	Untreated	Extrusion	Microwave	Gamma	NaOH	*p*-value
COMS (%)	94.1 ± 0.1	95.7 ± 0.1	95.9 ± 0.4	95.7 ± 0.2	96.4 ± 1.6	0.360
DOM (%)	89.1 ± 0.1	90.6 ± 0.1	90.8 ± 0.4	90.7 ± 0.19	91.3 ± 1.6	0.370
ME (MJ/kg)	14.0 ± 0.1	14.3 ± 0.1	14.4 ± 0.1	14.3 ± 0.1	14.1 ± 0.2	0.240

Note.
COMS, cellulase organic matter solubility; DOM, digestible organic matter; ME, metabolizable energy
Data are expressed as means ± SEM

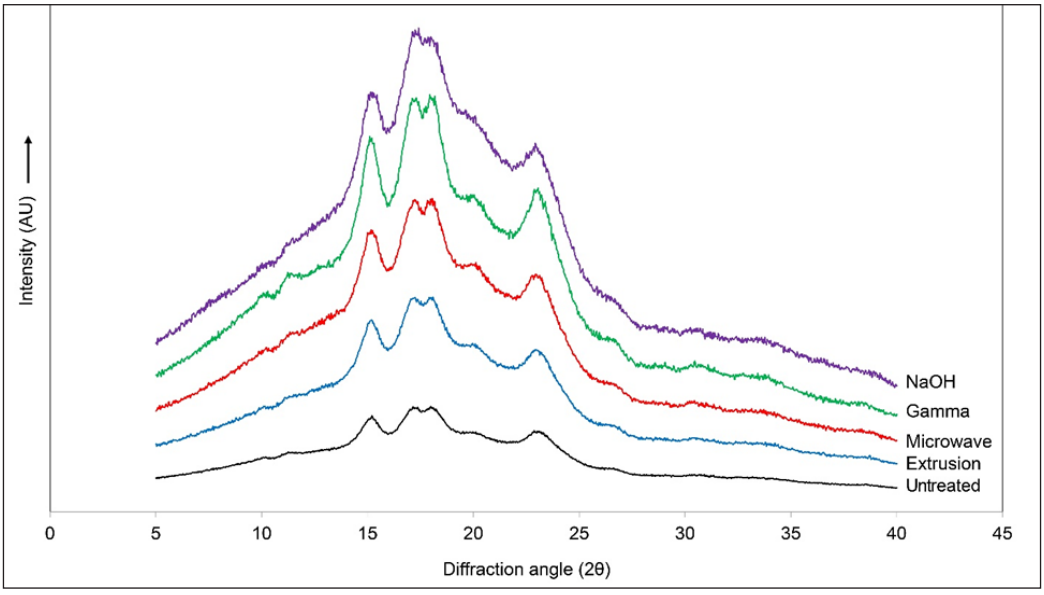

Figure 2. Diffraction patterns of untreated, extruded, microwave-irradiated, gamma-irradiated, and NaOH-treated corn samples

In Vitro Digestibility

Aquatic Animal and Poultry Models

Using Nile tilapia digestive enzymes, the corn treated with NaOH showed the maximum carbohydrate digestibility, followed by corn that was microwave-irradiated, extruded, and gamma-irradiated, respectively. All pretreated samples showed higher carbohydrate digestibility relative to untreated corn ($p < 0.05$; Figure 4a). There were no discernible variations in the protein digestibility between the untreated and treated samples ($p > 0.05$; Figure 4b). When using digestive enzymes from broiler chickens, the highest carbohydrate digestibility was observed in NaOH-treated corn, followed by extruded corn. Untreated corn, gamma-irradiated corn, and microwave-irradiated corn showed the lowest digestibility of carbohydrates ($p < 0.05$; Figure 4c), except for gamma-irradiated corn which showed no significant differences relative to extrusion ($p > 0.05$). Protein digestibility using broiler enzymes was unaffected by pretreatment ($p > 0.05$; Figure 4d).

Ruminant Model

No significant differences in COMS (94.1 to 96.4%), DOM (89.1 to 91.3%), and ME (14.0 to 14.4%) were observed among the four treatments and control ($p > 0.05$, Table 4).

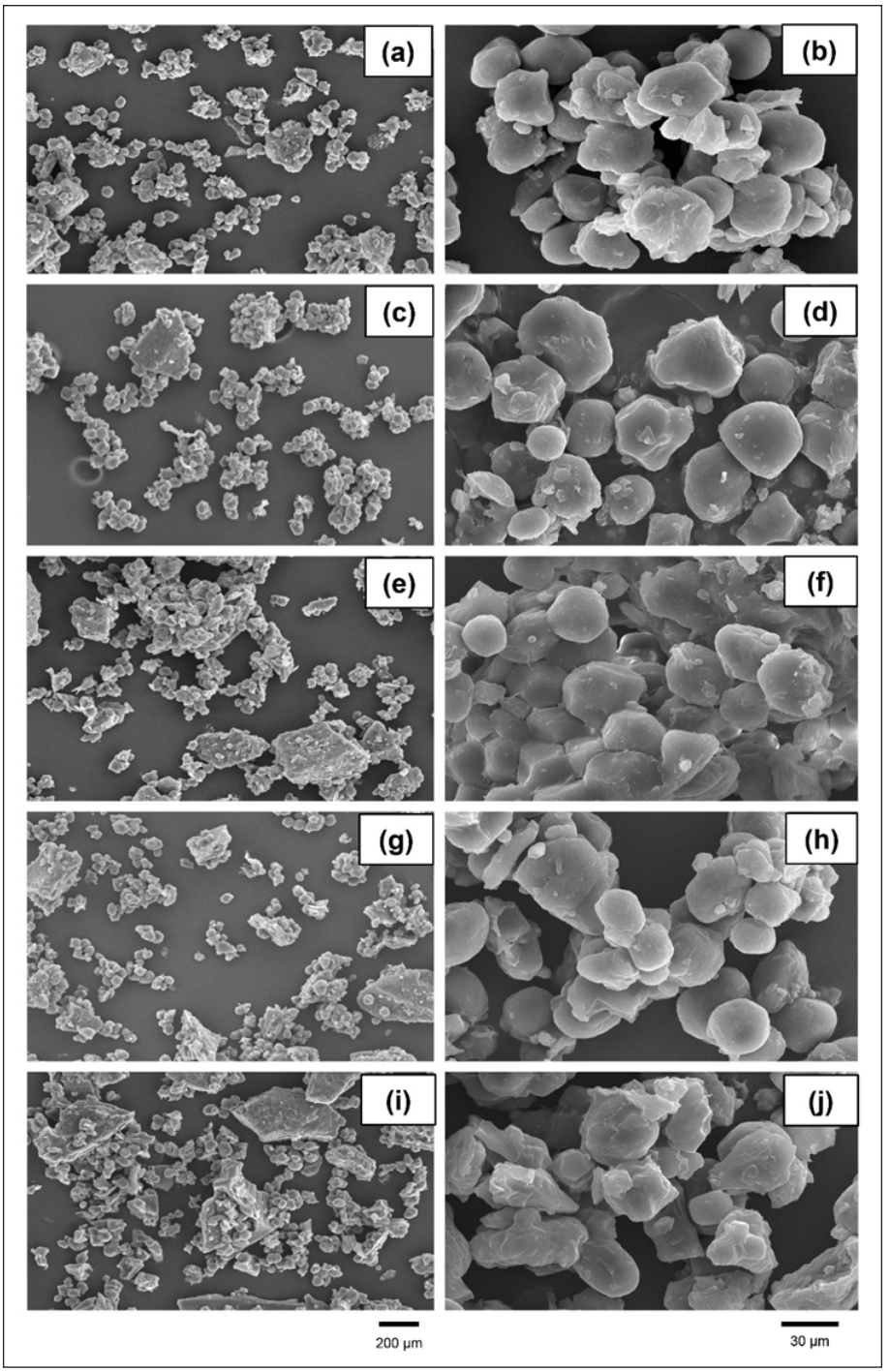

Figure 3. Microstructures of untreated (a and b), extruded (c and d), microwave-irradiated (e and f), gamma-irradiated (g and h), and NaOH-treated (i and j) corn. Micrographs were captured at 250× (left) and 1500× (right) magnifications

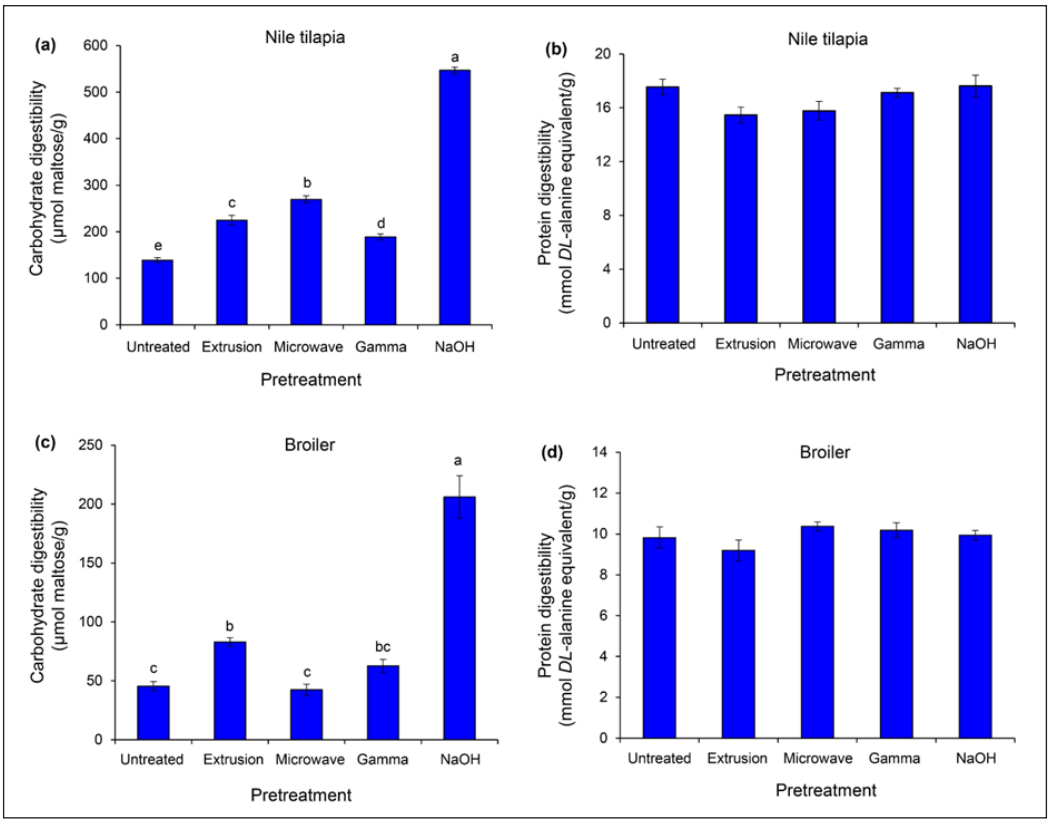

Figure 4. *In vitro* digestibility of untreated and treated corn samples for carbohydrates (µmol maltose/g sample, left) and protein (mmol *DL*-alanine equivalent/g sample, right). The Nile tilapia (a and b) and broiler (c and d) provided the enzymes for the *in vitro* tests. Means ± SEM ($n = 3$) are used to express the data. Different superscripts ($p < 0.05$) indicate significant differences between treatments

DISCUSSION

Chemical Compositions

The chemical compositions of the corn grain were significantly altered by the pretreatments. Changes in the chemical composition can be due to differences in dry matter content, or losses in some components, for example volatilization of organic matter can increase the ash content. CP and EE contents were lower in the NaOH treatment than in control and all other treatments. The average ranges of CP and EE (8.09 to 12.3% and 2.75 to 4.29%, respectively) were similar to previously reported ranges of 8.44 to 8.80% for CP and 4.70 to 4.95% for EE (Srakaew et al., 2021; Suksombat et al., 2007). In general, the thermo-alkaline NaOH process drastically changed the proteins, lipids and starch in the grain kernels, reducing the values of CP, EE, and NFC in treated samples (Palacios-Fonseca et al., 2013). These changes increased the amounts of NDF and ADF in the NaOH-treated corn. Furthermore, the results showed an increase in ash content when the samples were

treated with NaOH, perhaps due to Na is present in the oxide form. Nonetheless, grain corn contains very little ash and fibrous carbohydrates, so any loss will not have an impact on the composition of other ingredients or probably GE.

The increased CP in gamma-irradiated corn was consistent with findings reported for canola meal (Sekali et al., 2023) and palm kernel meal (Thongprajukaew et al., 2013). Proteins and other N-containing substances developed covalent cross-linkages upon exposure to gamma radiation, which changed them into greater molecular weight aggregates (Sadeghi & Shawrang, 2006). While NDF and ADF decreased, NFC increased, indicating the disruption of cell wall constituents, enabling the expansion of available carbohydrates (Thongprajukaew et al., 2013). The significant decrease in the ash content of gamma-irradiated corn is in agreement with studies of pretreatments of velvet bean seed (Bhat et al., 2008) and pigeon pea flour (Bamidele & Akanbi, 2013). In general, gamma irradiation can affect the amount of minerals and ash in certain materials. It might alter the mineral composition and impact the overall quantity of ash present, potentially leading to the amorphization of some phases (Hashim et al., 2024; Lowińska-Kluge & Piszora, 2008).

The proximate chemical composition of microwaved corn grain was different to the proximate chemical composition of gamma-irradiated corn. In general, EE-containing foods are sensitive to heating by microwave irradiation. However, since microwave irradiation can extract lipids, the increased EE contents in the present study might be due to improved extraction efficiency (Hahor et al., 2022). The creation of protein-fiber complexes during pretreatment may be the cause of the elevated NDF and ADF (Bressani, 1993). These changes would have a direct effect on the cellulose, hemicellulose, and lignin composition of the lignocellulosic barrier as well as the NFC (Thongprajukaew et al., 2015). Alteration in the structure and composition of cell walls and other components, such as the formation of new cell wall-bound protein or insoluble condensed tannin-protein polymers, can result from microwave treatment, increasing the amount of NDF and ADF in food (Jančík et al., 2017; Shishir et al., 2020). For hydrothermal extrusion, the amount of CP and EE in corn grain were increased by this treatment method. However, this method reduced the amount of ash and NFC while increasing NDF.

Differences among specific constituents between the four pretreatments did not affect GE in microwaved and NaOH-treated corns. However, FTIR spectral analysis indicated qualitative changes to corn grain after pretreatment. Changes in the characteristics of proteins, lipids, carbohydrates, and inorganic materials were found, as shown in the annotated spectra (Table S1).

Physicochemical Properties

Significantly increased pH was observed in corn pretreated with NaOH. NaOH contributes to the increased overall alkalinity of pretreated corn. Significant changes were also observed in the other treatments. The breakdown of larger molecules into smaller ones, particularly

proteins and carbohydrates, which results in the production of acidic carboxyl groups, is most likely the cause of the lowered pH of extruded and gamma-irradiated corn (Hahor et al., 2022; Thongprajukaew et al., 2015). Conversely, the possibility exists that the elevated pH in the microwave-irradiated corn results from the hydroxyl groups released during the decomposition of lignocellulosic components (Thongprajukaew et al., 2013).

The extruded and NaOH-treated corn had higher water solubility than other treatments. This characteristic is associated with the capacity of enzymes to hydrolyze substrates (Chung et al., 2010). Regarding interactions with water, the WAC of NaOH-treated corn was higher than control whereas WAC did not differ relative to control in the other treatments. The differences in fiber content might have impacted WAC since the fiber constituents, especially hydrophilic celluloses, contain a number of hydroxyl groups, producing a polarity which facilitates water absorption (Rashid et al., 2015).

The starch gelatinization is often quantified using DSC. In the present study, the T_p and T_c from Peak I showed upward trends, except for the corn pretreated by microwave irradiation. Amylose-amylose and amylose-amylopectin interactions, or the complexation between amylose and other substances may cause increased temperature (Caetano et al., 2019). However, similar changes in Peak II were found in the microwave-irradiated sample, suggesting that complexes form at higher temperatures. On the other hand, some thermal parameters in Peak II were lower than control in corn pretreated by extrusion or gamma irradiation. It is possible that these pretreatment methods disrupted the starch granule, which might be related to the lower temperature of gelatinization (Macarthur & Appolonia, 1984). Shifts in onset and conclusion points caused significantly changed $T_c - T_o$ ranges, indicating a wide range of cleaved polymer chain lengths after pretreatments (Thongprajukaew et al., 2015). Molecular transformation brought about by pretreatment can indicated by the ΔH. The reduced $\Sigma\Delta H$ of the extruded corn was significant, indicating the presence of low amounts of unaltered untreated corn. The hydrothermal extrusion pretreatment destroyed the ordered structure of starch granules. This characteristic is beneficial for enzymatic hydrolysis *in vitro*.

The crystal structure of the untreated and treated corn samples was determined by XRD analysis. The diffraction patterns exhibited intense peaks at 16.5, 18.3 and 24.6 °, respectively. This result was consistent with the intense peaks of corn starch at 15, 17, 18 and 23 ° reported by Wang et al. (2020) that indicated a classical A-type crystalline structure. However, this unique crystal structure can be altered by the pretreatment disruption of the crystallization region (Chang et al., 2013). Although some structural changes were observed via XRD, the four present pretreatment methods did not alter corn RC.

Surface roughness and the ability of enzymes to use feed components are directly related (Thongprajukaew et al., 2013). Fusion and aggregation characteristics in corn pretreated by microwave irradiation indicate the gelatinization of starch. Disruptions

causing rough, laminated, and abraded surfaces with shallow grooves were observed in corn treated with NaOH. On the other hand, extruded and gamma-irradiated corn samples showed similar characteristics to untreated corn, indicating small changes in the starch architecture. Based on overall physicochemical investigations, extrusion appears to be a suitable pretreatment method for corn grain.

In Vitro Digestibility

The qualitative changes in raw materials caused by the pretreatment process directly improve digestibility by digestive enzymes, whereas changes in proximate chemical composition have little impact on *in vitro* digestibility (Thongprajukaew et al., 2013). Significant improvements in carbohydrate digestibility were observed in the aquatic animal and poultry *in vitro* models. NaOH pretreatment increased carbohydrate digestibility most in both models, but NaOH can have hazardous effects and there is a lack of information about the consumption of corn pretreated in this way by monogastric animals (Han et al., 2022). The hydrothermal extrusion treatment appears to be suitable for these two model species, while microwave irradiation gave good results with digestive enzymes from Nile tilapia. Improved nutrient digestibility or feed utilization have been reported for these pretreatments in a number of studies (Hahor et al., 2022; Sansuwan et al., 2017; Thongprajukaew et al., 2015). Nutritive profiles and physicochemical changes support the increased *in vitro* carbohydrate digestibility in both models.

For ruminant model, we observed no differences in digestibility values between untreated and treated corn samples. Nevertheless, there are not many published comparisons of the molecular structures of variously treated corn. Xu et al. (2018) reported that steam-flaked corn had higher rumen degradable DM and starch, but lower rumen degradable protein, compared to untreated corn. Furthermore, Karami et al. (2018) used an *in vitro* gas test with two types of thermally treated corn demonstrating that the OM digestibility and ME of extruded corn were higher than those of steam-flaked corn. Moreover, based on the degradation of starch, the study of Han et al. (2022) found that steam flaking and extrusion were more beneficial than grinding. The starch gelatinization was increased during both processes (Boroojeni et al., 2016), possibly due to the swelling during steam flaking and extrusion. However, starch digestibility was not assessed in the present study and it is possible that physicochemical changes may have direct effects on starch digestibility, and classification by degrees of digestibility might clarify the results.

CONCLUSION

All of the observed proximate chemical compositions and nutritional values of corn grain were substantially altered by the pretreatment methods. Among four pretreatments, hydrothermal extrusion increased crude protein and ether extract contents but reduced ash

and non-fiber carbohydrate contents. In ways that were expected to increase enzymatic hydrolysis, pretreatment techniques improved physicochemical qualities. *In vitro* carbohydrate digestibility indicates that either hydrothermal extrusion or microwave irradiation should be utilized to prepare corn grain for aquatic animals, even if only extrusion was suitable for chicken feed. The use of pretreatment to improve corn grain for ruminant feed was supported by better chemical composition, nutritional values, and physicochemical features, even though the four pretreatment techniques did not affect the observed digestibility values. The data obtained in this study can be used to produce high-quality raw materials for sale to consumers or to prepare meals for animal farms. Nevertheless, this investigation altered raw materials under particular circumstances mentioned in previous studies. Changes to the pretreatment circumstances may also have an impact on the chemical composition, physicochemical characteristics, and digestibility.

ACKNOWLEDGMENT

A Postdoctoral Fellowship from Prince of Songkla University (Dr. Sukanya Poolthajit), and a Research Fellowship from the Faculty of Science (Contract No. SCIRF66001) provided partial funding for this study. The authors thank the International Relations Office, Faculty of Science, Prince of Songkla University, for guiding the manuscript development process.

REFERENCES

Association of Official Analytical Chemists. (1990). *Official methods of analysis* (15th ed.). AOAC.

Bamidele, O. P., & Akanbi, C. T. (2013). Effect of gamma irradiation on physicochemical properties of stored pigeon pea (*Cajanus cajan*) flour. *Food Science and Nutrition*, *1*(5), 377–383. https://doi.org/10.1002/fsn3.50

Benning, L. G., Phoenix, V. R., Yee, N., & Tobin, M. J. (2004). Molecular characterization of cyanobacterial silification using synchrotron infrared micro-spectroscopy. *Geochimica et Cosmochimica Acta*, *68*(4), 729–741. https://doi.org/10.1016/S0016-7037(03)00489-7

Berger, L. L., Ricke, S. C., & Fahey, G. C. (1981). Comparison of two forms and two levels of lasalocid with monensin on feedlot cattle performance. *Journal of Animal Science*, *53*(6), 1440–1445. https://doi.org/10.2527/jas1982.5361440x

Bhat, R., Sridhar, K. R., & Seena, A. (2008). Nutritional quality evaluation of velvet bean seed (*Mucuna pruriens*) exposed to gamma irradiation. *International Journal of Food Science and Nutrition*, *54*(4), 261–278. https://doi.org/10.1080/09637480701456747

Boroojeni, F. G., Svihus, B., von Reichenbach, H. G., & Zentek, J. (2016). The effects of hydrothermal processing on feed hygiene, nutrient availability, intestinal microbiota and morphology in poultry—A review. *Animal Feed Science and Technology*, *220*, 187–215. http://dx.doi.org/10.1016/j.anifeedsci.2016.07.010

Brandenburg, K., & Seydel, U. (1996). Fourier transform infrared spectroscopy of cell surface polysaccharides. In H. H. Mantsch, & D. Chapman (Eds.), *Infrared spectroscopy of biomolecules* (pp. 203–278). Wiley.

Bressani, R. (1993). Grain quality of common beans. *Food Reviews International*, *9*(2), 237–297. https://doi.org/10.1080/87559129309540960

Caetano, M., Goulart, R. S., Rizzo, P. M., Silva, S. L., Drouillard, J. S., Leme, P. R., & Lanna, D. P. D. (2019). Impact of flint corn processing method and dietary starch concentration on finishing performance of Nellore bulls. *Animal Feed Science and Technology*, *251*, 166–175. https://doi.org/10.1016/j.anifeedsci.2019.03.006

Chang, F., He, X., & Huang, Q. (2013). Effect of lauric acid on the V-amylose complex distribution and properties of swelled normal cornstarch granules. *Journal of Cereal Science*, *58*(1), 89–95. http://dx.doi.org/10.1016/j.jcs.2013.03.016

Chung, B. Y., Firth, A. E., & Atkins, J. F. (2010). Frameshifting in alphaviruses: A diversity of 3' stimulatory structures. *Journal of Molecular Biology*, *397*(2), 448-456. https://doi.org/10.1016/j.jmb.2010.01.044

De Boever, J. L., Cottyn, B. G., Buysse, F. X., Wainman, F. W., & Vanacker, J. M. (1986). The use of an enzymatic technique to predict digestibility, metabolizable and net energy of compound feedstuff for ruminant. *Animal Feed Science and Technology*, *14*(3–4), 203–214.

Dean, A. P., Martin, M. C., & Sigee, D. C. (2007). Resolution of codominant phytoplankton species in a eutrophic lake using synchrotron-based Fourier transform infrared spectroscopy. *Phycologia*, *46*(2), 151–159. https://doi.org/10.2216/06-27.1

Dean, M., Raats, M. M., & Shepherd, R. (2008). Moral concerns and consumer choice of fresh and processed organic foods. *Journal of Applied Social Psychology*, *38*(8), 2088–2107. https://doi.org/10.1111/j.1559-1816.2008.00382.x

Dozier, W. A., Gehring, C. K., Corzo, A., & Olanrewaju, H. A. (2011). Apparent metabolizable energy needs of male and female broilers from 36 to 47 days of age. *Poultry Science*, *90*(4), 804–814. https://doi.org/10.3382/ps.2010-01132

Falkeborg, M., Cheong, L. Z., Gianfico, C., Sztukiel, K. M., Kristensen, K., Glasius, M., Xu, X., & Guo, Z. (2014). Alginate oligosaccharides: enzymatic preparation and antioxidant property evaluation. *Food Chemistry*, *164*, 185–194. http://dx.doi.org/10.1016/j.foodchem.2014.05.053

Freitas, T. B., Felix, T. L., Shriver, W., Fluharty, F. L., & Relling, A. E. (2020). Effect of corn processing on growth performance, carcass characteristics, and plasma glucose-dependent insulinotropic polypeptide and metabolite concentrations in feedlot cattle. *Translational Animal Science*, *4*(2), 822-830. https://doi.org/10.1093/tas/txaa009

Giordano, M., Kansiz, M., Heraud, P., Beardall, J., Wood, B., & McNaughton, D. (2001). Fourier transform infrared spectroscopy as a novel tool to investigate changes in intracellular macromolecular pools in the marine microalga *Chaetoceros muellerii* (Bacillariophyceae). *Journal of Phycology*, *37*(2), 271–279. https://doi.org/10.1046/j.1529-8817.2001.037002271

Guzman, J., Esmail, R., Karjalainen, K., Malmivaara, A., Irvin, E., & Bombardier, C. (2001). Multidisciplinary rehabilitation for chronic low back pain: systematic review. *BMJ*, *322*(7301), 1511–1516. https://doi.org/10.1136/bmj.322.7301.1511

Hahor, W., Thongprajukaew, K., Nuntapong, N., Saekhow, S., Rungruangsak-Torrissen, K., Dumrongrittamatt, T., & Phonchai, A. (2022). Partial pretreatment of ingredient mixture effectively improved feed chemical

composition, physicochemical properties and *in vitro* digestibility. *Animal Feed Science and Technology, 285*, Article 115216. https://doi.org/10.1016/j.anifeedsci.2022.115216

Han, C., Guo, Y., Cai, X., & Yang, R. (2022). Starch properties, nutrients profiles, *in vitro* ruminal fermentation and molecular structure of corn processed in different ways. *Fermentation*, *8*(7), Article 315. https://doi.org/10.3390/fermentation8070315

Hashim, M. S., Yusop, S. M., & Rahman, I. A. (2024). The impact of gamma irradiation on the quality of meat and poultry: A review on its immediate and storage effects. *Applied Food Research*, *4*(2), Article 100444. https://doi.org/10.1016/j.afres.2024.100444

Jančík, F., Kubelková, P., Kubát, V., Koukolová, M., & Homolka, P. (2017). Effects of drying procedures on chemical composition and nutritive value of alfalfa. *South African Journal of Animal Science*, *47*(1), 96–101. http://dx.doi.org/10.4314/sajas.v47i1.14

Jitngarmkusol, S., Hongsuwankul, J., & Tananuwong, K. (2008). Chemical compositions, functional properties, and microstructure of defatted macadamia flours. *Food Chemistry*, *110*(1), 23–30. https://doi.org/10.1016/j.foodchem.2008.01.050

Karami, M., Palizdar, M., & Almasi, M. (2018). The effect of different processing of corn grain on gas production kinetics and *in vitro* digestibility in Taleshi cows. *Journal of Livestock Science*, *9*(2), 101–106.

Lewis, R. N., & McElhaney, R. N. (1996). Fourier transform infrared spectroscopy in the study of hydrated lipids and lipid bilayer membranes. In H. H. Mantsch, & D. Chapman (Eds.), *Infrared spectroscopy of biomolecules* (pp. 159–202). Wiley.

Li, W., Raoult, D., & Fournier, P. E. (2009). Bacterial strain typing in the genomic era. *FEMS Microbiology Reviews*, *33*(5), 892–916. https://doi.org/10.1111/j.1574-6976.2009.00182

Lowińska-Kluge, A., & Piszora, P. (2008). Effect of gamma irradiation on cement composites observed with XRD and SEM methods in the range of radiation dose 0–1409 MGy. *Acta Physica Polonica Series A, 114*(2), 399–411. https://doi.org/10.12693/APhysPolA.114.399

Ma, S., Wang, H., Yang, J., Liang, X., Xue, M., & Cheng, H. (2023). Effect of process parameters on the physical quality of low-starch extruded feed containing *Clostridium autoethanogenum* protein. *Animal Feed Science and Technology*, *304*, Article 115745. https://doi.org/10.1016/j.anifeedsci.2023.115745

Macarthur, L. A., & Appolonia, B. L. (1984). Gamma radiation of wheat. II. Effects of low-dosage radiations on starch properties. *Journal of Cereal Chemistry*, *61*(4), 321–326.

Maquelin, K., Kirschner, C., Choo-Smith, L. P., Braak, N. V. D., Ph Endtz, H., Naumann, D., & Puppels, G. J. (2002). Identification of medically relevant microorganisms by vibrational spectroscopy. *Journal of Microbiological Methods*, *51*(3), 255–271. https://doi.org/10.1016/S0167-7012(02)00127-6

Numoto, A. Y., Filho, P. S. V., Scapim, C. A., Franco, A. A. N., Ortiz, A. H. T., Marques, O. J., & Pelloso, M. F. (2019). Agronomic performance and sweet corn quality as a function of inoculant doses (*Azospirillum brasilense*) and nitrogen fertilization management in summer harvest. *Bragantia*, *78*(1), 26–37. https://doi.org/10.1590/1678-4499.2018044

Palacios-Fonseca, A. J., Castro-Rosas, J., Gómez-Aldapa, C. A., Tovar-Benítez, T., Millán-Malo, B. M., del Real, A., & Rodríguez-García, M. E. (2013). Effect of the alkaline and acid treatments on the physicochemical

properties of corn starch. *Journal of Food Science*, *11*(1), 67–74. https://doi.org/10.1080/19476337.2012.761651

Rashid, M. M., Al Mesfer, M. K., Naseem, H., & Danish, M. (2015). Hydrogen production by water electrolysis: A review of alkaline water electrolysis, PEM water electrolysis and high temperature water electrolysis. *International Journal of Engineering and Advanced Technology*, *4*(3), 80–93.

Sadeghi, A. A., & Shawrang, P. (2006). Effects of microwave irradiation on ruminal degradability and *in vitro* digestibility of canola meal. *Animal Feed Science and Technology*, *127*(1–2), 45–54. https://doi.org/10.1016/j.anifeedsci.2005.08.016

Sansuwan, K., Kovitvadhi, S., Thongprajukaew, K., Ozorio, R. O. A., Somsueb, P., & Kovitvadhi, U. (2017). Microwave irradiation and pelleting method affected feed chemical composition and growth performance and feed utilization of sex-reversed Nile tilapia, *Oreochromis niloticus* (L.). *Aquaculture Research*, *48*(4), 1836–1848. https://doi.org/10.1111/are.13021

Sekali, M., Mlambo, V., Marume, U., & Mathuthu, M. (2023). *In vitro* ruminal fermentation parameters of canola meal protein in response to incremental doses of gamma irradiation. *South African Journal of Animal Science*, *53*(1), 109–116. http://dx.doi.org/10.4314/sajas.v53i1.12

Shawrang, P., Nikkhah, A., Zare-Shahneh, A., Sadeghi, A. A., Raisali, G., & Moradi-Shahrebabak, M. (2008). Effects of gamma irradiation on chemical composition and ruminal protein degradation of canola meal. *Radiation Physics and Chemistry*, *77*(7), 918–922. https://doi.org/10.1016/j.radphyschem.2008.03.006

Shishir, M. S. R., Brodie, G., Cullen, B., Kaur, R., Cho, E., & Cheng, L. (2020). Microwave heat treatment induced changes in forage hay digestibility and cell microstructure. *Applied Sciences*, *10*(22), Article 8017. https://doi.org/10.3390/app10228017

Silva, T. M., de Medeiros, A. N., Oliveira, R. L., Neto, S. G., Queiroga, R. C. R. E., Ribeiro, R. D. X., Leão, A. G., & Bezerra, L. R. (2016). Carcass traits and meat quality of crossbred Boer goats fed peanut cake as a substitute for soybean meal. *Journal of Animal Science*, *94*(7), 2992–3002. https://doi.org/ 10.2527/jas.2016-0344

Soest, P. J. V., Robertson, J. B., & Lewis, B. A. (1991). Methods for dietary fibre, neutral detergent fibre and non-starch polysaccharides in relation to animal nutrition. *Journal of Dairy Science*, *74*(10), 3583–3597. https://doi.org/10.3168/jds.S0022-0302(91)78551-2

Sokhey, A. S., & Chinnaswamy, R. (1993). Chemical and molecular properties of irradiated starch extrudates. *Journal of Cereal Chemistry*, *70*(3), 260–268.

Srakaew, W., Wachirapakorn, C., & Wongnen, C. (2021). Dietary modified cassava chip and corn seed: Effect on growth performance, rumen production, and blood glucose and insulin in early fattening beef bulls. *Walailak Journal of Science and Technology*, *18*(7), Article 9217. https://doi.org/10.48048/wjst.2021.9217

Stuart, F. I. (1997). Supply-chain strategy: Organizational influence through supplier alliances. *British Journal of Management*, *8*(3), 223–236. https://doi.org/10.1111/1467-8551.00062

Suksombat, W., Boonmee, T., & Lounglawan, P. (2007). Effects of various levels of conjugated linoleic acid supplementation on fatty acid content and carcass composition of broilers. *Poultry Science*, *86*(2), 318–324. https://doi.org/10.1093/ps/86.2.318

Takaeh, S., Poolthajit, S., Hahor, W., Nuntapong, N., Ngampongsai, W., & Thongprajukaew, K. (2024). Physical pretreatments of cassava chips influenced chemical composition, physicochemical properties, and *in vitro* digestibility in animal models. *Animals*, *14*(6), Article 908. https://doi.org/10.3390/ani14060908

Thongprajukaew, K., Kovitvadhi, U., Kovitvadhi, S., Somsueb, P., & Rungruangsak-Torrissen, K. (2011). Effects of different modified diets on growth, digestive enzyme activities and muscle compositions in juvenile Siamese fighting fish (*Betta splendens* Regan, 1910). *Aquaculture*, *322–323*, 1–9. https://doi.org/10.1016/j.aquaculture.2011.10.006

Thongprajukaew, K., Rodjaroen, K., Tantikitti, C., & Kovitvadhi, U. (2015). Physicochemical modifications of dietary palm kernel meal affect growth and feed utilization of Nile tilapia (*Oreochromis niloticus*). *Animal Feed Science and Technology*, *202*, 90–99. https://doi.org/10.1016/j.anifeedsci.2015.01.010

Thongprajukaew, K., Yawang, P., Dudae, L., Bilanglod, H., Dumrongrittamatt, T., Tantikitti, C., & Kovitvadhi, U. (2013). Physical modification of palm kernel meal improved available carbohydrate, physicochemical properties and *in vitro* digestibility in economic freshwater fish. *Journal of the Science of Food and Agriculture*, *93*(15), 3832–3840. https://doi.org/10.1002/jsfa.6314

Wang, Y., Hu, B., Zhan, J., Xu, R., & Tian, Y. (2020). Effects of starchy seed crystals on the retrogradation of rice starch. *Food Chemistry*, *318*, Article 126487. https://doi.org/10.1016/j.foodchem.2020.126487

Wong, P., Goldstein, S., Grekin, R., Godwin, A., Pivik, C., & Riga, B. (1993). Distinct infrared spectroscopic pattern of human basel cell carcinoma of the skin. *Cancer Research*, *53*(4), 762–765.

Xu, N., Liu, J., & Yu, P. (2018). Alteration of biomacromolecule in corn by steam flaking in relation to biodegradation kinetics in ruminant, revealed with vibrational molecular spectroscopy. *Spectrochimica Acta*, *191*, 491–497. https://doi.org/10.1016/j.saa.2017.10.040

Zhou, P., Theil, P. K., Wu, D., & Knudsen, K. E. B. (2018). *In vitro* digestion methods to characterize the physicochemical properties of diets varying in dietary fiber source and content. *Animal Feed Science and Technology*, *235*(10), 87–96. https://doi.org/10.1016/j.anifeedsci.2017.11.012

Table S1
Tentative assignments of FTIR spectral peaks found in unprocessed (native) and pretreated corn grains

Wavenumber (cm^{-1})	Tentative band assignment	Macromolecule	References
2924	v_{as} (CH_2) stretching of methylene	Lipid	Lewis and McElhaney (1996) and Stuart (1997)
2852	v_s (CH_2) stretching of methylene	Lipid	Lewis and McElhaney (1996) and Stuart (1997)
1743	v (C=O) stretching of esters	Lipid	Giordano et al. (2001)
1652	v_s (C=O) stretching of amide I	Protein	Dean et al. (2008)
1542	δ (N-H) bending and v (C-N) stretching of amide II	Protein	Stuart (1997)
1462	δ_{as} (CH_2) bending of methyl	Lipid	Lewis and McElhaney (1996) and Stuart (1997)
	δ_{as} (CH_3) bending of methyl	Protein	Giordano et al. (2001)
1373	v_s (COO-) stretching of amino acid salt	Protein	Guzman et al. (2001)
	v_s (C=O) stretching vibrations of carboxylate	Carbohydrate	Falkeborg et al. (2014)
1240	N(C=O) stretching and (C-OH) bending of deprotonated amino acid	Protein	Li et al. (2009)
1157	v (C-O-C) stretching of polysaccharide	Carbohydrate	Brandenburg and Seydel (1996)
1059	v (C-O-C) stretching of polysaccharide	Carbohydrate	Brandenburg and Seydel (1996)
991	v (C-O-C) stretching of polysaccharide	Carbohydrate	Brandenburg and Seydel (1996)
927	C=C bending of alkene	Alkene	Guzman et al. (2001)
858	v_{as} (PO_4^{3-}) P-O asymmetric stretching of lipids	Lipid	Dean et al. (2007)
765	δ (CO_3^{2-}) Out of O-C=O bending of oxalate	Inorganic	Giordano et al. (2001)
711	(CH^{2-}), C-H rocking of lipids	Lipid	Stuart (1997)
574	C-Br stretching of halo compound	Inorganic	Wong et al. (1993)
526	N-C=O of amides	Amides	Maquelin et al. (2002)
437	v_4 (PO_4^{3-}) P-O stretching of tetrahedral inorganic molecules	Inorganic	Benning et al. (2004)

Pertanika J. Trop. Agric. Sci. 48 (6): 1733 - 1754 (2025)

PERTANIKA JOURNALS

TROPICAL AGRICULTURAL SCIENCE

Journal homepage: http://www.pertanika.upm.edu.my/

Feeding Behaviour of *Helopeltis theivora* on Tea and Alternate Host Plants

Shovon Kumar Paul[1, 2], Nur Azura Adam[1, 3]*, Syari Jamian[1], and Anis Syahirah Mokhtar[1]

[1]*Department of Plant Protection, Faculty of Agriculture, Universiti Putra Malaysia, 43400 UPM Serdang, Selangor, Malaysia*
[2]*Entomology Division, Bangladesh Tea Research Institute, Bangladesh Tea Board, Sreemangal-3210, Moulvibazar, Bangladesh*
[3]*Southeast Asian Regional Center for Graduate Study and Research in Agriculture, Los Baños, Laguna, Philippines*

ABSTRACT

The study was conducted to determine the feeding behavior of *Helopeltis theivora* on different host plants, i.e., tea, golden dewdrop, mikania, and china rose, under both no-choice and choice experiments in the laboratory. The results indicated that the female created the highest number of feeding spots on the tea leaves, followed by the male and the second instar nymph. The fourth and fifth nymphal instars, as well as adults, preferred the second leaf, whereas the first, second, and third instars chose the first leaf of tea shoot. There was a linear and positive relationship between the diameter of the feeding spots on tea leaves and the different growth stages. The highest number and diameter of feeding spots by *H. theivora* were observed on the tea leaves compared to the stem in no-choice and choice experiments. The result also revealed that the greatest extent of damage to the tea shoot area was caused by adult females, significantly different from other growth stages of *H. theivora* in both experiments. The order of choice of different host plants based on the number of feeding spots by nymphs and adults was tea>golden dewdrop>mikania>china rose in no-choice and choice experiments. The feeding behavior of different hosts confirms that *H. theivora* can survive when its primary food source is scanty. The result of this research may help plan an effective pest management strategy against *H. theivora* in tea.

Keywords: Alternate host, feeding behavior, *Helopeltis theivora*, tea

ARTICLE INFO

Article history:
Received: 27 December 2024
Accepted: 17 June 2025
Published: 25 November 2025

DOI: https://doi.org/10.47836/pjtas.48.6.04

E-mail addresses:
shovonbtri@gmail.com (Shovon Kumar Paul)
nur_azura@upm.edu.my (Nur Azura Adam)
syari@upm.edu.my (Syari Jamian)
anissyahirah@upm.edu.my (Anis Syahirah Mokhtar)
*Corresponding author

e-ISSN: 2231-8542

INTRODUCTION

Feeding means the consumption of food in an overarching, ecological sense (Song et al., 2021). Feeding is a fundamental ecological behavior in insects, especially within insect-host-plant interactions. Feeding by herbivorous insects may cause damage to the host plant through negative effects on the physiology. Herbivorous insects damage plants by physically consuming leaves, stems, and roots, which disrupts photosynthesis, nutrient transport, and growth. Additionally, their feeding can introduce toxins, transmit pathogens, and trigger costly plant defense responses, further weakening the plant's health and productivity (Yao et al., 2025).

Helopeltis theivora is an important polyphagous sucking insect pest and causes quality and quantity deterioration in tea as the nymphs and adults suck sap from young buds, leaves, and tender stems by inserting their labial stylet. In severe infestations, damaged leaves curl upward, desiccate, and cause dieback (Sireesha et al., 2020; Yao et al., 2025). The crop loss due to *H. theivora* infestation in tea is about 10-50% (Borthakur & Bora, 2023), which can sometimes reach up to 100% without taking proper control measures in time (Das, 2022; Suganthi et al., 2020). *Helopeltis theivora* is also a major leaf sucking insect pest of tea in Malaysia, and approximately 10-15% of the crop is lost due to this pest (Krishnan, 2000; Latip et al., 2010). It is a polyphagous sucking insect pest of tea, and more than 100 plant species, including both economic crops and weeds, have been identified as alternate hosts for it (Sankarganesh et al., 2020; Sivakumar & Yeshwanth, 2019). The abundance of alternate host plants in and around tea plantations is considered one of the major predisposing factors for the frequent resurgence of this pest (Roy et al., 2018). Alternate hosts, such as weeds, shrubs, or even trees, enable them to sustain feeding and breed throughout the year, even when the primary crop plants are not available or sprayed with pesticides (Amutha & Rani, 2022; Sivakumar & Yeshwanth, 2019). Previous studies have indicated that every year, the host range of the pest is expanding on a wide array of crops documented from different tea-growing countries (Sankarganesh et al., 2020; Sivakumar & Yeshwanth, 2019). The polyphagous nature of this mirid bug imposes pest management constraints since it can survive everywhere by alternating hosts between seasonal changes, both in the wild, cultivated, and ornamental plant species (Roy et al., 2018).

The investigation on feeding habits and host range of *H. theivora* was conducted on tea, cashew, eggplant, and amaranth in India (Bharathi et al., 2024; Borthakur & Bora, 2023; Sankarganesh et al., 2020; Sivakumar & Yeshwanth, 2019). Historically, Miller (1941) documented 39 host plants of *H. theivora* (identified initially as *H. theobromae* Miller), including cash crops, fruits, vegetables, ornamental, and weed species in Malaysia (then Malaya). Despite these records, there remains a significant gap in understanding the feeding behavior of *H. theivora* on tea and alternate host plants. The study of feeding behavior and host range is crucial in predicting and preventing the expansion of a particular

insect population, which will ultimately help formulate effective pest management strategies (Sivakumar & Yeshwanth, 2019; Xie et al., 2020). Therefore, the objectives of this study were (1) to determine the feeding behavior of *H. theivora* on different parts of tea shoots and (2) to ascertain the feeding behavior of *H. theivora* on different alternate host plants.

MATERIALS AND METHODS

The experiments were conducted from January to May 2021 in the insectary, Department of Plant Protection, Faculty of Agriculture, Universiti Putra Malaysia (UPM), under laboratory conditions with a temperature of 25.0 ± 2.0°C and 69.0 ± 5.0% relative humidity with a 12h:12h photoperiod. These conditions were maintained consistently throughout the experiments to ensure reproducibility. Different growth stages of *H. theivora* used in this experiment were obtained from the stock culture maintained in the insectary.

Feeding Behavior of *H. theivora* at Different Growth Stages on Tea Shoot and Different Alternate Host Plants

The feeding behavior of *H. theivora* on tea shoots and alternate host plants was determined through no-choice and choice experiments. Both methods are essential to understand the insect's host range, preference hierarchy, and ecological adaptability (Jamian et al., 2020; Thube et al., 2019). No-choice experiment assesses only the insect's host range, i.e., its ability to survive, feed, and reproduce on a given host under forced conditions (Song et al., 2021). In contrast, the choice experiment evaluates the insect's preference hierarchy when exposed to multiple host species simultaneously under field-like conditions (Awudzi et al., 2020). The method of feeding behavior of *H. theivora* in this study was adopted and modified (laboratory rearing condition, rearing technique, and tea variety were different) from Bhuyan & Bhattacharyya (2006) and Gogoi et al. (2012).

Tea shoots with a bud (tip of the new shoot, which is the youngest and most tender part of the shoot), first leaf (emerges after the bud on the shoot, which is usually small, delicate, and slightly unfolded compared to mature leaves), second leaf (following the first leaf, the second leaf is the next one to develop on the shoot that is slightly larger and more unfolded than the first leaf but still relatively tender), and third leaf (the third leaf is the leaf that follows the second leaf in the sequence of growth on the shoot which is more fully developed, larger, and less tender compared to the bud and the first two leaves) were used in this experiment. The bud and three leaves are the main yielding parts used for tea manufacturing (Roy et al., 2018). This ensures that the tea retains its delicate aroma and characteristics. *Helopeltis theivora* infested this tender part of the tea shoot. The leaves below this part are called maintenance or mother leaves, which support generating new shoots by supplying food after plucking. Tea shoots of the variety TV8 (Tocklai Vegetative 8, an Indian tea variety) were collected from the tea plot of University Agriculture Park, located on the UPM campus.

Three types of alternate host plants, such as hedges, ornamental plants, and weeds, were selected for this experiment (Table 1). The alternate host plants selected for this study represent the diversity of non-crop vegetation typically found in tea agroecosystems in Malaysia to provide a realistic evaluation of the host selection behavior of *H. theivora* under conditions that closely resemble the field environment. China rose, and golden dewdrops are commonly planted as ornamental and hedge plants, respectively, in and around tea plantations in Malaysia. The mikania is a common weed in tea plantations. The primary host plant, tea, was used to compare the feeding behavior of *H. theivora* with that of the alternate host plants.

Table 1
Alternate host plants used for the experiment

Plant type	Common name	Scientific name	Family	Growth habit
Beverage	Tea	*Camellia sinensis* (L) Kuntze	Theaceae	Perennial, tree
Hedge	Golden dewdrop	*Duranta erecta* L.	Verbenaceae	Evergreen, shrub
Ornamental	China rose	*Hibiscus rosa-sinensis* L.	Malvaceae	Evergreen, shrub
Weeds	Mikania	*Mikania micrantha* H.B. & K	Asteraceae	Perennial, vine

No-Choice Experiment

In this experiment, the bud, first, second, and third leaves of tea shoot (Figure 1) were kept separately (maintained by removing undesired leaves or whole leaves) in a glass vial and placed in individual cages measuring 30 cm × 30 cm × 30 cm. Shoots of different alternate

Figure 1. Different parts of the tea shoot (a) bud, (b) first leaf, (c) second leaf, (d) third leaf, and (e) stem were used for the no-choice experiment. Photos were taken under standard lab lighting using a digital camera

host plants were collected from the UPM campus (Figure 2). The shoots in glass vials are placed separately in each cage, measuring 30 cm × 30 cm × 30 cm.

Choice Experiment

In the choice experiment, the tea shoots containing bud, first, second, and third leaf (Figure 3) were kept in a glass vial and placed in individual cages measuring 30 cm × 30 cm ×

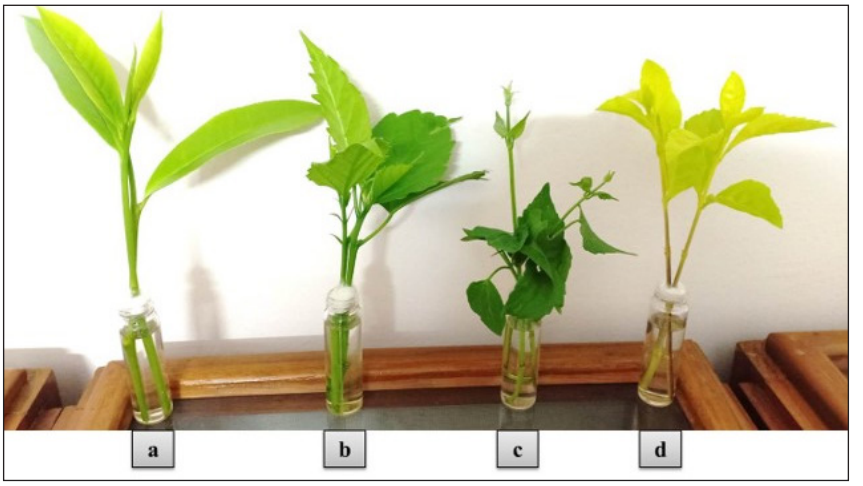

Figure 2. Shoots of different alternate host plants (a) tea, (b) china rose, (c) mikania, and (d) golden dewdrop were used for the no-choice and choice experiment. Photos were taken under standard lab lighting using a digital camera

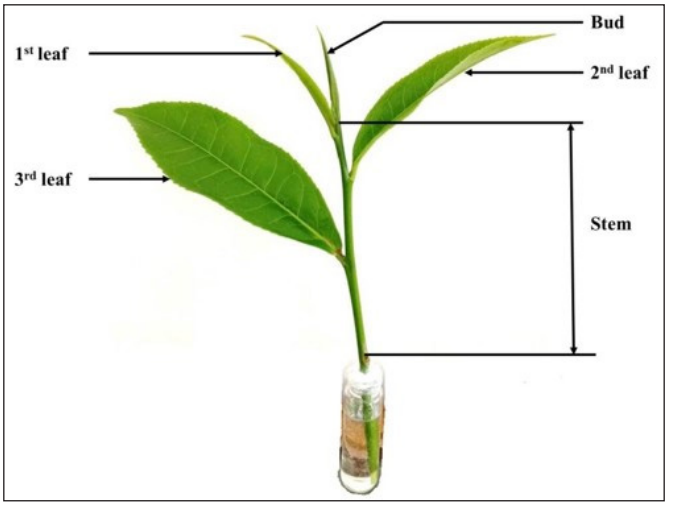

Figure 3. Tea shoot showing bud, 1st leaf, 2nd leaf, 3rd leaf, and stem used for the choice experiment. Photos were taken under standard lab lighting using a digital camera

30 cm. On the other hand, shoots of different alternate host plants were kept in glass vials separately, and all the shoots were placed together in one cage measuring 30 cm × 30 cm × 30 cm. A watch glass was placed in the middle of each cage to release the different growth stages of *H. theivora*. The glass vials containing alternate host plants are placed 10 cm apart from the watch glass.

Ten individual nymphal instars (first–fifth instars), adult males, and females of each stage (the total number of individuals was 70) of *H. theivora* were released in each cage for no-choice and choice experiments. The experimental design was a Complete Randomized Design (CRD) with ten replications.

Data Analysis

Data on the numbers and diameters of feeding spots were recorded in the leaves and stems of tea shoots and alternate host plants separately for different growth stages of *H. theivora* in both no-choice and choice experiments after 24 hours of releasing the insect into each cage. The number of spots was counted using a magnifying glass (10x). Photos of feeding spots were taken by a Dino-eye microscope eyepiece (AnMo Electronics Corporation, Taiwan) connected to a Wild Heerbrugg Microscope (M3Z Switzerland). The diameters were measured using Dino-capture 2.0 software. The mean diameter of feeding spots was calculated based on randomly selected three spots for every growth stage of *H. theivora* from different parts of the tea shoot and alternate host plants for no-choice and choice experiments. The number of feeding spots/individual/day and area damaged at every growth stage were also calculated for tea shoots in both experiments. In the case of alternate host plants, only the numbers of feeding spots/individual/day were calculated. All data were tested for normality using the normality test. The abnormal data on the feeding spots were normalized using the square root of x ($\sqrt{x}$) (non-zero data set) and $\sqrt{x+1}$ (zero data set) transformation. Data were statistically analyzed using two-way ANOVA, and the differences between individual means were compared using the LSD test in the SAS statistical program (version 9.4). Differences are considered significant at $p<0.05$ unless otherwise stated.

RESULTS

Feeding Behavior of *H. theivora* at Different Growth Stages on Tea Shoot

No-Choice and Choice Experiment

Number of Feeding Spots. Figure 4 shows that all growth stages of *H. theivora* caused more feeding spots on the first and second leaf than on the stem, bud, and third leaf, both in the no-choice (n= 350) and choice (n= 350) experiments.

Table 2 shows a significant difference (n=350; F = 3.61; df = 24, 349; P < 0.05) in the mean numbers of feeding spots according to insect growth stages and leaf ages of tea shoots

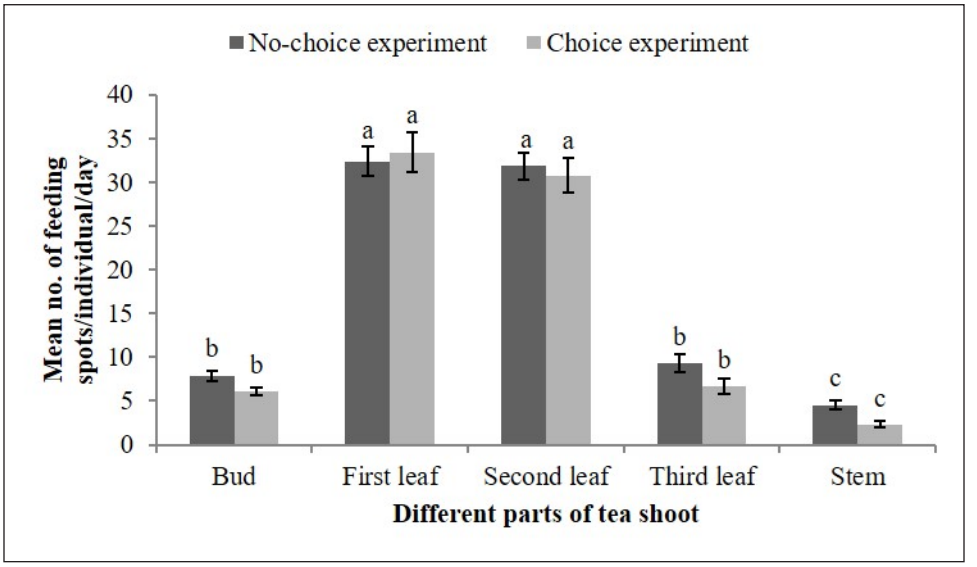

Figure 4. The mean number of feeding spots on different parts of the tea shoot caused by *H. theivora* in the no-choice and choice experiment. Vertical lines at each bar indicate the SE value. The same small letters on the bar are not significantly different (p>0.05) at 5% level of significance

in the no-choice experiment. Adult females produced a significantly the highest number of feeding spots across most leaf categories, with the maximum recorded on the second leaf (39.40 ± 4.59), followed by the buds (12.10 ± 1.47), third leaves (20.40 ± 2.64), and the stem (9.90 ± 1.79). In contrast, first instar nymphs exhibited the highest feeding spots on the first leaf (43.60 ± 5.19), while showing minimal feeding spots on the third leaf (2.30 ± 0.42) and stem (1.20 ± 0.47).

Table 2
The mean number of feeding spots on different parts of the tea shoot caused by different stages of H. theivora *in the no-choice experiment*

Growth stage	The mean number of feeding spots ± SE				
	Bud	First leaf	Second leaf	Third leaf	Stem
First instar	7.90±1.31abC	43.60±5.19aA	25.50±3.17bB	2.30±0.42cD	1.20±0.47cD
Second instar	8.80±2.26abC	40.90±4.13aA	28.60±3.26abB	3.70±1.03cD	2.10±0.69bcD
Third instar	6.80±1.30bC	34.10±4.30abA	26.10±2.97bB	5.50±1.29bcC	2.70±0.72bcC
Fourth instar	5.10±0.84bC	27.10±2.85cB	35.80±4.11abA	6.60±2.11bcC	3.50±0.83bcC
Fifth instar	6.30±1.27bC	22.70±2.94cB	32.50±3.96abA	10.50±1.49bC	4.10±0.90bC
Male	8.10±1.83abB	27.80±3.73cA	35.10±5.07abA	16.10±2.64aB	7.10±1.05aC
Female	12.10±1.47aBC	30.10±4.62bcA	39.40±4.59aA	20.40±2.64aB	9.90±1.79aC

Means within a column followed by the same small letter and means within a row followed by the same capital letter are not significantly different (p>0.05) at 5% level of significance

Among the nymphal stages, a general trend of decreasing feeding spots with increasing instar was observed on the first leaf, with the second (40.90 ± 4.13) and third instars (34.10 ± 4.30) showing moderately high activity. The fourth and fifth instars shifted their peak feeding to the second leaf (35.80 ± 4.11 and 33.30 ± 4.44, respectively), with comparatively lower feeding activity on the stem. Both adult males and females exhibited peak feeding on the second leaf, statistically comparable to the first leaf, indicating a strong preference for younger foliage.

In the case of the choice experiment, the mean numbers of feeding spots varied significantly (n=350; F = 8.83; df = 24, 349; P < 0.05) based on the insect growth stages and leaf ages of tea shoots (Table 3). Among all stages, adult females induced significantly greater feeding damage on buds (8.10 ± 1.35), whereas the third instar nymph recorded the lowest (3.90 ± 0.80). The first leaf consistently received the most intense feeding activity from the first instar nymph (50.90 ± 5.57). In contrast, feeding on the first leaf was lowest for the fifth (15.40 ± 1.80) and fourth instars (20.80 ± 3.12).

Table 3
The mean number of feeding spots on different parts of the tea shoot caused by different stages of H. theivora *in the choice experiment*

Growth stage	The mean number of feeding spots ± SE				
	Bud	First leaf	Second leaf	Third leaf	Stem
First instar	5.40±1.26abC	50.90±5.57aA	18.20±3.36cB	0.00cC	0.00dC
Second instar	6.40±1.28abC	48.00±5.25aA	23.40±2.71bcB	2.30±0.84bcC	0.00dC
Third instar	3.90±0.80bC	42.60±6.06abA	17.40±3.60cB	3.90±1.13bcC	1.10±0.38cdC
Fourth instar	5.70±1.35abC	20.80±3.12cdB	38.30±5.93aA	5.50±1.34bC	1.90±0.75cdC
Fifth instar	6.70±1.22abC	15.40±1.80dB	35.10±4.67abA	5.80±1.47bC	2.60±0.99bcC
Male	6.20±0.77abC	25.30±4.48cdB	40.50±5.42aA	12.20±2.14aC	4.10±0.75bC
Female	8.10±1.35aD	30.70±3.22bcB	42.50±4.74aA	16.70±2.92aC	6.30±1.36aD

Means within a column followed by the same small letter and means within a row followed by the same capital letter are not significantly different (p>0.05) at 5% level of significance

The second leaf was the most preferred site for older nymphs and adults. The highest number of feeding spots was recorded for adult females (42.50 ± 4.74), adult males (40.50 ± 5.42), and the fourth (38.30 ± 5.93) and fifth instar nymphs (35.10 ± 4.67), whereas the early instars (first to third) exhibited significantly lower activity. On the third leaf, adult females again produced the highest number of feeding spots (16.70 ± 2.92), followed by males (12.20 ± 2.14). Early instars showed minimal feeding, with the first instar producing none, while the second (2.30 ± 0.84) and third (3.90 ± 1.13) instars generated the fewest feeding marks. Notably, no feeding was observed on the stem by the first and second instars, reflecting a possible physical constraint in stylet penetration. However, the adult female

caused the most stem feeding (6.30 ± 1.36), followed by the adult male (4.10 ± 0.75) and the fifth instar (2.60 ± 0.99).

Diameter of Feeding Spots. The mean diameter (mm) of feeding spots on other leaves of tea shoots showed significant differences (n= 350; F = 11.87; df = 24, 349; P < 0.05) among the growth stages of *H. theivora* in the no-choice experiment (Table 4). Adult females produced the largest feeding spots (1.68 ± 0.02 mm) on the bud. In contrast, the smallest diameter of feeding spots was caused by the first instar nymph (0.40 ± 0.08 mm). Similar trends were observed on the first leaf, with adult females generating the largest spot (2.59 ± 0.04 mm), whereas the first instar nymph produced significantly smaller spots (0.84 ± 0.09 mm).

Table 4
The mean diameter (mm) of feeding spots on different parts of the tea shoot caused by different stages of H. theivora *in the no-choice experiment*

Growth stage	The mean diameter (mm) of feeding spots ± SE				
	Bud	First leaf	Second leaf	Third leaf	Stem
First instar	0.40±0.08eC	0.84±0.09fA	0.62±0.08fB	0.16±0.06eD	0.09±0.02dD
Second instar	1.12±0.03dB	1.33±0.05eA	1.22±0.06eAB	0.85±0.07dC	0.12±0.02dD
Third instar	1.27±0.04cdB	1.59±0.02dA	1.50±0.03dA	0.93±0.05dC	0.38±0.03cD
Fourth instar	1.33±0.06cC	1.97±0.06cB	2.19±0.08cA	1.42±0.05cC	0.84±0.04bD
Fifth instar	1.44±0.06bcC	2.20±0.07bcA	2.39±0.08bA	1.68±0.05bB	0.88±0.07bD
Male	1.54±0.05abC	2.42±0.03abA	2.57±0.07bA	2.07±0.06aB	1.03±0.0.05aD
Female	1.68±0.02aD	2.59±0.04aB	2.78±0.05aA	2.18±0.08aC	1.11±0.06aE

Means within a column followed by the same small letter and means within a row followed by the same capital letter are not significantly different (p>0.05) at 5% level of significance

The result also showed that the first instar nymph created significantly the smallest feeding spots (0.62 ± 0.08 mm) on the second leaf. It was determined that adult females had the largest mean diameter of feeding spots (2.78 ± 0.05 mm) on the second leaf than other growth stages of *H. theivora*. The mean diameter of feeding spots on the third leaf caused by adult females (2.18 ± 0.08 mm) was significantly larger than all nymphal instars, among which the fifth instar had the largest (1.68 ± 0.05 mm) and the first instar the smallest (0.16 ± 0.06 mm) feeding spots. In the case of the stem, the adult female created the larger diameter of the feeding spot (1.11 ± 0.06 mm). On the other hand, the first instar nymph created the smallest diameter of the feeding spot (0.09 ± 0.02 mm) on the stem.

The first instar nymph (0.84 ± 0.09 mm), second instar nymph (1.33 ± 0.05 mm), and third instar nymph (1.59 ± 0.02 mm) had the largest diameter of feeding spots on the first leaf next to the second leaf of the tea shoot (Table 4). The fourth instar nymph (2.19 ±

0.08 mm), fifth instar nymph (2.39 ± 0.08 mm), adult male (2.57 ± 0.07 mm), and female (2.78 ± 0.05 mm) produced the larger diameter of feeding spots on the second leaf next to the first leaf. For all the growth stages of *H. theivora*, the mean diameter of feeding spots formed on the stem of the tea shoot was the smallest.

A positive and linear correlation (R^2= 0.9628) was found between the growth stages of *H. theivora* and the diameter of the feeding spots (Figure 5). It suggests that the size of the feeding punctures increased proportionately as the insect underwent successive growth stages, from early instars to adulthood. According to this association, the degree of tissue damage caused to the host plant was directly affected by the insect's morphological growth, namely the rostrum's enlargement and related eating mechanisms. In field assessments, feeding spot diameter may be used as an indirect predictor of the pest's developmental stage.

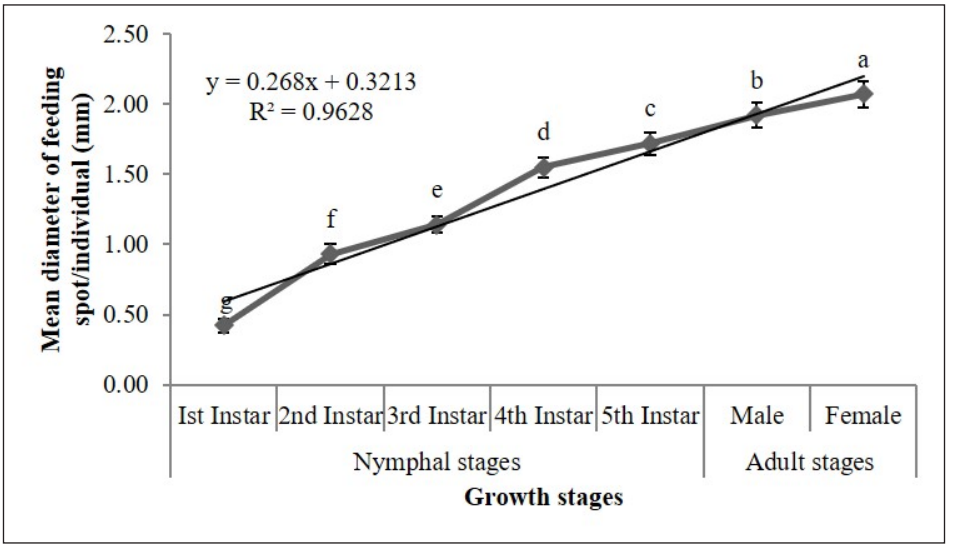

Figure 5. Relationship of the diameter (mm) of feeding spots produced by various growth stages of *H. theivora o*n tea shoots in the no-choice experiment. Vertical bars at lines indicate the SE value. Different small letters on the lines are significantly different ($p<0.05$) at 5% level of significance

On the other hand, the mean diameter of feeding spots on other leaves of tea shoots differed significantly (n= 350; F = 17.83; df = 24, 349; P < 0.05) among the growth stages of *H. theivora* in the choice experiment (Table 5). The largest mean diameter of feeding spots was caused by the adult female (1.62 ± 0.14 mm) on the bud. In comparison, the first instar nymph (0.35 ± 0.06 mm) created the smallest diameter of feeding spots. The females and males had the largest diameter of feeding spots on the first leaf, measuring 2.52 ± 0.08 mm and 2.37 ± 0.05 mm, respectively. The first instar nymph created significantly the smallest mean diameter of feeding spots on the first leaf (0.90 ± 0.05 mm), followed by the second (1.39 ± 0.05 mm) and third (1.64 ± 0.05 mm) instar nymph. Similar trends were

observed on the second leaf, where the first instar generated the smallest mean diameter (0.58 ± 0.04 mm), while adult females produced the largest (2.84 ± 0.09 mm), statistically comparable to adult males (2.64 ± 0.07 mm).

Table 5
The mean diameter (mm) of feeding spots on different parts of the tea shoot caused by different stages of H. theivora *in the choice experiment*

Growth stage	Mean diameter (mm) of feeding spots ± SE				
	Bud	**First leaf**	**Second leaf**	**Third leaf**	**Stem**
First instar	0.35±0.06eC	0.90±0.05eA	0.58±0.04eB	0.00eD	0.00dD
Second instar	1.06±0.09dB	1.39±0.05dA	1.18±0.06dB	0.80±0.07dC	0.00dD
Third instar	1.22±0.06cdC	1.64±0.05cdB	1.45±0.06cA	0.89±0.15dD	0.32±0.06cE
Fourth instar	1.27±0.07cC	1.91±0.14bcB	2.25±0.10bA	1.36±0.13cC	0.79±0.01bD
Fifth instar	1.38±0.11bcD	2.15±0.07bB	2.45±0.12bA	1.63±0.10bC	0.83±0.07bE
Male	1.48±0.11abD	2.37±0.05aB	2.64±0.07aA	2.01±0.10aC	0.97±0.15aE
Female	1.62±0.14aD	2.52±0.08aB	2.84±0.09aA	2.12±0.13aC	1.05±0.18aE

Means within a column followed by the same small letter and means within a row followed by the same capital letter are not significantly different (p>0.05) at 5% level of significance

The mean diameter of feeding spots made by adult females (2.12 ± 0.13 mm) and males (2.01 ± 0.10 mm) on the third leaf was significantly larger than the other nymphal instars. Among nymphal stages, the fifth instar nymph (1.63 ± 0.10 mm) made the larger diameter of feeding spots. The adult female created the largest diameter of the feeding spot (1.05 ± 0.18 mm) on the stem, next to the adult male (0.97 0.15 mm) and the fifth instar nymph (0.83 ± 0.07 mm). However, the third instar nymph made the smallest diameter of the feeding spot (0.32 ± 0.06 mm), followed by the fourth instar nymph (0.79 ± 0.01 mm).

The first, second, and third instar nymphs produced the largest diameter of feeding spots on the first leaf of the tea shoot, measuring 0.90 ± 0.05 mm, 1.39 ± 0.05 mm, and 1.64 ± 0.05 mm, respectively (Table 5). However, no feeding spots were made on the third leaf and stem of the tea shoot by the first instar nymph. Similarly, the second instar nymphs did not create feeding spots on the stem. The fourth and fifth instar nymphs, adult male and female, produced the larger diameter of feeding spots on the second leaf next to the first leaf. The mean diameter of feeding spots developed on the stem of the tea shoot was the smallest for all the growth stages. Figure 6 shows the positive and linear correlation (R^2= 0.9593) between the growth stages of *H. theivora* and the diameter of the feeding spots. This relationship indicates a proportional increase in feeding spot size with each successive instar, culminating in the adult stage.

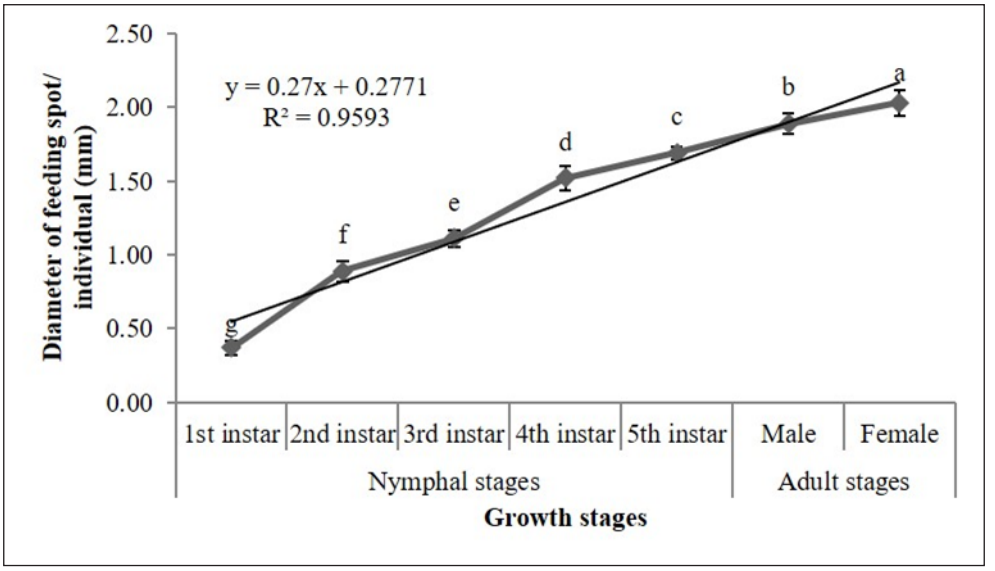

Figure 6. Relationship of the diameter (mm) of feeding spots produced by various growth stages of *H. theivora o*n tea shoots in the choice experiment. Vertical bars at lines indicate the SE value. Different small letters on the lines are significantly different ($p<0.05$) at 5% level of significance

Area of Damaged Shoots. The result of the no-choice experiment revealed that the total area damaged by the adult female was the maximum (409.55 ± 28.58 mm^2), significantly different from other growth stages of *H. theivora* (Table 6). At the same time, the lowest leaf area damage was calculated in the first instar nymph (19.32 ± 4.07 mm^2), followed by that of the second instar nymph (70.64 ± 4.33 mm^2). Similarly, adult females caused

Table 6
Shoot area damaged by different growth stages of H. theivora *reared on tea shoot in no-choice experiment*

Growth stage	The mean area damaged (mm^2)/ feeding spot/ individual (a)	Feeding spots/ individual/ day (b)	The total area damaged (mm^2) by feeding/ individual/ day (a × b)	Damage % by feeding/ individual/ day
First instar	0.24±0.03g	80.50±6.48bc	19.32±4.07e	1.54±0.34e
Second instar	0.84±0.04f	84.10±4.43bc	70.64±4.33d	5.64±0.43d
Third instar	1.17±0.03e	75.20±5.31c	87.98±5.75d	7.03±0.51d
Fourth instar	2.10±0.05d	78.10±5.76c	163.23±13.76c	13.04±0.83c
Fifth instar	2.58±0.07c	76.10±4.56c	196.34±9.23c	15.69±0.74c
Male	3.20±0.08b	95.20±7.67ab	304.64±27.03b	24.34±1.57b
Female	3.66±0.09a	111.90±6.54a	409.55±28.58a	32.72±1.13a

Means within columns followed by the same letter are not significantly different ($p>0.05$) at 5% level of significance

the highest percentage of shoot area damage (32.72%), followed by adult males (24.34%), fifth instar nymph (15.69%), and fourth instar nymph (13.04%). It was also observed that the percentage of area damage was the lowest by the first instar nymph (1.54%) next to the second instar nymph (5.64%) and third instar nymph (7.03%).

In the case of the choice experiment, the adult female caused the maximum total area damage (371.31 ± 37.26 mm^2), significantly different from other growth stages of *H. theivora* (Table 7). In addition, the lowest leaf area damage was assessed in the first instar nymph (16.39 ± 3.12 mm^2). In a similar pattern, adult females inflicted the most significant shoot damage (33.13%), with adult males causing the next highest amount (24.66%), followed by fifth instar nymphs (14.75%).

Table 7
Shoot area damaged by different growth stages of H. theivora *reared on tea shoot in the choice experiment*

Growth stage	The mean area damaged (mm^2)/ feeding spot/ individual (a)	Mean total feeding spots/ individual/ day (b)	The total area damaged (mm^2) by feeding/ individual/ day (a × b)	Damage % by feeding/ individual/ day
First instar	0.22±0.03g	74.50±6.87bc	16.39±3.12e	1.46±0.26e
Second instar	0.82±0.04f	80.10±7.41bc	65.68±5.87de	5.86±0.49d
Third instar	1.14±0.03e	68.90±7.50bc	78.55±8.06d	7.01±0.64d
Fourth instar	2.04±0.05d	72.20±5.92bc	147.29±10.07c	13.14±1.09c
Fifth instar	2.52±0.08c	65.60±4.69c	165.31±13.28c	14.75±1.26c
Male	3.13±0.09b	88.30±6.45ab	276.38±23.46b	24.66±1.49b
Female	3.56±0.07a	104.30±8.96a	371.31±37.26a	33.13±2.35a

Means within columns followed by the same letter are not significantly different ($p>0.05$) at 5% level of significance

Feeding Behavior of *H. theivora* at Different Growth Stages on Different Alternate Host Plants

No-Choice and Choice Experiment

Figure 7 demonstrates the overall mean number of feeding spots on different alternate host plants created by *H. theivora* in the no-choice and choice experiments. The results revealed that all growth stages of *H. theivora* caused more feeding spots on the tea leaf than on the golden dewdrop, mikania, and china rose leaves in both experiments. The significantly higher feeding activity by *H. theivora* on tea shoots in the no-choice experiment indicates its inherent host preference, morphological adaptation, nutritional quality, stress-induced nutritional changes, suppressed plant defenses, and limited defense activation under laboratory conditions.

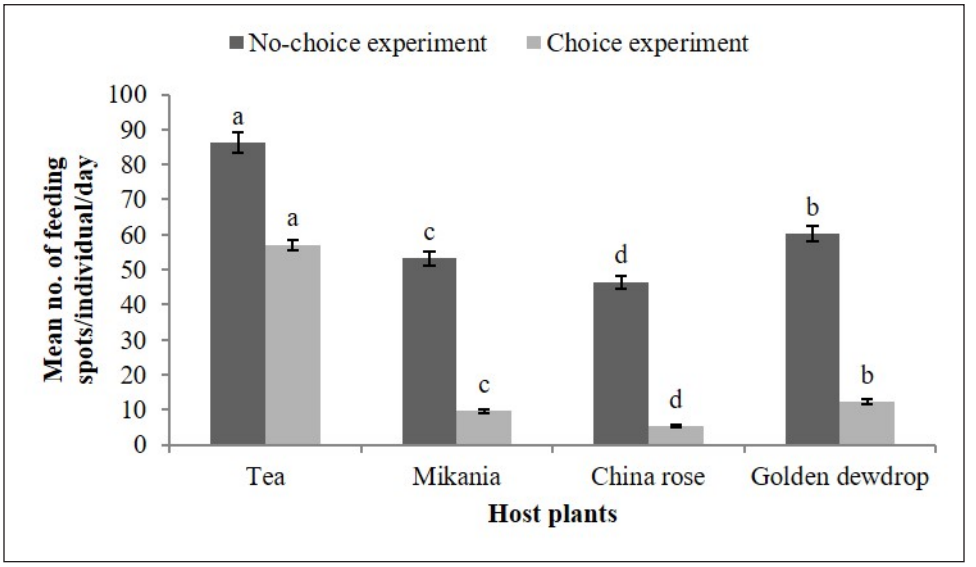

Figure 7. The mean number of feeding spots produced by various growth stages of *H. theivora* on different alternate host plants in the no-choice and choice experiments. Vertical lines at each bar indicate the SE value. Different small letters on the bar are significantly different ($p<0.05$) at 5% level of significance

The mean numbers of feeding spots in the no-choice experiment varied significantly ($F = 1.87$; $df = 18, 279$; $P < 0.05$) depending on the insect growth stages and alternate host plants (Table 8). On the tea leaves, adult females generated a significantly higher number of feeding spots (115.40 ± 8.36), followed by the adult male (103.90 ± 6.44) and the first instar nymph (85.60 ± 3.49). The third instar nymph made the lowest mean number of feeding spots (67.30 ± 5.18) compared to other growth stages. In the case of golden dewdrop leaves, the adult female made the highest feeding spots (81.50 ± 5.53), followed by the adult male (73.10 ± 3.84). The second instar nymph generated the lowest number of feeding spots (47.90 ± 3.59) on the golden dewdrop leaves. On the China rose leaf, however, the adult female created the highest feeding spots (61.50 ± 5.36). The first instar nymph (33.30 ± 5.57) had the lowest number of feeding spots next to the second instar nymph (34.60 ± 3.72). On the mikania leaf, the adult females made the highest number of feeding spots (69.80 ± 6.54), followed by the adult males (63.60 ± 4.59). Significantly, the second instar nymph (36.40 ± 5.05) created the lowest number of feeding spots, followed by the first instar nymph (45.60 ± 4.13).

The first instar nymph created the highest number of feeding spots (85.60 ± 3.49) on the tea leaf next to the golden dewdrop (51.70 ± 4.86) and mikania (45.60 ± 4.13) leaves (Table 8). In contrast, the lowest number of feeding spots was counted on the China rose leaf (33.30 ± 5.57). A similar pattern of feeding behavior was observed for the fifth instar nymph. The second instar nymph created the highest number of feeding spots on the tea leaf

Table 8
The mean number of feeding spots on the leaf of different alternate host plants caused by H. theivora *in the no-choice experiment*

Growth stage	Alternate host plants and mean number of feeding spots ± SE			
	Tea	Golden dewdrop	China rose	Mikania
First instar	85.60±3.49bA	51.70±4.86cdB	33.30±5.57cC	45.60±4.13cdB
Second instar	81.60±4.50bcA	47.90±3.59dB	34.60±3.72cC	36.40±5.05dC
Third instar	67.30±5.18cA	52.10±5.18cdB	46.20±4.70bcC	49.30±5.06cC
Fourth instar	78.20±4.67bcA	61.10±2.95bcAB	44.80±3.12bcC	56.20±3.40bcBC
Fifth instar	71.40±5.92bcA	54.70±4.83cdB	48.40±2.22bcC	51.30±5.74cB
Male	103.90±6.44aA	73.10±3.84abB	56.30±4.51abC	63.60±4.59abBC
Female	115.40a±8.36aA	81.50±5.53aB	61.50±5.36aC	69.80±6.54aBC

Means within a column followed by the same small letter and means within a row followed by the same capital letter are not significantly different ($p>0.05$) at 5% level of significance

(81.60 ± 4.50), followed by the golden dew drop leaf (47.90 ± 3.59). The lowest number of feeding spots was recorded on the China rose leaf (34.60 ± 3.72), similar to those of the mikania leaf (36.40 ± 5.05). The third instar nymph showed a similar feeding pattern. Similarly, the fourth instar nymph, as well as adult male and female, created the highest number of feeding spots on the tea leaf, significantly different from other host leaves.

Based on the insect growth stages and alternate host plants, the mean numbers of feeding spots varied significantly ($F = 3.10$; $df = 18, 279$; $P < 0.05$) in the choice experiment (Table 9). The adult female demonstrated the highest feeding intensity on the tea leaves (70.50 ± 4.27), whereas the fifth instar nymph made the lowest (49.10 ± 3.59). The second instar nymph caused the least feeding activity (4.50 ± 1.30) while the adult female had more feeding spots (18.40 ± 2.47) on the golden dew drop leaf. Feeding patterns in China rose followed a similar trend, with adult females being the most voracious (10.70 ± 3.05), whereas the first instar nymph (0.90 ± 0.79) created the least number of feeding spots. Similarly, adult females caused the most feeding spots on mikania leaves (16.60 ± 2.86), while the lowest feeding incidence was recorded for the second instar nymph (3.10 ± 0.73).

The first instar nymph produced the highest number of feeding spots (54.20 ± 5.30) on the tea leaf, followed by the golden dew drop leaf (5.10 ± 2.11) and mikania leaf (3.50 ± 1.16) (Table 9). The second instar nymph, fifth instar nymph, and adult male and female showed a similar trend of feeding choice. The third instar nymph produced the highest feeding spots on the tea leaves (53.30 ± 4.46), followed by the golden dew drop leaf (12.30 ± 2.39) and mikania leaf (10.40 ± 2.14). On the other hand, the fourth instar nymph made the highest number of feeding spots on the tea leaf, followed by the golden dew drop leaf (15.80 ± 2.77). All the growth stages of *H. theivora* made the least feeding damage on the China rose leaf.

Table 9
The mean number of feeding spots on different alternate host plants caused by H. theivora *in the choice experiment*

Growth stage	Alternate host plants and mean number of feeding spots ± SE			
	Tea	Golden dewdrop	China rose	Mikania
First instar	54.20±5.30bcA	5.10±2.11cB	0.90±0.79dC	3.50±1.16cBC
Second instar	55.80±4.76bcA	4.50±1.30cB	1.20±0.53dC	3.10±0.73cBC
Third instar	53.30±4.46cA	12.30±2.39bB	4.10±1.27bcC	10.40±2.14bB
Fourth instar	52.40±5.77cA	15.80±2.77abB	5.20±1.00bcC	8.90±1.78bC
Fifth instar	49.10±3.59cA	13.20±1.79bB	6.10±1.21bC	9.90±1.68bBC
Male	64.20±4.06abA	16.30±4.18abB	9.30±1.84aC	14.40±2.71aBC
Female	70.50±4.27aA	18.40±2.47aB	10.70±3.05aC	16.60±2.86aBC

Means within a column followed by the same small letter and means within a row followed by the same capital letter are not significantly different ($p>0.05$) at 5% level of significance

DISCUSSION

Number of Feeding Spots

The results revealed that various growth stages of *H. theivora* created different numbers of feeding spots on the tea shoot in no-choice and choice experiments. These findings are in line with the results of Sarkar et al. (2021), whom reported that during the growth of insects, digestive performance value changes, and the values for approximate digestibility tend to decrease from early to late instars. This is probably related to increased feeding rate and gut size when nymphs get older. The early nymphal stages, especially first and second-instar nymphs, created more feeding spots than late-instar nymphs. Because first-instar nymphs have a relatively higher nutritional demand compared to older nymphs, they can access more sap and nutrients by creating multiple feeding spots to support their rapid growth and development. Another reason may be that the stylet in the first instar nymphs is smaller than that of older nymphs, i.e., early instars have limited penetration ability. Creating multiple feeding spots allows them to access a larger surface area of plant tissues, compensating for their smaller stylet and limited ability to extract sap from a single puncture site.

Diameter of Feeding Spots

In the no-choice and choice experiments, the diameter of feeding spots showed an increasing trend with the advancement of their growth stages. Yao et al. (2025) also mentioned a direct correlation between growth stages and the diameter of the feeding spots by *H. theivora* in tea. Another study by Serrana et al. (2022) confirmed that at an early age, the nymphs of the cacao mirid bug (*H. bakeri* Poppius) (Hemiptera: Miridae) were smaller, and their stylet in the mouth parts was also small. Therefore, the feeding spots in plant tissue would be small.

The females created significantly higher numbers and larger diameters of feeding spots in the no-choice and choice experiments. The present observation could be corroborated by the findings of Gou et al. (2022), whom noted that females need more nutrition and energy to produce eggs.

The diameter of feeding spots was larger on the first and second leaves compared to other parts of the tea shoot. Different growth stages of *H. theivora* prefer younger leaves, so they suck longer, which may increase the diameter of feeding spots. This is consistent with the results from a previous study by Song et al. (2021), who observed that when the cotton leaves are young, a relatively shorter duration of cell rupturing (i.e., enzymatic salivary maceration) is needed to allow a longer time of ingestion by *Apolygus lucorum* (Meyer-Dür) (Hemiptera: Miridae). The length of the stylet also plays a vital role in the formation and area of feeding spots. An adult has a longer stylet and can extend the same to penetrate many cells at a time, resulting in a larger necrotic area (Das et al., 2017).

Feeding Behavior of *H. theivora* on Different Parts of Tea Shoots

The feeding behavior study showed that all the growth stages of *H. theivora* caused more feeding spots on the first and second leaves compared to the bud, third leaf, and stem of tea shoots in no-choice and choice experiments. This result was in agreement with the findings of Gou et al. (2022), Serrana et al. (2022), and Song et al. (2021). Gou et al. (2022) stated that *Lygus pratensis* preferred young plants since they could suck more easily on the tender tissues of young plants and make repeated feedings. A relatively higher amino acid concentration was recorded in young plants that ingest large amounts of plant sap. Serrana et al. (2022) also documented that *H. bakeri* preferred to feed on young shoots rather than inflorescences and old fruits in cacao.

Moreover, Song et al. (2021) found that *A. lucorum* tends to feed on young leaves of cotton plants. The first and second nymphal instars created more spots on the first leaf, indicating they stayed longer in one location. This could probably be because sap in each feeding area depletes more slowly for the earlier nymphal stages than the older ones (Serrana et al., 2022). First and second-instar nymphs are relatively less mobile than older nymphs and adults. They may not be able to move as far or access a wide range of plant tissues. By creating more feeding spots in a localized area, they can increase their chances of finding a sufficient food source.

The feeding behavior study also showed that the fourth and fifth nymphal instars and adults preferred the second leaf, whereas the first, second, and third nymphal instars chose the first leaf. This indicated that different growth stages of *H. theivora* preferred leaves of various ages of a tea shoot. The leaf surface morphology (trichomes), surface texture, the surface wax structure of different tea leaves, and chemical composition could be responsible for *H. theivora* feeding at different stages (Bharathi et al., 2024; Das et al., 2017). High

trichomes on younger leaves can serve as a physical barrier that hinders the insect's ability to access the leaf surface and penetrate the epidermal layer. As the leaves mature, the density of trichomes typically decreases, potentially making older leaves more susceptible to feeding due to easier access and reduced physical barriers (Bindu & Pramanik, 2017; Yasmin et al., 2021). The variation of the biochemical profile of the various parts of the tea shoot (bud, leaf, internode) may also play a vital role in influencing the feeding behavior of the different stages of *H. theivora* (Das et al., 2017). Another study by Sarkar et al. (2021) mentioned that the nutritional requirements of insects vary based on their growth and development, which are characteristically reflected in feeding behavior. Insects consume protein and carbohydrate-rich plant tissues to fulfill their nutrient requirements. These components are present in variable quantities in an individual plant, depending on the tissue type and age of the leaves. Similar findings were cited by Song et al. (2021), who mentioned that the cotton leaf age had a significant effect on the feeding behavior of *A. lucorum.* Another study showed that the nutrient supply of leaves at different growth stages varies greatly, affecting insects' feeding, oviposition, and survival rate (Borthakur & Bora, 2023).

Different growth stages of *H. theivora* created fewer feeding spots on the bud, though it is the most tender part of a tea shoot. This may be due to more trichomes and waxy layers on the bud (Sarkar et al., 2021; Serrana et al., 2022). In addition, the feeding spots caused by different stages of *H. theivora* are significantly less on the third leaf and stem of a tea shoot. Similar results were claimed by Song et al. (2021), who found that as the cotton leaves matured, the amounts of defensive compounds, such as gossypol, tannins, and soluble proteins, gradually increased. In contrast, the parts of nutritious compounds, such as amino acids and soluble sugars, gradually decreased. Tannins, gossypol, soluble proteins, and thick leaves were negatively correlated with stylet probing durations by *A. lucorum*, whereas soluble sugars, amino acids, and thin leaves were positively correlated with probing. Bharathi et al. (2024) and Borthakur & Bora (2023) also reported that metabolites such as flavonoids, phenolic acid, terpenoids, and soluble sugar content of various parts of the tea shoot also play a vital role in feeding site preference by *H. theivora*.

Feeding Behavior of *H. theivora* on Different Alternate Host Plants

The feeding behavior study of *H. theivora* on different alternate host plants showed different feeding preferences toward plants under different families and genera. The physical structure and chemical components of plants play a vital role in selecting host plants. The phytophagous insects use their olfactory sensilla to receive volatile plant odors, which are important chemical signals for insects to locate the host plants for either feeding or oviposition (Borthakur & Bora, 2023; Gou et al., 2022; Yin et al., 2022). Borthakur et al. (2016) noticed that the variations in feeding rates and oviposition potential of *H. theivora* among different alternate hosts indicated changes in the physical and chemical properties of the alternate host plants.

Borthakur & Bora (2023) documented that soluble sugar is a powerful feeding stimulant, and the carbon-based nutrient, carbohydrates in general, is a significant energy source for various insect activities. They also mentioned that the soluble sugar was a crucial factor for host acceptance and eventually for the growth of *H. theivora*. Zhang et al. (2025) reported that optimal sugar components provide essential cues for the formation of host-specialised cotton-melon aphids. Insects are likely to prefer plants or plant parts with higher sugar concentrations because these provide readily available energy essential for survival, development, and reproduction. It was estimated that both *Duranta erecta* and *D. repens* had high sugar content (Borthakur & Bora, 2023; Johnson et al., 2018). In another study by Borthakur et al. (2016) concerning the preference of *H. theivora* for alternate host plants among *Duranta erecta*, *Senna tora*, and *Lawsonia inermis*, they recorded *D. erecta* as the most preferred after *C. sinensis*. The metabolites flavonoids, phenolic acid, terpenoids, and soluble sugar content of the host plants may influence the host preference by *H. theivora* for feeding and reproduction (Bharathi et al., 2024). The lower choice for china rose leaves may be due to more trichomes, mucilage cells, and secondary metabolites (Raghu et al., 2019).

The early instar nymphs in the present study produced more feeding spots on tea leaves, whereas fewer on other alternate host plants, golden dewdrop, mikania, and china rose, than late instar nymphs and adults. This may be because the early instar nymph cannot detoxify the secondary metabolites properly associated with that host. Prasad & Roy (2017) confirmed that the primary criterion for selecting a host plant is whether the insect can detoxify plant secondary metabolites. They also mentioned that general esterase, glutathione-S-transferase, and cytochrome P450 are the detoxifying enzymes mainly associated with detoxifying plant secondary metabolites. Higher activities of these enzymes will enhance the capability of an insect to take a plant as a host.

CONCLUSION

The feeding behavior of *H. theivora* on tea shoots in both no-choice and choice experiments revealed distinct preferences among its developmental stages. Specifically, the fourth and fifth nymphal instars and adults preferred the second leaf, whereas the first, second, and third instar nymphs chose the first leaf of tea shoots. Furthermore, the feeding activity *H. theivora* was significantly higher on the first and second leaves compared to the bud, stem, or third leaf, indicating a developmental and structural influence on host part selection. When alternate host plants were evaluated, all developmental stages of *H. theivora* showed the highest preference for tea leaves, followed by golden dewdrop, mikania, and china rose. However, the ability of *H. theivora* to utilize alternate host plants allows it to maintain populations during the scarcity of tea shoots, making pest management challenging. These alternate hosts act as reservoirs, enabling the pest to persist in the agroecosystem

and subsequently re-infest tea crops when conditions become favorable. Hence, the polyphagous nature of *H. theivora* and its reliance on tea and alternate hosts demand a holistic management approach addressing both tea plantations and surrounding ecosystems. Identification and characterization of alternate host plants enables growers to implement proactive control measures, such as the removal or spatial separation of high-risk alternate hosts from the vicinity of tea fields. Additionally, such knowledge supports the design of trap cropping systems, where more attractive alternate hosts are strategically used to divert the pests away from tea plants as a part of the push-pull technique. Therefore, the information on host plant preference will enhance the ecological basis of pest control and reduce dependency on broad-spectrum insecticides, thereby promoting the eco-friendly and sustainable management of *H. theivora* in tea plantations.

ACKNOWLEDGEMENT

This study is funded by the National Agricultural Technology Program, Phase-II (NATP-2), Bangladesh Agricultural Research Council (BARC), Bangladesh (Research Vote No. 6282523). The authors are grateful to the Ministry of Commerce, Bangladesh Tea Board, and Bangladesh Tea Research Institute of the People's Republic of Bangladesh. The authors are thankful to the Department of Plant Protection, Faculty of Agriculture, Universiti Putra Malaysia, Selangor, Malaysia, for providing research facilities.

REFERENCES

Amutha, M., & Rani, S. U. (2022). Tea mosquito bug- A new threat to cotton crop. *Biotica Research Today*, *4*(1), 23–25.

Awudzi, G. K., Hadley, P., Hatcher, P. E., & Daymond, A. J. (2020). Mirid feeding preference as influenced by light and temperature-mediated changes in plant nutrient concentration in cocoa. *Annals of Applied Biology*, *177*(3), 395–403. https://doi.org/10.1111/aab.12636

Bharathi, N. S., Babu, A., Prabhu, A., Karan, S. R., Ajith, M. L., & Rabeesh, T. P. (2024). Feeding behavior and ovipositional preference of the tea mosquito bug, *Helopeltis theivora* (Hemiptera: Miridae) on Tea, *Camellia sinensis* (Theales: Theaceae). *Uttar Pradesh Journal of Zoology, 45*(23), 39-47. https://doi.org/10.56557/upjoz/2024/v45i234684

Bhuyan, M., & Bhattacharyya, P. R. (2006). Feeding and oviposition preference of *Helopeltis theivora* (Hemiptera: Miridae) on tea in North-East India. *Insect Science*, *13*(6), 485–488. https://doi.org/10.1111/j.1744-7917.2006.00119.x

Bindu, S. P., & Pramanik, A. (2017). Effect of leaf characteristics on different brinjal genotypes and their correlation on insects pests infestation. *International Journal of Current Microbiology and Applied Sciences*, *6*(11), 3752-3757. https://doi.org/10.20546/ijcmas.2017.611.439

Borthakur, S., & Bora, D. (2023). Identification of chemical cues of *Camellia sinensis* (Ericales: Theaceae) and alternate host plants for preference by tea mosquito bug *Helopeltis theivora* (Hemiptera: Miridae).

International Journal of Science and Research Archive, *8*(1), 710–719. https://doi.org/10.30574/ijsra.2023.8.1.0123

Borthakur, S., Bora, D., & Barman, M. P. (2016). Assessment of certain plants as alternate hosts of *Helopeltis theivora* (Hemiptera: Miridae) Waterhouse - A pest of *Camellia sinensis* (L.) Kuntge. *Agricultural Research Journal*, *53*(1), 62–68. http://dx.doi.org/10.5958/2395-146x.2016.00010.7

Das, P. P. (2022). Fabrication of a vertical Y-Tube olfactometer for the assessment of spatial repellency of essential oils against *Helopeltis theivora* Waterhouse. *International Journal of Tropical Insect Science*, *42*(1), 835–844. https://doi.org/10.1007/s42690-021-00607-3

Das, P., Kalita, S., & Hazarika, L. K. (2017). Tea clonal preference by *Helopeltis theivora* (Hemiptera: Miridae). *Journal of Entomology and Zoology Studies*, *5*(6), 97–103.

Gogoi, B., Choudhury, K., Sharma, M., Rahman, A., & Borthakur, M. (2012). Studies on the host range of *Helopeltis theivora*. *Two and a Bud*, *59*, 31–34.

Gou, C. Q., Hao, H. T., Wang, L., & Feng, H. Z. (2022). Preferences of *Lygus pratensis* (Hemiptera: Miridae) for four potential trap crop plants. *Journal of Entomological Science*, *57*(4), 548–560. https://doi.org/10.18474/jes22-01

Jamian, S., Adam, N. A., Noor, H. M., Zulperi, D., Asib, N., Muhamad, R., Mokhtar, A. S., Wahab, M. A. A., Azhar, B., Sidi, M., & Maamor, A. (2020). The effect of plant volatiles on plant preference by the predatory insect, *Sycanus dichotomus* Stal. (Hemiptera: Reduviidae) in oil palm plantation. *Journal of Oil Palm Research*, *32*(3), 471–479. https://doi.org/10.21894/jopr.2020.0053

Johnson, E., Udoh, A., Etim, E., Attih, E., & Williams, I. (2018). Phytochemical studies, proximate and mineral composition of ethanol leaf extract of *Duranta repens* Linn (Verbenaceae). *Research Journal of Phytochemistry*, *12*(1), 1–6. https://doi.org/10.3923/rjphyto.2018.1.6

Krishnan, T. S. (2000). *Forecasting tea production in Malaysia* [Unpublished master thesis]. University of Malaya.

Latip, S. N. H., Muhamad, R., Manjeri, G., & Tan, S. G. (2010). Development of microsatellite markers for *Helopeltis theivora* waterhouse (Hemiptera: Miridae). *African Journal of Biotechnology*, *9*(28), 4478–4481. https://doi.org/10.5897/AJB10.468

Miller, N. C. E. (1941). Insects associated with cocoa (*Theobroma cocoa*) in Malaya. *Bulletin of Entomological Research*, *32*, 1–15. https://doi.org/10.1017/s0007485300005186

Prasad, A. K., & Roy, S. (2017). Role of host switching in the development of pesticide tolerance in *Helopeltis theivora* (Hemiptera: Miridae), the major pest of tea in India. *Annales de La Societe Entomologique de France*, *53*(6), 428–433. https://doi.org/10.1080/00379271.2017.1396924

Raghu, K., Naidoo, Y., & Dewir, Y. H. (2019). Secretory structures in the leaves of *Hibiscus sabdariffa* L. *South African Journal of Botany*, *121*, 16–25. https://doi.org/10.1016/j.sajb.2018.08.018

Roy, S., Rahman, A., Sarma, M., Babu, A., & Deka, B. (2018). *Special bulletin on integrated management of tea pests of Northeast India*. Tea Research Association-Tocklai.

Sankarganesh, E., Lavanya, S. B., Rajeshwaran, B., & Mounika, M. N. (2020). Tea mosquito bug (*Helopeltis* spp.)- A pest of economically important fruit and plantation crops: Its status and management prospects. *Journal of Plant Health Issues*, *1*(1), 014–024. https://doi.org/10.54083/pha/1.2.2023/18-28

Sarkar, S., Babu, A., Chakraborty, K., Deka, B., Kashyap, B., & Adhikary, B. (2021). Study on varietal preference and nutritional indices of tea looper *Hyposidra talaca* (Lepidoptera: Geometridae) on ten selected tea varieties. *International Journal of Tropical Insect Science*, *41*(4), 3087–3098. https://doi.org/10.1007/s42690-021-00502-x

Serrana, J. M., Ormenita, L. A. C., Almarinez, B. J. M., Watanabe, K., Barrion, A. T., & Amalin, D. M. (2022). Life history and host plant assessment of the cacao mirid bug *Helopeltis bakeri* Poppius (Hemiptera: Miridae). *PhytopSarasitica*, *50*(1), 1-12. https://doi.org/10.1007/s12600-021-00957-1

Sireesha, U., Borah, R., Ramdam, D. S., Modak, B., & Pradhan, B. (2020). Review on destructive pest tea mosquito bug, *Helopeltis theivora* of tea (*Camellia sinensis*). *International Journal of Entomology Research*, *5*(6), 222–228. https://doi.org/10.5958/2249-524x.2020.00028.x

Sivakumar, T., & Yeshwanth, H. M. (2019). New hosts of tea mosquito bug, *Helopeltis theivora* Waterhouse on eggplant (*Solanum melongena* L.) and amaranth (*Amaranthus* sp. L.) from India. *Phytoparasitica*, *47*(4), 499–503. https://doi.org/10.1007/s12600-019-00750-1

Song, H., Dong, Z., Li, L., Lu, Z., Li, C., Yu, Y., & Men, X. (2021). Relationships among the feeding behaviors of a mirid bug on cotton leaves of different ages and plant biochemical substances. *Journal of Insect Science*, *21*(1), Article 15. https://doi.org/10.1093/jisesa/ieab007

Suganthi, M., Arvinth, S., & Senthilkumar, P. (2020). Comparative bioefficacy of *Bacillus* and *Pseudomonas* chitinase against *Helopeltis theivora* in tea (*Camellia sinensis* (L.) O.Kuntze. *Physiology and Molecular Biology of Plants*, *26*(10), 2053–2060. https://doi.org/10.1007/s12298-020-00875-2

Thube, S. H., Mahapatro, G. K., Mohan, C., Pandian, T. P. R., Apshara, E., & Jose, C. T. (2019). Biology, feeding and oviposition preference of *Helopeltis theivora*, with notes on the differential distribution of species of the tea mosquito bug species complex across elevations. *Animal Biology*, *70*(1), 67–79. https://doi.org/10.1163/15707563-20191083

Xie, R., Wu, B., Dou, H., Liu, C., Knox, G. W., Qin, H., & Gu, M. (2020). Feeding preference of crapemyrtle bark scale (*Acanthococcus lagerstroemiae*) on different species. *Insects*, *11*, 1–15. https://doi.org/10.3390/insects11070399

Yao, Q., Lin, Y. Z., Qin, S., Lin, Z. F., & Ji, X. C. (2025) Characterization of feeding damage by tea mosquito bug, *Helopeltis theivora* Waterhouse (Hemiptera: Miridae) on Hainan Dayezhong tea cultivar. *Frontiers in Plant Science*, *15*, Article 1529535. https://doi.org/10.3389/fpls.2024.1529535

Yasmin, F., Amin, M. R., Afroz, M., Swapon, M. A. H., & Hossain, M. M. (2021). Morpho-biochemical characteristics of brinjal germplasms affect the abundance and infestation of Jassid. *SAARC Journal of Agriculture*, *19*(1), 81-91. https://doi.org/10.3329/sja.v19i1.54780

Yin, H., Li, W., Xu, M., Xu, D., & Wan, P. (2022). The role of tetradecane in the identification of host plants by the pest bugs *Apolygus lucorum* and *Adelphocoris suturalis*. *Research Square*, 1–16. https://doi.org/10.21203/rs.3.rs-1532442/v1

Zhang, Y., Zhang, Y., Wang, X., Yan, H., Zhang, Z., Huo, R., Chen, A., Du, Y., & Guo, H. (2025). Optimal sugar components provide essential cues for the formation of host-specialised cotton-melon aphids. *Ecological Entomology*, *50*(3), 440-452. https://doi.org/10.1111/een.13414

Pertanika J. Trop. Agric. Sci. 48 (6): 1755 - 1767 (2025)

PERTANIKA JOURNALS

TROPICAL AGRICULTURAL SCIENCE

Journal homepage: http://www.pertanika.upm.edu.my/

Determination of the Whitefly (Hemiptera: Aleyrodidae) Damage Index in a White Cargamanto Bean Crop (*Phaseolus Vulgaris*, Fabaceae), in Antioquia, Colombia

Camilo Alcides Marín[1], Carlos Santiago Escobar-Restrepo[2]*, and Carlos Eduardo Giraldo[3]

[1]Study group BIOECO, Catholic University of the East. Rionegro, Antioquia. Sector 3 Cr 46 # 40B-50, Rionegro, Colombia
[2]INCA-CES Research Group, Faculty of Veterinary Medicine and Animal Science, CES University, Cl 10A #22 - 04, Medellín, Antioquia, Colombia
[3]Plant Health Research Group (GISAVE), Catholic University of the East. Rionegro, Antioquia. Sector 3 Cr 46 # 40B-50, Rionegro, Colombia

ABSTRACT

The whitefly is a prevalent pest in bean crops. Although it feeds on sap and can transmit phytopathogenic viruses, many farmers and existing literature do not fully acknowledge its potential harm to bean crops. To address this, it is crucial to quantify the Damage Index (DI), Economic Injury Level (EIL), and Economic Threshold (ET) to aid in decision-making and prevent economic losses. This study aimed to quantify the DI of whiteflies in a bean crop under field conditions. A bean plot was established with three treatments: Buffer Zone, Chemical Control, and No Control. Whitefly adults per leaflet were monitored every 14 days throughout the crop cycle. Yield per plant for each treatment was estimated and related to whitefly populations using linear regressions. The EIL and ET were calculated based on the region's socioeconomic context. The estimated DI was 3.52 grams of dry beans per plant (47 kg per hectare) for each whitefly adult found per leaflet. Consequently, the EIL and ET were 14 and 8 adult whiteflies per leaflet, respectively. Whitefly populations can significantly reduce yields and result in economic losses for local farmers if not properly managed.

Keywords: Crops, economic injury level (EIL), economic threshold (ET), integrated pest management (IPM), monitoring

ARTICLE INFO

Article history:
Received: 27 November 2024
Accepted: 14 April 2025
Published: 25 November 2025

DOI: https://doi.org/10.47836/pjtas.48.6.05

E-mail addresses:
camilomarin25@hotmail.com (Camilo Alcides Marín)
csescobar@ces.edu.co (Carlos Santiago Escobar-Restrepo)
cegiral0@gmail.com (Carlos Eduardo Giraldo)
* Corresponding author

e-ISSN: 2231-8542

INTRODUCTION

The common bean (*Phaseolus vulgaris*, Fabaceae) is one of the most important crops for the rural economy across the American continent. Belonging to the genus *Phaseolus*, which includes about 70 species, the bean has historically contributed to human well-being in Mesoamerica and the Andean regions of South America (Acosta-Gallegos et al., 2007). Its ability to adapt to various environments and climatic conditions, owing to its tropical and subtropical origins, sets it apart from other crops (Ligarreto & Gustavo, 2013). Common bean is the predominant legume crop globally, accounting for approximately 85% of total bean production worldwide (Machiani et al., 2019). With an annual global output exceeding 27 million tons, this crop is cultivated across 29 million hectares (Gepts et al., 2008). In Colombia, per capita consumption ranges between 3 and 4 kg annually. The regions with the highest production are Santander, Antioquia, Huila, and Nariño, yielding an average of 1.24 tons per hectare. Beyond its role in food security, the bean crop provides rural employment and income, with approximately 120,000 small-scale farmers cultivating 92,412 hectares and producing 114,408 tons annually (Ministerio de Agricultura y Desarrollo Rural, 2020).

However, the bean is also one of the crops most affected by insect pests, which can cause significant losses or result in excessive insecticide use during the production process. Whiteflies (Hemiptera: Aleyrodidae) are among the most damaging pests worldwide, affecting beans and many other crops. These sap-sucking insects cause damage in two ways: by directly feeding on the plant's sap, which weakens the plant, induces chlorosis, deforms foliage, and reduces crop productivity; and by transmitting leafroll viruses in the early stages of leaf development (Otzoy-Rosales & Rodas-Rodríguez, 2003). Additionally, whiteflies indirectly cause harm by excreting sugary honeydew, which promotes the growth of sooty mold (*Capnodium fungus*) (Rebolledo-Martínez et al., 2013). While this fungus does not damage plant tissues, it impairs photosynthesis by obstructing light penetration, reducing the marketable value of leaves, flowers, fruits, and other parts (Nombela & Muñiz, 2010). Thus, whitefly infestations can severely impact bean production. Furthermore, whiteflies have a broad geographic distribution and a wide range of host plants, increasing their economic impact. Although substantial research exists, some studies have misled bean growers, suggesting that whitefly infestations do not significantly reduce yields under field conditions (Bueno et al., 2005). Consequently, many bean producers in Eastern Antioquia appear unconcerned about the losses caused by whiteflies, possibly due to a lack of accurate population and yield quantification.

The technical term for the relationship between pest populations and crop yields is the Damage Index (DI), which represents the amount of damage (e.g., kilograms/plant, tons/hectare) per unit of pest population (individual or percentage unit) (Pedigo et al., 1986). For instance, Bueno et al. (2005) evaluated the DI of the whitefly *Trialeurodes vaporariorum* (Westwood) in snap bean crops in Valle del Cauca, Colombia, finding that

2.25 nymphs/leaflet/cm² led to losses of 158.4 kg per hectare. The DI is crucial in estimating the Economic Injury Level (EIL), which marks the pest population level where economic loss equals the cost of control measures. The EIL helps determine the Economic Threshold (ET), or the pest population level that requires intervention to avoid financial loss. These indices are vital for developing Integrated Pest Management (IPM) programs. However, no published data are available on yield losses in beans under field conditions caused by whitefly infestations.

Therefore, quantifying production losses due to whitefly in bean crops and assessing the economic impact of pest control measures are crucial for decision-making processes. This study aims to estimate the whitefly Damage Index in bean crops under field conditions, based on the hypothesis that plants with the highest whitefly populations will exhibit the lowest yields across various production parameters. Specifically, the study seeks to answer the following questions: 1) How much production loss do whiteflies cause in bean crops when populations are left uncontrolled? 2) What is the net economic profit margin in systems with and without whitefly control? 3) What are the Economic Injury Level and Economic Threshold for the growing conditions in this region?

MATERIAL AND METHODS

Location

The experiment was conducted in the municipality of San Vicente Ferrer, in the Alto de la Compañía area, on the "Curazaos" farm, Antioquia department, Colombia (6°15'56''N; -75°20'24"E), at an elevation of 2,201 meters above sea level (masl). The average temperature was 17°C, with a maximum of 25°C and a minimum of 13°C, and relative humidity of 70%.

Crop Establishment, Cultural Practices, and Harvest

A plot of approximately 500 m² was established. Land preparation involved plowing, row hilling, and the application of a soil conditioner (60 kg of dolomitic lime one month before planting). A total of 440 bean plants were sown at a spacing of 1.50 m between rows and 0.5 m between plants, with two seeds per site. A subplot of 220 sites (hereafter referred to as plants) was marked off, consisting of 11 rows of 20 plants each, to minimize edge effects. In the third week after sowing (WAS), 100 g of organic matter was applied to each plant, followed by staking and wiring in the fourth week. During the sixth week, weeding was performed, and each plant received 40 g of granular fertilizer, consisting of a 1:1 mixture of diammonium phosphate and micronutrients. In the tenth week, a second round of weeding and fertilization was performed, with each plant receiving 50 g of a granular mixture of 10-20-30 and potassium chloride in a 1:0.5 ratio.

The dry bean harvest was carried out in the 18th week, with pods from 15 plants per treatment being individually counted. The harvested pods were separated, placed into labeled plastic bags, and weighed before and after shelling. Total production for each row was recorded, based on the individual yields of the 45 plants across the three treatments.

Experimental Design

The experiment consisted of three treatments: buffer zone (BZ), chemical control (CC), and no control (NC). The BZ comprised 100 plants, arranged in five rows of 20 plants each, situated between the CC and NC treatments to mitigate drift from the CC applications. No whitefly control measures were implemented in the BZ. The CC treatment consisted of 60 bean plants, arranged in three rows of 20 plants, placed between the NC and BZ treatments. These plants were treated with a rotation of chemically synthesized insecticides traditionally used by local farmers for whitefly control: Malathion (1B), Sulfoxaflor (4C), and Lambdacyalothrin (3A), applied every 14 days. The NC treatment also included 60 plants, distributed in three rows of 20, located between the CC and BZ treatments, with no whitefly control applied.

In all three treatments, fungicide applications were performed every 14 days using the following active ingredients: Difenoconazole and Flutriafol (G1), Azoxystrobin (C3), and Chlorothalonil (M05), for Lepidoptera larvae management *Bacillus turigensis* var *kursaki* (Dipel®) was applied, every 15 days. All applications followed the dosages recommended by the manufacturers.

Whitefly Monitoring

The first whiteflies appeared during the third week (WAS). Adult and nymph samples were collected and sent to the "Instituto Colombiano Agropecuario" (ICA) for identification (sample number M4021M0004094). Monitoring began in the sixth week (WAS) and was conducted every 14 days. To count whiteflies while avoiding underestimation due to adult escape, six leaflets per plant from 15 randomly selected plants per treatment were photographed. The images were taken on the underside of the leaves using a mobile device camera with 13 megapixels of resolution, capturing two leaflets from the upper, middle, and lower parts of the plant to assess spatial distribution. The images were processed to count adults, and the data were recorded in spreadsheets. Images also allowed to confirm or discard the presence of any other pest insect species.

After each monitoring event, whitefly control measures were applied only in the CC treatment. Disease control was carried out across the entire plot. A total of six monitoring events were conducted, with the final one occurring in week 16, two weeks prior to harvest.

Data Analysis and Statistical Modeling

The analysis of production parameters and losses due to whitefly infestation was conducted by comparing treatments using box and whisker plots (Tukey, 1977). Whitefly population data and production outcomes (three and six parameters, respectively) were used to calculate the Damage Index (DI) via linear regression analysis (Pedigo et al., 1986). Confidence intervals were generated for each regression using 9,999 bootstrap pseudo-replicates. All analyses were performed using the PAST software, version 4.08 (Hammer et al., 2001).

Economic Injury Level (EIL) and Economic Thresholds (ET)

With the calculated DI and the control costs for whitefly management (including labor, insecticide costs, and equipment depreciation), the EIL was calculated using the formula:

$$EIL = \frac{\$ \text{ CONTROL/HA}}{\$ \text{ SALE KG} * \text{DI} * \% \text{ CONTROL EFFECTIVENESS}}$$

To determine this, economic calculations were made for chemically synthesized insecticide applications, and the sale price was estimated based on the monthly average for beans from the nearest local market.

RESULTS

The whitefly species identified was *Trialeurodes vaporariorum* Westwood (1856). A total of 8,108 individuals were recorded throughout the experiment: 1,658 in the Chemical Control (CC) treatment, 5,519 in the No Control (NC) treatment, and 931 in the Buffer Zone (BZ). The highest abundance of whiteflies occurred during week 12, with an average of 50 adults per leaflet in the NC treatment. By week 16, the population had decreased, coinciding with the onset of plant senescence. The average number of adults per plant across the entire growth cycle was 3.20 in the CC treatment, 10.80 in the NC treatment, and 3.80 in the BZ.

In the BZ, the upper leaflets exhibited an average of 6.77 adults per leaflet over the entire crop cycle, compared to 4.00 in the middle section and 0.79 in the lower section. A similar pattern was observed in the NC treatment, where the averages were 2.43, 0.88, and 0.33 adults per leaflet for the upper, middle, and lower sections, respectively. The CC treatment showed a higher whitefly distribution, with 18.50 adults per leaflet in the upper section, 7.81 in the middle, and 0.61 in the lower section, indicating a concentration of the pest in the middle and upper parts of the plants (Figure 1).

Total production of shelled dry beans was 16,354 g, with the CC treatment yielding 6,585 g (109.76 g/plant), the BZ treatment yielding 5,924 g (59.24 g/plant), and the NC treatment producing 3,845 g (64.8 g/plant). Individual measurements from the 15 plants sampled (Table 1) were 132.3 g (± 30.12) per plant for CC, 95 g (± 35.04) for BZ, and 82.8 g (± 33.89) for NC. The average unshelled weight per plant, calculated from the entire

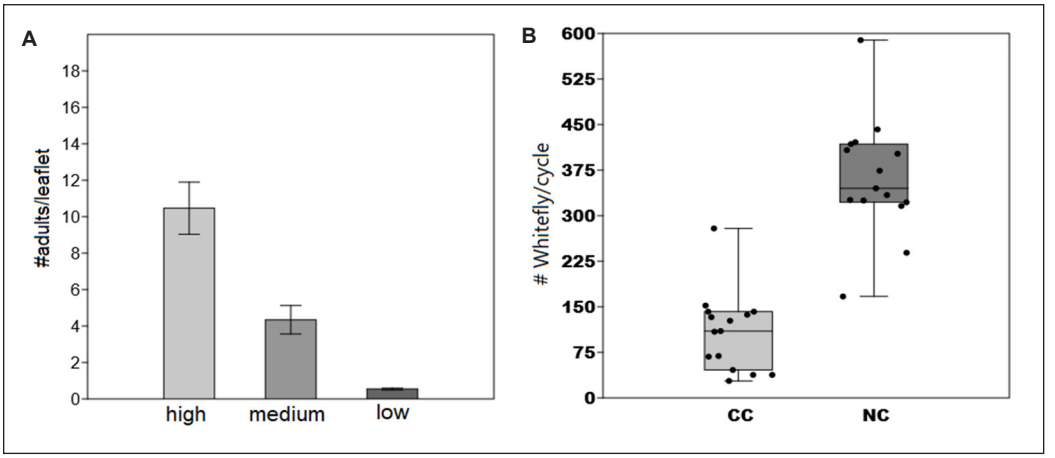

Figure 1. Whitefly adult population dynamics throughout the crop cycle: (A) Number of individuals per leaflet in the upper, middle, and lower thirds of the plant; and (B) Total number of adult individuals per plant in the NC and CC treatments

population of plants, was 203 g for CC, 154 g for BZ, and 136 g for NC. The number of pods per plant was 40 for CC, 35 for BZ, and 32 for NC. A summary of the whitefly population data and productive parameters by treatment is provided in Table 1.

There were no significant differences in the number of pods per plant ($F = 2.576$, $p = 0.08804$). However, significant differences were observed in both unshelled weight ($F = 7.276$, $p = 0.001935$) and dry weight ($F = 9.038$, $p = 0.0005332$). In the case of unshelled weight, the differences were found between the Chemical Control (CC) and No Control (NC) treatments ($p = 0.001874$) and between CC and the Buffer Zone (BZ) ($p = 0.02554$). For dry weight, significant differences were observed between CC and NC ($p = 0.0005332$) and between CC and BZ ($p = 0.01158$) (Figure 2).

A total of 18 linear regressions were conducted to relate production to pest population (Table 2) to estimate the Damage Index (DI). Of these, the regressions with the best fit and statistical significance were selected (Figure 3). The final regression suggested a DI of 3.52 g of dry beans per plant for each additional whitefly adult per leaflet (Figure 4). In our linear regressions, 30 data points were analyzed, resulting in 28 total degrees of freedom. Specifically, the degrees of freedom for treatment were 1, and the degrees of freedom for error were 28.

The average production of shelled dry beans in the CC treatment was 109.76 g/plant, compared to 64.8 g/plant in the NC treatment, showing a difference of 44.96 g/plant. This corresponds to the yield loss per plant due to the absence of whitefly control.

When extrapolated to a planting density of 13,333 plants/ha, this difference results in an estimated loss of approximately 600 kg/ha. Based on a local sale price of COP 6,000/kg, the economic loss per hectare without whitefly control would be around COP 3,600,000.

The Economic Injury Level (EIL) was calculated using a market price of COP 6,000/kg and a control cost of COP 3,130,285/ha, which included labor, insecticide costs, and equipment depreciation. The DI (3.52 g/plant) was adjusted to the estimated yield losses per hectare, with a planting density of 13,333 plants/ha. This resulted in an approximate loss of 46.90 kg/ha for every one whitefly adult per leaflet. The average control efficacy over the crop cycle was 80%. Substituting these values into the EIL equation:

Table 1
Summary of whitefly adult population indicators and bean crop production parameters

	Parameters	n	Min	Max	Median	Std. desv
Whitefly	**Total/cycle**	40	24	568	172.60	134.87
	WF/week6	30	6	247	64.73	55.88
	WF/week10	40	1	167	36.15	44.86
	Max/leaflet	40	5	134	54.23	32.02
	Avg-upper/cycle	40	0.25	39.88	9.544	9.30
	Avg/leaflet	40	1.39	31.56	10.92	7.10
Bean production	**CC**	15	67	203	132.33	33.89
	BZ	15	31	176	95.8	35.04
	NC	15	47	139	82.8	30.12

Note. WF: Whitefly; Avg: average; CC: Chemical Control; NC: No Control; BZ: Buffer Zone

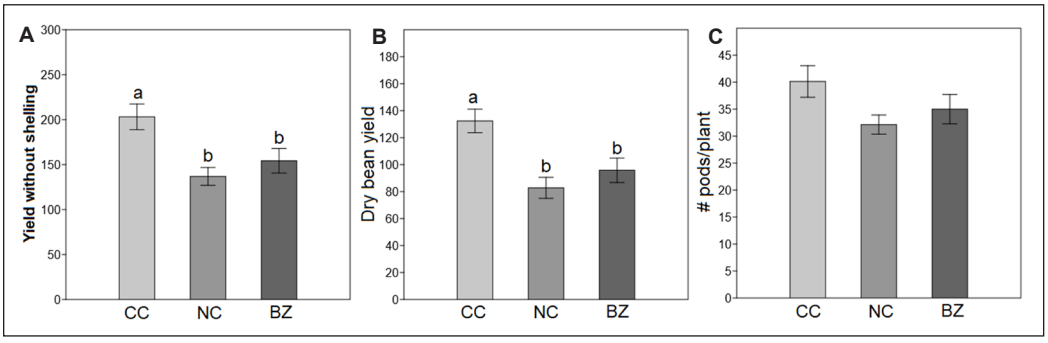

Figure 2. Production parameters of white cargamanto beans in eastern Antioquia under three whitefly management systems: Chemical Control (CC), No Control (NC), and Buffer Zone (BZ). (A) Unshelled bean production in grams per plant; (B) Dry-shelled bean production; and (C) Number of pods per plant

Table 2
Statistical analysis of linear regressions for whitefly populations and most significant production parameters

Parameters	Slope (DI)	Intercept	r^2	P value
Total/Cycle	-0.109(-0.18454; -0.011358)	126.46 (106.72; 143.44)	-0.38	0.0136
Whitefly/week10	-0.41(-0.61; -0.20)	122.5 (108.11; 136.49)	-0.48	0.0014
Unshelled weight	-0.56(-0.82; -0.30)	191.17 (168.92; 212.46)	-0.46	0.0027
Avg-upper/cycle	-2.44(-4.6747; 0.40765)	197.33 (162.1; 227.02)	-0.31	0.048

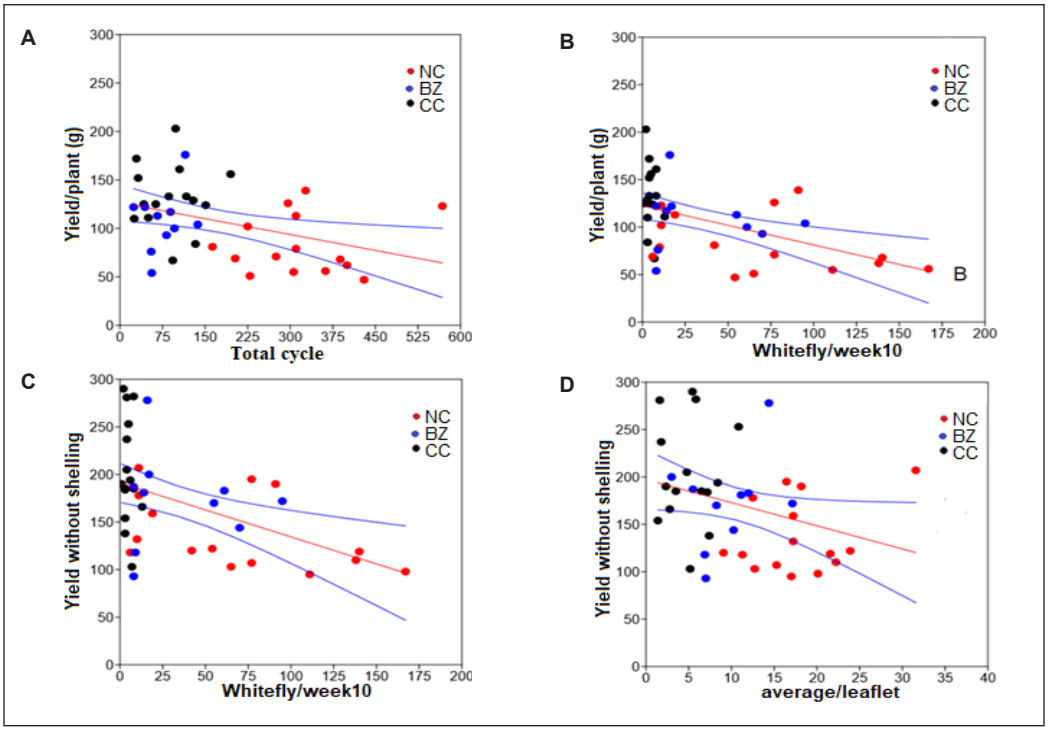

Figure 3. Relationship between whitefly population and production parameters of white cargamanto beans: (A) Total whitefly population throughout the crop cycle and production per plant (g); (B) Whitefly population at week ten and production per plan; (C) Whitefly population at week ten and unshelled bean weight; and (D) Average number of whiteflies per leaflet and unshelled bean weight

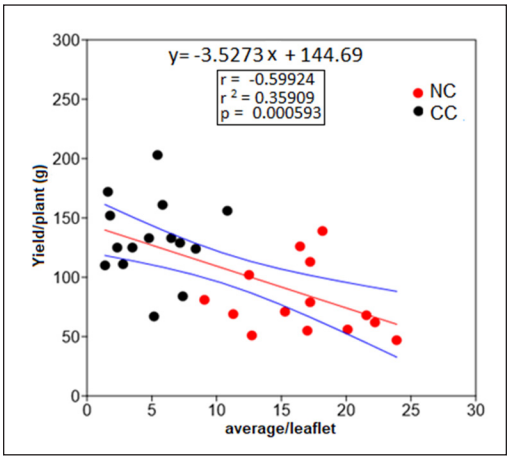

Figure 4. Damage index of white cargamanto bean plants estimated from linear regression of average whiteflies per leaflet and production per plant (in grams) for crops with Chemical Control (CC) and No Control (NC)

$$EIL = \frac{\$3130285}{\$6000 * 46.90kg * 0.8}$$

$$= 13.90 \text{ whitefly/leaflet}$$

Thus, the EIL was estimated to be approximately 14 adult whiteflies per leaflet.

DISCUSSION

Although whiteflies are a common pest in various crops, particularly beans, there is a lack of comprehensive monitoring methods and data to measure their populations and the associated crop damage. Despite the importance of the Damage Index (DI) in pest management, it is not well-established

for widely cultivated crops like beans. In this study, we estimated that each whitefly adult found per leaflet results in a loss of 3.52 grams of dry beans per plant. Extrapolating these data to the region's planting density of 13,333 plants per hectare, we calculate a potential decrease of 47 kilograms per hectare when an average of one adult whitefly per leaflet is present throughout the crop's production cycle.

Gonzalez et al. (2015) calculated the sap consumption rates of whiteflies on bean plants throughout their life cycle. They found that the first and second instars consumed 0.052 mg and 0.14 mg per day, respectively; the third instar consumed 0.19 mg/day, and adults consumed 0.27 mg/day. Over a lifespan of approximately 45 days (excluding egg incubation), the total sap consumption amounts to 6.35 mg per whitefly. Given that the sap's solute concentration is around 20% (Jensen et al., 2013), this translates to 1.27 mg of solutes consumed per whitefly. Thus, 114 whiteflies would be required to consume the equivalent of the bean production in the CC treatment, which averages 145 grams per plant.

Bueno et al. (2005) investigated whitefly sampling methods and spatial distribution in beans and snap beans. They estimated the DI for snap beans at 4.97 grams per whitefly nymph found in 2.25 cm^2, with an Economic Injury Level (EIL) of 12 nymphs per 2.25 cm^2 leaflet. Although these findings contribute to understanding pest dynamics, estimating nymphs in the field remains challenging for producers. The DI calculated in this study, based on adult whiteflies, can enhance decision-making processes. Previous research has provided valuable data on various aspects of whitefly biology and management, but there has been limited focus on calculating DI and EIL specifically for bean crops.

Campuzano-Martínez et al. (2010) proposed an intrinsic growth rate (r) for whiteflies of 0.04/day, which can be used to estimate the Economic Threshold (ET) of whiteflies in bean crops using the exponential growth equation (Stern et al., 1959). Assuming the final population as the EIL and the initial population as the ET, with a 14-day action time between indicators (Pérez-Marulanda & Giraldo-Sánchez, 2020), the calculation yields:

$$EIL = ET\ (\text{Economic Threshold})\ e^{r*t}, \text{ so,}$$

$$ET = \frac{13.90}{e\hat{}(0.04 * 14)} = 8.00\ \text{whitefly/leaflet/plant}$$

This suggests that control measures should be initiated when the average population reaches around eight whiteflies per leaflet, before it exceeds the EIL of approximately 14 adults per leaflet, to prevent economic losses. This value can be adjusted based on local conditions, including variations in sale prices and production costs, providing a practical decision rule for commercial bean production. Future research should focus on evaluating whitefly population parameters under diverse field conditions and climatic regimes to refine ET estimates for different regions, enhancing integrated pest management strategies.

While extensive research has been conducted on whitefly oviposition (de Jesus et al., 2011), preferred cultivars (Morales & Cermeli, 2007), population sampling (Bueno et al., 2005), resistance to insecticides (Campuzano-Martínez et al., 2010), and symbiosis with fungi and viruses (Otzoy-Rosales & Rodas-Rodríguez, 2003; Perea et al., 2003), few studies have focused on damage indices, Economic Injury Levels, or Economic Thresholds (Nava-Camberos & Cano-Ríos, 2000). This study provides valuable insights for managing whitefly populations in bean crops, offering useful information for decision-making in both current and future pest management practices in regions with moderate cold climates.

The observed variability in whitefly populations and crop yield can be explained by the inherent heterogeneity of field conditions and plant physiological responses. The influence of environmental factors such as microclimate variations, natural enemy activity, and plant resilience mechanisms can contribute to fluctuations in pest populations and yield outcomes. Despite this variability, our statistical analyses allowed us to establish a clear Damage Index, reinforcing the economic relevance of whitefly control in bean crops. Moreover, the use of extensive sampling and statistical modeling provided reliable estimates of the Economic Injury Level and Economic Threshold, ensuring their applicability in real-world production systems. These results highlight the importance of integrating population monitoring with decision-making tools to optimize pest management strategies while minimizing unnecessary pesticide applications.

The results of this study highlight the significant economic impact of whitefly infestations on bean crops and emphasize the importance of accurate monitoring and timely intervention. By establishing a clear relationship between whitefly populations and yield loss, this research provides a practical tool for growers to estimate potential damage and implement control measures before economic thresholds are exceeded. The calculated economic threshold (ET) of eight whiteflies per leaflet provides a practical benchmark for the initiation of pest management strategies which can be adapted to local conditions and market dynamics. Furthermore, incorporating these findings into integrated pest management (IPM) programs could improve the sustainability of bean production by reducing unnecessary pesticide use and minimizing crop losses. Future research should focus on validating these thresholds under different climatic conditions and bean varieties to ensure their applicability in different agricultural contexts, thereby supporting more resilient and efficient pest management practices of whitefly populations, not only in this region, but also in other temperate cold climate producing regions.

CONCLUSION

Under the evaluated field conditions, the Damage Index (DI) for whiteflies is 3.52 grams of dry beans per plant for each whitefly found per leaflet. Consequently, the Economic Injury Level (EIL) and the Economic Threshold (ET) for the study period and conditions

were determined to be 14 and 8 adult whiteflies per leaflet, respectively. This indicates that whitefly populations in bean crops can significantly reduce yields and lead to economic losses for local farmers if not properly managed.

ACKNOWLEDGEMENT

We extend our gratitude to the farm "Curazaos" owners for funding.

REFERENCES

Acosta-Gallegos, J. A., Kelly, J. D., & Gepts, P. (2007). Prebreeding in common bean and use of genetic diversity from wild germplasm. *Crop Science*, 47, S-44-S-59. https://doi.org/10.2135/cropsci2007.04.0008ipbs

Bueno, J. M., Cardona, C., & Chacón, P. (2005). Phenology, spatial distribution and development of sampling methods for *Trialeurodes vaporariorum* (Westwood) (Hemiptera: Aleyrodidae) on snap beans and beans (*Phaseolus vulgaris L.*). *Revista Colombiana de Entomología*, *31*(2), 161-169. https://doi.org/10.25100/socolen.v31i2.9439

Campuzano-Martínez, A., Rodríguez-Maciel, J. C., Lagunes-Tejeda, Á., Llanderal-Cázares, C., Terán-Vargas, A. P., Vera-Graziano, J., Vaquera-Huerta, H., & Silva-Aguayo, G. (2010). Aptitud biológica de poblaciones de *Bemisia tabaci* (Gennadius) biotipo B (Hemiptera: Aleyrodidae) con diferente susceptibilidad al insecticida thiametoxam [Fitness of *Bemisia tabaci* (Gennadius) B Biotype (Hemiptera: Aleyrodidae) populations with different levels of susceptibility to the thiametoxam insecticide]. *Neotropical Entomology, 39*(3), 430–435. https://doi.org/10.1590/S1519-566X2010000300018

de Jesus, F. G., Junior, B., Leal, A., Pitta, R. M., Campos, A. P., & Alves Tagliari, S. R. (2011). Fatores que afetam a oviposição de *Bemisia tabaci* (Genn.) Biótipo B (Hemiptera: Aleyrodidae) em feijoeiro [Factors Affecting Oviposition of *Bemisia tabaci* (Genn.) Biotype B (Hemiptera: Aleyrodidae) on Common Bean Plants]. *Bioscience Journal*, *37*(2), 190-195. https://doi.org/10.1590/s1519-566x2008000200012

Gepts, P., Aragão, F. J., Barros, E. D., Blair, M. W., Brondani, R., Broughton, W., Galasso, I., Hernandez, G., Kami, J., Lariguet, P., McClean, P., Melotto, M., Miklas, P., Pauls, P., Pedrosa-Harand, A., Porch, T., Sanchez, F., Sparvoli, F., & Yu, K. (2008). Genomics of *Phaseolus* beans, a major source of dietary protein and micronutrients in the tropics. In P. H. Moore & R. Ming (Eds.) *Genomics of tropical crop plants* (pp. 113–143). Springer. https://doi.org/10.1007/978-0-387-71219-2_5

Gonzalez, L. F. S., Tapias, M. A. D., Caicedo, D. R., & Rincón, F. C. (2015). Medición indirecta de la tasa de consumo de adultos e inmaduros de *Trialeurodes vaporariorum* (Hemiptera: Aleyrodidae) sobre fríjol [Indirect measurement of the consumption rate of adult and immature stages of *Trialeurodes vaporariorum* (Hemiptera: Aleyrodidae) on bean]. *Acta Biológica Colombiana, 20*(3), 99–109. https://doi.org/10.15446/abc.v20n3.44073

Hammer, Ø., & Harper, D. A. (2001). Past: Paleontological statistics software package for education and data analysis. *Palaeontologia electronica*, *4*(1), 1-9.

Jensen, K. H., Savage, J. A., & Holbrook, N. M. (2013). Optimal concentration for sugar transport in plants. *Journal of the Royal Society Interface*, *10*(83), Article 20130055. https://doi.org/10.1098/rsif.2013.0055

Ligarreto, M., & Gustavo, A. (2013). Componentes de variancia en variables de crecimiento y fotosíntesis en frijol común (*Phaseolus vulgaris* L.) [Components of variance in growth traits and photosynthesis in common bean (*Phaseolus vulgaris* L.)]. *Revista UDCA Actualidad & Divulgación Científica, 16*(1), 87–96. https://doi.org/10.31910/rudca.v16.n1.2013.862

Machiani, M. A., Rezaei-Chiyaneh, E., Javanmard, A., Maggi, F., & Morshedloo, M. R. (2019). Evaluation of common bean (*Phaseolus vulgaris* L.) seed yield and quali-quantitative production of the essential oils from fennel (*Foeniculum vulgare* Mill.) and dragonhead (*Dracocephalum moldavica* L.) in intercropping system under humic acid application. *Journal of Cleaner Production, 235,* 112–122. https://doi.org/10.1016/j.jclepro.2019.06.241

Ministerio de Agricultura y Desarrollo Rural. (2020). *Cadena del fríjol. Dirección de Cadenas Agrícolas y Forestales, Ministerio de Agricultura y Desarrollo Rural* [Bean value chain. Directorate of Agricultural and Forestry Chains, Ministry of Agriculture and Rural Development]. MINAGRICULTURA. https://sioc.minagricultura.gov.co/AlimentosBalanceados/Documentos/2020-03-31%20Cifras%20Sectoriales%20frijol.pdf

Morales, P., & Cermeli, M. (2001). Evaluación de la preferencia de la mosca blanca *Bemisia tabaci* (Gennadius) (Hemiptera: Aleyrodidae) en cinco cultivos agrícolas [Evaluation of the preference of the whitefly *Bemisia tabaci* (Gennadius) (Hemiptera: Aleyrodidae) in five agricultural crops]. *Entomotropica, 16*(2), 73–78.

Nava-Camberos, U., & Cano-Ríos, P. (2000). Umbral económico para la mosquita blanca de la hoja plateada en melón en la Comarca Lagunera, México [Economic threshold for the silverleaf whitefly on melon in the Lagunera region, Mexico]. *Agrociencia, 34*(2), 227–234.

Nombela, G., & Muñiz, M. (2010). Host plant resistance for the management of *Bemisia tabaci*: A multi-crop survey with emphasis on tomato. In P. A. Stansly & S. E. Naranjo (Eds.) *Bemisia: Bionomics and management of a global pest* (pp. 357–383). Springer. https://doi.org/10.1007/978-90-481-2460-2_14

Otzoy-Rosales, M., & Rodas-Rodríguez, C. (2003). Selección de cultivares nativos de tomate (*Lycopersicon esculentum* L.) resistentes y/o tolerantes a geminivirus [Selection of native tomato cultivars (*Lycopersicon esculentum* L.) resistant and/or tolerant to geminivirus]. *Universidad de San Carlos de Guatemala, 1*(1), Article 75.

Pedigo, L. P., Hutchins, S. H., & Higley, L. G. (1986). Economic injury levels in theory and practice. *Annual Review of Entomology, 31*(1), 341–368. https://doi.org/10.1146/annurev.en.31.010186.002013

Perea, E. I., Rojas, E., & Villalobos, A. (2003). Diagnóstico de *Trialeurodes vaporariorum* (Homoptera: Aleyrodidae) en tabaco y frijol de García Rovira, Santander [Diagnosis of *Trialeurodes vaporariorum* (Homoptera: Aleyrodidae) in tobacco and kidney beans of García Rovira, Santander]. *Revista Colombiana de Entomología, 29*(1), 7–11. https://doi.org/10.25100/socolen.v29i1.9571

Pérez-Marulanda, J. A., & Giraldo-Sánchez, C. E. (2020). Parámetros poblacionales de *Tuta absoluta* (Lepidoptera: Gelechiidae) y pérdidas asociadas en tomate de invernadero [Population parameters of *Tuta absoluta* (Lepidoptera: Gelechiidae) and associated losses in greenhouse tomato]. *Revista de Biología Tropical, 68*(4), 1025–1038. https://doi.org/10.15517/rbt.v68i4.40898

Rebolledo-Martínez, A., Ángel-Pérez, A. L. D., Peralta-Antonio, N., & Díaz-Padilla, G. (2013). Control de fumagina (*Capnodium mangiferae* Cooke & Brown) con biofungicidas en hojas y frutos de mango

"Manila" [Sooty mold control (*Capnodium mangiferae* Cooke and Brown) with biofungicides in leaves and fruits of mango "Manila"]. *Tropical and Subtropical Agroecosystems, 16*(3), 355–362. https://doi.org/10.56369/tsaes.1437

Stern, V. M., Smith, R. F., Bosch, R. V. D., & Hagen, K. S. (1959). The integrated control concept. *Hilgardia, 29*, 81–101. https://doi.org/10.3733/hilg.v29n02p081

Tukey, J. W. (1977). *Exploratory data analysis*. Addison-Wesley. https://doi.org/10.1126/science.200.4338.195.a

Pertanika J. Trop. Agric. Sci. 48 (6): 1769 - 1784 (2025)

PERTANIKA JOURNALS

TROPICAL AGRICULTURAL SCIENCE

Journal homepage: http://www.pertanika.upm.edu.my/

Updating Knowledge on Species Richness of the Tortoise Beetles (Coleoptera: Cassidinae) from Peninsular Malaysia through Their DNA Barcoding

Salmah Yaakop[1]*, Muhammad Afiq Senen[1], Anang Setyo Budi[2], Abdullah Muhaimin Mohammad Din[1], Audi Jamaluddin[3], Syari Jamian[3], and Aqilah Sakinah Badrulisham[1]

[1]Centre for Insect Systematics, Department of Biological Sciences and Biotechnology, Faculty of Science and Technology, Universiti Kebangsaan Malaysia, 43600 Bangi, Selangor, Malaysia
[2]Museum Zoologicum Bogoriense, Research Center for Biosystematics and Evolution, National Research and Innovation Agency (BRIN), Indonesia
[3]Department of Plant Protection, Faculty of Agriculture, Universiti Putra Malaysia, 43400 Serdang, Selangor, Malaysia

ABSTRACT

The Cassidinae family, comprising unique and beautiful leaf beetles, has been the subject of limited research regarding its diversity and richness in Malaysia. Consequently, this study aimed to perform DNA barcoding on the Cassidinae species collected from Peninsular Malaysia by using the cytochrome *c* oxidase subunit I (*COI*) gene. Prior to molecular work, each species was identified morphologically based on external morphological characteristics. This study reconfirmed the host plant record for only one species, *Silana farinosa*, which infests the curry leaf, *Murraya koenigii*. Notably, a total of ten species were morphologically identified, including those belonging to the tribe Aspidimorphini (*Aspidimorpha assimilis*, *Aspidimorpha elevata*, *Aspidimorpha malaccana*, *Aspidimorpha miliaris*, and *Laccoptera nepalensis*) and tribe Cassidini (*Chiridopsis punctata*, *Cassida circumdata*, *Chiridopsis scalaris*, *Notosacantha taeniata*, and *Silana farinosa*). In this study, only seven species were successfully barcoded, and the resulting data have been deposited in GenBank. Remarkably, the separation of species is clearly delineated within their respective lineages on the Neighbor-Joining tree, with the exception of several species that predominantly belong to the genus *Aspidimorpha.* The data gathered in this study are significant and contribute valuable information for genetic conservation and the preservation of plant species.

Keywords: Cassidines, *COI*, genetic information, leaf beetle, Malaysia

ARTICLE INFO

Article history:
Received: 06 December 2024
Accepted: 20 March 2025
Published: 25 November 2025

DOI: https://doi.org/10.47836/pjtas.48.6.06

E-mail addresses:
salmah78@ukm.edu.my (Salmah Yaakop)
muhammadafiq.senen@ukm.edu.my (Muhammad Afiq Senen)
anangsetyobudi@gmail.com (Anang Setyo Budi)
abdullahmuhaimin1990@gmail.com (Abdullah Muhaimin Mohammad Din)
audi@upm.edu.my (Audi Jamaluddin)
syari@upm.edu.my (Syari Jamian)
aqilah.sakinah01@gmail.com (Aqilah Sakinah Badrulisham)
* Corresponding author

e-ISSN: 2231-8542

INTRODUCTION

The tortoise beetle (Coleoptera: Cassidinae) comprises a group of coleopteran species that are notable for their unique and striking external morphology. These beetles exhibit a shining body pattern and possess a transparent body structure that covers the pronotum and elytral parts. In addition to their uniqueness and peculiar body features, tortoise beetles can sometimes be mistaken for ladybirds. The cassidines are herbivorous and can become significant pests of crops, particularly those from various plant families. They have been documented feeding on Poaceae, Convolvulaceae, Cyperaceae, and Rosaceae (Yang et al., 2023). Several studies conducted by Pathourm et al. (2021), Mohamedsaid and Sajap (1996), and Sajap and Mohamedsaid (1997) documented that the species *Silana farinosa* consumes the curry leaf, *Murraya koenigii* Thw. (Rutaceae). However, none of the cassidines have been recorded as pests or causing outbreaks in Malaysia. The Cassidinae species is also known to have very specific host preferences, often exhibiting monophagous feeding habits on several plant species, while others are polyphagous across various plant genera (Chaaboo, 2007). This particular species is also recognized as one of the more challenging species to collect and sample due to its solitary behavior.

In Malaysia, specifically in Peninsular Malaysia, research on Cassidinae species is quite limited. However, several studies dating back to 2010 focused on samples collected from Borneo, resulting in the description of new species, such as *Cassida malaysiana* (Borowiec, 2010). The taxonomic study of Cassidinae in Peninsular Malaysia concluded in 1993 with the work of Mohamedsaid (1993). Despite this, multiple studies were conducted by Borowiec (1998, 1999, 2010), primarily concentrating on Bornean species. However, research on this group of species remains sparse and underexplored (Buzzi, 1988). According to Mohamedsaid (2004), a total of 40 species under 10 genera of Cassidinae from Malaysia have been recorded, while the total numbers collected globally are relatively higher, with approximately 6,200 described species across 339 genera and 43 tribes (Borowiec & Świętojańska, 2024). This number represents a relatively low proportion of the total number of species recorded worldwide. The subfamily Cassidinae is derived from the family Chrysomelidae (Chaboo, 2007) and is categorized into several tribes based on their morphological structure (López-Pérez et al., 2018).

So far, none of the Cassidinae species has been barcoded in Malaysia to understand the diversity and genetics of each species, particularly for conservation purposes. Consequently, barcoding information is very useful for confirming species status due to the high variation observed in both interspecies and intraspecies relationships (López-Pérez et al., 2018). Several studies, such as those by Nie et al. (2020) and Leocádio et al. (2020) on the Chrysomelidae family, have also demonstrated that genetic information can address issues related to taxonomy and species classification.

In this study, the barcode information of the collected species is very crucial and valuable for precise species determination. The objectives of the study are to barcode the Cassidinae species collected from Peninsular Malaysia and to investigate the host preference of these species. The findings will be beneficial for the implementation of plant conservation efforts and will provide the first data or record on Cassidinae species' barcoding information from Peninsular Malaysia.

MATERIALS AND METHODS

Insect Sampling

The sampling of beetles was conducted across several states in Peninsular Malaysia. The locations were randomly selected based on records of the availability of host plants, and sampling was performed using active sampling (i.e. sweep netting) through observation of the potential host plant species, such as legumes and shrubs, following the methods of Muhaimin et al. (2017, 2019). The Cassidinae were collected either with a net or handpicked once the insects were spotted. Sampling took place on a clear day between 10:00 a.m. and 12:00 p.m. with several time intervals (every 10 min). The specimens were subsequently collected and preserved in 70% alcohol for morphological identification and molecular work.

Host Plant Records and Insect Rearing

The host plants or visited plant species of Cassidinae were recorded based on the locations where the beetles (both adult and larval stages) were spotted and captured. Information was collected regarding locality, altitude, collector, and date. The larvae that fed on the plants through observation in the field were reared in the laboratory until the emergence of the adult stages. Identification was also conducted based on the photographs of leaf samples by a plant taxonomist from the Herbarium of Universiti Kebangsaan Malaysia. After that, the specimens were collected and preserved in 70% alcohol for morphological identification and molecular work.

Morphological Identification

The specimens were identified based on morphological characteristics up to the species level, when possible, and categorized into morphospecies using a microscope (Stereomicroscope Stemi D4). This identification process referenced the works of Mohamedsaid (1993), Borowiec (1998, 1999, 2010), and a picture available at https://www.nickybay.com/cassidinae-checklist-tortoise-beetles. Additionally, assistance was obtained from Dr. Lukáš Sekerka, a Cassidinae taxonomist at the National History Museum in the Czech Republic. During morphological identification, the features on the pronotum, spots, and patterns (markings) on the elytra, and also coloration were observed and documented for

subsequent analysis. The specimens were also microscopically photographed using the stereomicroscope equipped with a DSLR camera and analyzed using the Image Analyser with ToupTek microscope camera and software.

DNA Barcode

DNA extraction, PCR Amplification and Sequencing Analysis

DNA samples were extracted from each species of all collected specimens using the DNeasy Blood and Tissue Kit (Qiagen, Germany). The extraction process adhered to the manufacturer's protocol, which involved initial soaking in Proteinase K and ATL buffer for the lysis process, followed by the remaining steps as outlined by the manufacturer. For several species with low collection numbers, a modified freezing method was employed, with slight adjustments to several steps as described by Yaakop et al. (2013). Then, PCR amplification was performed using the cytochrome *c* oxidase subunit I (*COI*) gene with primers developed by Folmer (1994), as well as the PCR conditions proposed by Halim et al. (2017) and Musa, Halim et al. (2024). The resulting PCR product was verified through gel electrophoresis using a 1.5% agarose gel and subsequently sent to Apical Sdn. Bhd., Selangor, Malaysia, for sequencing analysis.

DNA Editing and Alignment, and BLAST Analyses

The sequences obtained were edited manually using Sequencher 5.4.6 (Gene Codes Corporation, Ann Arbor, MI USA). Additionally, the Basic Local Alignment Search (BLAST) was employed for species confirmation and comparison based on several parameters, including the total score, expected value, maximum identical value, maximum score, and query coverage.

Genetic Distance

Genetic distance analysis was conducted using PAUP* version 4.0 (Sinauer Associates, Sunderland, Massachusetts) software, employing the Kimura-2-parameter (K2P) model (Zainudin et al., 2010). This analysis aims to investigate the genetic distance of the Cassidinae samples and the GenBank sequences utilized in this research.

Tree Reconstruction

The separation of species was visualized through tree reconstruction using distance criteria, specifically the Neighbor-Joining (NJ) method via phylogenetic analysis. The NJ tree was constructed using PAUP* version 4.0 software and employed using the K2P algorithm model with bootstrap analysis (1,000 replications). The outgroup species selected for this analysis belong to the subfamily Hispinae, and the ingroups are Cassidinae (Table 1).

Table 1
List of specimens along with the results obtained from the morphological and molecular identification of Cassidinae species in the current study and the GenBank information used for tree reconstruction, with the value of maximum score, total score, query coverage, E-value, similarity percentage, and accession number, and the additional Genbank sequences

No.	Code/ voucher no.	Locality	Tribe	Maximum score	Total score	Query cover (%)	E-value	Similarity percentage (%)	Species closely related to Genbank accession no.	Genbank accession no.	Species identified
1	425	Malaysia: Pahang, Fraser Hill	Hispinii	-	-	-	-	-	-	MW175466	Hispini sp.
2	USNM:ENT: 01117140	Myanmar	Aspidimorphini	-	-	-	-	-	-	MF804568	*Aspidimorpha* sp.
3	J	Vietnam	Aspidimorphini	-	-	-	-	-	-	MN845123	*Aspidimorpha furcata*
4	Cas-36-2019	Vietnam	Aspidimorphini	-	-	-	-	-	-	MZ303504	*Aspidimorpha furcata*
5	H	Vietnam	Aspidimorphini	-	-	-	-	-	-	MN845120	*Aspidimorpha dorsata*
6	13	Malaysia: Pahang, Cameron Highlands	Aspidimorphini	1050	1050	100	0.0	98.67	MN845123 *Aspidimorpha furcata*	PQ187448	*Aspidimorpha assimilis*
7	404	Malaysia: Pahang: Fraser Hill	Aspidimorphini	1077	1077	100	0.0	99.67	MF804566 *Aspidimorpha* sp.	MN897085	*Aspidimorpha assimilis*
8	479a	Malaysia: Pahang: Fraser Hill	Aspidimorphini	1077	1077	100	0.0	99.67	MF804566 *Aspidimorpha* sp.	MN897084	*Aspidimorpha assimilis*
9	22	Malaysia: Perak, Batu Kurau	Aspidimorphini	1011	1011	100	0.0	97.33	MN845121 *Aspidimorpha furcata*	PQ524205	*Aspidimorpha assimilis*
10	515d	Malaysia: Pahang, Fraser Hill	Aspidimorphini	902	902	100	0.0	93.19	KJ195294 *Aspidimorpha sanctaecrucis*	MN934809	*Aspidimorpha elevata*
11	7	Malaysia: Pahang, Cameron Highlands	Aspidimorphini	974	974	100	0.0	95.85	KJ195294 *Aspidimorpha sanctaecrucis*	PQ203305	*Aspidimorpha elevata*

Table 1 *(continue)*

No.	Code/ voucher no.	Locality	Tribe	Maximum score	Total score	Query cover (%)	E-value	Similarity percentage (%)	Species closely related to Genbank accession no.	Genbank accession no.	Species identified
12	531c	Malaysia: Pahang, Fraser Hill	Aspidimorphini	902	902	100	0.0	93.19	KJ195294 *Aspidimorpha sanctaecrucis*	MN934808	*Aspidimorpha elevata*
13	363b	Malaysia: Pahang, Fraser Hill	Aspidimorphini	902	902	100	0.0	93.19	KJ195294 *Aspidimorpha sanctaecrucis*	MN934810	*Aspidimorpha elevata*
14	1	Malaysia: Pahang, Cameron Highlands	Aspidimorphini	-	-	-	-	-	-	-	*Aspidimorpha elevata*
15	29	Malaysia: Perak, Zoo Taiping	Aspidimorphini	-	-	-	-	-	-	-	*Aspidimorpha elevata*
16	15	Malaysia: Selangor, Serdang, Ladang UPM	Aspidimorphini	1016	1016	100	0.0	97.01	KJ195294 *Aspidimorpha sanctaecrucis*	PQ203270	*Aspidimorpha malaccana*
17	16	Malaysia: Selangor, Serdang, Ladang UPM	Aspidimorphini	986	986	100	0.0	95.85	KJ195294 *Aspidimorpha sanctaecrucis*	PQ203271	*Aspidimorpha malaccana*
18	5	Malaysia: Pahang, Fraser Hill	Aspidimorphini	-	-	-	-	-	-	-	*Aspidimorpha miliaris*
19	19	Malaysia: Perak, Batu Kurau	Aspidimorphini	-	-	-	-	-	-	-	*Aspidimorpha miliaris*
20	RoLn1	India	Aspidimorphini		-	-	-	-	-	KM226876	*Laccoptera nepalensis*
21	F2	Malaysia: Pahang, Fraser Hill	Aspidimorphini	1028	1028	100	0.0	97.84	KM226876 *Laccoptera nepalensis*	MW168661	*Laccoptera nepalensis*
22	TB	India	Cassidini	-	-	-	-	-	-	OR416859	*Chiridopsis* sp.
23	L	Vietnam	Cassidini	-	-	-	-	-	-	MN845124	*Chiridopsis bowringii*

Table 1 *(continue)*

No.	Code/ voucher no.	Locality	Tribe	Maximum score	Total score	Query cover (%)	E-value	Similarity percentage (%)	Species closely related to Genbank accession no.	Genbank accession no.	Species identified
24	SSG-2014 C83	India	Cassidini	-	-	-	-	-	-	KJ195316	*Chiridopsis bipunctata*
25	C70	India	Cassidini	-	-	-	-	-	-	KJ195312	*Chiridopsis undecimnotata*
26	190	Malaysia: Pahang: Fraser Hill	Cassidini	938	938	100	0.0	94.52	OR416859 *Chiridopsis* sp.	MN955586	*Chiridopsis punctata*
27	21	Malaysia: Perak, Batu Kurau	Cassidini	762	762	100	0.0	88.04	OR416859 *Chiridopsis* sp.	PQ524206	*Chiridopsis scalaris*
28	30	Malaysia: Perak, Zoo Taiping	Cassidini	-	-	-	-	-	-	-	*Chiridopsis punctata*
29	SFV 1	India	Cassidini	-	-	-	-	-	-	PP373131	*Silana farinosa*
30	28	Malaysia: Kedah	Cassidini	1046	1046	100	0.0	98.83	PP373131 *Salina farinosa*	PQ549944	*Silana farinosa*
31	11	Malaysia: Johor, Benot Pontian	Cassidini	1055	1055	100	0.0	98.84	PP373131 *Salina farinosa*	PQ203298	*Silana farinosa*
32	32	Malaysia: Perak: Manong, Kpg. Bekor	Cassidini	1055	1055	100	0.0	98.84	PP373131 *Salina farinosa*	PQ549945	*Silana farinosa*
33	33	Malaysia: Perak, Manong, Kpg. Bekor	Cassidini	1046	1046	100	0.0	98.50	PP373131 *Salina farinosa*	PQ549946	*Silana farinosa*
34	10	Malaysia: Pahang, Cameron Highland	Cassidini	-	-	-	-	-	-	-	*Cassida circumdata*
35	43	Malaysia: Selangor: Serdang, Ladang UPM	Notosacanthini	-	-	-	-	-	-	-	*Notosacantha taeniata*

RESULTS

Morphological Identification

A total of ten species belonging to the Cassidinae subfamily, which is divided into two tribes namely Cassidini and Aspidimorphini, were successfully identified morphologically up to the genus and species levels. The species included in the Cassidini tribe were *Silana farinosa*, *Chiridopsis punctata*, *Cassida circumdata*, *Chiridopsis scalaris*, and *Notosacantha taeniata*. The Aspidimorphini tribe included *Aspidimorpha miliaris*, *Aspidimorpha assimilis*, *Aspidimorpha malaccana*, *Aspidimorpha elevata*, and *Laccoptera nepalensis*. Several species exhibited variation in characteristics, particularly in the genus *Aspidimorpha* (*A. malaccana* and *A. elevata*), which were collected from multiple locations.

Records on Host Plant Species

Based on observations made in the field and subsequently confirmed through laboratory investigations, the leaves of the curry plant (*M. koenigii*) were consumed by the larval stage of *S. farinosa*.

Molecular Identification

The barcoding analysis identified seven distinct species. All the sequences submitted to GenBank, NCBI, are listed in Table 1 with corresponding accession numbers. This table includes a list of specimens together with the results from the morphological and molecular identification of Cassidinae species in this study.

Genetic Distance

The genetic distances among the Cassidinae species are presented in Tables 2 and 3. In this study, the genetic separation between *A. malaccana* and *A. elevata* was observed to be between 0.053, with the range between the same species of *A. malaccana* of 0.007 and *A. elevata* of 0.04. The genetic separation between *A. assimilis* and *A. furcata* ranges between 0.083, with the range between the same species of *A. furcata* of 0.028 and *A. assimilis* of 0.10 (Tables 2 and 3).

Table 2
Genetic distance of Cassidinae sample implemented in the tree reconstruction (within group mean distance)

		d
1	*Hispini* sp.	-
2	*Aspidimorpha* sp.	-
3	*Aspidimorpha assimilis*	0.100
4	*Aspidimorpha dorsata*	-
5	*Aspidimorpha elevata*	0.040
6	*Aspidimorpha furcata*	0.028
7	*Aspidimorpha malaccana*	0.007
8	*Chiridopsis* sp.	-
9	*Chiridopsis bowringii*	-
10	*Chiridopsis bipunctata*	-
11	*Chiridopsis punctata*	-
12	*Chiridopsis scalaris*	-
13	*Chiridopsis undecimnotata*	-
14	*Laccoptera nepalensis*	0.021
15	*Silana farinosa*	0.006

Table 3
Genetic distance of Cassidinae samples implemented in the tree reconstruction (between group mean distance)

		1	2	3	4	5	6	7	8	9	10	11	12	13	14	15
1	*Hispini* sp.	-														
2	*Aspidimorpha* sp.	0.233	-													
3	*Aspidimorpha assimilis*	0.237	0.092	-												
4	*Aspidimorpha dorsata*	0.241	0.155	0.125	-											
5	*Aspidimorpha elevata*	0.197	0.207	0.204	0.196	-										
6	*Aspidimorpha furcata*	0.226	0.019	0.083	0.149	0.198	-									
7	*Aspidimorpha malaccana*	0.192	0.227	0.221	0.199	0.053	0.215	-								
8	*Chiridopsis* sp.	0.183	0.191	0.205	0.200	0.217	0.190	0.213	-							
9	*Chiridopsis bowringii*	0.181	0.226	0.232	0.240	0.210	0.226	0.198	0.167	-						
10	*Chiridopsis bipunctata*	0.188	0.194	0.207	0.210	0.217	0.195	0.216	0.018	0.169	-					
11	*Chiridopsis punctata*	0.199	0.198	0.207	0.194	0.232	0.198	0.227	0.052	0.177	0.059	-				
12	*Chiridopsis scalaris*	0.204	0.191	0.198	0.205	0.210	0.195	0.197	0.124	0.131	0.126	0.138	-			
13	*Chiridopsis undecimnotata*	0.220	0.233	0.232	0.233	0.226	0.226	0.213	0.170	0.175	0.172	0.161	0.179	-		
14	*Laccoptera nepalensis*	0.216	0.220	0.210	0.197	0.228	0.216	0.227	0.216	0.203	0.223	0.206	0.199	0.203	-	
15	*Silana farinosa*	0.201	0.222	0.228	0.237	0.228	0.223	0.226	0.229	0.242	0.224	0.225	0.227	0.229	0.242	-

Microscopic Figures

All the species collected in this study are presented in the microscopic figures and photographs in Figure 1.

Tree Reconstruction

The NJ tree showed a clear separation between the ingroup and outgroup, as supported by low bootstrap values. All the species were also separated from one another, as strongly

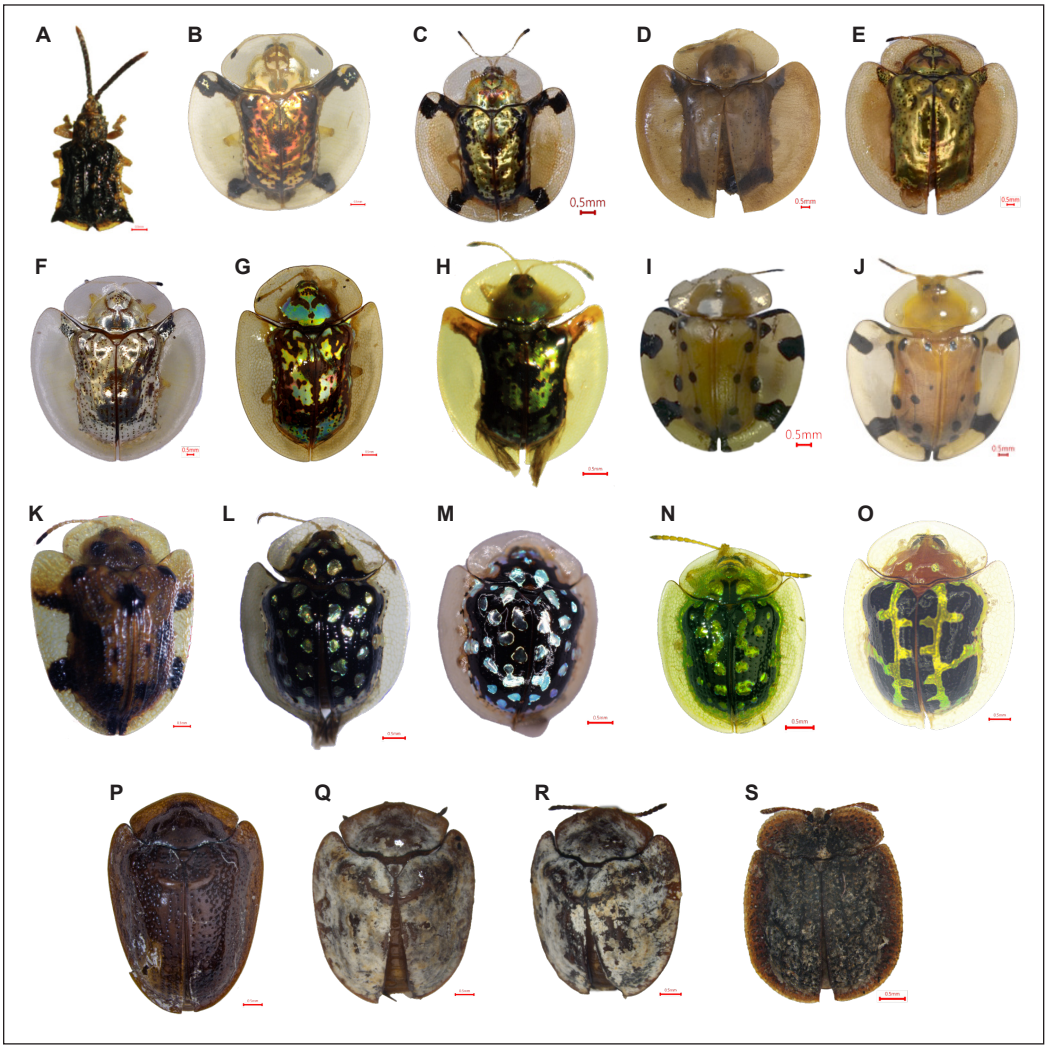

Figure 1. Cassidinae species collected in this study: A, Hispini sp. (425); B, *A. malaccana* (16); C, *A. malaccana* (15); D, *A. elevata* (7), E, *A. elevata* (1), F, *A. elevata* (29); G, *A. assimilis* (22); H, *A. assimilis* (404); I, *A. miliaris* (5); J, *A. miliaris* (19); K, *L. nepalensis* (F2); L, *C. punctata* (190); M, *C. punctata* (30); N, *C. circumdata* (10); O, *C. scalaris* (21); P, *S. farinosa* (28); Q, *S. farinosa* (33); R, *S. farinosa* (32); S, *N. taeniata* (43)

supported by the low to high bootstrap values ranging from 58% to 100%, except for several species under the genus *Aspidimorpha.* However, the separation among tribes was not distinctly evident, showing a mixture between them. The separation between Cassidinae and Hispinae was clear, but there was no clear separation between tribes, as both tribes (Cassidini and Aspidimorphini) were paraphyletic (Figure 2).

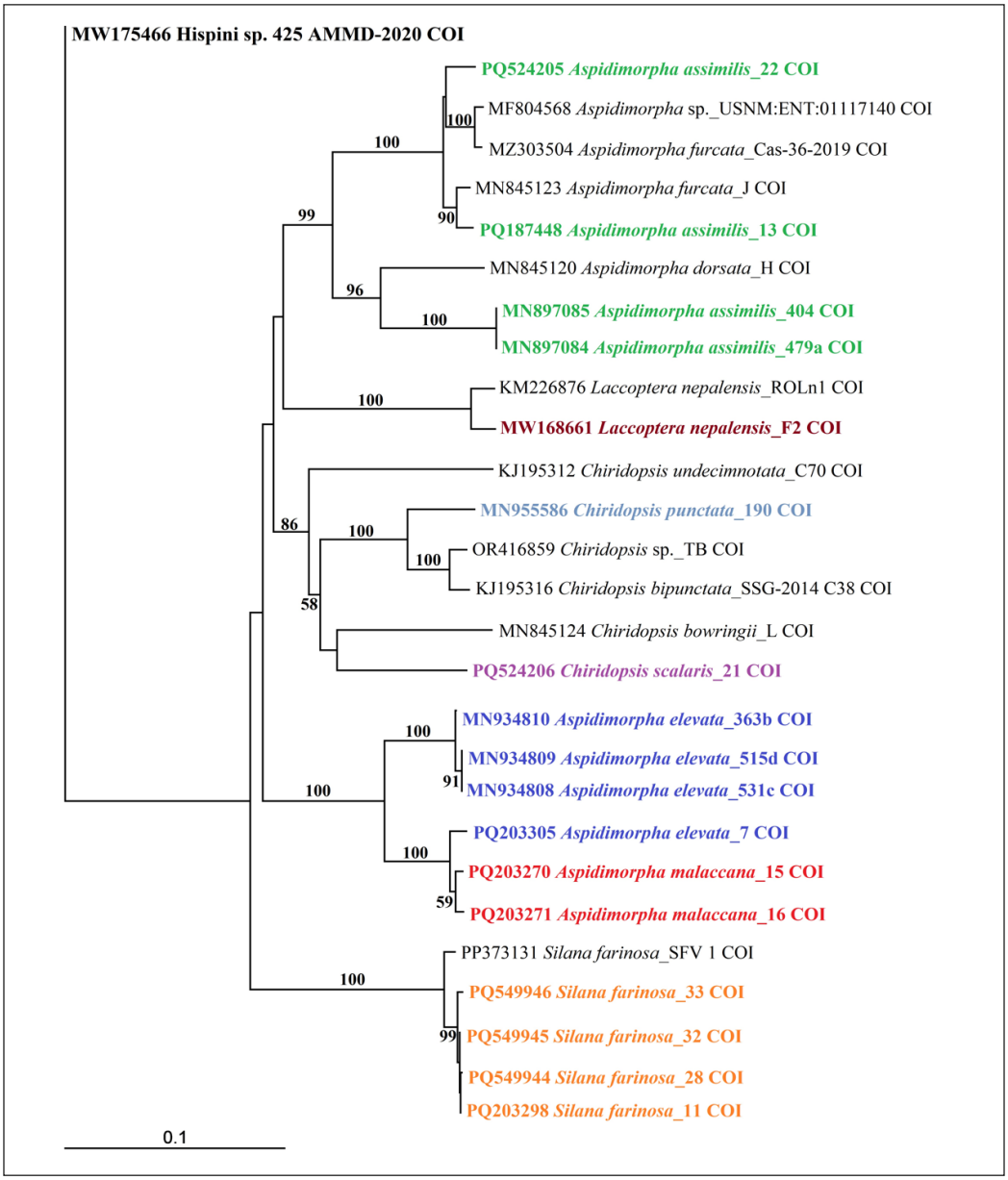

Figure 2. Neighbor-joining tree based on mitochondrial cytochrome C oxidase I (*COI)* sequences of Cassidinae species. The bootstrap values are indicated on the branches

DISCUSSION

The study of Cassidinae diversity and its interactions with plant species in Malaysia is quite limited due to the scarcity of available information and published research on these species. Therefore, it is urgently necessary to investigate the status of Cassidinae species in this geographical region. Only a few Cassidinae species have been barcoded from Malaysia, primarily through mitochondrial metagenomic studies of beetle species, particularly those from Borneo, as reported by Crampton-Platt et al. (2015). Research from neighboring countries mainly focused on new species records from specific areas, insect-plant interactions, and the taxonomy and phylogeny of Cassidinae species (López-Pérez et al., 2018; Yang et al., 2023).

This number is considered low compared to the species recorded in Malaysia, representing only 20%, comprising 10 species obtained from this study out of a total of over 50 species recorded in Malaysia by Mohamedsaid (1993), in addition to several papers published on new species from Malaysia, such as those by Borowiec and Świętojańska (2014). The numbers obtained from this study do not accurately reflect the diversity and richness of Peninsular Malaysia due to inconsistent sampling efforts in the selection of sampling sites. The sampling process employs active sampling, which is very time-consuming and requires significant human effort.

The record of host preferences or host plants of Cassidinae is important due to their functional role as leaf-eating beetles as herbivores that can potentially become pests in agriculture (Salem et al., 2020). However, information on many other species remains unexplored. In this study, the reconfirmation that *S. farinosa* infests curry leaves has been proven based on laboratory observation. A study by Begha and Oliveira (2024) also confirmed the host preference based on the immature stages of the Cassidinae species, *Hybosa acutangula* Spaeth, 1913 from Brazil. The records are very convincing as they are based on careful observation and rearing until the emergence of the adult samples. This study identified several plant families involved in the food webs of the Cassidinae, including Fabaceae, Convolvulaceae, Myristicaceae, and others, which are utilized as host plants. This finding is supported by Borowiec et al. (2013), Mohamedsaid and Sajap (1996), Sajap and Mohamedsaid (1997), and Yang et al. (2023), indicating that the same tribe shares several groups of plant families, demonstrating their role as generalist consumers.

In taxonomic contexts, the sister-species relationships between two subfamilies, Cassidinae s. str. and Hispinae s. str., are distinguished based on their distinct external morphological characteristics. Cassidinae have smooth, flat elytral edges, and a rounded shape, while Hispinae have spines, non-flattened elytral edges, and a non-rounded shape, and the separation of these subfamilies is supported in Figure 2. However, within the Cassidinae, only two tribes namely Cassidini and Aspidimorphini (Borowiec &

Świętojańska, 2014), were collected, and only seven species were barcoded in this study. Each species is located within a specific lineage, and each clade represents the same tribe and species, supported by morphological characteristics. The reconstruction of the NJ tree proved to be a viable method for clearly illustrating species separation, as corroborated by several studies on DNA barcoding (Rusinko & McPartlon, 2017).

In this study, many species were easily identified based on external morphology, except for several species that exhibit high resemblance, namely *A. malaccana* and *A. elevata*, and *A. assimilis* and *A. furcata*. These species show very low divergence between species based on genetic distance results when compared to other species included in the NJ tree. According to Borowiec (1998, 1999, 2010) and Mohamedsaid (1993), all species within the same genus possess specific species characteristics; however, *A. assimilis* was distinctly separated and also located quite far from the genus clade (*A. elevata* and *A. malaccana*). This situation may arise due to the limited number of sequences and other potential biases that affect the estimation of species divergence (Zheng et al., 2011). Additionally, the use of the single-gene *COI* as barcoding data is effective for species identification. However, it has limited resolution for closely related or recently diverged species, as evidenced by the low genetic divergence between species such as *A. elevata* and *A. malaccana*. Therefore, our results suggest that *COI* alone is unlikely to accurately delimit species. It should be combined and integrated with morphological identification for more precise species identification (Ranasinghe et al., 2022)

Interestingly, the barcode information for the *COI* of seven species of Cassidinae from Peninsular Malaysia has been firstly submitted and deposited in GenBank, NCBI. The barcode information obtained from this study is highly significant for confirming the species status of these organisms in Malaysia. Generally, these species exhibit high morphological variation, particularly in the patterns or spots on their elytra, such as on Coccinellidae in studies by Halim et al. (2017), Musa, Halim et al. (2024) and Musa, Hatta et al. (2024). By referring to their DNA barcodes, the diversity of the same species both in Malaysia and globally can be accurately identified. This identification is not limited to beetle species only, but it also extends to other insect species, as demonstrated by Nor-Atikah et al. (2019), Yaakop et al. (2020), Yaakop, Amiruddin et al. (2022) and Yaakop, Sabri et al. (2022).

CONCLUSION

The latest information on Cassidinae species in Peninsular Malaysia is urgently needed to investigate species richness, barcode information, and insect-host interactions. This information is essential for understanding the complex food webs of Cassidinae in Peninsular Malaysia, which are crucial for genetic conservation and the preservation of plant species.

ACKNOWLEDGEMENT

The authors would like to thank Nagao Natural Environment Foundation (NEF) for the research grant number ST-2022-013. We would also like to thank Dr. Lukáš Sekerka from National History Museum, Czech Republic for his help in morphological identification. Not to forget, Mr. Asyraf Aman for giving assistance and help in insect collection.

REFERENCES

Begha, B. P., & Oliveira, S. S. (2024). Description of larva, pupa, and genitalia of *Hybosa acutangula* Spaeth, 1913 (Coleoptera: Chrysomelidae: Cassidinae) from the Brazilian Cerrado. *Revista Brasileira de Entomologia*, *68*(1), Article e20230048. https://doi.org/10.1590/1806-9665-RBENT-2023-0048

Borowiec, L. (1998). *Megapyga minima*, n. sp. from Borneo (Coleoptera: Chrysomelidae: Cassidinae). *Serangga*, *3*(1), 103-106.

Borowiec, L. (1999). *Cassida kinabaluensis* n. sp. from Sabah, Malaysia (Coleoptera: Chrysomelidae: Cassidinae). *Serangga*, *4*(1), 1-5.

Borowiec, L. (2010). A new species of *Cassida* L. from Malaysia (Coleoptera: Chrysomelidae: Cassidinae). *Genus*, *21*(2), 279-286.

Borowiec, L., & Świętojańska, J. (2014). 2.7.2 Cassidinae Gyllenhal, 1813. In R. A. B. Leschen, & R. G. Beutel (Eds.) *Handbook of zoology Arthropoda: Insecta. Coleoptera, beetles. Volume 3: Morphology and systematics (Phytophaga)* (pp. 198–217). Walter de Gruyter.

Borowiec, L., & Świętojańska, J. (2024, September 24). *Cassidinae of the world - an interactive manual (Coleoptera: Chrysomelidae)*. University of Wroclaw. https://www.cassidae.uni.wroc.pl/katalog%20internetowy/index.htm

Borowiec, L., Takizawa, H., & Świętojańska, J. (2013). Five new species of *Notosacantha chevrolat* (Coleoptera: Chrysomelidae: Cassidinae) from Borneo, with a key to the Bornean species and new faunistic data. *Zootaxa, 3608*(3), 161-177. https://doi.org/10.11646/zootaxa.3608.3.1

Buzzi, Z. J. (1988). Biology of neotropical Cassidinae. In P. Jolivet, E. Petitpierre & T. H. Hsiao (Eds.) *Biology of Chrysomelidae* (pp. 559-580). Kluwer Academic Publishers.

Chaboo, C. S. (2007). Biology and phylogeny of the Cassidinae Gyllenhal sensu lato (tortoise and leaf-mining beetles) (Coleoptera: Chrysomelidae). *Bulletin of the American Museum of Natural History*, *305*, 1-250. https://doi.org/10.1206/0003-0090(2007)305[1:BAPOTC]2.0.CO;2

Crampton-Platt, A., Timmermans, M. J. T. N., Gimmel, M. L., Kutty, S. N., Cockerill, T. D., Khen, C. V., & Vogler, A. P. (2015). Soup to tree: The phylogeny of beetles inferred by mitochondrial metagenomics of a Bornean rainforest sample. *Molecular Biology and Evolution*, *32*(9), 2302–2316. https://doi.org/10.1093/molbev/msv111

Folmer, O., Black, M., Hoeh, W., Lutz, R., & Vrijenhoek, R. (1994). DNA primers for amplification of mitochondrial cytochrome *c* oxidase subunit I from diverse metazoan invertebrates. *Molecular Marine Biology and Biotechnology*, *3*(5), 294-299.

Halim, W. M. W., Aman-Zuki, A., & Yaakop, S. (2017). DNA barcoding and relationships of eight ladybugs species (Coleoptera: Coccinellidae) that infesting several crops from Peninsular Malaysia. *Journal of Asia-Pacific Entomology*, *20*, 814-820. http://dx.doi.org/10.1016/j.aspen.2017.05.009

Leocádio, M., Simões, M. V. P, Sekerka, L., Schrago, C. G., Mermudes, J. R. M., & Windsor, D. M. (2020). Molecular systematics reveals the origins of subsociality in tortoise beetles (Coleoptera, Chrysomelidae, Cassidinae). *Systematic Entomology*, *45*(4), 894-910. https://doi.org/10.1111/syen.12434

López-Pérez, S., Zaragoza-Caballero, S., Ochoterena, H., & Morrone, J. J. (2018). A phylogenetic study of the worldwide tribe Cassidini Gyllenhal, 1813 (Coleoptera: Chrysomelidae: Cassidinae) based on morphological data. *Systematic Entomology*, *43*(2), 372-386. https://doi.org/10.1111/syen.12280

Mohamedsaid, M. S. (1993). The tortoise beetles of Malaysia. *Nature Malaysiana*, *18*(2), 44-47.

Mohamedsaid, M. S. (2004). *Catalogue of the Malaysian Chrysomelidae (Insecta: Coleoptera)*. Pensoft.

Mohamedsaid, M. S., & Sajap, A. S. (1996). *Silana farinosa*, a new generic record of tortoise beetle for Malaysia (Coleoptera: Chrysomelidae Cassidinae). *Malayan Nature Journal*, *50*(1), 33-38.

Muhaimin, A. M. D., Halim, M., Zulaikha, S. S., & Yaakop, S. (2019). Habitat preferences of leaf beetles (Coleoptera: Chrysomelidae) based on abiotic factors: A study from Fraser's Hill, Pahang, Malaysia. *IOP Conference Series: Earth and Environmental Science, 269*(1), Article 012035. https://doi.org/10.1088/1755-1315/269/1/012035

Muhaimin, A. M. D., Norela, S., Halim, M., & Yaakop, S. (2017). Altitudinal accumulation and diversity of leaf beetle (Coleoptera: Chrysomelidae) at Fraser's Hill, Pahang. *Serangga*, *22*(2), 171-184.

Musa, N. N., Halim, M., & Yaakop, S. (2024). First insight on tritrophic interaction involving *Plukenetia volubilis* L., insects, and microbe as an early and crucial data for developing a pest management strategy. *Pakistan Journal of Agricultural Sciences*, *61*(1), 13-25. https://doi.org/10.21162/PAKJAS/24.144

Musa, N. N., Hatta, S. K. M., & Yaakop, S. (2024). Diversity and assemblage patterns of ladybirds (Coccinellidae) in different crop management practices in Peninsular Malaysia. *Arthropod-Plant Interactions*, *18*, 723–740. https://doi.org/10.1007/s11829-024-10070-9

Nie, R. E., Andújar, C., Gómez-Rodríguez, C., Bai, M., Xue, H. J., Tang, M., Tang, C. T., Tang, P., Yang, X. K., & Vogler, A. P. (2020). The phylogeny of leaf beetles (Chrysomelidae) inferred from mitochondrial genomes. *Systematic Entomology*, *45*(1), 188-204. https://doi.org/10.1111/syen.12387

Nor-Atikah, A. R., Halim, M., Syarifah-Zulaikha, S. A., & Yaakop, S. (2019). Molecular identification and first documentation of seven species of *Carpophilus* Stephens (Nitidulidae: Carpophilinae) in oil palm ecosystem, Peninsular Malaysia. *Journal of Asia-Pacific Entomology*, *22*(2), 619-624. https://doi.org/10.1016/j.aspen.2019.04.010

Pathourm, S. R., Rajgopal, N. N., Bhagyasreee, S.N., & Sreedevi, K. (2021). Sporadic outbreak of curry leaf tortoise beetle, *Silana farinosa* (Boheman) (Coleoptera: Chrysomelidae) in Shivamogga, Karnataka, India. *Pest Management in Horticultural Ecosystems*, *27*(2), 301-304.

Ranasinghe, S., Eberle, J., Thormann, J., Bohacz, C., Benjamin, S. P., & Ahrens, D. (2022). Multiple species delimitation approaches with coi barcodes poorly fit each other and morphospecies – An integrative

taxonomy case of Sri Lankan sericini chafers (Coleoptera: Scarabaeidae). *Ecology and Evolution, 12*(5), Article e8942. https://doi.org/10.1002/ece3.8942

Rusinko, J., & McPartlon, M. (2017). Species tree estimation using Neighbor Joining. *Journal of Theoretical Biology*, *414*, 5-7. https://doi.org/10.1016/j.jtbi.2016.11.005

Sajap, A. S., & Mohamedsaid, M. S. (1997). Biology of *Silana farinosa* (Boheman) (Coleoptera: Chrysomelidae), a new pest of *Murraya koenigii* Thw. (Rutaceae) in Peninsular Malaysia. *Malayan Nature Journal*, *50*, 167-171.

Salem, H., Kirsch, R., Pauchet, Y., Berasategui, A., Fukumori, K., Moriyama, M., Cripps, M., Windsor, D., Fukatsu, T., & Gerardo, N. M. (2020). Symbiont digestive range reflects host plant breadth in herbivorous beetles. *Current Biology*, *30*(15), 2875-2886. https://doi.org/10.1016/j.cub.2020.05.043

Yaakop, S., Amiruddin, P. A., Mohammed, M. A., Badrulisham, A. S., Zulkifli, N. A., & Nadzir, M. N. H. M. (2022). Molecular identification and species richness of flies (Diptera) and their associated Bovidae hosts at cattle farms in Selangor, Malaysia. *Pertanika Journal of Tropical Agricultural Science*, *43*(3), 611-630. http://dx.doi.org/10.47836/pjtas.45.3.05

Yaakop, S., Sabri, S., Kamaruddin, N. A. K., Norizam, N. N., & Mohammed, M. A. (2022). Species composition and DNA barcoding of hemipteran assemblages throughout paddy growing seasons. *Pertanika Journal of Tropical Agricultural Science*, *45*(3), 631–648. http://dx.doi.org/10.47836/pjtas.45.3.06

Yaakop, S., David-Dass, A., Shaharuddin, U. S., Sabri, S., Badrulisham, A. S., & Che-Radziah, C. M. Z. (2020). Species richness of leaf roller and stem borers (Lepidoptera) associated with different paddy growth and first documentation of its DNA barcode. *Pertanika Journal of Tropical Agricultural Science*, *43*(4), 523-535. https://doi.org/10.47836/pjtas.43.4.08

Yaakop, S., van Achterberg, C., Idris, A. B., & Araan, A. Z. (2013). Freezing method as a new non-destructive modification of DNA extraction. *Pertanika Journal of Tropical Agricultural Science*, *36*(4), 373-392.

Yang, C., Liao, C., Xu, J., Liu, P., Staines, C. L., & Dai, X. (2023). Field survey of Cassidinae beetles (Coleoptera, Chrysomelidae) and their host plants in southern Guangxi, China. *Biodiversity Data Journal, 11,* Article e107523. https://doi.org/10.3897/BDJ.11.e107523

Zainudin, R. (2010). Distance and parsimony inferences. In R. Zainudin, R. Hassan, Y. Esa & S. A. K. A. Rahim (Eds.) *Basic computational phylogenetic analysis manual* (pp. 42-67). Universiti Malaysia Sarawak.

Zheng, Y., Peng, R., Kuro-o, M., & Zeng, X. (2011). Exploring patterns and extent of bias in estimating divergence time from mitochondrial DNA sequence data in a particular lineage: A case study of salamanders (Order Caudata). *Molecular Biology and Evolution*, *28*(9), 2521–2535. https://doi.org/10.1093/molbev/msr072

Pertanika J. Trop. Agric. Sci. 48 (6): 1785 - 1802 (2025)

PERTANIKA JOURNALS

TROPICAL AGRICULTURAL SCIENCE

Journal homepage: http://www.pertanika.upm.edu.my/

Effect of Different Irrigation Solutions on Wound and Fracture Healing in a Rabbit Open Fracture Model—A Pilot and Feasibility Study

Wan Lye Cheong[1], Norazian Kamisan[1]*, Imma Isniza Ismail[1], Michelle Wai Cheng Fong[2], Rozanaliza Radzi[2], Nurul Izzati Uda Zahli[3], and Maria Syafiqah Ghazali[2]

[1]Department of Orthopaedics, Faculty of Medicine and Health Sciences, Universiti Putra Malaysia, 43400 Serdang, Selangor, Malaysia

[2]Department of Veterinary Clinical Studies, Faculty of Veterinary Medicine, Universiti Putra Malaysia, 43400 Serdang, Selangor, Malaysia

[3]Department of Veterinary Pathology & Microbiology, Faculty of Veterinary Medicine, Universiti Putra Malaysia, 43400 Serdang, Selangor, Malaysia

ABSTRACT

This study compares the microbiological, radiological and histological effects of irrigation with povidone-iodine, hydrogen peroxide or saline on wound and fracture healing in an animal open fracture model. This study used an open fracture tibia model in a New Zealand White rabbit treated with debridement and irrigation 24 hours after the initial fracture. Irrigation was performed via gravity flow with either 20 mL of 0.9% saline, povidone-iodine 10% or hydrogen peroxide 3%, followed by rinsing with 100 mL saline. Tissue samples were taken before and after debridement for microbiological assessment of bacterial clearance and histological evaluation of wound inflammation. Radiographs were performed at intervals to assess the progress of fracture union. Eight weeks later, the tibia and surrounding tissues were extracted to histologically evaluate fracture and wound healing. All wounds healed well with no clinical evidence of infection. Reduction of the bacterial load was seen with irrigation by povidone-iodine. Fractures irrigated with povidone-iodine had a relatively faster radiological progression of fracture union than saline. There was no histological difference in wound and fracture healing among the tested solutions. This study provides evidence that povidone-iodine does not impair fracture healing. However, as this was a pilot study with a small sample size, a larger study is required to confirm statistical significance and clinical relevance.

Keywords: Antiseptic, fracture healing, irrigation, open fracture, wound healing

ARTICLE INFO

Article history:
Received: 03 January 2025
Accepted: 08 April 2025
Published: 25 November 2025

DOI: https://doi.org/10.47836/pjtas.48.6.07

E-mail addresses:
wlcheong89@gmail.com (Wan Lye Cheong)
norazian.kamisan@upm.edu.my (Norazian Kamisan)
immaisniza@upm.edu.my (Imma Isniza Ismail)
michelle@upm.edu.my (Michelle Wai Cheng Fong)
rozanaliza@upm.edu.my (Rozanaliza Radzi)
nurulizzati.udazahli@upm.edu.my (Nurul Izzati Uda Zahli)
gs65767@student.upm.edu.my (Maria Syafiqah Ghazali)
* Corresponding author

e-ISSN: 2231-8542

INTRODUCTION

The incidence of open fracture is estimated at 30.7 per 10,000 persons per year and is bound to increase (Court-Brown et al., 2012). It is often associated with poor outcomes, with reported rates of 24% infection, 15% amputation and 11% non-union (Schade et al., 2021). These have a profound financial impact, costing up to £40,000 for treating infection and reconstructive procedures (Schade et al., 2021). Complications such as infection led to a six-fold increase in hospitalisation duration, decreased productivity and loss of financial earnings, where less than 50% of patients returned to work after one year (Flores et al., 2024; Hoekstra et al., 2017). These understandably cause substantial physical and psychosocial impacts on patients and significantly strain medical personnel and healthcare centres.

Hence, open fracture management focuses on preventing such complications from the outset. Studies and guidelines have been developed over the years to improve the outcome (Eccles et al., 2020). They advocate early antibiotic administration, adequate debridement, wound irrigation and fracture stabilisation. While irrigation mechanically removes foreign bodies and reduces the amount of potential pathological microorganisms, the choice of irrigation solutions is still subject to debate. A good irrigation solution is one that not only removes foreign materials but also kills harmful microorganisms without causing damage to host tissues. Antiseptic solutions such as povidone-iodine and hydrogen peroxide are widely used, as they are bactericidal and less selective, rendering them less susceptible to resistance. There have been concerns about their cytotoxicity, as reported by several in vitro studies (Kaysinger et al., 1995; Lineaweaver et al., 1985; Nicholson et al., 1998; Rueda-Fernández et al., 2022; Thomas et al., 2009). Nevertheless, irrigation of open fractures with antiseptics is a common clinical practice. In international surveys, up to a third of surgeons used antiseptics to irrigate severe open fractures, and almost half believed they were superior to saline (Petrisor et al., 2008; Puetzler et al., 2019).

Thus, our study investigates the effects of these antiseptics on wound and fracture healing *in vivo* in an experimental animal model. We designed a pilot study to assess the feasibility of this protocol. We hypothesised that povidone-iodine and hydrogen peroxide do not impair wound and fracture healing when used as irrigation solutions in a rabbit open fracture model.

MATERIALS AND METHODS

This pilot experimental animal study was conducted at the University Veterinary Hospital, Faculty of Veterinary Medicine, Universiti Putra Malaysia (UPM). The study design was approved by the Institutional Animal Care and Use Committee UPM (approval number: UPM/IACUC/AUP-R056/2023) and conducted in accordance with the Animal Welfare Act 2015.

Animals

Four healthy male New Zealand White rabbits of the species *Oryctolagus cuniculus* (A Sapphire Enterprise, Selangor, Malaysia), aged eight to ten weeks old and weighing between 2.0 to 2.35 kg, were used in this study. Exclusion criteria were rabbits with ongoing infection and a previous history of injury or fracture. The rabbits were allowed to acclimatise for one week before surgery in the exotic animal ward of the University Veterinary Hospital UPM. They were housed in individual cages in a 12:12 light-dark cycle. They were given an antibiotic-free diet, Timothy hay enrichments and tap water ad libitum. The rabbits were allocated into three groups: Group 1 (control group)—normal saline (NS); Group 2—hydrogen peroxide (HPO); and Group 3— povidone-iodine (PI). At the start of the acclimatisation period, the rabbits' right hindleg fur was trimmed and cast with fibreglass (ALTOCAST™) (Figure 1). Venous samples were sent for a complete blood count and renal profile. Their body weights were measured and recorded.

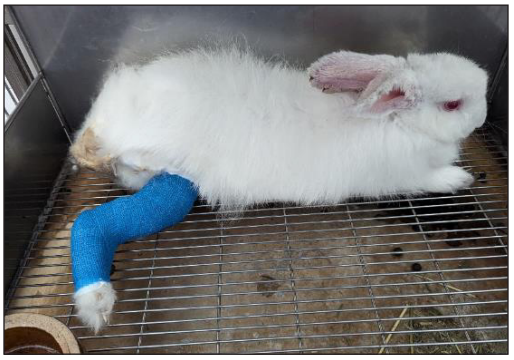

Figure 1. Rabbits allowed acclimatisation with the right hind leg cast one week prior to surgery

Irrigation Solutions

The irrigation solutions used in this study were sterile normal saline 0.9% (RinsCap®, Ain Medicare Sdn. Bhd.), povidone-iodine 10% w/v, containing 1% available iodine (Septidin 10%, AVANTE' Group Inc, USA), and hydrogen peroxide 3%.

Preparation of Open Fracture Model

The rabbits were anaesthetised with intramuscular injection (IM) of ketamine 20 mg/kg and midazolam 1 mg/kg. Anaesthesia was maintained with top-up doses of intravenous (IV) propofol 1–2 mg/kg, ketamine 1–2 mg/kg, and fentanyl 5–8 mcg/kg. Oxygenation was provided via facemask. The rabbits were placed in recumbency (Figure 2).

Using a cast cutter, a window measuring 5×2 cm was created over the anterior aspect of the rabbit's right hind leg cast. Through

Figure 2. Rabbit positioned recumbent after general anaesthesia with mask oxygenation

this window, a longitudinal skin incision approximately 2 cm in length was made over the anterior surface of the right hind leg (Figure 3). The tibial diaphysis was exposed via the anterolateral approach, and an oblique osteotomy of the mid-tibia was done using an oscillating saw cooled with saline irrigation. No skin preparation was done, and non-sterile equipment was used to simulate an open fracture environmental contamination. The wound was then loosely packed with gauze, and bandaging was applied. This phase marked the surgical creation of the open fracture model. Analgesia was given post-operatively with subcutaneous (SC) meloxicam 0.5–1.0 mg/kg SID and tramadol 5 mg/kg TID.

(a) (b)

Figure 3. Surgical creation of tibia open fracture model: (a) Window marked and created over right hind leg cast for surgical access; (b) Incision and fracture creation done through the window

Surgical Debridement and Irrigation

Twenty-four hours after open fracture creation, definitive surgery was performed. General anaesthesia was administered as described above. Prior to debridement, tissue samples (fascia and muscle layer) of approximately 0.5 g were taken from the wound for microbiological and histological analysis. The cast over the right hind leg was removed with a cast cutter. The right hind leg was shaved, and surgical skin preparation was performed with povidone-iodine 10%. A sterile surgical drape was prepared over the right hind leg. Subsequent procedures were done using an aseptic technique with sterile instruments. The wound over the right hind leg was thoroughly debrided, removing unhealthy tissues. The wound and fracture ends were then irrigated with the respective solutions according to their groups. The control group received 20 mL of normal saline 0.9% (n = 1); the HPO group received 20 mL of hydrogen peroxide 3% (n = 1); and the PI group received 20 mL of povidone 10% (n = 2). Then, another 100 mL of 0.9% saline irrigation followed to rinse off the residual solution. All irrigations were performed at low pressure via gravity flow, approximately 5 cm above the wound. Post debridement, tissue samples 0.5 g were taken for microbiological and histological comparison. The tibia fracture was stabilised using a single intramedullary Kirschner wire inserted retrograde. The wound was then closed with

Monosyn® 5/0 suture (B. Braun Surgical, Rubi, Spain). Gauze dressing and crepe bandage were applied over the right hind leg. Fibreglass cast was reapplied for further rotational stability, followed by window creation to facilitate wound inspection and dressing. A venous blood sample was taken from the contralateral hind leg for a post-operative haemogram.

Post-operative Treatment

Rabbits were isolated in their respective cages (Figure 4). Analgesia was given with SC meloxicam 0.5–1 mg/kg SID for up to five days and SC tramadol 5 mg/kg TID for up to two weeks, with further doses as clinically appropriate. IV cefuroxime 20 mg/kg 8-hourly was given as a post-operative antibiotic for three days. Oral metoclopramide 0.5 mg/kg BID, oral simethicone 20 mg/kg BID and oral multivitamin 0.2 mL SID were given for five days post-operatively to enhance gut motility and feeding. The rabbits were monitored clinically for signs of local or systemic infection. Weight measurements were performed weekly. Wounds were dressed daily with normal saline and non-adherent dressing until healing, and signs of erythema, swelling, exudate or dehiscence were observed. Casts were removed on day 42. At day 56 post-operatively, the rabbits were euthanised with IV propofol 10mg/kg and pentobarbital sodium 135–140 mg/kg. Tissue samples from the wound site were taken, and the right tibiae were extracted for histological analysis.

(a) (b)

Figure 4. Rabbits are placed in individual cages and allowed feeding and water ad libitum post-operatively

Radiological Analysis

Serial radiographs of the right tibia were taken immediately post-operatively and at 21, 42 and 56 days post-operatively. Anteroposterior and lateral views of each tibia were taken at each interval. Both the radiographic views provided a combined Radiographic Union Scale in Tibial fracture (RUST) score with a minimum score of four and a maximum of twelve (Table 1) (Whelan et al., 2010). Interpretation of the scores provided an estimate of the healing of the fracture (Table 2) (Leow et al., 2020).

Table 1
Radiographic union score for tibial fractures (RUST)

Score per Cortex	Radiographic Criteria	
	Callus	**Fracture line**
1	Absent	Visible
2	Present	Visible
3	Present	Invisible

Note. Two criteria are evaluated for each cortex (anterior, posterior, medial and lateral) from two radiographic views. The sum of all four cortical scores gives the total RUST score (Whelan et al., 2010)

Table 2
Interpretation of RUST score

Score	**4**	**5**	**6**	**7**	**8**	**9**	**10**	**11**	**12**
Interpretation	Not healed		Possible non-union			Not non-union, not healed	Possibly healed	Healed	

Note. Union is defined as three cortices with a RUST score of 3, with a value higher than 10 indicating definite fracture healing (Leow et al., 2020)

Microbiological Analysis

Tissue samples of approximately 0.05 g collected pre-debridement and post-debridement were placed in 0.1 mL of saline in Eppendorf Tubes® with a dilution ratio of 1:10. Fluid taken from this tube was serially diluted with saline, subsequently inoculated onto agar plates and then incubated at 37°C for 24 hours. Colony-forming units (CFU) were counted, representing the bacterial count per gram of tissue (CFU/g). Colonies were also microscopically identified and further sub-cultured on agar plates to identify the type of microorganisms present.

Histological Analysis

Tissue samples collected pre-debridement and post-debridement were fixed in 10% neutral-buffered formalin and embedded in paraffin. 4µm thick tissue sections were stained with hematoxylin and eosin (H&E) and examined under a light microscope for heterophils count to evaluate wound inflammation.

Tissue samples were collected after euthanasia for histological assessment of wound healing. These tissue samples were taken perpendicular to the initial surgical incision, incorporating the skin, fascia and muscle. They were subjected to similar processing as above, with additional Masson's trichrome stain for evaluation of wound healing (Table 3) (Sultana et al., 1970). The parameters assessed included the amount of granulation tissue, inflammatory infiltrate, collagen fibre orientation, pattern of collagen, and amount of early and mature collagen. The summation of all six parameters gave a total wound healing score. Good wound healing is denoted by scores of 16–19, fair 12–15 and poor 8–11.

Extracted tibiae were stored in 10% neutral-buffered formalin for three days and decalcified in 10% formic acid solution for 8–14 days before further processing. The samples were embedded in paraffin, sliced longitudinally, perpendicular to the diaphyseal axis, into 4 μm thick sections, and stained with H&E and Masson's trichrome. These bone sections were scored for fracture healing based on the quantity and type of predominant tissue, i.e., fibrous, cartilaginous, immature or mature bone, in ascending order of bone healing (Table 4) (Huo et al., 1991).

Table 3
Histological scoring system for wound healing

Number	Histological Parameter
1	Amount of granulation tissue (profound-1, moderate-2, scanty-3, absent-4)
2	Inflammatory infiltrate (plenty-1, moderate-2, a few-3)
3	Collagen fibre orientation (vertical-1, mixed-2, horizontal-3)
4	Pattern of collagen (reticular-1, mixed-2, fascicle-3)
5	Amount of early collagen (profound-1, moderate-2, minimal-3, absent-4)
6	Amount of mature collagen (minimal-1, moderate-2, profound-3)

Note. Interpretation: Good (16–19); Fair (12–15); Poor (8–11) (Sultana et al., 1970)

Table 4
Histological scoring system for fracture healing

Score	Findings at the fracture site
1	Fibrous tissue
2	Predominant fibrous tissue with minimal cartilage tissue
3	Cartilage tissue and fibrous tissue in a uniform manner
4	Predominant cartilage tissue with minimal fibrous tissue
5	Cartilage tissue
6	Predominant cartilage tissue with minimal immature bone
7	Immature bone and cartilage tissue in a uniform manner
8	Predominant immature bone with minimal cartilage tissue
9	Bone healing with immature bone
10	Bone healing with matured bone

Note. Cartilaginous and bony tissue types are associated with progressive stages of fracture healing (Huo et al., 1991)

Data Measurement

Radiological scoring was recorded by an orthopaedic surgeon who was blinded to the treatment groups. Microbiological and histological analyses were performed by a veterinary pathologist who was blinded to the treatment groups.

RESULTS

General Observations

All wounds healed well by 7 to 10 days after surgery (Figure 5). There were no signs of infection, such as erythema, exudate, swelling or wound dehiscence. There were two mortalities: (1) one death (HPO group) on day 10 due to gut stasis and (2) another (PI group) on day 39 due to bronchopneumonia, likely infection from an environmental source. Increasing analgesic frequency and duration up to a minimum of two weeks resulted in reduced stress and improved gut motility in subsequent rabbits. All the rabbits in the PI and control group showed normal appetite, bowel and urinary functions, and locomotion up until their death or euthanasia.

Microbiological Evaluation

Only one wound tissue sample in the PI group demonstrated a bacterial colony pre-debridement, which was reduced by 2.8×10^3 CFU/g following irrigation with povidone-iodine (Table 5). The colony culture grew S*taphylococcus aureus*. The other wound tissue samples did not detect any CFU.

(a) (b)

Figure 5. Clinically healed wound of two different rabbits at (a) two weeks and (b) eight weeks

Table 5
Microbiological evaluation of tissue sample before and after debridement

Rabbit	Group	Bacterial count (CFU/g)		Culture	
		Pre-debridement	Post-debridement	Pre-debridement	Post-debridement
1	HPO	0	NA	0	NA
2	PI	3.2×10^3	4.0×10^2	*Staphylococcus aureus*	*Staphylococcus aureus*
3	NS	0	0	0	0
4	PI	0	0	0	0

Note. The bacterial count and the microorganism culture before and after debridement
HPO = hydrogen peroxide; PI = povidone-iodine; NS = normal saline; NA = not available

Radiological Evaluation

RUST scores to evaluate fracture healing were determined from four cortices seen on anteroposterior and lateral radiographic views of the tibia (Figure 6) (Whelan et al., 2010). Criteria for scoring included the presence of a callus and visibility of the fracture line. A score of eight or less implied possible non-union; nine was indeterminate, while ten and above signified a healed fracture.

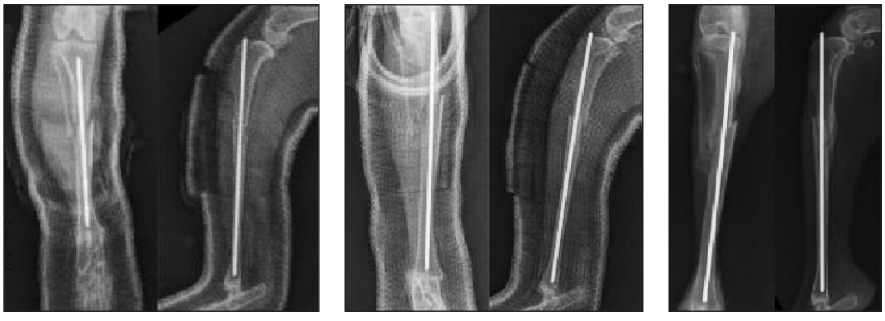

(a) (b) (c)

Figure 6. Anteroposterior and lateral radiographic views of the right tibia were taken: (a) post-operative; (b) at three weeks; and (c) at eight weeks. Radiographic healing was assessed using the RUST method, giving a score of 4, 6 and 8, respectively

On days 21, 42, and 56, both rabbits in the PI group noted comparable or slightly higher scores than the control (Table 6). No score was recorded for the HPO group due to the rabbit's premature death.

Table 6
Radiological evaluation of fracture healing at post-operative day 1, week 3, 6 and 8

Rabbit	Group	RUST score at a time interval			
		D1	Week 3	Week 6	Week 8
1	HPO	4	NA	NA	NA
2	PI	4	5	8	NA
3	NS	4	5	6	6
4	PI	4	6	7	8

Note. HPO = hydrogen peroxide; PI = povidone-iodine; NS = normal saline; RUST score = Radiographic union scale in tibial fracture; NA = not available

Histological Evaluation

Histological examination of tissue samples under light microscopy found a reduction of heterophils count in both the PI and control groups post-debridement (Figure 7). However, one of the samples in the PI group noted a moderate amount of heterophils post-irrigation despite recording a nil heterophil count pre-debridement (Table 7).

Both the PI and control groups demonstrated good wound healing, although one tissue sample in the PI group had a fair score due to the lack of cutaneous tissue for a complete assessment (Figure 8, Table 7).

Macroscopically, all the extracted tibiae demonstrated features of bone union (Figure 9). Histologically, all rabbits in the PI and control groups showed evidence of bone healing by the sixth and eighth weeks, with predominant immature bone noted (Figure 10, Table 7). There was no evidence of bone infection. No tissue sample was available for histological evaluation from the HPO group due to the rabbit's premature death.

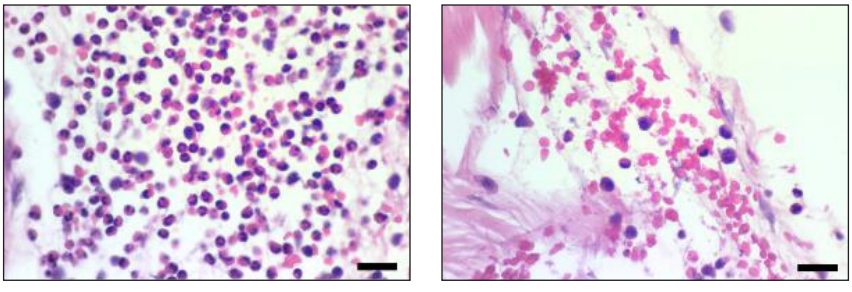

(a) (b)

Figure 7. Wound tissue histology showing heterophils count (a) pre-irrigation and (b) post-irrigation. H&E stain, magnification ×800, bar: 20 µm

Table 7
Histological evaluation of wound inflammation, wound healing and fracture healing

Rabbit	Group	Death/ Euthanasia	Heterophils count		Wound healing score	Fracture healing score
			Pre-irrigation	Post-irrigation		
1	HPO	D10	NA	NA	NA	NA
2	PI	D39	2+	1+	18/20	7/10
3	NS	D62	3+	2+	17/20	8/10
4	PI	D58	NA	2+	15/20	8/10

Note. HPO = hydrogen peroxide; PI = povidone-iodine; NS = normal saline; NA = not available; 1+ = low, < 10/HPF; 2+ = moderate, 10-100/HPF; 3+ = high, > 100/HPF; HPF = high power field

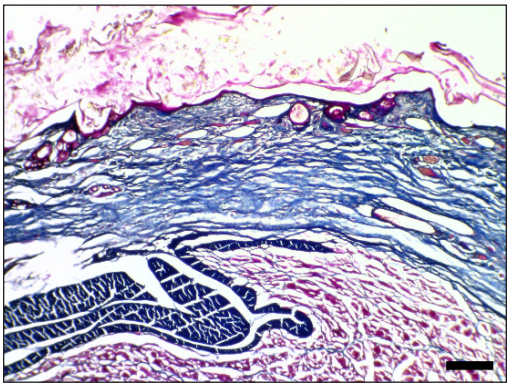

Figure 8. Histology of tissue from the previous wound site after eight weeks shows moderate mature collagen with horizontal orientation. Masson's trichrome stain, magnification ×800, bar: 20 µm

(a) (b)

Figure 9. The extracted tibia was processed for histological evaluation: (a) macroscopic features of fracture union indicated by callus formation and immobile fracture site; (b) longitudinal cut section at fracture site showing callus formation

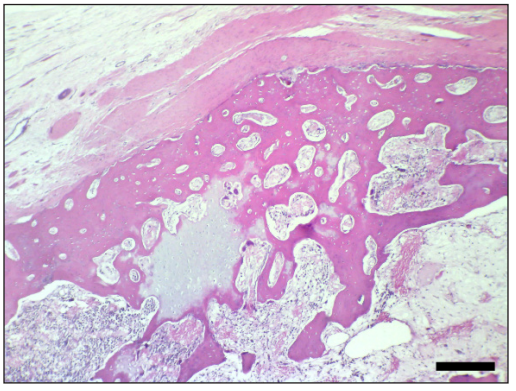

Figure 10. After eight weeks, bone histology at the fracture site shows a predominant amount of mature bone interspersed with cartilage tissue. H&E stain, magnification ×200, bar: 100 µm

DISCUSSION

There have been a substantial number of studies on the effects of antiseptics on bacterial count and wound healing. Despite their ability to reduce the number of bacteria on wound surfaces, they are also known to be detrimental to the viability and functions of cellular units essential to wound and fracture healing, such as fibroblasts, osteoblasts, and osteoclasts (Bhandari et al., 2001; Kaysinger et al., 1995; Lineaweaver et al., 1985; Thomas et al., 2009). Even *in vivo* studies showed a rebound in bacterial count

48 hours and 14 days after the initial irrigation (Owens et al., 2009; Penn-Barwell et al., 2012). This rebound could be theorised to result from the toxic effects of these solutions, thus allowing the proliferation of bacteria in damaged host tissues. However, these studies cannot account for the complex interplay of host immune response and regenerative capabilities of cellular tissues *in vivo*. Earlier *in vivo* studies on fracture healing described the effect of povidone-iodine, hydrogen peroxide and chlorhexidine in a rat fracture model, but these were closed fractures with no bacterial contamination (Husodo et al., 2016; Özbay, 2021). Therefore, we designed our study protocol to replicate an actual open fracture scenario, where the effectiveness of antiseptics in promoting wound and fracture healing depends on its ability to clear harmful bacteria while avoiding cytotoxicity to host tissues.

We chose rabbits, considered closest to human phylogeny after primates, for the study due to their similarity to humans in terms of bone attributes, such as spontaneous Haversian remodelling, bone metabolism, bone mineral density and resistance to fracture (Sengupta & Dutta, 2020; X. Wang et al., 1998). Axial forces and bending moments of rabbit tibia also approach that of humans (Reifenrath et al., 2012). They have a systemic and local inflammatory response comparable to that of humans, and antibiotics demonstrate similar pharmacokinetics. These characteristics make them popular candidates for bone infection and pharmacology studies (An et al., 2006; Bottagisio et al., 2019). The size of the rabbit tibia and the limited soft tissues surrounding the bone allow a more accessible surgical approach and implant insertion, which resembles that of the human orthopaedic scenario (Pearce et al., 2007). In addition, rabbits are easier to handle due to their docile nature and size. Their size allows for the standardisation of fracture creation and repeatability of protocol at a lower cost.

The current study performed definitive debridement 24 hours after the initial 'injury' in contrast to other *in vivo* studies where debridement was performed two to six hours later (Cheng et al., 2015; Owens et al., 2009; Penn-Barwell et al., 2012). Moreover, none of the studies evaluated fracture healing. Owens et al. (2009) performed irrigation with surfactants and antibiotics, such as bacitracin, castile soap and benzalkonium chloride, which have largely fallen out of favour in current practice. The 24-hour period in our study more accurately reflects real clinical scenarios, especially in developing countries or even developed countries with limited resources or in polytrauma patients whose resuscitation attempts precede surgical debridement, where often, the time to first debridement may extend more than 24 hours (Hadizie et al., 2022; Mener et al., 2020; Yusof et al., 2013).

The solutions used in the current study are the standard formulations found in clinical use. Iodine has long been known for its bactericidal properties. However, its use alone is limited by its low solubility in water and the caustic effect on skin and mucosal membranes. Complexing iodine with a polymer thus makes it stable and less irritating to tissues. We used povidone-iodine 10% solution with 1% available iodine for our study, the commonly

available commercial option. A full-strength povidone-iodine 1% destroyed all fibroblasts in an *in vitro* study (Lineaweaver et al., 1985). Another study demonstrated toxic effects on embryonic chick tibia and osteoblasts with povidone-iodine above one-tenth of the usual strength and with hydrogen peroxide from as low as one-thousandth of the usual strength. Removal of the offending solutions did not cause a return of the cellular functional activity (Kaysinger et al., 1995). However, the findings of *in vitro* studies do not necessarily correlate with those of *in vivo* studies. A clinical study of appendicectomy wounds in children noted a reduced wound infection rate using 1% povidone-iodine but a worse outcome with a 5% concentration (Viljanto, 1980). Even a 10% povidone-iodine solution applied for 15 minutes was safe for decontaminating bone grafts (Bauer et al., 2011; Yaman et al., 2007). These may be partly due to factors such as inactivation of the active solution by body fluids such as blood (Docherty et al., 2005).

Hydrogen peroxide is another commonly used antiseptic solution. Its bactericidal property is conferred by the generation of hydroxyl free radicals, which attack essential cell components. The usual concentration is 3%, as lower concentrations may be less effective, especially in the presence of organisms with catalase or peroxidase enzymes (McDonnell & Russell, 1999). However, 3% or even lower concentrations are cytotoxic *in vitro* (Kaysinger et al., 1995; Lineaweaver et al., 1985; Nicholson et al., 1998; Rueda-Fernández et al., 2022; Thomas et al., 2009). On the other hand, *in vivo* studies noted conflicting results. Gruber et al. (1975) reported accelerated healing of experimental animal wounds and human skin graft donor sites. Tur et al. (1995) described increased vascular perfusion in ischemic ulcers in guinea pigs after applying hydrogen peroxide cream. This contradictory effect may be partly explained by catalase enzymes in normal tissue, which partially degrades the available hydrogen peroxide (Brown & Zitelli, 1993). Data from the current study regarding the effect of hydrogen peroxide is unavailable due to the premature death of the rabbit in the HPO group. The cause of the premature mortality was gut stasis. Increasing the analgesic dose frequency and duration and providing oral prokinetic agents improved gut motility in subsequent rabbits.

Overall, *in vivo* studies comparing the efficacy of irrigation solutions on bacterial clearance and wound healing are limited (Cheng et al., 2015; Owens et al., 2009; Penn-Barwell et al., 2012). Cheng et al. (2015) induced a rat open femur fracture model by using blunt force and leaving the wound exposed for two hours before debridement and irrigation with saline, iodophor and hydrogen peroxide. They showed significant bacterial clearance with all tested solutions and the least wound inflammation by saline (Cheng et al., 2015). Interestingly, they achieved a high bacterial count ($> 10^5$ CFU/mL) from the environmental exposure before debridement. Our study could not obtain consistent contamination despite the environmental exposure and use of non-sterile equipment for fracture creation. This disparity may be due to the different methods of fracture creation; a blunt force may induce greater tissue damage, which renders it more susceptible to bacterial colonisation. An

improvement to our study will be the direct inoculation of microorganisms during fracture creation. In our PI group with recorded CFU pre-debridement, povidone-iodine reduced bacterial count, but S*taphylococcus aureus* was still cultured post-irrigation. It is doubtful if the remaining bacteria could cause a clinically significant infection, as the wound healed well. The histological evaluation noted similar wound healing scores between the PI and control group, although a full study will be required for a proper analysis.

Our results showed a similar radiological score between the PI and control groups, with slightly faster healing in the PI group beginning week three and a higher final score at week eight. Macroscopically, all extracted tibiae appeared united. Histologically, callus at the fracture sites in both groups found a mixture of immature bone and small amounts of cartilaginous tissue. Conversion of cartilage to woven bone suggests good fracture healing, implying minimal or no toxicity to bone *in vivo*. However, a larger sample size will be needed for a definite analysis. Our study can also provide a correlation between the radiographic RUST scale and histological data of fracture union for further validation of the scale (Leow et al., 2020; Whelan et al., 2010).

The positive effect of povidone-iodine on fracture healing can be attributed to the direct antimicrobial activity of PI and other mechanisms that contribute to bone and wound healing. A bacterial load of more than 10^5 has a strong predisposition to clinical infection in an open fracture (Sen et al., 2000). Naturally, a reduced bacterial load will lead to a favourable environment for bone healing, with reduced inflammatory stress brought on by substantial infection. Even subclinical colonisation of bacteria in deeper tissues can elicit an inflammatory response such as vasculitis, which interferes with healing (Piérard-Franchimont et al., 1997). In addition, iodine was found to activate macrophages and modulate their cytokine and growth factor secretions, which then regulate mesenchymal stem cell (MSC) proliferation and differentiation. In a favourable environment, in the absence of infection, macrophage production of cytokines, including bone morphogenetic proteins (BMP) such as BMP-2 and BMP-6, is increased (Moore et al., 1997). These osteoinductive cytokines are critical to bone healing (Champagne et al., 2002). *In vitro*, BMP-2 increased osteoblastic activity and differentiation even after an initial retardation (Schmidlin et al., 2009). Of note, this effect was only observed if there were osteogenic cells in the adjacent area, the most important source of which is the periosteum (Knight & Hankenson, 2013). Furthermore, iodine stimulates the upregulation of transforming growth factor beta (TGF-β) and vascular endothelial growth factor (VEGF), which have roles in endothelial cell migration and angiogenesis, while downregulating the production of interleukin 6 (IL-6), which reduces congestion and oedema (D. Wang et al., 2022; L. Wang et al., 2017). This effectively converts the inflammatory phase of healing to the proliferative phase, which is beneficial for wound healing. However, the positive effect of PI in this study could also be explained by variability due to the small sample size. Therefore, a larger sample needs to be studied to confirm the significance of the findings.

The preliminary results suggest PI as a viable adjunct for irrigation in open fractures. A cost-effective approach is ideal, given the enormous economic burden of treating open fractures and their complications. Since irrigation is already standard practice in treating open fractures, optimising the irrigation solution is an obvious choice, considering it is one of the cheapest and easily modifiable variables, without relying on expensive methods to improve the outcome. The results of this study can also be applied to treating fracture-related infections.

The current study does have limitations. We did not investigate different fracture types, concentrations and contact times of the irrigation solutions. Testing these would present ethical concerns due to the huge sample involved and the difficulty in achieving standardisation. Our open fracture model does not encompass other factors, such as polytrauma injury, multiple surgical treatments, and soft tissue damage, which may be seen in clinical scenarios and affect the outcome. Further biomechanical wound tensile and bone strength testing may provide information regarding the functional outcome. There was inconsistent microbial contamination during the open fracture creation phase, which can be improved by directly inoculating a fixed quantity of bacteria. We performed tissue biopsies for organism culture and detection, which is considered the gold standard (Serena et al., 2021). However, these may be subject to sampling error, and fastidious organisms that are difficult to culture may be missed. Newer and more advanced techniques, such as bioluminescence or fluorescence imaging, can provide real-time quantification of bacteria and repeated measurement. The effects of the irrigation solutions were studied in a diaphyseal open fracture model. Peri-articular fractures, in the presence of articular cartilage, may behave differently. A critical-size bone defect or significant loss of periosteum, often seen in high-grade open fractures, is outside the scope of this study. This experimental model also exhibits a translational barrier. Although there is good representation similarity in terms of micro and macro anatomy and molecular and biochemical interactions, there are differences which may not translate directly (Marmor et al., 2020). Rabbits have different bone shapes and sizes, flexed limbs with different weight loading and faster bone turnover, which may not be fully representative of bone healing response in adult humans (Li et al., 2015). The parameters evaluated, such as *ex vivo* bone histology, provided valuable information to guide treatment strategy. However, there is no comparable analysis in humans, which is impossible in a clinical setting.

CONCLUSION

These findings suggest that povidone-iodine may be a safe irrigation solution for open fractures. However, given the small sample size, further research with larger cohorts must validate these results before clinical recommendations can be made.

ACKNOWLEDGEMENT

We thank the University Veterinary Hospital Universiti Putra Malaysia staff for assistance with the study. We also thank veterinary assistant Muhammad Nur Iman bin Aminuddin for his contributions during the study. The authors declared no conflicts of interest concerning this article's authorship and/or publication.

REFERENCES

An, Y. H., Kang, Q. K., & Arciola, C. R. (2006). Animal models of osteomyelitis. *The International Journal of Artificial Organs*, *29*(4), 407–420. https://doi.org/10.1177/039139880602900411

Bauer, J., Liu, R. W., Kean, T. J., Dennis, J. E., Petersilge, W., & Gilmore, A. (2011). A comparison of five treatment protocols for contaminated bone grafts in reference to sterility and cell viability. *Journal of Bone and Joint Surgery*, *93*(5), 439–444. https://doi.org/10.2106/JBJS.J.00418

Bhandari, M., Adili, A., & Schemitsch, E. H. (2001). The efficacy of low-pressure lavage with different irrigating solutions to remove adherent bacteria from bone. *The Journal of Bone and Joint Surgery-American Volume*, *83*(3), 412–419. https://doi.org/10.2106/00004623-200103000-00014

Bottagisio, M., Coman, C., & Lovati, A. B. (2019). Animal models of orthopaedic infections. A review of rabbit models used to induce long bone bacterial infections. *Journal of Medical Microbiology*, *68*(4), 506–537. https://doi.org/10.1099/jmm.0.000952

Brown, C. D., & Zitelli, J. A. (1993). A review of topical agents for wounds and methods of wounding: Guidelines for wound management. *The Journal of Dermatologic Surgery and Oncology*, *19*(8), 732–737. https://doi.org/10.1111/j.1524-4725.1993.tb00417.x

Champagne, C. M., Takebe, J., Offenbacher, S., & Cooper, L. F. (2002). Macrophage cell lines produce osteoinductive signals that include bone morphogenetic protein-2. *Bone*, *30*(1), 26–31. https://doi.org/10.1016/S8756-3282(01)00638-X

Cheng, Q., Zhang, X. F., Di, D. H., Zhao, G. Y., & Cui, X. W. (2015). Efficacy of different irrigation solutions on the early debridement f open fracture in rats. *Experimental and Therapeutic Medicine*, *9*(5), 1589–1592. https://doi.org/10.3892/etm.2015.2325

Court-Brown, C. M., Bugler, K. E., Clement, N. D., Duckworth, A. D., & McQueen, M. M. (2012). The epidemiology of open fractures in adults. A 15-year review. *Injury*, *43*(6), 891–897. https://doi.org/10.1016/j.injury.2011.12.007

Docherty, J. G., McGregor, J. R., Purdie, C. A., Galloway, D. J., & O'Dwyer, P. J. (2005). Efficacy of tumoricidal agents in vitro and in vivo. *British Journal of Surgery*, *82*(8), 1050–1052. https://doi.org/10.1002/bjs.1800820816

Eccles, S., Handley, B., Khan, U., Nanchahal, J., Nayagam, S., & McFadyen, I. (2020). *Standards for the management of open fractures* (1st ed.). Oxford University Press. https://doi.org/10.1093/med/9780198849360.001.0001

Flores, M. J., Brown, K. E., Haonga, B., Morshed, S., & Shearer, D. W. (2024). Estimating the economic impact of complications after open tibial fracture: A secondary analysis of the pilot Gentamicin Open Tibia trial

(pGO-Tibia). *OTA International: The Open Access Journal of Orthopaedic Trauma*, *7*(1), Article e290. https://doi.org/10.1097/OI9.0000000000000290

Gruber, R. P., Vistnes, L., & Pardoe, R. (1975). The effect of commonly used antiseptics on wound healing. *Plastic and Reconstructive Surgery*, *55*(4), 472–476. https://doi.org/10.1097/00006534-197555040-00013

Hadizie, D., Kor, Y. S., Ghani, S. A., & Mohamed-Saat, M. A. (2022). The incidence of fracture-related infection in open tibia fracture with different time interval of initial debridement. *Malaysian Orthopaedic Journal*, *16*(3), 24–29. https://doi.org/10.5704/MOJ.2211.005

Hoekstra, H., Smeets, B., Metsemakers, W. J., Spitz, A. C., & Nijs, S. (2017). Economics of open tibial fractures: The pivotal role of length-of-stay and infection. *Health Economics Review*, *7*(1), Article 32. https://doi.org/10.1186/s13561-017-0168-0

Huo, M. H., Troiano, N. W., Pelker, R. R., Gundberg, C. M., & Friedlaender, G. E. (1991). The influence of ibuprofen on fracture repair: Biomechanical, biochemical, histologic, and histomorphometric parameters in rats. *Journal of Orthopaedic Research*, *9*(3), 383–390. https://doi.org/10.1002/jor.1100090310

Husodo, K., Kamal, A. F., & Yusuf, A. A. (2016). Effect of povidone iodine and hydrogen peroxide on fracture healing: A histomorphometric study on rats. *Journal of Orthopaedic Surgery*, *24*(2), 245–249. https://doi.org/10.1177/1602400224

Kaysinger, K. K., Nicholson, N. C., Ramp, W. K., & Kellam, J. F. (1995). Toxic effects of wound irrigation solutions on cultured tibiae and osteoblasts: *Journal of Orthopaedic Trauma*, *9*(4), 303–311. https://doi.org/10.1097/00005131-199509040-00006

Knight, M. N., & Hankenson, K. D. (2013). Mesenchymal stem cells in bone regeneration. *Advances in Wound Care*, *2*(6), 306–316. https://doi.org/10.1089/wound.2012.0420

Leow, J. M., Clement, N. D., & Simpson, A. H. W. R. (2020). Application of the radiographic union scale for tibial fractures (RUST): Assessment of healing rate and time of tibial fractures managed with intramedullary nailing. *Orthopaedics & Traumatology, Surgery & Research*, *106*(1), 89–93. https://doi.org/10.1016/j.otsr.2019.10.010

Li, Y., Chen, S. K., Li, L., Qin, L., Wang, X. L., & Lai, Y. X. (2015). Bone defect animal models for testing efficacy of bone substitute biomaterials. *Journal of Orthopaedic Translation*, *3*(3), 95–104. https://doi.org/10.1016/j.jot.2015.05.002

Lineaweaver, W., McMorris, S., Soucy, D., & Howard, R. (1985). Cellular and bacterial toxicities of topical antimicrobials. *Plastic and Reconstructive Surgery*, *75*(3), 394–396. https://doi.org/10.1097/00006534-198503000-00016

Marmor, M. T., Dailey, H., Marcucio, R., & Hunt, A. C. (2020). Biomedical research models in the science of fracture healing—Pitfalls & promises. *Injury*, *51*(10), 2118–2128. https://doi.org/10.1016/j.injury.2020.06.025

McDonnell, G., & Russell, A. D. (1999). Antiseptics and disinfectants: Activity, action, and resistance. *Clinical Microbiology Reviews*, *12*(1), 147–179. https://doi.org/10.1128/CMR.12.1.147

Mener, A., Staley, C. A., Lunati, M. P., Pflederer, J., Reisman, W. M., & Schenker, M. L. (2020). Is operative debridement greater than 24 hours post-admission associated with increased likelihood of post-operative infection?. *Journal of Surgical Research*, *247*, 461–468. https://doi.org/10.1016/j.jss.2019.09.059

Moore, K., Thomas, A., & Harding, K. G. (1997). Iodine released from the wound dressing iodosorb modulates the secretion of cytokines by human macrophages responding to bacterial lipopolysaccharide. *The International Journal of Biochemistry & Cell Biology*, *29*(1), 163–171. https://doi.org/10.1016/S1357-2725(96)00128-8

Nicholson, N. C., Ramp, W. K., Kneisl, J. S., & Kaysinger, K. K. (1998). Hydrogen peroxide inhibits giant cell tumor and osteoblast metabolism in vitro. *Clinical Orthopaedics and Related Research*, *347*, 250–260.

Owens, B. D., White, D. W., & Wenke, J. C. (2009). Comparison of irrigation solutions and devices in a contaminated musculoskeletal wound survival model. *The Journal of Bone and Joint Surgery-American Volume*, *91*(1), 92–98. https://doi.org/10.2106/JBJS.G.01566

Özbay, H., Yüksel, S., Güleç, M. A., Atçı, T., Küçükyıldırım, B. O., & Çay, T. (2021). The effect of different irrigation solutions on fracture healing in a rat femur fracture model. *Joint Diseases and Related Surgery*, *32*(1), 144–151. https://doi.org/10.5606/ehc.2021.77358

Pearce, A. I., Richards, R. G., Milz, S., Schneider, E., & Pearce, S. G. (2007). Animal models for implant biomaterial research in bone: A review. *European Cells and Materials*, *13*, 1–10. https://doi.org/10.22203/eCM.v013a01

Penn-Barwell, J. G., Murray, C. K., & Wenke, J. C. (2012). Comparison of the antimicrobial effect of chlorhexidine and saline for irrigating a contaminated open fracture model. *Journal of Orthopaedic Trauma*, *26*(12), 728–732. https://doi.org/10.1097/BOT.0b013e31826c19c4

Petrisor, B., Jeray, K., Schemitsch, E., Hanson, B., Sprague, S., Sanders, D., & Bhandari, M. (2008). Fluid lavage in patients with open fracture wounds (FLOW): An international survey of 984 surgeons. *BMC Musculoskeletal Disorders*, *9*(1), Article 7. https://doi.org/10.1186/1471-2474-9-7

Piérard-Franchimont, C., Paquet, P., Arrese, J. E., & Piérard, G. E. (1997). Healing rate and bacterial necrotizing vasculitis in venous leg ulcers. *Dermatology*, *194*(4), 383–387. https://doi.org/10.1159/000246156

Puetzler, J., Zalavras, C., Moriarty, T. F., Verhofstad, M. H. J., Kates, S. L., Raschke, M. J., Rosslenbroich, S., & Metsemakers, W. J. (2019). Clinical practice in prevention of fracture-related infection: An international survey among 1197 orthopaedic trauma surgeons. *Injury*, *50*(6), 1208–1215. https://doi.org/10.1016/j.injury.2019.04.013

Reifenrath, J., Gottschalk, D., Angrisani, N., Besdo, S., & Meyer-Lindenberg, A. (2012). Axial forces and bending moments in the loaded rabbit tibia in vivo. *Acta Veterinaria Scandinavica*, *54*(1), Article 21. https://doi.org/10.1186/1751-0147-54-21

Rueda-Fernández, M., Melguizo-Rodríguez, L., Costela-Ruiz, V. J., Luna-Bertos, E. D., Ruiz, C., Ramos-Torrecillas, J., & Illescas-Montes, R. (2022). Effect of the most common wound antiseptics on human skin fibroblasts. *Clinical and Experimental Dermatology*, *47*(8), 1543–1549. https://doi.org/10.1111/ced.15235

Schade, A. T., Khatri, C., Nwankwo, H., Carlos, W., Harrison, W. J., & Metcalfe, A. J. (2021). The economic burden of open tibia fractures: A systematic review. *Injury*, *52*(6), 1251–1259. https://doi.org/10.1016/j.injury.2021.02.022

Schmidlin, P. R., Imfeld, T., Sahrmann, P., Tchouboukov, A., & Weber, F. E. (2009). Effect of short-time povidone-iodine application on osteoblast proliferation and differentiation. *The Open Dentistry Journal*, *3*(1), 208–212. https://doi.org/10.2174/1874210600903010208

Sen, R. K., Murthy, N., Gill, S. S., & Nagi, O. N. (2000). Bacterial load in tissues and its predictive value for infection in open fractures. *Journal of Orthopaedic Surgery*, *8*(2), 1–5. https://doi.org/10.1177/230949900000800202

Sengupta, P., & Dutta, S. (2020). Mapping the age of laboratory rabbit strains to human. *International Journal of Preventive Medicine*, *11*, Article 194. https://doi.org/10.4103/ijpvm.IJPVM_530_18

Serena, T. E., Bowler, P. G., Schultz, G. S., D'souza, A., & Rennie, M. Y. (2021). Are semi-quantitative clinical cultures inadequate? Comparison to quantitative analysis of 1053 bacterial isolates from 350 wounds. *Diagnostics*, *11*(7), Article 1239. https://doi.org/10.3390/diagnostics11071239

Sultana, J., Molla, M. R., Kamal, M., Shahidullah, M., Begum, F., & Bashar, M. A. (1970). Histological differences in wound healing in maxillofacial region in patients with or without risk factors. *Bangladesh Journal of Pathology*, *24*(1), 3–8. https://doi.org/10.3329/bjpath.v24i1.2874

Thomas, G. W., Rael, L. T., Bar-Or, R., Shimonkevitz, R., Mains, C. W., Slone, D. S., Craun, M. L., & Bar-Or, D. (2009). Mechanisms of delayed wound healing by commonly used antiseptics. *Journal of Trauma: Injury, Infection & Critical Care*, *66*(1), 82–91. https://doi.org/10.1097/TA.0b013e31818b146d

Tur, E., Bolton, L., & Constantine, B. E. (1995). Topical hydrogen peroxide treatment of ischemic ulcers in the guinea pig: Blood recruitment in multiple skin sites. *Journal of the American Academy of Dermatology*, *33*(2), 217–221. https://doi.org/10.1016/0190-9622(95)90238-4

Viljanto, J. (1980). Disinfection of surgical wounds without inhibition of normal wound healing. *Archives of Surgery*, *115*(3), Article 253. https://doi.org/10.1001/archsurg.1980.01380030009003

Wang, D., Huang, X., Lv, W., & Zhou, J. (2022). The toxicity and antibacterial effects of povidone-iodine irrigation in fracture surgery. *Orthopaedic Surgery*, *14*(9), 2286–2297. https://doi.org/10.1111/os.13422

Wang, L., Qin, W., Zhou, Y., Chen, B., Zhao, X., Zhao, H., Mi, E., Mi, E., Wang, Q., & Ning, J. (2017). Transforming growth factor β plays an important role in enhancing wound healing by topical application of povidone-iodine. *Scientific Reports*, *7*(1), Article 991. https://doi.org/10.1038/s41598-017-01116-5

Wang, X., Mabrey, J. D., & Agrawal, C. M. (1998). An interspecies comparison of bone fracture properties. *Bio-Medical Materials and Engineering*, *8*(1), 1–9.

Whelan, D. B., Bhandari, M., Stephen, D., Kreder, H., McKee, M. D., Zdero, R., & Schemitsch, E. H. (2010). Development of the radiographic union score for tibial fractures for the assessment of tibial fracture healing after intramedullary fixation. *Journal of Trauma: Injury, Infection & Critical Care*, *68*(3), 629–632. https://doi.org/10.1097/TA.0b013e3181a7c16d

Yaman, F., Ünlü, G., Atilgan, S., Celik, Y., Özekinci, T., & Yaldiz, M. (2007). Microbiologic and histologic assessment of intentional bacterial contamination of bone grafts. *Journal of Oral and Maxillofacial Surgery*, *65*(8), 1490–1494. https://doi.org/10.1016/j.joms.2006.10.027

Yusof, N. M., Khalid, K. A., Zulkifly, A. H., Zakaria, Z., Amin, M. A. M., Awang, M. S., Ahmad, A. C., & Akter, S. F. U. (2013). Factors associated with the outcome of open tibial fractures. *The Malaysian Journal of Medical Sciences: MJMS*, *20*(5), 47–53.

Pertanika J. Trop. Agric. Sci. 48 (6): 1803 - 1815 (2025)

PERTANIKA JOURNALS

TROPICAL AGRICULTURAL SCIENCE

Journal homepage: http://www.pertanika.upm.edu.my/

Seed Yield and Nutritional Content of *Mucuna pruriens* in Different Doses of NPK Fertiliser and Plant Density

Ismail Saleh*, Umi Trisnaningsih, Ida Setya Wahyu Atmaja, and Muhamad Nizar Maulid Junaedi

Department of Agrotechnology, Faculty of Agriculture, Universitas Swadaya Gunung Jati, 45132 Cirebon, West Java, Indonesia

ABSTRACT

Mucuna pruriens is a member of Leguminosae family with the potential to be developed into a source of vegetable protein. Despite the significant potential, plant commonly has not been cultivated by good agriculture practices. Therefore, this study aimed to analyze the effect of different doses of NPK fertilizer and plant density on yield, nutritional, and bioactive content of *M. pruriens* seed. The experiment was conducted in Kuningan Regency, West Java, Indonesia (6°48'0.31"S, 108°28'17.5"E), from June to December 2024. A randomized complete block design was used, with treatments containing the combination of NPK fertilizer doses and plant density. The NPK fertilizer doses used consisted of four levels, namely 0, 0.5, 1, and 1.5 recommended doses. The recommended doses for N, P_2O_5, and K_2O were 112.5, 90, and 108 kg/ha, respectively, with plant densities of 1, 2, and 3 seeds per planting hole. There were 12 treatment combinations, and each was repeated three times. The results showed that the treatment had a significant effect on *M. pruriens* yield, sugar, and starch content, as well as antioxidant activity ($P<0.05$). The combination of 1.5 recommended doses (168.75 kg N/ha, 135 kg P_2O_5/ha, and 162 kg K_2O/ha) and 1 seed per hole gave a higher number of pods per plant, pod weight per plant, and seed weight per plant although not significantly different from 1 and 0.5 recommended doses with the same plant density. This combination of treatments also produced higher starch and sugar levels. Seed protein content was not affected by the treatment, including total phenol and flavonoid levels. Furthermore, the highest antioxidant activity was obtained in the combination of 1.5 recommended doses and 3 seeds per hole.

Keywords: Antioxidant, fatty acid, Leguminosae, protein, starch

ARTICLE INFO

Article history:
Received: 12 January 2025
Accepted: 24 April 2025
Published: 25 November 2025

DOI: https://doi.org/10.47836/pjtas.48.6.08

E-mail addresses:
ismail.saleh68@gmail.com (Ismail Saleh)
umitrisna@gmail.com (Umi Trisnaningsih)
iedaatmaja@gmail.com (Ida Setya Wahyu Atmaja)
nizarmaulid98@gmail.com (Muhamad Nizar Maulid Junaedi)
* Corresponding author

e-ISSN: 2231-8542

INTRODUCTION

Mucuna pruriens is one type of plant from the Leguminosae family that is still underutilized. This plant is known as velvet bean and "koro benguk" in Indonesia, which is rarely consumed as food compared to another legume plant like soybeans with potential as raw materials for making tofu, tempeh, and soy sauce. The use of *M. pruriens* seed includes as raw materials for making tempeh and tofu (Gravitiani et al., 2022), although the level of public preference for koro tempeh is still lower than soybean tempeh (Suwasono et al., 2022).

In addition to serving as a source of vegetable protein, *M. pruriens* seed has significant medicinal properties, including antidiabetic, aphrodisiac, antimicrobial, and anti-inflammatory (Rai et al., 2020). The use of *M. pruriens* seed as a medicinal plant and a source of protein is due to the presence of bioactive content such as alkaloids, flavonoids, tannins, saponins, and phenols (Jadhav et al., 2022). This bioactive content shows potential of *M. pruriens* as a source of antioxidants that are beneficial for human health (Jimoh et al., 2020). Due to its bioactive contents, *M. pruriens* can be classified as functional food. There were some definitions of functional food by the expert. In general, functional foods contain ingredients that provide health benefits (Baker et al., 2022).

Due to the potential of *M. pruriens* as a functional food which is still underutilized, several efforts are needed to increase the yield and seed quality. One important aspect of cultivation is fertilization, which should be performed in appropriate dose to enhance plant growth and optimal production. Fertilizer provides important nutrients for plants such as N, P, and K which are essential macronutrients. The availability of these nutrients in sufficient quantities can support plant growth and yield. The functions of the three nutrients include supporting vegetative growth, increasing CO_2 assimilation and photosynthesis, and playing a role in seed formation (Zewdie & Hassen, 2021). However, excessive application can affect content and quality of seed. Previous studies on wheat reported that increasing nitrogen level caused a rise in seed protein content (Nasiroleslami et al., 2021). Excess of nitrogen will reduce bioactive content and antioxidant capacity, affecting the composition of fatty acid in seed (Elhanaf et al., 2019). The decrease in bioactive content and antioxidant activity is often caused by increasing levels of nutrients, reducing the activity of the PAL enzyme which catalyzes the formation of phenolic compound precursors (Li et al., 2021).

High crop yields can be obtained by increasing the number of plant populations per unit area to a certain limit. However, increasing the population or high density reduced plant biomass, yield caused by a lower photosynthetic rate and low nutrients (Postma et al., 2021). Previous studies have shown that increasing the population of soybean plant due to increasing the number of seed per hole can reduce the number of pods and the weight of soybean seed (Xu et al., 2021). This showed the need to determine the right population to optimize the yield of *M. pruriens* by regulating the number of seed per hole.

MATERIALS AND METHODS

Study Area

The study was conducted at Kuningan District, West Java, Indonesia at coordinates 6°48'0.31" S, 108°28'17.5" E from June to December 2024. This location has an altitude of 296 m above sea level. Laboratory analysis was carried out at the Laboratory of Department of Agronomy and Horticulture IPB University (Seed nutrient, starch, sugar, protein, phenolic, and flavonoid content), Integrated Laboratory IPB (Fatty acid content), Food and Biochemistry Laboratory Universitas Negeri Sebelas Maret (Fiber content and antioxidant activity), and Laboratory of Plant Physiology, Universitas Swadaya Gunung Jati (Sample preparation).

Materials

The material used were *M. pruriens* seed obtained from wild *M. pruriens* plant at Banyumas District, Central Java, Indonesia. Fertilizer as source of nitrogen, phosphorus, and potassium used urea, SP-36, and KCl, respectively. Furthermore, the bamboo used as a pole to support growth of plant.

Procedures

The experiment used a randomized complete block design, with treatment containing the combination of NPK fertilizer dose and plant density. Dose of fertilizer consisted of four levels, namely 0, 0.5, 1, and 1.5 recommended dose. Moreover, the recommended doses for N, P_2O_5, and K_2O were 112.5, 90, and 108 kg ha^{-1}, respectively, based on doses of NPK fertilizer that was used in cowpea (Gustiningsih et al., 2023). Urea, SP-36, and KCl were used as source of nutrient with rates 250, 250, and 180 kg ha^{-1}, respectively. Plant density consisted of three levels, namely 1, 2, and 3 seeds per planting hole and each treatment combination was repeated three times. There were 36 experimental units and each unit was a plot of 2 m × 3 m. Furthermore, 12, 24, and 36 plants were put in the treatment 1, 2, and 3 seeds per planting hole, respectively.

Seed was planted with a spacing of 100 cm × 50 cm. Phosphorus and potassium fertilizer were applied at 3 weeks after planting. Nitrogen fertilizer was applied twice at 3 and 5 weeks after planting with 50% dose in each application.

The pods were harvested starting at 18 weeks after planting and harvested four times. Subsequently, the criteria of pods that could be harvested was brownish colored pods. The yield observation included pods number per plant, pods weight per plant, and seed weight per plant, as well as weight of 100 seeds. These pods were harvested from all plants in each plot.

The observation of nutritional and bioactive content in *M. pruriens* seed included nutrient content (N (titrimetric), P (spectrophotometric), and K (AAS)), protein (Calculation by 5.30 as factor) (Mariotti et al., 2008), crude fat (AOAC 2005: 4.5.06),

starch (spectrophotometric), sugar (spectrophotometric), and crude fiber (gravimetric). Other contents included fatty acid profile (AOAC (2012): 969.33), total phenolic (Folin-Ciocalteau), and total flavonoid (Aluminum chloride colorimetric) (Vongsak et al., 2013), and antioxidant activity (DPPH).

Data Analysis

The data were analyzed using analysis of variance (ANOVA) at α =5%. When treatment had a significant effect, the analysis continued with DMRT post hoc with α=5%, although fatty acid profile was not analyzed statistically.

RESULTS AND DISCUSSION

Soil Properties and Climate Conditions at Experimental Location

The result of soil analysis showed pH value of 5.95 (slightly acid), content of C-organic was 1.48% (low), and N-total was 0.16% (low). Meanwhile, the P_2O_5 content was 73.43 mg 100 g^{-1} (very high) and K_2O was 19.43 mg 100 g^{-1} (moderate). The soil texture at the study location was silty clay loam (Table 1). Generally, nitrogen is a macro essential nutrient that is needed by plant for vegetative growth. *M. pruriens* that belongs to Leguminosae has the ability to fix nitrogen from the air into a form available to plant (Magadlela et al., 2021). Phosphorus and potassium are also essential macronutrients needed by plant. Specifically, phosphorus is one of the components of nucleic acid and phospholipids (Lambers, 2022). Potassium plays a role in several biochemical processes such as stomatal regulation, photosynthesis, and increasing plant tolerance to abiotic stress (Johnson et al., 2022).

Table 1
Soil properties at experimental location

Parameters	Value	Status
pH H_2O	5.95	Slightly acid
C-organic (%)	1.48	Low
N-total (%)	0.16	Low
P_2O_5 (mg 100 g^{-1})	73.43	Very high
K_2O (mg 100 g^{-1})	19.43	Medium
Soil Texture		
Clay (%)	65	Silty Clay Loam
Silt (%)	28	
Sand (%)	7	

In the early of plant growth, rainfall conditions were low because it was in the dry season with an average rainfall of 131.85 mm $month^{-1}$. Therefore, watering was carried out every day to prevent drought stress. When plant entered harvest time, rainfall was approximately 488 mm $month^{-1}$ or in the rainy season. There were no significant pests and diseases attacking plant, thereby no control activity was not carried out.

Yield Component of *M. pruriens*

The yield component of *M. pruriens* seed production was pod number, pod weight, weight of 100 seeds, and seed weight per plant. These components affected the yield of *M. pruriens*,

including the treatment combinations of NPK fertilizer dose and plant density, as shown in Table 2. The combinations of 1.5 recommended dose and 1 seed per plant hole produced the highest value. Yield component of *M. pruriens* tended to increase with high fertilizer doses. In each dose of NPK fertilizer, there was a decrease of yield component with increasing plant density. Weight of 100 seeds was not affected by treatment.

High plant density caused competition for nutrients, water, and sunlight for plant. The high competition caused decreasing of plant growth and yield. Nutrient competition also occurs when plant population increases. The previous studies on white lupine showed that lower plant density increased the number of seed per pod and seed weight per plant (Tobiasz-Salach et al., 2023). High number of seed per plant hole also increases intraspecific competition. At low plant density, the rate of photosynthesis per plant increases, thereby the supply of C to the root nodules has an impact on increasing nodulation and the rate of nitrogen fixation (Luca & Hungria, 2014).

Table 2
Effect of NPK fertilizer and plant density on yield component of M. pruriens

Treatment	Pod number per plant	Pod weight per plant (g)	100 seeds weight (g)	Seed weight per plant (g)
0 RD, 1 seed	35.6 ± 9.57 bc	156.28 ± 38.59 bc	78.17 ± 3.47 a	85.16 ± 21.38 bc
0 RD, 2 seed	19.9 ± 10.12 ab	90.52 ± 36.47 ab	74.36 ± 4.92 a	47.57 ± 23.25 ab
0 RD. 3 seed	16.0 ± 3.90 a	67.01 ± 17.30 a	72.77 ± 4.31 a	42.67 ± 15.77 ab
0.5 RD, 1 seed	50.4 ± 20.97 cd	233.37 ± 117.14 cd	75.95 ± 5.59 a	125.79 ± 63.86 cd
0.5 RD, 2 seed	18.7 ± 1.83 ab	79.88 ± 9.00 ab	75.29 ± 2.82 a	43.72 ± 5.46 ab
0.5 RD, 3 seed	13.9 ± 4.55 a	54.25 ± 17.75 a	69.37 ± 3.87 a	29.92 ± 10.08 a
1 RD, 1 seed	52.5 ± 15.09 cd	217.77 ± 58.65 cd	75.06 ± 2.78 a	119.95 ± 31.18 cd
1 RD, 2 seed	21.9 ± 3.77 ab	96.27 ± 14.53 ab	76.60 ± 3.76 a	52.78 ± 8.40 ab
1 RD, 3 seed	12.8 ± 10.69 a	54.75 ± 46.02 a	74.99 ± 8.27 a	30.89 ± 26.52 a
1.5 RD, 1 seed	61.1 ± 21.11 d	260.23 ± 96.88 d	74.74 ± 4.40 a	141.13 ± 53.37 d
1.5 RD, 2 seed	23.9 ± 3.57 ab	103.91 ± 22.22 ab	69.16 ± 1.65 a	57.12 ± 11.37 ab
1.5 RD, 3 seed	16.7 ± 5.80 a	71.90 ± 22.54 ab	73.38 ± 6.99 a	39.65 ± 12.60 ab

Note. The number followed by the same letter in a column is not significantly different by the DMRT test at the level of α=5%. Numbers were followed by ± standard deviation. RD = recommended dose of NPK fertilizer

Nutritional dan Bioactive Content of *M. pruriens* Seed

The nitrogen and phosphorus content in *M. pruriens* seed were not affected by dose of fertilization and plant density. More importantly, the potassium content was found to be higher in the control treatment (without fertilization) in all treatments of the number of seed per planting hole (Table 3). The potassium accumulation in seed function plant resistance to oxidative stress (Johnson et al., 2022). When plant is not fertilized, there is a tendency to face nutrient stress, leading to the accumulation of potassium in the seed.

Table 3
Effect of NPK fertilizer and plant density on nutrient content of M. pruriens *seed*

Treatment	N (%)	P (%)	K (%)
0 RD, 1 seed	4.57 ± 0.04 a	0.27 ± 0.03 a	1.66 ± 0.26 b
0 RD, 2 seed	4.47 ± 0.08 a	0.27 ± 0.01 a	1.72 ± 0.11 b
0 RD, 3 seed	4.42 ± 0.26 a	0.29 ± 0.01 a	1.86 ± 0.13 b
0.5 RD, 1 seed	4.48 ± 0.11 a	0.28 ± 0.01 a	1.35 ± 0.07 a
0.5 RD, 2 seed	4.38 ± 0.19 a	0.28 ± 0.01 a	1.15 ± 0.08 a
0.5 RD, 3 seed	4.40 ± 0.17 a	0.25 ± 0.02 a	1.20 ± 0.10 a
1 RD, 1 seed	4.34 ± 0.17 a	0.26 ± 0.02 a	1.22 ± 0.10 a
1 RD, 2 seed	4.76 ± 0.30 a	0.26 ± 0.03 a	1.24 ± 0.03 a
1 RD, 3 seed	4.58 ± 0.34 a	0.27 ± 0.03 a	1.29 ± 0.20 a
1.5 RD, 1 seed	4.60 ± 0.10 a	0.28 ± 0.04 a	1.27 ± 0.14 a
1.5 RD, 2 seed	4.50 ± 0.16 a	0.25 ± 0.00 a	1.35 ± 0.10 a
1.5 RD, 3 seed	4.61 ± 0.14 a	0.27 ± 0.03 a	1.21 ± 0.08 a

Note. The number followed by the same letter in a column is not significantly different by the DMRT test at the level of α=5%. Numbers were followed by ± standard deviation. RD = recommended dose of NPK fertilizer

The nitrogen content in seed is related to protein content (Lu et al., 2020). Based on Pearson correlation analysis, there was a positive correlation between protein and nitrogen ($P < 0.01$, $r = 0.650$) (Figure 1). The nitrogen and phosphorus content in seed was also positively correlated with the weight of 100 seeds with correlation coefficients of $r = 404$ and $r = 0.503$, respectively. In this study, protein content was not significantly different between treatments (Table 4). This was because the nitrogen content in seed did not differ between treatments. Previous studies showed that the enhanced protein levels were affected by nitrogen delivery to seed (Lu et al., 2020).

Legume plants are able to fix free nitrogen from the air, thereby meeting their needs. The ability to fix atmospheric nitrogen shows the potential of plant to be included in low-input agricultural systems (Kebede, 2021). In this study, protein content of *M. pruriens* ranged from 22-25%. Previous studies have shown that protein content of white *M. pruriens* seed was 28.82 % and black was 26.26% (Baby et al., 2023). However, protein content of *M. pruriens* was lower than soybeans, which ranged 33-37% (Kudelka et al., 2021).

Crude fat content of *M. pruriens* seed was affected by combination of fertilizer dose and plant density, although there was no clear trend regarding those treatment. The highest fat content was found in the 1 recommended dose and 2 seeds per plant hole. At the same dose, the treatment of 1 and 3 seeds per plant hole gave the lowest crude fat content. In this study, crude fat content was 2.21-6.92% in line with previous report, where content of lipids in *M. pruriens* seed without processing was 4.69% (Ezegbe et al., 2023).

The analysis of fatty acid profile in *M. pruriens* showed that linoleic acid was found in higher concentrations (Figure 2), followed by palmitic acid. The composition of linoleic acid

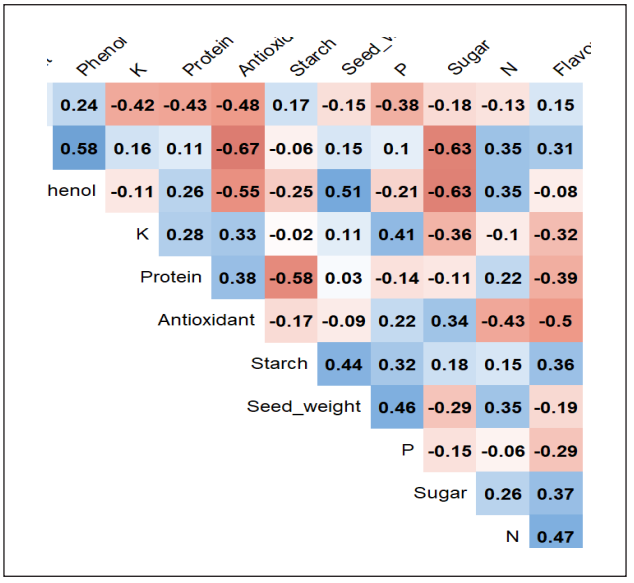

Figure 1. Pearson correlation analysis of seed weight and nutritional content of *M. pruriens* seed

Table 4
Effect of NPK fertilizer and plant density on protein, crude fat, and starch content of M. pruriens *seed*

Treatment	Protein (%)	Crude fat (%)	Starch (%)
0 RD, 1 seed	24.23 ± 0.16 a	5.03 ± 0.20 cd	8.97 ± 0.20 bcd
0 RD, 2 seed	23.71 ± 0.43 a	4.97 ± 0.24 cd	7.23 ± 1.15 ab
0 RD, 3 seed	23.46 ± 1.38 a	5.00 ± 1.21 cd	7.04 ± 1.02 ab
0.5 RD, 1 seed	23.73 ± 0.59 a	5.78 ± 0.43 de	7.92 ± 1.41 abc
0.5 RD, 2 seed	23.21 ± 0.99 a	5.07 ± 0.47 cd	7.43 ± 2.10 ab
0.5 RD, 3 seed	23.34 ± 0.89 a	5.24 ± 0.47 cd	7.63 ± 1.41 ab
1 RD, 1 seed	23.06 ± 0.97 a	2.82 ± 0.67 a	7.54 ± 0.58 ab
1 RD, 2 seed	23.54 ± 0.44 a	6.57 ± 0.39 e	6.98 ± 0.24 ab
1 RD, 3 seed	23.16 ± 1.12 a	3.67 ± 0.34 ab	9.72 ± 0.09 cd
1.5 RD, 1 seed	22.54 ± 0.06 a	4.69 ± 1.06 bcd	10.55 ± 0.59 d
1.5 RD, 2 seed	23.82 ± 0.84 a	4.54 ± 0.73 bc	5.87 ± 1.50 a
1.5 RD, 3 seed	24.45 ± 0.77 a	3.75 ± 0.79 ab	5.90 ± 1.25 a

Note. The number followed by the same letter in a column is not significantly different by the DMRT test at the level of α=5%. Numbers were followed by ± standard deviation. RD = recommended dose of NPK fertilizer

was relatively the same in each treatment, which was approximately 34.5%. Meanwhile, palmitic acid had a higher concentration in the 0.5 of the recommended doses with 1 seed planted per hole (Figure 2). The presence of linoleic acid, palmitic acid, and oleic acid in *M. pruriens* seed has the potential to be used as a source of vegetable oil (Baby et al., 2023). Linoleic acid is included in the n-6 polyunsaturated fatty acid (PUFA) with 18

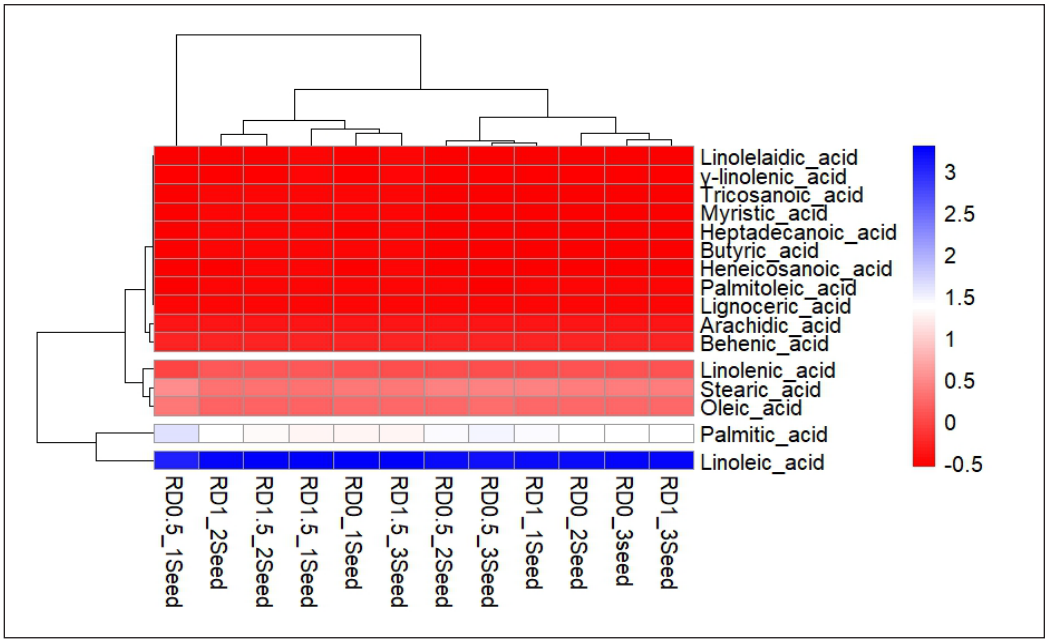

Figure 2. Heatmap profile of fatty acid in *M. pruriens* seed
Note. RD = Recommended dose

carbon atoms. It is also found in high concentrations in nuts and lower concentrations in some cereals including legumes (Marangoni et al., 2020).

Starch is a form of carbohydrate storage in seed (MacNeill et al., 2017). The highest starch content is found in the treatment of 1.5 recommended doses and 1 seed per hole. Increasing the number of seed per hole decreases the starch content in seed. The decrease in starch levels with increasing plant density is attributed to competition between plant which has an impact on reducing the rate of photosynthesis and its derivative product such as starch. Like protein, starch is positively correlated with the weight of 100 seed ($P<0.05$, $r = 0.330$). Starch plays a role during seed development (Liu, Luo et al., 2021).

Sugar (sucrose) is the product of photosynthesis in plant (Aluko et al., 2021) and is converted into stored starch during seed development (Li et al., 2022). Based on the ANOVA results, the sugar content in *M. pruriens* seed was affected by fertilizer dose treatment. Compared to potassium content in seed, the highest sugar content was found in the treatment of 1.5 recommended doses (Table 5). In this study, there was a negative correlation between sugar and fat content ($P <0.01$, $r = -0.509$). Fat content in seed is mainly synthesized from sugar (Kaur et al., 2021). Therefore, high sugar accumulation reduces the fat content in seed.

The crude fiber content in *M. pruriens* seed was affected by the treatment. Based on the results, the highest crude fiber content was found in the treatment of 0.5 recommended doses

Table 5
Effect of NPK fertilizer and plant density on sugar and crude fiber content of M. pruriens *seed*

Treatment	Sugar (%)	Crude fiber (%)
0 RD, 1 seed	5.11 ± 0.26 ab	5.25 ± 0.14 ab
0 RD, 2 seed	4.90 ± 0.27 ab	5.49 ± 1.62 ab
0 RD, 3 seed	4.94 ± 0.42 ab	4.75 ± 0.32 a
0.5 RD, 1 seed	4.87 ± 0.33 a	4.36 ± 0.77 a
0.5 RD, 2 seed	4.97 ± 0.05 ab	6.86 ± 0.50 c
0.5 RD, 3 seed	5.13 ± 0.61 ab	6.93 ± 0.59 c
1 RD, 1 seed	5.73 ± 0.10 b	5.42 ± 0.47 ab
1 RD, 2 seed	4.76 ± 0.19 a	6.07 ± 0.41 bc
1 RD, 3 seed	6.72 ± 0.47 c	6.28 ± 0.44 bc
1.5 RD, 1 seed	6.99 ± 0.55 c	5.32 ± 0.50 ab
1.5 RD, 2 seed	6.71 ± 0.59 c	5.32 ± 0.54 ab
1.5 RD, 3 seed	6.93 ± 0.70 c	4.51 ± 0.16 a

Note. The number followed by the same letter in a column is not significantly different by the DMRT test at the level of α=5%. Numbers were followed by ± standard deviation. RD = recommended dose of NPK fertilizer

with 2 and 3 seeds per planting hole, but not significantly different from 1 recommended dose. Increasing fertilizer dose to 1.5 recommended doses reduced the crude fiber content in seed. The components of crude fiber include cellulose and lignin (Liu et al., 2022; Yang et al., 2021). Previous studies on rice showed that the addition of nitrogen fertilizer reduced the cellulose level in the endosperm (Midorikawa et al., 2014). Lignin, cellulose, and hemicellulose also decreased with the increase of nitrogen fertilizer in maize (Liu, Gu et al., 2021).

The development of *M. pruriens* seed into a functional food needs to consider bioactive content that has the potential to act as an antioxidant. Previous studies have shown that *M. pruriens* has a function as an antioxidant, antidiabetic, and anti-inflammatory agent (Kumbhare et al., 2023; Yadav et al., 2024). The main compounds that function as antioxidant includes phenolics and flavonoids. Total flavonoids and total phenolics in *M. pruriens* seed were not affected by treatment (Table 6). However, antioxidant activity was affected by the treatment of fertilizer doses and the number of seed per plant hole. The highest antioxidant activity was found in the treatment of 1.5 recommended doses and 3 seeds per hole. Furthermore, the average percentage of inhibition of DPPH free radical compounds produced by antioxidant compounds in *M. pruriens* seed was 90.97%. The high antioxidant activity in *M. pruriens* seed allows for incorporation into human diet to promote healthy living (Jimoh et al., 2020). In this study, the antioxidant activity of *M. pruriens* seed did not correlate with the phenolic and flavonoid content (Figure 1), which varied significantly from several previous reports.

Table 6.
Effect of NPK fertilizer and plant density on total phenolic content, total flavonoid content, and antioxidant activity of M. pruriens *seed*

Treatment	TPC (mg GAE 100 g^{-1} dw)	TFC (mg QE 100 g^{-1} dw)	Antioxidant activity (% inhibition)
0 RD, 1 seed	4221.20 ± 503.82 a	62.87 ± 11.11. a	91.51 ± 1.08 bc
0 RD, 2 seed	4078.00 ± 455.38 a	64.75 ± 5.09 a	91.48 ± 0.68 bc
0 RD, 3 seed	3849.14 ± 385.40 a	59.15 ± 1.79 a	91.29 ± 0.28 bc
0.5 RD, 1 seed	4089.88 ± 477.87 a	65.47 ± 6.08 a	90.89 ± 0.52 bc
0.5 RD, 2 seed	4194.04 ± 356.85 a	61.82 ± 6.12 a	91.03 ± 0.69 bc
0.5 RD, 3 seed	3978.34 ± 272.83 a	67.61 ± 5.95 a	90.04 ± 1.42 ab
1 RD, 1 seed	4061.95 ± 140.60 a	60.77 ± 1.22 a	91.48 ± 0.28 bc
1 RD, 2 seed	4623.95 ± 968.47 a	69.26 ± 20.26 a	88.90 ± 0.76 a
1 RD, 3 seed	3849.14 ± 514.03 a	64.78 ± 13.10 a	91.02 ± 0.12 bc
1.5 RD, 1 seed	3763.21 ± 100.93 a	75.95 ± 10.95 a	90.55 ± 1.27 bc
1.5 RD, 2 seed	3906.86 ± 282.87 a	70.10 ± 9.39 a	91.56 ± 0.38 bc
1.5 RD, 3 seed	3946.23 ± 171.05 a	61.90 ± 5.82 a	91.93 ± 0.32 c

Note. The number followed by the same letter in a column is not significantly different by the DMRT test at the level of α=5%. Numbers were followed by ± standard deviation. RD = recommended dose of NPK fertilizer; TPC = Total phenolic contents; TFC = Total flavonoid contents; GAE = Gallic acid equivalent; QE = Quercetin equivalent; dw = dry weight

CONCLUSION

In conclusion, this study showed that an increase in plant density decreased seed yield of *M. pruriens.* The combination of 1.5 recommended doses (168.75 kg N/ha, 135 kg P_2O_5/ha, and 162 kg K_2O/ha) and 1 seed per plant hole gave a higher number of pods per plant, pod weight per plant, and seed weight per plant. These treatments combination also produced higher starch and sugar levels in the seed. Protein content was not affected by the treatment, including total phenol and flavonoid levels. The highest antioxidant activity was obtained in the combination of 1.5 recommended doses and 3 seeds per hole. Moreover, further studies were recommended to analyze the effect of organic fertilizer on the yield and quality of *M. pruriens* seed.

ACKNOWLEDGMENT

The authors are grateful to the Minister of Education, Culture, Research, and Technology of the Republic of Indonesia under the Fundamental Research funding program number 0667/E5/AL.04/2024.

REFERENCES

Aluko, O. O., Li, C., Wang, Q., & Liu, H. (2021). Sucrose utilization for improved crop yields: A review article. *International Journal of Molecular Sciences*, *22*, Article 4704. https://doi.org/10.3390/ijms22094704

Baby, C., Kaur, S., Singh, J., & Prasad, R. (2023). Velvet bean (*Mucuna pruriens*): A sustainable protein source for tomorrow. *Legume Science*, *5*, Article e178. https://doi.org/10.1002/leg3.178

Baker, M. T., Lu, P., & Parrella, J. A. (2022). Consumer acceptance toward functional foods: A scoping review. *International Journal of Environmental Research and Public Health*, *19*, Article 1217. https://doi.org/10.3390/ijerph19031217

Elhanaf, L., Houhou, M., Rais, C., Mansouri, I., Elghadraoui, L., & Greche, H. (2019). Impact of excessive nitrogen fertilization on the biochemical quality, phenolic compounds, and antioxidant power of *Sesamum indicum* L seeds. *Journal of Food Quality, 2019*(1), Article 9428092. https://doi.org/10.1155/2019/9428092

Ezegbe, C. C., Nwosu, J. N., Owuamanam, C. I., Victor-Aduloju, T. A., & Nkhata, S. G. (2023). Proximate composition and anti-nutritional factors in *Mucuna pruriens* (velvet bean) seed flour as affected by several processing methods. *Heliyon*, *9*, Article e18728. https://doi.org/10.1016/j.heliyon.2023.e18728

Gravitiani, E., Sari, D. M., Setiyanto, D. O., Ashar, A. F., Hayati, C. N., Rahmahita, D. B., Rofi'atullaili, Mustajab, I., Putri, B. C. T., Sadewa, D. M., & Ramono, B. G. (2022). Penyuluhan inovasi packaging dan branding produk tempe benguk sebagai upaya pengembangan UMKM bagi masyarakat Desa Pagak Kecamatan Sumberlawang Kabupaten Sragen [Counseling on packaging innovation and branding of benguk tempeh products as an effort to develop MSMEs for the people of Pagak Village, Sumberlawang District, Sragen Regency]. *Kreasi: Jurnal Inovasi Dan Pengabdian Kepada Masyarakat*, *2*(1), 13–22.

Gustiningsih, D., Purnamawati, H., Lubis, I., & Syukur, M. (2023). Morphophysiological characters and production of cowpea due to variation in the number of seeds and fertilization combination. *Ecology Journal*, *5*(1), 19–26.

Jadhav, S. N., Nayyar, S., Hundal, J. S., Bedi, J. S., & Singh, C. (2022). In-vitro evaluation of *Mucuna pruriens* seeds by nutritional and phytochemical analysis, assessment of antioxidant property and estimation of L-DOPA content by RP-HPLC. *The Pharma Innovation Journal*, *11*(1), 289–294.

Jimoh, M. A., Idris, O. A., & Jimoh, M. O. (2020). Cytotoxicity, phytochemical, antiparasitic screening, and antioxidant activities of *Mucuna pruriens* (Fabaceae). *Plants*, *9*, Article 1249. https://doi.org/10.3390/plants9091249

Johnson, R., Vishwakarma, K., Hossen, M. S., Kumar, V., Shackira, M., Puthur, J. T., Abdi, G., Sarraf, M., & Hasanuzzaman, M. (2022). Potassium in plants: Growth regulation, signaling, and environmental stress tolerance. *Plant Physiology and Biochemistry*, *172*, 56–69. https://doi.org/10.1016/j.plaphy.2022.01.001

Kaur, M., Tak, Y., Bhatia, S., Asthir, B., Lorenzo, J. M., & Amarowicz, R. (2021). Crosstalk during the carbon–nitrogen cycle that interlinks the biosynthesis, mobilization and accumulation of seed storage reserves. *International Journal of Molecular Sciences*, *22*, Article 12032. https://doi.org/10.3390/ijms222112032

Kebede, E. (2021). Contribution, utilization, and improvement of legumes-driven biological nitrogen fixationin agricultural systems. *Frontiers in Sustainable Food Systems*, *5*, Article 767998. https://doi.org/10.3389/fsufs.2021.767998

Kudelka, W., Kowalska, M., & Popis, M. (2021). Quality of soybean products in terms of essential amino acids composition. *Molecules*, *26*, Article 5071. https://doi.org/10.3390/ molecules26165071

Kumbhare, S. D., Ukey, S. S., & Gogle, D. P. (2023). Antioxidant activity of *Flemingia praecox* and *Mucuna pruriens* and their implications for male fertility improvement. *Scientific Reports*, *13*, Article 19360. https://doi.org/10.1038/s41598-023-46705-9

Lambers, H. (2022). Phosphorus acquisition and utilization in plants. *Annual Review of Plant Biology*, *73*, 17–42. https://doi.org/10.1146/annurev-arplant-102720- 125738

Li, P., Wang, L., Liu, H., & Yuan, M. (2022). Impaired SWEET-mediated sugar transportation impacts starch metabolism in developing rice seeds. *The Crop Journal*, *10*, 98–108. https://doi.org/10.1016/j.cj.2021.04.012

Li, Z., Jiang, H., Qin, Y., Yan, H., Jiang, X., & Qin, Y. (2021). Nitrogen deficiency maintains the yield and improves the antioxidant activity of *Coreopsis tinctoria* Nutt. *Bioscience, Biotechnology, and Biochemistry*, *85*(6), 1492–1505. https://doi.org/10.1093/bbb/zbab048

Liu, X., Gu, W., Li, C., Li, J., & Wei, S. (2021). Effects of nitrogen fertilizer and chemical regulation on spring maize lodging characteristics, grain filling and yield formation under high planting density in Heilongjiang Province, China. *Journal of Integrative Agriculture*, *20*(2), 511–526. https://doi.org/10.1016/S2095-3119(20)63403-7

Liu, X., Luo, J., Li, T., Yang, H., Wang, P., Su, L., Zheng, Y., Bao, C., & Zhou, C. (2021). *SDG711* is involved in rice seed development through regulation of starch metabolism gene expression in coordination with other histone modifications. *Rice*, *14*(1), Article 25. https://doi.org/10.1186/s12284-021-00467-y

Liu, Z., Zeng, Z., Yang, X., Zhu, S., Liu, T., & Wang, Y. (2022). Genetic insights into the crude protein and fiber content of ramie leaves. *Frontiers in Plant Science*, *13*, Article 969820. https://doi.org/10.3389/fpls.2022.969820

Lu, M., Snyder, R., Grant, J., & Tegeder, M. (2020). Manipulation of sucrose phloem and embryo loading affects pea leaf metabolism, carbon and nitrogen partitioning to sinks as well as seed storage pools. *The Plant Journal*, *101*, 217–236. https://doi.org/10.1111/tpj.14533

Luca, M. J., & Hungria, M. (2014). Plant densities and modulation of symbiotic nitrogen fixation in soybean. *Scientia Agricola*, *71*(3), 181–187.

MacNeill, G. J., Mehrpouyan, S., Minow, M. A. A., Patterson, J. A., Tetlow, I. J., & Emes, M. J. (2017). Starch as a source, starch as a sink: The bifunctional role of starch in carbon allocation. *Journal of Experimental Botany*, *68*(16), 4433–4453. https://doi.org/10.1093/jxb/erx291

Magadlela, A., Makhaye, N., & Pérez-Fernández, M. (2021). Symbionts in *Mucuna pruriens* stimulate plant performance through nitrogen fixation and improved phosphorus acquisition. *Journal of Plant Ecology*, *14*, 310–322. https://doi.org/10.1093/jpe/rtaa098

Marangoni, F., Agostoni, C., Borghi, C., Catapano, A. L., Cena, H., Ghiselli, A.,Vecchia, C. L., Lercker, G., Manzato, E., Pirillo, A., Riccardi, G., Rise, P., Visioli, F., & Poli, A. (2020). Dietary linoleic acid and human health: Focus on cardiovascular and cardiometabolic effects. Atherosclerosis, 292, 90–98. https://doi.org/10.1016/j.atherosclerosis.2019.11.018

Mariotti, F., Tomé, D. D., & Mirand, P. P. (2008). Converting nitrogen into protein – beyond 6.25 and Jones' Factors. *Critical Reviews in Food Science and Nutrition*, *48*(2), 177–184. https://doi.org/10.1080/10408390701279749

Midorikawa, K., Kuroda, M., Terauchi, K., Hoshi, M., Ikenaga, S., Ishimaru, Y., Abe, K., & Asakura, T. (2014). Additional nitrogen fertilization at heading time of rice down-regulates cellulose synthesis in seed endosperm. *Plos One*, *9*(6), Article e98738. https://doi.org/10.1371/journal.pone.0098738

Nasiroleslami, E., Mozafari, H., Sadeghi-Shoae, M., Habibi, D., & Sani, B. (2021). Changes in yield, protein, minerals, and fatty acid profle of wheat (*Triticum aestivum* L.) under fertilizer management involving application of nitrogen, humic acid, and seaweed extract. *Journal of Soil Science and Plant Nutrition*, *21*(4), 2642–2651. https://doi.org/10.1007/s42729-021-00552-7

Postma, J. A., Hecht, V. L., Hikosaka, K., Nord, E. A., Pons, T. L., & Poorter, H. (2021). Dividing the pie: A quantitative review on plant density responses. *Plant Cell Environment*, *44*, 1072–1094. https://doi.org/10.1111/pce.13968

Rai, S. N., Chaturvedi, V. K., Singh, P., Singh, B. K., & Singh, M. P. (2020). *Mucuna pruriens* in Parkinson's and in some other diseases: Recent advancement and future prospective. *Biotech*, *10*, Article 522. https://doi.org/10.1007/s13205-020-02532-7

Suwasono, S., Jayus, & Sari, P. (2022). Pengembangan produk tempe berbasis koro di Desa Banjarsengon, Kecamatan Patrang, Jember [Development of koro-based tempeh products in Banjarsengon Village, Patrang District, Jember]. *Jurnal Hasil Pengabdian Kepada Masyarakat Universitas Jember*, *1*(1), 36–43.

Tobiasz-Salach, R., Janczak-Pieniazek, M., & Augustynska-Prejsnar, A. (2023). Effect of different row spacing and sowing density on selected photosynthesis indices, yield, and quality of white lupine seeds. *Agriculture*, *13*, Article 1845. https://doi.org/10.3390/ agriculture13091845

Vongsak, B., Sithisarn, P., Mangmool, S., Thongpraditchote, S., Wongkrajang, Y., & Gritsanapan, W. (2013). Maximizing total phenolics, total flavonoid contents, and antioxidant activity of *Moringa oleifera* leaf extract by the appropriate extraction method. *Industrial Crops and Products*, *44*, 566–571. https://doi.org/10.1016/j.indcrop.2012.09.021

Xu, C., Li, R., Song, W., Wu, T., Sun, S., Hu, S., Han, T., & Wu, C. (2021). Responses of branch number and yield component of soybean cultivars tested in different planting densities. *Agriculture*, *11*, Article 69. https://doi.org/10.3390/agriculture 11010069

Yadav, J. P., Pathak, P., Yadav, S., Singh, A., Palei, N. N., & Verma, A. (2024). In-Vitro evaluation of antidiabetic, antioxidant, and anti-inflammatory activities in *Mucuna pruriens* seed extract. *Clinical Phytoscience*, *10*, Article 21. https://doi.org/10.1186/s40816-024-00381-y

Yang, C., Zhang, F., Jiang, X., Yang, X., He, F., Wang, Z., Long, R., Chen, L., Yang, T., Wang, C., Gao, T., Kang, J., & Yang, Q. (2021). Identification of genetic loci associated with crude protein content and fiber composition in alfalfa (*Medicago sativa* L.) using QTL mapping. *Frontiers in Plant Science*, *12*, Article 608940. https://doi.org/10.3389/fpls.2021.608940

Zewdie, T., & Hassen, E. (2021). Review on effects of phosphorus fertilizer rates on growth, yield components and yield of common bean (*Phaseolus vulgaris* L.). *Journal of Current Research in Food Science*, *2*(1), 34–39.

Pertanika J. Trop. Agric. Sci. 48 (6): 1817 - 1829 (2025)

PERTANIKA JOURNALS

TROPICAL AGRICULTURAL SCIENCE

Journal homepage: http://www.pertanika.upm.edu.my/

Behavioural Indicators of Stress in Cats During Veterinary Visits: Effects of Transportation and Clinical Examinations

Ahmed Abubakar Abubakar[1], Ubedullah Kaka[2], Ngiow Ee Wen[2], and Yong-Meng Goh[1,3]*

[1]Laboratory of Sustainable Animal Production and Biodiversity, Institute of Tropical Agriculture and Food Security, Universiti Putra Malaysia, 43400 UPM Serdang, Selangor, Malaysia
[2]Department of Companion Animal Medicine and Surgery, Faculty of Veterinary Medicine, Universiti Putra Malaysia, 43400 UPM Serdang, Selangor, Malaysia
[3]Department of Preclinical Sciences, Faculty of Veterinary Medicine, Universiti Putra Malaysia, 43400 UPM Serdang, Selangor, Malaysia

ABSTRACT

Cats experience stress when visiting novel environments, including veterinary clinics. Stress can impact physiological indicators, which are crucial for assessing patients. Prolonged stress affects the immune system, health, and behaviour. The current study assesses cat stress using behavioural indicators after transportation to the university veterinary hospital for clinical examinations. A total of 35 cats of different sexes, including males, females and neutered, and ages between 6 to 36 months, were recruited for the study conducted at the Universiti Veterinary Hospital UPM. The study employed cat behavioural stress scores to monitor stress remotely. Cats were assessed on a scale ranging from 1 (indicating a state of relaxation) to 6 (indicating a state of extreme fear). Behavioural assessments were conducted in consultation rooms, and the cats were removed from the cage, examined physically, and carefully put back into the cage. Information regarding the patients' attributes, consultation, and distances travelled to the UVH was documented and analysed. Results indicated that long-distance transportation substantially impacted clinical stress levels, even after waiting at UVH reception. No significant ($P>0.05$) changes were observed in stress levels following handling events, case presentation, consultation time, procedures, sexes, breeds, and ages. Overall, cats experience significant stress in clinical environments, particularly during physical examinations, with transportation playing a key role in eliciting stress-related behaviours that persist even after rest.

Keywords: Behaviour, clinical environment stress, cats, stress, transportation

ARTICLE INFO

Article history:
Received: 24 October 2024
Accepted: 08 May 2025
Published: 25 November 2025

DOI: https://doi.org/10.47836/pjtas.48.6.09

E-mail addresses:
ahmed@upm.edu.my (Ahmed Abubakar Abubakar)
dr_ubedkaka@upm.edu.my (Ubedullah kaka)
ahmadsadeeq7@gmail.com (Ngiow Ee Wen)
ymgoh@upm.edu.my (Yong-Meng Goh)
* Corresponding author

e-ISSN: 2231-8542

INTRODUCTION

Veterinary visits are often perceived as stressful events for cats, with numerous factors contributing to their stress levels. This stress can significantly affect critical physiological measures such as blood pressure, heart rate, and respiration rate, which are essential for accurate patient assessments (Pereira et al., 2015; Conti et al., 2017). Furthermore, prolonged stress in cats can have detrimental effects on their overall health, including immune function and behaviour (Moberg and Mench, 2000). This issue is not just of scientific concern but also influences the behaviour of pet owners, as many avoid regular veterinary visits due to the perceived stress experienced by their cats. It has been noted that only 40% of cat owners regularly bring their cats to veterinary clinics, compared to 90% of dog owners (Bir et al., 2020).

The behavioural signs of stress during veterinary visits are widely observed, including reluctance to enter carriers, aggression, vocalisation, and anxiety, especially when unfamiliar animals, such as dogs, are present (Riemer et al., 2021; Tuozzi et al., 2021). These stress responses can persist even after the visit, with cats exhibiting uncharacteristic behaviours and aggression at home. This situation highlights the urgent need to better understand and manage stress in veterinary settings, as well as to improve the overall experience for both cats and their owners.

The goal of veterinary care is to prioritise the welfare of its patients (Dawson et al., 2016). Reducing stress during veterinary visits is crucial, as it aids in more accurate health assessments, reduces the risk of stress-induced health complications, and enhances the safety of both staff and animals (Trevorrow, 2013). The current study seeks to investigate stress intensity in cats within the clinical environment, particularly during consultation and examination. By identifying key behavioural indicators of stress, this research aims to implement best practices for stress management in veterinary clinics, improving the clinical environment for both pets and staff and fostering greater confidence in veterinary care from clients.

MATERIALS AND METHODS

Ethical Note

The present work received clearance from the Institutional Animal Use and Ethics Committee (IACUC) of Universiti Putra Malaysia, with approval number UPM/IACUC-U021/2019, dated June 13, 2019, after complying with the committee's criteria for animal research.

Design of the Experiment and Study Location

This study was conducted with cats brought in seeking outpatient care at the University Veterinary Hospital (UVH) of Universiti Putra Malaysia (UPM), located at coordinates

2°98'N and 101°71'E on Persiaran Mardi-UPM. A total of 35 cats of different sexes, including males, females and neutered, and ages between 6 to 36 months, were recruited for the study conducted at the Universiti Veterinary Hospital UPM.

Experimental Procedure

The current study uses the cat behavioural stress scores published by Kessler and Turner (1997) and modified by Nibblet et al. (2015) to monitor and assess the behavioural stress scores in cats. It is worth noting that the observation differed between animals depending on the case presented and the level of cooperation from the cat during an examination. Within an average of 3-10 minutes, depending on the procedure and complaints, the cats' level of cooperation, behavioural observation and scoring were noted, and no physical contact was made between the investigator and the participants. A score of 1 (relaxed) and 6 (extreme fear) was used to measure the cats' behaviour and responses to the events. Behavioural stress scores were recorded during handling events in the consultation room, including the process of removing cats from their carriers, performing physical examinations, and returning them to the carriers. Data regarding patients, including signalment, total consultation time, complaints, procedures performed, distance travelled from home to the UVH, age, breeds, and sexes, were recorded and analysed.

Cat Behavioural Stress Score

This study employed the cat behavioural stress score model developed by Kessler and Turner (1997) and Nibblet et al. (2015) to monitor and evaluate stress through behavioural stress scores in cats remotely.

Data and Statistical Analysis

The analysis was conducted with SPSS Version 22.0 (IBM SPSS Inc, USA), employing two-way Analysis of Variance (ANOVA) to calculate the mean of a quantitative variable change according to the levels of two categorical variables and the Kruskal-Wallis Test (handling events and stress score) to compare means when data is non-parametric (not normally distributed). Statistical analyses were performed at a 95% confidence ($P<0.05$).

RESULTS

It is worth mentioning that the cats that partake in the current study are of different ages, ranging from 24-36 months. No notable changes were observed in cat stress levels between age ($P = 0.194$) and handling events ($P = 0.068$). Furthermore, no interaction effect was observed between age and cat stress levels after handling events ($P = 0.945$; Table 1).

The cats in this study comprise various breeds, including Bengal, Domestic Shorthair, Mixed, Persian, Scottish Fold, and Domestic Longhair. No considerable changes were observed between handling events and stress levels (P=0.164) and between the cat breed and the stress level (P=0.280). Similarly, no significant difference was observed between breeds and handling events in the stress levels of cats (P = 0.998), as shown in Table 2.

No considerable alterations were observed between gender and handling events on cats' stress levels (P=0.414). No significant difference was found between the cat's gender and stress level (P = 0.501). Additionally, no significant interaction (P = 0.898)

Table 1
The effect test between age and handling events on stress levels in cats

Tests of Between-Subjects Effects Dependent Variable: Stress					
Source	**Type III Sum of Squares**	**df**	**Mean Square**	**F**	**Sig.**
Corrected Model	3.798[a]	5	.760	1.502	.196
Intercept	983.150	1	983.150	1944.692	.000
Event	2.800	2	1.400	2.769	.068
age_cat	.864	1	.864	1.710	.194
Event * age_cat	.057	2	.029	.057	.945
Error	50.050	99	.506		
Total	1066.000	105			
Corrected Total	53.848	104			
a. R Squared = .071 (Adjusted R Squared = .024)					

Note. Means within columns with distinct superscripts revealed substantial changes at p<0.05

Table 2
The effect test between breed and handling events on stress levels in cats

Tests of Between-Subjects Effects Dependent Variable: Stress					
Source	**Type III Sum of Squares**	**df**	**Mean Square**	**F**	**Sig.**
Corrected Model	7.181[a]	17	.422	.787	.702
Intercept	325.607	1	325.607	607.024	.000
event	1.981	2	.991	1.847	.164
BREED	3.431	5	.686	1.279	.280
event * BREED	.874	10	.087	.163	.998
Error	46.667	87	.536		
Total	1066.000	105			
Corrected Total	53.848	104			
a. R Squared = .133 (Adjusted R Squared = -.036)					

Note. Means within columns with distinct superscripts revealed substantial changes at p<0.05

was observed between gender and handling events on the cat's stress levels, as shown in Table 3.

No significant changes (P = 0.478) were observed in the duration of consultation and handling events on the cats' stress levels. Similarly, there were no significant differences (P = 0.085) in the duration of the consultation with the cats and their stress levels. Additionally, there was no significant interaction (P = 0.886) between the duration of consultation and handling events on the cats' stress levels (Table 4).

Results observed following handling differed significantly (P=0.026) between the cat's stress levels. No significant difference (P = 0.109) was observed between the complaints

Table 3
The effect test between gender and handling events on stress levels in cats

Tests of Between-Subjects Effects Dependent Variable: Stress					
Source	**Type III Sum of Squares**	**df**	**Mean Square**	**F**	**Sig.**
Corrected Model	4.153[a]	8	.519	1.003	.439
Intercept	424.260	1	424.260	819.582	.000
event	.921	2	.460	.889	.414
GENDER	.721	2	.361	.697	.501
event * GENDER	.555	4	.139	.268	.898
Error	49.695	96	.518		
Total	1066.000	105			
Corrected Total	53.848	104			
a. R Squared = .077 (Adjusted R Squared = .000)					

Note. Means within columns with distinct superscripts revealed substantial changes at p<0.05

Table 4
The effect test between the duration in the consultation room and handling events on stress levels in cats

Tests of Between-Subjects Effects Dependent Variable: Stress					
Source	**Type III Sum of Squares**	**df**	**Mean Square**	**F**	**Sig.**
Corrected Model	16.344[a]	29	.564	1.127	.332
Intercept	490.371	1	490.371	980.658	.000
Event	.746	2	.373	.746	.478
Duration consultation	8.032	9	.892	1.785	.085
Event*duration consultation	5.436	18	.302	.604	.886
Error	37.503	75	.500		
Total	1066.000	105			
Corrected Total	53.848	104			
a. R Squared = .304 (Adjusted R Squared = .034)					

Note. Means within columns with distinct superscripts revealed substantial changes at p<0.05

and procedures on the cats' stress levels. Furthermore, there was no significant interaction (P = 0.577) between handling events and complaints and procedures on stress levels in cats (Table 5).

Table 6 shows significant interactions between presenting complaints and procedures carried out with handling events on stress levels.

No significant differences (P = 0.066) were observed between handling events and transportation in terms of cats' stress levels. However, transportation distance significantly affected stress levels in cats (P = 0.009). No significant (P=0.835) interaction between transportation and handling events on cats' stress levels, as shown in Table 7.

Table 8 shows that no significant difference (P = 0.071) was observed between handling events and stress levels following the Kruskal-Wallis test in cats.

Table 5
The effect of complaints and procedures carried out on handling events on cat stress levels

Tests of Between-Subjects Effects Dependent Variable: stress					
Source	**Type III Sum of Squares**	**df**	**Mean Square**	**F**	**Sig.**
Corrected Model	6.539[a]	8	.817	1.659	.119
Intercept	806.284	1	806.284	1636.135	.000
event	3.750	2	1.875	3.805	.026
Presenting complaints	2.234	2	1.117	2.266	.109
Event*presenting complaints	1.429	4	.357	.725	.577
Error	47.309	96	.493		
Total	1066.000	105			
Corrected Total	53.848	104			
a. R Squared = .121 (Adjusted R Squared = .048)					

Note. Means within columns with distinct superscripts revealed substantial changes at p<0.05

Table 6
The interaction effects between presenting complaints and procedures carried out and handling events on stress levels in cats

Handling event * Presenting complaints Dependent Variable: Stress					
Event	**Presenting complaint**	**Mean**	**Std. Error**	**95% Confidence Interval**	
				Lower Bound	**Upper Bound**
Taken out of the cage	vaccination and general PE	2.882	.170	2.544	3.220
	short, non-invasive, and minimally painful procedures	2.923	.195	2.537	3.310
	longer duration and potentially painful procedure	2.800	.314	2.177	3.423

Table 6 *(continue)*

Handling event * Presenting complaints Dependent Variable: Stress					
Event	**Presenting complaint**	**Mean**	**Std. Error**	**95% Confidence Interval**	
				Lower Bound	**Upper Bound**
Start PE	vaccination and general PE	3.059	.170	2.721	3.397
	short, non-invasive, and minimally painful procedures	3.462	.195	3.075	3.848
	longer duration and potentially painful procedure	3.600	.314	2.977	4.223
Before putting them back into the cage	vaccination and general PE	2.941	.170	2.603	3.279
	short, non-invasive, and minimally painful procedures	3.231	.195	2.844	3.617
	longer duration and potentially painful procedure	3.600	.314	2.977	4.223

Table 7
The effect test between estimated transportation distance out and handling events on stress levels in the cat

Tests of Between-Subjects Effects Dependent Variable: Stress					
Source	**Type III Sum of Squares**	**df**	**Mean Square**	**F**	**Sig.**
Corrected Model	8.213[a]	8	1.027	2.160	.037
Intercept	954.713	1	954.713	2008.384	.000
event	2.655	2	1.327	2.792	.066
distance cat	4.649	2	2.325	4.890	.009
event * distance cat	.687	4	.172	.361	.835
Error	45.635	96	.475		
Total	1066.000	105			
Corrected Total	53.848	104			

a. R Squared = .153 (Adjusted R Squared = .082)

Note. Means within columns with distinct superscripts revealed substantial changes at $p<0.05$

Table 8
The Kruskal-Wallis test between handling events and stress levels in the cat

Kruskal-Wallis Test	
	Stress
Kruskal Walis	5.286
df	2
Asymp. Sig	.071

Cats demonstrated the highest stress levels during the initial phase of the physical examination and the lowest when removed from the carrier or cage. The stress levels recorded when the cats returned to their cages decreased compared to those obtained during the physical examination and when they were removed, as illustrated in Figure 1.

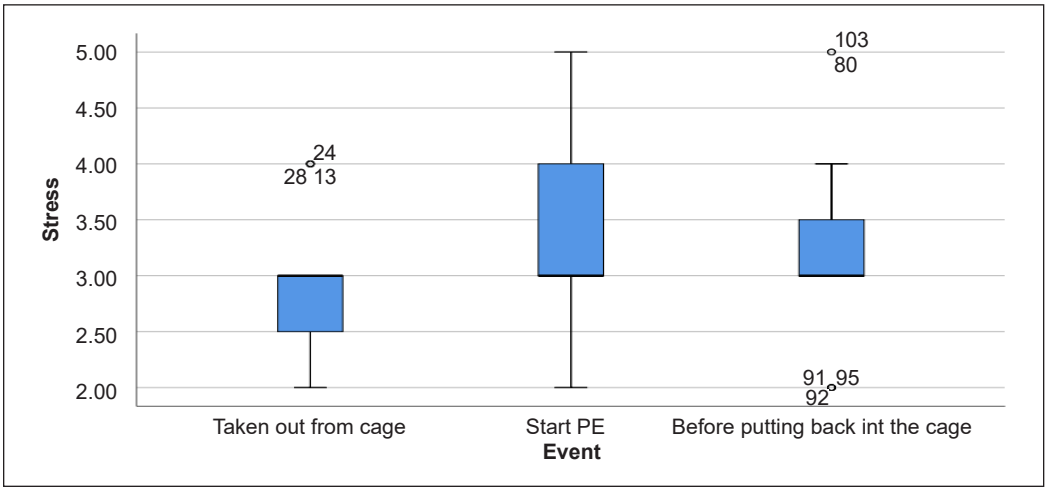

Figure 1. Graph showing stress level caused by each handling event

DISCUSSION

The current investigation assessed the behavioural indicators of stress in cats following transportation and clinical examinations during visits to the university veterinary hospital. Sex, breed, and age did not affect the cat's stress score. This is supported by Ramos et al. (2012), who assessed the cat's stress level by measuring the mean faecal glucocorticoid metabolites (mGCM). Adrenocortical activity, a valuable physiological indicator of arousal underlying potential emotional stress, was evaluated through the mGCM of cats. The associations between mGCM and age, sex, and breed were not detected (Ramos et al.,2012). Additionally, age, breed, and gender did not significantly influence the urinary corticoid: creatinine ratio (UCCR), which is used to assess stress levels (Cauvin et al., 2003).

This study revealed that age did not affect the observed stress levels ($P>0.05$), with no significant difference in stress levels between adult cats and kittens visiting the clinic. These findings highlight the importance of handling a cat's initial visit in a manner that minimises negative associations with the clinic and examination process. Palestrini (2009) emphasises that the first visit is particularly critical, as negative experiences during this early exposure can lead to behavioural issues in the future, such as increased anxiety, aggression, or avoidance of the veterinary environment.

Veterinarians should ensure that patients have a positive experience at the veterinary clinic and continue to monitor the emotional states of their cat patients during subsequent

visits, as the perception of cats deteriorates with each negative experience. Additionally, the environment of the consultation room itself does not directly affect the stress levels of the cats. This could be attributed to various activities during the specified time frame. For instance, certain cats may require more thorough physical examinations and extended waiting periods.

Consequently, the stress level may fluctuate depending on the duration required to complete a specific procedure within a designated time frame. Afterwards, a significant difference in stress level ($P < 0.05$) is observed when handling events, presenting complaints, and performing procedures are tested in relation to stress level. This suggested that handling events solely influenced stress levels, with no interaction between handling events and presenting complaints and procedures; this demonstrates the importance of handling cats effectively. Veterinarians sometimes prioritise the physical needs of patients, perhaps overlooking their behavioural requirements in routine care (Dawson et al., 2016). Hence, veterinary assistants should pay attention to how their interaction affects the patients and learn to choose the best way of handling the animals while working positively and calmly (Lloyd, 2017).

Additionally, transportation distance affects cat stress levels ($P <0.05$). This study demonstrates that transportation plays a significant role in stress behaviour. Most cats are rarely taken to unfamiliar locations, such as veterinary clinics. Consequently, individuals often perceive transportation as intimidating and anxiety-inducing. Shu and Gu (2021) indicate that transport stress can be alleviated by minimising disturbances and employing familiar scents, pheromones, dietary supplements (Beck, 2013), engaging distractions, and cat carriers to establish a concealed space for the cats, thus reducing excessive movement during transit. Pratsch et al. (2018) also found that the training effectively reduced stress during the car ride.

To alleviate stress during veterinary appointments, owners should be encouraged and provided with guidance on carrier-training their pets (Pratsch et al., 2018). Making an effort to acclimatise the cat to travel and handling can assist in decreasing the stress associated with veterinary appointments throughout the cat's lifetime. Cats were the most stressed at the start of the physical exams and the least stressed when initially taken out of the carrier. Cats' stress levels were measured upon their return to the cage between these events. Cats exhibit stress behaviours in a variety of handling settings. Consequently, understanding the best way to approach the animals minimises stress and makes the clinic visit a pleasurable experience (Karn-Buehler & Kuhne, 2021).

The study's limitations encompass the possibility of assessor bias, given that stress behaviours were recorded subjectively by clinic staff. Future research must address this limitation by integrating objective stress measures and examining additional variables pertinent to the clinical experience. Understanding and addressing the sources of stress allows veterinary practices to create more comfortable environments for cats, thereby enhancing their overall well-being during visits.

CONCLUSION

This study highlights that cats undergo significant stress during veterinary visits, especially during transportation, handling, and physical examinations. The stress identified in this study was mainly associated with handling events, such as the removal of cats from their carriers, conducting physical examinations, and returning them to the carriers. Despite resting and waiting in the reception area, stress-related behaviours continued, suggesting that these experiences substantially influence overall stress levels. The results indicate that transportation, waiting, and handling during clinical consultations are significant factors affecting stress levels in cats. Veterinary personnel must comprehend these dynamics and implement proactive measures to alleviate stress. Modifying handling techniques and minimising prolonged waiting periods for cats may effectively reduce stress levels. Cats may benefit from being situated in species-specific environments, away from visual stimuli like dogs or other animals, which can increase anxiety. The recommendation for future studies is to increase the sample size to improve the reliability of the findings. Additional research may investigate the application of advanced techniques, including electroencephalography, for a more objective and real-time assessment of stress. Analysing the effects of waiting and resting durations on stress levels will yield important insights for optimising the clinical environment.

ACKNOWLEDGEMENT

The authors are thankful to pet owners for allowing us to conduct the survey using their pets and to members and staff of the University Veterinary Hospital (UVH) Faculty of Veterinary Medicine, Universiti Putra Malaysia, for their unwavering support in ensuring the conduct of the work.

REFERENCES

Beck, A. (2013). Use of pheromones to reduce stress in sheltered cats. *Journal of Feline Medicine and Surgery*, *15*(9), 829–830. https://doi.org/10.1177/1098612x13500882

Bir, C., Ortez, M., Widmar, N. J. O., Wolf, C. A., Hansen, C., & Ouedraogo, F. B. (2020). Familiarity and use of veterinary services by us resident dog and cat owners. *Animals*, *10*(3), 483. https://doi.org/10.3390/ani10030483

Cauvin, A., Witt, A., Groves, E., Neiger, R., Martinez, T., & Church, D. (2003). The urinary corticoid: Creatinine ratio (UCCR) in healthy cats undergoing hospitalisation. *Journal of Feline Medicine and Surgery*, *5*(6), 329–333. https://doi.org/10.1016/s1098-612x(03)00067-6

Conti, L. M., Champion, T., Guberman, Ú. C., Mathias, C. H., Fernandes, S. L., Silva, E. G., Lázaro, M. A., Lopes, A. D., & Fortunato, V. R. (2017). Evaluation of environment and a feline facial pheromone analogue on physiologic and behavioural measures in cats. *Journal of feline medicine and surgery*, *19*(2), 165-170.

Dawson, L., Dewey, C., Stone, E., Guerin, M., & Niel, L. (2016). A survey of animal welfare experts and practicing veterinarians to identify and explore key factors thought to influence canine and feline welfare in relation to veterinary care. *Animal Welfare*, *25*(1), 125–134. https://doi.org/10.7120/09627286.25.1.125

Gourkow, N. (2012). *Emotions, mucosal immunity and respiratory disease in shelter cats*. https://doi.org/10.14264/uql.2017.1004

Herron, M. E., & Shreyer, T. (2014). The Pet-friendly veterinary practice. *Veterinary Clinics of North America Small Animal Practice*, *44*(3), 451–481. https://doi.org/10.1016/j.cvsm.2014.01.010

Karn-Buehler, J., & Kuhne, F. (2021). Perception of stress in cats by German cat owners and influencing factors regarding veterinary care. *Journal of Feline Medicine and Surgery*, *24*(8), 700-708. doi:10.1177/1098612X211041307

Lavendel, G. A., & Sapolsky, R. M. (1995). *Why zebras don't get ulcers: a guide to shess-related diseases and coping*. *Competitive Intelligence Review*, *6*(1), 84. Wiley. https://doi.org/10.1002/cir.3880060119

Levine, E. D. (2008). Feline fear and anxiety. *Veterinary Clinics of North America Small Animal Practice*, *38*(5), 1065–1079. https://doi.org/10.1016/j.cvsm.2008.04.010

Minimising Stress for patients in the veterinary hospital: why it is important and what can be done about it. *Veterinary Sciences*, *4*(4), 22. https://doi.org/10.3390/vetsci4020022

Lloyd, J. (2017). Minimising stress for patients in the veterinary hospital: why it is important and what can be done about it. *Veterinary Sciences*, *4*(4), 22. https://doi.org/10.3390/vetsci4020022

Mariti, C., Bowen, J. E., Campa, S., Grebe, G., Sighieri, C., & Gazzano, A. (2016). Guardians' perceptions of cats' welfare and behaviour regarding visiting veterinary clinics. *Journal of Applied Animal Welfare Science*, *19*(4), 375–384. https://doi.org/10.1080/10888705.2016.1173548

Mariti, C., Gazzano, A., Moore, J. L., Baragli, P., Chelli, L., & Sighieri, C. (2012). Perception of dogs' stress by their owners. *Journal of Veterinary Behavior*, *7*(4), 213–219. https://doi.org/10.1016/j.jveb.2011.09.004

McCobb, E. C., Patronek, G. J., Marder, A., Dinnage, J. D., & Stone, M. S. (2005). Assessment of stress levels among cats in four animal shelters. *Journal of the American Veterinary Medical Association*, *226*(4), 548–555. https://doi.org/10.2460/javma.2005.226.548

Miller, D. B., & O'Callaghan, J. P. (2002). Neuroendocrine aspects of the response to stress. *Metabolism*, *51*(6), 5–10. https://doi.org/10.1053/meta.2002.33184

Moberg, G. P. & Mench, J. A. (2000). *The biology of animal stress: basic principles and implications for animal welfare.* CABI Publishing. https://doi.org/10.1079/9780851993591.0000

Moffat, K. (2008). Addressing canine and feline aggression in the veterinary clinic. *Veterinary Clinics of North America Small Animal Practice*, *38*(5), 983–1003. https://doi.org/10.1016/j.cvsm.2008.04.007

Möstl, K., Egberink, H., Addie, D., Frymus, T., Boucraut-Baralon, C., Truyen, U., Hartmann, K., Lutz, H., Gruffydd-Jones, T., Radford, A. D., Lloret, A., Pennisi, M. G., Hosie, M. J., Marsilio, F., Thiry, E., Belák, S., & Horzinek, M. C. (2013). Prevention of infectious diseases in cat shelters. *Journal of Feline Medicine and Surgery*, *15*(7), 546–554. https://doi.org/10.1177/1098612x13489210

Nibblett, B. M., Ketzis, J. K., & Grigg, E. K. (2014). Comparison of stress exhibited by cats examined in a clinic versus a home setting. *Applied Animal Behaviour Science*, *173*, 68–75. https://doi.org/10.1016/j.applanim.2014.10.005

Palestrini, C. (2009). *Situational sensitivities. In bsava manual of canine and feline behavioural medicine* (pp. 169-181). BSAVA Library. https://doi.org/10.22233/9781905319879.16

Pereira, J. S., Fragoso, S., Beck, A., Lavigne, S., Varejão, A. S., & Da Graça Pereira, G. (2015). Improving the feline veterinary consultation: the usefulness of Feliway spray in reducing cats' stress. *Journal of Feline Medicine and Surgery*, 18(12), 959–964. https://doi.org/10.1177/1098612x15599420

Perego, R., Proverbio, D., & Spada, E. (2014). Increases in heart rate and serum cortisol concentrations in healthy dogs are positively correlated with an indoor waiting-room environment. *Veterinary Clinical Pathology*, *43*(1), 67–71. https://doi.org/10.1111/vcp.12118

Phillips, M., Jeyaretnam, J., & Jones, H. (2000). Disease and injury among veterinarians. *Australian Veterinary Journal*, *78*(9), 625–629. https://doi.org/10.1111/j.1751-0813.2000.tb11939.x

Pratsch, L., Mohr, N., Palme, R., Rost, J., Troxler, J., & Arhant, C. (2018). Carrier training cats reduces stress on transport to a veterinary practice. *Applied Animal Behaviour Science*, *206*, 64–74. https://doi.org/10.1016/j.applanim.2018.05.025

Pruett, S. B. (2003). Stress and the immune system. *Pathophysiology*, *9*(3), 133–153. https://doi.org/10.1016/s0928-4680(03)00003-8

Quimby, J. M., Smith, M. L., & Lunn, K. F. (2011). Evaluation of the effects of hospital visit stress on physiologic parameters in the cat. *Journal of Feline Medicine and Surgery*, *13*(10), 733–737. https://doi.org/10.1016/j.jfms.2011.07.003

Ramos, D., Arena, M., Reche-Junior, A., Daniel, A., Albino, M., Vasconcellos, A., Viau, P., & Oliveira, C. (2012). Factors affecting faecal glucocorticoid levels in domestic cats (Felis catus): a pilot study with single and large multi-cat households. *Animal Welfare*, *21*(2), 285–291. https://doi.org/10.7120/09627286.21.2.285

Ramos, D., & Mills, D. S. (2009). Human directed aggression in Brazilian domestic cats: Owner reported prevalence, contexts and risk factors. *Journal of Feline Medicine and Surgery*, *11*(10), 835–841. https://doi.org/10.1016/j.jfms.2009.04.006

Riemer, S., Heritier, C., Windschnurer, I., Pratsch, L., Arhant, C., & Affenzeller, N. (2021). A review on mitigating fear and aggression in dogs and cats in a veterinary setting. *Animals*, *11*(1), 158. https://doi.org/10.3390/ani11010158

Rodan, I. (2010). Understanding feline behavior and application for appropriate handling and management. *Topics in Companion Animal Medicine*, *25*(4), 178–188. https://doi.org/10.1053/j.tcam.2010.09.001

Shu, H., & Gu, X. (2021). Effect of a synthetic feline facial pheromone product on stress during transport in domestic cats: a randomised controlled pilot study. *Journal of Feline Medicine and Surgery*, *24*(8), 691–699. https://doi.org/10.1177/1098612x211041305

Stella, J., Croney, C., & Buffington, T. (2012). Effects of stressors on the behaviour and physiology of domestic cats. *Applied Animal Behaviour Science*, *143*(2–4), 157–163. https://doi.org/10.1016/j.applanim.2012.10.014

Trevorrow, N. (2014). Helping cats cope with stress in veterinary practice. *Veterinary Nursing Journal*, *28*(10), 327–329. https://doi.org/10.1111/vnj.12074

Tuozzi, A., Arhant, C., Anderle, K., Backes, J., Cords, C., Magierski, V., Rault, J., & Windschnurer, I. (2021). Effects of human presence and voice on the behaviour of shelter dogs and cats: a preliminary study. *Animals*, *11*(2), 406. https://doi.org/10.3390/ani11020406

Volk, J. O., Felsted, K. E., Thomas, J. G., & Siren, C. W. (2011). Executive summary of phase 2 of the bayer veterinary care usage study. *Journal of the American Veterinary Medical Association*, *239*(10), 1311–1316. https://doi.org/10.2460/javma.239.10.131.

Pertanika J. Trop. Agric. Sci. 48 (6): 1831 - 1846 (2025)

PERTANIKA JOURNALS

TROPICAL AGRICULTURAL SCIENCE

Journal homepage: http://www.pertanika.upm.edu.my/

Review Article

Q Fever in Small Ruminants: A Review on Epidemiology, Risk Factors, and Diagnostic Approaches

Khaiyal Vili Palani and Rozaihan Mansor*

Department of Farm and Exotic Animal Medicine and Surgery, Faculty of Veterinary Medicine, Universiti Putra Malaysia, 43400 Serdang, Selangor, Malaysia

ABSTRACT

Coxiella burnetii, which causes Q fever, is a significant zoonotic disease targeting livestock, particularly sheep and goats, with global implications for public health and agriculture. The disease presents diverse epidemiological patterns across regions, with goats often exhibiting higher seroprevalence rates compared to sheep. Transmission occurs primarily through breathing in contaminated airborne particles, with environmental determinants such as farm management practices and wind speed playing crucial roles in disease spread. Risk factors include animal age, flock size, tick infestations, environmental conditions, and poor biosecurity measures. Serological methods, primarily enzyme-linked immunosorbent assay (ELISA), remain widely used for large-scale surveillance due to their cost-effectiveness, sensitivity, and ability to detect past exposure. On the other hand, polymerase chain reaction (PCR) offers higher specificity. It is preferred for detecting active infections and environmental contamination, whereas the immunofluorescence assay (IFA) is a reliable confirmatory test. Emerging molecular techniques, including metagenomic next-generation sequencing (mNGS), surface plasmon resonance (SPR) biosensors, and up-converting phosphor technology-based lateral flow (UPT-LF) assay, demonstrate promise for enhancing diagnostic accuracy and early detection. However, regional disparities in diagnostic approaches, insufficient surveillance data, and gaps in epidemiological research continue to pose significant challenges. Addressing these gaps through integrated diagnostic strategies, affordable PCR implementation, and targeted research on transmission dynamics in livestock, wildlife, and environmental reservoirs is essential. Such efforts will strengthen Q fever control and prevention measures, minimising its impact on public health and livestock productivity.

Keywords: Coxiella burnetii, diagnostic methods, epidemiology, Q fever, risk factors, small ruminants, zoonotic disease

ARTICLE INFO

Article history:
Received: 10 February 2025
Accepted: 10 June 2025
Published: 25 November 2025

DOI: https://doi.org/10.47836/pjtas.48.6.10

E-mail addresses:
khaiyalvilivet@gmail.com (Khaiyal Vili Palani)
rozaihan@upm.edu.my (Rozaihan Mansor)
* Corresponding author

e-ISSN: 2231-8542

INTRODUCTION

Coxiella burnetii, of the order *Legionellales*, causes Q fever, a highly contagious zoonotic disease in livestock. Its chronic effects pose significant challenges to veterinary and healthcare surveillance and care systems (Villari et al., 2018; Clark & Magalhães, 2018; Larson et al., 2019). *C. burnetii* is a widespread intracellular bacterium causing acute and chronic disease, with cattle, sheep, and goats as its main hosts (Yohannes & Mekonen, 2018). Q fever affects arthropods, wildlife, companion animals, and livestock, often asymptomatic in the latter (Salifu et al., 2019). Q fever in livestock is mostly subclinical, where infected animals are mostly asymptomatic with no obvious signs of illness. Symptoms, when present, may include fever, conjunctivitis, arthritis, mastitis, and reproductive issues such as abortion and infertility. In the acute phase*, C. burnetii* tends to localise in certain organs like the liver, lungs, spleen, and bloodstream. In contrast, ongoing bacterial shedding in urine and faeces marks the chronic phase. Reproductive complications like abortions, usually in late pregnancy, with rates ranging from 3% to 80%, stillbirths, low birth weight, and neonatal mortality are common in goats and sheep (Saglam & Sahin, 2016; Tagesu, 2019).

Following a large Q fever outbreak in the Netherlands from 2007 to 2011, a cross-sectional study involving 478 human patients revealed that the health issues extended up to a decade post-infection. About 50% had serious work and physical limitations, over 25% struggled with daily and social activities, and over one-third were found to have stopped working permanently, while fatigue affected 91.2% (Bronner et al., 2020). A Q fever outbreak in 2011 linked to a goat farm in Washington involved 17 herds across Washington, Montana, and Oregon, and the outbreak caused by *C. burnetii* led to 21 human cases. Polymerase chain reaction (PCR) testing confirmed bacterial shedding in 25% of 629 goats, while enzyme-linked immunosorbent assay (ELISA) showed a 12% seroprevalence. This outbreak highlighted the need for strong collaboration between veterinary, medical, and public health sectors for effective zoonotic disease control (Anderson et al., 2015).

C. burnetii can be detected in the air and dust on livestock farms (Espí et al., 2021) while enduring extreme conditions and adhering to dust, increasing the risk of environmental dispersal and outbreaks (Clark & Magalhães, 2018). Q fever is a highly contagious illness that can appear as occasional outbreaks or larger epidemics. It poses a significant health risk, especially to veterinarians, laboratory technicians, farmers, and abattoir workers. In humans, acute infections typically present as self-limiting fever, pneumonia, or hepatitis, while chronic cases can lead to endocarditis (Yohannes & Mekonen, 2018). In Southern Belgium, veterinarians who had frequent contact with livestock showed a higher seroprevalence of Q fever (58.5%) compared to those who dealt exclusively only with companion animals like dogs, cats, and horses (6.25%), indicating that occupational exposure significantly influences the risk of the infection (Pozzo et al., 2016). A Q fever outbreak in an abattoir in Sydney affected eight male workers, with common symptoms including fever (87.5%),

lethargy (75%), headaches (62.5%), and nausea or vomiting (62.5%). Notably, one of them died, whereby Q fever was identified as the main contributing factor. The cases were linked to high-risk exposures such as handling birthing materials and slaughtering pregnant animals (Lord et al., 2016). *C. burnetii*, primarily linked to domestic small ruminants as the key origin of human infections, has been weaponised due to its high infectivity, environmental persistence in a spore-like form, and windborne transmission potential, posing a biological warfare threat (Tagesu, 2019). The Centres for Disease Control and Prevention (CDC) has designated *C. burnetii* as a Category B bioterrorism agent, making Q fever reportable in many countries, including the USA, and highlighting its higher prevalence than previously recognised (Bioterrorism Agents/Diseases, 2018; Eldin et al., 2017).

In northwest Italy, a cross-sectional study assessed the individual and flock seroprevalence of *C. burnetii* in small ruminants, addressing the limited data previously based almost solely on records of breeding issues in livestock farms (Rizzo et al., 2016). Coxiellosis results in substantial losses due to miscarriages and the birth of dead offspring in small ruminants (Zahid et al., 2016). Another study in Southeast Iran assessed *C. burnetii* antibody prevalence in small ruminants, revealing high antibody positivity and identifying sheep and goats as significant Q fever reservoirs on the spot (Ezatkhah et al., 2015). Research in Ethiopia detected antibodies against *C. burnetii* in small grazers slaughtered at a slaughterhouse (Yohannes & Mekonen, 2018). Similarly, a study in The Gambia's Kiang West district assessed the extent of *C. burnetii* antibodies in adults and small ruminants, along with *C. burnetii* shedding in small grazers within domestic settings and associated risk factors. Results showed that *C. burnetii* infection is local in humans and animals in the region, with exposure linked to specific settings and shared environments (Bok et al., 2017). Q fever is known to cause abortion in livestock and febrile illness in humans. Outbreaks in Australia and the Netherlands have been related to miscarriages in small ruminant herds. However, limited information exists on Q fever in livestock and humans in Ghana. Therefore, a study was conducted in the Tongu area of Ghana's Volta region to determine the prevalence of Q fever in cattle, sheep, and goats (Johnson et al., 2019).

In South Africa, Q fever is often overlooked as a zoonosis, resulting in substantial losses in livestock and game animals due to reproductive issues (Mangena et al., 2021). A study in Egypt aimed to address the limited data on Q fever by assessing *C. burnetii*-specific antibodies in 299 herds of ruminants and camels. The review also called for more epidemiological studies to better understand Q fever's impact on human health and the market in Egypt (Klemmer et al., 2018). Q fever has drawn renewed attention, particularly following the large outbreak in the Netherlands from 2007 to 2009, emphasising its significance as a looming public health concern. New Zealand is the only country where Q fever is not reported (Pexara et al., 2018). The biggest human Q fever epidemic happened in the Netherlands between 2006 and 2009, rooted in dairy goat herds with abortion matters caused by the infection (Bontje et al., 2016). A study investigated the hosts, origins, and modes of spread associated with the significant Q

fever occurrence in the Serbia-Montenegro frontier region (Debeljak et al., 2018). Between 2013 and 2015, an outbreak of abortions in grazing animals linked to Q fever affected the Jimma zone and the city of Ethiopia (Proboste et al., 2021).

EPIDEMIOLOGY

The distribution of Q fever differs significantly across regions and livestock species, based on Table 1. In Asia, studies in Iran and Turkey show sheep are more affected than goats (Ezatkhah et al., 2015; Karagul et al., 2019), whereas in Jordan, goats exhibit a higher seroprevalence than sheep (Lafi et al., 2020). In the Middle Eastern and Sub-Saharan African countries, goats are generally more vulnerable, with a particularly high seroprevalence of

Table 1
Epidemiology of Q fever across different regions

Continent	Country	Species	Sample Size	Seroprevalence (%)	Year of Study	Reference
Africa	Egypt	Goat	311	6.8	2015–2016	Klemmer et al. (2018)
		Sheep	716	8.9		
		Cattle	840	19.3		
		Buffalo	304	11.2		
		Camel	528	40.7		
	Egypt	Goat	39	28.2	2016–2017	Abushahba et al. (2017)
		Sheep	109	25.68		
		Human	35	25.71		
	Ethiopia	Goat	297	48.8	2016	Ibrahim et al. (2021)
		Sheep	269	28.9		
		Cattle	135	9.6		
		Camel	171	55.7		
		Human	190	27.0		
	Ethiopia	Goat	385	51.9	2017–2022	Oakley et al. (2024)
		Sheep	323	39.9		
		Cattle	340	8.8		
		Camel	369	16.3		
		Human (Pastoralist)	323	25.0		
	Ghana	Goat	100	10.0	Not Stated	Johnson et al. (2019)
		Sheep	158	28.4		
		Cattle	204	21.7		
	Guinea	Goat	408	4.4	2017–2019	Troupin et al. (2022)
		Sheep	486	2.3		
		Cattle	463	20.5		
	Kenya	Goat	132	0.76	2019	Kiptanui et al. (2022)
		Sheep	283	1.41		
		Cattle	725	8.14		
	Kenya	Goat	280	18.2	2013	Larson et al. (2019)
		Sheep	100	13.0		

Table 1 *(continue)*

Continent	Country	Species	Sample Size	Seroprevalence (%)	Year of Study	Reference
		Cattle	157	5.7	2013	Larson et al. (2019)
		Camel	312	19.9		
	Kenya	Goat	83	83.1	Not Stated	Nakeel et. al. (2016)
		Sheep	80	57.5		
		Cattle	156	89.7		
		Human	90	26.0		
	South Africa	Sheep	69	4.3	Not Stated	Mangena et al. (2021)**
		Cattle	331	9.4		
		Pig	107	0.9		
	The Gambia	Small Ruminants (Goat & Sheep)	615	24.9	2014	Bok et al. (2017)
		Human	599	3.8-9.7		
Asia	Iran	Goat	241	22.4	2011	Ezatkhah et al. (2015)
		Sheep	127	33.9		
	Jordan	Goat	250	43.3	2015–2017	Lafi et al. (2020)
		Sheep	480	27.0		
	Malaysia	Goat	132	9.9	2019	Jesse et al. (2020)
		Sheep	140	14.3		
	Malaysia	Goat	100	70%	Not Stated	Ahmad et al. (2024)
	Saudi Arabia	Goat	423	34.04	2012–2013	Jarelnabi et al. (2018)
		Sheep	630	12.38		
		Cattle	428	30.67		
		Camel	489	51.53		
	Turkey	Goat	205	10.24	Not Stated	Karagul et al. (2019)
		Sheep	627	14.19		
Europe	France	Goat	349*	41.5	2012–2015	Gache et al. (2017)
		Sheep	522*	25.7		
		Cattle	731*	22.2		
	Italy	Goat	206	19.5	2012	Rizzo et al. (2016)
		Sheep	111	38.7		
		Mixed Flocks (Goat & Sheep)	94	15.9		
	Spain	Goat	135	24.4	2015–2018	Espí et al. (2021)
		Sheep	154	8.4		
		Cattle	163	18.4		
		Iberian Red Deer	83	8.4		
		Cantabrian Chamois	41	7.3		
		Fallow Deer	73	6.9		
		European Wild Boar	73	5.5		
		Roe Deer	57	3.5		
		Human	1312	15.9		

Note. *Number of herds: Seroprevalence (%) calculated between-herds/within-herds
**Study on slaughter-livestock

34.04% reported in Saudi Arabia (Jarelnabi et al., 2018). In Kenya, however, findings are more variable, with one study reporting a lower prevalence in goats (0.76%) compared to sheep (1.41%) (Kiptanui et al., 2022), while the other two studies observed significantly greater rates in goats than in sheep (Nakeel et al., 2016; Larson et al., 2019). This likely reflects regional differences in livestock management and environmental conditions rather than methodological variation.

Research from Italy, Spain, and France in Europe highlights variability across species. In Italy, sheep showed higher seroprevalence than goats (38.7% vs. 19.5%) (Rizzo et al., 2016). In Spain, goats had higher rates (24.4%) than sheep (8.4%) (Espí et al., 2021), while France also reported goats again leading (41.5%) over sheep (25.6%), although the prevalence of the disease in sheep remains notably high (Gache et al., 2017). These differences may reflect variations in veterinary practices or disease surveillance systems between the countries.

In Southeast Asia, limited studies on Q fever have provided valuable insights. One study conducted on goats in Peninsular Malaysia revealed an extremely high seropositivity of 70% among dairy goats from Besut (Ahmad et al., 2024). In contrast, another study in Malaysia found that sheep (14.3%) had higher seroprevalence rates than goats (9.9%) (Jesse et al., 2020). However, the region lacks comprehensive data, highlighting the need for further investigations to better understand the disease's dynamics across species and locations.

A test done on sheep and goats in Egypt found a relatively high seroprevalence of Q fever in sheep (25.68%) and goats (28.2%) but no notable correlation between factors such as location, age, reproductive condition, or history of miscarriages and the rates of Q fever infection (Abushahba et al., 2017). In Nandi County, Kenya, a study found that animal species was the only notable predictor for Q fever, with cattle being more susceptible than sheep and goats. Other factors showed no statistical relevance (Kiptanui et al., 2022). The prevalence in cattle also varies widely, with higher rates in European countries like France (22.2%) (Gache et al., 2017) compared to lower rates in Asian and African countries such as Iran (9.6%) (Ezatkhah et al., 2015) and Kenya (8.14%) (Kiptanui et al., 2022). This variation might result from differences in climate, livestock production systems, or diagnostic practices.

No clear global trend identifies one species as consistently exhibiting the highest Q fever seroprevalence. Rather, species dominance varies by region, underscoring the need for targeted disease control and prevention strategies adapted to local contexts.

RISK FACTORS

Various animal and management-related factors have been linked to Q fever seropositivity across different regions, which can be seen in Table 2. Larger flock size was consistently identified as a risk factor in multiple studies from Jordan (Lafi et al., 2020) and Italy (Rizzo et al., 2016; Villari et al., 2018). Age was another recurring factor, with older goats and sheep tending to be more seropositive in The Gambia, Jordan, and Saudi Arabia (Bok

et al., 2017; Lafi et al., 2020; Aljafar et al., 2020). However, a study in Malaysia found that younger animals were more at risk, highlighting that age-related susceptibility to Q fever may vary based on study populations or local management practices (Jesse et al., 2020). Certain exposure-related factors, such as proximity to other flocks, environmental contamination, and contact with companion animals, were also identified as predisposing factors to Q fever risk in small ruminants in some studies (Rizzo et al., 2016; Opaschaitat et al., 2018; Lafi et al., 2020). Many studies identified risk factors unique to their local settings with limited overlap across countries. This suggests that the epidemiology of Q fever is highly context-specific, shaped by regional husbandry practices, environmental conditions, species dynamics, and geographical factors.

Table 2
Reported risk factors for Q fever

Continent	Country	Species	Risk Factors	Reference
Africa	Ethiopia	Goat, Sheep, Cattle, Camel	None	Oakley et al. (2024)
		Human (Pastoralist)	Age (<15, ≥49) in households having goats with a history of abortion	
	South Africa	Sheep, Cattle, Pig*	Auction-sourced animals	Mangena et al. (2021)*
	The Gambia	Goat, Sheep	Grazing in village areas, recent lambing, old (age not specified)	Bok et al. (2017)
		Human	The presence of a seropositive animal within their compound	
Asia	Jordan	Goat, Sheep	Large flock size (≥100 animals), older animals (≥2 years), loaned breeding bucks/rams, presence of cats, goats (animal-level)	Lafi et al. (2020)
	Malaysia	Goat, Sheep	Young (age not specified), breed (Barbados Black Belly sheep), production purpose (meat > dairy)	Jesse et al. (2020)
	Saudi Arabia	Goat, Sheep, Cattle	Old (>1 year old), species (goat > sheep/cattle)	Aljafar et al. (2020)
	Saudi Arabia	Sheep	Tick infestation, history of Q fever	Elsohaby et al. (2021)
	Thailand	Goat, Sheep, Cattle, Buffalo, Wild ruminants	Contamination from bedding, manure, and the environment	Opaschaitat et al. (2018)
Europe	Italy	Goat, Sheep	Flock size (>12 animals), mixed flocks, contact with other flocks, farms in the western area, history of infertility	Rizzo et al. (2016)
	Italy	Sheep	Large flock size (>50 animals), high-altitude farms (501–1200 m)	Villari et al. (2018)

Note. *Study on slaughter-livestock

DIAGNOSTIC METHODS

Table 3 refers to the recent diagnostic approaches used for Q fever detection in small ruminants where it shows a dominance of serological methods. ELISA appears to be the most preferred method for screening and determining seroprevalence in studies across different countries, indicating past exposure to infection (Ibrahim et al., 2021). This preference may be attributed to ELISA's cost-effectiveness compared to molecular techniques, particularly large-scale surveillance (Lafi et al., 2020). The method also allows the processing of many samples simultaneously, making it ideal for estimating exposure in populations even when the infection is no longer active. Additionally, ELISA kits are widely available and have been validated for specific animal species. Indirect ELISA remains the most widely utilised, with several commercial kits such as ID Screen®, PrioCHECK™, and IDEXX tests being selected multiple times across diverse geographical settings (Lafi et al., 2020; Abbass et al., 2020; Espí et al., 2021; Ibrahim et al., 2021; Mangena et al., 2021; Ahmad et al., 2024; Saadullah et al., 2024).

Immunofluorescence assay (IFA) is another diagnostic test used to confirm seropositivity by detecting phase-specific antibodies, and it was reported only once in recent studies (Abbass et al., 2020). On the other hand, molecular techniques such as conventional PCR and real-time quantitative PCR (RT-qPCR) are used to detect any ongoing active infection by amplifying specific *C. burnetii* DNA. They were less frequently used in recent years of study and typically in combination with ELISA rather than as standalone diagnostics (Abbass et al., 2020; Mangena et al., 2021). PCR has also been proven to analyse dust and aerosol samples collected from livestock farms, confirming the presence of *C. burnetii* DNA in the environment (Espí et al., 2021).

A study from Malaysia was the only one that used a commercial sandwich-ELISA kit to determine the seroprevalence of Q fever in small ruminants. It was also the only study to report the sensitivity and specificity of the diagnostic kit, demonstrating high diagnostic accuracy with 100% sensitivity and 99.6% specificity (Jesse et al., 2020). Almost no other study reported the sensitivity and specificity of the different diagnostic methods used, which presents a major limitation in assessing and comparing diagnostic tools' performance.

Overall, ELISA remains the primary diagnostic approach for Q fever surveillance in small ruminants. In contrast, molecular diagnostic and confirmatory tests like PCR and IFA are used alongside serological screening rather than independently. Future studies should emphasise reporting the diagnostic accuracy of various diagnostic methods used and consider combining serological and molecular methods to improve the reliability of Q fever detection in small ruminants.

Beyond the commonly used diagnostic methods, a few studies have explored more advanced methods with potential relevance to small ruminants. Metagenomic next-generation sequencing (mNGS) was highlighted for its efficiency in *C. burnetii* pathogen

Table 3
Diagnostic methods used for detection of Coxiella burnetii *in small ruminants*

Diagnostic Method	Type/Model	Target	Sample	Species	Sensitivity/ Specificity	Country	References
ELISA (Indirect)	ID Screen® Q Fever Indirect Multi-species (FQS-MS, IDvet, Grabels, France)	Antigen-specific antibodies against *C. burnetii*	Serum	Goat, Sheep	Not reported	Pakistan	Saadullah et al. (2024)
	PrioCHECK™ Ruminant Q Fever Ab Plate Kit (Thermo Fisher Scientific, France)	Q fever-specific antibodies (Phases I+II purified antigens)	Serum	Goat	Not reported	Malaysia	Ahmad et al. (2024)
	PrioCHECK™ Ruminant Q Fever Ab Plate Kit (Thermo Fisher Scientific)	Antibodies against *C. burnetii* (Phases I and II antigens)	Serum	Goat, Sheep, Cattle	Not reported	Spain	Espí et al. (2021)
	ID-vet Q Fever (FQS-MS ver 0514 GB, Grabels, France)	Phases I and II strain	Serum	Goat, Sheep, Cattle, Camel	Not reported	Ethiopia	Ibrahim et al. (2021)
	IDEXX Q Fever 2/Strip Ab test kit (IDEXX Laboratories, Liebefeld-Bern, Switzerland)	IgG antibodies	Serum	Sheep, Cattle, Pig	Not reported	South Africa	Mangena et al. (2021)
	CHEKIT *C. burnetii* Ab ELISA test kit (IDEXX Laboratories, Broomfield, CO, USA)	Phases I and II antibodies	Serum	Goat, Sheep	Not Reported	Jordan	Lafi et al. (2020)
	ID Screen® Q Fever Indirect Multi-species (FQS-MS-2P, IDvet, Grabels, France)	Phase II antibodies (IgM, IgG)	Serum, Milk	Goat, Sheep, Cattle, Human	Not reported	Egypt	Abbass et al. (2020)
ELISA (Sandwich)	*Coxiella burnetii* Q Fever ELISA Kit (Sunlong Biotech Co., Ltd., China)	Q fever specific-antibodies	Serum	Goat, Sheep	100%/99.6%	Malaysia	Jesse et al. (2020)

Table 3 *(continue)*

Diagnostic Method	Type/Model	Target	Sample	Species	Sensitivity/ Specificity	Country	References
PCR	Conventional PCR targeting the IS1111 element	Multi-copy transposase *C. burnetii* IS1111 gene	**Sheep:** Pooled foetal tissues (liver, spleen, lung); **Cattle:** Tissue samples (Mammary gland, uterus, penis, testes, ovary)	Sheep, Cattle	Not reported	South Africa	Mangena et al. (2021)
	Real-Time Quantitative PCR (RT-qPCR)	*C. burnetii* IS1111 repetitive gene	Whole-blood	Goat, Sheep, Cattle, Human	Not reported	Egypt	Abbass et al. (2020)
IFA	*Coxiella burnetii* I+II IFA IgG/IgM/ IgA (Vircell, Spain)	Phase II IgG and IgM anti-*C. burnetii* antibodies	Serum	Goat, Sheep, Cattle, Human	Not reported	Egypt	Abbass et al. (2020)

detection in China's human Q fever outbreak investigation. Although the diagnostic method was primarily applied to human plasma samples, the study also performed mNGS and IFA on goat and cattle blood samples. The detection of *C. burnetii* by mNGS was verified by IFA, supporting the reliability and effectiveness of mNGS as a diagnostic tool for acute Q fever (Huang et al., 2021). Another human Q fever case study from China also proved the application of mNGS in detecting *C. burnetii* within 48 hours, with results validated by IFA (Yang et al., 2022). This highlights the method's rapidity, comprehensiveness, and ability to detect low pathogen loads, which suggests potential for application in livestock animals, including goats and sheep, the key hosts of *C. burnetii,* for early diagnosis and outbreak surveillance when traditional methods fall short.

A study conducted in Bulgaria developed a Surface Plasmon Resonance (SPR)-based biosensor to detect *C. burnetii* antibodies in human serum. Despite being designed for human samples, it underscores the potential of biosensor platforms for rapid, on-site, and user-friendly serological detection of *C. burnetii* by offering a promising alternative to conventional methods requiring proper laboratory settings (Genova-Kalou et al., 2024). Given the challenges of diagnosing Q fever in livestock under field conditions, such biosensor technologies could be great solutions for early detection and surveillance in small ruminants.

An Up-converting Phosphor Technology-based Lateral Flow (UPT-LF) assay was developed in China for rapid and quantitative detection of *C. burnetii* phase I strains, demonstrating high sensitivity, specificity, and field applicability, with successful testing on experimentally infected mice and naturally infected tick samples. Based on the assay's reliable performance in tissue and tick samples and its suitability for field use, it could also potentially be adapted for detecting *C. burnetii* in livestock, including small ruminants, especially in on-site or low-resource settings (Zhang et al., 2020).

CONCLUSION

Q fever remains a significant zoonosis with varying prevalence, particularly in goats and sheep across Africa, Asia, and Europe. Due to its feasibility and cost-effectiveness, ELISA is widely used for serological screening, especially in countries like Malaysia. At the same time, PCR and IFA offer a higher specificity and a valuable and reliable confirmatory test, respectively. However, critical knowledge gaps persist, especially in Southeast Asia, where the detailed epidemiology of *C. burnetii* and risk factors are still unclear. This lack of data hinders disease control, particularly among small ruminants, the primary reservoirs of *C. burnetii.* Holistic studies on seroprevalence and risk factors in this population are urgently needed.

Moreover, the disparity in diagnostic methods across regions is a challenge. ELISA is suitable for large-scale screening, but PCR should be prioritised in high-risk areas for active infection detection. While ELISA is vital in resource-limited settings, complementing

it with PCR when feasible will improve diagnostic accuracy. Research into affordable PCR and more advanced methods with rapid on-site detection capability, like SPR-biosensor or UPT-LF implementation in such settings, is crucial. Future studies should also investigate transmission dynamics in wildlife and environmental reservoirs to enhance outbreak control. Addressing these diagnostic and transmission gaps will be essential for preventing future outbreaks and reducing the impacts of Q fever on public health and livestock production.

ACKNOWLEDGEMENT

This review was performed under the Faculty of Veterinary Medicine, Universiti Putra Malaysia, with funding support from GP-IPS/2025/9816400. The authors acknowledge the Department of Veterinary Services (DVS), Malaysia, for their collaborative support.

REFERENCES

Abbass, H., Selim, S. A. K., Sobhy, M. M., El-Mokhtar, M. A., Elhariri, M., & Abd-Elhafeez, H. H. (2020). High prevalence of *Coxiella burnetii* infection in humans and livestock in Assiut, Egypt: A serological and molecular survey. *Veterinary World, 13*(12), 2578. https://doi.org/10.14202/vetworld.2020.2578-2586

Abushahba, M. F., Abdelbaset, A. E., Rawy, M. S., & Ahmed, S. O. (2017). Cross-sectional study for determining the prevalence of Q fever in small ruminants and humans at El Minya Governorate, Egypt. *BMC Research Notes, 10*, 1–6. https://doi.org/10.1186/s13104-017-2868-2

Ahmad, K., Mustaffa, N. D. A. N., Azmi, N. S., Ariffin, S. M. Z., Ghazali, M. F. B., & Ibrahim, N. S. (2024). Detection and seroprevalence of Q fever infection in dairy goats in Besut district, Malaysia. *Journal of Advanced Veterinary and Animal Research, 11*(2), 231. https://doi.org/10.5455/javar.2024.k768

Aljafar, A., Salem, M., Housawi, F., Zaghawa, A., & Hegazy, Y. (2020). Seroprevalence and risk factors of Q fever (*Coxiella burnetii* infection) among ruminants reared in the eastern region of the Kingdom of Saudi Arabia. *Tropical Animal Health and Production, 52*, 2631–2638. https://doi.org/10.1007/s11250-020-02295-6

Anderson, A. D., Szymanski, T. J., Emery, M. P., Kohrs, P. H., Bjork, A. C., Marsden-Haug, N., Nett, R. J., Woodhall, D. M., Self, J. S., Fitzpatrick, K. A., Priestley, R. A., & Kersh, G. J. (2015). Epizootiological investigation of a Q fever outbreak and implications for future control strategies. *Journal of the American Veterinary Medical Association*, *247*(12), 1379-1386. https://doi.org/10.2460/javma.247.12.1379

Bioterrorism Agents/Diseases (by category). (2018). Centers for Disease Control and Prevention: Emergency Preparedness and Response. https://emergency.cdc.gov/agent/agentlist-category.asp

Bok, J., Hogerwerf, L., Germeraad, E. A., Roest, H. I. J., Faye-Joof, T., Jeng, M., Nwakanma, D., Secka, A., Stegeman, A., Goossens, B., Wegmüller, R., van der Sande, M. A. B., van der Hoek, W., & Secka, O. (2017). *Coxiella burnetii* (Q fever) prevalence in associated populations of humans and small ruminants in The Gambia. *Tropical Medicine & International Health, 22*(3), 323–331. https://doi.org/10.1111/tmi.12827

Bontje, D. M., Backer, J. A., Hogerwerf, L., Roest, H. I. J., & van Roermund, H. J. W. (2016). Analysis of Q fever in Dutch dairy goat herds and assessment of control measures by means of a transmission model. *Preventive Veterinary Medicine, 123*, 71–89. https://doi.org/10.1016/j.prevetmed.2015.11.004

Bronner, M. B., Haagsma, J. A., Dontje, M. L., Barmentloo, L., Kouwenberg, R. M., Loohuis, A. G. O., De Groot, A., Erasmus, V., & Polinder, S. (2020). Long-term impact of a Q-fever outbreak: An evaluation of health symptoms, health-related quality of life, participation and health care satisfaction after ten years. *Journal of psychosomatic research*, *139*, 110258. https://doi.org/10.1016/j.jpsychores.2020.110258

Clark, N. J., & Soares Magalhães, R. J. (2018). Airborne geographical dispersal of Q fever from livestock holdings to human communities: A systematic review and critical appraisal of evidence. *BMC Infectious Diseases, 18*, 1–9. https://doi.org/10.1186/s12879-018-3135-4

Debeljak, Z., Medić, S., Baralić, M., Andrić, A., Tomić, A., Vidanović, D., Šekler, M., Matović, K., & Vasković, N. (2018). Clinical, epidemiological, and epizootic features of a Q fever outbreak in the border region between Serbia and Montenegro. *The Journal of Infection in Developing Countries, 12*(05), 290-296. https://doi.org/10.3855/jidc.9918

Eldin, C., Mélenotte, C., Mediannikov, O., Ghigo, E., Million, M., Edouard, S., Mége, J.-L., Maurin, M., & Raoult, D. (2017). From Q fever to *Coxiella burnetii* infection: A paradigm change. *Clinical Microbiology Reviews, 30*(1), 115–190. https://doi.org/10.1128/cmr.00045-16

Elsohaby, I., Elmoslemany, A., El-Sharnouby, M., Alkafafy, M., Alorabi, M., El-Deeb, W. M., Al-Marri, T., Qasim, I., Alaql, F. A., & Fayez, M. (2021). Flock management risk factors associated with Q fever infection in sheep in Saudi Arabia. *Animals, 11*(7), 1948. https://doi.org/10.3390/ani11071948

Espí, A., Del Cerro, A., Oleaga, Á., Rodríguez-Pérez, M., López, C. M., Hurtado, A., Rodríguez-Martínez, L. D., Barandika, J. F., & García-Pérez, A. L. (2021). One health approach: An overview of Q fever in livestock, wildlife, and humans in Asturias (Northwestern Spain). *Animals, 11*(5), 1395. https://doi.org/10.3390/ani11051395

Ezatkhah, M., Alimolaei, M., Khalili, M., & Sharifi, H. (2015). Seroepidemiological study of Q fever in small ruminants from Southeast Iran. *Journal of Infection and Public Health, 8*(2), 170-176. https://doi.org/10.1016/j.jiph.2014.08.009

Gache, K., Rousset, E., Perrin, J. B., De Cremoux, R., Hosteing, S., Jourdain, E., Guatteo, R., Nicollet, P., Touratier, A., Calavas, D., & Sala, C. (2017). Estimation of the frequency of Q fever in sheep, goat, and cattle herds in France: Results of a 3-year study of the seroprevalence of Q fever and excretion level of *Coxiella burnetii* in abortive episodes. *Epidemiology & Infection, 145*(15), 3131–3142. https://doi.org/10.1017/s0950268817002308

Genova-Kalou, P., Dyankov, G., Krumova, S., Simeonov, K., Valkov, T., Baymakova, M., Tsachev, I., & Fournier, P.-E. (2024). Applicability of biosensor technologies in the detection of *Coxiella burnetii* infection in clinical samples. *Biotechnology & Biotechnological Equipment, 38*(1), 2350163. https://doi.org/10.1080/13102818.2024.2350163

Huang, M., Ma, J., Jiao, J., Li, C., Chen, L., Zhu, Z., Ruan, F., Xing, L., Zheng, X., Fu, M., Ma, B., Gan, C., Mao, Y., Zhang, C., Sun, P., Liu, X., Lin, Z., Chen, L., Lu, Z. … Xia, J. (2021). The epidemic of Q fever in 2018 to 2019 in Zhuhai city of China determined by metagenomic next-generation sequencing. *PLoS Neglected Tropical Diseases, 15*(7), e0009520. https://doi.org/10.1371/journal.pntd.0009520

Ibrahim, M., Schelling, E., Zinsstag, J., Hattendorf, J., Andargie, E., & Tschopp, R. (2021). Sero-prevalence of brucellosis, Q-fever and Rift Valley fever in humans and livestock in Somali Region, Ethiopia. *PLoS Neglected Tropical Diseases, 15*(1), e0008100. https://doi.org/10.1371/journal.pntd.0008100

Jarelnabi, A. A., Alshaikh, M. A., Bakhiet, A. O., Omer, S. A., Aljumaah, R. S., Harkiss, G. D., Mohammed, O. B., & Hussein, M. F. (2018). Seroprevalence of Q fever in farm animals in Saudi Arabia. *Biomedical Research, 29*(5), 895-900. https://doi.org/10.4066/biomedicalresearch.29-17-770

Jesse F. F. A., Paul, B. T., Hashi, H. A., Lim, E. T. C., Abdurrahim, N. A., & Mohd Lila, M. A. (2020). Seroprevalence and risk factors of Q fever in small ruminant flocks in selected States of Peninsular Malaysia. *The Thai Journal of Veterinary Medicine, 50*(4), 511-517. https://doi.org/10.56808/2985-1130.3056

Johnson, S. A. M., Kaneene, J. B., Asare-Dompreh, K., Tasiame, W., Mensah, I. G., Afakye, K., Simpson, S. V., & Addo, K. (2019). Seroprevalence of Q fever in cattle, sheep, and goats in the Volta region of Ghana. *Veterinary Medicine and Science, 5*(3), 402-411. https://doi.org/10.1002/vms3.160

Karagul, M. S., Malal, M. E., & Akar, K. (2019). Seroprevalence of Q fever in sheep and goats from the Marmara region, Turkey. *Journal of Veterinary Research*, *63*(4), 527-532. https://doi.org/10.2478/jvetres-2019-0070

Kiptanui, J., Gathura, P. B., Kitala, P. M., & Bett, B. (2022). Seroprevalence estimates of Q fever and the predictors for the infection in cattle, sheep, and goats in Nandi County, Kenya. *Veterinary Medicine International*, *2022*(1), 3741285. https://doi.org/10.1155/2022/3741285

Klemmer, J., Njeru, J., Emam, A., El-Sayed, A., Moawad, A. A., Henning, K., Elbeskawy, M. A., Sauter-Louis, C., Straubinger, R. K., Neubauer, H., & El-Diasty, M. M. (2018). Q fever in Egypt: Epidemiological survey of *Coxiella burnetii*-specific antibodies in cattle, buffaloes, sheep, goats, and camels. *PLoS ONE, 13*(2), e0192188. https://doi.org/10.1371/journal.pone.0192188

Lafi, S. Q., Talafha, A. Q., Abu-Dalbouh, M. A., Hailat, R. S., & Khalifeh, M. S. (2020). Seroprevalence and associated risk factors of Coxiella burnetii (Q fever) in goats and sheep in northern Jordan. *Tropical Animal Health and Production*, *52*, 1553-1559. https://doi.org/10.1007/s11250-019-02153-0

Larson, P. S., Espira, L., Grabow, C., Wang, C. A., Muloi, D., Browne, A. S., Deem, S. L., Fèvre, E. M., Foufopoulos, J., Hardin, R., & Eisenberg, J. N. (2019). The sero-epidemiology of *Coxiella burnetii* (Q fever) across livestock species and herding contexts in Laikipia County, Kenya. *Zoonoses and Public Health*, 66(3), 316-324. https://doi.org/10.1111/zph.12567

Lord, H., Fletcher-Lartey, S., Weerasinghe, G., Chandra, M., Egana, N., Schembri, N., & Conaty, S. (2016). AQ fever cluster among workers at an abattoir in south-western Sydney, Australia, 2015. *Western Pacific surveillance and response journal: WPSAR*, *7*(4), 21-27. https://doi.org/10.5365/wpsar.2016.7.2.012

Mangena, M., Gcebe, N., Pierneef, R., Thompson, P. N., & Adesiyun, A. A. (2021). Q fever: Seroprevalence, risk factors in slaughter livestock and genotypes of *Coxiella burnetii* in South Africa. *Pathogens*, 10(3), 258. https://doi.org/10.3390/pathogens10030258

Nakeel, M. J., Arimi, S. M., Kitala, P., Nduhiu, G., Njenga, J. M., & Wabacha, J. K. (2016). A sero-epidemiological survey of brucellosis, Q-fever and leptospirosis in livestock and humans and associated risk factors in kajiado county-Kenya. *Journal of Tropical Diseases*, *4*(3), 8. https://doi.org/10.4172/2329-891X.1000215

Oakley, R. B., Gemechu, G., Gebregiorgis, A., Alemu, A., Zinsstag, J., Paris, D. H., & Tschopp, R. (2024). Seroprevalence and risk factors for Q fever and Rift Valley fever in pastoralists and their livestock in Afar, Ethiopia: A One Health approach. *PLoS Neglected Tropical Diseases*, 18(8), e0012392. https://doi.org/10.1371/journal.pntd.0012392

Opaschaitat, P., Ramrin, L., & Yingst, S. L. (2018). Epidemiology of Q fever in ruminants in the north-east and the north region of Thailand, 2012 to 2013. *KKU Veterinary Journal*, 28(1), 19-25.

Pexara, A., Solomakos, N., & Govaris, A. (2018). Q fever and seroprevalence of *Coxiella burnetii* in domestic ruminants. *Veterinaria Italiana*, 54(4), 265-279. https://doi.org/10.12834/vetit.1113.6046.3

Pozzo, F. D., Martinelle, L., Léonard, P., Renaville, B., Renaville, R., Thys, C., Smeets, F., Czaplicki, G., Van Esbroeck, M., & Saegerman, C. (2016). Q Fever serological survey and associated risk factors in veterinarians, Southern Belgium, 2013. *Transboundary and Emerging Diseases*, *64*(3), 959–966. https://doi.org/10.1111/tbed.12465

Proboste, T., Deressa, F. B., Li, Y., Kal, D. O., Gelalcha, B. D., & Soares Magalhães, R. J. (2021). Geographical variation in *Coxiella burnetii* seroprevalence in dairy farms located in South-Western Ethiopia: Understanding the broader community risk. *Pathogens*, 10(6), 646. https://doi.org/10.3390/pathogens10060646

Rizzo, F., Vitale, N., Ballardini, M., Borromeo, V., Luzzago, C., Chiavacci, L., & Mandola, M. L. (2016). Q fever seroprevalence and risk factors in sheep and goats in northwest Italy. *Preventive Veterinary Medicine, 130*, 10-17. https://doi.org/10.1016/j.prevetmed.2016.05.014

Saadullah, M., Ahmed, I., Kashif, M., Rafique, M. K., Yousaf, M. S., Meraj, M. T., Tehreem, A., Saeed, M. A., Saleemi, M. K., Nazir, S., & Rehman, T. U. (2024). Antioxidant Status and Biochemical Alterations in *Chlamydia abortus* and *Coxiella burnetii* Infected Small Ruminants. *Pakistan Veterinary Journal*, *44*(4). https://doi.org/10.29261/pakvetj/2024.283

Saglam, A. G., & Sahin, M. (2016). *Coxiella burnetii* in samples from cattle herds and sheep flocks in the Kars region of Turkey. *Veterinarni Medicina, 61*(1), 17–22. https://doi.org/10.17221/8678-vetmed

Salifu, S. P., Bukari, A. R. A., Frangoulidis, D., & Wheelhouse, N. (2019). Current perspectives on the transmission of Q fever: Highlighting the need for a systematic molecular approach for a neglected disease in Africa. *Acta Tropica, 193*, 99-105. https://doi.org/10.1016/j.actatropica.2019.02.032

Tagesu, T. (2019). Fever in small ruminants and its public health importance. *Journal of Dairy & Veterinary Sciences, 9*(1), 555752. https://doi.org/10.19080/jdvs.2019.09.555752

Troupin, C., Ellis, I., Doukouré, B., Camara, A., Keita, M., Kagbadouno, M., Bart, J.-M., Diallo, R., Lacôte, S., Marianneau, P., Groschup, M. H., & Tordo, N. (2022). Seroprevalence of brucellosis, Q fever and Rift Valley fever in domestic ruminants in Guinea in 2017–2019. *BMC Veterinary Research, 18*(1), 64. https://doi.org/10.1186/s12917-022-03159-x

Villari, S., Galluzzo, P., Arnone, M., Alfano, M., Geraci, F., & Chiarenza, G. (2018). Seroprevalence of *Coxiella burnetii* infection (Q fever) in sheep farms located in Sicily (Southern Italy) and related risk factors. *Small Ruminant Research, 164*, 82-86. https://doi.org/10.1016/j.smallrumres.2018.05.006

Winter, F., Schoneberg, C., Wolf, A., Bauer, B. U., Prüfer, T. L., Fischer, S. F., Gerdes, U., Runge, M., Ganter, M., & Campe, A. (2021). Concept of an active surveillance system for Q fever in German small ruminants—conflicts between best practices and feasibility. *Frontiers in Veterinary Science, 8*, 623786. https://doi.org/10.3389/fvets.2021.623786

Yang, Y., Shi, Q., Jin, Q., Yang, Z., Li, W., Han, J., Mao, J., & Zheng, B. (2022). Case report: metagenomic next-generation sequencing clinches the diagnosis of acute Q fever and verified by indirect immunofluorescence assay. *Frontiers in Medicine*, 9, 846526. https://doi.org/10.3389/fmed.2022.846526

Yohannes, G., & Mekonen, S. (2018). Review on Q fever in small ruminants and its public health importance. *Biomedical Journal of Scientific & Technical Research*, 9(1), 6914-6922. https://doi.org/10.26717/bjstr.2018.09.001754

Zahid, M. U., Hussain, M. H., Saqib, M., Neubauer, H., Abbas, G., Khan, I., Mansoor, M. K., Asi, M. N., Ahmad, T., & Muhammad, G. (2016). Seroprevalence of Q fever (Coxiellosis) in small ruminants of two districts in Punjab, Pakistan. *Vector-Borne and Zoonotic Diseases, 16*(7), 449-454. https://doi.org/10.1089/vbz.2015.1852

Zhang, P., Jiao, J., Zhao, Y., Fu, M., Wang, J., Song, Y., Zhou, D., Wang, Y., Wen, B., Yang, R., & Xiong, X. (2020). Development and evaluation of an up-converting phosphor technology-based lateral flow assay for rapid and quantitative detection of *Coxiella burnetii* phase I strains. *BMC Microbiology*, *20*, 1-10. https://doi.org/10.1186/s12866-020-01934-0

Pertanika J. Trop. Agric. Sci. 48 (6): 1847 - 1860 (2025)

PERTANIKA JOURNALS

TROPICAL AGRICULTURAL SCIENCE

Journal homepage: http://www.pertanika.upm.edu.my/

Hydrogen Peroxide as a Potential Priming Agent to Reinvigorate Deteriorated Sweet Corn Seed

Sharif Azmi Abdurahman[1,2], Uma Rani Sinniah[1]*, Azizah Misran[1], Muhamad Hazim Nazli[1], and Indika Weerasekara[3]

[1]Department of Crop Science, Faculty of Agriculture, Universiti Putra Malaysia, 43400 UPM Serdang, Selangor, Malaysia
[2]Fakulti Pertanian Lestari, Universiti Malaysia Sabah, 90509 Sandakan, Sabah, Malaysia
[3]Seed and Planting Material Development Centre, Department of Agriculture, 20400 Peradeniya, Sri Lanka

ABSTRACT

Sweet corn (*Zea mays* L. *Saccharata* Sturt) seeds, like other crops, often experience deterioration during storage, which can negatively impact their germination and performance. This study investigated the impact of hydrogen peroxide (H_2O_2) priming on the germination, vigour, and antioxidant activities of deteriorated sweet corn seeds. A one-year-old GSH1005Y sweet corn seed sample, with a germination of 48%, was primed in H_2O_2 concentrations ranging from 1 mM to 20 mM for 24 hours, followed by drying. Seed germination and vigour were assessed through germination and electrical conductivity (EC) tests. Antioxidant activities, including catalase (CAT), peroxidase (POD), superoxide dismutase (SOD), and malondialdehyde (MDA) content, were also evaluated. Results showed that priming with H_2O_2 significantly improved seed germination. Seeds treated with 10 mM H_2O_2 achieved 69% germination, a 21% increase compared to the untreated seeds. Priming with 5 mM and 7.5 mM H_2O_2 also enhanced germination (67% and 66%, respectively). Seedling performance was best at 10 mM H_2O_2, reducing mean germination time by 16%, increasing the coefficient of velocity of germination, and resulting in longer seedlings and higher shoot dry weight (45.5% increase over untreated seeds). Higher concentrations (12.5 mM to 20 mM) did not improve performance and negatively affected seedlings. H_2O_2 priming increased SOD activity while reducing MDA content, indicating less oxidative stress. EC measurements showed improved membrane integrity, especially at 10 mM H_2O_2. In conclusion, H_2O_2 priming at 10

ARTICLE INFO

Article history:
Received: 17 February 2025
Accepted: 06 May 2025
Published: 25 November 2025

DOI: https://doi.org/10.47836/pjtas.48.6.11

E-mail addresses:
sh.azmi@ums.edu.my | shazmiey.abdurahman@me.com (Sharif Azmi Abdurahman)
umarani@upm.edu.my (Uma Rani Sinniah)
azizahm@upm.edu.my (Azizah Misran)
m_hazim@upm.edu.my (Muhamad Hazim Nazli)
weerasekaradoa@gmail.com (Indika Weerasekara)
*Corresponding author

mM for 24 hours significantly improved seed quality and vigour, offering a cost-effective solution for enhancing deteriorated seeds.

Keywords: antioxidant activity, hydrogen peroxide priming, membrane integrity, sweet corn seed, seed priming.

INTRODUCTION

Corn (*Zea mays* L.) is among the top three crops cultivated worldwide for multiple purposes ranging from feedlot to biofuel production (Erenstein et al., 2022). Several types of corn are being cultivated such as flint, dent, waxy and sweet corn. Corn is cultivated using seeds as planting materials however, as biological material seeds will eventually undergo deterioration, and planting deteriorated seeds will lead to poor stand establishment (Weerasekara et al., 2021). Seed deterioration is an inevitable process that is influenced by various factors such as seed maturity at harvest, seed moisture content during storage, and the genetic makeup of the species. Seeds rely on stored carbon for survival and seedling establishment. In most seeds, this reserve is primarily in the form of starch, which is derived from the partitioning of assimilated carbon (typically as sucrose). Starch serves as an inert, water-insoluble storage compound. However, genetic mutations in certain crops, such as the endosperm of sweet corn (*Zea mays* L. *Saccharata* Sturt), can alter seed storage composition. Sweet corn is unique as it has several mutated genes such as *shrunken2* (*sh2*), *sugary1* (*su1*), *sugary enhancer* (*se*) that are responsible in preventing conversion of soluble sucrose into starch, resulting in high sucrose content and low starch as storage compound in seed endosperm. In addition to low storage compounds in the seeds, drying of sweet corn seed causes air pockets to form between the seed's endosperm, embryo, and seed coat. This leads to poor seed quality, resulting in low and inconsistent germination, reduced seed vigour, and hindered seedling establishment in sweet corn (Pairochteerakul et al., 2018; Styer et al., 1980; Suo et al., 2017; Tracy, 2000).

Seed pre-treatment methods, such as priming, have been shown to improve seed quality, particularly for aged or deteriorated seeds, by enhancing their germination or vigour prior to sowing. Priming involves a controlled process of hydration and drying, allowing seeds to undergo early metabolic processes without initiating radicle emergence. This process helps seeds achieve more rapid and uniform germination when re-imbibed increases seed vigour, which enhances seedling establishment (Bradford, 1986; Raj & Raj, 2019). Priming enhances seed performance through various physiological mechanisms. It activates or elevates the levels of specific enzymes and proteins associated with germination, stimulates cellular repair mechanisms, and boosts the antioxidant defence system, which collectively contribute to improved stress tolerance and seed vigour (Gammoudi et al., 2020). These changes help accelerate germination and improve overall seedling development. Among the different priming techniques, osmo-priming is a specific method that involves soaking

seeds in solutions with controlled osmotic potential, such as osmotic solutions or solutions containing substances like polyethylene glycol or hydrogen peroxide (H_2O_2). After soaking in such solution and dried to initial seed moisture content, the seeds is ready to use for germination (Chen & Arora, 2011). Osmo-priming is an effective, cost-efficient approach widely used globally to enhance seedling establishment (Farooq et al., 2019).

Today, the use of hydrogen peroxide, H_2O_2, as pre-treatment to improve plant growth is gaining attention. Lariguet et al. (2013) stated that H_2O_2 at proper concentration helps in breaking seed dormancy and improves germination while over-accumulation would lead to cell injury which can be detrimental to the seeds (Jeevan Kumar et al., 2015). Many studies had reported that the application of H_2O_2 alone or a combination with other compounds as seed or seedling pre-treatment induced and activated plant abiotic stress protective mechanisms such as accumulation of latent defence mechanism, by maintaining non-toxic levels just enough to signal stress ROS scavenging actions (Hossain et al., 2015). Many antioxidant mechanisms by plants such as superoxide dismutase (SOD), catalase (CAT) and guaiacol peroxidase (POD) have been attributed to redox balance from the act of signalling by H_2O_2 in plants (Ślesak et al., 2007). H_2O_2 has been used as foliar spray and for priming in many plants (Banerjee & Roychoudhury, 2019). Among the crops, wheat (Hameed & Iqbal, 2014), rice (Jira-Anunkul & Pattanagul, 2020), and sunflower (Silva et al., 2020) showed that concentrations ranging between 1μM to 100 mM of H_2O_2 as priming agent improved seed viability, vigour as well as seedling performance, however, the effect of H_2O_2 on deteriorated sweet corn seeds have never been tested. Therefore, this study was conducted to investigate the potential of H_2O_2 as a priming agent to invigorate deteriorated sweet corn seed by observing viability, vigour, seedling performance, and antioxidant activity particularly seed antioxidant enzymes.

MATERIALS AND METHODS

Seed Sample

The experiment was carried out at the Seed Technology Laboratory, Universiti Putra Malaysia, Selangor, Malaysia. A year-old GSH1005Y sweet corn seeds harvested at 35 days after pollination, dried, and stored in an ambient room (26±3°C, moisture content =8%) was used. Seed germination upon retrieval under the aforementioned condition was 48%.

Priming Treatment

The initial seed moisture content (MC) was determined using the high constant temperature oven method at 130±3°C for 4 hours (ISTA, 2021). Then, the seeds were soaked in different concentrations of H_2O_2 i.e. 1, 2.5, 5, 7.5, 10, 12.5, 17.5, and 20 mM for 24 hours at a temperature of 26±3°C. After 24 hours, the seeds were removed from the priming solution

and dried for 3 to 4 days at a temperature of 26±3°C until they reached the initial MC, following which the seeds were subjected to germination within 24 hours. Germination test was carried out using sand as the substrate. Seed germination was observed, and daily germination was recorded. Final Germination Percentage (FGP) was recorded on the seventh day (ISTA, 2021).

Seed Germination, Vigour and Seedling Performance

Seven days after the initiation of the germination test, Mean Germination Time (MGT) and Coefficient Velocity of Germination (CVG) based on daily seed germination count were calculated using the formula by Kader (2005) as follows:

$$\text{MGT (day)} = \frac{\Sigma\,(n \times d)}{\Sigma\,N}$$

where n = number of seeds germinated on each day, d = number of days from the beginning of the test, and N = total number of seeds germinated at the termination of the experiment.

$$\text{CVG} = \frac{(G_1+G_2+\cdots+G_n)}{(1\times G_1+2\times G_2+\cdots+n\times G_n)} \times 100$$

Where G is the number of germinated seeds and n is the last day of germination

Then, all germinated seedlings on the seventh day after sowing were arranged based on the length, and five median seedlings per replicate were selected for seedling performance analysis. Root length was measured from the tip of the longest root to the base of the hypocotyl while shoot length was measured from the end of the longest primary leaf to the base of the hypocotyl. Samples used for seedling length measurement were separated into shoot and root and dried at 65°C for 48 hours to get the root and shoot dry weight (Brar et al., 2019).

Antioxidant Enzymatic Activities

For antioxidant enzyme analysis, the sample was prepared using the method of Abuelsoud et al., (2020). Seed sample was ground into a powder form using liquid nitrogen. Then, a sample of 0.15 grams of the ground sample was mixed with 1.5 mL of ice-cold 2-Morpholinoethanesulfonic acid potassium salt (MES-KOH) (50 mM, pH 6.0) extraction buffer in 2 mL microcentrifuge tube followed by centrifuging at 16,000 × *g* in 4°C for 20 minutes. A sample of supernatant was taken for the antioxidant enzymatic assay. Catalase

(CAT) activity was measured using the method described by Aebi (1984) where the absorbance at 240 nm was used and the result was expressed in µmol/min/mg FW. Guaiacol Peroxidase (POD) assay was measured using protocol by Maehly & Chance (1954) with absorbance reading at 470 nm before POD activity was calculated and expressed in nmol/min/mg FW. Superoxide Dismutase (SOD) activity was measured using the method by Gupta et al., (1993) and the absorbance reading of SOD activity was taken at 560 nm and the activity was expressed in unit/mg FW. All absorbance reading was made using a micro-plate spectrophotometer (Thermo scientific MULTISKAN GO).

Electrical Conductivity Test and Malondialdehyde Content Measurement

To measure the oxidative damage on the seed membrane, electrical conductivity test was conducted where 25 seeds for each treatment were weighed, following which it was placed in 75 mL of deionized water in a beaker and left for 24 hours at 20°C. After 24 hours, the seed leachate was measured using a digitalized conductivity meter (labCHEM-CP conductivity meter) and expressed in µS/cm/g (Thant et al., 2017). To estimate the lipid peroxidation, Malondialdehyde (MDA) content was measured using Stewart & Bewley, (1980). The seed sample was homogenized using 2 mL distilled water and centrifuged 10,000 × *g* for 15 minutes to get supernatant. A reaction mixture of 1 mL of supernatant, 2 mL of TBA/TCA (0.5% thiobarbituric acid (TBA) in 20% trichloroacetic acid (TCA)) was incubated for 30 minutes in a water bath at temperature of 95±3°C. It was placed in an ice tray immediately after the incubation to stop the reaction before reading was taken at 450, 532 and 600 nm using a micro-plate spectrophotometer (Thermo scientific MULTISKAN GO) and MDA was calculated and expressed in mmol/g FW.

Statistical Analysis

Analysis of variance (ANOVA) was carried out for all parameters and if significant difference was found, means comparison was done using Tukey Test with minimum 95% confidence interval. All statistical analysis were carried out using statistical software, Statistical Analysis System, SAS 9.4 (SAS Institute, Cary, NC).

RESULTS AND DISCUSSION

Seed Germination, Vigour and Seedling Performance

In this study, priming with H_2O_2 significantly affected seed germination, as illustrated in Figure 1. A substantial increase in germination percentage can be observed with H_2O_2 concentrations ranging from 0 to 20 mM, compared to untreated seeds, which exhibited 48% of germination. Priming with H_2O_2 concentrations between 5 mM and 10 mM has led to significant improvements in seed germination, whereas lower or higher concentrations did

not differ substantially from untreated seeds. The greatest enhancement in seed germination was observed in seeds treated with 10 mM H_2O_2 for 24 hours, which showed 69% seed germination, reflecting a 21% increase relative to untreated seeds. Seeds primed with 5 mM and 7.5 mM H_2O_2 exhibit 67% and 66% seed germination, respectively, corresponding to 19% and 18% increase in germination compared to untreated seeds. No significant differences in germination were found between these three concentrations. In contrast, treatments with 1 mM, 2.5 mM, 12.5 mM, 15 mM, 17.5 mM and 20 mM resulted in no significant change in seeds germination, to the untreated control (48%). Priming with H_2O_2 is not new as many other crops also showed positive improvements in seed germination for example priming with H_2O_2 in rice improved seed germination by 13% and 14% in cotton (Hemalatha et al., 2017).

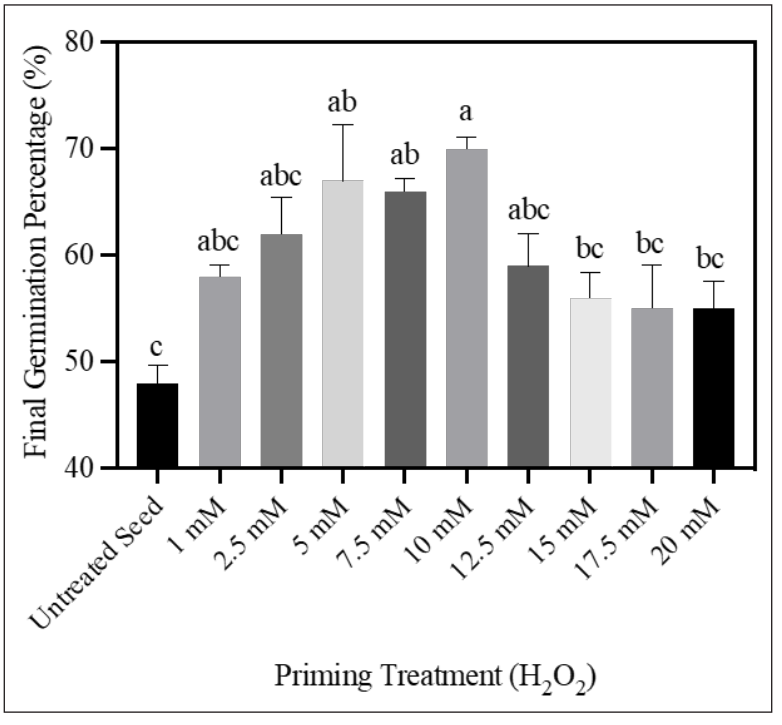

Figure 1. Final germination percentage of sweet corn seed primed with 0 to 20 mM hydrogen peroxide for 24 hours. Means with same letter on the bars are not significantly different at $P > 0.05$ using the Tukey Test

Apart from the seed viability, there was a significant difference observed in MGT and CVG when seeds were primed with different H_2O_2 concentration as illustrated in Figure 2. Priming at 10 mM of H_2O_2 reduces time of germination up to 16% from the untreated seed germination time. There was no clear trend in seed's CVG, however, the study showed that the highest CVG was obtained when the seeds were primed in 10 mM of H_2O_2 (25.2) for 24 hours. compared to untreated seeds (21.31).

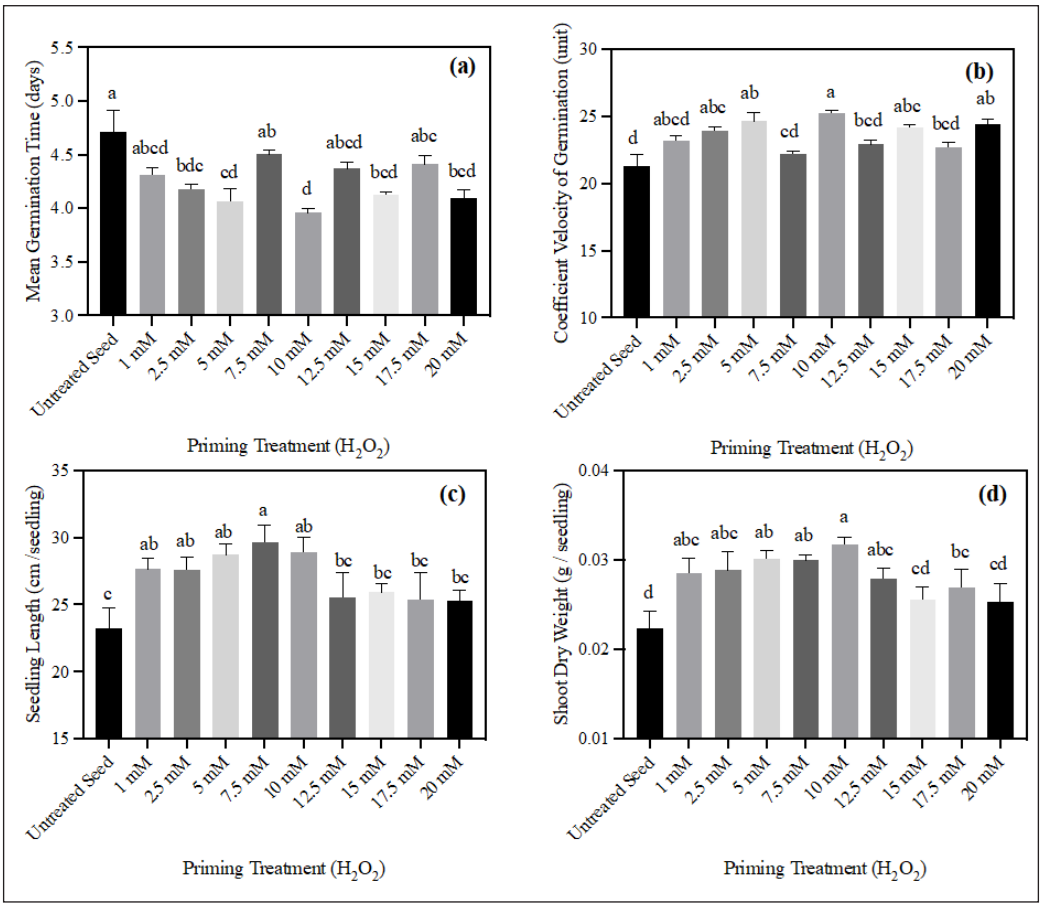

Figure 2. Seed vigour parameters, Mean Germination Time (a) and Coefficient Velocity of Germination (b) with seedling performance based on Seedling Length (c) and Shoot Dry Weight (d) of deteriorated sweet corn seed primed with different concentrations of hydrogen peroxide. Means with the same letter in each parameter are not significantly different at $P > 0.05$ using the Tukey Test

Seedling performance parameters such as seedling length showed a significant difference when the sweet corn seeds were treated with different priming concentrations of H_2O_2 for 24 hours. Seedling length shows an increasing trend and peaks at 7.5 mM of H_2O_2 which was around 29.66 cm/seedling, followed by seeds primed at 10 mM H_2O_2 at 28.93 cm/seedling. However, seedling length after 12.5 mM declines and does not differ statistically with untreated seeds at 23.23 cm/seedling. The same trend is observed in shoot dry weight where priming between 1 mM to 12.5 mM improved the shoot dry weight but higher concentrations cause a decline. Priming at 10 mM improves seedling performance, with 45.5% increment in shoot dry weight compared to untreated seeds (0.022 g / seedling). In contrast with parameters mentioned earlier, priming with different concentrations of H_2O_2 shows no improvement and no significant difference in root dry weight.

For comparison, in pepper seed invigoration, priming with 10 mM of H_2O_2 improved MGT, Germination Rate and Germination Index while under salinity stress (Gammoudi et al., 2020). In a study by Jira-Anunkul & Pattanagul, (2020), priming on rice seeds using H_2O_2 showed improvement in seedling length, and root and shoot dry mass when primed with less than 10 mM of H_2O_2 and an increase of more than 15 mM had detrimental effect on seedling performance. Another finding by Ashraf et al., (2015) showed seed priming using H_2O_2 improved shoot and root dry mass of maize in water deficit stress study, indicating there were some roles of exogenous H_2O_2 responsible in the improvement observed in all of those studies.

A research by Neto et al. (2005) showed better plant growth in terms of shoot dry mass, root dry mass and leaf area when the plant was supplemented with exogenous H_2O_2 three days after sowing, as the study observed the increase in SOD content in plant root and leaves resulting in lower lipid peroxidation in the plant seedling. In rice plants, it was observed that plant shoot and root decreased, however application of H_2O_2 improved seedling growth especially on the shoot due to an increase in glutathione level in the plant (Hu et al., 2009) and there was an increase of antioxidant enzymes in rice seedling leaves (Chou et al., 2012), therefore improving the seedling growth. Verma et al., (2015) also suggested that H_2O_2 production during germination would activate reserve mobilization by signalling storage organ to mobilize its reserve to promote axis growth which explains the higher shoot and root dry mass in this study. Most of these studies showed alleviation in antioxidant defence mechanism.

Antioxidant Enzymatic Activities

Priming with H_2O_2 for 24 hours significantly affected the activities of catalase (CAT), peroxidase (POD), and superoxide dismutase (SOD) in sweet corn seeds as summarized in Table 1. Untreated seeds exhibited a baseline CAT activity of 10.75 μmol/min/mg FW. Priming with H_2O_2 has led to a decrease in CAT activity across all concentrations. Seeds primed with 5 mM H_2O_2 showed the highest CAT activity (8.89 μmol/min/mg FW), a 17.3% reduction, while the lowest activity was observed at 17.5 mM H_2O_2 (7.43 μmol/min/mg FW), a 30.4% reduction. Seeds treated with 10 mM H_2O_2, which show the highest seed germination with 24.9% also has reduced CAT activity (8.07 μmol/min/mg FW). There are no significant differences in CAT activity between the 1 mM to 15 mM concentrations and 20 mM. Priming with H_2O_2 generally reduces POD activity. Seeds primed with 5 mM and 7.5 mM show a reduction of 18.3% and 19.1% in POD activity, respectively. The most significant reductions (31.3% to 41.1%) are observed at 1 mM, 2.5 mM, and 20 mM. However, seeds primed with 10 mM, 12.5 mM, and 15 mM show minimal reductions (3.6% to 7.4%) compared to untreated seeds, indicating that moderate H_2O_2 concentrations (10 mM to 15 mM) may help preserve POD activity. SOD activity increase significantly

following priming. The untreated seeds have 5.33 units/mg FW, which have increased by 20.5% at 1 mM, 31.7% at 5 mM, and 42.8% at 10 mM H_2O_2. SOD activity peaked at 10 mM (7.61 units/ mg FW) and the activity decreases at 20 mM (5.92 units/mg FW), with 10.1% reduction compared to the untreated seeds. These results suggest that moderate H_2O_2 concentrations (up to 10 mM) enhance antioxidant defences, while higher concentrations higher concentrations may cause oxidative stress.

Table 1.
Summary of analysis of variance (ANOVA) of different priming concentration of hydrogen peroxide on biochemical activities focusing on on electrical conductivity of seed leachate, malondialdehyde and antioxidant enzymes of one year old sweet corn seeds

			Antioxidant Enzymes Activities		
Priming Concentration	**Electrical Conductivity of Seed Leachate**	**Malondialdehyde (MDA)**	**Catalase (CAT)**	**Guaiacol Peroxidase (POD)**	**Super Oxide Dismutase (SOD)**
	µS/cm/g	**mmol /g FW**	**µmol/min/mg FW**	**nmol/min/mg FW**	**unit/mg FW**
F Test	**	**	**	**	**
Control	106.22 a	5.91 a	10.78 a	12.28 a	5.33 d
1.0 mM	53.94 bc	3.16 bc	8.68 bc	7.66 e	6.42 bc
2.5 mM	55.37 bc	2.42 cd	8.37 bc	8.34 de	6.41 bc
5.0 mM	55.37 b	2.33 cd	8.89 b	9.89 bc	7.02 ab
7.5 mM	62.18 b	2.133 cd	7.63 bc	9.91 bc	7.25 ab
10.0 mM	61.09 b	1.64 d	8.07 bc	11.32 ab	7.61 a
12.5 mM	52.54 bc	3.49 bc	7.85 bc	11.35 ab	6.38 bc
15.0 mM	49.31 bc	4.19 b	7.74 bc	11.78 a	6.55 bc
17.5 mM	54.60 bc	4.31 b	7.43 c	9.66 cd	6.04 cd
20.0 mM	40.13 c	4.25 b	7.59 bc	7.22 e	5.92 cd

** indicates highly significant differences at $P \leq 0.0001$
n.s indicates no significant differences means with same letter vertically in each of parameters are not significantly different at $P > 0.05$ using Tukey Test

The decrease in CAT and POD activities, coupled with the increase in SOD, suggests that H_2O_2 priming alters the antioxidant balance in seeds. CAT and POD likely work to neutralize excess H_2O_2, while SOD helps mitigate oxidative damage by converting superoxide anions to H_2O_2, which is further detoxified by CAT and POD. This shift in enzymatic activity likely helps seeds cope with oxidative stress during priming. H_2O_2 is known to regulate the expression of genes involved in ROS production and scavenging (Hossain et al., 2015), and priming with H_2O_2 may trigger seeds to activate stress-responsive mechanisms more efficiently. This is supported by studies showing increased antioxidant

activities in various crops after H_2O_2 priming, such as maize (Neto et al., 2005) and sunflower (Silva et al., 2020). In line with these findings, our results suggest that H_2O_2 priming, particularly at 10 mM, activates stress-resilience pathways, leading to improved seed quality and stress tolerance. Similar studies have shown that H_2O_2 priming enhances SOD and APX activity, while maintaining or reducing CAT and POD activities, indicating a complex regulatory mechanism for oxidative stress management (Jira-Anunkul & Pattanagul, 2020; Hameed & Iqbal, 2014).

Seed Oxidative Damage Measurement

The electrical conductivity (EC) test, which measures the extent of seed leachate as an indicator of membrane integrity, showed that untreated seeds had the highest EC value of 106.22 µS/cm/g. This indicates poor membrane stability with a high degree of leakage. In contrast, seeds primed with H_2O_2 at concentrations ranging from 1 mM to 20 mM displayed a significant reduction in EC, suggesting that H_2O_2 priming improved membrane integrity and reduced leakage. Seeds treated with 10 mM H_2O_2 exhibited the highest viability and reduced EC to 61.09 µS/cm/g, representing a 42.5% reduction in seed leachate compared to untreated seeds. Seeds primed with 20 mM H_2O_2 showed the smallest EC value measure which is 40.13 µS/cm/g, reflecting a 62.3% reduction in leachate. Despite the differences in absolute values, Tukey's test revealed no significant differences between the various H_2O_2 concentrations, suggesting that all priming treatments are similarly effective in reducing EC and improving membrane integrity. The reduction in EC values following priming reflects a membrane stabilization, which is crucial for seed quality, as damaged membranes can lead to excessive leakage and poor germination potential. Membrane repair and integrity are crucial for maintaining seed vitality, and the reduction in EC upon H_2O_2 priming indicates that H_2O_2 activates repair mechanisms within the seed. Khaliq et al. (2015) suggested that a reduction in EC is an indicator of improved membrane stability, which is essential for successful seed germination. The results of this study were in line with this concept, showing that H_2O_2 priming can effectively restore membrane integrity and mitigate damage caused by oxidative stress.

Lipid peroxidation, as measured by malondialdehyde (MDA) content, is also significantly affected by H_2O_2 priming. Untreated seeds exhibit the elevated MDA content (5.91 mmol/g FW), indicating substantial oxidative damage to the seed membrane and cellular components. In contrast, all priming treatments with H_2O_2 lead to a significant reduction in MDA levels, reflecting a decreased lipid peroxidation and improved seed quality. The lowest MDA content is observed in seeds primed with 10 mM H_2O_2, which shows an MDA value of 1.64 mmol/g FW. This reduction in MDA represents a 72% decrease compared to untreated seeds, indicating that 10 mM H_2O_2 priming is the most effective at reducing oxidative stress. Seeds treated with H_2O_2 concentrations between 2.5

mM and 7.5 mM show similar reductions in MDA content, ranging from 2.13 mmol/g FW to 2.42 mmol/g FW, which are significantly lower than untreated seeds but still higher than the 10 mM treatment. Seeds primed with 1 mM H_2O_2 exhibited an MDA content of 3.16 mmol/g FW, which is statistically similar to those primed with higher concentrations (12.5 mM to 20 mM), where MDA contents ranges from 3.49 mmol/g FW to 4.25 mmol/g FW. The reduction in MDA content across all priming concentrations suggests that H_2O_2 priming helps mitigate oxidative stress by activating antioxidant defence mechanisms that neutralize reactive oxygen species (ROS) and prevent lipid peroxidation. These findings are consistent with previous studies, such as those by Hameed and Iqbal (2014), Jira-Anunkul and Pattanagul (2020), and Ashraf et al. (2015), who reported reduced MDA levels in various crops following H_2O_2 priming. Specifically, in maize, Terzi et al. (2014) found that a 10 mM H_2O_2 pre-treatment significantly reduced MDA levels, which mirrors the results observed in this study. The reduction in MDA levels is indicative of decreased oxidative damage, which is crucial for maintaining seed quality. Lipid peroxidation, measured by MDA content, is a key marker of cellular damage due to oxidative stress. The significant reduction in MDA after priming, especially with 10 mM H_2O_2, suggests that H_2O_2 activates cellular repair and antioxidant mechanisms, leading to improved seed health and germination capability.

CONCLUSION

This study demonstrated the effectiveness of H_2O_2 as a priming agent for revitalizing deteriorated sweet corn seeds when used at an optimal concentration. Priming seeds at 10 mM H_2O_2 for 24 hours resulted in improved seed germination, increasing from 48% (untreated) to 69% (treated) in year-old GSH1005Y sweet corn seeds. Additionally, this treatment reduced germination time by 16%, enhanced the CVG, promoted longer seedlings, and improved shoot dry weight by 45.46% compared to untreated seeds. When H_2O_2 was added during seed priming, it was neutralized by the enzymes CAT and POD. This process also triggered the activation of other antioxidant enzymes like SOD, which helped improve the seed's condition. As a result, there was a reduction in lipid peroxidation, shown by lower levels of MDA content and less seed membrane leakage.

ACKNOWLEDGMENT

The authors would like to acknowledge and to express their gratitude to Green World Genetics Sdn. Bhd. (GWG) for their assistance in facilitating the conduct of this research in their research and field facilities in Batu Arang Farm, Rawang, Selangor.

REFERENCES

Abuelsoud, W., Cortleven, A., & Schmülling, T. (2020). Photoperiod stress induces an oxidative burst-like response and is associated with increased apoplastic peroxidase and decreased catalase activities. *Journal of Plant Physiology*, *253*, 153252. https://doi.org/10.1016/j.jplph.2020.153252

Aebi, H. (1984). Catalase in vitro. *Methods in enzymology. 105*,121-126. https://doi.org/10.1016/s0076-6879(84)05016-3

Ashraf, M. A., Rasheed, R., Hussain, I., Iqbal, M., Haider, M. Z., Parveen, S., & Sajid, M. A. (2015). Hydrogen peroxide modulates antioxidant system and nutrient relation in maize (*Zea mays* L.) under water-deficit conditions. *Archives of Agronomy and Soil Science*, *61*(4), 507–523. https://doi.org/10.1080/03650340.2014.938644

Banerjee, A., & Roychoudhury, A. (2019). Abiotic stress tolerance in plants by priming and pretreatment with hydrogen peroxide. In *Priming and Pretreatment of Seeds and Seedlings* (pp. 417–426). Springer, Singapore. https://doi.org/10.1007/978-981-13-8625-1_20

Bradford, K. J. (1986). Manipulation of seed water relations via osmotic priming to improve germination under stress conditions. *HortScience*, *21*(5), 1105–1112. https://doi.org/10.21273/hortsci.21.5.1105

Brar, N. S., Kaushik, P., & Dudi, B. S. (2019). Assessment of natural ageing related physio-biochemical changes in onion seed. *Agriculture (Switzerland)*, *9*(8). https://doi.org/10.3390/agriculture9080163

Chen, K., & Arora, R. (2011). Dynamics of the antioxidant system during seed osmopriming, post-priming germination, and seedling establishment in Spinach (*Spinacia oleracea*). *Plant Science*, *180*(2), 212–220. https://doi.org/10.1016/j.plantsci.2010.08.007

Chou, T. S., Chao, Y. Y., & Kao, C. H. (2012). Involvement of hydrogen peroxide in heat shock- and cadmium-induced expression of ascorbate peroxidase and glutathione reductase in leaves of rice seedlings. *Journal of Plant Physiology*, *169*(5), 478–486. https://doi.org/10.1016/j.jplph.2011.11.012

Erenstein, O., Jaleta, M., Sonder, K., Mottaleb, K., & Prasanna, B. M. (2022). Global maize production, consumption and trade: trends and R&D implications. *Food Security 2022 14:5*, *14*(5), 1295–1319. https://doi.org/10.1007/S12571-022-01288-7

Farooq, M., Usman, M., Nadeem, F., Rehman, H. ur, Wahid, A., Basra, S. M. A., & Siddique, K. H. M. (2019). Seed priming in field crops: Potential benefits, adoption and challenges. *Crop and Pasture Science*, *70*(9), 731–771. https://doi.org/10.1071/CP18604

Gammoudi, N., Karmous, I., Zerria, K., Loumerem, M., Ferchichi, A., & Nagaz, K. (2020). Efficiency of pepper seed invigoration through hydrogen peroxide priming to improve in vitro salt and drought stress tolerance. *Horticulture Environment and Biotechnology*, *61*(4), 703–714. https://doi.org/10.1007/s13580-020-00260-8

Gupta, A. S., Heinen, J. L., Holaday, A. S., Burke, J. J., & Allen, R. D. (1993). Increased resistance to oxidative stress in transgenic plants that overexpress chloroplastic Cu/Zn superoxide dismutase.*Proceedings of the National Academy of Sciences, 90*(4), 1629-1633. https://doi.org/10.1073/ pnas.90.4.1629

Hameed, A., & Iqbal, N. (2014). Chemo-priming with mannose, mannitol and H_2O_2 mitigate drought stress in wheat. *Cereal Research Communications*, *42*(3), 450–462. https://doi.org/10.1556/CRC.2013.0066

Hemalatha, G., Renugadevi, J., & Eevera, T. (2017). Studies on seed priming with hydrogen peroxide for mitigating salt stress in rice. *International Journal of Current Microbiology and Applied Sciences*, *6*(6), 691–695. https://doi.org/10.20546/ijcmas.2017.606.081

Hossain, M. A., Bhattacharjee, S., Armin, S. M., Qian, P., Xin, W., Li, H. Y., Burritt, D. J., Fujita, M., & Tran, L. S. P. (2015). Hydrogen peroxide priming modulates abiotic oxidative stress tolerance: Insights from ROS detoxification and scavenging. *Frontiers in Plant Science*, *6*(6), 420. https://doi.org/10.3389/fpls.2015.00420

Hu, Y., Ge, Y., Zhang, C., Ju, T., & Cheng, W. (2009). Cadmium toxicity and translocation in rice seedlings are reduced by hydrogen peroxide pretreatment. *Plant Growth Regulation*, *59*(1), 51–61. https://doi.org/10.1007/s10725-009-9387-7

International Seed Testing Association (2021). International Rules for Seed Testing, International Seed Testing Association, Bassersdorf, CH-Switzerland. https://www.seedtest.org/

Jeevan Kumar, S. P., Rajendra Prasad, S., Banerjee, R., & Thammineni, C. (2015). Seed birth to death: Dual functions of reactive oxygen species in seed physiology. *Annals of Botany*, *116*(4), 663–668. https://doi.org/10.1093/aob/mcv098

Jira-Anunkul, W., & Pattanagul, W. (2020). Seed priming with hydrogen peroxide alleviates the effects of drought stress in rice (*Oryza sativa* L.) seedlings. *Notulae Botanicae Horti Agrobotanici Cluj-Napoca*, *48*(1), 273–283. https://doi.org/10.15835/NBHA48111829

Kader, M. (2005). A comparison of seed germination calculation formulae and the associated interpretation of resulting data. *Journal and proceedings of the Royal Society of New South Wales.* 138. 65-75. https://doi.org/10.5962/p.361564

Khaliq, A., Aslam, F., Matloob, A., Hussain, S., Geng, M., Wahid, A., & Ur Rehman, H. (2015). Seed priming with selenium: Consequences for emergence, seedling growth, and biochemical attributes of rice. *Biological Trace Element Research*, *166*(2), 236–244. https://doi.org/10.1007/s12011-015-0260-4

Lariguet, P., Ranocha, P., de Meyer, M., Barbier, O., Penel, C., & Dunand, C. (2013). Identification of a hydrogen peroxide signalling pathway in the control of light-dependent germination in Arabidopsis. *Planta*, *238*(2), 381–395. https://doi.org/10.1007/s00425-013-1901-5

Maehly, A. C., & Chance, B. (1954). The assay of catalases and peroxidases. *Methods of Biochemical Analysis*, *1*, 357–424. https://doi.org/10.1002/9780470110171.ch14

Neto, A. D. D. A., Prisco, J. T., Enéas-Filho, J., Rolim Medeiros, J. V., & Gomes-Filho, E. (2005). Hydrogen peroxide pre-treatment induces salt-stress acclimation in maize plants. *Journal of Plant Physiology*, *162*(10), 1114–1122. https://doi.org/10.1016/j.jplph.2005.01.007

Pairochteerakul, P., Jothityangkoon, D., Ketthaisong, D., Simla, S., Lertrat, K., & Suriharn, B. (2018). Seed germination in relation to total sugar and starch in endosperm mutant of sweet corn genotypes. *Agronomy*, *8*(12), 299. https://doi.org/10.3390/agronomy8120299

Raj, A. B., & Raj, S. K. (2019). Seed priming: An approach towards agricultural sustainability. *Journal of Applied and Natural Science*, *11*(1), 227–234. https://doi.org/10.31018/jans.v11i1.2010

Silva, P. C. C., Azevedo Neto, A. D. de, Gheyi, H. R., Ribas, R. F., Silva, C. R. dos R., & Cova, A. M. W. (2020). Salt tolerance induced by hydrogen peroxide priming on seed is related to improvement of ion homeostasis and antioxidative defense in sunflower plants. *Journal of Plant Nutrition*, *44*(8), 1207–1221. https://doi.org/10.1080/01904167.2020.1862202

Ślesak, I., Libik, M., Karpinska, B., Karpinski, S., & Miszalski, Z. (2007). The role of hydrogen peroxide in regulation of plant metabolism and cellular signalling in response to environmental stresses. In *Acta Biochimica Polonica* (Vol. 54, Issue 1, pp. 39–50). Acta Biochimica Polonica. https://doi.org/10.18388/abp.2007_3267

Styer, R. C., Cantliffe, D. J., & Hannah, L. C. (1980). Differential seed and seedling vigor in shrunken-2 compared to three other genotypes of corn at various stages of development. *Journal of the American Society for Horticultural Science, 105*(3), 329-332. http://dx.doi.org/10.21273/jashs.105.3.329

Stewart, R. R. C., & Bewley, J. D. (1980). Lipid Peroxidation Associated with Accelerated Aging of Soybean Axes. *Plant Physiology*, *65*(2), 245–248. https://doi.org/10.1104/pp.65.2.245

Suo, H. C., Li, W., Wang, K. H., Ashraf, U., Liu, J. H., Hu, J. G., Li, Z. J., Zhang, X. L., Xie, J., & Zheng, J. R. (2017). Plant growth regulators in seed coating agent affect seed germination and seedling growth of sweet corn. *Applied Ecology and Environmental Research*, *15*(4), 829–839. https://doi.org/10.15666/aeer/1504_829839

Terzi, R., Kadioglu, A., Kalaycioglu, E., & Saglam, A. (2014). Hydrogen peroxide pretreatment induces osmotic stress tolerance by influencing osmolyte and abscisic acid levels in maize leaves. *Journal of Plant Interactions*, *9*(1), 559–565. https://doi.org/10.1080/17429145.2013.871077

Thant, P. S., Puteh, A. B., Sinniah, U. R., & Ismail, M. F. (2017). Physiological and chromosomal changes of delayed harvest soybean (*Glycine max* L. Merr.) seeds. *Seed Science and Technology*, *45*(2), 340–353. https://doi.org/10.15258/sst.2017.45.2.13

Tracy, W. F. (2000). Sweet Corn. In Hallauer, A. R., *Specialty Corns, Second Edition* (pp. 160–204). CRC Press. https://doi.org/10.1201/9781420038569

Verma, G., Mishra, S., Sangwan, N., & Sharma, S. (2015). Reactive oxygen species mediate axis-cotyledon signaling to induce reserve mobilization during germination and seedling establishment in Vigna radiata. *Journal of Plant Physiology*, *184*, 79–88. https://doi.org/10.1016/j.jplph.2015.07.001

Weerasekara, I., Sinniah, U. R., Namasivayam, P., Nazli, M. H., Abdurahman, S. A., & Ghazali, M. N. (2021). The influence of seed production environment on seed development and quality of Soybean (*Glycine max* (L.) Merrill). *Agronomy*, *11*(7), 1430. https://doi.org/10.3390/agronomy11071430

Pertanika J. Trop. Agric. Sci. 48 (6): 1861 - 1882 (2025)

PERTANIKA JOURNALS

TROPICAL AGRICULTURAL SCIENCE

Journal homepage: http://www.pertanika.upm.edu.my/

Carbon Footprint Assessment in *Acacia crassicarpa* Plantation Forests on Peatlands by Quantifying Emission Sources and Mitigation Potential

Ambar Tri Ratnaningsih[1]*, Sukendi[1], Thamrin[1], and Besri Nasrul[2]

[1]Doctor of Environmental Science, Postgraduate Program, Universitas Riau, Jalan Pattimura No. 9, Pekanbaru, 28127 Riau, Indonesia
[2]Department of Soil Science, Faculty of Agriculture, Universitas Riau, Jalan HR. Soebrantas Km. 12.5, Pekanbaru, 28293 Riau, Indonesia

ABSTRACT

Peatland forestry plantations significantly contribute to carbon dynamics, yet long-term carbon emissions from industrial timber plantations remain understudied. This study quantifies CO_2 emissions from peat subsidence, soil respiration following fertilization, logging residue decomposition, and fossil fuel combustion in an *Acacia crassicarpa* plantation in Siak Regency, Riau, Indonesia. Carbon emissions were measured through field observations and empirical models. The total peat carbon stock in the 43,538 ha study area was 137.733 megatons, equivalent to 505.023 megatons CO_2e. Peat subsidence rates from 2021 to 2023 averaged 0.29 cm/year, resulting in 3.058 tons CO_2e/ha annually. Fertilization-induced soil respiration contributed 2.552×10^{-4} tons CO_2e/ha/year, leading to 42.139 tons CO_2e over 20 years. Logging residue decomposition released 2.002 tons CO_2e/ha, with a 20-year cumulative emission of 280,984.70 tons CO_2e. Fossil fuel use required 4.02 liters per ton of wood, contributing 5,192.319 tons CO_2e per harvest cycle. Over 20 years, total emissions from all sources were substantial, highlighting peat subsidence as the dominant contributor. Optimizing fertilization practices, managing logging residues, and improving fuel efficiency could mitigate emissions. Future research should explore carbon sequestration strategies such as alternative fertilization, residue utilization, and water table management for sustainable peatland forestry.

Keywords: carbon footprint; *Acacia crassicarpa*; peatland; carbon emissions; sustainable forestry

ARTICLE INFO

Article history:
Received: 10 March 2025
Accepted: 17 June 2025
Published: 25 November 2025

DOI: https://doi.org/10.47836/pjtas.48.6.12

E-mail addresses:
ambar@unilak.ac.id | p.sukendims@yahoo.com (Ambar Tri Ratnaningsih)
p.sukendims@yahoo.com (Sukendi)
thamrin@lecturer.unri.ac.id (Thamrin)
besrinasrul@lecturer.unri.ac.id (Besri Nasrul)
*Corresponding author

INTRODUCTION

Peatlands are among the most significant terrestrial carbon sinks, storing approximately 550 gigatons of carbon,

which accounts for nearly 30% of the world's soil carbon (Harris et al., 2022; Girkin et al., 2023). However, land-use changes, including industrial plantation forestry, have substantially altered peatland ecosystems, contributing to significant greenhouse gas (GHG) emissions (Deshmukh et al., 2018). Drainage, biomass removal, fertilization, and decomposition processes in managed peatlands have been identified as key factors in carbon flux alterations, making peatlands a major global source of carbon dioxide (CO_2) emissions (Mander et al., 2024). Indonesia, home to one of the largest tropical peatland ecosystems, has recognized this challenge and committed to reducing 140 million tons of CO_2e emissions by 2030 through the Forestry and Other Land Use Net Sink 2030 (FOLU Net Sink 2030) strategy (Ministry of Environment and Forestry, 2022). Given this policy framework, a deeper understanding of carbon emissions from managed peatland forests is essential to ensure that plantation forestry aligns with national and global climate commitments.

Among various plantation species, *Acacia crassicarpa* has gained widespread adoption in Indonesia's industrial plantation forests, particularly in Riau Province, which serves as a hub for the country's pulpwood industry. This species is preferred due to its rapid growth, adaptability to acidic and waterlogged soils, and high biomass productivity (Hardiyanto et al., 2024). However, the environmental trade-offs associated with A. crassicarpa plantations on peatlands remain poorly understood. While oil palm plantations have been extensively studied for their impacts on peatland carbon emissions (Jaafar et al., 2020) industrial tree plantations have received significantly less attention, despite their growing footprint. The extent to which these plantations contribute to peat subsidence, soil carbon loss, and overall CO_2 emissions remains unclear, necessitating a more detailed investigation.

Previous studies on carbon fluxes in peatlands have largely focused on natural forests, degraded peatlands, and agricultural land-use changes (Houghton & Castanho, 2020; Girkin et al., 2023). While some research has examined carbon dynamics in plantation forests, such studies often generalize carbon emissions from large-scale forestry without differentiating specific emission sources (Suharto et al., 2017; Firyadi et al., 2018). In particular, studies have emphasized peat oxidation and subsidence as primary sources of emissions, but fewer have integrated multiple emission pathways, including soil respiration due to fertilization, logging residue decomposition, and fossil fuel use in harvesting operations. Furthermore, there is a significant lack of long-term projections on carbon fluxes in plantation forests, which limits the ability to align forest management practices with global climate mitigation goals.

Another major gap in the literature is the absence of empirical data quantifying emissions from industrial tree plantations on peatlands. Unlike natural forests, where carbon sequestration often offsets emissions, plantation forests undergo regular harvesting cycles that alter their carbon balance over time. While previous studies have attempted to quantify carbon stock fluctuations in plantation forests (Ratnaningsih et al., 2024), they have not

comprehensively addressed the net carbon emissions from different plantation management activities. Additionally, while logging residue decomposition has been recognized as a potential carbon source in tropical forests (Yuniwati & Suhartana, 2014), its contribution to the carbon footprint of plantation forestry remains largely unquantified. This research aims to address these gaps by providing a comprehensive assessment of CO_2 emissions across multiple processes in A. crassicarpa plantations on peatlands.

This study aims to comprehensively assess the carbon footprint of A. crassicarpa plantation forests on peatlands by quantifying emissions from multiple sources, including peat subsidence, fertilization-induced soil respiration, logging residue decomposition, and fossil fuel combustion during harvesting operations. By integrating these emission sources into a single, comprehensive analysis, this study provides a more detailed and accurate account of carbon emissions in industrial plantation forests, an area that has been underexplored in previous research. Additionally, this research seeks to identify the most significant emission sources in A. crassicarpa plantations and evaluate their relative contributions to the overall carbon balance. Beyond short-term emissions, this study also examines long-term carbon flux projections over a 20-year plantation cycle, an aspect that has been largely overlooked in previous studies. Repeated plantation cycles alter peatland carbon dynamics, with cumulative emissions from peat subsidence, fertilization, and residue decomposition gradually accumulating over time. The long-term perspective adopted in this research provides a more realistic estimation of the total carbon footprint of industrial plantation forests, offering valuable insights for future land-use planning and emission reduction strategies.

The findings are expected to provide crucial insights into potential mitigation strategies, including optimized fertilization practices, efficient residue management, and improved logging operations, contributing to the development of sustainable peatland forestry practices. Furthermore, this study contributes to the broader scientific and policy discussions on climate change mitigation in peatland forestry by offering empirical data that aligns with Indonesia's FOLU Net Sink 2030 strategy. The results will serve as a reference for policymakers, plantation managers, and researchers in formulating data-driven strategies to reduce emissions from industrial plantation forests while ensuring economic viability. Given the increasing global pressure to balance economic productivity with environmental sustainability, this research provides a critical foundation for developing evidence-based land-use policies that support climate resilience in peatland ecosystems.

MATERIALS AND METHODS

Study Area and Site Description

This study was conducted in an industrial plantation forest located in Siak Regency, Riau Province, Indonesia, a region characterized by extensive peatland ecosystems managed for large-scale forestry. The study area covers 43,538 ha, with plantations dominated by *A.*

crassicarpa, a fast-growing tree species widely cultivated for pulp and paper production. The study site experiences a tropical humid climate, with an annual average temperature of 26–28°C and mean annual precipitation of 2,500–3,000 mm, with a distinct dry season occurring from June to September. The soil is classified as ombrotrophic peat with depths ranging from 0.5 to 11 m, exhibiting an average pH of 4.0–4.5.

The plantation operates under a rotational harvesting system, with trees being harvested at approximately 4–5 years of age. Standard silvicultural practices include controlled drainage, mechanized harvesting, and periodic fertilization. To quantify the carbon footprint of these plantations, emissions from peat subsidence, fertilization-induced soil respiration, logging residue decomposition, and fossil fuel combustion from harvesting operations were assessed using field measurements, laboratory analysis, and secondary data sources.

Peat Characteristics Analysis

To characterize the physical and chemical properties of the peat, samples were collected from the study site at 50 cm depth intervals using an Eijkelkamp peat auger. Peat characteristics were analyzed for bulk density, fiber content, moisture content, ash content, and organic carbon content, following Indonesian National Standard (Badan Standardisasi Nasional [BSN], 2011).

Bulk Density (BD)

Bulk density (g/cm3) was determined using the oven-drying method (BSN, 2011). Peat samples were weighed before and after drying at 105°C for 48 h, and bulk density was calculated as:

$$BD = \frac{M_d}{V} \quad [1]$$

where:
BD = Bulk density (g/cm^3)
M_d = Dry mass of the sample (g)
V = Sample volume (cm^3)

Moisture Content (%)

Peat moisture content was determined using the gravimetric method, by calculating the difference between fresh and oven-dried weight:

$$MC = \frac{M_f - M_d}{M_d} \times 100 \quad [2]$$

where:
MC = Moisture content (%)
M_f = Fresh weight of the sample (g)
M_d = Dry weight of the sample (g)

Ash Content (%)

Ash content was measured by combusting 2 g of dried peat in a muffle furnace at 550°C for 6 h, and calculating the remaining mineral content:

$$AC = \frac{M_{ash}}{M_d} \times 100 \quad [3]$$

where:
AC = Ash content (%)
M_{ash} = Weight of residual ash after combustion (g)

Organic Carbon Content (%)

The organic carbon content (C_{org}) in peat was determined using the Walkley-Black method. The percentage of organic carbon was calculated based on the mass of oxidized carbon in the sample using the following equation:

$$C_{org} = \frac{(M_f - M_d) \times OC_{conc}}{M_f} \times 100 \quad [4]$$

where:
C_{org} = Organic carbon content in peat (%)
OC_{org} = Organic carbon concentration from titration (mg/g)

Fiber Content (%)

Fiber content was determined using the sieving method, classifying peat as fibric (>67% fibers), hemic (33–67% fibers), or sapric (<33% fibers) following USDA classification (Chmielewska, 2023).

Peat Subsidence and Carbon Emission Estimation

Carbon emissions due to peat subsidence were estimated using secondary data from 2021–2023, with an average subsidence rate of 0.29 cm/year, following the correlation between peat depth, subsidence rate, and carbon release as proposed by Aswandi et al.

(2016). The decomposition rate due to subsidence was calculated using the model adapted from Triadi et al. (2014):

$$T_s = \frac{D}{S} \quad [5]$$

$$E_{\text{subsidence}} = \frac{C_{\text{peat}}}{T_s} \quad [6]$$

where:
T_s = Peat subsidence period (years)
D = Peat depth (cm)
S = Average subsidence rate (cm/year)
$E_{subsidence}$ = Annual carbon emission from peat subsidence (Mt CO_2 /year)
C_{peat} = Total carbon stored in peat (Mt CO_2)

Soil Respiration from Fertilization

CO_2 emissions from fertilized peat soils were measured in A. crassicarpa plantations one week after NPK fertilizer application. Gas flux measurements were conducted at three different times (morning, noon, and afternoon) using a modified Verstraete method (Lestari et al., 2024; Suhesti et al., 2024). In each observation plot, film canisters filled with 10 ml of 0.1N KOH solution were placed inside open chambers made of transparent plastic jars with known dimensions. The chambers were left for 1 h, during which CO_2 released from soil respiration was absorbed by the KOH solution. The absorbed CO_2 was then analyzed through acid-base titration, following the method of Andelia et al. (2020).

CO_2 emission rates were calculated using the following equation:

$$C_{CO_2} = \frac{(a - b) \times t \times 12}{T \times \pi \times r^2} \quad [7]$$

where:
C_{CO2} = Soil CO_2 respiration rate (mg CO_2 /m^2/ h^1)
a = Volume of HCl used for the sample titration (mL)
b = Volume of HCl used for the blank titration (mL)
t = Normality of HCl (N)
T = Incubation time (h)
r = Radius of the chamber (m)
12 = Atomic mass of carbon

Fossil Fuel Emissions from Logging Operations

CO_2 emissions from fossil fuel consumption were calculated by measuring fuel usage during logging activities, including harvesting, skidding, and transportation. The amount of fuel consumed was recorded and converted into CO_2 emissions using the method proposed by Suharto et al. (2017). The following equation was applied:

$$E_{fuel} = FUEL_a \times EF_a \quad [8]$$

where:
E_{fuel} = CO_2 emissions from fossil fuel consumption (tons CO_2)
$FUEL_a$ = Energy generated from fuel type aa (TJ)
EF_a = Emission factor for fuel type a (t CO_2/TJ)

The energy content of the fuel was determined using:

$$FUEL_a = \text{Liters of fuel}_a \times \text{Density of fuel}_a \times NCV_a \times 10^{-3} \quad [9]$$

where:
Liters of $fuel_a$ = Amount of fuel consumed (liters)
Density of $fuel_a$ = Fuel density (kg/liter)
NCV_a = Net calorific value of fuel (TJ/Gg)

Default emission factors were based on IPCC Guidelines (Buendia et al., 2019), as shown in Table 1.

Table 1
Default IPCC emission factors for fossil fuels

Fuel Type	Density (kg/liter)	NCV (TJ/Gg)	Emission Factor (t CO_2/TJ)
Gasoline	0.7407	44.3	69.3
Diesel	0.8439	43.0	74.1

Total CO_2 emissions from fossil fuel use were estimated using:

$$E_{transport} = FUEL_a \times EF_a \quad [10]$$

where $E_{transport}$ represents CO_2 emissions from transportation activities.

Carbon Estimation from Logging Residues

To assess CO_2 emissions from logging residues, circular sampling plots (0.04 ha each) were established across three different harvested stands, representing variations in tree density

and biomass distribution. Within each plot, tree diameter at breast height (DBH) and total tree height were recorded to estimate the total biomass left as logging residues. Logging residues were categorized into four components: stumps, branches, sorting residues, and upper trunk sections, following the classification by Yuniwati & Suhartana (2014). The carbon content of each residue category was estimated using allometric models as follows:

$$C_{stump} = 0.000141D^{3.084} \quad [11]$$

$$C_{branch} = 1.26979 \times 10^{-10}D^{6.908} \quad [12]$$

$$C_{sorting} = 1.13411 \times 10^{-10}D^{6.645} \quad [13]$$

$$C_{upper\ trunk} = 2.01512 \times 10^{-8}D^{4.767} \quad [14]$$

where:
C_{stump},C_{branch},$C_{sorting}$,$C_{upper\ trunk}$ = Carbon stock in different tree components (tons C)
D = Diameter at breast height (m)

The CO_2 emissions from decomposing residues were estimated using an exponential decay model:

$$E_{residue} = C_{residue} \times (1 - e^{-kt}) \times \frac{44}{12} \quad [15]$$

where:
$E_{residue}$ = CO_2 emissions from residue decomposition (tons CO_2 /ha/year)
$C_{residue}$ = Carbon stock in logging residues (tons C/ha)
k = Decomposition rate constant ($year^{-1}$)
t = Time (years)
44/12 = Carbon-to-CO_2 conversion factor

Decomposition rates were determined through periodic residue sampling over 12 months, with litterbag collections at 1, 3, 6, and 12 months. The cumulative carbon emissions from logging residues were then projected over a 20-year plantation cycle, assuming a four-year rotation period for harvested stands.

Data Analysis

Carbon emissions were expressed as tons CO_2e per hectare per year. Peat subsidence emissions were analyzed using linear regression models, while soil respiration was evaluated through two-way ANOVA. Logging residue decomposition was modeled using an exponential decay function, and fossil fuel emissions were analyzed using IPCC default

conversion factors. All statistical analyses were performed using R software (v4.2.1), with significance levels set at $p < 0.05$.

RESULTS AND DISCUSSION

Peat Characteristics and Carbon Content

Peat characteristics at the study site were analyzed to understand their role in carbon storage and emission dynamics. The peat characteristics observed in the study site are summarized in Table 2, which presents variations in bulk density, moisture content, ash content, organic carbon content, and fiber content across different peat depths. Bulk density values ranged from 0.06 to 0.14 g/cm³, with an average of 0.082 g/cm³. This indicates that the peat has a highly porous structure, which influences its ability to retain water and store carbon. Bulk density is a critical parameter in determining peat subsidence rates, as lower bulk density values correspond to higher compressibility and greater susceptibility to decomposition when exposed to air. Lower bulk density also implies that carbon loss per unit volume of peat may be significant upon drainage and oxidation (Hooijer et al., 2011).

Moisture content ranged from 550.51 to 1260.26 percent, showing high water retention capacity, which is a typical characteristic of tropical peatlands. High moisture content plays a crucial role in limiting oxygen diffusion, thereby slowing microbial decomposition and reducing carbon release. However, when the water table drops, aeration increases, leading to accelerated oxidation of organic matter and greater CO_2 emissions. The variability in moisture content across different depths suggests that water retention decreases in deeper layers due to compaction and structural changes in peat composition (McCarter et al., 2020).

Ash content varied from 0.61 to 5.04 percent, indicating that the peat is primarily organic with minimal mineral content. The lower ash content suggests limited mineral input from external sources, which is characteristic of ombrotrophic peatlands. The presence of higher ash content in the upper layers may be attributed to external sediment deposition or organic matter decomposition over time. Peat with low ash content tends to have higher carbon storage potential but is also more vulnerable to rapid degradation when drained (Pardede et al., 2021).

Organic carbon content ranged between 51.09 and 57.65 percent, confirming the high carbon storage capacity of the study site. Deeper peat layers exhibited slightly higher organic carbon concentrations, which aligns with previous studies indicating that decomposition is less intense in deeper layers due to reduced microbial activity and oxygen availability. Organic carbon levels are a key factor in determining the carbon sequestration potential of peatlands, with variations in carbon content affecting total carbon stock estimates. The strong correlation between peat depth and organic carbon content reinforces the importance of maintaining natural peat hydrology to prevent excessive carbon loss (Nurzakiah, 2014).

Table 2
Peat characteristics at the study site

Peat Depth (cm)	Bulk Density (g/cm³)	Moisture Content (%)	Ash Content (%)	Organic Carbon (%)	Fiber Content (%)
0-50	0.14	550.51	5.04	55.08	50.56
50-100	0.10	879.32	3.09	56.21	51.33
100-150	0.06	1095.59	2.98	56.28	51.44
150-200	0.07	1141.40	1.61	57.05	52.14
200-250	0.08	1108.44	1.56	57.10	53.43
250-300	0.08	1174.18	1.98	56.61	55.43
300-350	0.07	1260.26	1.86	56.93	56.00
350-400	0.07	1103.76	1.71	54.21	56.17
400-450	0.07	1108.35	1.52	54.80	56.50
450-500	0.08	1132.51	0.61	57.65	57.33
500-550	0.08	1134.45	0.84	57.52	58.00
550-600	0.09	1030.16	0.83	57.52	58.33
600-650	0.07	988.39	0.93	51.09	59.67
650-700	0.10	1035.72	0.89	54.74	60.00

The relationship between organic carbon content and peat depth demonstrates that deeper layers tend to retain higher carbon concentrations, likely due to lower decomposition rates and minimal exposure to aerobic conditions, as shown in Figure 1. Regression analysis indicated a significant correlation between peat depth and total carbon content, represented by the equation $Y = 192.8127 + 4.460X$, where X is peat depth (m) and Y is total carbon content (tons). The model yielded a high coefficient of determination ($R^2 = 0.99$) and a statistically significant P-value < 0.05, confirming that peat depth has a significant effect on carbon storage at a 5% significance level. The study area, covering 43,538 hectares, was estimated to contain a total peat carbon stock of 137.733 megatons, which is equivalent to 505.023 megatons of CO_2e. The distribution of carbon content across different peat depths is illustrated in Figure 1, further highlighting the role of deep peat layers in long-term carbon sequestration. The inverse correlation between bulk density and organic carbon stock emphasizes the importance of maintaining natural peatland conditions to prevent excessive carbon loss and minimize greenhouse gas emissions.

Fiber content ranged from 50.56 to 60 percent, indicating that the peat in the study area is predominantly hemic. Hemic peat is characterized by a moderate level of decomposition, where plant structures are still recognizable but have undergone partial breakdown. Peat with higher fiber content tends to have greater water retention capacity, reducing decomposition rates under natural conditions. However, once drained, hemic peat can become highly susceptible to degradation, contributing to long-term CO_2 emissions. The fiber content values observed in this study align with previous findings on tropical peat characteristics and their role in carbon cycling (Ahmad et al., 2021).

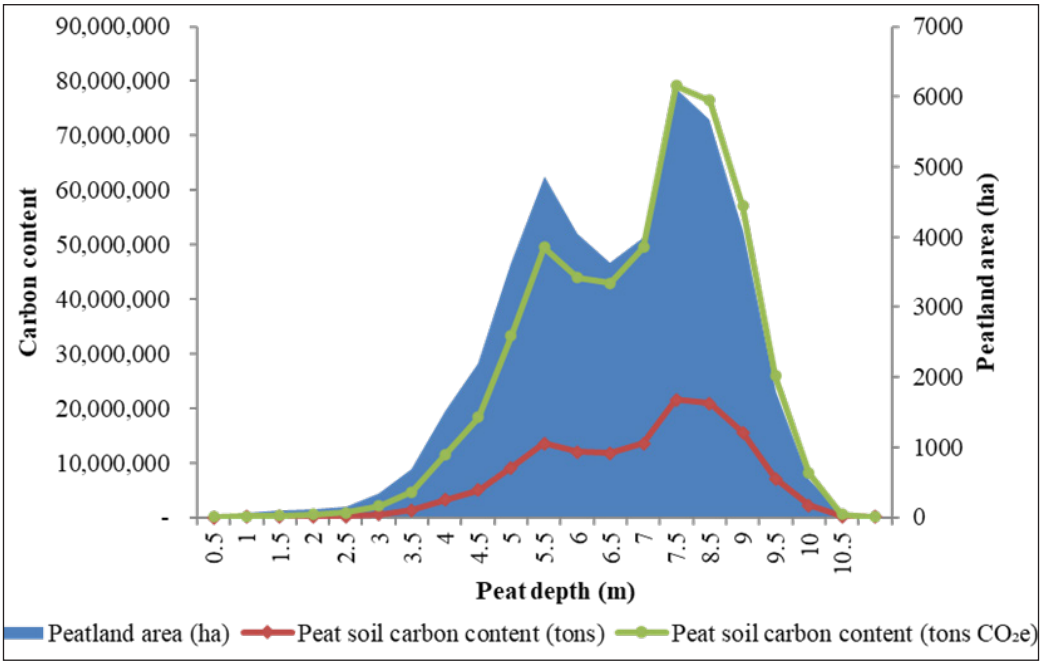

Figure 1. Organic carbon content distribution across peat depths

These findings emphasize the critical role of peat depth and composition in maintaining ecosystem carbon balance. Given the high carbon stock observed in the study area, it is essential to implement sustainable peatland management practices to minimize carbon loss. Future studies should investigate the influence of hydrological management on peat decomposition rates and explore potential carbon sequestration strategies such as controlled water table regulation and alternative peatland restoration methods.

Carbon Emissions from *A. crassicarpa* Plantation Management

CO_2 Emissions from Peat Subsidence

Peat subsidence is the process of surface lowering due to compaction, oxidation, or decomposition, which is primarily driven by drainage construction that facilitates water loss from peat soils. As water drains, oxygen infiltrates the peat matrix, accelerating microbial decomposition of organic matter into inorganic compounds, thereby releasing CO_2 emissions (McCarter et al., 2020). This process reduces peat biomass and bulk density, ultimately leading to subsidence. Peatland drainage for plantation forestry has been widely recognized as a significant contributor to soil carbon loss and increased emissions (Mander et al., 2024; McCalmont et al., 2021; Hooijer et al., 2011).

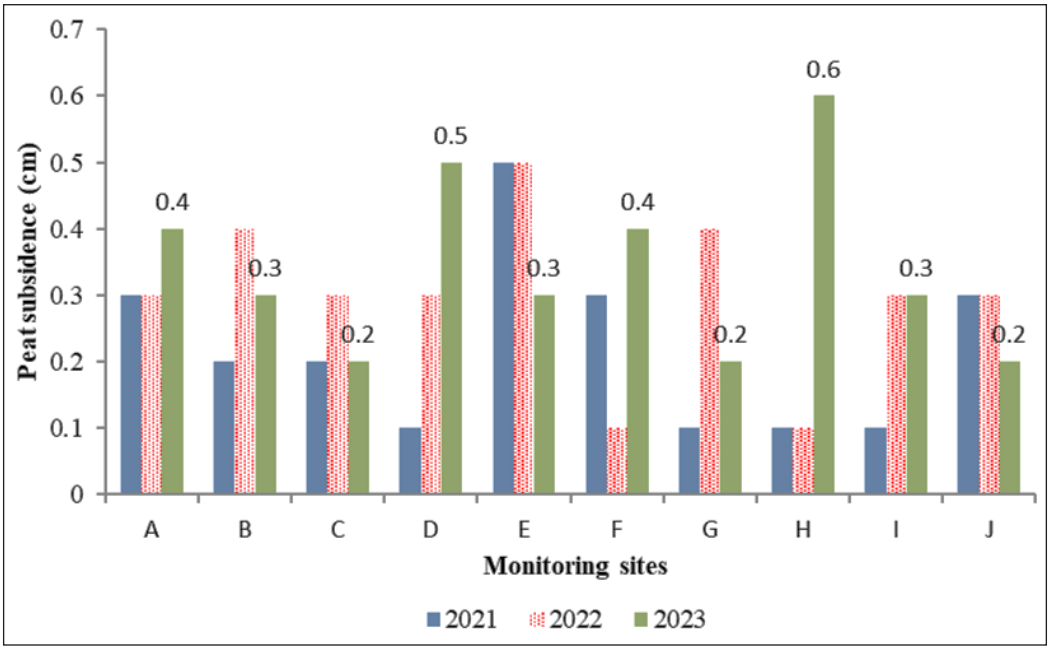

Figure 2. Peat subsidence at 10 monitoring sites in the study area

To quantify peat subsidence in this study, secondary data were collected from 10 monitoring sites distributed across the research site. The observed fluctuations in peat subsidence over three years are presented in Figure 2. The average subsidence rates were 0.34 cm in 2023, 0.3 cm in 2022, and 0.22 cm in 2021, yielding a three-year mean subsidence rate of 0.29 cm/year. This rate is significantly lower than the 5.5 cm/year reported by Lisnawati et al. (2015) in Rasau Kuning, Riau Province, where subsidence was strongly correlated with groundwater table fluctuations.

Hooijer et al. (2011) established a link between peat subsidence and carbon loss, as subsidence directly corresponds with organic matter degradation and peat compaction, leading to increased CO_2 emissions. The estimated total carbon stock in the study area, with a peat depth of 11 meters, was 505,022,898.29 tons CO_2e.. Annual carbon emissions from peat subsidence were estimated at 133,142.40 tons CO_2e, equivalent to 3.058 tons CO_2e/ha/year. Over a 20-year projection, total emissions from peat subsidence alone were estimated at 2,662,848 tons CO_2e, as illustrated in Figure 3.

The emission rate reported in this study is lower than previous findings in other land-use types. Aswandi et al. (2016) documented 5.96 tons CO_2e/ha/year in secondary forests and 7.45 tons CO_2e/ha/year in oil palm plantations, while degraded tropical forests were found to emit up to 65 tons CO_2e/ha/year (Hooijer et al., 2010). The lower emissions observed in the managed A. crassicarpa plantation suggest that while drainage-induced subsidence

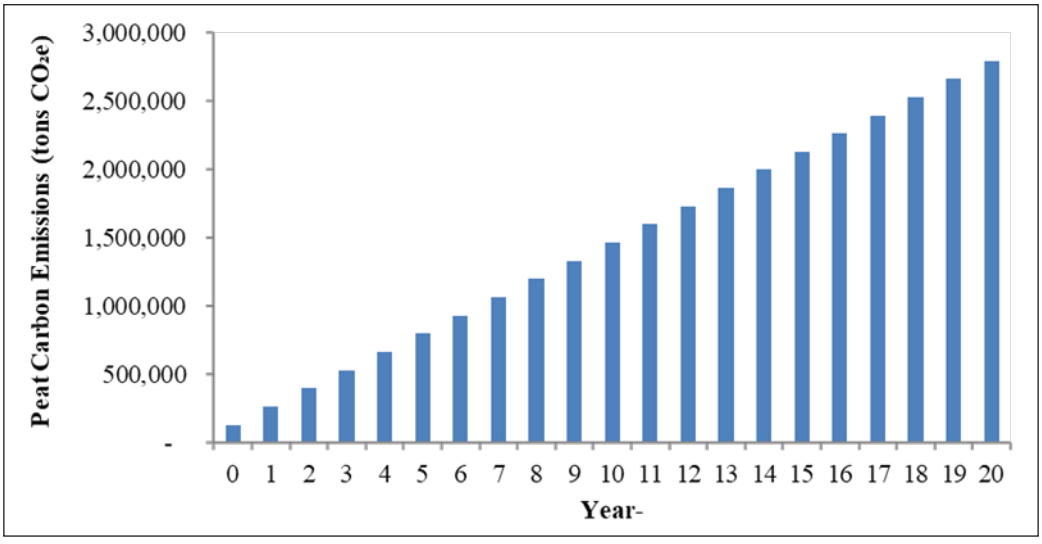

Figure 3. CO_2 emissions from peat subsidence over 20 years

occurs, it is not as severe as in other more intensively disturbed land-use systems. The rate of subsidence is influenced by multiple factors, including drainage depth and peat thickness. Deeper drainage channels and thicker peat layers typically result in higher subsidence rates, leading to greater carbon emissions. This finding underscores the need for improved water table management in plantation forestry to minimize peat oxidation and CO_2 release.

CO_2 Emissions from Fertilized Peat Soil Respiration

To enhance soil fertility and improve the productivity of A. crassicarpa plantations, fertilization is commonly applied. The main purpose of fertilization is to increase soil nutrient availability, thereby supporting optimal tree growth (Purnama et al., 2023). Zincobor fertilizer has been reported to enhance tree height, stem straightness, and prevent shrubby growth in A. crassicarpa plantations (Hidayat et al., 2022). However, fertilization on peatlands may also influence microbial activity, potentially leading to increased CO_2 emissions (Shi et al., 2025). Serrano-Silva et al., (2011) found that urea application enhances soil microbial activity, consequently increasing soil respiration and CO_2 release into the atmosphere.

At the study site, fertilization was applied twice during the plantation cycle. The first application, or basal fertilization, consisted of BTA 12 (1 kg per tree) and NPK (80 g per tree), while the second application, or topdressing, involved NPK (80 g per tree). CO_2 emissions were measured one week after fertilization at 1-, 3-, 5-, and 7-days post-application, with the results presented in Figure 4. The average soil CO_2 emissions from

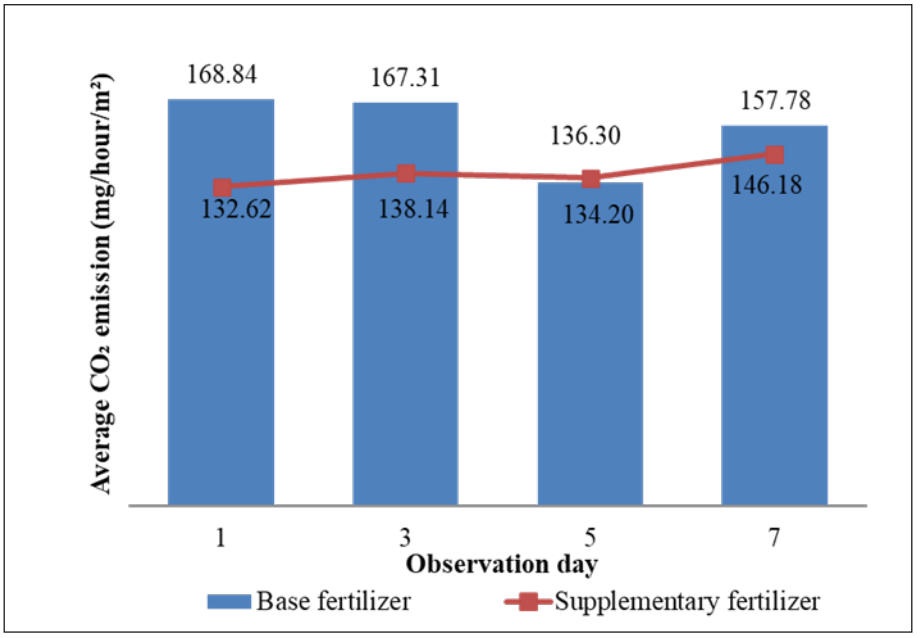

Figure 4. CO_2 emissions following fertilization

basal fertilization were 157.036 mg/m²/h, whereas topdressing resulted in slightly lower emissions of 138.308 mg/m²/h. The total estimated annual CO_2 emissions from fertilization were 2.552×10^{-4} tons/ha/year. The temporal pattern of emissions showed an initial increase immediately after fertilization, followed by a gradual decline over time.

The emissions observed in this study are significantly higher than those reported by Andelia et al. (2020), who found soil CO_2 emissions of 29.56 mg/m²/h in green bean cultivation fertilized with manure and NPK. In contrast, NPK application in oil palm plantations has been reported to generate CO_2 emissions ranging from 1.090 to 230 mg/m²/h (Riyani et al., 2021). The higher emissions in A. crassicarpa plantations may be attributed to peat soil conditions, fertilizer type, and microbial activity associated with decomposition processes. In this study, fertilization was assumed to follow a four-year harvesting cycle, where fertilizer application occurred at 14 and 90 days after planting. Annual CO_2 emissions from fertilization were estimated at 2.107 tons in the first year, with emissions remaining consistent from year 2 to year 20. Over a 20-year plantation cycle, the total CO_2 emissions from fertilization were calculated at 42.139 tons. The cumulative emissions over this period are illustrated in Figure 5.

The results highlight the necessity of refining fertilization strategies in peatland forestry to reduce carbon emissions while sustaining soil fertility and enhancing productivity. Future studies should investigate the effectiveness of alternative fertilization approaches,

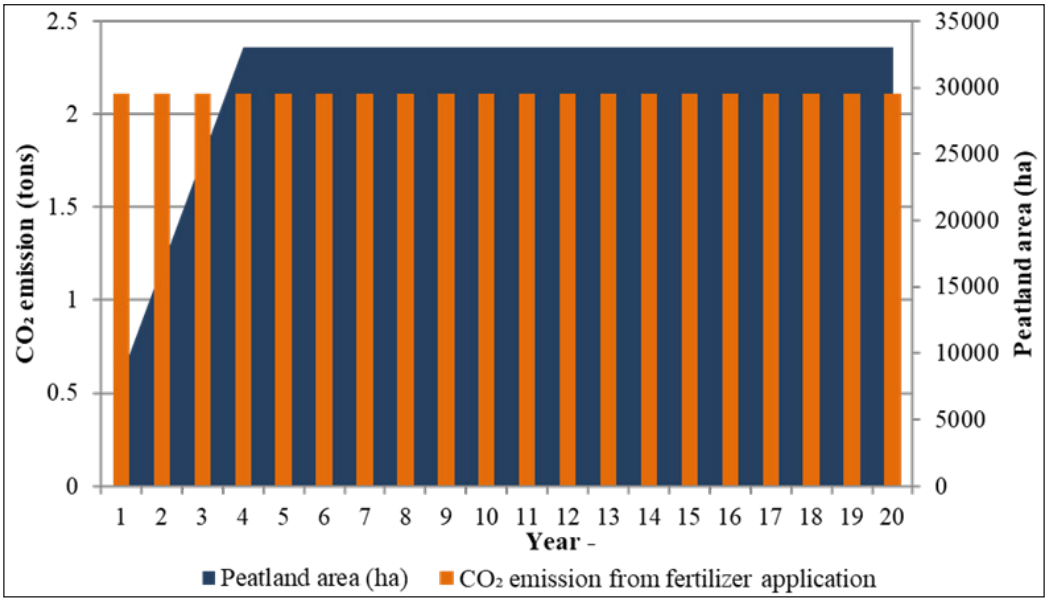

Figure 5. Cumulative CO_2 emissions from fertilization over a 20-year cycle.

such as slow-release fertilizers or biochar amendments, in mitigating CO_2 emissions from fertilized peat soils.

CO_2 Emissions from Logging Residue Decomposition

One of the major sources of carbon emissions in A. crassicarpa plantation management is logging operations. According to Yuniwati & Suhartana (2014), timber harvesting in tropical forests across Asia can reduce carbon stocks by 22–67% due to the decomposition of residual biomass left after harvesting. Logging residues typically consist of stumps, branches, short wood pieces, and upper trunk sections (Surasana et al., 2020). These residues decompose over time, releasing carbon into the atmosphere (Yuniwati & Suhartana, 2014).

Table 3
Emissions from logging residues

No plot	Number of Trees (trees/ ha)	Stump Carbon Mass (ton/ha)	Branch Carbon Mass (ton/ha)	Sorting Carbon Mass (ton/ha)	Upper Trunk Carbon Mass (ton/ha)	Total Carbon Mass (ton/ha)	Carbon Mass (ton CO_2e)
1	1266	0.507	0.017	0.007	0.007	0.538	1.972
2	1385	0.460	0.013	0.006	0.006	0.484	1.776
3	1464	0.571	0.025	0.011	0.009	0.616	2.258
Average		**0.513**	**0.018**	**0.008**	**0.007**	**0.546**	**2.002**

The estimation of carbon emissions from A. crassicarpa logging residue decomposition was conducted using an allometric equation from Yuniwati & Suhartana (2014). The estimated carbon storage and emission potential from logging residues are presented in Table 3. The total estimated carbon emissions from logging residues were 0.546 tons/ha, equivalent to 2.002 tons CO_2e/ha. Assuming a four-year harvesting cycle, the total emissions from logging residues in the fourth year would reach 4,507.78 tons CO_2e. From year 4 to year 20, emissions remain relatively stable as plantation management follows a continuous cycle. Over a 20-year period, the cumulative emissions from logging residue decomposition were estimated at 76,632.19 tons of carbon, equivalent to 280,984.70 tons CO_2e. The long-term emission trend from logging residue decomposition is illustrated in Figure 6.

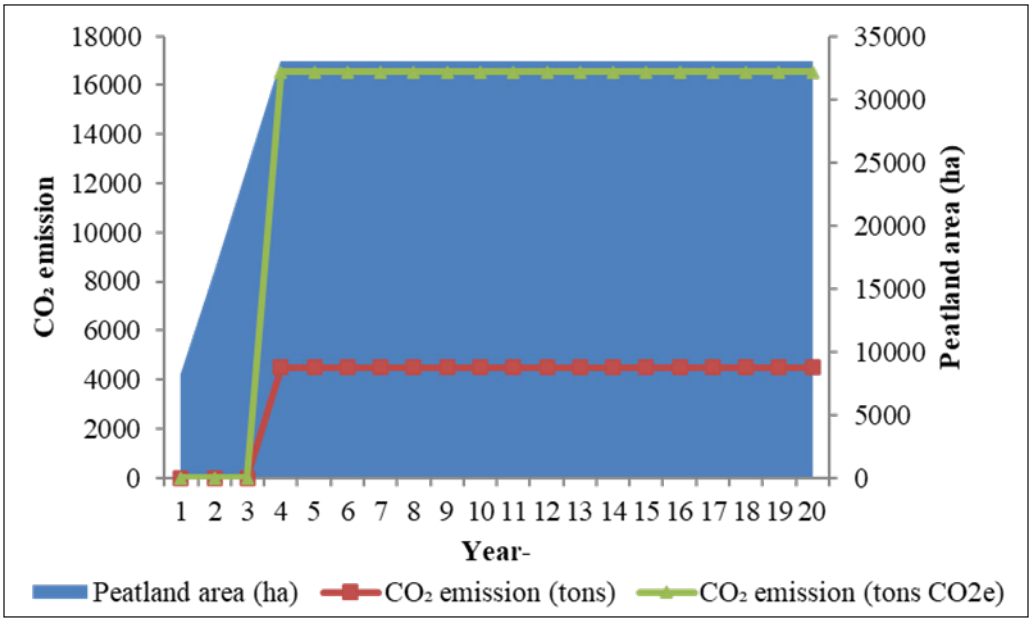

Figure 6. Carbon emissions from logging residue decomposition

These findings underscore the importance of optimizing logging residue management to minimize emissions from decomposing biomass. Future studies should explore alternative methods such as biochar conversion or residue repurposing to enhance carbon sequestration while maintaining sustainable forest productivity.

CO_2 Emissions from Fossil Fuel Use in Logging Operations

Timber harvesting in A. crassicarpa plantation management involves multiple stages, including felling, delimbing, skidding, loading, and transportation (Mohamad-Amini,

2024). In large-scale operations, mechanized harvesting is the standard approach, requiring significant fossil fuel consumption for operating heavy machinery and transport vehicles (McEwan et al., 2020). Fossil fuel combustion from these activities contributes to CO_2, NO_x, and SO_2 emissions (Mohammed et al., 2024). The carbon footprint of fossil fuel use in industrial timber harvesting has been estimated at 1,100 tons CO_2e (Suharto et al., 2017). The fossil fuel consumption required for logging A. crassicarpa plantations is summarized in Table 4.

Table 4
Fossil fuel consumption in logging operations of A. crassicarpa

Activity	Equipment	Fuel Type	Trials	Fuel Consumption (L)	Wood Transported (tons)	Average Fuel Consumption per Ton (L)	CO_2 Emissions (tons)
Felling	Excavator with feller buncher	Diesel	1	65	78	0.8266	0.0022
			2	61	67		
			3	53	72		
Pre-Bunching	Excavator with fixed grapple	Diesel	1	55	70	0.7620	0.0020
			2	57	77		
			3	57	75		
Delimbing & Cut-to-Length	Chainsaw	Gasoline	1	20	35	0.5516	0.0012
			2	30	40		
			3	16	48		
Skidding	Excavator with fixed grapple	Diesel	1	57	57	0.9872	0.0027
			2	50	52		
			3	55	55		
Log Transport	Tug boat	Diesel	1	51	210	0.243	0.0022
			2	50	202		
			3	55	230		
	Truck	Diesel	1	30	50	0.572	
			2	31	60		
			3	33	55		
Loading	Excavator with rotary grapple	Diesel	1	33	384	0.0799	0.0002
			2	38	480		
			3	43	576		
Total						**4.0227**	**0.0106**

Based on Table 4, the total fuel consumption for harvesting 1 ton of A. crassicarpa timber was 4.02 liters, resulting in CO_2 emissions of 0.0106 tons per ton of harvested wood. The amount of fuel required for logging operations is influenced by annual production targets, with emissions estimated at 5,192.319 tons CO_2e, consistent with findings by Suharto et al. (2017). Among all activities, skidding required the highest fuel consumption,

as it involves transporting logs from the felling site to temporary storage areas (Surasana et al., 2020). Conversely, log loading required the least fuel consumption.

Fuel consumption in heavy machinery is influenced by engine power, machine type, and workload intensity (Purwanto et al., 2021). Additionally, the type of machinery used and the operational workload directly affect fuel efficiency (Banggur et al., 2023). These findings suggest that improving fuel efficiency and optimizing transport logistics could reduce CO_2 emissions in large-scale forestry operations.

CONCLUSION

This study quantified CO_2 emissions from *A. crassicarpa* plantations on peatlands, identifying peat subsidence as the dominant emission source, contributing 3.058 tons CO_2e/ha annually, followed by logging residue decomposition (2.002 tons CO_2e/ha), fertilization-induced soil respiration (2.552×10^{-4} tons CO_2e/ha/year) and fossil fuel used contributing 5,192.319 tons CO_2e per harvest cycle. Over a 20-year projection, cumulative emissions from all sources were substantial, highlighting the long-term impact of plantation forestry on peat carbon stocks. To mitigate emissions, optimizing fertilization practices, improving residue management, and enhancing fuel efficiency are essential. Maintaining higher water table levels and integrating carbon sequestration strategies such as alternative fertilization and biochar application could further reduce emissions while ensuring sustainability. Future research should refine long-term carbon flux models, explore adaptive land-use strategies, and develop science-based policies to align plantation forestry with global climate commitments.

REFERENCES

Ahmad, A., Sutanto, M. H., Al-Bared, M. A. M., Harahap, I. S. H., Abad, S. V. A. N. K., & Khan, M. A. (2021). Physio-chemical properties, consolidation, and stabilization of tropical peat soil using traditional soil additives—A state of the art literature review. *KSCE Journal of Civil Engineering*, *25*(10), 3662-3678. https://doi.org/10.1007/s12205-021-1247-7

Andelia, P., Yusnaini, S., Buchorie, H., & Niswati, A. (2020). Pengaruh sistem olah tanah dan pemupukan terhadap respirasi tanah pada pertanaman kacang hijau (*Vigna radiat*a L.) di laboratorium lapang terpadu [Effect of tillage system and fertilization on soil respiration in mung bean (*Vigna radiata* L.) cultivation at the integrated field laboratory]. *Journal of Tropical Upland Resources*, *2*(2), 287-294.

Aswandi, A., Sadono, R., Supriyo, H., & Hartono, H. (2016). Kehilangan karbon akibat drainase dan degradasi lahan gambut tropika di Trumon dan Singkil Aceh [Carbon loss from drainaged and degradation of tropical peatland in Trumon and Singkil, Aceh]. *Jurnal Manusia dan Lingkungan*, *23*(3), 334-341. https://doi.org/10.22146/jml.18807

Banggur, L., Wijaya, L. H., Aaminullah, A., & Kusmianti, K. (2023). Analisis produktifitas penggunaan alat berat excavator pada penambangan pasir di Desa Kediri Kecamatan Kediri Kabupaten Lombok Barat

[Productivity analysis of excavator utilization in sand mining in Kediri Village, Kediri District, West Lombok Regency]. *Sosial Sains dan Teknologi*, *3*(1), 38-45. https://doi.org/10.35327/sosintek.v3i1.423

Badan Standardisasi Nasional. 2011. Pengukuran dan penghitungan cadangan karbon - Pengukuran lapangan untuk penaksiran cadangan karbon hutan [Measurement and calculation of carbon stocks – Field measurement for forest carbon stock estimation]. SNI 7724:2011

Buendia, E. C., Guendehou, S., Limmeechokchai, B., Pipatti, R., Rojas, Y., Sturgiss, R., Tanabe, K., Wirth, T., Romano, D., Witi, J., Garg, A., Weitz, M. M., Cai, B., Ottinger, D. A., Dong, H., MacDonald, J. D., Ogle, S. M., Rocha, M. T., Sanz Sanchez, M. J., & Bartram, D. M. (2019). *2019 refinement to the 2006 IPCC guidelines for national greenhouse gas inventories: Overview*. Intergovernmental Panel on Climate Change (IPCC).

Chmielewska, I. (2023). Effect of fibre content on the geotechnical properties of peat. *Studia Geotechnica et Mechanica*, *45*(1), 133-143. https://doi.org/10.2478/sgem-2023-0003

Deshmukh, C. S., Julius, D., Evans, C. D., Nardi, Susanto, A. P., Page, S. E., Gauci, V., Laurén, A., Sabiham, S., Agus, F., Asyhari, A., Kurnianto, S., Suardiwerianto, Y., & Desai, A. R. (2020). Impact of forest plantation on methane emissions from tropical peatland. *Global Change Biology*, *26*(4), 2477-2495. https://doi.org/10.1111/gcb.15019

Firyadi, F., Widiatmaka, W., Iswati, A., Muhamad, A., & Mulyanto, B. (2018). Neraca karbon, emisi dan serapan historis CO_2 karena perubahan penggunaan lahan di Kabupaten Banyuasin, Sumatera Selatan [Carbon balance, historical CO_2 emissions and absorption due to land use changes in banyuasin regency, south sumatra]. *Jurnal Pengelolaan Sumberdaya Alam dan Lingkungan*, *8*(2), 178-187.

Girkin, N. T., Burgess, P. J., Cole, L., Cooper, H. V., Honorio Coronado, E., Davidson, S. J., Hannam, J., Harris, J., Holman, I., McCloskey, C. S., Mc.Keown, M. M., Milner, A. M., Page, S., Smith, J., & Young, D. (2023). The three-peat challenge: business as usual, responsible agriculture, and conservation and restoration as management trajectories in global peatlands. *Carbon management*, *14*(1), 2275578. https://doi.org/10.1080/17583004.2023.2275578

Hardiyanto, E. B., Inail, M. A., Nambiar, S., & Mendham, D. S. (2024). Sustaining plantation forest productivity in Sumatra over three decades: From acacias to eucalypts. *Forest Ecology and Management*, *553*, 121613. https://doi.org/10.1016/j.foreco.2023.121613

Harris, L. I., Richardson, K., Bona, K. A., Davidson, S. J., Finkelstein, S. A., Garneau, M., McLaughlin, J., Nwaishi, F., Olefeldt, D., Packalen, M., Roulet, N. T., Southee, F. M., Strack, M., Webster, K. L., Wilkinson, S. L., & Ray, J. C. (2022). The essential carbon service provided by northern peatlands. *Frontiers in Ecology and the Environment*, *20*(4), 222-230. https://doi.org/10.1002/fee.2437

Hidayat, R., Effendi, A., & Nasrul, B. (2022). pengaruh pemberian pupuk zincobor dan kombinasi zincobor + dolomit terhadap pertumbuhan akasia di lahan gambut [Effect of zincobor fertilizer and its combination with dolomite on the growth of acacia in peatlands]. *Photon: Journal of Natural Sciences and Technology*, *13*(1), 29-35. https://doi.org/10.37859/jp.v13i1.3919

Hooijer, A., Page, S., Jauhiainen, J., Lee, W. A., Lu, X. X., Idris, A., & Anshari, G. (2011). Subsidence and carbon loss in drained tropical peatlands: reducing uncertainty and implications for CO_2 emission reduction options. *Biogeosciences Discussions*, *8*(5). https://doi.org/10.5194/bg-9-1053-2012

Hooijer, A., Page, S., Canadell, J. G., Silvius, M., Kwadijk, J., Wösten, H., & Jauhiainen, J. (2010). Current and future CO_2 emissions from drained peatlands in Southeast Asia. *Biogeosciences*, *7*(5), 1505-1514. https://doi.org/10.5194/bg-7-1505-2010

Houghton, R. A., & Castanho, A. (2022). Annual emissions of carbon from land use, land-use change, and forestry 1850–2020. *Earth System Science Data Discussions*, *2022*, 1-36. https://doi.org/10.5194/essd-15-2025-2023

Jaafar, W. S. W. M., Said, N. F. S., Abdul Maulud, K. N., Uning, R., Latif, M. T., Muhmad Kamarulzaman, A. M., Mohan, M., Pradhan, B., Saad, S. N. M., Broadbent, E. N., Cardil, A., Silva, C. A., & Takriff, M. S. (2020). Carbon emissions from oil palm induced forest and peatland conversion in sabah and Sarawak, Malaysia. *Forests*, *11*(12), 1285. https://doi.org/10.3390/f11121285

Lestari, S. U., Roeswitawati, D., Syafrani, S., Maftuchah, M., & Purnama, I. (2024). Addressing Nitrogen-rich Biomass Production Challenges in Azolla microphylla Cultivation from Varying Shading and Water Depth Dynamics. *Pertanika Journal of Tropical Agricultural Science*, *47*(3). https://doi.org/10.47836/pjtas.47.3.18

Lisnawati, Y., Suprijo, H., Poedjirahajoe, E., & Musyafa, M. (2015). Dampak pembangunan hutan tanaman industri *Acacia crassicarpa* di lahan gambut terhadap tingkat kematangan dan laju penurunan permukaan tanah [The impact of development of industrial plantation forest *Acacia Crassicarpa* in peatland towards the maturity]. *Jurnal manusia dan lingkungan*, *22*(2), 179-186. https://doi.org/10.22146/jml.18740

Mander, Ü., Espenberg, M., Melling, L., & Kull, A. (2024). Peatland restoration pathways to mitigate greenhouse gas emissions and retain peat carbon. *Biogeochemistry*, *167*(4), 523-543. https://doi.org/10.1007/s10533-023-01103-1

McCalmont, J., Kho, L. K., Teh, Y. A., Lewis, K., Chocholek, M., Rumpang, E., & Hill, T. (2021). Short-and long-term carbon emissions from oil palm plantations converted from logged tropical peat swamp forest. *Global Change Biology*, *27*(11), 2361-2376. https://doi.org/10.1111/gcb.15544

McCarter, C. P. R., Rezanezhad, F., Quinton, W. L., Gharedaghloo, B., Lennartz, B., Price, J., Connon, R., & Van Cappellen, P. (2020). Pore-scale controls on hydrological and geochemical processes in peat: Implications on interacting processes. *Earth-Science Reviews*, *207*, 103227. https://doi.org/10.1016/j.earscirev.2020.103227

McEwan, A., Marchi, E., Spinelli, R., & Brink, M. (2020). Past, present and future of industrial plantation forestry and implication on future timber harvesting technology. *Journal of Forestry Research*, *31*, 339-351. https://doi.org/10.1007/s11676-019-01019-3

Ministry of Environment and Forestry (2022). FOLU Net Sink: Indonesia's Climate Actions Towards 2030. https://www.menlhk.go.id/cadmin/uploads/PHOTO_BOOK_FOLU_NET_SINK_Indonesia_s_Climate_Actions_Towards_2030_a3d4f1fa43.pdf#:~:text=The%20Operational%20Plan%20of%20Indonesia's%20FOLU%20Net,equivalent%20to%201.6%20tonnes%20CO2%20per%20capita.

Mohamad-Amini, M. H. (2024). Forest and agricultural biomass. *Plant biomass derived materials: Sources, extractions, and applications*, 271-290. https://doi.org/10.1002/9783527839032.ch11

Mohammed, A., Alsagheer, F., Ghaithan, A. M., & Mazher, K. M. (2024). An optimization of hybrid renewable energy system for seawater desalination in Saudi Arabia. *International Journal of Environmental Science and Technology*, 1-18. https://doi.org/10.1007/s13762-024-05904-1

Nurzakiah, S. (2014). *Prediksi potensi emisi karbon pada lapisan gambut akrotelmik dan katotelmik*. [Master's thesis, IPB University] http://repository.ipb.ac.id/handle/123456789/70314

Pardede, A. E., Yulianti, N., Sajarwan, A., & Adji, F. F. (2021). Kajian C-organik gambut pedalaman pada berbagai tutupan lahan [Study of organic carbon in inland peat under different land covers]. *Jurnal Penelitian UPR*, *1*(2), 63-72. https://doi.org/10.52850/jptupr.v1i2.4090

Purnama, I., Mutryarny, E., & Wijaya, R. T. (2023). Avanzando en el crecimiento de porang (*Amorphophallus muelleri*) en suelos podzólicos rojo-amarillos: un análisis experimental de la interacción entre el guano sólido y el fertilizante orgánico líquido [Advancing porang (*Amorphophallus muelleri*) growth in red-yellow podzolic soils: an experimental analysis of solid guano and liquid organic fertilizer interaction]. *Idesia (Arica)*, *41*(3), 9-14. http://dx.doi.org/10.4067/S0718-34292023000300009

Purwanto, S., Mu'min, M. A., & Amaludin, D. (2021). Analisa kebutuhan penggunaan alat berat pada pekerjaan pembentukan lahan proyek cluster duo perumahan Talaga Bestari untuk tercapainya efisiensi biaya proyek [Analysis of heavy equipment requirements for land development in the cluster duo housing project, Talaga Bestari, to achieve project cost efficiency]. *Structure*, *3*(2), 138-147. http://dx.doi.org/10.31000/civil.v3i2.7164

Ratnaningsih, A. T., Sukendi, Thamrin, Nasul, B. 2024. The role of *Acacia crassicarpa* plantation forest in Peatland in reducing CO_2 emissions. 8th International Conference on Agriculture, Environment, and Food Security (AEFS 2024). IOP Conf. Series: Earth and Environmental Science 1413 (2024) 012011. https://doi.org/10.1088/1755-1315/1413/1/012011

Riyani, D., Gusmayanti, E., & Pramulya, M. (2021). Dampak pemberian pupuk hayati dan npk terhadap emisi CO_2 pada perkebunan kelapa sawit di lahan gambut [Impact of biofertilizer and NPK application on CO_2 emissions in oil palm plantations on peatlands]. *Jurnal Ilmu Lingkungan*, *19*(2), 219-226. https://doi.org/10.14710/jil.19.2.219-226

Shi, Y., Wei, X., Sheng, L., & Yang, X. (2025). Effects of nitrogen fertilization on soil CH_4, CO_2, and N^2O emissions and their global warming potential in agricultural peatlands. *Agronomy*, *15*(1), 115. https://doi.org/10.3390/agronomy15010115

Serrano-Silva, N., Luna-Guido, M., Fernández-Luqueno, F., Marsch, R., & Dendooven, L. (2011). Emission of greenhouse gases from an agricultural soil amended with urea: a laboratory study. *Applied Soil Ecology*, *47*(2), 92-97. https://doi.org/10.1016/j.apsoil.2010.11.012

Suharto, A., Nurrochmat, D. R., & June, T. (2017). Neraca karbon pra dan post HTI di blok khusus kesatuan pengelolaan hutan tasik besar serkap Riau [Pre- and post-industrial timber plantation carbon balance in the special block of the Tasik Besar Serkap forest management unit, Riau]. *Jurnal Pengelolaan Sumberdaya Alam dan Lingkungan*, *7*(1), 19-28. https://doi.org/10.29244/jpsl.7.1.19-28

Suhesti, E., Zalizar, L., Triwanto, J., Ervayenri, E., & Purnama, I. (2024). Effects of harvest time and *Acacia crassicarpa* age on the physicochemical characteristics of *Apis mellifera* L. honey in tropical Indonesian forests. *Pertanika Journal of Tropical Agricultural Science*, *47*(4), 1205-1219. https://doi.org/10.47836/pjtas.47.4.10

Surasana, I. N., Limbong, K. D., & Yosep, Y. (2020). Limbah penebangan kayu di perusahaan PT. Dwimajaya Utama [Logging waste at PT. Dwimajaya Utama]. *Journal of Environment and Management*, *1*(3), 253-258. https://doi.org/10.37304/jem.v1i3.2571

Triadi, B. Marpang, M.F., Khardiman, Y. 2014. Korelasi antar parameter penurunan gambut-kedalaman air tanah - emisi karbon. output kegiatan penelitian pengaruh perubahan iklim terhadap Daerah Rawa. Kementrian Pekerjaan Umum, Badan Penelitian dan Pengembangan. Pusat Penelitian dan Pengembangan Sumberdaya Alam. https://simantu.pu.go.id/personal/img-post/adminkms/post/20210301095701__F__030_2014_Korelasi_Antar_Parameter_Penurunan_Gambut_Kedalaman_Air_Tanah.pdf

Yuniwati, Y., & Suhartana, S. (2014). Potensi karbon pada limbah pemanenan kayu *Acacia Crassicarpa* [Carbon potential of waste timber harvesting *Acacia Crassicarpa*]. *Jurnal Ilmu Lingkungan*, *12*(1), 21-31. https://doi.org/10.14710/jil.12.1.21-31

Pertanika J. Trop. Agric. Sci. 48 (6): 1883 - 1914 (2025)

PERTANIKA JOURNALS

TROPICAL AGRICULTURAL SCIENCE

Journal homepage: http://www.pertanika.upm.edu.my/

Review Article

Herbal Medicine Efficacy in Enhancing Crustacean Growth, Ovarian Maturation, and Immunity: A Review

Ariffin Hidir[1], Mohd Amran Aaqillah-Amr[2], Alias Redzuari[1], Zulkifli Hajar-Azira[1], Muyassar H. Abualreesh[3], Hanafiah Fazhan[1,4], Khor Waiho[1,4], Hongyu Ma[4,5], and Mhd Ikhwanuddin[1, 4, 6]*

[1]*Higher Institution Centre of Excellence (HICoE), Institute of Tropical Aquaculture, Universiti Malaysia Terengganu, 21030 Kuala Nerus, Terengganu, Malaysia*
[2]*WorldFish, Jalan Batu Maung, 11960 Bayan Lepas, Penang, Malaysia*
[3]*Department of Marine Biology, Faculty of Marine Sciences, King Abdulaziz University, Jeddah 21589, Saudi Arabia*
[4]*STU-UMT Joint Shellfish Research Laboratory, Shantou University, Shantou, China*
[5]*Guangdong Provincial Key Laboratory of Marine Biotechnology, Shantou University, Shantou, China*
[6]*Faculty of Fisheries and Marine, Campus C, Airlangga University, Mulyorejo, 60115 Surabaya, Indonesia*

ABSTRACT

Crabs, lobsters, prawns, and shrimp are among the most highly prized crustaceans in the aquaculture industry and contribute significantly to the global economy. In crustacean farming, artificial chemotherapeutic drugs have been used to improve growth, ovarian maturation, and immunity. However, dependence on chemotherapeutics promotes antibiotic-resistant bacteria, pollutes the environment, and poses risks for human consumption. Therefore, the primary goal of this review article is to identify the various plants used to improve the growth, spawning, and immunity of crustaceans. The findings indicate that plants and herbs such as amaranth, soursop leaf, mulberry leaf, olive, cajuput, bitterweed, Shepherd's needle, Indian borage, Chinese skullcap, and Indian gooseberry can enhance crustacean growth. Herbs like common senduduk can promote ovarian maturation, resulting in 100% spawned crustaceans. Plants such as guava leaves, tall-stilt mangrove leaves, chaihu, Indian ginseng, rosemary, mangrove cannonball trees, lechuguilla, moringa, neem, screw pine, Indian gooseberry, solanum, buton forest onion, roselle, giant sensitive trees, and Tasmanian blue gum

ARTICLE INFO

Article history:
Received: 17 March 2025
Accepted: 22 May 2025
Published: 25 November 2025

DOI: https://doi.org/10.47836/pjtas.48.6.13

E-mail addresses:
hidirariffin@umt.edu.my (Ariffin Hidir)
aaqillahamr_92@yahoo.com (Mohd Amran Aaqillah-Amr)
redzuary@gmail.com (Alias Redzuari)
ejaieyra@yahoo.com (Zulkifli Hajar-Azira)
Mabulreesh1@kau.edu.sa (Muyassar H. Abualreesh)
fazhan@umt.edu.my (Hanafiah Fazhan)
waiho@umt.edu.my (Khor Waiho)
mahy@stu.edu.cn (Hongyu Ma)
ikhwanuddin@umt.edu.my (Mhd Ikhwanuddin)
*Corresponding author

have been verified to have medicinal properties that can boost crustacean immunity. In conclusion, the knowledge gained from these findings may drive future research aimed at developing natural supplements or treatments to enhance growth, reproduction, and immune functions, ultimately benefiting crustacean farming.

Keywords: Crustacean, growth, immunity, ovarian maturation, plant extract

INTRODUCTION

Aquatic animals such as crustaceans are highly valued in the commercial market because of their delicious taste and rich in essential nutrients like vitamins, minerals, protein, amino acids, and fatty acids, which significantly contribute to their economic importance (Ahmadifar et al., 2021). Crabs, lobsters, prawns, and shrimp are among the highly prized crustaceans in the aquaculture industry and contribute significantly to the global economy (FAO, 2024). In 2022, global crustacean production surged to 12.7 million tonnes with penaeids shrimp stand out as the primary contributors to crustacean production, comprising 7.9 million tonnes, followed by crayfish (2.9 million tonnes) and crabs (1.2 million tonnes) (FAO, 2024). Main crustacean species being cultured in the world including white-leg shrimp (*Litopenaeus vannamei*), red swamp crayfish (*Procambarus clarkii*), Chinese mitten crab (*Eriocheir sinensis*), river prawn (*Penaeus monodon* and *Macrobrachium rosenbergii*) and swimming crabs (*Portunus* sp.) (FAO, 2024).

In crustacean farming, output or productivity could be increased by enhancing crustacean growth. Farmers tend to utilize synthetic hormones as the primary option to increase growth performance during crustacean farming. However, artificial hormone applications face challenges due to uncertain supply and rising prices, which undermines their usage (Hasnidar et al., 2021). The aquaculture industry has experienced consequences resulting from the use of synthetic hormones, which disrupt the health of surrounding aquatic animals and alter the sex ratio of affected species. This was evidenced by the spread of hormonal compounds through wastewater in aquaculture farming. Similarly, in modern times, the use of synthetic hormones in crustacean farming has resulted in significant consequences for humans, who consume these hormone-treated crustaceans, which affects human health. Since 2006, Europe has addressed such issues by implementing a ban on the use of drugs or chemicals in farmed animals (Lu et al., 2023a). Hence, plant products have been widely used in aquaculture to stimulate growth replacing drugs and chemical due to plants offer active compounds, such as alkaloids, terpenoids, saponins, and flavonoids (Ahmadifar et al., 2019). However, information regarding the use of plants on crustaceans needs to be gathered to reveal the mechanisms through which various plants affect crustacean growth.

In addition, seeds constitute one of the basic necessities or foundations of crustacean farming; hence, broodstock spawning is vital for initiating mass seed cultivation. To address the slow gonadal maturation of broodstock in aquaculture, eyestalk ablation is often introduced to suppress endogenous gonad-inhibiting hormone release by the eyestalk, which ultimately stimulates ovarian maturation in the broodstock (Farizah et al., 2017). However, several issues have arisen regarding ethics and the decreasing quality of eggs and larvae from broodstock with ablated eyestalks (Alam et al., 2017). The use of natural plants helps maintain crustacean welfare as an alternative to eyestalk ablation (Ahmadifar et al., 2019). Herbs and plant extracts are considered potential enhancers of ovarian maturation when applied to crustacean broodstock. For example, plant extracts contain numerous bioactive substances, such as vitamins and polyphenols, that may improve ovarian maturation in a variety of crustacean species (Dawood et al., 2017). Likewise, these herbs can promote the growth of beneficial microbial colonies in the digestive tract of broodstock, improving feed intake and providing the necessary nutrients for ovarian development (Moustafa et al., 2020). However, few studies have been conducted to explore the impact of these plants on improving ovarian maturation in crustaceans to date.

Disease outbreaks are frequent and significant challenges in the field of crustacean farming. Wu et al. (2021) indicated that *Vibrio* poses a difficulty in crab farming, resulting in an outbreak of milky disease. Similarly, other significant diseases that infect crabs include reovirus, dicisrovirus-1, bacterial pathogens and ciliate protozoans (Linh et al., 2017; Yue et al., 2023). Moreover, in shrimp farming, white spot syndrome is a disease that can affect the entire white-leg shrimp industry. In the prawn industry, nodavirus and extrasmall virus-like particles can cause white tail disease, which reduces the survival of larvae, postlarvae or juvenile prawns (Farook et al., 2016). Disease outbreaks in crustacean farming affect farming productivity to an extent, which has caused the aquaculture industry to collapse within a short period (Zhou et al., 2022). To overcome this issue, antibiotics are often used to control outbreaks (Wu et al., 2021). Antibiotics can be defined as substances that have the ability to kill or inhibit the growth of microorganisms while being safe for the host (Dawood et al., 2017). However, dependence on antibiotics in crustacean farming promotes antibiotic-resistant bacteria, leading to the emergence of drug-resistant strains (Ahmadifar et al., 2022), pollutes the environment and poses risks for human consumption (Yue et al., 2023). Thus, it is necessary to search for a non-chemotherapeutic method that serves a similar role as antibiotics, with the ability to kill microorganisms without affecting the crustacean as the host. Hence, the use of natural plants may improve crustacean health, as plants contain important phytochemical and plant secondary metabolites which act as antioxidants, antivirals, and antibacterials that activate specific immune system (Ahmadifar et al., 2021)

Given the beneficial effects of various plant on crustaceans and the great developments achieved through previous studies on crustaceans, the objective of present review is to identify all the plants that are potentially useful for commercial crustaceans, such as blue swimming crabs, mud crabs, crayfish, giant freshwater prawns, black tiger prawns and white-leg shrimp, and then to determine the ability of these specific plants to improve growth, ovarian maturation and immunity. This review also offers insight into the application of specific plant extracts in crustacean farming, including the conditions and techniques for introducing these specific plants to cultured crustaceans.

APPLICATION OF PLANT EXTRACTS IN CRUSTACEAN FARMING

Conditions for Choosing Plants

Several conditions should be taken into consideration before the commercialization of plants in the aquaculture industry. Certain conditions should be considered to ensure that the plants can be used for their medicinal properties for a prolonged period. The first condition is that plants should have antioxidant, antiviral, and antibacterial activities that promote growth, gonad maturation or immunity in crustaceans (Yue et al., 2023). These medicinal properties of plants are reflected by several active compounds inside them, such as phenols, polyphenols, alkaloids, quinones, triterpenoids, steroids, lectins, and polypeptides, all of which play a role in stimulating growth and immunity in crustaceans (Hasnidar et al., 2021). Plants have been verified to contain active compounds, such as phytoestrogens, which act as inducers of gonad maturation and antifertility, to stimulate the gonads of crustaceans. Phytoestrogens are vital active compounds that have a structure similar to that of oestradiol with a low molecular weight, allowing them to pass through cell membranes easily to bind with oestrogen receptors and stimulate an oestrogenic effect (Farizah et al., 2018). Determining the active compounds in plants could be achieved through compound screening via modern technologies, such as gas chromatography or conventional chromatography, before further experimentation with plants on crustaceans. To expedite this process, the use of plants that have previously been recognized as traditional local herbs (Table 1) with medicinal properties for humans could be effective for aquatic animals as well. For example, *Melastoma malabathricum L.*, known as a medicinal plant that promotes fertility and strengthens the human womb, has been proven effective in promoting ovary maturation in the mud crab *Scylla olivacea* (Farizah et al., 2018). Additionally, Chi et al. (2017) utilized herbs known to cure liver diseases in humans to treat hepatopancreas infection in aquaculture shrimp. Since the efficacy of plant supplementation is dose dependent, the optimal dose should be determined as the second condition. Administering plant concentrations below optimal doses does not affect crustacean growth or immunity, whereas too high a dose may sometimes act as an inhibitor of the immune response (Lu et al., 2023a). For example, Leite et al. (2021) reported that a too high rosemary concentration

Table 1
Previous herbs used in commercial aquaculture crustaceans

Commercialization of herbs	Crustacean species	Herbs	Reference
Commercialized as advanced product	Red claw crayfish, *Cherax quadricarinatus*	Coumarin extract from orchids and black beans (Sigma–Aldrich)	Zhou et al., 2022
	Giant freshwater prawn, *M. rosenbergii*	Polyherbal formulation (AquaImmu, Indian Herbs Supply and Research Company Limited) containing mixed herbs: • Basil, *Ocimum sanctum* • Indian ginseng, *Withania somnifera* • Heart-leaved moonseed, *Tinospora cordifolia* • Emblica, *Emblica officinalis*)	Kumari et al., 2004
	Black tiger shrimp, *P. monodon*	Polyherbal formulation (AquaImmu, Indian Herbs Supply and Research Company Limited) containing mixed herbs: • Basil, *O. sanctum* • Indian ginseng, *W. somnifera* • Heart-leaved moonseed, *T. cordifolia* • Emblica, *E. officinalis*	Chandran et al., 2016
	White-leg shrimp, *L. vannamei*	Polyherbal feed supplement (Ban-V trilobatum, Ideal Biosciences Private Limited) containing mixed herbs: • Turmeric, *Curcuma longa* • Guava, *Psidium guajava* • Holy basil, *O. sanctum* • Neem, *Azadirachta indica* • Birch-leaved cat tail, *Acalypha fruticose* • Indian pennywort, *Centella asiatica* • Waterhyssop, Bacopa *monnieri* • Sireh, *Piper betle* • Thumbai, *Leucas aspera*	Iyapparaj et al., 2021

Table 1 *(continue)*

Commercialization of herbs	Crustacean species	Herbs	Reference
		Polyherbal supplements (Phycurma Aquatic, Agrinusa Jaya Santosa company) containing mixed herbs: • Turmeric, *Cucurma domestica* • Javanese ginger, *Cucurma xanthorrhiza* • Gale of the wind, *Phyllantus niruri*	Putra et al., 2024
	Shrimp (NA species)	Cinnamon, *Cinnamomum cassia* (Ningbo Hangjing Biological Technology Co., LTD)	Zhang et al., 2023
Commercialized as traditional herbs, these are typically purchased from traditional medicine shops or commonly used in human food	Mud crab, *S. paramamosain*	Chinese gallnut, *G. chinensis*	Wu et al., 2021
	Red claw crayfish, *Cherax quadricarinatus*	Tochu, *Eucommia ulmoides* (leaf)	Lu et al., -2023a
	Giant freshwater prawn, *M. rosenbergii*	Peppermint, *Mentha piperita* (leaf)	Kawamura et al., 2019
		Lemongrass, *Cymbopogon citratus* (rhizome)	Adnan et al., 2021
		Rosemary, *Rosmarinus officinalis* (leaf)	Leite et al., 2021
	Black tiger shrimp, *P. monodon*	Ginger, *Boesenbergia pandurata* (rhizome)	Hardi et al., 2022
		Hairy-fruited eggplant, *Solanum ferox* (fruit)	Hardi et al., 2022
		Aloe vera (leaf)	Aftabuddin et al., 2017
		Green chiretta, *Andrographis pariculata* (leaf)	Aftabuddin et al., 2017
		Sugar apple, *Annona squamosa* (fruit)	Aftabuddin et al., 2017
		Neem, *A. indica* (leaf)	Aftabuddin et al., 2017
		Key lime, *Citrus aurantifolia* (leaf)	Aftabuddin et al., 2017
		Coriander, *Coriandrum sativum* (leaf)	Aftabuddin et al., 2017
		Holy basil, *Ocimum sanctum* (leaf)	Aftabuddin et al., 2017
		Onion, *Allium sepa*	Aftabuddin et al., 2017
		Guava, *P. guajava* (leaf)	Aftabuddin et al., 2017

Table 1 *(continue)*

Commercialization of herbs	Crustacean species	Herbs	Reference
	White-leg shrimp, *L. vannamei*	Dokudami, *Houttuynia cordata* (leaf)	Kawamura et al., 2019
		Peppermint, *M. piperita* (leaf)	Kawamura et al., 2019
		Red chilli, *C. annuum* (fruit)	Kawamura et al., 2019
		Ginger, *Zingiber officinale* (rhizome)	Kawamura et al., 2019
		Ginger, *Z. officinale* (rhizome)	Widowati et al., 2022
		Turmeric, *Cucurma domestica* (rhizome)	Widowati et al., 2022
		Temulawak, *Curcuma zanthorrhiza* (rhizome)	Widowati et al., 2022
		Green tea, *Camellia sinensis* (leaf)	Kongchuma et al., 2016
		Chinese skullcap, *Scutellaria baicalensis* (root)	Maurus et al., 2023
		Nightshades, *Solanum procumbens* (leaf)	Hong et al., 2022
		Cat's claw, *Uncaria tomentosa* (bark)	Junior, 2017
		Buton forest onion, *Eleutherine bulbosa* (bulb)	Munaeni et al., 2020
Collected from wild	Blue swimming crab, *Portunus pelagicus*	Common senduduk, *M. malabathricum* (leaf)	Alam et al., 2019
	Mud crab, *S. paramamosain*	Soursop, *A. muricata* (leaf)	Yue et al., 2023
	Mud crab, *S. olivacea*	Common senduduk, *M. malabathricum* (leaf)	Farizah et al., 2017
		Common senduduk, *M. malabathricum* (leaf)	Farizah et al., 2018
		Common senduduk, *M. malabathricum* (leaf)	Iromo et al., 2021
		Mulberry, *Morus alba* (leaf)	Fujaya et al., 2018
		Tall-stilt mangrove, *R. apiculata* (leaf)	Linh et al., 2017
	Red claw crayfish, *C. quadricarinatus*	Lempuyang, *Zingiber zerumbet* (flower)	Hardi et al., 2021
		Chaihu, *Radix bupleuri* (root)	Lu et al., 2023b
	Giant freshwater prawn, *M. rosenbergii*	Bermuda grass, *Cynodon dactylon* (leaf)	Farook et al., 2016

Table 1 *(continue)*

Commercialization of herbs	Crustacean species	Herbs	Reference
		Fiddlehead fern, *Diplazium esculentum* (leaf)	Hajar-Azira et al., 2023
		Indian ginseng, *W. somnifera* (root)	Harikrishnan et al., 2012
		Cajeput, *Melaleuca cajuputi* (leaf)	Sahimi et al., 2022
	Black tiger shrimp, *P. monodon*	Mangrove holly, *Acanthus ilicifolius* (leaf)	Saptiani et al., 2021
		Cannonball mangrove, *Xylocarpus granatum* (leaf)	Saptiani et al., 2020
	White-leg shrimp, *L. vannamei*	Buton forest onion, *E. bulbosa* (bulb)	Munaeni et al., 2019
		Papaya, *Carica papaya* (leaf)	Supono et al., 2019
		Ketapang, Terminalia catappa (leaf)	Supono et al., 2019
		Tall-stilt mangrove, R. apiculata (leaf)	Supono et al., 2019
		King of Bitters, *Andrographis paniculata* (leaf)	Yin et al., 2023
		Shepherd's Needles, *Bidens alba* (leaf)	Huang et al., 2022
		Mexican mint, *Plectranthus amboinicus* (leaf)	Huang et al., 2022
		Purple coneflower, *Echinacea purpurea* (root, leaf and flower)	Medina-Beltrán et al., 2012
		Cat's claw, *U. tomentosa* (bark)	Medina-Beltrán et al., 2012
		Indian ginseng, *W. somnifera* (root)	Abdel-Tawwab et al., 2022
		Moringa, *Moringa oleifera* (seeds and pods)	Lugo-Rubio et al., 2022
		Croton, *Croton californicus* (Petiole, leaves, and flowers)	Lugo-Rubio et al., 2022
		Moringa, *M. oleifera* (leaf)	Abidin et al., 2022
		Roselle, *Hibiscus sabdariffa* (fruit)	Nguyen et al., 2023
		Giant sensitive tree, *Mimosa pirga* (leaf)	Nguyen et al., 2023
		Tasmanian blue gum, *Eucalyptus globulus* (leaf)	Nguyen et al., 2023
Agricultural waste (byproduct)	Crayfish, *A. leptodactylus*	Olive, *Olea europaea* (wastewater of olive mill)	Parrillo et al., 2017
	White-leg shrimp, *L. vannamei*	Lechuguilla, *Agave lechuguilla* (bagasse)	Quiroz-Guzman et al., 2023
		Cacao, *Theobroma cacao* (Pod husk)	Chang et al., 2023

of 15% fed to the giant freshwater prawn *M. rosenbergii* promoted the production of reactive oxygen species that led to cell damage due to lipid peroxidation and decreased prawn growth. Similarly, Munaeni et al. (2020) reported lower intestinal microbe diversity through gel electrophoresis for fish given a higher dosage of rosemary extract at 25 g kg^{-1}, which slowed the immune response mechanism. The third condition is the availability of wild plants, which are freely accessible in vast quantities at no cost (Table 1). For example, Linh et al. (2017) utilized a mangrove plant leaf from *Rhizophora apiculata* to cure the megalopa of a mud crab, *S. paramamosain,* that was infected by ciliate protozoans. Sahimi et al. (2022) also utilized *Melaleuca cajuput* leaves as a feed additive to improve the growth of the giant freshwater prawn *M. rosenbergii.* Certainly, these tall-stilt mangrove and cajuput leaves are available at no cost and can be found in abundance, allowing farmers to use these plants without any constraints. A fourth condition is that plants and herbs could be obtained from industrial waste as part of an effort to eradicate waste from industries (Table 1). Parrillo et al. (2017) used wastewater from an olive processing mill to coat fish flesh before being fed crayfish, *Astacus leptodactylus*, resulting in improved moulting. Similarly, several previous studies have used leaves from commercial trees such as mulberry, guava, and roselle for enhancing growth and the immune system of mud crabs, *S. olivacea* (Fujaya et al., 2018) and *S. paramamosain* (Yue et al., 2023), and the white-leg shrimp, *Littopenaeus vannamei* (Nguyen et al., 2023), respectively. In conclusion, these third and fourth conditions, such as using wild plants or utilizing waste from the plantation industry, are imperative to reduce the costs of raw materials, making them viable for commercial use in crustacean farming. However, the efficacy of plants (first condition and second condition) in promoting the growth, spawning or immunity of crustaceans should be prioritized. Because a wide variety of herbs have been proven effective for use on commercial crustaceans, herbs could be further commercialized not only by involving a single herb but also by combining different herbs to increase their efficacy while offering various functions (Table 1).

Processing and Implementation of Plants

Previous studies often used leaf parts that were air dried, powdered and used directly for medicinal treatments. Additionally, the plant powder is further extracted by soaking (sometimes stirring) with a solvent such as ethanol (70–85%) or methanol with a ratio of 5- to 10-fold the solvent for 4 to 48 hours (Leite et al., 2021). Other solvents can be used to extract the plant by boiling it with distilled water or deionized water at 100 °C for 1 to 2 hours at a ratio of 5-fold solvent (Wu et al., 2021). The extract is then filtered through muslin cloth or Whatman paper no. 1 or centrifuged before being evaporated via a rotary evaporator at 40–50 °C and stored at 4–20 °C for further use (Hajar-Azira et al., 2023; Zhang et al., 2023). After plant extraction, four different techniques are applied to introduce

the plants to cultured crustaceans: pelleting, coating, immersion, or injection. The most common technique used involves incorporating the plant powder in formulated pellets within a range of concentrations of 0.5–2 g/kg. For ready-made pellets, coating techniques can be used to encapsulate feeds with plant extracts via two different coatings. This dual-layer coating process prevents any leaching of the plant extract into the surrounding water. The feed can be initially coated with a plant extract as the first layer, followed by a second layer coating with either chitosan (1% or 3%) (Ali et al., 2023; Fujaya et al., 2018) or squid oil (2%) (Nguyen et al., 2023). The chitosan solution is prepared by using acetic acid as a solvent (Fujaya et al., 2018). After the first layer of coating, the pellet was dried at room temperature for 30 minutes before the second layer was applied and then dried at room temperature for 5 hours (Medina-Beltrán et al., 2012). Additionally, instead of pellets, raw materials such as fish can be coated by soaking them with plant extracts for 20 to 30 minutes, air dried and layered with a chitosan solution or squid oil (Ali et al., 2023). The dosage of plant extract typically ranges from 0.8 to 10 g of plant extract per kilogram of feed (Lu et al., 2023b; Nguyen et al., 2023). For the immersion technique, medicinal treatment is achieved by dissolving the plant powder within the range of 1000 to 6000 mg per litre of seawater (Anirudhan et al., 2021; Linh et al., 2017), with the main purpose of using this technique to cure cultured crustaceans from any disease or parasite infection. Another technique is injection, which is specialized for stimulating the gonads and spawning of broodstock. Given that this technique demands skilled labour and is applicable only to a restricted number of broodstock, it has been used primarily for crabs, as a single mother crab can yield over a million eggs. Previously, several doses of plant extract were applied, ranging from 20 µg to 1 mg of plant extract per gram of crab body weight (Alam et al., 2019; Farizah et al., 2018). Overall, four techniques can be applied for plant or herb administration in crustacean farming, either through pellets, coatings, immersion, or injection; all these techniques should be in accordance with the purpose of plant use.

ROLE OF PLANT ADDITIVES ON CRUSTACEAN GROWTH AND FEEDING

Herbs or medicinal plants contain compounds that can enhance growth performance in terms of survival, growth, and moulting. To improve the growth of crabs, several herbs, such as amaranth (*Amaranthus* sp.), soursop leaf (*A. muricata*), and mulberry leaf (*M. alba*), have been identified and shown to increase growth. For crayfish (*A. leptodactylus*) and giant freshwater prawn (*Macrobrachium rosenbergii*), plants such as cajaput (*M. cajuputi*), olive (*O. europaea*) and fiddlehead fern (*D. esculentum*) have been verified to positively affect their growth. Moreover, for white-leg shrimp, several plants are able to improve shrimp growth, such as bitterweed (*Andrographis paniculate*) shepherd's needles (*B. alba*), Indian borage (*P. amboinicus*)*, Mexican mint (P. amboinicus),* Chinese skullcap (*S. baicalensis),*

and Indian gooseberry (*Phyllanthus amarus*), as well as commercial products such as Ban-V. Interestingly, plants that can benefit the survival of crustaceans, such as mud crab (*S. olivacea*), crayfish (*A. leptodactylus*), and white-leg shrimp (*L. vannamei*) given plant additives such as soursop leaf (*A. muricata*), olive (*O. europaea*) and the king of bitters (*A. paniculata*), reach survival rates of more than 80%, 81.5%, and 93.3%, respectively (Ali et al., 2023; Parrillo et al., 2017; Yin et al., 2023). In addition to survival, crustaceans fed plant additives are more likely to show significant growth in terms of weight gain and specific growth rate. Table 2 shows that crustaceans such as mud crab (*S. olivacea*) had a greater growth rate percentage after being provided with soursop leaf (*A. muricata*) (16.5%) than after being provided the control diet (15.8%). Other studies by Parrillo et al. (2017) revealed a greater specific growth rate (SGR) for crayfish (*A. leptodactylus*) supplemented with 15 g/kg olive (*O. ueropaea*) additive (SGR: 0.32% day^{-1}) than for the control (SGR: 0.21% day^{-1}). Similarly, a study by Sahimi et al. (2022) and Hajar-Azira et al. (2023) reported a weight increase of approximately 2-fold for giant freshwater prawns (*M. rosenbergii*) fed with cajuput (*M. cajuputi*) and fiddlehead fern (*Diplazium esculentum*) with weight gains of 1.1 g and 50 mg, respectively, compared with the control treatment (weight gains of 0.5 g and 20 mg, respectively). For white-leg shrimp, several listed plant additives, such as bitterweed (*A. paniculata*), shepherd's needle (*B. alba*), Indian borage (*P. amboinicus*), Chinese skullcap (*S. baicalensis*) and Indian gooseberry (*P. amarus*), have been verified to increase their growth (Table 2). Interestingly, the use of plant additives such as Shepherd's needle (*B. alba*) (SGR: 16% day^{-1}) and Indian borage (*P. amboinicus*) (SGR: 17% day^{-1}) increased the SGR approximately 2-fold compared with that of the control group (SGR: 9.34% day^{-1}) (Huang et al., 2022).

Plant extracts aid in promoting crustacean growth through a vital compound known as phytoecdysteroid, which is found in the leaves of plants (Hajar-Azira et al., 2023). Phytoecdysteroids have a four-ring skeleton composed of 27, 28, 29, or 30 carbon atoms (derived from plant sterols), and the most common phytoecdysteroid is 20-hydroxyecdysone (Arif et al., 2022). In crustaceans, 20-hydroxyecdysone is known as a moulting hormone, which is imperative for promoting ecdysis in crustaceans (Fujaya et al., 2018). Instead of depending on the Y-organ for the secretion of the moulting hormone, providing plant leaves that contain high levels of phytoecdysteroids leads to ecdysteroid elevation in the crustacean haemolymph and acts as a signal for triggering moulting occurrence in crustaceans (Hasnidar et al., 2021). The moulting process is required for the crustacean to shed the old carapace and grow in size, and the moulting process ends with the formation of a new carapace that slowly hardens. In addition, plant extracts improve crustacean growth performance by optimizing feed absorption through a healthy digestive tract (Quiroz-Guzman et al., 2023). Through qPCR, the incorporation of plant extracts in the crustacean diet caused the upregulation of the expression of several genes related to amylase, protease,

and lipase in the hepatopancreas, stomach, and intestine, leading to the secretion of more digestive enzymes (Yin et al., 2023). The increase in digestive enzyme activity promotes the catabolism of glycogen, protein, and lipids for better absorption and, subsequently, increases the feed conversion ratio of crustaceans (Abdel-Tawwab et al., 2022; Lu et al., 2023b). Additionally, the presence of plant extracts in crustacean feed positively influences the morphology of the hepatopancreas and intestines to improve the absorptive ability of various nutrients (Lu et al., 2023a). Crustaceans fed with plant extracts presented increased numbers of intestinal goblet cells, intestinal villus heights, widths of the intestinal lamina propria, and mucosal folds; all of these morphological enhancements increase the surface area available for efficient nutrient absorption, thus promoting crustacean growth (Abdel-Tawwab et al., 2022). One of the active compounds, especially polyphenols in plant extracts, stimulates digestion activity, which increases crustacean appetite (Hajar-Azira et al., 2023; Yue et al., 2023;). Since these phenolic compounds have antimicrobial characteristics, they may have bactericidal effects on the gut microflora. The microbial properties of the plant extract shift the microbial ecology in the crustacean gut by preventing pathogen colonization and providing a diverse gut ecosystem (Sahimi et al., 2022). This increase in bacterial diversity leads to a greater level of intra- and interspecific competition, thereby reducing the niches available for the colonization of pathogenic microorganisms (Quiroz-Guzman et al., 2023). This phenomenon has also been observed in pathogen-infected crustaceans, where plant additives shift the dominance of *Vibrio* in the crustacean gut and intestine to a greater abundance of *Bacilli* and cyanobacteria (Quiroz-Guzman et al., 2023). Plant incorporation into the crustacean diet not only reduces pathogen infection in the digestive system but also serves oligosaccharides as a feed source for the microbial community, enhancing crustacean digestion and leading to increased growth performance (Quiroz-Guzman et al., 2023).

ROLE OF PLANT ADDITIVES ON CRUSTACEAN REPRODUCTION

Current research on crustacean reproduction has focused only on crab species, such as the blue swimming crab (*P. pelagicus*) and mud crabs from two species, *S. serrata* and *S. olivacea (Table 3)*. All three studies used common senduduk with an injection technique to substantially improve the ovarian maturation of crabs, and these experiments were verified through several analyses, including hormone levels (i.e., oestradiol), gonad volume (i.e., gonadosmatic index (GSI) and oocyte size) and the spawning rate. Farizah et al. (2018) reported that the oestradiol level in the haemolymph of the mud crab *S. olivacea,* injected with 1.00 mg/g (oestradiol: 48.6 pg/ml) of common senduduk, was more than double that of the mud crab in the control group (oestradiol: 25.5 pg/ml). This, in turn, induced oocyte growth in the mud crab ovary, as evidenced by the greater oocyte diameter (113 μm) and GSI (14.1). Similarly, another study by Iromo et al. (2021) demonstrated an increase in the

Table 2
Effects of plant extracts on the growth performance and feeding of crustaceans

Crustacean species	Plant extract	Optimal dose	Growth indicators				Reference
			Survival	WG	SGR	Moulting	
Mud crab, *S. olivacea*	Amaranth, *Amaranthus sp.*	42 µg/ml*	●			●	Hasnidar et al., 2021
	Soursop, *A. muricata* (leaf)	0.6 g/kg	●			●	Ali et al., 2023
	Mulberry, *M. alba* (leaf)	2.7 g/kg				●	Fujaya et al., 2018
Crayfish, *A. leptodactylus*	Olive, *O. europaea* (wastewater of olive mill)	5.0 g/kg	●		●		Parrillo et al., 2017
Giant freshwater prawn, *M. rosenbergii*	Fiddlehead fern, *D. esculentum* (leaf)	10 g/kg	●	●			Hajar-Azira et al., 2023
	Cajeput, *M. cajuputi* (leaf)	15 g/kg		●			Sahimi et al., 2022
Black tiger shrimp, *P. monodon*	AquaImmu product (mixed herbs, refer Table 1)	300 g/kg			●		Chandran et al., 2016
	Mix of ginger, *B. pandurata* (rhizome) and hairy-fruited eggplant, *S. ferox* (fruit) with ratio 2:1	30 g/kg	●		●		Hardi et al., 2022
White-leg shrimp, *L. vannamei*	King of Bitters, *A. paniculata* (leaf)	5 g/kg	●	●			Yin et al., 2023
	Shepherd's Needles, *B. alba* (leaf)	20 g/kg			●		Huang et al., 2022
	Mexican mint, *P. amboinicus* (leaf)	20 g/kg			●		Huang et al., 2022
	Chinese skullcap, *S. baicalensis* (root)	10 g/kg		●			Maurus et al., 2023)
	Indian gooseberry, *P. amarus* (leaf)	20 g/kg	●	●			Ngo et al., 2020
	Ban-V product (mixed herbs, refer Table 1)	20 g/kg	●		●		Iyaparaj et al., 2020
	Buton forest onion, *E. bulbosa* (bulb)	40 g/kg		●			Munaeni et al., 2019
	Mixed herbs consisting ginger, *Z. officinale* (rhizome), turmeric, *Cucurma domestica* (rhizome), temulawak, *Curcuma zanthorrhiza* (rhizome)	NA		●			Widowati et al., 2022

Note: SGR: Specific growth rate. Many of the crustaceans were given plant extract through feeding, while those given plant extract via injection are indicated by the symbol *. The green circle indicates results of growth performance that are better than the control treatment (without the plant extract)

gonadosomatic index (GSI) for the mud crab *S. serrata* injected with 0.01 mg/g of common senduduk (GSI: 18.1) compared with that of crabs without common senduduk injection (GSI: 15.2). The use of common senduduk not only ensures that the ovarian stimulation of crabs occurs at the highest rate but also aids in increasing the number of spawned crabs. This occurrence was reported by Alam et al. (2019), who reported that all blue swimming crabs, *P. pelagicus,* injected with common senduduk at concentrations of 15 and 20 µg/g were completely spawned (100%), whereas those crabs given 5 and 10 µg/g had spawning rates of 67 and 67%, respectively. In contrast, the control groups presented the lowest spawning rate, at only 33%. To date, only one herb has been used to promote the ovarian growth of crabs. More studies are needed to collect information from other potential herbs or plants that could enhance the ovarian maturation of crustaceans or perhaps expand the use of common senduduk on other crustacean groups to obtain more data on this herb's efficacy for increasing spawning, either in lobsters, prawns, or shrimp.

Table 3
Effects of plant extracts on the reproductive performance of crustaceans

Crustacean species	Plant extract	Optimal dose	Reproductive indicators				Reference
			Spawning rate	GSI	Oocyte size	Oestradiol	
Blue swimming crab, *P. pelagicus*	Common senduduk, *M. malabathricum*	15-20 µg/g	●				Alam et al., 2019
Mud crab, *S. serrata*	Common senduduk, *M. malabathricum*	0.01 mg/g		●			Iromo et al., 2021
Mud crab, *S. olivacea*	Common senduduk, *M. malabathricum*	1.00 mg/g		●	●	●	Farizah et al., 2018

Note: GSI: The green circle indicates result of reproductive indicators better than control treatment (without given plant extract). All the crabs here were given plant extract via injection

Plant extracts contain bioactive compounds, especially phytoestrogens, that have a similar structure to oestradiol, resulting in effects similar to those of steroid hormones in stimulating reproduction in crustaceans (Iromo et al., 2021). Since these phytoestrogens have a low molecular weight, they easily move in crustacean haemolymph, pass through cell membranes and bind with oestrogen receptors to induce Vtg expression in the ovary oocyte (Farizah et al., 2017) and hepatopancreas (Iromo et al., 2021). This expression then stimulates vitellin deposition and the proliferation of yolk globules in crustacean ovaries,

leading to ovary volume enlargement and colour changes from white to deep orange (Farizah et al., 2018). In addition, hormones such as ecdysteroid, known for regulating moulting in crustaceans, are known to promote reproduction (Sumiya et al., 2014). The expression of ecdysone commonly commences in the Y-organ and becomes 20-hydroxyecdysone (20E), the biologically active form of ecdysteroid that promotes vitellogenesis for ovarian growth (Gong et al., 2015). Although without endogenous 20-hydroxyecdysone, the incorporation of plant extract (containing phytoecdysteroids) in crustacean feed causes an increase in this hormone in crustacean haemolymph. In plants, phytoecdysteroids play a role in enhancing plant immunity against predators, particularly during the reproductive stage, when their concentration is highest, and these compounds accumulate in reproductive organs such as seeds and roots (Arif et al., 2022). Since phytoecdysteroids are polyhydroxylated steroids with a structure resembling that of the crustacean-moulting hormone, such steroids are able to improve gonad maturation in crustaceans when included in their diet (Dinan et al., 2021). These phytoecdysteroids are sent via haemolymph into ovarian tissue and bind with EcR (ecdysone receptor), activating the ecdysteroid signalling pathway (Gong et al., 2015). After binding with phytoecdysteroid, EcR forms a heterodimer that interacts with the 50-promoter region of the Vg gene, promoting its transcription (Gong et al., 2015). This leads to the synthesis of vitellogenin in the ovary, resulting in yolk accumulation, and the ovary undergoes gradual changes, transitioning from white to an orange–reddish colour (Farizah et al., 2018). Other bioactive compounds from plant extracts that play important roles in ovarian development include α-tocopherol. Since α-tocopherol (known as vitamin E) is lipid soluble, it easily accumulates in the ovary oocyte and acts as a natural antioxidant (Li et al., 2018). In the oocyte, α-tocopherol protects membranes and organelles from oxidation by scavenging organic free radicals (Wouters et al., 2001) and prevents peroxides resulting from lipid metabolism (Lebold & Traber. 2014). This biological role of α-tocopherol subsequently aids in ovarian maturation, fertilization, and egg hatchability in crustacean female broodstock (Li et al., 2018). The role of α-tocopherol does not cease during the postspawning event, as a previous study reported a high level of α-tocopherol in crustacean larvae, providing evidence for the importance of α-tocopherol in larval development as well (Wouters et al., 2001).

ROLE OF PLANT ADDITIVES ON CRUSTACEAN IMMUNITY

Increasing prices, along with the increasing demand for crustaceans, have led to the mass culture of crustacean species. Unfortunately, currently, the greatest challenge in crustacean farming is maintaining the health of commercial crustaceans in the aquaculture industry. Many studies have focused on commercial crustacean species such as the mud crab (*S. paramamosain*), red claw crayfish (*C. quadrinatus*), giant freshwater prawn (*M. rosenbergii*), and black tiger shrimp (*P. monodon*). White-leg shrimp is the most

attractive species for use as experimental specimens because this aquatic animal is the most crustacean farmed, and disease outbreaks have halted aquaculture operations to the extent that entire farms have collapsed, resulting in millions of losses. To ensure the efficacy of the plants, a challenge test was conducted, and the crustacean specimens were exposed to several harmful pathogens, such as *Vibrio harveyi, V. parahaemolyticus, V. alginolyticus, Aeromonas hydrophilia* and microcystin-LR (Table 4). Previous evidence verified that several medicinal plants, such as mangrove cannonball trees, lechuguilla deserts, neems, screw pines, Indian gooseberries, solanum, buton forest onion, giant sensitive trees, and tall-stilt mangroves, were able to cure *Vibrio* sp. infection. Moreover, medicinal plants such as tochu and chaihu are able to resist microcystin-LR, and herbs such as Indian ginseng can cure diseases caused by *A. hydrophila*. Interestingly, despite white-leg shrimp being infected with *Vibrio*, the survival of shrimps fed lechuguillas (Quiroz-Guzmán et al., 2023), neems (Morales-Covarrubias et al., 2016) and Indian gooseberries (Ngo et al., 2020) was 100, 75.8 and 72.6%, respectively, greater than that of shrimp in the control treatment (>50%). In addition to conducting challenge tests, plant efficacy was tested via immunity-related analyses, such as alkaline phosphatase (AKP), catalase (CAT), glutathione peroxidase (GPx), glutathione S transferase (GST), malondialdehyde (MDA), phenoloxidase (PO), reduced glutathione (GSH), superoxide dismutase (SOD) and total antioxidant capacity (T-AOC) analyses. Some of these components are part of the body's antioxidant defence system, working together to neutralize reactive oxygen species and minimize oxidative damage to cells and tissues in crustaceans. For crabs, Yue et al. (2023) reported that an increase in SOD and GST simultaneously reduced the MDA content after the mud crab, and *S. paramamosain* fed leaf guava as a feeding additive at a concentration of 230 mg/kg. For lobster, Lu et al. (2023a, 2023b) reported that red claw crayfish *C. quadrinatus* provided with tochu and chaihu at concentrations of 1.0 and 0.8 g/kg, respectively, presented relatively higher AKP, CAT, GPx, GSH, GST, PO, SOD, and T-AOC and, at the same time, reduced MDA levels (Table 4). For prawn species, giant freshwater prawns (*M. rosenbergii*) presented increased PO (absorbance: 3.09) and SOD (4.66 U/mg $prot^{-1}$) levels in response to Indian ginseng fed a concentration of 1.0% (Harikrishnan et al., 2012). Moreover, giant freshwater prawns fed with rosemary at a concentration of 5% presented relatively high GSH, GR and GST contents, with values of 80 mmol mL^{-1}, 501 nmol mL^{-1}, and 0.41 mmol min^{-1} mg $prot^{-1}$, respectively (Leite et al., 2021). For shrimp, the incorporation of plant additives such as Indian ginseng at a concentration of 2.0 g/kg into white-leg shrimp (*L. vannamei*) builds a better immune system by increasing the levels of CAT, GPx, GSH, and T-AOC and reducing the levels of MDA (Table 4).

To date, only one study has addressed the larval stage of crustaceans, referring to a study by Linh et al. (2017), which used tall-stilt mangrove leaves, *R. apiculata, t*o alleviate ciliate and protozoan infection during the Megalopal stage of the mud crab. It is imperative

to carry out experiments related to crustacean larvae since this phase is considered a fragile stage due to the incomplete development of the immune system, which increases susceptibility to disease and pathogen infection. The crustacean larval phase is often vulnerable to *Vibrio* infection, which decreases larval survival in a hatchery within a short period. Therefore, to make substantial improvements in crustacean larval farming, plants and herbs such as mangrove cannonball trees, lechuguilla, Indian ginseng, neem, screw pine, Indian gooseberry, and *Solomon procumbens*, as well as forest onions, and giant sensitive trees should have their applications expanded to crustacean larvae to ensure larval resilience against *Vibrio* infection. Established products such as AquaImmu, Ban-V, and Phycurma aquatic could also be used for larval rearing because of their ability to promote bactericidal, antioxidant and lysozyme activities. The two best possible techniques that could be implemented for larval farming are immersion, by dissolving plant powder in the larval tank, or enrichment, by enriching the artemia with medicinal plants before feeding the artemia to crustacean larvae. The effect of the disease is minimized with high-yield larval output, which could be improved in crustacean farming. Additionally, this is one of the initiatives to curb antibiotic usage, especially in crustacean species with very low larval survival, such as mud crabs, blue swimming crabs, and spiny lobsters.

Phenolic compounds such as polyphenols, flavonoids, and tannins (see Table 5) are some of the natural compounds derived from plants that have potent antimicrobial activity against several strains of bacteria (Parrillo et al., 2017). Phenolic compounds inactivate microbial adhesions that are vital for facilitating the attachment of microorganisms to host tissues or cells. Additionally, the phenolic–lipophilic characteristics cause the cytoplasmic membrane of bacteria to dissolve, leading to the leakage of intracellular constituents, killing the bacteria (Sahimi et al., 2022). In addition to damaging the bacterial cell membrane, phenolic compounds offer bacteriolytic properties, including preventing the cell division of bacteria and reducing their biofilm-forming ability (Quiroz-Guzman et al., 2023). Phenolic compounds also act as prebiotic agents for the growth of the gut microbiota. Polyphenols increase the number of good bacteria while simultaneously inhibiting the proliferation of pathogenic bacteria in the intestinal tract (Lu et al., 2023b). Good bacteria, such as *Lactobacillus*, can metabolize polyphenol compounds to generate energy. Some phenolic compounds, such as flavonoids, tannins, and saponins, can reduce cholesterol levels since these phenolic compounds compete with cholesterol for the same receptors, preventing its absorption in the crustacean digestive tract and reducing blood cholesterol levels (Ali et al., 2023). The accumulation of cholesterol increases oxidative stress and may block blood flow, thus decreasing the oxygen supply to target cells. Since phenolic compounds can stimulate the secretion of bile salts, which are crucial for emulsifying fats in the intestine, these findings indicate that phenolic compounds indirectly contribute to the elimination of LDL cholesterol via the digestion process (Ali et al., 2023). Additionally, plant additives

Table 4
Effects of plant extracts on the immunity of crustaceans

Crustacean	Plant extract	Opt dose	Antioxidant indicators							Other immunity indicators					Challenge test				Reference
			CAT	GSH	GPx	GST	SOD	T-AOC	MDA	PO	AKP	Haemocyte count	Lysozyme	Phagocytic activity	*Aeromonas*	Microcystin-LR	Protozoan	*Vibrio*	
Mud crab, *S. paramamosain*	Guava, *P. guajava* (L)	0.3 g/kg				●	●		●										Yue et al., 2023
	Tall-stilt mangrove, *R. apiculata* (L)	1.0 g/l*															●		Linh et al., 2017
Red claw crayfish, *C. quadrinatus*	Tochu, *E. ulmoides* (L)	1.0 g/kg	●	●	●	●	●	●		●	●					●			Lu et al., 2023a
	Chaihu, *R. bupleuri* (R)	0.8 g/kg	●		●	●	●	●	●	●	●					●			Lu et al., 2023b
Giant freshwater prawn, *M. rosenbergii*	Indian ginseng, *W. somnifera* (R)	1 g/kg					●			●					●				Harikrishnan et al., 2016
	Rosemary, *R. officinalis* (L)	5 g/kg		●		●													Leite et al., 2021
	Cannonball mangrove, *X. granatum* (L)	1.25 g/kg												●				●	Saptiani et al., 2020
	AquaImmu product (Table 1)	1 g/kg								●			●						Sahoo et al., 2004
	Ban-V product (Table 1)	20 g/kg					●			●		●	●						Iyaparaj et al., 2020
Black tiger shrimp, *P. monodon*	AquaImmu product (Table 1)	300 g/kg								●		●							Chandran et al., 2016
	Mixed of nine herbs, (Table 1)	2.5 ml/kg	●	●	●		●							●				●	Aftabuddin et al., 2017
White-leg shrimp *L. vanname*	Indian ginseng, *W. somnifera* (R)	1.0 g/kg																●	Abdel-Tawwab et al., 2022
	Neem, *A. indica* (L)	0.5 g/kg																●	Morales-Covarrubias et al., 2016
	Lechuguilla, *A. lechuguilla* (L)	1-3 g/kg																●	Quiroz-Guzman et al., 2023

Table 4 *(continue)*

Crustacean	Plant extract	Opt dose	Antioxidant indicators							Other immunity indicators					Challenge test			Reference
			CAT	GSH	GPx	GST	SOD	T-AOC	MDA	PO	AKP	Haemocyte count	Lysozyme	Phagocytic activity	*Aeromonas*	Microcystin-LR	Protozoan	*Vibrio*	
	Buton forest onion, *E. bulbosa* (B)	12.5 g/kg								●		●						●	Munaeni et al., 2020
	Nightshades, *S. procumbens* (L)	15 g/kg										●						●	Hong et al., 2022
	Screw pine, *P. tectorius* (F)	6 g/l*																●	Anirudhan et al., 2021
	Indian gooseberry, *P. amarus* (L)	40 g/kg								●		●		●				●	Ngo et al., 2020
	Roselle, *H. sabdariffa* (fruit), Giant sensitive tree, *M. pirga* (L), Tasmanian blue gum, *E. globulus* (leaf)	10 g/kg																●	Nguyen et al., 2023
	Phycurma aquatic product (Table 1)	5 ml/kg					●		●									●	Putra et al., 2024
	Papaya, *Carica papaya* (L), Ketapang, *Terminalia catappa* (L), and tall-stilt mangrove, *R. apiculata* (L)	0.7 g/l*																●	Supono et al., 2019

Note: B: bulb, F: fruit, L: leaf, R: root, AKP: alkaline phosphatase, CAT: catalase, GSH: reduced glutathione, GPx: glutathione peroxidase, GR: glutathione reductase, GST: glutathione S transferase, MDA: malondialdehyde, PO: phenoloxidase, SOD: superoxide dismutase, T-AOC: total antioxidant capacity. Many of the crustaceans were given plant extract through feeding, while those given plant extract via immersion are indicated by the symbol *. The green circle indicates immune indicator results that are better than those of the control treatment (without the plant extract), while the blue circle indicates the ability to cure the infection.

Table 5
Imperative compounds that could enhance the immunity and growth of crustaceans

Crustacean species	Plant extract	Bioactive compounds									Challenge test								Reference
		Alkaloids	**Coumarin**	**Flavonoids**	**Phenols**	**Saponins**	**Steroids**	**Tannins**	**Terpenoids**	**Ciliate protozoans**	**Microcystein-LR**	***Pseudomonas***	***Vibrio***	***Acinobacter***	***Aeromonas***	***Stenotrophomonas***	***Morganella***	**WSS virus**	
Mud crab, *S. paramamosain*	Tall-stilt mangrove, *R. apiculata*			●	●	●		●	●	●									Linh et al., 2017
Lobster, *C. quadrinatus*	Tochu leaf, *E. ulmoides*					●					●								Lu et al., 2023a
Giant freshwater prawn, *M. rosenbergii*	Fiddlehead fern, *D. esculentum*			●	●	●	●	●	●										Hajar-Azira et al., 2023
	Soapbush, *Clidemia Hirta*			●		●			●			●	●	●	●	●	●		Musa et al., 2011
Black tiger shrimp,*P. monodon*	Mangrove cannonball leaf, *X. granatum*	●		●	●			●					●						Saptiani et al., 2020
White-leg shrimp, *Litopenaeus vannamei*	Lechuguilla, *A. Lechuguilla*			●									●						Quiroz-Guzman et al., 2023
	Cat's claw, *Uncaria tomentosa*	●	●	●	●			●	●									●	Junior et al., 2017

Note: Phytochemical screening of compounds in previous studies was conducted thoroughly via advanced chromatography techniques such as high-performance liquid chromatography (HPLC) and gas chromatography–mass spectrometry (GC–MS) or via conventional chromatography techniques such as thin-layer chromatography. The green circle indicates the presence of bioactive compounds in the plant, while the blue circle indicates that the plant is able to cure infection

can induce the expression of antimicrobial peptides involved in strengthening the innate immunity of crustaceans, such as penaeidin (Pen2, Pen3, Pen4), anti-lipopolysaccharide factor (ALF), anti-crustin protein (ACP Crus), and lysozyme (Lyz), with these peptides participating in antimicrobial activities through several mechanisms. For example, penaeidin, also known as an antimicrobial peptide with chitin-binding activity, is secreted in haemolymph granulocytes to eliminate microorganisms that are engulfed by granulocytes (Anirudhan et al., 2021). Other peptides, such as ACP, are involved in enhancing the recognition and phagocytosis of foreign bodies (Yue et al., 2023), whereas Lyz peptides are involved in cleaving β-1,4 glycosidic bonds between N-acetylmuramic acid and N-acetylglucosamine, which causes lysis of the bacterial cell wall (Abidin et al., 2022).

The bioactive compounds in plant extracts improve antioxidant enzyme activities to withstand reactive oxygen species (ROS) that are harmful to host cells. ROS-induced damage in crustaceans is neutralized via enzymatic antioxidant defence mechanisms such as catalase (CAT), glutathione peroxidase (GPx), glutathione reductase (GR), glutathione S-transferase (GST), phenoloxidase (PO), reduced glutathione (GSH), and superoxide dismutase (SOD). Many researchers have reported that these antioxidant enzymes increase in crustacean haemolymph, ovaries, or hepatopancreas after supplementation with plant extracts. Lu et al., (2023b) reported an increase in the mRNA expression levels of antioxidant enzymes such as CAT, SOD (cMN-SOD), GST, and GPx (GPx, GPx3P, Se-GPx), which are involved in key pathways to eliminate unnecessary free superoxide anion radicals in crustaceans. The SOD enzyme converts superoxide radicals (O2) into hydrogen peroxide (H2O2), which is then detoxified by CAT and GPx enzymes (Harikrishnan et al., 2012; Li et al., 2021). Other antioxidant enzymes, such as GST, play a role in converting xenobiotics (foreign compounds) to xenobiotic-GSH conjugates that are less toxic and more easily excreted (Cheng et al., 2020), whereas GR enzymes function to catalyse the conversion of oxidized glutathione into reduced glutathione (GSH), allowing the antioxidant function of GSH to continue. GSH donates electrons to neutralize ROS, preventing oxidative stress in crustacean tissues. In addition to these mechanisms, phenolic compounds in plants upregulate proPO and ProPO2 expression, thereby activating the PO enzyme for melanization (a process in which phenol interacts with quinone, which is then polymerized to form melanin) in the haemolymph or hepatopancreas, which encapsulates and immobilizes any pathogen (Anirudhan et al., 2021; Munaeni et al., 2020; Scherping & Watson, 2021).

ROLE OF PLANT ADDITIVES AGAINST ENVIRONMENTAL STRESS

With ongoing climate change worldwide, alterations in temperature, salinity, and pH are increasingly exceeding the tolerance limits of crustaceans. Even slight temperature changes can have detrimental effects on the physiological balance of crustaceans, potentially

leading to mortality. In shrimp aquaculture, temperature fluctuations are common, and it has been documented that white-leg shrimp (*Litopenaeus vannamei*) stop feeding when exposed to unfavorable temperatures. Both excessively high and low temperatures can induce oxidative stress, overwhelm antioxidant defense mechanisms, and suppress immune function (Zabolinia et al., 2024). Salinity stress can increase gill Na^+/K^+-ATPase activity, cause swelling in gill filaments and in response to this severe condition, the transcription levels of 272 genes related to ion transport, energy metabolism, osmolyte metabolism, and methyltransferase activity are upregulated to enhance the osmoregulatory capacity of crustaceans (Xu et al., 2023). Similarly, pH fluctuations may disrupt the ionic balance in the gills, leading to decreased metabolic activity (Castro, 2022). Due to these vulnerabilities, there is growing interest in incorporating medicinal plants and herbs to enhance crustacean resilience against environmental stress. Several studies have evaluated the use of plants such as Indian ginseng (*Withania somnifera*), ginger (*Zingiber officinale*), red seaweed (*Gracilaria tenuistipitata* and *Kappaphycus alvarezii*), mesquite (*Prosopis juliflora*), green seaweed (*Ulva ohnoi*), noni fruit (*Morinda citrifolia*) and Moringa (*Moringa oleifera*) through dietary supplementation or immersion to improve stress resistance in crustaceans, particularly in white-leg shrimp (see Table 6). Overall, previous studies have shown that crustaceans, particularly white-leg shrimp, fed with plant extracts exhibit higher tolerance and increased survival under salinity, temperature or ammonia stress.

Upon exposure to environmental stressors, compounds in the plant including phenol, flavonoid and carotenoid activate a suite of protective responses, involving heat shock protein 70 (Hsp70). Hsp70 is stress protein belongs to a family of highly conserved stress proteins (~70 kDa) that are critical for protein biogenesis and homeostasis, and their functions include maintaining protein structure, repairing damaged cytoskeletal elements, and assisting in protein folding and hormone receptor function (Castro, 2022). For example, *Artemia* treated with Indian ginseng, *W. somnifera* showed a 3.5-fold upregulation of Hsp70 expression compared to the control group after exposure to stressors such as temperature, pH, and salinity (Castro, 2022). Hsp70 further initiates the activation of various defense mechanisms, including superoxide dismutase (SOD), glutathione peroxidase (GPx), phenoloxidase (PO), and lysozyme, which are essential for neutralizing harmful reactive oxygen species in crustaceans (Yeh et al., 2010; Zabolinia et al., 2024). Overall, the compounds in the plant play an essential role in scavenging reactive oxygen species and reducing oxidative damage, allowing lipids, proteins, and DNA to carry out their functions even when the crustacean exposed to environmental stress (Romadhoni et al., 2020).

GAP STUDY, CONCLUSION, AND FUTURE PERSPECTIVE

In aquaculture, two crucial matters should be prioritized: producing spawning broodstock and mass rearing of seeds. Milder research has been carried out in these two field areas,

Table 6
Effects of plant extracts on the environmental stress of crustaceans

Crustacean species	Plant extract	Optimal dose	Environmental stress treatment	Environmental stress indicators								Reference
				Survival	Hyaline cell	Granular cell	Haemocyte count	SOD activity	GPx	Lysozyme	PO	
Artemia	Indian ginseng, *W. somnifera* (R)	1000 mg/l*	Temperature (41 °C, 15 min)	●								Castro, 2022
	Indian ginseng, *W. somnifera* (R)	1000 mg/l*	pH (5.5, 24 h)	●								Castro, 2022
	Indian ginseng, *W. somnifera* (R)	1000 mg/l*	Salinity (100 ppt, 48 h)	●								Castro, 2022
White-leg shrimp, *L. vannamei*	Ginger, *Z. officinale* (rhizome)	1 g/kg	Ammonia (40 mg/L, 96 h)	●								Tu et al., 2023
	Red seaweed, *Gracilaria Tenuistipitata*	400 mg/l*	Temperature (28 °C, 120 h)		●	●	●	●				Yeh et al., 2010
	Mesquite, *Prosopis juliflora* (L)	50 mg/kg	Temperature (7 °C, 12 h)	●				●	●	●	●	Zabolinia et al., 2024
	Green algae, *Ulva ohnoi*	20 mg/kg	Temperature (11.5 °C, 1 h)	●								Coelho et al., 2023
	Noni, *Morinda citrifolia* (F)	15 ml/L**	Salinity (5 ppt, 96 h)	●								Phan et al., 2023
	Noni, *Morinda citrifolia* (F)	15 ml/L**	Ammonia (40 mg/L, 96 h)	●								Phan et al., 2023
	Red Seaweed, *Kappaphycus alvarezii*	0.5 g/L***	Salinity (0 ppt, 30 min)	●								Suantika et al., 2017
	Moringa, *Moringa oleifera* (L)	50 g/kg	Salinity (0 ppt, 24 h)	●								Baniesmaeili et al., 2023
	Moringa, *Moringa oleifera* (L)	50 g/kg	Salinity (55 ppt, 24 h)	●								Baniesmaeili et al., 2023

Note. F: fruit, L: leaf, R: root, GPx: glutathione peroxidase, PO: phenoloxidase, SOD: superoxide dismutase. Many of the crustaceans were given plant extract through feeding, while those given plant extract via immersion, spray and artemia enrichment are indicated by the symbol *, **, ***, respectively. The green circle indicates environmental stress indicator results that are better than those of the control treatment (without the plant extract)

especially regarding seed production or, more specifically, the crustacean larval phase. Farmers often face barriers to increasing seed output because of the occurrence of larval mass mortalities caused by pathogen infection. Furthermore, researchers have yet to take the initiative to increase publications regarding plant efficacy on gonads for rapid reproduction during crustacean farming. Additionally, regarding spiny lobsters, past studies have poorly documented any implications of plants or herbs for the growth, reproduction or immunity of spiny lobsters, probably due to constraints in the researcher's ability to rear spiny lobsters while conducting an experiment. Currently, neither spiny lobster domestication nor spiny lobster landing from the fishery sector has fully recovered; in this context, researchers should commit to further participation in any research relevant to the relationship between plant additives and spiny lobster.

As a whole, several conditions should be taken into consideration before the commercialization of plants in the aquaculture industry, with the most important conditions encompassing plant efficacy and plant dosage. Additionally, this review explains the common process of obtaining plant extracts, starting with collection, followed by maceration, extraction and evaporation. Several techniques are then applied to introduce plant extracts into crustaceans via pellets, coatings, immersions or injections. Plants and herbs such as amaranth, soursop leaf, mulberry leaf, olive, cajuput, bitterweed, Shepherd's needle, Indian borage, Chinese skullcap, and Indian gooseberry have been verified to improve crustacean growth. A bioactive compound in plant extracts that resembles a moulting hormone, an ecdysteroid, may promote the growth of crustaceans through moulting stimulation. Bioactive compounds in plants also promote digestive enzyme secretion, intestinal morphology and the gut microbiota, which are crucial for better absorptive function, increasing appetite, and ultimately improving crustacean growth. Moreover, herbs such as common senduduk can promote ovarian maturation, ultimately resulting in the production of 100% spawned crustaceans. Compounds such as phytoestrogen, phytoecdysteroid and α-tocopherol might stimulate ovarian growth. Plants such as guava leaf, talt-silt mangrove leaf, tochu, chaihu, Indian ginseng, rosemary, mangrove cannonball tree, lechuguilla, moringa, neem, screw pine, Indian gooseberry, solanum, buton forest onion, roselle, giant sensitive tree and Tasmanian blue gum have been verified to contain phenolic compounds such as polyphenols, flavonoids, and tannins that have potent antimicrobial activity against several strains of bacteria while also promoting antioxidant defence mechanisms via CAT, GPx, GR, GST, GSH and SOD.

Knowledge gained from collected findings might drive more research to develop supplements or cures for increasing growth, reproduction, and immune systems to benefit crustacean farming since there is a pressing need to overcome rising issues, especially in curbing disease infections. Each plant has a specific function; for example, some plants or herbs may promote growth but are unable to strengthen the crustacean immune system, thus

devaluing plants for development as pharmaceutical supplements. However, a combination of different plants may provide an impressive supplement or cure for the crustacean farming industry in the future. The development of well-balanced supplements is imperative, as they must be capable of performing different functions simultaneously. For example, we should prioritize plant additives that can enhance crustacean egg development and, at the same time, protect vulnerable eggs from disease infections since many crustaceans bear their eggs underneath their abdomen, which is susceptible to external pathogens.

ACKNOWLEDGEMENT

This study was funded by the Ministry of Higher Education under the Higher Institution Center of Excellence (HICoE) grant for the development of future food through sustainable shellfish aquaculture (Vot No. 63933 and 56062). The authors express their gratitude to all the staff at the Institute of Tropical Aquaculture and Fisheries for their support. Ariffin Hidir designed the study, gathered information, analyzed data, and drafted the paper; Aaqillah-Amr reviewed the paper; Redzuari Alias and Hajar-Azira also contributed to the study design and drafting; Muyassar H. Abualreesh, Hanafiah Fazhan, Khor Waiho, and Hongyu Ma were involved in conceptualization and validation; and Mhd Ikhwanuddin reviewed the paper, acquired funding, and provided project administration and supervision.

REFERENCES

Abdel-Tawwab, M., Selema, A. M., Khalil, R. H., El-Sabbagh, N., Eldessouki, E. A. A., Fawzy, R. M., & El-Naby, A. S. A. (2022). The growth performance, antioxidant and immune responses, and disease resistance of *Litopenaeus vannamei* fed on diets supplemented with Indian ginseng (*Withania somnifera*). *Fish & Shellfish Immunology 128*, 19–27. https://doi.org/10.1016/j.fsi.2022.07.061

Abidin, Z., Huang, H. T., Liao, Z. H., Chen, B. Y., Wu, Y. S., Lin, Y. J., & Nan, F. H. (2022). *Moringa oleifera* leaves' extract enhances nonspecific immune responses, resistance against *Vibrio alginolyticus*, and growth in white leg shrimp (*Penaeus vannamei*). *Animals, 12*(1), Article 42. https://doi.org/10.3390/ani12010042

Adnan, W. N. W., Karim, N. U., Yusof, N. A. H., Zakariah, M. I., & Hassan, M. (2021). Effect of *Cymbopogon citratus* essential oil (EO) on handling stress in giant freshwater prawn (*Macrobrachium rosenbergii*). *Pakistan Journal of Biological Sciences, 24*(1), 13–18. https://doi.org/10.3923/pjbs.2021.13.18

Aftabuddin, S., Siddique, M. A. M., Romkey, S. S., & Shelton, W. L. (2017). Antibacterial function of herbal extracts on growth, survival, and immunoprotection in the black tiger shrimp *Penaeus monodon*. *Fish & Shellfish Immunology, 65*, 52–58. https://doi.org/10.1016/j.fsi.2017.03.050

Ahmadifar, E., Fallah, P. H., Yousefi, M., Dawood, M. A. O., Hoseinifar, S. H., Adineh, H., Yilmaz, S., Paolucci, M., & Doan, H. V. (2021). The gene regulatory roles of herbal extracts on the growth, immune system, and reproduction of fish. *Animals, 11*(8), Article 2167. https://doi.org/10.3390/ani11082167

Ahmadifar, E., Mohammadzadeh, S., Kalhor, N., Yousefi, M., Moghadam, M. S., Naraballobh, W., Ahmadifar, M., Hoseinifar, S. H., & Doan, H. V. (2022). Cornelian cherry (*Cornus mas* L.) fruit extract improves

growth performance, disease resistance, and serum immune-and antioxidant-related gene expression of common carp (*Cyprinus carpio*). *Aquaculture, 558*, 738372–738372. https://doi.org/10.1016/j.aquaculture.2022.738372

Ahmadifar, E., Sheikhzadeh, N., Roshanaei, K., Dargahi, N., & Faggio, C. (2019). Can dietary ginger (*Zingiber officinale*) alter biochemical and immunological parameters and gene expression related to growth, immunity and antioxidant system in zebrafish (Danio rerio)? *Aquaculture, 507*, 341–348. https://doi.org/10.1016/j.aquaculture.2019.04.049

Alam, N., Fujaya, Y., Haryati, Sari, D. K., Achmad, M., Rusdi, M., & Farizah, N. (2019). The effect of *Melastoma malabathricum* leaf extract on growth and spawning of blue swimming crab (*Portunus pelagicus*). *IOP Conference Series: Earth and Environmental Science, 370*(1), Article 012029. https://doi.org/10.1088/1755-1315/370/1/012029

Ali, M., Saade, E., & Tandipayuk, H. (2023). Utilization of soursop leaf, *Annona Muricata* extract for improving growth performance and reducing cholesterol levels in fattening mangrove crab, *Scylla olivacea*. *Journal of Pharmaceutical Negative Results, 14*(2), 804–814. https://doi.org/10.47750/pnr.2023.14.02.101

Anirudhan, A., Okomoda, V. T., Iryani, M. T. M., Andriani, Y., Wahid, M. E. A., Tan, M. P., Danish-Daniel, M., Wong, L. L., Tengku-Muhammad, T. S., Mok, W. J., Sorgeloos, P., & Sung, Y. Y. (2021). *Pandanus tectorius* fruit extract promotes Hsp70 accumulation, immune-related genes expression, and *Vibrio parahaemolyticus* tolerance in the white-leg shrimp *Penaeus vannamei*. *Fish & Shellfish Immunology, 109*, 97–105. https://doi.org/10.1016/j.fsi.2020.12.011

Arif, Y., Singh, P., Bajguz, A., & Hayat, S. (2022). Phytoecdysteroids: Distribution, structural diversity, biosynthesis, activity, and crosstalk with phytohormones. *International Journal of Molecular Sciences, 23*, Article 8664. https://doi.org/10.3390/ijms23158664

Baniesmaeili, Y., Akbarzadeh, A., Abdollahi, F., & Niroomand, M. (2023). Effectiveness of dietary *Moringa oleifera* leaf powder and extract in the Pacific white shrimp (*Litopenaeus vannamei). Iranian Journal of Fisheries Sciences, 22*(3), 547–565.

Castro, A. A. (2022). *Effect of a plant-derived nutraceutical on the tolerance of axenically-cultured Artemia towards abiotic or biotic stressor* [Unpublished doctoral thesis] Swedish University of Agricultural Sciences.

Chandran, M. N., Moovendhan, S., Suganya, A. M., Tamilselvi, A., Bebin, Immanuel, G., & Palavesam, A. (2016). Influence of polyherbal formulation (AquaImmu) as a potential growth promoter and immunomodulator in shrimp *Penaeus monodon*. *Aquaculture Reports, 4*, 143–149. https://doi.org/10.1016/j.aqrep.2016.10.002

Chang, C., Kuo, H., & Cheng, W. (2023). Effectiveness of various cacao pod husk extraction byproducts in promoting growth and immunocompetence in *Litopenaeus vannamei*. *Fish & Shellfish Immunology, 134*, Article 108632. https://doi.org/10.1016/j.fsi.2023.108632

Cheng, C. H., Ma, H. L., Deng, Y. Q., Chen, X. L., Feng, J., Chen, X. L. & Guo, Z. X. (2020-). The role of Mu-type glutathione S-transferase in the mud crab (*Scylla paramamosain*) during ammonia stress. *Comparative Biochemistry and Physiology Part C: Toxicology & Pharmacology, 227*, Article 108642. https://doi.org/10.1016/j.cbpc.2019.108642

Chi, T. T. K., Clausen, J. H., Van, P. T., Tersbøl, B., & Dalsgaard, A. (2017). Use practices of antimicrobials and other compounds by shrimp and fish farmers in Northern Vietnam. *Aquaculture Reports, 7*, 40–47. https://doi.org/10.1016/j.aqrep.2017.05.003

Coelho, J. D. R., Santos, U. R. A. D., Rezenda, P. C., Ramirez, N. C. B., & Viera, F. D. N. (2023). Increased resistance to thermal shock in pacific white shrimp fed on green algae and its effect in conjunction with probiotics. *International Aquatic Research, 15*, 123–134. https://doi.org/10.22034/iar.2023.1968874.1337

Dawood, M. A. O., Koshio, S., & Esteban, M. Á. (2017). Beneficial roles of feed additives as immunostimulants in aquaculture: a review. *Reviews in Aquaculture, 10*(4), 950–974. https://doi.org/10.1111/raq.12209

Dinan, L., Mamadalieva, N. Z., & Lafont, R. (2021). Dietary phytoecdysteroids. In J. Xiao, S. D. Sarker & Y. Asakawa (Eds.) *Handbook of dietary phytochemicals (pp. 1541–1593).* Springer. https://doi.org/10.1007/978-981-15-4148-3_35

FAO. (2024). *The state of world fisheries and aquaculture*. Food and Agriculture Organization of the United Nations. https://doi.org/10.4060/cd0683en

Farizah, N., Zairin, J. M., Darusman, L. K., Boediono, A., & Suprayadi, M. A. (2017). The application of thyroxine hormone and *Melastoma malabathricum* leaf extract as stimulators in gonadal maturation of *Scylla serrata* in traditional ponds. *Aquaculture, Aquarium, Conservation & Legislation - International Journal of the Bioflux Society, 10*(4), 911–921.

Farizah, N., Zairin, J. R. M., Darusman, L. K., Boediono, A., & Suprayudi, M. A. (2018). The side effect of the *Melastoma malabathricum* L ethanol extract on the gonad maturation of female orange mud crab (*Scylla olivacea*). *HAYATI Journal of Biosciences, 25*(4), Article 188. https://doi.org/10.4308/hjb.25.4.188

Farook, M. A., Vimal, S., Madan, N., Taju, G., Majeed, S. A., Nambi, K. S. N., Balasubramanian, G., & Hameed, A. S. S. (2016). Immunomodulatory effect of *Cynodon dactylon* against white tail disease of giant freshwater prawn *Macrobrachium rosenbergii* (de Man, 1879). *Aquaculture Research, 47*(11), 3421–3431. https://doi.org/10.1111/are.12789

Fujaya, Y., Trijuno, D. D., Haryati, Hasnidar, Rusdi, M., & Usman, Z. (2018). Efektivitas ekstrak daun Murbei dalam menstimulasi peningkatan kandungan ekdisteroid hemolimph dan molting kepiting bakau (*Scylla olivacea*) [The effectiveness of mulberry leaf extract in stimulating an increase in the ecdysteroid content of hemolymph and molting of mangrove crabs (Scylla olivacea)]. *Journal of Fisheries and Marine Science, 2*(1), 32–43.

Gong, J., Yu, K., Shu, L., Ye, H., Li, S., & Zeng, C. (2015). Evaluating the effects of temperature, salinity, starvation, and autotomy on molting success, molting interval, and expression of ecdysone receptor in early juvenile mud crabs, *Scylla paramamosain*. *Journal of Experimental Marine Biology and Ecology, 464*, 11–17. https://doi.org/10.1016/j.jembe.2014.12.008

Hajar-Azira, Z., Aaqillah-Amr, M. A., Rasdi, N. W., Ma, H., & Ikhwanuddin, M. (2023). Preliminary investigation on the effect of fiddlehead fern, *Diplazium esculentum*, extract to the growth performance of giant freshwater prawn, *Macrobrachium rosenbergii*, postlarvae. *Aquaculture International*, *31*, 81–101. https://doi.org/10.1007/s10499-022-00965-w

Hardi, E. H., Nugroho, R. A., Agriandini, M., Rizki, M., Falah, M. E. M., Almadi, I. F., Susmiyati, H. R., Diana, R., Palupi, N. P., Saptiani, G., Agustina, A., Asikin, A. N., & Sukarti, K. (2022). Application

of phyto-stimulants for growth, survival rate, and meat quality improvement of tiger shrimp (*Penaeus monodon*) maintained in a traditional pond. *Pathogens*, *11*(11), Article 1243. https://doi.org/10.3390/pathogens11111243

Hardi, E. H., Pagoray, H., & Harefa, N. J. K. (2021). Use of lempuyang extract (*Zingiber zerumbet*) to prevent *Aerococcus viridans* bacterial infection in freshwater lobster (*Cherax quadricarinatus*). *Aquaculture Indonesia*, *22*(2), Article 20. https://doi.org/10.21534/ai.v22i2.204

Harikrishnan, R., Balasundaram, C., Jawahar, S., & Heo, M. S. (2012). Immunomodulatory effect of *Withania somnifera* supplementation diet in the giant freshwater prawn *Macrobrachium rosenbergii* (de Man) against *Aeromonas hydrophila*. *Fish & Shellfish Immunology*, *32*(1), 94–100. https://doi.org/10.1016/j.fsi.2011.10.027

Hasnidar, H., Tamsil, A., & Wamnebo, M. I. (2021). The effect of Amaranth extract (*Amaranthus spp.*) on the molting of orange mud crab (*Scylla olivacea*). *Aquaculture, Aquarium, Conservation & Legislation - International Journal of the Bioflux Society*, *14*(2), 1036–1045.

Hong, T. T. T., Nhi, N. T. H., & Day, P. V. (2022). Effect of *Solanum procumbens* Lour. extract on survival, growth performances, immune responses and against *Vibrio parahaemolyticus* causing acute hepatopancreas necrosis disease in white leg shrimp (*Litopenaeus vannamei*). *Indian Journal of Animal Research, 56(12), 1513-1518.* https://doi.org/10.18805/ijar.bf-1566

Huang, H. T., Liao, Z. H., Wu, Y. S., Lin, Y. J., Kang, Y. S., & Nan, F. H. (2022). Effects of *Bidens alba* and *Plectranthus amboinicus* dietary supplements on nonspecific immune responses, growth, and resistance to *Vibrio alginolyticus* in white leg shrimp (*Penaeus vannamei*). *Aquaculture*, *546*, Article 737306. https://doi.org/10.1016/j.aquaculture.2021.737306

Iromo, H., Farizah, N., & Puryono. (2021). The application of thyroxine hormone and *Melastoma malabathricum* leaf extract as stimulators in gonadal maturation of *Scylla serrata* in traditional ponds. *Aquaculture, Aquarium, Conservation & Legislation - International Journal of the Bioflux Society*, *14*(3), 1769–1777.

Iyapparaj, P., Revathi, P., Divakar, S., Marudhupandi, T., & Niroshan, S. (2021). Evaluation of polyherbal feed supplement (Ban-V) on the enhancement of growth and non-specific immune responses in shrimp *Penaeus vannamei*. *Aquaculture International*, *29*(3), 1091–1101. https://doi.org/10.1007/s10499-021-00680-y

Júnior, O. S., Kuhn, F., Padilla, P. J. M., Vicente, L. R. M., Costa, S. W. D., Silva, B. C. D., Schleder, D. D., Nesi, C. N., Magro, J. D., & Lamo-Castellví, S. D. (2017). Survival of white spot syndrome virus–infected *Litopenaeus vannamei* fed with ethanol extract of *Uncaria tomentosa*. *Journal of the World Aquaculture Society*, *49*(1), 165–174. https://doi.org/10.1111/jwas.12483

Kawamura, G., Yong, A. S. K., Au, H. L., Doison, A., Ooi, S. Y., & Lim, L. S. (2019). Malaysian herbs as feeding attractants and enhancers for the giant freshwater prawn (*Macrobrachium rosenbergii*) and the whiteleg shrimp (*Litopenaeus vannamei*). *Borneo Journal of Marine Science and Aquaculture 3*(2), 57–67. https://doi.org/10.51200/bjomsa.v3i2.1793

Kongchum, P., Chimtong, S., Chareansak, N., & Subprasert, P. (2016). Effect of green tea extract on *Vibrio parahaemolyticus* inhibition in pacific white-leg shrimp (*Litopenaeus vannamei*) postlarvae. *Agriculture and Agricultural Science Procedia*, *11*, 117–124. https://doi.org/10.1016/j.aaspro.2016.12.020

Kumari, J., Sahoo, P. K., Giri, S. S., & Pillai, B. R. (2004). Immunomodulation by "Immuplus (AquaImmu)" in giant freshwater prawn, *Macrobrachium rosenbergii* (De Man). *Indian Journal of Experimental Biology*, *42*(11), 1073–1077.

Lebold, K. M., & Traber, M. G. (2014). Interactions between α-tocopherol, polyunsaturated fatty acids, and lipoxygenases during embryogenesis. *Free Radical Biology and Medicine*, *66*, 13–19. https://doi.org/10.1016/j.freeradbiomed.2013.07.039

Leite, K., Kurosaki, J. K. D. A., J., Retcheski, M. C., Tormen, L., Romão, S., Pinto, V. Z., & Cazarolli, L. H. (2021). Effect of rosemary (*Rosmarinus officinalis*) extract on the antioxidant status and proximate composition of prawn (*Macrobrachium rosenbergii*) meat. *Journal of Aquatic Food Product Technology*, *30*(6), 683–693. https://doi.org/10.1080/10498850.2021.1924908

Li, Y., Fan, B., Huang, Y., Wu, D., Zhang, M., & Zhao, Y. (2018). Effects of dietary vitamin E on reproductive performance and antioxidant capacity of *Macrobrachium nipponense* female shrimp. *Aquaculture Nutrition*, *24*(6), 1698–1708. https://doi.org/10.1111/anu.12804

Li, Y., Zhan, F., Li, F., Lu, Z., Xu, Z., Yang, Y., Shi, F., Zhao, L., Qin, Z., & Lin, L. (2021). Molecular and functional characterization of mitochondrial manganese superoxide dismutase from *Macrobrachium rosenbergii* during bacterial infection. *Fish & Shellfish Immunology*, *118*, 94–101. https://doi.org/10.1016/j.fsi.2021.08.025

Linh, N. K., Khoa, T. N. D., Zainathan, S. C., Musa, N., Shaharom-Harrison, F. (2017). Development of mud crab crablet, the identification of ciliate and the bioefficacy of leaf extract of *Rhizophora apiculata* as anti-protozoal agent. *Journal of Sustainability Science and Management*, *12*(2), 52–62.

Lu, Y. P., Zheng, P. H., Xu, J. R., Cao, Y. L., Li, J. T., Hao, C. G., Zhang, Z. L., Xian, J. A., Zhang, X. X., & Wang, A. L. (2023a). Effects of dietary *Eucommia ulmoides* leaf extract on growth, muscle composition, hepatopancreas histology, immune responses and *Microcystin-LR* resistance of juvenile red claw crayfish (*Cherax quadricarinatus*). *Fishes*, *8*, Article 20. https://doi.org/10.3390/fishes8010020

Lu, Y. P., Zheng, P. H., Zhang, Z. L., Li, J. T., Li, J. J., Li, T., Wang, X., Xu, J. R., Wang, D. M., Xian, J. A., Zhang, X. X. (2023b). Effects of dietary *Radix bupleuri* root extract on the growth, muscle composition, histology, immune responses and *Microcystin-LR* stress resistance of juvenile red claw crayfish (*Cherax quadricarinatus*). *Aquaculture Reports*, *33*, Article 101822. https://doi.org/10.1016/j.aqrep.2023.101822

Lugo-Rubio, J. Y., López-Álvarez, E. S., Vázquez-Montoya, N., Escamilla-Montes, R., Félix-Ortiz, J. S., Lugo-Medina, E., Herrera-Moreno, M. N., Nava-Pérez, E., & Valenzuela-Quiñónez, W. (2022). Extracts of *Moringa oleifera* and *Croton californicus* against infections of *Vibrio parahaemolyticus* (IPNGS16) in juvenile Pacific white-leg shrimp (*Penaeus vannamei*). *Latin American Journal of Aquatic Research*, *50*(4), 541–552. https://doi.org/10.3856/vol50-issue4-fulltext-2825

Maurus, G., Ho, T. H., & Po-Tsang, L. (2023). Effects of dietary *Scutellaria baicalensis* extract on growth performance, immune-related genes expression, and resistance of *Penaeus monodon* shrimp to *Vibrio harveyi* infection. *Animals*, *13*(10), Article 1621. https://doi.org/10.3390/ani13101621

Medina-Beltrán, V., Luna-González, A., Fierro-Coronado, J. A., Campa-Córdova, A. I., Peraza-Gómez, V., Flores-Miranda, M. D. C., & Rivera, J. N. G. (2012). Echinacea purpurea and *Uncaria tomentosa* reduce the prevalence of WSSV in whiteleg shrimp (*Litopenaeus vannamei*) cultured under laboratory conditions. *Aquaculture*, *358-359*, 164–169. https://doi.org/10.1016/j.aquaculture.2012.06.030

Morales-Covarrubias, M. S., García-Aguilar, N., Bolan-Mejía, M., Del C, & Puello-Cruz, A. C. (2016). Evaluation of medicinal plants and colloidal silver efficiency against *Vibrio parahaemolyticus* infection in *Litopenaeus vannamei* cultured at low salinity. *Diseases of Aquatic Organisms*, *122*(1), 57–65. https://doi.org/10.3354/dao03060

Moustafa, E. M., Dawood, M. A. O., Assar, D. H., Omar, A. A., Elbialy, Z. I., Farrag, F. A., Shukry, M., & Zayed, M. M. (2020). Modulatory effects of fenugreek seeds powder on the histopathology, oxidative status, and immune related gene expression in Nile tilapia (*Oreochromis niloticus*) infected with *Aeromonas hydrophila*. *Aquaculture, 515,* Article 734589. https://doi.org/10.1016/j.aquaculture.2019.734589

Munaeni, W., Disnawati, Yuhana, M., Setiawati, M., Bujang, A., Abidin, L. O. B., & Kurniaji, A. (2019). Buton forest onion extract (*Eleutherine bulbosa* (Mill.)) potential on growth performance of *Vannamei* shrimp (*Litopenaeus vannamei*). *Pakistan Journal of Biological Sciences*, *22*(1), 15–20. https://doi.org/10.3923/pjbs.2019.15.20

Munaeni, W., Widanarni, Yuhana, M., Setiawati, M., & Wahyudi, A. T. (2020). Effect in white-leg shrimp *Litopenaeus vannamei* of *Eleutherine bulbosa* (Mill.) Urb. powder on immune genes expression and resistance against *Vibrio parahaemolyticus* infection. *Fish & Shellfish Immunology*, *102*, 218–227. https://doi.org/10.1016/j.fsi.2020.03.066

Musa, N., Musa, N., Ibrahim, W. N., Shariat, M. Z. A., Zamani, A., I., Abdullah, M. R., Wee, T. L., Marip, M., Razak, L. A., & Soh, A. S. A. (2011). Methanolic activities of selected weeds on bacteria isolated from *Macrobrachium rosenbergii* larvae. *Tropical Journal of Veterinary Medicine*, *41*(4), 535–540. https://doi.org/10.56808/2985-1130.2348

Ngo, H. V. T., Huang, H. T., Lee, P. T., Liao, Z. H., Chen, H. Y., & Nan, F. H. (2020). Effects of *Phyllanthus amarus* extract on nonspecific immune responses, growth, and resistance to *Vibrio alginolyticus* in white-leg shrimp *Litopenaeus vannamei*. *Fish & Shellfish Immunology*, *107*, 1–8. https://doi.org/10.1016/j.fsi.2020.09.016

Nguyen, T. T. L., Luu, T. T. H., Nguyen, T. T., Pham, V. D., Nguyen, T. N., Truong, Q. P., & Hong, M. H. (2023). A comprehensive study in efficacy of Vietnamese herbal extracts on whiteleg shrimp (*Penaeus vannamei*) against *Vibrio parahaemolyticus* causing acute hepatopancreatic necrosis disease (AHPND). *International Journal of Aquaculture*, *75*(2), 1-22. https://doi.org/10.46989/001c.81912

Parrillo, L., Coccia, E., Volpe, M. G., Siano, F., Pagliarulo, C., Scioscia, E., Varricchio, E., Safari, O., Eroldogan, T., & Paolucci, M. (2017). Olive mill wastewater-enriched diet positively affects growth, oxidative and immune status, and intestinal microbiota in the crayfish, *Astacus leptodactylus*. *Aquaculture*, *473*, 161–168. https://doi.org/10.1016/j.aquaculture.2017.02.013

Phan, T. C. T., Nguyen, T. K. L., Truong, T. P. T., Pham, T. T. N., Huynh, T. G., & Doan, X. D. (2023). Effects of noni fruit extract on the growth performance, digestive enzymes, and stress tolerance of juvenile whiteleg shrimp (*Litopenaeus vannamei*). *Egyptian Journal of Aquatic Research*, *49*(4), 549–554. https://doi.org/10.1016/j.ejar.2023.08.003

Putra, T., Widanarni, Wahjuningrum, D., & Yuhana, M. (2024). Commercial herbal administration for preventing *Vibrio parahaemolyticus* infection in *Vannamei* shrimp (*Litopenaeus vannamei*). *Indonesian Aquaculture Journal*, *19*(1), 11–23. https://doi.org/10.15578/iaj.19.1.2024.11-23

Quiroz-Guzmán, E., Morreeuw, Z. P., Peña-Rodríguez, A., Barajas-Sandoval, D. R., Magallón-Servín, P., Mejía, A., Reyes, A. G. (2023). Flavonoid-enriched extract of *Agave lechuguilla* bagasse as a feed supplement to prevent vibriosis in Pacific white-leg shrimp *Penaeus vannamei*. *Aquaculture*, *562*, 738867–738867. https://doi.org/10.1016/j.aquaculture.2022.738867

Romadhoni, A., Subekti, S., & Kismiyati. (2020). The effect of Cosmos caudatus extract on the survival rate of *Litopenaeus vannamei* post larvae against salinity. *Aquaculture, Aquarium, Conservation & Legislation*, *13*(4), 1820–1826.

Sahimi, B. M. K., Nagi, A. M., Hamdan, N. A., Zakariah, M. I., Yusoff, N. A. H., Tosin, O. V., & Hassan, M. (2022). Cajeput *Melaleuca cajuputi* extract supplementation in diets of *Macrobrachium rosenbergii*: Insight on the growth, immunological responses, and resistance against *Aeromonas hydrophila*. *Aquaculture Research*, *53*(9), 3441–3452. https://doi.org/10.1111/are.15851

Saptiani, G., Prayitno, S. B., & Anggarawati, S. (2021). Effect of mangrove leaf extract (*Acanthus ilicifolius*) on non-specific immune status and vibriosis resistance of black tiger shrimps (*Penaeus monodon*) challenged with *Vibrio harveyi*. *Veterinary World*, *14*(8), 2282–2289 https://doi.org/10.14202/vetworld.2021.2282-2289

Saptiani, G., Sidik, A. S., Ardhani, F., & Hardi, E. H. (2020). Response of hemocytes profile in the black tiger shrimp (*Penaeus monodon*) against *Vibrio harveyi* induced by *Xylocarpus granatum* leaves extract. *Veterinary World*, *13*(4), 751–757. https://doi.org/10.14202/vetworld.2020.751-757

Scherping, F. D., & Watson, M. J. (2021). A standardized protocol for measuring phenoloxidase in captive and wild Murray crayfish *Euastacus armatus*. *Fish & Shellfish Immunology*, *111*, 140–144. https://doi.org/10.1016/j.fsi.2021.01.008

Suantika, G., Situmorang, M. L., Aditiawati, P., Khakim, A., Suryanaray, S., Nori, S. S., Kumar, S., & Putri, F. (2017). Effect of red seaweed Kappaphycus alvarezii on growth, salinity stress tolerance and vibriosis resistance in shrimp *Litopenaeus vannamei* hatchery. *Journal of Fisheries and Aquatic Science*, *12*(3), 127–133. https://doi.org/10.3923/jfas.2017.127.133

Sumiya, E., Ogino, Y., Miyakawa, H., Hiruta, C., Toyota, K., Miyagawa, S., & Iguchi, T. (2014). Roles of ecdysteroids for progression of reproductive cycle in the freshwater crustacean *Daphnia magna*. *Frontiers in Zoology*, *11*(1), Article 60. https://doi.org/10.1186/s12983-014-0060-2

Supono, Wardiyanto, Harpeni, E., Khotimah, A. H., & Ningtyas, A. (2019). Identification of *Vibrio sp.* as a cause of white feces diseases in white-leg shrimp *Penaeus vannamei* and handling with herbal ingredients in East Lampung Regency, Indonesia. *Aquaculture, Aquaria, Conservation and Legislation*, *12*(2), 417–425.

Tu, P. T. C., Lien, N. T. K., Diep, D. X., & Ly, T. H. (2023). Effect of ginger, *Zingiber officinale* extract on growth performance, digestive enzyme and stress tolerance of whiteleg shrimp, *Litopenaeus vannamei* juveniles. *Israeli Journal of Aquaculture - Bamidgeh., 75*(2), 1-8. https://doi.org/10.46989/001c.90973

Widowati, H., Sutanto, A., Sulistiani, W. S., & Dewi, A. F. (2022). *Utilization of probiotics and spices to improve water quality*. *Universitas Muhammadiyah Metro.*

Wouters, R., Molina, C. A., Lavens, P., & Calderón, J. (2001). Lipid composition and vitamin content of wild female *Litopenaeus vannamei* in different stages of sexual maturation. *Aquaculture*, *198*(3-4), 307–323. https://doi.org/10.1016/s0044-8486(01)00522-1

Wu, Q., Jiang, Y., Chen, E., Mu, C., & Waiho, K. (2021). Chinese gallnut (*Galla chinensis*) against *Vibrio parahaemolyticus*: In vitro activity and the use of medicated bath method to treat infected mud crab *Scylla paramamosain*. *Aquaculture*, *539*, Article 736632. https://doi.org/10.1016/j.aquaculture.2021.736632

Xu, W. B., Zhang, Y. M., Li, B. Z., Lin, C. Y., Chen, D. Y., Cheng, Y. X., Guo, X. L., Dong, W. R., & Shu, M. A. (2023). Effects of low salinity stress on osmoregulation and gill transcriptome in different populations of mud crab *Scylla paramamosain*. *Science of the Total Environment*, *867*, Article 161522. https://doi.org/10.1016/j.scitotenv.2023.161522

Yeh, S. T., Li, C. C., Tsui, W. C., Lin, Y. C., & Chen, J. C. (2010). The protective immunity of white shrimp *Litopenaeus vannamei* that had been immersed in the hot-water extract of *Gracilaria tenuistipitata* and subjected to combined stresses of Vibrio alginolyticus injection and temperature change. *Fish & Shellfish Immunology, 29*(2), 271–278. https://doi.org/10.1016/j.fsi.2010.04.014

Yin, X., Zhuang, X., Liao, M., Cui, Q., Yan, C., Huang, J., Jiang, Z., Huang, L., Luo, W., Liu, Y., & Wang, W. (2023). *Andrographis paniculata* improves growth and non-specific immunity of shrimp *Litopenaeus vannamei*, and protects it from *Vibrio alginolyticus* by reducing oxidative stress and apoptosis. *Data in Brief*, *139*, 104542–104542. https://doi.org/10.1016/j.dci.2022.104542

Yue, Y., Ma, H. L., Cheng, C. H., Liu, G. X., Fan, S. G., Jiang, J. J., & Guo, Z. X. (2023). Effects of dietary guava leaf aqueous extract supplementation on growth, antioxidant capacity, and non-specific immunity in mud crab *Scylla paramamosain*. *Israeli Journal of Aquaculture-Bamidgeh, 75*(1), 1-13. https://doi.org/10.46989/001c.77654

Zabolinia, M., Abdoli, L., & Akbarzadeh, A. (2024.). Dietary ethanolic extract of Prosopis juliflora improved immuneantioxidant capacity and resistance to cold water stress in Pacific white shrimp, *Litopenaeus vannamei*. *Iranian Journal of Fisheries Sciences, 23*(3), 473–484. https://doi.org/10.22092/ijfs.2024.131222

Zhang, X., Hu, L., Liu, H., Song, D., Shen, Y., Liu, L., Hu, Y., & Chen, J. (2023). Cinnamaldehyde, a major component of *Cinnamomum cassia* Presl ethanol extract, has the potential to unlock the outbreak of WSSV. *Aquaculture*, *575*, 739761–739761. https://doi.org/10.1016/j.aquaculture.2023.739761

Zhou, X., Gong, J., Zhuang, Y., & Zhu, F. (2022). Coumarin protects *Cherax quadricarinatus* (red claw crayfish) against white spot syndrome virus infection. *Fish & Shellfish Immunology*, *127*, 74–81. https://doi.org/10.1016/j.fsi.2022.06.005

Pertanika J. Trop. Agric. Sci. 48 (6): 1915 - 1939 (2025)

PERTANIKA JOURNALS

TROPICAL AGRICULTURAL SCIENCE

Journal homepage: http://www.pertanika.upm.edu.my/

Review Article

The Multifaceted Roles of Microorganisms in Promoting Sustainable Plant Growth in Agriculture

Yakubu Iliya Appollm[1,5], Norida Mazlan[2,4]*, Dzarifah Mohamed Zulperi[1], and Noraini Md Jaafar[3]

[1]*Department of Plant Protection, Faculty of Agriculture, Universiti Putra Malaysia, 43400 Serdang, Selangor, Malaysia*
[2]*Department of Agriculture Technology, Faculty of Agriculture, Universiti Putra Malaysia, 43400 Serdang, Selangor, Malaysia*
[3]*Department of Land Management, Faculty of Agriculture, Universiti Putra Malaysia. 43400 Serdang, Selangor, Malaysia*
[4]*Laboratory of Climate-Smart Food Production, Institute of Tropical Agriculture and Food Security, Universiti Putra Malaysia, 43400 Serdang, Selangor, Malaysia*
[5]*Department of Agricultural Education, Federal College of Education (Tech), Gombe, Gombe State, Nigeria*

ABSTRACT

Sustainable agricultural productivity increasingly relies on plant growth-promoting microorganisms (PGPMs), which include plant growth-promoting rhizobacteria (PGPR) and fungi (PGPF). These beneficial microbes enhance crop growth by improving nutrient acquisition through processes such as nitrogen fixation, phosphate solubilization, and the synthesis of phytohormones. As a result, they help reduce the need for chemical fertilizers and pesticides. Additionally, PGPMs mitigate plant pathogens by producing antimicrobial compounds, inducing systemic resistance, and competing for ecological niches, resulting in significant reductions in disease incidence and severity. However, despite their demonstrated effectiveness in controlled environments, the performance of PGPMs in real-world agricultural systems is often inconsistent, with efficacy declining by 30-50% due to factors such as abiotic stressors, ecological incompatibilities, and reduced microbial viability. To overcome these challenges, this review presents a strategic framework focused on strain-specific adaptation to local soil and climate conditions, optimized co-inoculation strategies, and omics-guided selection of resilient microbial consortia. These approaches aim to bridge the gap between laboratory success and field performance, enhancing the stability and reliability of PGPM-based solutions. By identifying and addressing

ARTICLE INFO

Article history:
Received: 30 October 2024
Accepted: 09 October 2025
Published: 25 November 2025

DOI: https://doi.org/10.47836/pjtas.48.6.14

E-mail addresses:
appollmiliya@yahoo.com (Yakubu Iliya Appollm)
noridamz@upm.edu.my (Norida Mazlan)
dzarifah@upm.edu.my (Dzarifah Mohamed Zulperi)
j_noraini@upm.edu.my (Noraini Md Jaafar)
*Corresponding author

critical barriers to PGPM adoption, this review seeks to advance microbial technologies that promote sustainable farming, improve crop quality, and ensure global food security despite climate variability.

Keywords: Disease suppression, microbial inoculation, PGPMs, plant growth, sustainable agriculture

INTRODUCTION

The global population's continuous growth necessitates increased food production. However, sustaining this demand using conventional methods such as, chemical fertilizers presents financial and environmental challenges (Asghari et al., 2020). Agrochemical companies promote these practices, but their reliance on non-renewable fossil fuels and associated health concerns raises doubts about long-term viability. In contrast, farmers are increasingly adopting biopesticides for their affordability and effectiveness as biocontrol agents (Hulot & Hiller, 2021). To mitigate the negative impacts of agrochemicals in agriculture, plant growth-promoting microorganisms (PGPMs) have emerged as an environmentally friendly and sustainable alternative (Etesami, 2020).

Biocontrol agents (BCAs), including microorganisms such as *Azotobacter* sp., *Cyanobacteria*, fungi, and algae, show promise in enhancing agricultural productivity (Mensah et al., 2018). Notable examples include *Azospirillum*, *Bacillus*, *Rhizobium*, and *Trichoderma*. These PGPMs function as BCAs by converting nitrogen into plant-usable forms and improving the solubilization of key soil nutrients like phosphorus and potassium. Bhat et al. (2019) demonstrated that these microorganisms produce siderophores to enhance iron uptake and act as phytostimulants by influencing plant hormone levels. Additionally, Khan et al. (2020) reported that PGPMs indirectly serve as biopesticides by inducing systemic resistance against phytopathogens. When applied to soil, biofertilizers colonize the rhizosphere and internal plant structures, increasing nutrient accessibility and improving soil properties (Chatterjee et al., 2017). This eco-friendly approach supports sustainable development and environmental protection, offering a viable alternative to chemical fertilization (Etesami, 2020). Furthermore, PGPMs or biofertilizers can act as biocontrol agents through indirect mechanisms, such as enhancing plant vigor and enabling competition between plant growth-promoting rhizobacteria (PGPR) and pathogens in the root zone (Saeed et al., 2021). By colonizing plant roots, seedlings, or seed surfaces, BCAs improve growth by making essential nutrients available and enhancing soil physical, chemical, and biological conditions through microbial exudates that facilitate nutrient uptake (Chatterjee et al., 2017).

This article explores the mechanisms by which PGPM inoculation enhances plant growth, the influence of inoculation techniques on microbial effectiveness, and the role of PGPMs in suppressing disease development by antagonizing plant pathogens. It also lays a foundation for future research on sustaining plant-beneficial microbe interactions. The

uniqueness of this review lies in its practical framework for sustainable agriculture tailored to diverse environmental conditions, integrating recent advances in PGPM applications, including innovative inoculation techniques and their synergistic effects.

The reliance of chemical fertilizers on non-renewable fossil fuels poses significant environmental and health risks (Hulot & Hiller, 2021). In contrast, plant growth-promoting microorganisms (PGPMs) offer a sustainable alternative by enhancing nutrient cycling and reducing pesticide use (Etesami, 2020). Comparative studies reveal substantial variability in the efficacy of PGPMs, with field experiments demonstrating inconsistent crop yields. For instance, *Azospirillum* increased maize yields by 15–20% under optimal conditions (Al-Tammar & Khalifa, 2022), but its effectiveness declined by 30% under water stress (Asghari et al., 2020). This inconsistency presents a significant challenge to large-scale adoption, influenced by specific bio-ecological factors. To address these variations, targeted research is needed to connect PGPM mechanisms, such as nitrogen fixation and biocontrol, to sustainability outcomes like yield consistency and reduced chemical inputs.

PGPMs function through various mechanisms that promote agricultural sustainability. Nitrogen fixation contributes to yield stability but is affected by soil pH and moisture levels. However, there is a critical gap in understanding the long-term stability of nitrogen release under field conditions. Phosphate solubilization improves soil health, with its effectiveness influenced by soil type and microbial density. Nevertheless, its performance is limited by pH-dependent efficacy, highlighting the need for targeted strain selection. In terms of biocontrol, PGPMs help lower chemical inputs by suppressing pathogen loads, with the method of inoculation playing a vital role. A current gap exists in understanding how PGPMs interact or synergize with existing pathogens. Also, phytohormone production enhances plant stress tolerance and is influenced by crop genotype and stress type, but the underlying molecular interaction pathways remain inadequately explored.

To provide holistic synthesis and guide future research, this review adopts a conceptual framework that integrates validated PGPM mechanisms and highlights critical knowledge gaps, particularly in translating laboratory-based efficacy into field performance. This framework also forms the basis for the thematic structure of the review outlined below.

ADVANCING PGPM APPLICATION: A CONCEPTUAL FRAMEWORK TO OVERCOME PRACTICAL BARRIERS

The widespread adoption of plant growth-promoting microorganisms (PGPMs) faces three major barriers: ecological mismatches, technological limitations, and regulatory inconsistencies. First, incompatibility between soil, plants, and microbes is a significant challenge, as microbial efficacy can decrease by up to 20% when inoculants are applied to different soil types (Brown et al., 2020). Second, access to advanced technologies, particularly omics-based tools, is uneven; about 30% of developing regions lack access to

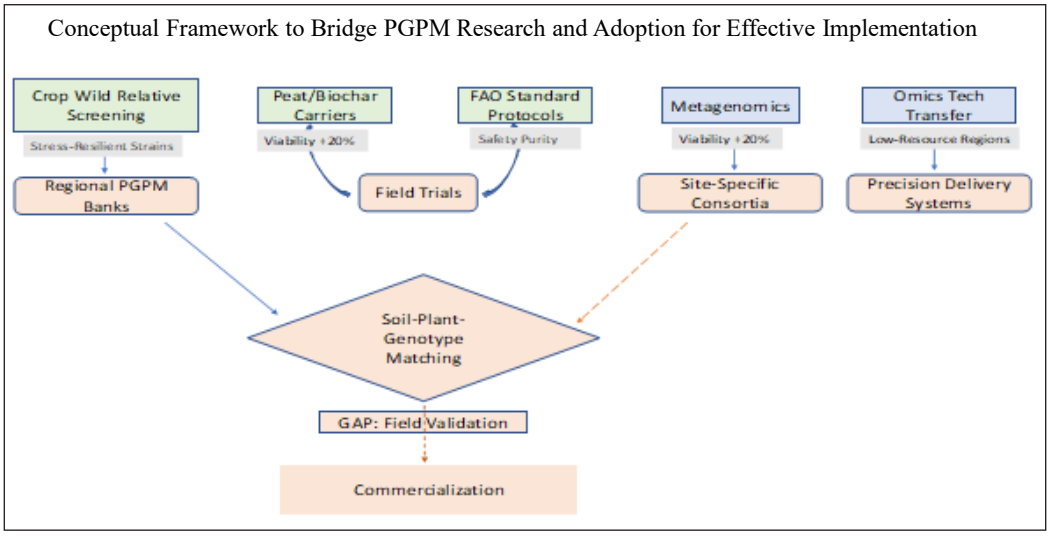

Figure 1. Integrated PGPM implementation framework. Green nodes: short-term priorities; blue nodes: long-term strategies. Dashed arrows indicate key research gaps (e.g., field validation of omics-guided consortia). Framework informed by FAO (2017); Muller et al. (2022)

these innovations (Reis et al., 2024). Finally, the lack of globally standardized protocols for evaluating inoculant purity, shelf-life, safety, and genetic stability undermine regulatory confidence and hampers market scalability. To address these constraints, we propose a dual-phase implementation framework (Figure 1) consisting of Short-term priorities and Long-term strategies:

Short-Term Priorities

1. Develop enhanced carrier materials, such as peat-based microcapsules, to improve microbial viability during storage and delivery.
2. Initiate regionally adapted PGPM screening programs, focusing on crop wild relatives, to identify stress-resilient strains.
3. Standardize evaluation protocols for assessing safety, microbial purity, and genetic stability before commercialization (FAO, 2017).

Long-Term Strategies

1. Utilize metagenomics and omics-guided selection to create site-specific PGPM consortia tailored to specific crop genotype and soil environments.
2. Expand molecular biology and omics infrastructure in low-resource regions through global technology transfer programs.

3. Integrate PGPMs into precision agriculture platforms for real-time, targeted delivery based on field conditions (Muller et al., 2022).

This framework highlights the importance of utilizing microbial diversity from crop wild relatives, which have developed superior phytostimulant traits, including improved nutrient uptake and drought tolerance. It also stresses the essential role of environmental compatibility, particularly soil characteristics and plant genotype in determining the survival and effectiveness of plant growth-promoting microorganisms (PGPM). While this approach is promising, its successful implementation will require a careful balance between agricultural productivity and ecological conservation, especially in areas rich in biodiversity.

PLANT GROWTH-PROMOTING MICROORGANISMS (PGPMS)

Plant growth-promoting microorganisms (PGPMs), encompassing plant growth-promoting rhizobacteria (PGPR) and plant growth-promoting fungi (PGPF), serve as beneficial biofertilizers, biocontrol agents, and decomposers (Dhawi, 2023). The term "rhizobacteria" was coined by Kloepper and Schroth (1978) to describe soil bacteria that colonize plant roots, enhance growth, and protect against disease. In 1980, they further defined "plant growth-promoting rhizobacteria" (PGPR) to characterize these microbes. To qualify as PGPR, a bacterial strain must fulfill at least two of the following criteria: effective root colonization, plant growth promotion, or disease suppression. PGPR can exist as endophytes within plant tissues or as rhizospheric bacteria on root surfaces, depending on their host interaction. Endophytic PGPR colonize the apoplastic region, while rhizospheric PGPR inhabits the root surface or superficial intercellular spaces (Vandana et al., 2021). Several symbiotic and nitrogen-fixing bacteria, including *Rhizobium*, *Azospirillum*, *Azotobacter*, *Mycobacterium*, *Bacillus*, *Serratia*, *Xanthomonas*, *Proteus*, *Pseudomonas*, and *Clostridium*, are recognized as PGPR. These microorganisms convert nitrogen into plant-usable forms.

In contrast, plant growth-promoting fungi (PGPF) includes beneficial species such as *Aspergillus*, *Penicillium*, *Fusarium*, *Trichoderma*, *Rhizoctonia*, and *Talaromyces*. Their hyphal networks and enzymatic capabilities enable them to degrade organic matter, solubilize nutrients, and stabilize soil aggregates (Corbu et al., 2023). PGPMs colonize the root zone and enhance plant growth through mechanisms such as nitrogen fixation, production of indole-3-acetic acid (IAA) and siderophores, phosphate solubilization, increased resistance to biotic and abiotic stresses, 1-aminocyclopropane-1-carboxylate (ACC) deaminase activity, quorum sensing (QS), and disease suppression (Cortivo et al., 2017).

Multiple studies indicate that PGPMs differ in their functional capabilities. *Trichoderma* improves phosphate solubilization, increasing tomato growth by 25% in acidic soils

(Tripathi et al., 2020), while *Azotobacter* is excellent at nitrogen fixation in microaerobic conditions, increasing wheat yields by 18% (Meena et al., 2017). Contradictions do arise, however, since strain-related siderophore synthesis varies by 40% under drought stress (Syed et al., 2023), suggesting limitations specific to the soil. Given that field observations show a 15–20% reduction in efficacy after a year (Mukhtar et al., 2017), research on long-term nutrient retention is lacking. A prolonged, strain-targeted study is necessary to improve long-term effects.

PLANT GROWTH-PROMOTING MECHANISMS OF PGPMS

This section discusses the mechanisms by which Plant Growth-Promoting Microorganisms (PGPMs) enhance crop growth, highlighting both direct and indirect processes. These mechanisms, influenced by factors such as soil type, host genotype, and plant developmental stage, play a crucial role in increasing agricultural yields (Brown et al., 2020). Direct mechanisms include nutrient acquisition through nitrogen fixation and phosphate solubilization, alongside the production of growth-promoting compounds like indole-3-acetic acid (IAA) and siderophores. Indirect mechanisms involve biocontrol activities that protect plants from phytopathogens (Elekhtyar, 2015).

Together, these mechanisms enhance plant vigor, nutrient uptake, and disease resistance. Their effectiveness has been demonstrated across a variety of crops, highlighting their importance in promoting sustainable agriculture (Kumar et al., 2022; Singh et al., 2019).

Biological Fixation of Nitrogen

Nitrogen is a crucial component of proteins and chlorophyll, essential for photosynthesis and plant growth. However, intensive agricultural practices often deplete soil nitrogen reserves, highlighting the need for microbial solutions (Saritha & Tollamadugu, 2019). Nitrogen-fixing bacteria, such as *Azotobacter* sp., *Rhizobium* sp., and *Azospirillum* sp., tackle this issue by converting atmospheric nitrogen into forms usable by plants, like nitrates and amines, through the nitrogenase enzyme and its FeMo cofactor (Meena et al., 2017). This microbial process not only maintains soil fertility but also adapts well to varying environmental conditions. The effectiveness of nitrogen-fixing microbes differs significantly among species and ecosystems. For instance, *Azotobacter* can boost maize yields by 18% in microaerobic soils (Al-Tammar & Khalifa, 2022), but its effectiveness drops by 30% in water-stressed conditions (Asghari et al., 2020). In contrast, Rhizobium-legume systems achieve stable nitrogen fixation through specialized oxygen-regulation mechanisms, such as the production of leghemoglobin, which protects nitrogenase activity (Reis et al., 2024). These physiological differences highlight the importance of selecting specific strains based on context, especially in arid regions where fluctuations in moisture and oxygen can significantly impact microbial function. Table 1 summarizes the agronomic

performance and stress adaptation mechanisms of major nitrogen-fixing PGPM strains, highlighting their yield benefits and limitations under field conditions.

Table 1
Performance and stress tolerance of key nitrogen-fixing PGPM strains

Strain	Optimal Condition	Yield Increase	Stress Tolerance Mechanism	Key Limitations	Reference
Azotobacter sp.	Microaerobic soils	18%	EPS production maintains hydration	30% decline under drought	Al-Tammar & Khalifa (2022)
Rhizobium sp.	Legume symbiosis	25%	Leghemoglobin protects nitrogenase from O_2	Host-specific	Poria et al. (2022)
Azospirillum brasilense	Well-drained soils	15–20%	ACC deaminase reduces ethylene stress	Sensitive to salinity (>6 dS/m)	Bashan & de-Bashan (2023)
Bradyrhizobium japonicum	Soybean symbiosis	22%	Heat-shock proteins (HSPs) stabilize enzymes	Low persistence in acidic soils	Reed & Glick (2023)
Paenibacillus polymyxa	Wide pH range (5–9)	12%	Biofilm formation enhances drought resistance	Competes poorly with native flora	Kumar et al. (2022)

PGPM = Plant Growth-Promoting Microorganisms; EPS = Exopolysaccharides; ACC = 1-Aminocyclopropane-1-Carboxylate. Data represent field-scale observations under optimal vs. stressed conditions

Phosphate Solubilization

Phosphorus is essential for energy transfer and plant development, but its availability is often restricted due to fixation as insoluble inorganic phosphates in soils and losses through runoff and leaching (Tripathi et al., 2020). Phosphate-solubilizing microorganisms, such as*Rhizobium* sp., *Bacillus* sp., and *Azotobacter* sp., utilize various biochemical strategies to enhance phosphorus availability. These microbes secrete organic acids, including gluconic and citric acid, which chelate metal cations (Ca^{2+}, Fe^{3+}, Al^{3+}) and release bound phosphate ions (Mukhtar et al., 2017). The acidification of the rhizosphere not only solubilize phosphorus but also increases the availability of other micro-nutrients. Furthermore, these microorganisms produce enzymes like Phytase and acid phosphatase, which mineralize organic phosphorus compounds from plant residues and soil organic matter. The *pqq* gene cluster is vital as it regulates gluconic acid production, a key factor in solubilization efficiency (Tripathi et al., 2020). Collectively, these processes convert inaccessible phosphorus into plant-available forms, enhancing nutrient uptake and reducing reliance on chemical fertilizers.

Production of Siderophores

Siderophores are vital for iron acquisition in iron-limited environments, commonly found in calcareous and high-pH soils. These low molecular weight compounds, produced by microorganisms such as *Pseudomonas* sp. and *Trichoderma* sp., have a very high affinity for ferric iron (Fe^{3+}), with formation constants exceeding 10^{30} (Syed et al., 2023). The structural diversity of siderophores (e.g., pyoverdines, catecholates, hydroxamates) allows different microbial species to thrive in various ecological niches within the rhizosphere. Specific siderophores, like pyoverdine and catechol-based compounds, facilitate iron uptake through specialized transport systems encoded by genes such as *fepA* and *fhuA* (Meena et al., 2017). In addition to their nutritional role, siderophores enhance plant health by sequestering iron from potential pathogens, thereby limiting their growth and virulence (Syed et al., 2023). This iron competition creates selective pressure in the rhizosphere, favoring beneficial organisms over pathogens. The dual role of siderophores-promoting plant iron nutrition while suppressing pathogens, highlights the sophisticated biocontrol capabilities of beneficial microbes and their potential to reduce reliance on pesticides.

Production of Phytohormones

Plant growth-promoting microorganisms significantly affect plant physiology through the production of various phytohormones, creating a complex signaling network that coordinates growth and stress responses. These microbial-derived hormones, including auxins, cytokinins, gibberellins, and abscisic acid, function at much lower concentrations than synthetic plant growth regulators while causing significant physiological changes (Chakraborty et al., 2021). Notably, indole-3-acetic acid (IAA), synthesized via the indole-3-pyruvate pathway in microbes such as *Pseudomonas* sp. and *Trichoderma* sp., plays a crucial role. The *ipdC* gene, which encodes indole-3-pyruvate decarboxylase, is essential in this process, directly impacting root architecture by stimulating lateral root formation and root hair development (Chakraborty et al., 2021). This morphological adaptation greatly increases the root surface area, enhancing nutrient and water acquisition. Additionally, cytokinins synthesized by PGPMs, produced through *ipt* gene activity, help modulate plant stress responses by upregulating key regulatory genes such as *DREB* and *MYB* (Singh et al., 2019). These hormonal interactions enSable plants to optimize growth under both favorable and stressful conditions, showcasing the sophisticated regulatory capacity of plant growth-promoting microorganisms (PGPMs). The balanced production of multiple phytohormones by microbial communities helps maintain plant homeostasis, preventing excessive vegetative growth or premature senescence often associated with synthetic hormone applications.

Production of Antibiotics and Enzymes

Microbial biofertilizers, including *Pseudomonas*, *Bacillus*, and *Streptomyces* spp., are well-known for their antagonistic effects against phytopathogens, primarily through the production of various secondary metabolites. These metabolites, which include antibiotics and cell wall-degrading enzymes, not only directly suppress pathogens but also induce systemic resistance in host plants (Kumar et al., 2022). For instance, *Pseudomonas* spp. produces 2,4-diacetylphloroglucinol (2,4-DAPG), an antibiotic regulated by the *phl* gene cluster, that effectively inhibits fungal pathogens. Similarly, *Bacillus* spp. secretes hydrolytic enzymes, such as chitinases and β-glucanases, regulated by the *chi* and *bgl* genes, which disrupt fungal cell walls. *Streptomyces* spp. also contributes by producing antibiotics like streptomycin, whose biosynthesis is modulated by quorum-sensing pathways to enhance effectiveness.

However, relying too heavily on single-strain biocontrol agents can lead to pathogen resistance. For example, repeated applications of 2,4-DAPG-producing *Pseudomonas* have resulted in *Fusarium oxysporum* populations developing *phl*-resistance genes, with a reported threefold increase in resistance after multiple inoculation cycles (Daigham et al., 2024). To mitigate this issue, we recommend rotating plant growth-promoting microorganisms (PGPMs) with distinct and complementary mechanisms. For instance, combining the chitinase activity of *Bacillus* with the antibiotic production of *Streptomyces* can strategically diversify approaches, reducing selective pressure, maintaining long-term efficacy, and promoting sustainable disease management.

Indole Acetic Acid Production

Bacillus species, especially *Bacillus thuringiensis*, are well-known for their ability to produce indole-3-acetic acid (IAA), a key phytohormone in the auxin group. The biosynthesis of IAA in these microorganisms typically occurs through the tryptophan-dependent pathway, where tryptophan is converted into IAA via intermediates such as indole-3-pyruvate. This conversion is facilitated by indole-3-pyruvate decarboxylase, encoded by the *ipdC* gene, which is crucial for enhancing IAA production. IAA functions to promote root elongation, lateral root formation, and cell division, thereby improving water and nutrient uptake—critical processes for developing a strong root system, particularly in nutrient-poor or stressed soils. Research on the *B. thuringiensis* strain RZ2MS9 has demonstrated that the IAA produced by the bacteria stimulates the expression of plant genes related to growth, nutrient transport, and stress tolerance. Moreover, the improved root architecture fosters better seedling establishment, resulting in enhanced biomass accumulation and increased crop yields. When combined with other beneficial traits such as phosphate solubilization or nitrogen fixation, IAA production significantly enhances the overall effectiveness of plant growth-promoting microorganisms (PGPMs). Thus,

IAA-producing strains like *B. thuringiensis* present a promising strategy for minimizing reliance on synthetic agrochemicals and promoting environmentally sustainable farming practices (Figueredo et al., 2023).

Hydrogen Cyanide Production

Beneficial microorganisms such as *Pseudomonas* sp., *Bacillus* sp., and *Trichoderma* sp. produce hydrogen cyanide (HCN) as a sophisticated biocontrol mechanism. Regulated by the *hcnABC* gene cluster, these microbes inhibit pathogenic organisms by disrupting cytochrome oxidase activity, thereby impairing their energy metabolism (Khoso, 2023). This natural pesticide action is further enhanced by the microbial release of ammonia (NH_3), a byproduct of amino acid degradation that serves dual purposes in soil ecosystems. The released NH_3 is rapidly converted to plant-available ammonium (NH_4^+) and simultaneously raises soil pH, creating conditions favorable for many crops. This pH modification can improve nutrient availability while suppressing acid-loving pathogens (Khoso, 2023). The combined effects of HCN and NH_3 offer a comprehensive approach to plant health management: HCN directly suppresses pathogens, while NH_3 enhances soil fertility and indirectly controls disease through environmental modification.

Zinc Solubilization

Zinc availability is a critical limiting factor in agricultural systems worldwide, despite its essential role in numerous enzymatic processes and protein synthesis. Plant growth-promoting microorganisms (PGPMs) tackle this challenge through various solubilization pathways. *Trichoderma* sp., *Providencia* sp., and *Anabaena* sp. secrete organic acids, particularly citric acid, to chelate zinc ions from insoluble compounds like ZnO. Additionally, their production of siderophores offers another pathway for zinc mobilization (Kumar, Sindhu et al. 2022). The efficiency of these systems is enhanced by high-affinity zinc transporters encoded by the *znuABC* genes, which facilitate plant uptake of the solubilized zinc. This microbial-mediated zinc cycling is particularly significant in alkaline soils, where conventional zinc fertilizers often fail. The resulting improvement in zinc nutrition not only boosts crop yields but also enhances nutritional quality, which is crucial for addressing human micronutrient deficiencies through bio-fortification (Kumar, Sindhu et al. 2022).

These mechanisms illustrate how PGPMs create integrated systems for promoting plant growth. The HCN/NH_3 systems provide both nutrition and protection, while zinc solubilization addresses a common micronutrient limitation. Importantly, these processes occur simultaneously in the rhizosphere, yielding synergistic benefits that surpass those achieved through single-mechanism approaches. The effectiveness of these natural systems suggests significant potential for reducing synthetic inputs in agriculture while maintaining

or improving productivity. Figure 2 illustrates the interconnections of these diverse mechanisms in promoting plant growth, emphasizing the multifunctional role of PGPMs in agricultural systems. This system-level understanding is essential for developing effective microbial inoculants that perform reliably across various field conditions.

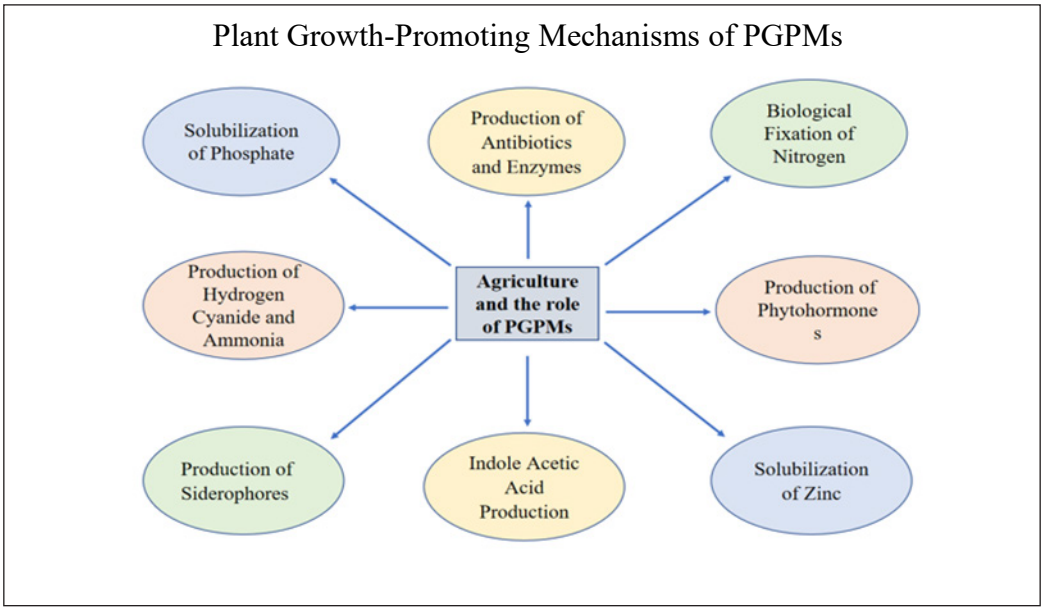

Figure 2. Plant growth-promoting mechanisms of PGPMs (PGPR and PGPF). The figure highlights key mechanisms such as nutrient solubilization (phosphate, zinc), biological nitrogen fixation, siderophore production, and synthesis of phytohormones (e.g., Indole Acetic Acid), antibiotics, and enzymes

These processes enhance plant growth, improve nutrient uptake, and increase resistance to pathogens, contributing to sustainable agriculture by boosting yield and reducing reliance on chemical inputs (Elekhtyar, 2015; Kumar et al., 2022; Singh et al., 2019).

APPROACH FOR SUCCESSFUL PLANT INOCULATION WITH PGPMS IN AGRICULTURE

Inoculation techniques are pivotal in ensuring the successful establishment, persistence, and growth-promoting activities of plant growth-promoting microorganisms (PGPMs) in the rhizosphere when introduced to host plants (Hernández-Montiel et al., 2017). These microorganisms enhance plant growth by inducing systemic resistance, producing growth regulators, and solubilizing nutrients. PGPMs can be applied individually or in mixtures via leaves, seeds, seedlings, roots, or soil. Such inoculations enable colonization of the plant interior or rhizosphere, promoting growth and improving adaptability to abiotic stress. For instance, inoculation with *Trichoderma* sp. through seed treatment or soil application has

demonstrated significant suppression of plant diseases and enhancement of plant growth. Dual inoculation with *Trichoderma harzianum* and *Azotobacter chroococcum* has proven more effective as a combined strategy for biological control in plant protection (Lopes et al., 2021). To optimize success, the following factors should be considered:

Proximity to Rhizosphere

Rhizosphere, with exudates of roots being present, enables colonization and activity of PGPMs such as *Pseudomonas* and *Bacillus* spp., enhancing plant growth through increased solubilization of nutrients and plant protection (Hernández-Montiel et al., 2017). Due to the low microbial mobility, inoculation near the root zone is necessary to achieve successful colonization. As they carry microorganisms on their cuticle or inside them, *Steinernema* and *Heterorhabditis* nematodes also facilitate PGPM transmission to allow root-targeted delivery (Hernández-Montiel et al., 2017; Knox et al., 2007). PGPM efficiency is enhanced, and farm-based sustainable food production is increased through combining nematode-delivery assisted with traditional inoculation techniques such as seed coating and soil drenching, as elaborated by Backer et al. (2018).

Inoculum Density and Method

The efficacy of plant growth-promoting microorganisms (PGPMs) inoculation depends on inoculum density, application method, and root colonization, which are influenced by microbial proliferation, soil conditions, and plant physiological state. For instance, applying solutions of *Trichoderma ghanense* and *Trichoderma tomentosum* at 10^9 conidia/mL significantly enhanced rye seedling growth in both grassland and arable soils. This can be achieved through seed inoculation or soil drenching, where *Trichoderma* is mixed with water and applied around plant bases during seedling and panicle initiation stages. Soil drenching with *Trichoderma* improves soil pH, nutrient uptake, and protection against root diseases (Msimbira & Smith, 2020).

The decline in microbial populations after inoculation poses a significant challenge to the efficacy of plant growth-promoting microorganisms (PGPMs). Research indicates that viability can decrease by up to 50% within 60 days due to environmental stressors (Msimbira & Smith, 2020). This decline results from both biotic factors, such as competition with native microbiota, and abiotic challenges, including fluctuations in soil pH and moisture extremes. Consequently, careful selection of site-adapted strains is essential (Etesami, 2020).

The choice of inoculation method also plays a critical role in outcomes. For example, seed inoculation can enhance rice germination by 20% (Ullah et al., 2017), while soil drenching with *Trichoderma* can boost tomato yields by 30% (Hernández-Montiel et al., 2017). Furthermore, root inoculation can achieve 40% greater rhizosphere colonization

in cucumbers (Gouda et al., 2020). Emerging technologies, such as micro-encapsulation, show particular promise, demonstrating 15% greater efficacy than liquid inoculants in tomato systems (Hernández-Montiel et al., 2017). However, to maintain field performance, it is crucial to optimize inoculum densities and develop strain-specific delivery protocols tailored to the specific crop and environmental conditions.

Single Vs. Co-Inoculation

Inoculation can involve a single isolate or co-inoculation with multiple isolates. Co-inoculation entails the simultaneous application of several microorganisms, promoting synergistic interactions that enhance efficacy. Research demonstrates that co-inoculation stimulates root development, boosting growth and productivity across various plant species (Asghari et al., 2020; Bakhshandeh et al., 2020; Lopes et al., 2018; Samaddar et al., 2019;). For example, Khan et al. (2023) compared single inoculation with *Trichoderma* sp. to co-inoculation with arbuscular mycorrhizal fungi (AMF) on tomato (*Solanum lycopersicum* L.) growth. The results showed that co-inoculation significantly improved plant development and nutrient absorption compared to single inoculation, highlighting the benefits of microbial synergy. Co-inoculated plants also exhibited enhanced growth parameters, including greater plant height, root length, and chlorophyll content, suggesting a synergistic effect on plant development.

Co-inoculation strategies show significant but context-dependent synergies. When *Trichoderma* is combined with arbuscular mycorrhizal fungi (AMF), tomato growth increases by 35% under optimal conditions with co-inoculation, more than double the 15% improvement observed with single inoculation (Khan et al., 2023). However, this advantage drops to just 5% under severe drought stress, highlighting critical limitations in stress adaptation. This variability in performance likely arises from three factors: (1) microbial competition for limited resources, (2) host-specific compatibility issues, and (3) insufficient expression of stress-responsive traits in sub-optimal consortia (Bakhshandeh et al., 2020).

Emerging omics approaches are shedding light on these interactions. Guzmán-Guzmán et al. (2024) found a 25% upregulation of antifungal genes in *Trichoderma*-PGPR combinations, indicating molecular pathways that facilitate synergy. However, a translational gap persists; although laboratory studies demonstrate promise, there is still limited field validation of these mechanisms. To tackle this issue, the following strategy is recommend:

Targeted Consortia Design

Where pairing microbes with complementary stress-response traits enhances plant resilience in adverse environments. For example:

- Drought-tolerant *Pseudomonas* species, which produce exopolysaccharides and ACC deaminase, when combined with nitrogen-fixing *Azospirillum brasilense*, are less effective under water scarcity and improve crop performance in arid conditions (Bashan et al., 2023).
- Salinity-resistant *Bacillus subtilis*, known for expressing osmolyte synthesis genes, paired with phosphate-solubilizing *Rhizobium*, helps mitigate salt stress in legumes (Etesami & Maheshwari, 2023).

Molecular Screening

Omics technologies, such as genomics and transcriptomics, facilitate the identification of strains with strong symbiotic potential and stress resilience through:

- CRISPR-based editing of *Bradyrhizobium japonicum* has enhanced its nitrogenase activity under heat stress (Reed et al., 2023).
- Metagenomic profiling of root microbiomes has uncovered *Paenibacillus polymyxa* strains with upregulated biofilm-related genes (*epsB*, *pelA*), contributing to improved drought tolerance (Kumar et al., 2023).

Condition-Specific Formulations

Tailored inoculants are designed to address specific agroecological challenges. For example:

- Under optimal conditions, high-performance consortia, such as *Azotobacter chroococcum* and *Trichoderma harzianum*, enhance nutrient uptake and promote plant growth (Singh et al., 2023).
- In stressed environments, specialized blends, like HCN-producing *Pseudomonas* combined with siderophore-producing *Streptomyces*, effectively suppress soil-borne pathogens, particularly in saline soils (Elekhtyar et al., 2023).

INOCULATION TECHNIQUES

Various techniques, including seed, root, soil, and foliar inoculation, are employed to introduce beneficial microorganisms to plants. Seed inoculation is the most widely used method, whereas foliar inoculation is the least common (Arora et al., 2020). The efficacy of microbial inoculation can be influenced by the composition and quantity of root exudates, as well as environmental stresses during plant growth. Seed inoculation involves applying beneficial microorganisms directly to seeds before planting, while soil inoculation disperses them throughout the soil. In contrast, root inoculation targets the plant roots specifically. The different inoculation methods used in screening trials are illustrated in Figure 3.

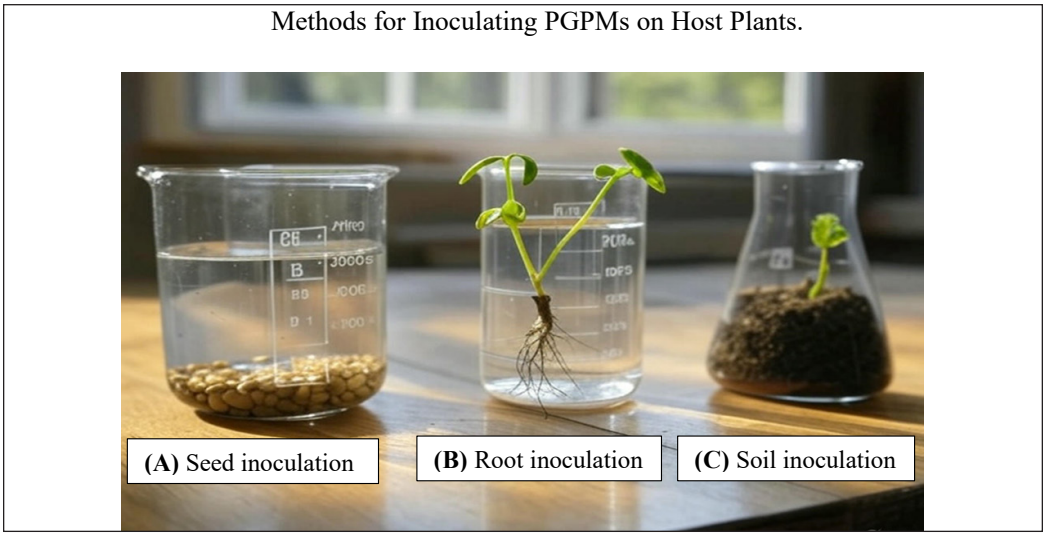

Figure 3. Methods for inoculating PGPMs on host plants.

The figure illustrates three key methods for inoculating PGPMs on host plants: (a) seed inoculation, where seeds are soaked in a microbial suspension to enhance germination and early seedling growth; (b) root inoculation, where seedling roots are submerged in microbial solutions to ensure direct colonization of the rhizosphere and facilitate nutrient uptake; and (c) soil inoculation, where microbial formulations are applied to the soil, promoting rhizosphere activity and disease suppression.

These techniques have been shown to improve plant growth, nutrient absorption, and pathogen resistance, supporting sustainable agriculture (Arora et al., 2020).

Seed Inoculation

Microbial inoculation methods, one of which involves immersing seeds in a solution of microorganisms with a defined concentration, and secretion occurs when carbohydrates and amino acids are released during seed germination (Lopes et al., 2018). This process has been shown to improve biomass production in species such as *Cicer arietinum* L. (Khan et al., 2019) and *Oryza sativa*. The inoculum remains dormant in the soil until it is activated by the growing root tips, which helps maintain effective cell density under field conditions. Additionally, *Pseudomonas fluorescens* was found to improve vigor, biomass, and water stress tolerance in *Vigna radiata* (Ullah et al., 2017).

Soil Inoculation

Soil inoculation delivers PGPMs directly into the soil through irrigation, soil addition, or microcapsules (Hernández-Montiel et al., 2017; Lopes et al., 2021). Soil soaking places the

microorganism solution near host roots (Lopes et al., 2018) to promote critical functions such as phosphate solubilization and phytohormone synthesis (Gouda et al., 2018). For *Brachiaria brizantha,* soil soaking with *Burkholderia pyromania* and *Pseudomonas fluorescens* promoted growth, while seed inoculation did not, due to a reduction in allelochemicals (Lopes et al., 2018). Soil inoculation with *Bacillus* increased nodule formation and development of *Cicer arietinum* L. compared to seed inoculation. The addition of PGPRs to the soil improved the growth of *Ranunculus asiaticus* by increasing nutrient and water absorption (Lopes et al., 2021). Inoculation via soil with *Pseudomonas putida* in microcapsules improved the development of *Lycopersicum esculentum* by providing gradual release and improved root colonization (Hernández-Montiel et al., 2017).

Root Inoculation

Root inoculation, which involves immersing seedling roots in a suspension of plant growth-promoting microorganisms (PGPM), offers a direct and effective method for delivering beneficial microbes to the rhizosphere. This technique ensures close contact between the inoculum and the root surface, enhancing both root colonization and microbial establishment. Research shows that root inoculation can lead to up to 40% higher rhizosphere colonization compared to seed coating (Gouda et al., 2020), significantly improving the consistency and effectiveness of plant growth promotion. Additionally, this method allows for the standardization of seedling size, enabling uniform inoculation of plants at similar developmental stages.

However, manual root inoculation can be labor-intensive, which limits its scalability in commercial agriculture. Fortunately, advancements in automated seedling dip systems, like those used in nurseries, have decreased labor costs by 25%, providing a practical balance between efficiency and affordability (Backer et al., 2018). These developments underscore the potential for integrating precision inoculation technologies to enhance the large-scale application of PGPMs in sustainable crop production systems. Table 2 below summarizes the impact of various PGPM inoculation techniques on plant growth parameters.

Table 2 outlines the impact of different PGPMs and their inoculation methods on various crops, demonstrating notable enhancements in plant growth, yield, and stress resilience. The effectiveness of these techniques varies based on the specific PGPM and the targeted plant.

The functions of PGPR and PGPF are to improve plant development, leading to increased production while maintaining environmental safety. They do this by producing phytohormones such as IAA, ABA, cytokinins, and ethylene, which facilitate processes like cell division, elongation, seedling emergence, and flower/fruit development (Meena et al., 2017). In addition to hormone production, PGPR and PGPF contribute to phosphate solubilization, nitrogen fixation, siderophore generation, and the synthesis of essential vitamins like niacin and biotin (Cortivo et al., 2017). Studies have shown that specific

Table 2
Effects of PGPM inoculation techniques on plant growth

PGPM	Plant	Inoculation Type	Effect of Inoculation	Reference
PGPR consortium	*Triticum aestivum* (wheat)	Soil application	Enhanced wheat productivity and nitrogen use efficiency with PGPR and nitrogen doses.	Gaspareto et al. (2023)
Pseudomonas fluorescens, *Bacillus licheniformis*	*Amaranthus hybridus(smooth pigweed)*	Soil application	Reduced plant stress and increased production with co-inoculation and seaweed bio-stimulant.	Ngoroyemoto et al. (2020)
Pseudomonas putida	*Lycopersicon esculentum (tomato)*	Soil microcapsules, liquid medium	Increased growth and yield with microcapsule and liquid medium inoculation.	Hernández-Montiel et al. (2017)
Rhizobial	*Oryza sativa (rice)*	Seed, root	Improved plant growth with seed inoculation.	Ullah et al. (2017)
Bacillus subtilis, *Pseudomonas putida*	*Cucumis sativus* (cucumber)	Soil application	Enhanced root growth and yield with combined inoculation and seaweed extracts.	Kakbra (2024)
Pseudomonas burkholderia	*Brachiaria brizantha (signal grass)*	Seed, soil	Improved plant development with seed inoculation.	Lopes et al. (2018)

species like *Klebsiella sp., B. spumilus, Acinetobacter sp.*, and *B. subtilis* enhance maize productivity through nitrogen fixation, phosphate solubilization, and IAA production (Kuan et al., 2016). Biofertilizers containing *B. mojavensis, B. subtilis, B. pumilus*, and *B. pseudomycoides* increased sweet maize yield and improved grain protein and fiber content (Katsenios et al., 2022). Furthermore, *Trichoderma* rhizosphere-competent varieties have equally expressed effectiveness in promoting plant growth, enhancing nutrient uptake, accelerating seed germination, and activating plant defense mechanisms. Numerous studies have reported the functions of PGPR and PGPF on plant growth, as highlighted in Tables 3 and 4.

Table 3 summarizes the effect of various PGPRs on different crops, highlighting their notable contributions to plant growth, nutrient uptake, and stress resilience. Observations indicate that PGPR can enhance root development, improve disease resistance, and promote crop yield, supporting their role as biological agents.

Table 3
PGPR and their impact on plant growth

PGPR	Crop	Observation	Reference
Azospirillum sp., *Azoarcus sp.*	*Triticum aestivum* (wheat)	Improved root growth, stress tolerance, and reduced nitrogen losses.	Bashan & de-Bashan (2023)
Bacillus subtilis	*Solanum lycopersicum* (tomato)	Enhanced growth and yield via nutrient uptake and disease resistance.	Souza et al. (2015)
Flavobacterium johnsoniae, *Pseudomonas putida*, *Azotobacter chroococcum*	*Triticum aestivum* (wheat)	Improved bacterial growth and seed germination under salt stress.	Rai et al. (2018)
Azospirillum brasilense	*Zea mays* (maize)	Enhanced root development and nutrient absorption, increasing yields.	Al-Tammar & Khalifa (2022)
Rhizobium leguminosarum	*Pisum sativum* (pea)	Increased nitrogen fixation, biomass, and yield.	Poria et al. (2022)
Enterobacter cloacae	*Oryza sativa* (rice)	Promoted growth under saline conditions via stress tolerance.	Katsenios et al. (2022)
Serratia marcescens	*Glycine max* (soybean)	Improved seed germination and early seedling growth.	Reed & Glick (2023)

Table 4
PGPF and their impact on plant growth

PGPF	Crop	Observation	Reference
Pleurotus tuber-regium, *Lentinus squarrosulus*, *Ganoderma sp.*	*Triticum aestivum* (wheat), *Solanum lycopersicum* (tomato)	Enhanced growth via siderophore production, phosphate solubilization, and enzyme activities.	Kumar et al. (2022)
Trichoderma harzianum	*Solanum lycopersicum* (tomato)	Improved growth and fungal pathogen resistance.	Aamir et al. (2023)
Penicillium chrysogenum	*Solanum lycopersicum* (tomato)	Promoted growth through phosphate solubilization and growth-promoting substances.	Adedayo & Babalola (2023)
Aspergillus chevalieri	*Solanum lycopersicum* (tomato)	Protected against *Alternaria solani*, enhancing growth and health.	Daigham et al. (2024)
Penicillium olsonii	*Nicotiana tabacum* (tobacco)	Enhanced salt tolerance and reduced fertilizer needs.	Tarroum et al. (2022)
Trichoderma spp.	*Arabidopsis thaliana (*thale-cress)	Potentiated antifungal and growth-promoting traits with PGPR.	Guzmán-Guzmán et al. (2024)

Table 4 presents various PGPF and their observed effects on different crops, highlighting significant impacts on plant growth, nutrient uptake, and stress tolerance. The findings highlight the potential of PGPF as effective biological agents.

The growth enhancement is demonstrated by increased plant material production, promoted lateral root development, higher yields, improved seed germination rates, and better growth parameters. *Azospirillum* sp.*, Azoarcus* sp and *Bacillus* sp highly improved root development, ability to withstand unfavorable conditions, reduced losses in N, and disease resistance in wheat and tomato. Similarly, *Trichoderma* sp has shown beneficial effects on multiple plant species, including tomato and Arabidopsis, suggesting its versatility in promoting growth across different plant types. Likewise, the application of *Trichoderma harzianum* has led to improvements in yield quality parameters, such as improved salt tolerance in tobacco. In addition, *Trichoderma* sp. and *Pleurotustuber-regium*, *Lentinus squarrosulus*, and *Ganoderma* sp., have demonstrated disease protection capabilities, providing resistance against various plant pathogens. Consequently, overall findings suggest that the application of PGPMs can be a promising strategy for enhancing plant growth, improving yield, and protection against plant diseases across various crop species. Despite the proven benefits of PGPMs, their large-scale adoption remains limited.

CONCLUSION

Plant growth-promoting microorganisms (PGPMs) play a crucial role in achieving sustainable crop production and enhancing soil health. By improving nutrient uptake and activating plant immune responses such as induced systemic resistance and antibiosis PGPMs can reduce reliance on chemical fertilizers and pesticides by 40–60% (Kumar et al., 2022). This reduction supports ecological balance, fosters soil biodiversity, and aligns with organic farming principles. However, the real-world adoption of PGPMs is still limited due to practical challenges. One major issue is strain resilience; studies have shown that microbial populations can decline by up to 50% after inoculation, highlighting the need for better delivery systems and formulations (Msimbira & Smith, 2020). Additionally, farmer education is essential pilot programs in Malaysia saw a doubling of PGPM uptake when paired with training modules (Lopes et al., 2021). Policy support also plays a significant role in adoption rates, as evidenced in India, where subsidies for biofertilizers resulted in a 25% increase in PGPM use (Saritha & Tollamadugu, 2019).

To bridge the gap between laboratory efficacy and field performance, future research should focus on advancing co-inoculation techniques that utilize complementary microbial strains and employ molecular omics to better understand plant–microbe–soil interactions. At the same time, developing low-cost, user-friendly inoculation technologies tailored for smallholder contexts will be vital. Implementing these strategies can unlock the full potential of PGPMs, contributing to sustainable agriculture and long-term food security.

ACKNOWLEDGMENT

We are grateful to the Ministry of Higher Education and University Putra Malaysia for providing financial support under the Malaysia Research University Network (MRUN) research grant, MRUN/ITAFOS/2022 (Vote No: 5539310) to conduct this research project.

REFERENCES

Aamir, M., Shanmugam, V., Dubey, M. K., Husain, F. M., Adil, M., Ansari, W. A., & Sah, P. (2023). Transcriptomic characterization of Trichoderma harzianum T34 primed tomato plants: Assessment of biocontrol agent-induced host-specific gene expression and plant growth promotion. *BMC Plant Biology, 23*(1), Article 552. https://doi.org/10.1186/s12870-023-03728-7

Adedayo, A. A., & Babalola, O. O. (2023). Fungi that promote plant growth in the rhizosphere boost crop growth. *Journal of Fungi (Basel), 9*(2), Article 239. https://doi.org/10.3390/jof9020239

Al-Tammar, F. K., & Khalifa, A. Y. Z. (2022). Plant growth-promoting bacteria drive food security. *Brazilian Journal of Biology, 82*, Article e267257. https://doi.org/10.1590/1519-6984.267257

Arora, N. K., Fatima, T., Mishra, I., & Verma, S. (2020). Microbe-based inoculants: Role in next green revolution. In V. Shukla & N. Kumar (Eds.) *Environmental concerns and sustainable development: volume 2: Biodiversity, soil and waste management* (pp. 191-246). Springer. https://doi.org/10.1007/978-981-13-6358-0_9

Asghari, B., Khademian, R., & Sedaghati, B. (2020). Plant growth-promoting rhizobacteria (PGPR) confer drought resistance and stimulate biosynthesis of secondary metabolites in pennyroyal (Mentha pulegium L.) under water shortage conditions. *Scientia Horticulturae, 263*, Article 109132. https://doi.org/10.1016/j.scienta.2019.109132

Backer, R., Rokem, J. S., Ilangumaran, G., Lamont, J., Praslickova, D., Ricci, E., Subramanian, S., & Smith, D. L. (2018). Plant growth-promoting rhizobacteria: Context, mechanisms of action, and roadmap to commercialization. *Frontiers in Plant Science*, *9,* Article 1473. https://doi.org/10.3389/fpls.2018.01473

Bakhshandeh, E., Gholamhosseini, M., Yaghoubian, Y., & Pirdashti, H. (2020). Plant growth-promoting microorganisms can improve germination, seedling growth, and potassium uptake of soybeans under drought and salt stress. *Plant Growth Regulation, 90*, 123-136. https://doi.org/10.1007/s10725-019-00556-5

Bashan, Y., & de-Bashan, L. E. (2023). Azospirillum: A plant growth-promoting bacterium for sustainable agriculture. *FEMS Microbiology Reviews*, *47*(1), Article fuad002. https://doi.org/10.1093/femsre/fuad002

Bashan, Y., de-Bashan, L. E., Prabhu, S. R., & Hernandez, J. P. (2023). Synergistic consortia for abiotic stress alleviation in crops. *Frontiers in Microbiology, 14*, Article 1125689. https://doi.org/10.3389/fmicb.2023.1125689

Bhat, M. A., Rasool, R., & Ramzan, S. (2019). Plant growth promoting rhizobacteria (PGPR) for sustainable and eco-friendly agriculture. *Acta Scientific Agriculture, 3*(1), 23-25.

Brown, S. P., Grillo, M. A., Podowski, J. C., & Heath, K. D. (2020). Soil origin and plant genotype structure distinct microbiome compartments in the model legume *Medicago truncatula*. *Microbiome, 8*(1), Article 139. https://doi.org/10.1186/s40168-020-00915-9

Chakraborty, A., Dastogeer, K. M. G., Tumpa, F. H., Sultana, A., Chakraborty, S., & Hoque, M. A. (2021). Microbial phytohormones and their role in plant growth regulation: A comprehensive review. *Frontiers in Plant Science, 12*, Article 678945. https://doi.org/10.3389/fpls.2021.678945

Chatterjee, A., Singh, S., Agrawal, C., Yadav, S., Rai, R., & Rai, L. C. (2017). Role of algae as a biofertilizer. In R. P. Rastogi, D. Madamwar & A. Pandey (Eds.) *Algal green chemistry: Recent progress in biotechnology* (pp. 189-200). Elsevier. https://doi.org/10.1016/B978-0-444-63784-0.00010-2

Corbu, V. M., Gheorghe-Barbu, I., Dumbravă, A. Ș., Vrâncianu, C. O., & Șesan, T. E. (2023). Current insights in fungal importance. A comprehensive review. *Microorganisms, 11*(6), Article 1384. https://doi.org/10.3390/microorganisms11061384

Cortivo, C. D., Ferrari, M., Visioli, G., Lauro, M., Fornasier, F., Barion, G., Panozzo, A., & Vamerali, T. (2017). Effects of seed-applied biofertilizers on rhizosphere biodiversity and growth of common wheat (*Triticum aestivum* L.) in an organic agroecosystem. *Plant and Soil, 421(1-2)*, 113-130. https://doi.org/10.1007/s11104-017-3445-0

Daigham, G. E., Mahfouz, A. Y., Abdelaziz, A. M., Nofel, M. M., & Attia, M. S. (2024). Protective role of plant growth-promoting fungi *Aspergillus chevalieri* OP593083 and *Aspergillus egyptiacus* OP593080 as biocontrol approach against Alternaria leaf spot disease of Vicia faba plant. *Biomass Conversion and Bio-refinery, 14*, 23073–23089. https://doi.org/10.1007/s13399-023-04510-4

Dhawi, F. (2023). The role of plant growth-promoting microorganisms (PGPMs) and their feasibility in hydroponics and vertical farming. *Metabolites, 13*(2), Article 247. https://doi.org/10.3390/metabo13020247

Elekhtyar, N. M. (2015). Impact of three strains of Bacillus as bio NPK fertilizers and three levels of mineral NPK fertilizers on growth, chemical compositions and yield of Sakha 106 rice cultivar. *International Journal of Chem Tech Research, 8*(4), 2150-2156.

Elekhtyar, N. M., Al-Tammar, J. K., & Khalifa, A. Y. Z. (2023). Stress-specific PGPR formulations for saline soils: Pathogen suppression and growth promotion. *Journal of Plant Growth Regulation, 42*(1), 45–60. https://doi.org/10.1007/s00344-022-10765-4

Etesami, H. (2020). Plant–microbe interactions in plants and stress tolerance. In G. Azzarello (Ed.) *Plant life under changing environment* (pp. 355-396). Academic Press. https://doi.org/10.1016/B978-0-12-818204-8.00018-7

Etesami, H., & Maheshwari, D. K. (2023). Use of plant growth promoting rhizobacteria (PGPRs) for salinity stress management in crops. *Microbiological Research, 267*, Article 127272. https://doi.org/10.1016/j.micres.2022.127272

FAO. (2017). *Protocol for the evaluation of microbial plant bio-stimulants* (2nd ed.). Food and Agriculture Organization of the United Nations. https://doi.org/10.4060/cb3125en

Figueredo, E. F., Cruz, T. A. D., Almeida, J. R. D., Batista, B. D., Marcon, J., Andrade, P. A. M. D., & Quecine, M. C. (2023). The key role of indole-3-acetic acid biosynthesis by *Bacillus thuringiensis* RZ2MS9 in promoting maize growth revealed by the ipdC gene knockout mediated by the CRISPR-Cas9 system. *Microbiological Research, 266*, Article 127218. https://doi.org/10.1016/j.micres.2023.127218

Gaspareto, R. N., Felici, B. G., Kichik, V., Buzinaro, R., & Souza, J. S. D. (2023). Inoculation with plant growth-promoting bacteria and nitrogen doses improves wheat productivity and nitrogen use efficiency. *Microorganisms, 11*(4), Article 1046. https://doi.org/10.3390/microorganisms11041046

Gouda, S., Das, G., Sen, S. K., Shawl, A. S., & Kaur, H. (2020). Revitalization of plant growth-promoting rhizobacteria for sustainable agriculture. *Frontiers in Sustainable Food Systems, 4*, 1-18. https://doi.org/10.3389/fsufs.2020.00001

Gouda, S., Kerry, R. G., Das, G., Paramithiotis, S., Shin, H. S., & Patra, J. K. (2018). Revitalization of plant growth promoting rhizobacteria for sustainable development in agriculture. *Microbiological Research, 206*, 131-140. https://doi.org/10.1016/j.micres.2017.08.016

Guzmán-Guzmán, P., Valencia-Cantero, E., & Santoyo, G. (2024). Plant growth-promoting bacteria potentiate antifungal and plant-beneficial responses of *Trichoderma atroviride* by upregulating its effector functions. *PLoS One, 19*(3), Article e0301139. https://doi.org/10.1371/journal.pone.0301139

Hernández-Montiel, L. G., Contreras, C. J. C., Amador, B. M., Hernández, L. V., Quiñones Aguilar, E. E., & Contreras, R. G. C. (2017). The efficiency of two inoculation methods of *Pseudomonas putida* on growth and yield of tomato plants. *Journal of Soil Science and Plant Nutrition, 17*(4), 1003–1012. https://doi.org/10.4067/S0718-95162017000400012

Hulot, J. F., & Hiller, N. (2021). *Exploring the benefits of biocontrol for sustainable agriculture - A literature review on biocontrol in light of the European green deal*. Institute for European Environmental Policy.

Kakbra, R. F. (2024). Effect of seaweed, moringa leaf extract, and biofertilizer on growth, yield, and fruit quality of cucumber (*Cucumis sativus* L.) under greenhouse conditions. *arXiv preprint arXiv:2403.17984*. https://doi.org/10.48550/arXiv.2403.17984

Katsenios, N., Andreou, V., Sparangis, P., Koutouki, S., & Koutouki, A. (2022). Assessment of plant growth promoting bacteria strains on growth, yield, and quality of sweet corn. *Scientific Reports, 12*(1), Article 11598. https://doi.org/10.1038/s41598-022-16044-2

Khan, M. I., Sharma, S., & Khan, M. W. (2023). Effects of single inoculation and co-inoculation of Trichoderma spp. with arbuscular mycorrhizal fungi on growth of tomato (*Solanum lycopersicum* L.). *Journal of Plant Growth Regulation, 42*(1), 87-98. https://doi.org/10.3390/plants12173101

Khan, N., Bano, A., Ali, S., & Babar, M. A. (2020). Crosstalk among phytohormones from planta and PGPR under biotic and abiotic stresses. *Plant Growth Regulation, 90*, 189-203. https://doi.org/10.1007/s10725-020-00571-x

Khan, S. A. R., Sharif, A., Golpîra, H., & Kumar, A. (2019). A green ideology in Asian emerging economies: From environmental policy to sustainable development. *Sustainable Development, 27*(6), 1063-1075. https://doi.org/10.1002/sd.1958

Khoso, M. A., Wagan, S., Alam, I., Hussain, A., Ali, Q., Saha, S., & Liu, F. (2023). Impact of plant growth-promoting rhizobacteria (PGPR) on plant nutrition and root characteristics: Current perspective. *Plant Stress, 11*, Article 100341. https://doi.org/10.1016/j.stress.2023.100341

Kloepper, J. W., & Schroth, M. N. (1978). Plant growth-promoting rhizobacteria on radishes. *Proceedings of the 4th International Conference on Plant Pathogenic Bacteria, 2*, 879–882.

Knox, O. G. G., Killham, K., & Leifert, C. (2007). Nematode-enhanced microbial colonization of the wheat rhizosphere. *FEMS Microbiology Ecology*, *62*(2), 123–129. https://doi.org/10.1111/j.1574-6941.2007.00376.x

Kuan, K. B., Othman, R., Rahim, K. A., & Shamsuddin, Z. H. (2016). Plant growth-promoting rhizobacteria inoculation to enhance vegetative growth, nitrogen fixation and nitrogen re-mobilization of maize under greenhouse conditions. *PloS One, 11*(3), Article e0152478. https://doi.org/10.1371/journal.pone.0152478

Kumar, A., Verma, J. P., & Singh, R. P. (2023). Metagenomic insights into drought-adaptive biofilm genes in *Paenibacillus polymyxa*. *Applied and Environmental Microbiology, 89*(3), Article e01822-22. https://doi.org/10.1128/aem.01822-22

Kumar, M., Ahmad, S., & Singh, R. P. (2022). Plant growth-promoting microbes: Diverse roles for sustainable and eco-friendly agriculture. *Energy Nexus, 7,* Article 100133. https://doi.org/10.1016/j.nexus.2022.100133

Kumar, S., Sindhu, S. S., & Kumar, R. (2022). Biofertilizers: An eco-friendly technology for nutrient recycling and environmental sustainability. *Current Research in Microbial Sciences, 3*, Article 100094. https://doi.org/10.1016/j.crmicr.2022.100094

Lopes, M. J. D. S., Dias-Filho, M. B., & Gurgel, E. S. C. (2021). Successful plant growth-promoting microbes: Inoculation methods and abiotic factors. *Frontiers in Sustainable Food Systems, 5*, Article 606454. https://doi.org/10.3389/fsufs.2021.606454

Lopes, M. J. D. S., Filho, M. B. D., Castro, T. H. D. R., Filippi, M. C. C. D., & Silva, G. B. D. (2018). Effect of *Pseudomonas fluorescens* and *Burkholderia pyrrocinia* on the growth improvement and physiological responses in *Brachiaria brizantha*. *American Journal of Plant Sciences, 9(*2), 250-265.

Meena, V. S., Meena, S. K., Verma, J. P., Kumar, A., Aeron, A., Mishra, P. K., & Dotaniya, M. L. (2017). Plant beneficial rhizospheric microorganisms (PBRM) strategies to improve nutrients use efficiency: A review. *Ecological Engineering, 107*, 8-32. https://doi.org/10.1016/j.ecoleng.2017.06.058

Mensah, D. L. N., Duponnois, R., Bourillon, J., Gressent, F., & Prin, Y. (2018). Biochemical characterization and efficacy of *Pleurotus, Lentinus,* and *Ganoderma* parent and hybrid mushroom strains as biofertilizers of attapulgite for wheat and tomato growth. *Biocatalysis and Agricultural Biotechnology, 16*, 63-72. https://doi.org/10.1016/j.bcab.2018.06.019

Msimbira, L. A., & Smith, D. L. (2020). The roles of plant growth-promoting microbes in enhancing plant tolerance to acidity and alkalinity stresses. *Frontiers in Sustainable Food Systems, 4*, Article 106. https://doi.org/10.3389/fsufs.2020.00106

Mukhtar, S., Shahid, I., Mehnaz, S., & Malik, K. A. (2017). Assessment of two carrier materials for phosphate-solubilizing biofertilizers and their effect on the growth of wheat (*Triticum aestivum* L.). *Microbiological Research, 205*, 107-117. https://doi.org/10.1016/j.micres.2017.08.011

Muller, D. B., Vogel, C., Bai, Y., & Vorholt, J. A. (2022). The plant microbiota: Systems-level insights and perspectives. *Nature Reviews Microbiology, 20*(5), 291-305. https://doi.org/10.1038/s41579-021-00668-8

Ngoroyemoto, N., Mudyiwa, S., & Bower, S. T. (2020). Interactions between microorganisms and a seaweed-derived bio-stimulant on the growth and biochemical composition of Amaranthus hybridus L. *Natural Product Communications, 15*(7), Article 1934578X20934228. https://doi.org/10.1177/1934578X20934228

Poria, V., Dębiec-Andrzejewska, K., Fiodor, A., Lyzohub, M., Ajijah, N., Singh, S., & Pranaw, K. (2022). Plant growth-promoting bacteria (PGPB) integrated phytotechnology: A sustainable approach for remediation of marginal lands. *Frontiers in Plant Science, 13*, Article 999866. https://doi.org/10.3389/fpls.2022.999866

Rai, V. K., Dutta, P., Sinha, R., Yadav, S. K., & Kumar, P. (2018). Salt stress tolerance in wheat (Triticum aestivum L.) improved by plant growth-promoting rhizobacteria (PGPR): A sustainable approach. *Journal of Plant Stress Physiology, 12*(3), 143–153. https://doi.org/10.1016/j.plsp.2018.05.007

Reed, L., & Glick, B. R. (2023). The recent use of plant-growth-promoting bacteria to promote the growth of agricultural food crops. *Agriculture, 13*(5), Article 1089. https://doi.org/10.3390/agriculture130501089

Reis, G. A. D., Martínez-Burgos, W. J., Pozzan, R., Pastrana Puche, Y., Ocán-Torres, D., de Queiroz Fonseca Mota, P., & Soccol, C. R. (2024). A comprehensive review of microbial inoculants: Agricultural applications, technology trends in patents, and regulatorframeworks. *Sustainability,16*(19), Article 8720. https://doi.org/10.3390/su16198720

Saeed, Q., Xiukang, W., Haider, F. U., Kučerik, J., Mumtaz, M. Z., Holatko, J., & Mustafa, A. (2021). Rhizosphere bacteria in plant growth promotion, biocontrol, and bioremediation of contaminated sites: A comprehensive review of effects and mechanisms. *International Journal of Molecular Sciences, 22*(19), Article 10529. https://doi.org/10.3390/ijms221910529

Samaddar, S., Chatterjee, P., Choudhury, A. R., Ahmed, S., & Sa, T. (2019). Interactions between Pseudomonas spp. and their role in improving the red pepper plant growth under salinity stress. *Microbiological Research, 219*, 66-73. https://doi.org/10.1016/micres.2018

Saritha, M., & Tollamadugu, N. P. (2019). The status of research and application of biofertilizers and biopesticides: Global scenario. In V. Buddolla (Ed.) *Recent developments in applied microbiology and biochemistry* (pp. 195-207). Academic Press. https://doi.org/10.1016/B978-0-12-816328-3.00015-5

Singh, M., Singh, D., Gupta, A., Pandey, K. D., Singh, P. K., & Kumar, A. (2019). Plant growth promoting rhizobacteria: Application in biofertilizers and biocontrol of phytopathogens. In A. K. Singh, A. Kumar & P. K. Singh (Eds.) *PGPR amelioration in sustainable agriculture* (pp. 41-66). Woodhead Publishing. https://doi.org/10.1016/B978-0-12-815879-1.00003-3

Singh, R. P., Shelake, G. M., & Sharma, S. (2023). Microbial inoculants for precision agriculture: Current status and future prospects. *Applied Soil Ecology, 184*, Article 104789. https://doi.org/10.1016/j.apsoil.2022.104789

Souza, R. D., Ambrosini, A., & Passaglia, L. M. (2015). Plant growth-promoting bacteria as inoculants in agricultural soils. *Genetics and Molecular Biology, 38*(4), 401-419. https://doi.org/10.1590/S1415-475738420150053

Syed, A., Elgorban, A. M., Bahkali, A. H., Eswaramoorthy, R., Iqbal, R. K., & Danish, S. (2023). Metal-tolerant and siderophore-producing *Pseudomonas fluorescens* and *Trichoderma* sp. improved the growth, biochemical features, and yield attributes of chickpeas by lowering Cd uptake. *Scientific Reports, 13*(1), Article 4471. https://doi.org/10.1038/s41598-023-31330-3

Tarroum, M., Romdhane, W. B., Al-Qurainy, F., Ali, A. A. M., Al-Doss, A., Fki, L., & Hassairi, A. (2022). A novel PGPF *Penicillium olsonii* isolated from the rhizosphere of *Aeluropus littoralis* promotes plant growth, enhances salt stress tolerance, and reduces chemical fertilizer inputs in the hydroponic system. *Frontiers in Microbiology, 13*, Article 996054. https://doi.org/10.3389/fmicb.2022.996054

Tripathi, S., Singh, M., & Singh, S. (2020). Advances in phosphate solubilizing microorganism (PSM)-based biofertilizers: Mechanisms and applications. *Acta Physiologiae Plantarum, 42(*3), 1-17. https://doi.org/10.1007/s11738-020-3041-1

Ullah, M. A., Mahmood, I. A., Ali, A., Nawaz, Q., & Sultan, T. (2017). Effect of inoculation methods of biozone-max (plant growth promoting rhizobacteria-PGPR) on growth and yield of rice under naturally salt-affected soil. *Research in Plant Biology, 7*(1), 24-26. https://doi.org/10.25081/ripb.2017.v7.3602

Vandana, U. K., Rajkumari, J., Singha, L. P., Satish, L., Alavilli, H., Sudheer, P. D. V. N., Chauhan, S., Ratnala, R., Satturu, V., Mazumder, P. B., & Pandey, P. (2021). The endophytic microbiome as a hotspot of synergistic interactions, with prospects of plant growth promotion. *Biology, 10*(2), Article 101. https://doi.org/10.3390/biology10020101

Pertanika J. Trop. Agric. Sci. 48 (6): 1941 - 1959 (2025)

PERTANIKA JOURNALS

TROPICAL AGRICULTURAL SCIENCE

Journal homepage: http://www.pertanika.upm.edu.my/

Assessing Resistance to Powdery Mildew in Mung Bean: The Role of Phenolic Compounds and Phenylalanine Ammonia-lyase (PAL) Activity

Alfi Inayati*, Trustinah, Rudy Soehendi, and Eriyanto Yusnawan

Research Centre for Food Crops, Research Organization for Agriculture and Food, National Research and Innovation Agency (BRIN), Jalan Raya Bogor Km. 46 Cibinong, West Java 16911, Indonesia

ABSTRACT

Powdery mildew caused by *Erysiphe polygoni* is one of the main pathogens on mung bean that causes significant yield loss. This study determined the agronomic performance and physio-biochemical activities of twelve mung bean genotypes under powdery mildew infection. The experimental design was arranged in a completely randomized block design with three replicates. Initial disease symptoms appeared 14 days after planting (DAP) and then progressed to 31.7% in the moderate genotype (Sampeong) and 87.2% in the susceptible genotype (G2). The study suggested no significant correlation between chlorophyll contents and the severity of powdery mildew in mung bean genotypes; however, the disease negatively affected the yield in susceptible genotypes. Total phenolic and flavonoid contents in leaves showed a positive relationship with disease severity and mung bean resistance in the G6 genotype, in Vima 1. and Sampeong cultivars. Our findings showed that the phenolic compounds including phenylalanine ammonia-lyase (PAL) and tyrosine ammonia-lyase (TAL) activities in the leaves were important factors for mung bean resistance to powdery mildew and this interaction impacted the growth and productivity of mung bean plants.

Keywords: Mung bean, phenolic, phenylalanine ammonia-lyase (PAL), powdery mildew

ARTICLE INFO

Article history:
Received: 24 March 2025
Accepted: 09 October 2025
Published: 25 November 2025

DOI: https://doi.org/10.47836/pjtas.48.6.15

E-mail addresses:
alfi013@brin.go.id (Alfi Inayati)
trus001@brin.go.id (Trustinah)
rudy007@brin.go.id (Rudy Soehendi)
eriy001@brin.go.id (Eriyanto Yusnawan)
* Corresponding author

INTRODUCTION

Powdery mildew is an obligate biotrophic pathogen caused by *Erysiphe polygoni* D.C. fungus. The incidence of powdery mildew increases particularly during the cool-dry season in Indonesia (Indiati, 2012). The initial disease symptom develops from the upper side of the leaves with white floury patches, then changes to brown. This disease

e-ISSN: 2231-8542

causes significant yield and quality losses in several important crops, including legumes such as peas and mung beans (Pandey et al., 2018). Yield losses due to this disease have been reported up to 40% at the reproductive stages, but the damage can be more intense when the infection occurs at the seedling phase (Mishra et al., 2024). Currently, there are 55 superior mung bean cultivars have been released in Indonesia; however, no resistant cultivars against powdery mildew are available, although some cultivars showed their tolerance in the field. Screening approximately 4,000 mung bean accessions at the Asian Vegetable Research and Development Center (AVRDC) in Taiwan revealed that less than 12% exhibited resistance to powdery mildew, with only a small number classified as highly resistant over multiple years (Reddy et al., 1994). In Indonesia, several mung bean lines have been developed for their resistance against powdery mildew in the field using a naturally infected plant approach (Hapsari et al., 2018). In addition, resistance evaluation conducted under a controlled environment is needed to confirm repeatable and consistent results of the plant pathogen interaction analysis (Sillero et al., 2010). Until now, resistant assessments to powdery mildew infection in legumes under controlled conditions and certain qualitative scales are still limited.

Genetics and variability of mung bean resistance to powdery mildew have been studied (Kasettranan et al., 2009; Pavithra et al., 2023). However, there is limited information about the physiological and biochemical mechanisms of mung bean resistance to *Erysiphe polygoni*. During the pathogen infection, physiological, biochemical, and metabolites in plants are changed (Kaur, Bhardwaj, et al., 2022). The changes noted in plant reactions are greatly influenced by the plant's genotype, the specific pathogen involved, and the interplay between these elements. A study by Mohapatra et al. (2016) demonstrated that the levels of enzymes that scavenge reactive oxygen species (ROS), such as superoxide dismutase (SOD) and catalase, as well as the amounts of total phenols (TP) and malondialdehyde (MDA), increased in both resistant and susceptible plant genotypes after being infected with powdery mildew. In addition, research conducted by Soundhiriyan et al. (2018) found that susceptible genotypes impacted by powdery mildew showed higher levels of total phenols, proteins, and non-reducing sugars. Phenolic compounds play an important role as defense agents in plants (Kumar et al., 2020). They act as phytoalexins and phytoanticipins as well as perform structural defenses against pathogens that effectively inhibit microbial entry, restrict pathogen growth, and reduce oxidative stress caused by infections (Kaur, Samota, et al., 2022; Kumar et al., 2020). The production of phenolic compounds in plants is influenced by the activity of phenylalanine ammonia-lyase (PAL) (Barros & Dixon, 2020). Moreover, PAL plays a key role in activating the precursors needed for synthesizing lignin and salicylic acid (SA), both of which are essential for developing acquired systemic resistance (SAR) and act as a substrate for oxidative enzymes such as peroxidase and polyphenol oxidase (Ampofo & Ngadi, 2021; Wang et al., 2022). In this study, we observed the resistance of mung bean breeding lines from two different parents with different resistance to powdery

mildew, Vima 1 and Sampeong. Further analysis of the biochemical compounds present in infected plants and the relationship between these parameters and resistance to powdery mildew in mung beans was conducted.

MATERIALS AND METHODS

Plant Materials, Artificial Inoculation, and Disease Scoring

Ten mung bean breeding lines from nine generations (F9) with high productivity (> 2 t/ha) derived from the crossing of Sampeong and Vima 1 cultivars were assessed for screening against powdery mildew. The breeding lines and their parents were grown in pots (16 × 50 × 30 cm) filled with a mixture of soil and organic fertilizer (5:1 v/v) inside a greenhouse (8°02'50.0"S 12°37'31.7"E, 345 m above the sea level). The media was fertilized with the recommended dosage (12.5:25:0 NPK kg/ha). Each genotype was planted in triplicates. Artificial inoculation was conducted by harvesting *E. polygoni* conidia in distilled water using a fine brush and filtering to remove impurities. The inoculum was adjusted to 10^6 conidia/mL and Tween 20 (0.1 ml/100 ml solution) was added to the suspension. The suspension was then sprayed on the upper and lower leaf surfaces 14 days after sowing.

Disease Assessment and Evaluation of Growth and Yield Parameters

Disease assessment of powdery mildew was monitored a week after inoculation using rating scales of 0 to 5 as described by Reddy et al. (1994). Disease assessment was carried out by calculating the percentage of leaves impacted on a single plant. The number of samples used to observe disease progression, growth, and yield consisted of three plants per replication, resulting in a total of 9 plants for each genotype. Percent Disease Index (PDI) was calculated according to the following formula:

$$\text{PDI} = \frac{\text{Sum of grades}}{\text{Total number of leaves analyzed} \times \text{maximum disease grade}} \times 100$$

PDI was used to determine the resistance level of mung beans to powdery mildew. Genotypes with PDI = 0% were considered as immune (I), PDI = 1-30% was considered as Resistance (R), PDI = 31-50% was considered as Moderately Resistant (MR)/tolerant (T), and PDI > 51% was considered as Susceptible (S).

The area under the disease progress curve (AUDPC) was calculated for each genotype based on the standard scale's measurement of disease severity using the following formula:

$$AUDPC = \sum_{i=1}^{n-1} \left(\frac{y_i + y_{i+1}}{2}\right)(t_{i+1} - t_i)$$

Where y = disease severity, t = time (day), n= number of observations

Growth and yield parameters were determined per plant. The average plant height was determined 56 days after planting. Plant biomass (fresh weight/plant), and the average numbers of pods and grains were assessed at harvesting based on the genotype maturity.

Determination of Plant Defense-related Enzymes

Biochemical parameters of mung bean genotypes, including chlorophylls, Phenylalanine ammonia-lyase (PAL), Tyrosine ammonia-lyase (TAL), and total phenolic content, were measured 14 days after artificial infection. The treatments were performed in triplicate. The mung bean leaves were ground into a fine powder using a mortar and liquid nitrogen and then stored at -20°C for future research.

Chlorophyll Content

The amount of chlorophyll was measured by Lichtenthaler and Buschmann (2001). The 90% methanol (1:10 w/v) was used to extract 0.5 g of mung bean leaves, which was used to further dilute the samples (1:5 v/v). At 470 nm, 652.4 nm, and 665.2 nm, three distinct wavelengths were used to measure the absorbance values. The following equations were used to determine the concentrations of carotenoid and chlorophyll:

$$Chlorophyll\ a\ [Ch\ a](\mu g\ ml^{-1}) = (16.82 \times Abs_{665.2}) - (9.16 \times Abs_{652.4})$$

$$Chlorophyll\ b\ [Ch\ b](\mu g\ ml^{-1}) = (34.92 \times Abs_{652.4}) - (16.54 \times Abs_{665.2})$$

Phenylalanine and Tyrosine Ammonia-Lyase Activities

PAL and TAL activities were determined according to Dogbo et al. (2012). Mung bean leaves (0.5 g) were extracted with 0.1 M borate buffer (pH 8.8) (1:10. v/v). Following centrifugation, 3.5 mL of distilled water, 30 mM L-phenylalanine, and 300 mM sodium borate were combined with the supernatant. L-tyrosine was used in place of L-phenylalanine for the TAL assay. After 60 minutes of incubation at 30 °C, the absorbance values were then measured at 290 nm and 330 nm, respectively. The amount of coumaric acid for TAL and cinnamic acid for PAL produced per gram of fresh tissue per hour was used to measure the enzyme activities.

Total Phenolic and Flavonoids Content

The ground samples (0.5 g) were extracted with 80% methanol (1:10 w/v). The mung bean extract was then diluted in distilled water (1:60 v/v) and mixed with 250 µL Folin Ciocalteu's reagent, 750 µL sodium carbonate, and distilled water. The mixture was then incubated for 90 minutes, and the total phenolic content was measured at 765 nm (Yusnawan et al., 2021). The phenolic content was expressed as milligrams of gallic acid equivalents per gram of sample (mg GAE/g sample).

Total flavonoid was measured according to a method by Lee et al. (2011). As many as 2500 µL of distilled water and 15 µL $NaNO_2$ 5% were used to react with the mung bean extract. After six minutes of incubation, 300 µL of 10% AlCl3 was added to the mixture. Following the addition of 1000 µL of 1 M NaOH and 550 µL, the total flavonoid content was determined at 513 nm.

Statistical Analysis

Statistical analysis of the data was subjected to ANOVA using the R Studio software (R v.4.2.2), and mean values were separated by the LSD at a probability level of 0.05%. The correlation matrix and the principal component analysis (PCA) were also made using R Studio software.

RESULTS AND DISCUSSION

Disease Symptoms and Severity

The first signs of infected mung beans were white, powder-like spores on the upper surface of the leaves, which grew and spread to cover the entire leaf surface (Figure 1b-d). Under a light microscope, the type of conidial formation (single or chain) as well as the presence of fibrosin bodies could be observed on fresh leaves (Figure 1d). Mycelia were formed on the young plants within two weeks after planting. In heavy infections, mycelia covered most of the leaf surface and stems up to 100%. This led to significant photosynthetic area reduction, thereby causing leaf drying and early leaf fall. The development of disease symptoms varied among genotypes. Several genotypes performed a very low percentage of infected leaf area (Figure 1a), while moderately resistant genotypes limited the pathogen growth on the lower leaves and performed hypersensitive reactions and necrotic symptoms (Figure 1b). Meanwhile, on the susceptible genotypes, leaves were covered by powdery mildew blotches (Figure 1c).

The resistance to powdery mildew on mung bean was expressed by a low score of disease severity and prolonged the augmentation of disease incidence. Different genotypes responded differently to powdery mildew infection. In greenhouse conditions, initial disease symptoms appeared in the early stages of the vegetative phase at 14 DAP and developed in the older plants until they reached maturity. During this period, disease progress was recorded at weekly intervals (Table 1). From the initial observation, several genotypes, such as G1, G2, G4, G7, and G9, showed high disease severity. Another genotype of the G6 showed low severity at the beginning (1.1%), but it rose to 77.8% at 56 DAP. Only G5 and G8 exhibited low infection rates that were comparatively stable. Meanwhile, G2 and G3 performed high disease severity at the first rating and the severity rose to 87.2% in the G2 and only 52.8% in the G3 at 49 DAP.

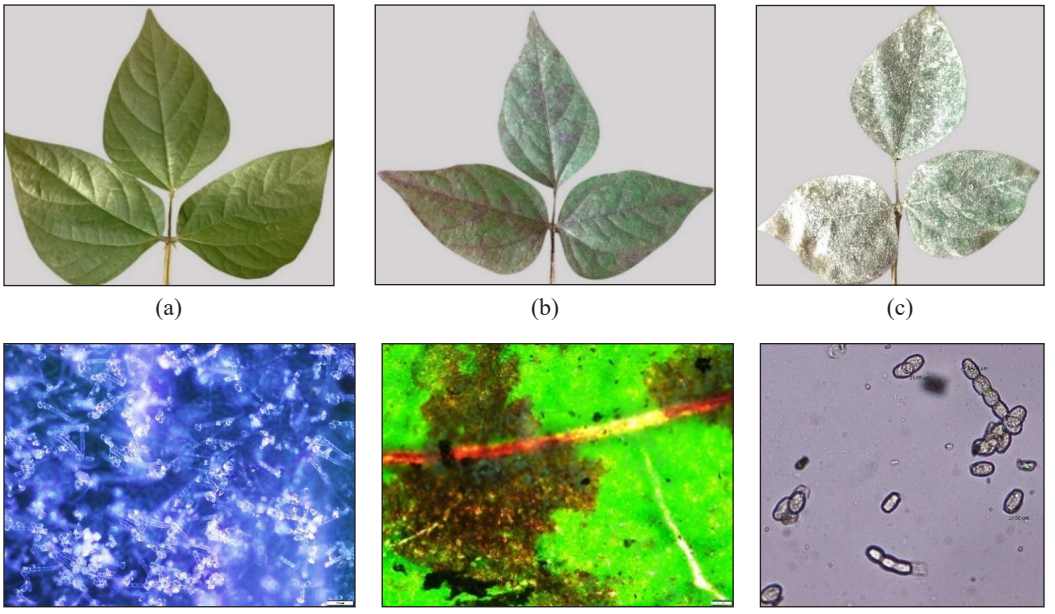

Figure 1. Mung bean leaves infected by powdery mildew: (a) No symptom; (b) moderate intensity; (c) and leaves covered by powdery mildew on susceptible genotypes; (d) micrographs of the powdery mildew fungi on the mung bean upper leaves; (e) hypersensitive reaction; (f) and chain of conidia

Table 1
Disease progress and resistant criteria of mung bean genotypes to powdery mildew

Genotypes	Disease Severity (%) 21 DAP	Disease Severity (%) 49 DAP	AUDPC	PDI	Resistant Criteria
G1	3.6 ± 1.3 ^{ab}	68.9 ± 7.6 $^{a-d}$	228.7 ± 33.4 $^{a-d}$	74.07	S
G2	4.6 ± 0.5 ^{a}	87.2 ± 5.2 ^{a}	289.3 ± 40.4 ^{a}	92.59	S
G3	4.8 ± 1.5 ^{a}	52.8 ± 9.8 $^{b-e}$	168.0 ± 26.3 $^{b-e}$	59.26	S
G4	2.6 ± 1.3 ^{ab}	73.3 ± 1.3 ^{abc}	247.7 ± 30.1 ^{abc}	77.78	S
G5	1.4 ± 0.8 ^{b}	43.3 ± 6.1 ^{cde}	146.6 ± 54.2 ^{cde}	48.15	MR
G6	1.1 ± 0.8 ^{b}	77.8 ± 2.1 ^{ab}	268.3 ± 41.8 ^{ab}	85.19	S
G7	4.4 ± 1.1 ^{a}	63.9 ± 6.7 $^{a-d}$	208.1 ± 51.9 $^{a-e}$	74.07	S
G8	1.2 ± 0.6 ^{b}	50.0 ± 8.3^{b-e}	170.7 ± 33.2 $^{b-e}$	59.26	S
G9	3.8 ± 1.1 ^{ab}	78.3 ± 2.3 ^{ab}	260.9 ± 38.2 ^{ab}	88.89	S
G10	2.8 ± 0.4 ^{ab}	42.2 ± 2.6 ^{de}	138.1 ± 43.7 ^{de}	48.15	MR
Vima 1	1.3 ± 0.8 ^{b}	51.7 ± 5.9 $^{b-e}$	176.2 ± 51.6 $^{b-e}$	55.56	S
Sampeong	1.6 ± 0.4 ^{b}	31.7 ± 6.4 ^{e}	105.4 ± 37.1 ^{e}	40.74	MR

Note. DAP = day after planting, AUDPC = area under the disease progress curve, PDI = percent disease index, S= Susceptible, MR = Moderately resistance. Values followed by the same letter within a column are not significantly different according to the Least Significant Difference (LSD) test ($p \leq 0.05$)

Based on the PDI analysis, none of the twelve mung bean genotypes exhibited resistance to powdery mildew. Three genotypes, namely Sampeong, G10, and G5 were classified as moderately resistant (MR). In contrast, the other nine genotypes were considered susceptible, showing PDI values higher than 50%. Moderately resistant genotypes showed chlorotic, limited sporulation, and exhibited a hypersensitive response. In the field tests, the Vima 1 cultivar was categorized as resistant to powdery mildew. However, when this cultivar was exposed to extremely high levels of stress in the greenhouse, the severity level rose to 51.7%, suggesting that this cultivar was susceptible. Meanwhile, the performance of the Sampeong cultivar against powdery mildew in this study was confirmed as moderately resistant, which was consistent with cultivar descriptions.

There were significant differences among the genotypes based on AUDPC values as shown in Table 1. The AUDPC values ranged from 105.39 to 334.40. Five genotypes (G1, G4, G6, G7, G9) had high AUDPC values as G2 genotypes, while low AUDPC values were observed in G3, G5, G7, G8, G10, Vima and Sampeong. At initial observation, five genotypes, including G5, G6, G8, Vima 1, and Sampeong, had disease severity lower than 2%. However, subsequent disease progression varied among genotypes. For instance, G6 disease severity was initially observed to be relatively low, but then disease progression increased rapidly, as indicated by a high AUDPC value. On the other hand, G3 was initially a relatively high severity, but subsequent observations revealed that the AUDPC value was comparatively low. This study showed that the crossing between Vima 1 and Sampeong, which was expected to inherit resistance traits, was not successful due to the new breeding lines being susceptible to powdery mildew.

Research by Rana et al. (2023) reported that resistance to powdery mildew in legumes was hereditary and could be passed down through hybridization. Variations in resistant responses to pathogens might arise from several factors, including environmental influences, durability of resistance, and pathogen virulence (Mundt, 2014). Notably, the powdery mildew observed in this study might be attributed to a new species or more aggressive populations of the pathogens. Kelly et al. (2021) reported that mung beans infected by two distinct pathogens, *Podosphaera xanthii* and *Erysiphe vignae*, exhibited similar symptoms but could only be differentiated through molecular methods. These two pathogens had not been reported to infect mung bean plants in Indonesia. Therefore, precise identification of the pathogens responsible for powdery mildew in Indonesia is essential. Unfortunately, molecular study related to the causal agents of the powdery mildew was not performed in this study. Furthermore, Sulima and Zhukov (2022) highlighted that even the strongest natural resistance to date is not universal, and previously effective alleles may lose their effectiveness against newly emerging pathogens, making taxonomic ambiguity and difficulties in identifying powdery mildew increasingly significant barriers for researchers and breeders.

Growth Performance and Yield

Powdery mildew affected the growth performance and yield of mung bean. There were significant differences among genotypes in terms of plant height and biomass as well as yield components (Table 2). Sampeong cultivar showed the highest plant height (68.0 ± 3.3 cm) and the lowest plant height was noted in G5 (37.1 ± 3.0 cm), G8 (38.0 ± 3.2 cm), G4 (40.0 ± 2.2 cm), Vima 1 (39.0 ± 1.5 cm), and G1 (41.0 ± 1.7 cm). However, plant height was dominantly affected by plant genetics rather than disease development. Disease severity was negatively correlated with plant biomass and yield. Powdery mildew, which infected from vegetative growth affecting generative growth, disrupting leaf development and causing premature defoliation. Consequently, the flowering process, formation, and pod filling were also affected. The highest yields were produced by G3 (15.6 ± 1.9 g), G5 (15.0 ± 6.5 g), G7 (14.9 ± 1.6 g), G8 (13.4 ± 0.9 g), G1 (13.4 ± 1.3 g), and Vima 1 (11.3 ± 0.2 g) genotypes, respectively. Meanwhile, the lowest yields were observed in Sampeong (7.6 ± 3.8 g), G4 (7.3 ± 1.8 g), G6 (8.8 ±6.7 g), G9 (9.4 ± 2.7 g), G10 (9.7 ± 0.6 g), and Vima 1 (11.3 ± 0.2 g) genotypes, respectively.

Powdery mildew infection also affected the yield quality as expressed by a reduced number of filling pods and seed weight as well as an increased number of empty or abnormal pods. The number of intact pods varied between 3.2 pods per plant (G10 genotype) and 7.6 ± 2.4 pods (G7 genotype). Although plant resistance did not directly influence the yield, low disease resistance affected the production of bean pods below their potential production (Basavaraja et al., 2020).

Table 2
Growth performance and yield components of mung bean genotypes infected by powdery mildew

Genotype	Plant height (cm)	Biomass (g)	Grain (g plant^{-1})	Number of Intact Pods per plant	Number of Empty Pods per plant
G1	41.0 ± 1.7 $^{d-g}$	69. 6 ± 5.5 ^{b}	13.4 ± 1.3 $^{a-d}$	6.7 ± 2.3 ^{ab}	3.9 ± 1.4 $^{a-d}$
G2	43.0 ± 3.5 $^{c-f}$	51.1 ± 5.0 ^{e}	14.1 ± 1.4 ^{abc}	5.3 ± 0.6 ^{abc}	5.4 ± 0.8 ^{ab}
G3	45.0 ± 4.2 ^{cd}	66.9 ± 1.1 ^{b}	15.6 ± 1.9 ^{a}	6.2 ± 2.0 ^{abc}	4.3 ± 2.0 ^{abc}
G4	40.0 ± 2.2 ^{efg}	55.8 ± 2.6 ^{de}	8.3 ± 1.9 ^{def}	4.0 ± 2.4 ^{bc}	5.7 ± 1.8 ^{a}
G5	37.1 ± 3.0 ^{g}	63.9 ± 2.4 ^{bc}	15.0 ± 6.5 ^{a}	5.1 ± 2.7 ^{abc}	3.9 ± 1.2 $^{a-d}$
G6	43.4 ± 4.9 $^{c-f}$	55.4 ± 6.7 ^{de}	8.8 ±6.7 $^{c-f}$	4.4 ± 2.9 ^{abc}	3.1 ± 2.7 ^{bcd}
G7	52.1 ± 2.3 ^{b}	90.2 ± 2.4 ^{a}	14.9 ± 1.6 ^{ab}	7.6 ± 2.4 ^{a}	1.8 ± 0.7 ^{d}
G8	38.0 ± 3.2 ^{g}	53.2 ± 5.7 ^{de}	13.4 ± 0.9 $^{a-d}$	5.3 ± 3.2 ^{abc}	3.3 ± 2.0 $^{a-d}$
G9	43.6 ± 2.6 ^{cde}	56.9 ± 2.7 ^{cde}	9.4 ± 2.7 $^{c-f}$	4.2 ± 1.9 ^{bc}	4.9 ± 1.4 ^{abc}
G10	47.4 ± 2.5 ^{bc}	53.3 ± 4.7 ^{de}	9.7 ± 0.6 $^{b-f}$	3.2 ± 0.8 ^{abc}	4.9 ± 0.5 ^{abc}
Vima 1	39.0 ± 1.5 ^{fg}	58.5 ± 2.5 ^{cd}	11.3 ± 0.2 $^{a-f}$	5.6 ± 2.1 ^{abc}	4.7 ± 1.2 ^{abc}
Sampeong	68.0 ± 3.3 ^{a}	86.5 ± 4.7 ^{a}	8.0 ± 4.1 ^{ef}	6.2 ± 2.2 ^{abc}	3.3 ± 1.9 $^{a-d}$

Note. Values followed by the same letter within a column are not significantly different based on the Least Significant Difference (LSD) test ($p < 0.05$)

Effect of Powdery Mildew Infections on Plant Pigments and Defence-related Enzymes

The chlorophyll content in mung bean plants infected with powdery mildew varied among different genotypes (Figure 2). The total pigments were from 0.73 µg g^{-1} (G10 genotype) to 1.33 mg g^{-1} (G7 genotype). Recent findings indicated that the correlation between chlorophyll content and the severity of powdery mildew in mung beans depended on genotypes. Some genotypes with lower disease severity, such as G4, G6, and G9 genotypes, exhibited higher chlorophyll levels compared to the G10 and Sampeong cultivars, which had relatively lower AUDPC values and disease severity. Conversely, G1, G2, and G7

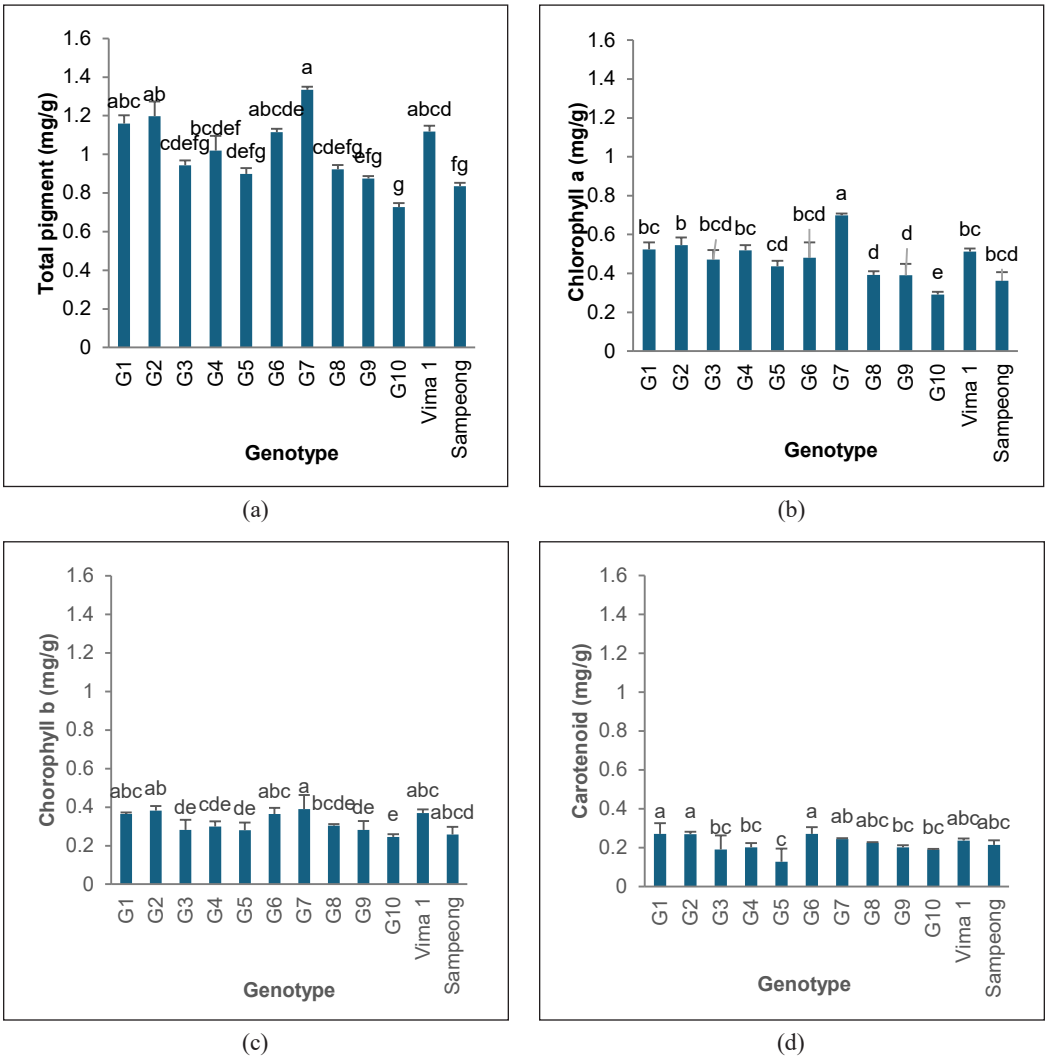

Figure 2. Mung bean genotypes infected by powdery mildew: (a) Total pigment; (b) chlorophyll a concentration; (c) chlorophyll b concentration; and (d) carotenoid

genotypes, which showed moderate disease severity and higher AUDPC values, also showed elevated chlorophyll content. Research conducted by Alwutayd et al. (2023) showed negative correlations between the severity of powdery mildew and the levels of chlorophylls a, b, and carotenoids in wheat. However, another study by Lobato et al. (2010) revealed that *Colletotrichum lindemuthianum* infection did not affect the contents of chlorophylls a and b in bean leaves. These findings suggested that both the type of pathogen and the plant species could influence chlorophyll levels in leaves.

Biochemical analyses showed that the enzyme activities associated with the defense mechanism varied among different genotypes. This study demonstrated a positive correlation between PAL and TAL activities in mung bean genotypes during powdery mildew infection. The concentration of PAL in the infected mung bean genotypes was higher than that of TAL. The G3 genotype exhibited relatively high activities for both enzymes, measuring 17.6 ± 0.4 mmol/g/FW/h for PAL and 9.5 ± 0.1 mmol/g/FW/h for TAL (Figure 3). Conversely, relatively low accumulation of PAL was observed in the G9 (12.1 ± 0.05 mmol/g/FW/h) and relatively low TAL activity was observed in the G6 (0.52 ± 0.06 mmol/g/FW/h). Phenylalanine ammonia-lyase and tyrosine ammonia-lyase are two critical enzymes involved in the pentose phosphate pathway (PPP). These two enzymes are essential for synthesizing defense-related secondary metabolites (Barros & Dixon, 2020). Both PAL and TAL can be induced in response to pathogen infections, and their coordinated activity can significantly enhance plant resistance to pathogens (Wang et al., 2022).

An assessment was conducted to determine whether variations in PAL and TAL activities correlated with the resistance of mung bean genotypes to powdery mildew. The

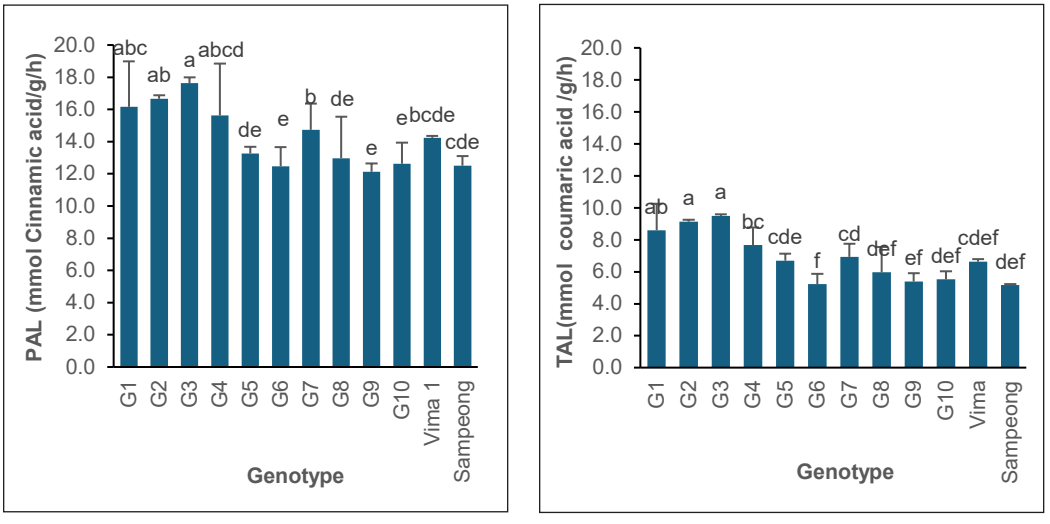

(a) (b)

Figure 3. Mung bean genotypes in response to powdery mildew infection: (a) Phenylalanine ammonia-lyase; (b) and Tyrosine ammonia-lyase

study found a dynamic relationship between PAL and TAL activities and the resistance of mung bean genotypes to powdery mildew. This was shown by disease severity and AUDPC values. Most genotypes with severe powdery mildew infections and high AUDPC values exhibited significantly high PAL and TAL activities. High levels of phenylalanine ammonia lyase (PAL) and tyrosine ammonia lyase (TAL) are typically associated with plant defense mechanisms; however, their relationship with increased disease occurrence indicates potential complex regulatory or mechanistic imbalances. These may arise from temporal discrepancies in the timing of defense activation (Boonchitsirikul et al., 1998), disrupting in metabolic channeling (Jun et al., 2018), and pathogen-derived counter-defense strategies (Kunkel & Brooks, 2002). In such cases, delayed activation of defense enzymes may allow pathogens to establish infections prior to the full mobilization of host defenses, potentially inhibiting downstream defense signaling pathways despite elevated PAL/TAL activity. Ten of the twelve genotypes showed a positive correlation between PAL and TAL activities with disease severity. The G3 genotype demonstrated low disease severity and slow disease progression but maintained high PAL and TAL activities. In contrast, G9 showed low PAL and TAL activities despite being severely infected by the pathogen. These results suggested that genotypes played a crucial role in the accumulation of PAL and TAL. Previous research by Mahatma et al. (2021) highlighted variations in PAL and TAL activities between resistant and susceptible groundnut genotypes during *Alternaria* leaf blight infection. Similar findings in PAL and TAL variants were observed in barley infected by stripe rust (Singla et al., 2020) and pepper infected by viruses (Sran et al., 2023).

Powdery mildew infection led to an increase in the total phenolic content (TPC) of mung bean genotypes. There was a significant variation in TPC among mung bean genotypes infected by powdery mildew (Figure 4a). The total phenolic content in the mung bean genotypes ranged from 0.84 mg GAE g^{-1} to 1.88 mg GAE g^{-1}, with the highest levels observed in the G1 genotype and the lowest in the G5 genotype. Elevated total phenolic accumulation in mung bean genotypes that were severely infected by the necrotrophic pathogen *Erysiphe polygonii* represented a plant response to suppressing the pathogen development. The stimulation of phenolic compounds was directly triggered when plants recognize the potential pathogens, and it was interconnected with disease resistance against fungal plant pathogens (Kaur, Samota, et al., 2022).

Our study showed that high phenolic accumulation was not consistently related to suppressing the development of powdery mildew disease as indicated by high AUDPC values. On the other hand, low phenolic accumulation in genotypes with low disease incidence was also observed. This was possibly due to reprogramming of the phenylpropanoid pathway to accumulate certain phenolic compounds. Differences in phenolic accumulation in plants can be influenced by plant genotype. As reported by Ampofo and Ngadi (2021), common beans (*Phaseolus vulgaris*) had variations in phenolic

concentration depending on the cultivar and growing conditions. Different plant genotypes could affect the phenolic content in leaves due to variations in gene expression involved in the biosynthesis of phenolic compounds. This variation caused differences in the quantity and quality of phenolic compounds produced (Yeluguri et al., 2022). The current study revealed that the highly infected genotype (G1 and G2) had higher total phenolic contents. On the other hand, G4 and G9 genotypes exhibited high disease severity and AUDPC values, but low accumulation of total phenolic contents. The G5 genotype showed both low AUDPC value and low total phenolic content.

In addition to TPC, changes in one of the polyphenolic groups, namely flavonoids, were also observed. The results showed that powdery mildew infection affected the total flavonoid contents in mung bean leaves (Figure 4b). High concentration of total flavonoids was observed in susceptible genotypes, G1 and G2, measuring approximately 1.36 ± 0.11 mg CE g^{-1} and 1.06 ± 0.02 mg CE g^{-1}, respectively. Conversely, low quantity of flavonoid content was observed in moderately resistant genotypes, G5 (0.59 ± 0.02 mg CE g^{-1}) and G10 (0.62 ± 0.01 mg CE g^{-1}). A similar genotype trend was also observed in total phenolic contents. Although in the Sampoeng cultivar which was also resistant, there was a positive correlation between TPC and flavonoids with the disease severity.

Several studies have documented higher levels of phenolic and flavonoid groups in resistant genotypes compared to susceptible ones during infections caused by foliar diseases (Ramaroson et al., 2022; Reddy et al., 1994; Soundhiriyan et al., 2018). The lower flavonoid and total phenolic contents in resistant genotypes compared to susceptible ones could be explained by the activation of efficient alternative defense mechanisms

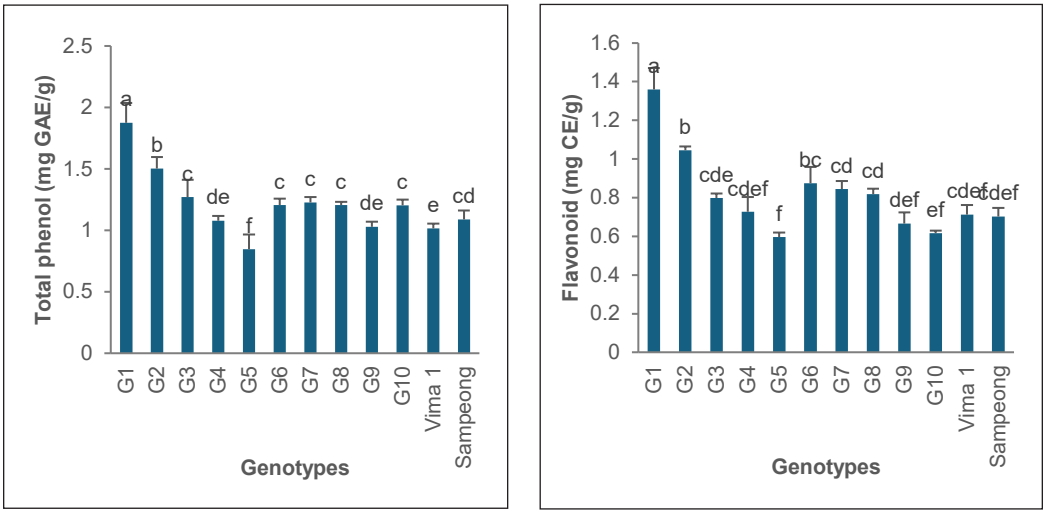

(a) (b)

Figure 4. Mung bean genotypes infected by powdery mildew: (a) Total phenolic contents; and (b) flavonoid contents

and rapid response strategies. The mechanism prioritized direct resistance rather than the accumulation of these compounds (Yeluguri et al., 2022). Flavonoids play a key role in defense mechanisms mainly through increased levels of protective compounds such as isoflavones and phytoalexins (Ramaroson et al., 2022).

Correlations Between Defense-Related Enzymes and Mung Bean Growth and Yield

A principal component analysis (PCA) and a correlation study on defense parameters and plant growth were carried out to determine the direct or indirect influence of the measured defense enzymes on plant growth and yield. Pearson's correlations showed that all defense parameters and plant pigments, namely PAL, TAL, phenolics, flavonoids, and chlorophyll content, had a positive correlation with the growth and yield of mung bean genotypes (Figure 5). The correlation analysis showed that flavonoids positively correlated with total phenolic content (r=0.89), PAL (r=0.56), and TAL (r=0.59). Furthermore, there were differences in the relationship between flavonoids and the severity of the disease, which were impacted by various factors such as plant species and genotypes. The current study showed that flavonoid accumulation in the G1 genotype was high, in line with disease severity and disease progress. In addition, several genotypes of G2, G3, G5, G7, G8, Vima 1, and Sampeong showed high flavonoid accumulation and low AUDPC values. Wang et al. (2022) stated that several flavonoids are classified as phytoalexins due to their accumulation in plant tissues upon pathogen infection; therefore, the increase in concentration triggers increasing plant resistance. Another similar study conducted by Steinkellner and Mammerler (2007) showed that a low increase in flavonoid concentrations exhibited antimicrobial properties against *Fusarium oxysporum* f. sp. *lycopersici*. Thus, it is also interesting to observe a comprehensive mechanism of genotypes with higher flavonoid and phenolic contents as well as higher PAL and TAL activities against powdery mildew infection.

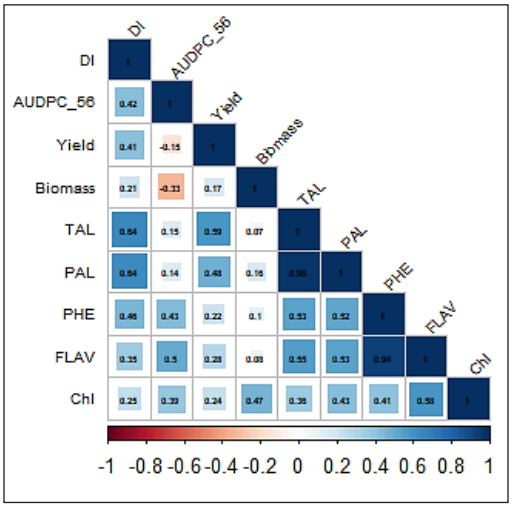

Figure 5. Matrix correlation of growth parameters yields and its related traits. IP: intact pods, FEN: total phenolic content, FLAV: total flavonoid content, PAL: PAL activity, TAL; TAL activity, AUDPC: AUDPC at 56 DAP

PAL was positively correlated with yield (r=0.62) and number of filled pods (r=0.52). However, there was no correlation with plant biomass. Apart from being reported to play an important role in plant resistance mechanisms, PAL also influenced

plant growth, such as the formation and development of roots and the addition of biomass (Cass et al., 2015). Total phenolic and flavonoid contents also play a crucial role in plant growth and development. A study conducted by Shen et al. (2022) revealed that flavonoids played essential roles in numerous biological processes, such as plant development, growth, and ripening. Another study by Tanase et al. (2019) highlighted the impact of several physiological processes involved in plant growth and development, including the synthesis of photosynthetic pigments, cell division, flower development, and seed germination. Interestingly, a positive correlation between chlorophyll content and the number of seeds (yield) as well as filled pods was observed. Chlorophylls play a crucial role in photosynthesis, which affects plant development and productivity. Surprisingly, severe powdery mildew infection on several mung bean genotypes had high chlorophyll content; however, it negatively affected the seed yield. This was in line with several previous studies, which stated that high chlorophyll contents did not correlate with high yields due to various physiological and environmental factors. These factors affected plant performance such as the allocation of energy and nutrient resources to produce defense compounds (Li et al., 2023).

Principal Component Analysis (PCA) was conducted on data related to mung bean growth and yield, disease severity, and the activity of defense-related enzymes (Figure 6a). The first principal component (PC1) accounted for 39.7% of the overall variation, with two variables linked to disease susceptibility, namely AUDPC and DI, showing significant contributions. The second principal component (PC2) explained 23.6% of the variation, with variables related to resistance mechanisms, such as TAL and PAL, exhibiting strong impacts on PC2.

The relationships among these four resistance-related variables indicated a positive correlation, suggesting that the activities of defense-related enzymes tent to increase simultaneously. In the PCA biplot, all mung bean genotypes were spread across all quadrants, revealing certain clustering patterns. In terms of resistance to powdery mildew, genotypes with elevated PC1 scores, such as G1 and G2, exhibited high DI and AUDPC values, suggesting a higher susceptibility to the disease. In contrast, genotypes such as Sampeong and G10, positioned far from the vectors related to disease and negatively correlated with PC1, were likely more resistant to powdery mildew.

The contributions of each variable to the PCA were shown in Figure 6b. Variables particularly TAL, FLAV, and plant height (PH) accounted for the most significant contributions (marked in red/orange) to Dimension 1 (Dim 1). PAL and FLAV notably influenced the positive direction of Dim 1, while biomass and plant height had a strong influence on its negative direction. These variables could serve as essential indicators for differentiating genotypes based on the growth characteristics and phytochemical contents. Variables such as the number of empty pods (EP; yellow color) showed moderate

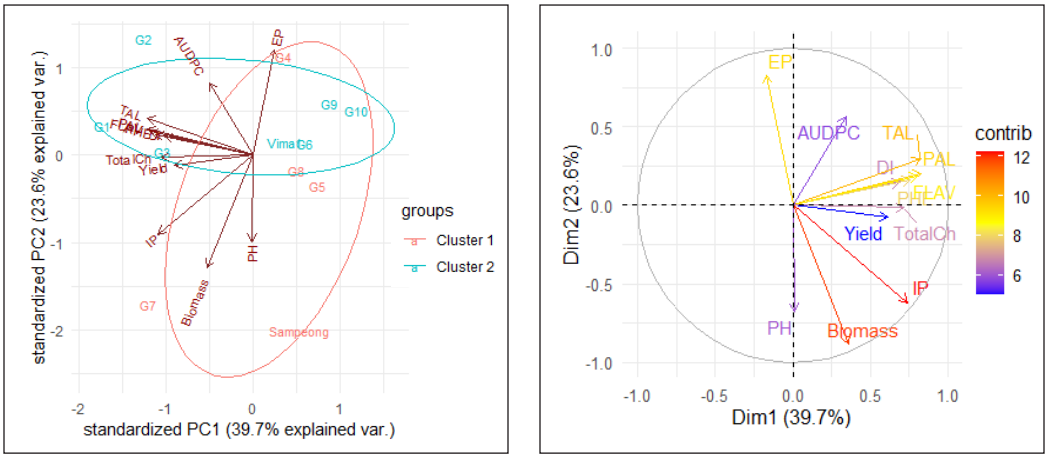

(a) (b)

Figure 6. (a) Principle component analysis (PCA); and (b) contributions of 12 trait measurement variables to the first 2 dimensions of the principal components analysis of mung bean leaves. The first dimension (Dim1) is composed primarily of biochemical traits related to mung bean resistant (PAL, TAL, PHE, FLAV), and the second dimension (Dim2) is composed primarily of resistant variables traits (AUDPC, DI). EP: empty pod; DI: disease incidence; Tot Ch: total chlorophyll, PH: plant height, IP: intact pods, FEN: total phenolic content, FLAV: total flavonoid content, PAL: PAL activity, TAL: TAL activity, AUDPC: AUDPC at 56 DAP

contributions, whereas yield (indicated in blue) had weaker contributions due to its negative correlation with Dimension 2 (Dim 2). The PCA revealed a distinct relationship between genotype traits and disease resistance. The clustering of genotypes based on PCA could be used in selecting superior varieties by considering both disease resistance and agronomic attributes such as yields.

Our research indicated that the resistance of mung beans to powdery mildew was affected by the physiological and biochemical states of the plants during the pathogen infection process. *Erysiphe polygoni*, a biotrophic pathogen, requires tissue penetration for survival and growth. Consequently, effective resistance strategies involve inhibiting the pathogen entry into the tissue through structural barriers such as lignin and the activation of systemic acquired resistance (SAR). Thus, the rapid accumulation of total phenolics at elevated levels is crucial for the resistance mechanism against powdery mildew. Genotypes that respond quickly to increased phenolic compounds exhibit greater resistance compared to those that respond slowly. Furthermore, a swift rise in PAL activity is essential since this enzyme is vital for initiating the synthesize of lignin and salicylic acid (SA). Both of which are critical for establishing acquired systemic resistance (SAR) and serve as substrates for oxidative enzymes such as peroxidase and polyphenol oxidase. Therefore, a breeding strategy can be implemented that focuses on selecting genotypes with inherent and swift induction of PAL/TAL expression following infection to guarantee prompt defense activation.

CONCLUSION

None of the genotypes from the Vima 1 and Sampeong cultivar progeny exhibited high resistance to powdery mildew disease. However, two selected genotypes of G10 and G5 were identified moderately resistance, suggesting some levels of defense capability against this pathogen. The PAL and TAL enzymes, along with the accumulation of total phenolics, were crucial components of the defense response in mung bean to powdery mildew infection. It was noteworthy that the effectiveness of these biochemical responses varied among different genotypes, highlighting the complexity of resistance mechanisms in mung beans. Based on our findings, it was suggested that the resistance mechanism in mung bean against powdery mildew primarily followed the phenylpropanoid pathway with the roles of PAL, TAL, and phenolic content. In addition, marker-assisted selection, particularly phenylpropanoid pathway genes may be taken into account for mung bean breeding resistance against powdery mildew.

ACKNOWLEDGMENT

The author would like to thank the Ministry of Agriculture of Indonesia for supporting the genetic materials and partially funding this research.

REFERENCES

Alwutayd, K. M., Esmail, S. M., Saad-El-Din, H. I., Abd El-moneim, D., & Draz, I. S. (2023). Metabolic and genotypic mechanisms involved in early defensive response of powdery mildew-infected wheat. *Physiological and Molecular Plant Pathology*, *126*, Article 102035. https://doi.org/10.1016/j.pmpp.2023.102035

Ampofo, J. O., & Ngadi, M. (2021). Stimulation of the phenylpropanoid pathway and antioxidant capacities by biotic and abiotic elicitation strategies in common bean (*Phaseolus vulgaris*) sprouts. *Process Biochemistry*, *100*, 98-106. https://doi.org/10.1016/j.procbio.2020.09.027

Barros, J., & Dixon, R. A. (2020). Plant phenylalanine/tyrosine ammonia-lyases. *Trends in Plant Science*, *25*(1), 66-79. https://doi.org/10.1016/j.tplants.2019.09.011

Basavaraja, T., Pratap, A., Dubey, V., Gurumurthy, S., Gupta, S., & Singh, N. P. (2020). Molecular and conventional breeding strategies for improving biotic stress resistance in common bean. In S. S. Gosal & S. H. Wani (Eds.), *Accelerated Plant Breeding, Volume 3: Food Legumes* (pp. 389-421). Springer. https://doi.org/10.1007/978-3-030-47306-8_13

Boonchitsirikul, C., Wasano, K., & Nose, A. (1998). Activities of Phenylalanine Ammonia-lyase (PAL) and Tyrosine Ammonia-lyase (TAL) in young rice panicles inoculated with *Pyricularia grisea*. *Japanese Journal of Tropical Agriculture*, *42*(1), 39-45. https://doi.org/10.11248/jsta1957.42.39

Cass, C. L., Peraldi, A., Dowd, P. F., Mottiar, Y., Santoro, N., Karlen, S. D., Bukhman, Y. V., Foster, C. E., Thrower, N., Bruno, L. C., Moskvin, O. V., Johnson, E. T., Willhoit, M. E., Phutane, M., Ralph, J., Mansfield, S. D., Nicholson, P., & Sedbrook, J. C. (2015). Effects of *phenylalanine ammonia lyase* (PAL)

knockdown on cell wall composition, biomass digestibility, and biotic and abiotic stress responses in *Brachypodium*. *Journal of Experimental Botany*, *66*(14), 4317-4335. https://doi.org/10.1093/jxb/erv269

Dogbo, D. O., Gogbeu, S. J., N'zue, B., Ya, K. A., Zohouri, G. P., Mamyrbekova-Bekro, J. A., & Bekro, Y. A. (2012). Comparative activities of phenylalanine ammonia-lyase and tyrosine ammonia-lyase and phenolic compounds accumulated in cassava elicited cell. *African Crop Science Journal*, *20*(2), 85-94.

Hapsari, R. T., Trustinah, & Iswanto, R. (2018). Diversity of local Indonesian mung bean germplasm based on morphological quantitative and qualitative traits. *IOP Conference Series: Earth and Environmental Science, 197*, Article 012036. https://doi.org/10.1088/1755-1315/197/1/012036

Indiati, S. W. (2012). Pengaruh insektisida nabati dan kimia terhadap hama thrips dan hasil kacang hijau [The effect of botanical and chemical insecticides on thrips pests and mung bean yield] . *Jurnal Penelitian Pertanian Tanaman Pangan*, *31*(3), 152-157.

Jun, S. Y., Sattler, S. A., Cortez, G. S., Vermerris, W., Sattler, S. E., & Kang, C. (2018). Biochemical and structural analysis of substrate specificity of a phenylalanine ammonia-lyase. *Plant Physiology*, *176*(2), 1452-1468. https://doi.org/10.1104/pp.17.01608

Kasettranan, W., Somta, P., & Srinives, P. (2009). Genetics of the resistance to powdery mildew disease in mung bean (*Vigna radiata* (L.) Wilczek). *Journal of crop science and biotechnology*, *12*, 37-42.

Kaur, S., Bhardwaj, R. D., Kaur, J., & Kaur, S. (2022). Induction of defense-related enzymes and pathogenesis-related proteins impart resistance to barley genotypes against spot blotch disease. *Journal of Plant Growth Regulation, 41*, 682-696. https://doi.org/10.1007/s00344-021-10333-2

Kaur, S., Samota, M. K., Choudhary, M., Choudhary, M., Pandey, A. K., Sharma, A., & Thakur, J. (2022). How do plants defend themselves against pathogens-Biochemical mechanisms and genetic interventions. *Physiology and Molecular Biology of Plants*, *28*(2), 485-504. https://doi.org/10.1007/s12298-022-01146-y

Kelly, L. A., Vaghefi, N., Bransgrove, K., Fechner, N. A., Stuart, K., Pandey, A. K., Sharma, M., Németh, M. Z., Liu, S.-Y., Tang, S.-R., Nair, R. M., Douglas, C. A., & Kiss, L. (2021). One crop disease, how many pathogens? *Podosphaera* xanthii and *Erysiphe vignae* sp. nov. identified as the two species that cause powdery mildew of mung bean (*Vigna radiata*) and black gram (*V. mungo*) in Australia. *Phytopathology®*, *111*(7), 1193-1206. https://doi.org/10.1094/PHYTO-12-20-0554-R

Kumar, S., Abedin, M. M., Singh, A. K., & Das, S. (2020). Role of phenolic compounds in plant-defensive mechanisms. *Plant Phenolics in Sustainable Agriculture* (Vol. 1, pp. 517-532). Springer. https://doi.org/10.1007/978-981-15-4890-1_22

Kunkel, B. N., & Brooks, D. M. (2002). Cross talk between signaling pathways in pathogen defense. *Current Opinion in Plant Biology*, *5*(4), 325-331. https://doi.org/10.1016/S1369-5266(02)00275-3

Lee, J. H., Jeon, J. K., Kim, S. G., Kim, S. H., Chun, T., & Imm, J.-Y. (2011). Comparative analyses of total phenols, flavonoids, saponins and antioxidant activity in yellow soybeans and mung beans. *International Journal of Food Science and Technology*, *46*(12), 2513-2519. https://doi.org/10.1111/j.1365-2621.2011.02775.x

Li, D., Wu, X., Huang, C., Lin, Q., Wang, Y., Yang, X., Wang, C., Xuan, Y., Wei, S., & Mei Q. (2023). Enhanced rice resistance to sheath blight through *nitrate transporter 1.1B* mutation without yield loss under NH4+

fertilization. *Journal of Agricultural and Food Chemistry, 71*(50), 19958-19969. https://doi.org/10.1021/acs.jafc.3c05350

Lichtenthaler, H. K., & Buschmann, C. (2001). Extraction of photosynthetic tissues: chlorophylls and carotenoids. *Current Protocols in Food Analytical Chemistry*, *1*(1), F4.2.1-F4.2.6. https://doi.org/10.1002/0471142913.faf0402s01

Lobato, A. K. S., Gonçalves-Vidigal, M. C., Vidigal Filho, P. S., Andrade, C. A. B., Kvitschal, M. V., & Bonato, C. M. (2010). Relationships between leaf pigments and photosynthesis in common bean plants infected by anthracnose. *New Zealand Journal of Crop and Horticultural Science*, *38*(1), 29-37. https://doi.org/10.1080/01140671003619308

Mahatma, M. K., Thawait, L. K., Jadon, K. S., Thirumalaisamy, P. P., Bishi, S. K., Rathod, K. J., Verma, A., Kumar, N., & Golakiya, B. A. (2021). Metabolic profiling for dissection of late leaf spot disease resistance mechanism in groundnuts. *Physiology and Molecular Biology of Plants*, *27*(5), 1027-1041. https://doi.org/10.1007/s12298-021-00985-5

Mishra, G., Yadav, N., Manasa, L. S., Biswal, D. P., Rout, G. R., & Panigrahi, K. C. (2024). Chromium stress induced alterations in leaf physiology and morphology in mung bean (*Vigna radiata* L.). *Journal of Crop Health*, *76*(6), 1735-1744. https://doi.org/10.1007/s10343-024-01043-2

Mohapatra, C., Chand, R., Navathe, S., & Sharma, S. (2016). Histo-chemical and biochemical analysis reveals association of *er1* mediated powdery mildew resistance and redox balance in pea. *Plant Physiology and Biochemistry*, *106*, 54-63. https://doi.org/10.1016/j.plaphy.2016.04.035

Mundt, C. C. (2014). Durable resistance: A key to sustainable management of pathogens and pests. *Infection, Genetics and Evolution*, *27*, 446-455. https://doi.org/10.1016/j.meegid.2014.01.011

Pandey, A. K., Burlakoti, R. R., Kenyon, L., & Nair, R. M. (2018). Perspectives and challenges for sustainable management of fungal diseases of mungbean [*Vigna radiata* (L.) R. Wilczek var. radiata]: A review. *Frontiers in Environmental Science*, *6*, Article 53. https://doi.org/10.3389/fenvs.2018.00053

Pavithra, B. S., Behera, L., & Samal, K. C. (2023). Genetic diversity analysis and validation of microsatellite markers linked with tolerance to powdery mildew disease in mung bean [*Vigna radiata* (L.) Wilczek]. *Legume Research, 46*(12), 1658-1667. https://doi.org/10.18805/LR-4472

Ramaroson, M.-L., Koutouan, C., Helesbeux, J.-J., Le Clerc, V., Hamama, L., Geoffriau, E., & Briard, M. (2022). Role of phenylpropanoids and flavonoids in plant resistance to pests and diseases. *Molecules*, *27*(23), Article 8371. https://doi.org/10.3390/molecules27238371

Rana, C., Sharma, A., Rathour, R., Bansuli, Banyal, D. K., Rana, R. S., & Sharma, P. (2023). In vivo and in vitro validation of powdery mildew resistance in garden pea genotypes. *Scientific Reports*, *13*, Article 2243. https://doi.org/10.1038/s41598-023-28184-0

Reddy, K. S., Pawar, S. E., & Bhatia, C. R. (1994). Inheritance of powdery mildew (*Erysiphe polygoni* DC) resistance in mung bean (*Vigna radiata* L. Wilczek). *Theoretical and Applied Genetics*, *88*, 945-948. https://doi.org/10.1007/BF00220800

Shen, N., Wang, T., Gan, Q., Liu, S., Wang, L., & Jin, B. (2022). Plant flavonoids: Classification, distribution, biosynthesis, and antioxidant activity. *Food Chemistry*, *383*, Article 132531. https://doi.org/10.1016/j.foodchem.2022.132531

Sillero, J. C., Villegas-Fernández, A. M., Thomas, J., Rojas-Molina, M. M., Emeran, A. A., Fernández-Aparicio, M., & Rubiales, D. (2010). Faba bean breeding for disease resistance. *Field Crops Research, 115*(3), 297-307. https://doi.org/10.1016/j.fcr.2009.09.012

Singla, P., Bhardwaj, R. D., Kaur, S., & Kaur, J. (2020). Stripe rust induced defence mechanisms in the leaves of contrasting barley genotypes (*Hordeum vulgare* L.) at the seedling stage. *Protoplasma*, *257*, 169-181. https://doi.org/10.1007/s00709-019-01428-5

Soundhiriyan, P. V., Kamalakannan, A., Jeyakumar, P., Paranidharan, V., & Latha, T. K. S. (2018). Morphology and biochemical parameters associated with powdery mildew resistance in mungbean. *Green Farming*, *9*(4), 704-709.

Sran, T. S., Jindal, S. K., Sharma, A., & Chawla, N. (2023). Genetics of novel leaf curl virus disease resistant pepper genotypes and antioxidative profile analysis of their progenies. *Scientia Horticulturae*, *308*, Article 111563. https://doi.org/10.1016/j.scienta.2022.111563

Steinkellner, S., & Mammerler, R. (2007). Effect of flavonoids on the development of *Fusarium oxysporum f. sp. lycopersici*. *Journal of Plant Interactions*, *2*(1), 17-23. https://doi.org/10.1080/17429140701409352

Sulima, A. S., & Zhukov, V. A. (2022). War and peas: Molecular bases of resistance to powdery mildew in pea (*Pisum sativum* L.) and other legumes. *Plants*, *11*(3), Article 339. https://doi.org/10.3390/plants11030339

Tanase, C., Bujor, O.-C., & Popa, V. I. (2019). Phenolic natural compounds and their influence on physiological processes in plants. In R. R. Watson (Ed.), *Polyphenols in plants: Isolation, purification and extract preparation* (pp. 45-58). Academic Press. https://doi.org/10.1016/B978-0-12-813768-0.00003-7

Wang, L., Chen, M., Lam, P.-Y., Dini-Andreote, F., Dai, L., & Wei, Z. (2022). Multifaceted roles of flavonoids mediating plant-microbe interactions. *Microbiome*, *10*, Article 233. https://doi.org/10.1186/s40168-022-01420-x

Yeluguri, S., Tejaswini, P., Upreti, K. K., Sriram, S., Seetharamu, G. K., Devappa, V., & Mythili, J. B. (2022). Biochemical characterization of defense responses in rose genotypes in response to artificial inoculation with black spot pathogen *Diplocarpon rosae*. *Journal of Horticultural Sciences*, *17*(1), 209-219. https://doi.org/10.24154/jhs.v17i1.1027

Yusnawan, E., Inayati, A., & Baliadi, Y. (2021). Total phenolic content and antioxidant activity in eight cowpea (*Vigna unguiculata*) genotypes. *IOP Conference Series: Earth and Environmental Science, 924,* Article 012047. https://doi.org/10.1088/1755-1315/924/1/012047

Pertanika J. Trop. Agric. Sci. 48 (6): 1961 - 1981 (2025)

PERTANIKA JOURNALS

TROPICAL AGRICULTURAL SCIENCE

Journal homepage: http://www.pertanika.upm.edu.my/

An Assessment of Trace Metal Accumulation in the Fish Genus *Barbonymus* sp. from a Former Mining Lake in Kg. Gajah, Perak, Malaysia, and Its Potential Human Health Risk

Fathin Shakira Abdul Azhar[1], Nazatul Shima Azmi[1], Rohasliney Hashim[2], Ferdaus Mohamat-Yusuff[1], Mohamad Faiz Zainuddin[1], Ong Meng Chuan[3,4], and Zufarzaana Zulkeflee[1]*

[1]Department of Environmental Science and Technology, Faculty of Forestry and Environment, Universiti Putra Malaysia, 43400 UPM Serdang, Selangor, Malaysia
[2]Department of Environmental Management, Faculty of Forestry and Environment, Universiti Putra Malaysia, 43400 UPM Serdang, Selangor, Malaysia
[3]Faculty of Science and Marine Environment, Universiti Malaysia Terengganu, 21030 Kuala Nerus, Terengganu, Malaysia
[4]Ocean Pollution and Ecotoxicology (OPEC) Research Group, Universiti Malaysia Terengganu, 21030 Kuala Nerus, Terengganu, Malaysia

ABSTRACT

Ex-mining lakes are known to have elevated metal levels from past mining activities, thus, consuming fish originating from these lakes may pose potential health risks. The ability of fish to accumulate metals from the surrounding environment raised public concern about the health risks posed when consuming fish from former mining lakes. An investigation was carried out to quantify the concentrations of iron (Fe), zinc (Zn), and lead (Pb) in the water and organs (gills and muscle) of twenty *Barbonymus* sp. found in a former mining lake. Metal levels were measured using ICP-MS, and the results obtained were compared with their respective standards. A comparable Fe>Zn>Pb pattern was observed in the metal concentrations of both samples. Although the concentration of Pb in the water samples surpassed the limit of 0.166 mg/L, the levels of Fe and Zn were within the range set by the National Lake Water Quality Standards for Malaysia (NLWQS). The concentrations of iron in the fish muscles and gills are beyond the established thresholds set by the World Health Organisation (WHO) and Food and Agriculture Organisation (FAO). The concentration of Zn in the fish gills exceeded the FAO standard limit, and the levels of Pb in both organs exceeded the acceptable limits set

ARTICLE INFO

Article history:
Received: 06 February 2025
Accepted: 20 August 2025
Published: 25 November 2025

DOI: https://doi.org/10.47836/pjtas.48.6.16

E-mail addresses:
fathinshakira.aa@gmail.com (Fathin Shakira)
nazatulshimazmi@gmail.com (Nazatul Shima Azmi)
rohasliney@upm.edu.my (Rohasliney Hashim)
ferdius@upm.edu.my (Ferdaus Mohamat-Yusuff)
z_faiz@upm.edu.my (Mohamad Faiz Zainuddin)
ong@umt.edu.my (Ong Meng Chuan)
zufarzaana@upm.edu.my (Zufarzaana Zulkeflee)
* Corresponding author

by all regulations, including the Malaysian Food Act 1983 (MFA). Notably, the incremental life cancer risk (ILCR) for lead (Pb) was determined to be within the threshold limit, and the hazard index (HI) of consuming *Barbonymus* sp. is less than 1, thus indicating a low potential health risk.

Keywords: Bioaccumulation, cancer risk, freshwater fish, heavy metals, non-cancer risk, target hazard quotient

INTRODUCTION

The lakes in Sg. Galah, Kg. Gajah, Perak, Malaysia, are the result of tin ore mining operations that lasted until 1984. Mining activities resulted in the formation of nine interconnected man-made lakes that serve as habitats for various fish, aquatic plants, and organisms. The lakes are now used as a source of income for local inland fishermen. Fishermen rely on lake fish catches for food and income from selling the fish at markets or to fishmongers.

Correspondingly, former mining lakes pose a significant trace metal risk. The common trace metals linked to former mining water bodies are arsenic (As), iron (Fe), cadmium (Cd), chromium (Cr), copper (Cu), manganese (Mn), nickel (Ni), lead (Pb), and zinc (Zn) (Baharim et al., 2022; Pistelli et al., 2017). These trace metals, if present in high concentrations, may endanger human health either directly through ingestion or dermal contact with the water (Koki et al., 2018; Low et al., 2016; Medunić et al., 2019) or indirectly through the consumption of fish caught from the lakes that may have bioaccumulated the metals over time (Ashraf et al., 2012; Dalzochio et al., 2018; Saat et al., 2014). Aside from the common metals found in lakes due to mining operations, the lakes in the study area receive continuous metal input from agricultural activities in the surrounding areas (Kamari et al., 2017; Okereafor et al., 2020). Runoffs containing metal fertilisers and pesticide residues may increase metal contamination in lakes (Hembrom et al., 2019; Müller et al., 2020; Xie et al., 2016).

The assortment of macro and micronutrients that is present in fish renders it an indisputable protein source in a well-balanced human diet (Liu et al., 2020; Mishra et al., 2007; Tacon & Metian, 2013). Their ability to accumulate trace metals in their tissues, however, has sparked worldwide concern, and the health risk posed by eating fish has been called into question. The amount of trace metal accumulation in fish varies according to metal, fish species, and tissues of concern (Petrović et al., 2013). Sex, age, size, reproductive cycle, swimming habits, eating behaviour, and habitat quality are all other factors that influence metal uptake in fish.

Therefore, determining the levels of metal pollution in the ex-mining lake water and fish is critical in order to analyse bioaccumulation events and predict the potential human health risk caused by metal contamination, particularly to ensure food security when consuming fish.

The Cyprinidae family contains the most abundant genera and species of freshwater fish in Malaysia (Kamarudin & Esa, 2009). The genus *Barbonymus*, formerly referred to as *Barbus, Barbodes, Puntius*, or *Systomus*, can be classified into ten species: *B. altus, B. balleroides, B. collingwoodii, B. gonionotus, B. schawenfeldii, B. belinka, B. mahakkamensis, B. platysoma*, and *B. sunieri* (Batubara et al., 2021, Kottelat, 2013; Yang et al., 2012; Zheng et al., 2016). Two species, the *Barbonymus schawenfeldii* (tinfoil barb) and the *Barbonymus gonionotus* (Java barb), are frequently encountered in the freshwater ecology of Malaysia (Kusmini et al., 2021; Rashid, 2014). These species have been primary targets for inland fishers as food and ornamental fish due to the stunning colours of their caudal and ventral fins (Eslamloo et al., 2012; Isa et al., 2012; Muchlisin et al., 2015). The Malaysian Department of Fisheries (DOF, 2021) has confirmed that the total number of *Barbonymus* sp. landings, particularly in the public water bodies in Perak, exhibited an upward trend from 2013 to 2020, with a slight decrease in 2015. *Barbonymus* sp., or pointedly to river carp and Javanese carp, was discovered in more ex-mining lakes, lakes, and rivers in Perak alone in 2020 than in any other year before, with landings totalling up to 352.77 tonnes that year. The *Barbonymus* sp. was chosen for this study because of its large population and the local community's keen attention.

The objectives of this present study are to:

(i) quantify the concentrations of trace metals in the water of the lake and in the muscles and gills of *Barbonymus* sp., a regularly encountered fish species in this lake.

(ii) investigate the relationship between metal concentrations in water and fish.

(iii) compare metal concentrations in water to the National Lake Water Quality Standard (NLWQS) and in fish organs to the World Health Organisation (WHO), 2004, Food and Agriculture Organisation (FAO), 1983, and Malaysian Food Act (MFA), 1983.

(iv) utilising the incremental life cancer risk (ILCR) for prospective cancer effects and the hazard index (HI) for undesirable non-cancer effects to calculate the potential harm to human health. The results provide an initial assessment of the magnitude of trace metal contamination in the study region, as well as the possible risk to human health from fish ingestion.

MATERIALS AND METHODS

Sampling Location

Figure 1 depicts Sg. Galah, Kg. Gajah's public waters for inland fishermen, which consist of nine interconnected lakes (Lake A – Lake I). The Kinta River near Lakes B, H, and I supply the lakes' water through three culverts. However, due to a lack of management in the culvert areas, siltation, solid debris, and invasive macrophyte infestation significantly

restrict the flow of water entering and exiting the lakes. As a result, except during river flooding, which occurs once a year during an extraordinarily high rain event, the water within the lakes is circulated between them. Furthermore, in recent years, the invasion of invasive macrophytes, particularly water hyacinth (*Pontederia crassipes*), has become more serious. This invasive weed covers 70% of the lake areas, preventing local inland fishermen from fishing. Lake B was the only one still open for fishing. Because the lakes are interconnected and have limited fishing access, this study assumes that one lake can serve as a representative of all lakes due to the natural migration of fish between them. Therefore, in this study, the sampling at Lake B is representative of all the lakes.

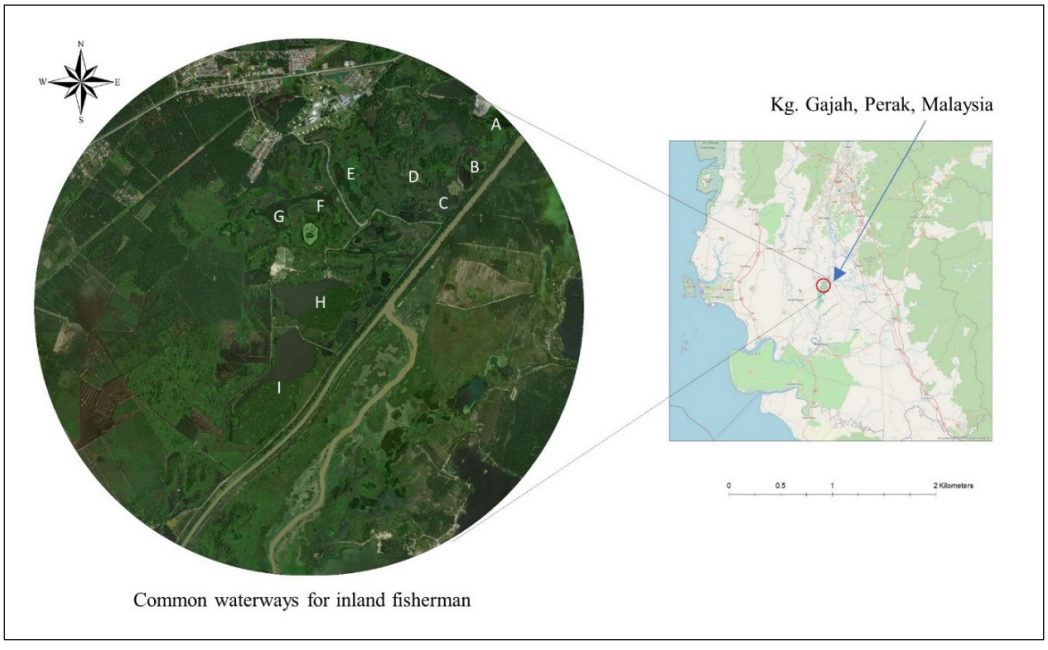

Figure 1. Ex-mining lakes of Sg. Galah, Kg. Gajah, Perak

Water Quality Determination and Water Sample Collection

Acid-washed bottles were used to collect water samples at three different locations, each representing Lake B's inlet, middle, and outlet. The samples were kept in a cool box at 4^{o}C until further analysis. These samples were stored at a pH level below 2 in order to minimise the incidence of precipitation, adsorption, or microbiological activity by the addition of nitric acid (HNO_3). The quality of the lake water was assessed using a handheld multiparameter instrument model 556 (YSI, USA) to measure in-situ water quality parameters such as pH, temperature, salinity, dissolved oxygen (DO), conductivity (EC), and total dissolved solids (TDS); turbidity was assessed using a turbidity meter model 2100P (HACH, USA).

Fish Sampling

Fish samples were collected using gill nets with the assistance of local inland fishermen, washed with distilled water, and placed in separate polyethylene bags. The fish were measured for length (mm) and weight (g), and fish with a similar average length and weight were collected. Uneven numbers of fish in each species prevented species-level identification. As a result, the fish samples will be reported as *Barbonymus* sp. samples. Around 20 fish samples were collected. All the samples were stored at -20 °C until they were further analysed.

Acid Digestion of the Water and Fish Samples

Prior to the analysis for trace metals using Inductively Coupled Plasma Mass Spectrometry (ICP-MS), both the fish and water samples underwent acid digestion (USEPA, 1991).

The water samples were allowed to evaporate up to one-fourth of their original volume after being boiled for 5-10 minutes on a hot plate through a 0.45 µm cellulose nitrate membrane filter. The samples were subsequently filled to a volume of 10 mL by washing the vials with a 2% HNO_3 solution to prevent any possibility of sample loss. The samples were then placed in a refrigerator for two weeks to allow the metals to stabilise. Trace metal concentrations were then analysed for Fe, Zn, and Pb in triplicate using ICP-MS (USEPA, 1991).

The fish samples were pre-treated by being washed in distilled water, and the muscle and liver were dried in an oven at 105^{o}C for 24 hours. The fish bones and scales were removed after drying, and the muscles and gills were collected. These fish parts were then ground separately with a mortar and pestle before being dried in a crucible and stored until further digestion.

Approximately 0.5 g of fish muscles and 0.2 g of fish gills, respectively, were added with 5 mL of HNO_3 and, correspondingly, subjected to heating on a hot plate within a digestive tube. The sample was then heated to 40^{o}C for one minute and then gradually heated to 100^{o}C for 10 minutes until it reached the maximum temperature of 140^{o}C. The digestion continued for 3 hours at a temperature of 140^{o}C. Before dilution with distilled water, the digested residues were cooled and then filtered into a 50 mL centrifuge tube using a 0.45 µm nylon syringe filter. The filtrates were then refrigerated before ICP-MS metal analysis of Fe, Zn, and Pb.

Trace Metal Analysis Using ICP-MS

The presence of trace metals Fe, Zn, and Pb in digested samples was determined using ICP-MS. The trace metal levels were given in mg/kg dry weight for the fish samples and mg/L for the water. The following standard concentrations were used: 10 ppb, 30 ppb, 50 ppb, 100 ppb, and 300 ppb to prepare the calibration curve.

The per cent recovery for the fish extraction was calculated using the Equation 1

$$Recovery\ (\%) = \left[\frac{x - y}{z}\right] \times 100 \quad [1]$$

Where x represents the average concentration of trace metal after a spike, y denotes the average concentration of trace metal before a spike, and z represents the concentration of trace metal that has been spiked.

The recovery percentages for Fe, Zn, and Pb were 81.8%, 82.8%, and 83.3%, respectively, which constituted acceptable results.

Analytical blanks, consisting of reagents without the sample matrix, were processed alongside the samples to monitor for potential contamination. Internal standards and calibration curves with $R^2 > 0.999$ were used for instrument validation.

Bioconcentration Factor and Health Risk Assessment

The ratio of the fish's steady-state metal ion concentrations to the concentration in the water is known as the bioconcentration factor (BCF). BCF values were measured according to Equation 2 proposed by Gobas et al., (2009):

$$BCF = \frac{Concentration\ \ of\ trace\ metal\ in\ fish\ (\frac{mg}{kg})}{Concentration\ \ of\ trace\ metal\ in\ water\ (\frac{mg}{L})} \quad [2]$$

The BCF values were calculated to demonstrate the possibility of metal uptake by the fish from the metal present in the lake water.

Finally, a health risk assessment was carried out. The potential health risks associated with fish eating were calculated by utilising the data on trace metal concentration in the fish and the anticipated consumption rate according to USEPA (2012) guidelines (Ashraf et al., 2012; Azmi et al., 2019). Therefore, the consumption rate is predicted based on the following assumptions:

- the ingestion rate (IR) of fish per day was 0.16 kg/day/person (FAO, 2009; Idriss & Ahmad, 2015).
- both men and women in Malaysia weigh an average of 62 kg for their adult body weight (BW) ((Ahmad et al., 2016)).
- bioavailability and maximum absorption rate are at 100%.

The Target Hazard Quotient (THQ) was determined for the non-carcinogenic risk using the Equation 3 (Khoshnood et al., 2014; Javed & Usmani, 2019):

$$Target\ Hazard\ Quotient\ (THQ) = \frac{EDI}{RfD} \quad [3]$$

To calculate the Estimated Daily Intake (EDI), the following equation (Equation 4) was used:

$$Estimated\ Daily\ Intake\ (EDI) = \frac{[EFr \times ED \times IR \times C]}{[BW \times AT]} \quad [4]$$

In the present study, the exposure frequency was set at 365 days per year and is denoted as EFr. According to USEPA (2012), the ED stands for the exposure duration, which is set at 70 years, to evaluate the impacts of the non-carcinogens. The IR represents the daily fish ingestion rate assumed to be 0.16 kg/day/person for Malaysians. The C represents the metal concentrations (mg/kg wet weight) in the muscles and gills of the fish samples. The average body weight (BW) for Malaysian adults was set at 65 kg. The averaging time (AT) for non-carcinogens was 365 days/year × ED. The oral reference dose (RfD) for each metal is expressed as mg/kg/day (Table 1).

From the THQ of each metal, the Hazard Index was determined using the Equation 5.

$$Hazard\ Index\ (HI) = \ sum\ of\ THQs\ of\ every\ metals \quad [5]$$

Values greater than 1 indicate that the exposure concentration exceeds the reference concentration and may have significant negative consequences. Values less than 1 suggest that the population being exposed is unlikely to suffer any detrimental health effects.

The Incremental Life Cancer Risk (ILCR) was calculated using the Equation 6 (Bacigalupo & Hale, 2012, Cao et al., 2015; Sultana et al., 2017), to determine the potential target cancer risk for metals that exceeded the standards.

$$Incremental\ Life\ Cancer\ Risk\ (ILCR) = CDI \times CSF \quad [6]$$

The CDI, similar to EDI in the THQ calculation, estimates the average daily dose of exposure to the metal carcinogen over a person's lifetime and is measured as the chronic daily intake of the chemical carcinogen in milligrams per kilogram of body weight per day. CSF is an abbreviation for the cancer slope factor. Only Pb was measured for the ILCR with the CSF of 8.5×10^{-3} mg/kg/day (Ahmad et al., 2016; USEPA, 1989; Orisakwe et al., 2017). The ILCR value that ranges between 1.0×10^{-6} to 1.0×10^{-4} (around 1 probability risk out of every 1,000,000 lifetime exposures) is recommended by USEPA (2012).

Table 1
Non-cancer oral reference dose (RfD) for the investigated metals

Element	RfD (mg/kg/day)	References
Fe	0.7000	Harmanescu et al., 2011
Zn	0.3000	Harmanescu et al., 2011; Korkmaz et al., 2017; USEPA, 1989
Pb	0.0035	Harmanescu et al., 2011; Orisakwe et al., 2017

Data Analysis

All samples collected and metal analysis were conducted with a minimum of three replicates. Descriptive statistics, including mean and standard deviation, were then determined. An assessment was conducted to compare the water quality parameters and trace metal concentrations with the National Lake Water Quality Standard (NLWQS) established by the National Hydraulic Research Institute of Malaysia (NAHRIM) for Category C lakes, which are designated for the conservation of aquatic life and biodiversity. The fish muscles and gills were analysed for trace metal concentration in accordance with the guidelines established by the World Health Organisation (WHO) in 2004, the Food and Agriculture Organisation (FAO) in 1983, and the Malaysia Food Act (MFA) in 1983.

The correlation between trace metal levels in lake water, fish muscles and gills was conducted using Pearson Product Moment Correlation in SPSS. Statistical analysis using one-way ANOVA and Kruskal-Wallis tests was employed to ascertain the presence of any statistical disparity between the sampling locations and water quality parameters.

RESULTS AND DISCUSSION

Water Quality Status of the Lake

The physicochemical properties of water are necessary for the monitoring of water quality (Alonso Castillo et al., 2013; Javed et al., 2016). With the exception of pH and DO, the physicochemical characteristics of the water samples shown in Table 2 were found to be generally within Malaysia's NLWQS permissible level for Category C lakes.

The pH of the limnetic zone of the lake was below pH 6.0, which was acidic and slightly contaminated. These acidic conditions might have originated from the commonly produced sulphide from the previous mining operations (Khalid et al., 2017). Higher or lower pH influences the water taste as well as the damage to the fish skin and eyes (Dirisu et al., 2016), while pH levels above 9.0 are similarly toxic to fish and other aquatic animals (Stone et al., 2013; Wurts, 2003). Although the effect of pH does not directly correspond

Table 2
In-situ water quality parameters of the lake

Point	Inlet	Middle	Outlet	NLQWS (NAHRIM) Category C
pH	6.77±0.03	3.89±0.50	6.57±0.01	6.0 – 9.0
EC (µS/cm)	161.33±0.49	159.30±0.70	167.50±0.00	2000
Salinity (%)	0.10±0.00	0.10±0.00	0.10±0.00	<1
Temperature (°C)	30.17±0.06	29.70±0.10	28.30±0.00	28
Turbidity (NTU)	8.98±0.14	9.30±0.41	11.43±0.61	70
DO (mg/L)	1.44±0.76	0.52±0.02	0.49±0.04	55-130

to human health, the pH level does impact metal solubility and concentration (Miao et al., 2021; Muhammad et al., 2011). Under slightly acidic circumstances (pH=5.0), higher metal solubilities were detected, which rose when pH was held at 3.3 (Başak & Alagha, 2010; Chuan et al., 1996). Therefore, the acidic conditions of the water were deemed unfavourable for the fish and may impact the lake ecosystem in the long run.

It was found that the dissolved oxygen (DO) levels in some areas of the lake were below the ideal threshold established by the NLWQS. Low DO is common in ex-mining ponds and lakes (Orji et al., 2013; Srivastava et al., 2009). Low DO values could be due to a decrease in aquatic plant activity and a high level of organic material content (Breitburg et al., 1997; Seitaj et al., 2017). Conversely, aquatic plants proliferate in the lake ecosystem in the study area. Therefore, as the DO level measures the water's assimilative capacity, its depletion may also indicate pollution of biological or chemical origins (Chiejine et al., 2015). Depleted DO levels threaten aquatic life as DO is crucial for the metabolism of all aquatic organisms. If low DO conditions are prolonged in the study area, metal contamination might not be the only concern.

EC, pH, and temperature were significantly different among the sampling points ($p<0.05$). A drastic decrease in pH levels in the middle of the lake compared to the inlet and outlet could be due to water flowing into the lake and passing over or through soil or bedrock of different mineral compositions. In terms of EC, although the differences between the level measured at the middle point and the two other points were significant, the difference was less than 5%, hence it was still considered negligible. Equally, the temperature measurements varied by around 1-2°C across each location and may have been influenced by the shadowing caused by cloud cover on the lake surface during the sampling process. In contrast, turbidity and dissolved oxygen levels measured for all points were similar ($p>0.05$). Therefore, the condition for the whole lake was representative of the values measured for both parameters.

Trace Metals in Water

Ex-mining waters are usually enriched with many elements. Determining the metal concentrations in the lakes is essential for the risk assessment, especially if the water is being used for human consumption. Table 3 shows the results of metal concentration that are detected in the ex-mining lake for the inlet, middle, and outlet. It is noticeable that there are differences between the Fe, Zn, and Pb concentrations in the inlet, middle, and outlet ($p<0.05$).

The major element in the mining area sediment and soil is usually Fe, which is present in high concentrations compared to other trace metals because in most of the earth's upper and lower crust, Fe is one of the most abundant elements. This is true because Fe has the most significant quantities of trace metals among the tested metals. Agriculture wastewater,

Table 3
Trace metal concentration in water

Point	Inlet	Middle	Outlet
Fe (mg/L)	0.80±12.02	0.57±15.11	0.64±22.74
Zn (mg/L)	0.10±0.28	0.53±0.34	0.18±2.47
Pb (mg/L)	0.13±0.38	0.18±0.01	0.19±0.09

prior mining and metallurgical operations that used zinc, as well as the use of commercial products containing zinc, contributed as anthropogenic sources of zinc in the water (ATSDR, 2005). Despite being lower than the guideline's value, Zn was detected in high concentration in the middle part of the lake as compared to the inlet and outlet (p<0.05). This could be due to the poor water flow, whereby a higher concentration of pollutants accumulated at the lake's centre. Different flow rates can significantly affect water quality parameters at any point in the lake (Pourfallah Koushali et al., 2021).

The comparison between metal concentrations in water and NLWQS is illustrated in Figure 2. The metal levels in the lake were all within the NLWQS's acceptable limits, except for Pb at 0.121 mg/L. It was discovered that the water's Pb levels were 33.3% higher than the recommended limit. Possible sources of Pb could include leftover residual metals from the mining activities (Paul, 2017) and agricultural runoff (Hamzah et al., 2018).

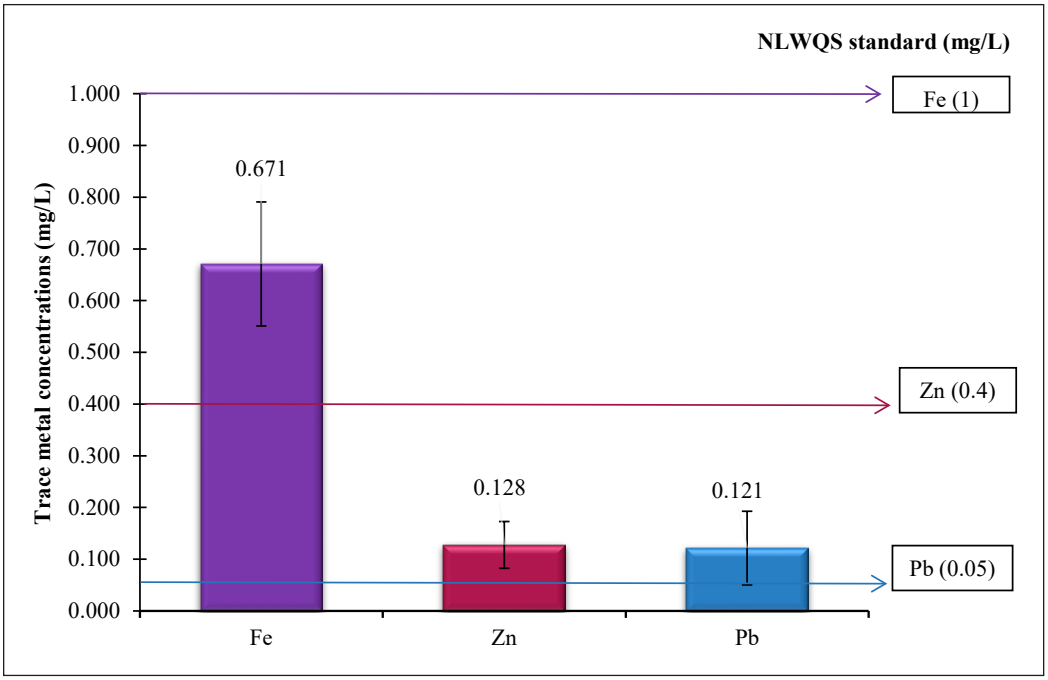

Figure 2. A comparison of the amount of trace metals in water with NLWQS

The present study has focused on the analysis of Fe and Zn because they are essential trace elements for biological functions but can pose a danger at elevated levels. Pb was included as well due to its known toxicity and prevalence in anthropogenic environments, especially in mining and industrial areas. On top of that, these metals are commonly monitored in food safety and environmental health guidelines, making them relevant indicators for risk assessment. However, the study acknowledged that the exclusion of other highly toxic metals, such as As and Cd, limits its ability to fully assess the accumulative health risk associated with metal contamination in the studied fish species. Therefore, future studies should cover a larger range of metals to provide a more complete risk assessment.

Trace Metal Concentration in Fish and the Bioconcentration Factor

The mean concentration of trace metals in the muscles and gills of the *Barbonymus* sp. followed a decreasing order of Fe > Zn > Pb. Metal concentrations observed in the *Barbonymus* sp. gills and muscles were compared to WHO, FAO, and MFA guidelines in Table 4. The Fe concentration in the muscles and gills of the *Barbonymus* sp. exceeded the maximum limits set by the FAO and World Health Organisation. The concentration of Pb recorded in this study also surpassed the safe range set by MFA, WHO, and FAO. Zn concentration in the *Barbonymus* sp. gills was less than the MFA and FAO limits of 100 mg/kg and 30 mg/kg, respectively. However, the amount of Zn in the *Barbonymus* sp. muscle was slightly greater than the FAO limit of 30 mg/kg, but this was still considered to be low compared to the values in MFA.

Table 5 presents the bioconcentration factors (BCF) of trace metals computed for the gills and muscles of *Barbonymus sp.* The BCF values among the studied trace metals showed a descending trend of Fe>Zn>Pb for its gills and Zn>Fe>Pb for the muscles of the *Barbonymus* sp. For both the gills and muscles of *Barbonymus* sp., the BCF values of all studied metals were greater than 1.0, indicating the propensity to accumulate Fe, Pb, and Zn from the water (Ju et al., 2017).

Metal accumulation in fish is a complex process influenced by both internal and external variables (Griboff et al., 2017; Jabeen & Chaudhry, 2010). Metal bioavailability, alkalinity, and ambient temperature are listed as external factors, whereas the feeding

Table 4
Trace metal concentrations in Barbonymus *sp. (mg/kg)*

Metal	Mean concentration		WHO	FAO	MFA
	Gills	Muscles			
Fe	267.66	132.76	43	2.5	-
Zn	18.65	31.85	-	30	100
Pb	9.82	10.19	1.5	0.5	2

habit of the fish is an example of internal factors affecting the metal accumulation in fish. Major pathways for metals to enter the fish are through surface exposure to water, the food chain, and respiratory activity (Adegbola et al., 2021).

Table 5
Bioconcentration Factor (BCF) of trace metal in muscles and gills of Barbonymus *sp.*

Trace metals	Organs	BCF
Iron (Fe)	Gills	398.90
	Muscles	197.85
Lead (Pb)	Gills	81.16
	Muscles	84.21
Zinc (Zn)	Gills	145.70
	Muscles	248.83

Gills are chosen in this study for assessing metal accumulation, as they reflect the metal pollution in water. Higher metals can usually be found in the gills as they are more exposed to the outer environment (water) than the muscle (Bebianno et al., 2004; Rajeshkumar & Li, 2018). Moreover, metal accumulation in gills is also due to the larger surface areas, which allow rapid metal diffusion and metal ion exchange process from the surrounding aquatic environment (Bebianno et al., 2004; El-Moselhy et al., 2014). Since muscles are frequently consumed when people eat fish, it was chosen as the organ of concern, even though it is not thought to be an active tissue in terms of accumulating trace metals (Agah et al., 2009; Aytekin et al., 2019; Mohammad Ali et al., 2021). In this study, a statistically significant difference was observed in Fe levels ($p < 0.05$), while no significant difference was found in Zn levels, although the concentration in the muscles was somewhat higher ($p < 0.05$). However, there were no statistically significant differences in Pb levels between the organs ($p > 0.05$). Kalay et al. (1999) argued that after a contaminant has passed through the body's defence barrier, it will begin to accumulate in the fish muscle.

It should be emphasised that, due to sampling constraints, this study has grouped all the fish samples under *Barbonymus* sp., which restricts the ability to generalise the results because various species within the genus can exhibit differing physiological traits and ecological niches. These changes may alter heavy metal uptake, accumulation, and detoxification mechanisms, potentially resulting in variations in the observed patterns (Cordeli et al., 2023; Oros, 2025). Future research on particular species within the genus may provide more detailed insights into metal accumulation.

Human Health Risk Assessment

The rate of fish consumption reported in Malaysia (both for inland and marine sources) in 2016 was about 59 kg per capita, making it among the world's highest demands for fish (FAO, 2020). As the demand for fish rises, it becomes increasingly important to assess the health risks connected with eating seafood that has been contaminated with trace metals (Mansour et al., 2009). Table 6 shows the estimated possible health hazards that are associated with consuming *Barbonymus* sp. that is polluted with Fe, Zn, and Pb from

the former mining lake. All THQ values for metals analysed were less than 1, indicating that the people consuming *Barbonymus* sp. from the former mining lake were not exposed to health risk (Ahmad & Sarah, 2015; Lemly, 1996; Wang et al., 2005). However, humans exposed to the effects of the combination of more than one metal or interactive effects can be higher (Li et al., 2013).

Table 6
Target Hazard Quotient (THQ) and Increment Lifetime Carcinogenic Risk (ILCR) by consuming Barbonymus *sp.*

Element	Risk Assessment	
	THQ	ILCR
Fe	0.0014	-
Zn	0.0004	-
Pb	0.0141	$1.05E^{-06}$

Due to their toxicity and frequent association with ex-mining metal contamination, the only carcinogenic risk for Pb was investigated pertaining to the consumption of *Barbonymus* sp. (Ghnaya et al., 2015; Oke & Vermeulen, 2017). According to Silbergeld et al. (2000), Pb poisoning can cause oxidative DNA damage, direct DNA damage, and suppression of DNA synthesis. It can also produce reactive oxygen species. The US EPA's tolerable risk range, which is 1×10-6 to 1×10-4, is still within the increased lifetime cancer risk (ILCR) for Pb, 1.05 ×10-6, indicating negligible carcinogenic risk to the consumer (USEPA, 1989). Nevertheless, Pb contamination remains particularly hazardous to vulnerable populations such as children and pregnant women. Their physiological differences, including rapid development in children and the unique vulnerability of the fetus, can lead to greater sensitivity to Pb exposure, potentially amplifying the long-term health consequences that are associated with even low-level contamination. Children are known to be more affected by Pb than adults, even at a low concentration. The risk to the infant from a pregnant woman should not be overlooked, as Pb can cross the placental barrier, potentially causing harm to the developing neurological system of the newborn (ATSDR, 2017). As a result, while the immediate carcinogenic risk to the general population may appear to be small, the possibility of long-term harm, particularly to the developing systems of children and the unborn, necessitates ongoing monitoring and risk communication.

Other similar studies on the health risk assessment of fish from the ex-mining lake also reported coinciding results. According to the evaluation by Ishak et al. (2020), while the computed HQ levels for both Pb and Cd showed no known health risk to humans, it is important to exercise caution, as there is still the possibility of other trace metals being present in the lake which potentially endanger human health if not monitored.

It should be noted that vulnerable individuals who are susceptible to long-term trace element exposure, such as children, pregnant or nursing mothers, and their infants, are not taken into account in the human health risk assessment in this study (Javed & Usmani, 2019).

CONCLUSION

This study sets out to evaluate the accumulation of trace metals in the populations of *Barbonymus* sp. that are obtained from a former mining lake in Sg. Galah, Kg. Gajah, Perak, Malaysia. Analysis revealed that the gills of *Barbonymus sp*. contained higher levels of Fe, Zn, and Pb than the muscles. However, both organs exhibited the same pattern of Fe > Zn > Pb accumulation. Iron (Fe) and lead (Pb) concentrations in the gills and muscles of *Barbonymus sp*. surpassed many established thresholds. Nevertheless, according to the findings of the health risk assessment, it can be concluded that the potential of harmful effects (including cancer and non-cancerous conditions) on human health that are linked to prolonged consumption of fish is still low. However, it is important to note that the present study is based on samples that have been collected at a single time point, which may not account for potential seasonal variations. Given the tropical environment of the study area in Perak, future research should consider the potential impact of seasonal fluctuations in precipitation and temperature on the solubility and bioavailability of metals in the lake, as these factors could subsequently affect their accumulation patterns in fish tissues. Other investigations on the movement of metals between different trophic levels or mediums are necessary to enhance the obtained findings.

ACKNOWLEDGEMENT

This research is financially supported by the Ministry of Higher Education, Malaysia, under the Fundamental Research Grant Scheme (FRGS) with grant reference number FRGS/1/2020/WAB02/UPM/02/4 and project number 07-01-20-2238FR.The authors would like to thank Persatuan Perikanan Air Tawar Sg. Galah, Kg. Gajah (PENIAT), Perak, Malaysia, for their cooperation, help and support and Ms. Nur Rohmawati Supardi for her involvement.

REFERENCES

Adegbola, I. P., Aborisade, B. A., & Adetutu, A. (2021). Health risk assessment and heavy metal accumulation in fish species (*Clarias gariepinus* and *Sarotherodon melanotheron*) from industrially polluted Ogun and Eleyele Rivers, Nigeria. *Toxicology Reports*, *8*, 1445–1460. https://doi.org/10.1016/j.toxrep.2021.07.007

Agah, H., Leermakers, M., Elskens, M., Fatemi, S. M. R., & Baeyens, W. (2009). Accumulation of trace metals in the muscle and liver tissues of five fish species from the Persian Gulf. *Environmental Monitoring and Assessment*, *157*(1–4), 499–514. https://doi.org/10.1007/s10661-008-0551-8

Agency for Toxic Substances and Disease Registry (ATSDR). (2005). Public Health Statement – Zinc. Division of Toxicology, Department of Health and Human Services. https://www.atsdr.cdc.gov/ToxProfiles/tp60-c1-b.pdf

Agency for Toxic Substances and Disease Registry (ATSDR). (2017, June 12). Lead toxicity. U.S. Department of Health and Human Services. https://www.atsdr.cdc.gov/hec/csem/lead/docs/lead.pdf

Ahmad, A. K., & Sarah, A.-M. (2015). Human Health Risk Assessment of Heavy Metals in Fish Species Collected from Catchments of Former Tin Mining. *International Journal of Research Studies in Science, Engineering and Technology*, *2*(4), 9–21.

Ahmad, N. I., Mahiyuddin, W. R. W., Mohamad, T. R. T., Ling, C. Y., Daud, S. F., Hussein, N. C., Abdullah, N. A., Shaharudin, R., & Sulaiman, L. H. (2016). Fish consumption pattern among adults of different ethnics in Peninsular Malaysia. *Food and Nutrition Research*, *60*. https://doi.org/10.3402/fnr.v60.32697

Alonso Castillo, M. L., Sánchez Trujillo, I., Vereda Alonso, E., García de Torres, A., & Cano Pavón, J. M. (2013). Bioavailability of heavy metals in water and sediments from a typical Mediterranean Bay (Málaga Bay, Region of Andalucía, Southern Spain). *Marine Pollution Bulletin*, *76*(1–2), 427–434. https://doi.org/10.1016/j.marpolbul.2013.08.031

Ashraf, M. A., Maah, M. J., & Yusoff. (2012). Bioaccumulation of Heavy Metals in Fish Species Collected from Former Tin Mining Catchment. *International Journal of Environmental Research*, *6*(1), 209–218. https://doi.org/10.22059/ijer.2011.487

Aytekin, T., Kargın, D., Çoğun, H. Y., Temiz, Ö., Varkal, H. S., & Kargın, F. (2019). Accumulation and health risk assessment of heavy metals in tissues of the shrimp and fish species from the Yumurtalik coast of Iskenderun Gulf, Turkey. *Heliyon*, *5*(8). https://doi.org/10.1016/j.heliyon.2019.e02131

Azmi, W. N. F. W., Ahmad, N. I., & Mahiyuddin, W. R. W. (2019). Heavy Metal Levels and Risk Assessment from Consumption of Marine Fish in Peninsular Malaysia. *Journal of Environmental Protection*, *10*(11), 1450–1471. https://doi.org/10.4236/jep.2019.1011086

Bacigalupo, C., & Hale, B. (2012). Human health risks of Pb and as exposure via consumption of home garden vegetables and incidental soil and dust ingestion: A probabilistic screening tool. *Science of the Total Environment*, *423*, 27–38. https://doi.org/10.1016/j.scitotenv.2012.01.057

Baharim, N. H., Tuan Daud, T. A., Hashim, H., & Dzulkafli, N. F. (2022). Lake Water Quality Assessment in Universiti Selangor Bestari Jaya Campus: A Preliminary Study. *Jurnal Pena Sains*, *9*(1), 1–6. https://doi.org/10.21107/jps.v9i1.11583

Başak, B., & Alagha, O. (2010). Trace metals solubility in rainwater: Evaluation of rainwater quality at a watershed area, Istanbul. *Environmental Monitoring and Assessment*, *167*(1–4), 493–503. https://doi.org/10.1007/s10661-009-1066-7

Batubara, A. S., Muchlisin, Z. A., Efizon, D., Perikanan, F., Kelautan, D., Riau, U., & Elvyra, R. (2021). DNA barcoding (COI genetic marker) revealed hidden diversity of Cyprinid fish (*Barbonymus* spp.) from Aceh Waters, Indonesia. *Biharean Biologist*, *1*(15), 39–47. https://www.researchgate.net/publication/343892635

Bebianno, M. J., Géret, F., Hoarau, P., Serafim, M. A., Coelho, M. R., Gnassia-Barelli, M., & Roméo, M. (2004). Biomarkers in *Ruditapes decussatus*: A potential bioindicator species. *Biomarkers*, *9*(4–5), 305–330. https://doi.org/10.1080/13547500400017820

Breitburg, D. L., Loher, T., Pacey, C. A., & Gerstein, A. (1997). Varying effects of low dissolved oxygen on trophic interactions in an estuarine food web. *Ecological Monographs*, *67*(4), 489–507. https://doi.org/10.1890/0012-9615(1997)067[0489:VEOLDO]2.0.CO;2

Cao, S., Duan, X., Zhao, X., Wang, B., Ma, J., Fan, D., Sun, C., He, B., Wei, F., & Jiang, G. (2015). Health risk assessment of various metal(loid)s via multiple exposure pathways on children living near a

typical lead-acid battery plant, China. *Environmental Pollution*, *200*, 16–23. https://doi.org/10.1016/j.envpol.2015.02.010

Chiejine, C. M., Igboanugo, A. C., & Ezemonye, L. I. N. (2015). Modelling Effluent Assimilative Capacity of IKPOBA River, Benin City, Nigeria. *Nigerian Journal of Technology*, *34*(1), 133–141. https://doi.org/https://doi.org/10.4314/njt.v34i1.17

Chuan, M. C., Shu, G. Y., & Liu, J. C. (1996). Solubility of heavy metals in a contaminated soil: Effects of redox potential and pH. *Water, Air and Soil Pollution*, *90*, 543–556. https://doi.org/https://doi.org/10.1007/BF00282668

Cordeli, A. N., Oprea, L., Crețu, M., Dediu, L., Coadă, M. T., & Mînzală, D. N. (2023). Bioaccumulation of metals in some fish species from the Romanian Danube River: A review. *Fishes*, *8*(8), 387. https://doi.org/10.3390/fishes8080387

Dalzochio, T., Rodrigues, G. Z. P., Simões, L. A. R., de Souza, M. S., Petry, I. E., Andriguetti, N. B., Silva, G. J. H., da Silva, L. B., & Gehlen, G. (2018). In situ monitoring of the Sinos River, southern Brazil: water quality parameters, biomarkers, and metal bioaccumulation in fish. *Environmental Science and Pollution Research*, *25*(10), 9485–9500. https://doi.org/10.1007/s11356-018-1244-7

Department of Fisheries Malaysia (DOF). (2021). Annual fisheries statistics, 2013-2020. Ministry of Agriculture and Agro-based Industry Malaysia. Retrieved from http://www.dof.gov.my. on 31 October 2022.

Dirisu, C. G., Mafiana, M. O., Dirisu, G. B., & Amodu, R. (2016). Level of pH in Drinking Water of an Oil and Gas Producing Community and Perceived Biological and Health Implications. *European Journal of Basic and Applied Sciences*, *3*(3). www.idpublications.org

El-Moselhy, Kh. M., Othman, A. I., Abd El-Azem, H., & El-Metwally, M. E. A. (2014). Bioaccumulation of heavy metals in some tissues of fish in the Red Sea, Egypt. *Egyptian Journal of Basic and Applied Sciences*, *1*(2), 97–105. https://doi.org/10.1016/j.ejbas.2014.06.001

Eslamloo, K., Morshedi, V., Azodi, M., Ashouri, G., Ali, M., & Iqbal, F. (2012). Effects of Starvation and Re-Feeding on Growth Performance, Feed Utilization and Body Composition of Tinfoil Barb (*Barbonymus schwanenfeldii*). *World Journal of Fish and Marine Sciences*, *4*(5), 489–495. https://doi.org/10.5829/idosi.wjfms.2012.04.05.6465

Food and Agriculture Organization (FAO). (2009) Fishery and aquaculture statistics. Retrieved from http://www.fao.org/3/aq187t/aq187t.pdf.

Food and Agriculture Organization (FAO). (2020) Fishery and Aquaculture Country Profiles. Malaysia. Food and Agriculture Organization of the United Nations. Assessed on 11 March 2022. Retrieved from: [Online Resource] http://www.fao.org/fishery/facp/MYS/en

Ghnaya, T., Mnassri, M., Ghabriche, R., Wali, M., Poschenrieder, C., Lutts, S., & Abdelly, C. (2015). Nodulation by *Sinorhizobium meliloti* originated from a mining soil alleviates Cd toxicity and increases Cd-phytoextraction in Medicago sativa L. *Frontiers in Plant Science*, *6*(October). https://doi.org/10.3389/fpls.2015.00863

Gobas, F. A. P. C., De Wolf, W., Burkhard, L. P., Verbruggen, E., & Plotzke, K. (2009). Revisiting bioaccumulation criteria for POPs and PBT assessments. *Integrated Environmental Assessment and Management*, *5*(4), 624–637. https://doi.org/10.1897/IEAM_2008-089.1

Griboff, J., Wunderlin, D. A., & Monferran, M. V. (2017). Metals, As and Se determination by inductively coupled plasma-mass spectrometry (ICP-MS) in edible fish collected from three eutrophic reservoirs. Their consumption represents a risk for human health? *Microchemical Journal*, *130*, 236–244. https://doi.org/10.1016/j.microc.2016.09.013

Hamzah, N., Diman, C. P., Ahmad, M. A. N., Lazim, M. I. H. M., Zakaria, M. F., & Bashar, N. M. (2018). Water quality assessment of abandoned mines in Selangor. *AIP Conference Proceedings*, *2020*. https://doi.org/10.1063/1.5062672

Harmanescu, M., Alda, L. M., Bordean, D. M., Gogoasa, I., & Gergen, I. (2011). Heavy metals health risk assessment for population via consumption of vegetables grown in old mining area; a case study: Banat County, Romania. *Chemistry Central Journal*, *5*(1). https://doi.org/10.1186/1752-153X-5-64

Hembrom, S., Singh, B., Gupta, S. K., & Nema. Arvind Kumar. (2019). A comprehensive evaluation of heavy metal contamination in foodstuff and associated human health risk: A global perspective. In P. Singh, R. P. Singh, & V. Srivastava (Eds.), *Contemporary Environmental Issues and Challenges in Era of Climate Change* (pp. 33–63). Springer. https://doi.org/https://doi.org/10.1007/978-981-32-9595-7_2

Idriss, A. A., & Ahmad, A. K. (2015). Heavy metal concentrations in fishes from Juru River, estimation of the health risk. *Bulletin of Environmental Contamination and Toxicology*, *94*(2), 204–208. https://doi.org/10.1007/s00128-014-1452-x

Isa, M. M., Md-Shah, A.-S., Mohd-Sah, S.-A., Baharudin, N., & Abdul-Halim, M.-A. (2012). Population Dynamics of Tinfoil Barb, *Barbonymus schwanenfeldii* (Bleeker, 1853) in Pedu Reservoir, Kedah. *Journal of Biology, Agriculture and Healthcare*, *2*(5), 55–69.

Ishak, A. R., Zuhdi, M. S. M., & Aziz, M. Y. (2020). Determination of lead and cadmium in tilapia fish (*Oreochromis niloticus*) from selected areas in Kuala Lumpur. *Egyptian Journal of Aquatic Research*, *46*(3), 221–225. https://doi.org/10.1016/j.ejar.2020.06.001

Jabeen, F., & Chaudhry, A. S. (2010). Environmental impacts of anthropogenic activities on the mineral uptake in *Oreochromis mossambicus* from Indus River in Pakistan. *Environmental Monitoring and Assessment*, *166*(1–4), 641–651. https://doi.org/10.1007/s10661-009-1029-z

Javed, M., Ahmad, I., Usmani, N., & Ahmad, M. (2016). Studies on biomarkers of oxidative stress and associated genotoxicity and histopathology in Channa punctatus from heavy metal polluted canal. *Chemosphere*, *151*, 210–219. https://doi.org/10.1016/j.chemosphere.2016.02.080

Javed, M., & Usmani, N. (2019). An overview of the adverse effects of heavy metal contamination on fish health. *Proceedings of the National Academy of Sciences India Section B - Biological Sciences*, *89*(2), 389–403. https://doi.org/10.1007/s40011-017-0875-7

Ju, Y. R., Chen, C. W., Chen, C. F., Chuang, X. Y., & Dong, C. Di. (2017). Assessment of heavy metals in aquaculture fishes collected from southwest coast of Taiwan and human consumption risk. *International Biodeterioration and Biodegradation*, *124*, 314–325. https://doi.org/10.1016/j.ibiod.2017.04.003

Kalay, M., Ay, Ö., & Canli, M. (1999). *Heavy Metal Concentrations in Fish Tissues from the Northeast Mediterranean Sea*. https://www.researchgate.net/publication/360484399

Kamari, A., Yusof, N., Abdullah, H., Haraguchi, A., & Abas, M. F. (2017). Assessment of heavy metals in water, sediment, *Anabas testudineus* and *Eichhornia crassipes* in a former mining pond in Perak, Malaysia. *Chemistry and Ecology*, *33*(7), 637–651. https://doi.org/10.1080/02757540.2017.1351553

Kamarudin, K. R., & Esa, Y. (2009). Phylogeny and phylogeography of *Barbonymus schwanenfeldii* (Cyprinidae) from Malaysia inferred using partial cytochrome b mtDNA gene. *Journal of Tropical Biology and Conservation 5*, 1-13.

Khalid, S. A., Fauziah, S., Draman, S., Rozaimah, S., Abdullah, S., Anuar, N., Azraf, M. F., & Radzi, M. (2017). *In Situ Analysis of Water Quality Monitoring in Ex-Mining Lake Tasik Puteri (Terengganu, Malaysia)* (Vol. 12, Issue 10). http://epublisiti.townplan.gov.my/rkk/RKK_Bukit%2

Khoshnood, R., Jaafarzadeh, N., Khoshnood, Z., Ahmadi, M., & Teymouri, P. (2014). Estimation of target hazard quotients for metals by consumption of fish in the North Coast of the Persian Gulf, Iran. *Journal of Advances in Environmental Health Research*, *2*(4), 263–272. https://doi.org/https://doi.org/10.22102/jaehr.2014.40177

Koki, I. B., Low, K. H., Juahir, H., Abdul Zali, M., Azid, A., & Zain, S. M. (2018). Consumption of water from ex-mining ponds in Klang Valley and Melaka, Malaysia: A health risk study. *Chemosphere*, *195*, 641–652. https://doi.org/10.1016/j.chemosphere.2017.12.112

Korkmaz, C., Ay, Ö., Çolakfakioğlu, C., Cicik, B., & Erdem, C. (2017). Heavy Metal Levels in Muscle Tissues of *Solea solea, Mullus barbatus*, and *Sardina pilchardus* Marketed for Consumption in Mersin, Turkey. *Water, Air, and Soil Pollution*, *228*(8). https://doi.org/10.1007/s11270-017-3503-5

Kottelat, M. (2013). The fishes of the inland waters of Southeast Asia: A catalogue and core bibliography of the fishes known to occur in freshwaters, mangroves and estuaries. *The Raffles Bulletin of Zoology*, *27*, 1–663.

Kusmini, I. I., Gustiano, R., Radona, D., & Kurniawan, K. (2021). Domestication Strategies of Tinfoil Barb *Barbonymus schwanenfeldii* (Bleeker, 1854): Potential Candidate for Freshwater Aquaculture Development. *IOP Conference Series: Earth and Environmental Science*, *934*(1). https://doi.org/10.1088/1755-1315/934/1/012003

Lemly, A. D. (1996). *Evaluation of the Hazard Quotient Method for Risk Assessment of Selenium*. https://doi.org/https://doi.org/10.1006/eesa.1996.0095

Li, J., Huang, Z. Y., Hu, Y., & Yang, H. (2013). Potential risk assessment of heavy metals by consuming shellfish collected from Xiamen, China. *Environmental Science and Pollution Research*, *20*(5), 2937–2947. https://doi.org/10.1007/s11356-012-1207-3

Liu, M., Xu, Y., Nawab, J., Rahman, Z., Khan, S., Idress, M., Ud din, Z., Ali, A., Ahmad, R., Khan, S. A., Khan, A., Khan, M. Q., Tang, Y. T., & Li, G. (2020). Contamination features, geo-accumulation, enrichments and human health risks of toxic heavy metal(loids) from fish consumption collected along Swat River, Pakistan. *Environmental Technology and Innovation*, *17*. https://doi.org/10.1016/j.eti.2019.100554

Low, K. H., Koki, I. B., Juahir, H., Azid, A., Behkami, S., Ikram, R., Mohammed, H. A., & Zain, S. M. (2016). Evaluation of water quality variation in lakes, rivers, and ex-mining ponds in Malaysia (review). *Desalination and Water Treatment*, *57*(58), 28215–28239. https://doi.org/10.1080/19443994.2016.1185382

Mansour, S. A., Belal, M. H., Abou-Arab, A. A. K., & Gad, M. F. (2009). Monitoring of pesticides and heavy metals in cucumber fruits produced from different farming systems. *Chemosphere*, *75*(5), 601–609. https://doi.org/10.1016/j.chemosphere.2009.01.058

Medunić, G., Fiket, Ž., & Ivanić, M. (2019). Arsenic Contamination Status in Europe, Australia, and Other Parts of the World. In *Arsenic in Drinking Water and Food* (pp. 183–233). Springer Singapore. https://doi.org/10.1007/978-981-13-8587-2_6

Miao, X., Hao, Y., Liu, H., Xie, Z., Miao, D., & He, X. (2021). Effects of heavy metals speciations in sediments on their bioaccumulation in wild fish in rivers in Liuzhou—A typical karst catchment in southwest China. *Ecotoxicology and Environmental Safety*, *214*. https://doi.org/10.1016/j.ecoenv.2021.112099

Mishra, S., Bhalke, S., Saradhi, I. V., Suseela, B., Tripathi, R. M., Pandit, G. G., & Puranik, V. D. (2007). Trace metals and organometals in selected marine species and preliminary risk assessment to human beings in Thane Creek area, Mumbai. *Chemosphere*, *69*(6), 972–978. https://doi.org/10.1016/j.chemosphere.2007.05.013

Mohammad Ali, M., Hossain, D., Al-Imran, Suzan Khan, Md., Begum, M., & Hasan Osman, M. (2021). Environmental pollution with heavy metals: A public health concern. In M. K. Nazal & H. Zhao (Eds.), *Heavy metals - Their environmental impacts and mitigation*. IntechOpen. https://doi.org/10.5772/intechopen.96805

Muchlisin, Z. A., Akyun, Q., Rizka, S., Fadli, N., Sugianto, S., Halim, A., & Siti-Azizah, M. N. (2015). Ichthyofauna of tripa peat swamp forest, Aceh province, Indonesia. *Check List*, *11*(2). https://doi.org/10.15560/11.2.1560

Muhammad, S., Shah, M. T., & Khan, S. (2011). Health risk assessment of heavy metals and their source apportionment in drinking water of Kohistan region, northern Pakistan. *Microchemical Journal*, *98*(2), 334–343. https://doi.org/10.1016/j.microc.2011.03.003

Müller, A., Österlund, H., Marsalek, J., & Viklander, M. (2020). The pollution conveyed by urban runoff: A review of sources. *Science of the Total Environment*, *709*. https://doi.org/10.1016/j.scitotenv.2019.136125

Oke, S., & Vermeulen, D. (2017). Geochemical modeling and remediation of heavy metals and trace elements from artisanal mines discharge. *Soil and Sediment Contamination: An International Journal*, *26*(1), 84–95. https://doi.org/https://doi.org/10.1080/15320383.2017.1241216

Okereafor, U., Makhatha, M., Mekuto, L., Uche-Okereafor, N., Sebola, T., & Mavumengwana, V. (2020). Toxic metal implications on agricultural soils, plants, animals, aquatic life and human health. *International Journal of Environmental Research and Public Health*, *17*(7). https://doi.org/10.3390/ijerph17072204

Orisakwe, O. E., Dagur, E. A., Mbagwu, H. O. C., & Udowelle, N. A. (2017). Lead levels in vegetables from artisanal mining sites of Dilimi River, Bukuru and Barkin Ladi north central Nigeria: Cancer and non-cancer risk assessment. *Asian Pacific Journal of Cancer Prevention*, *18*(3), 621–627. https://doi.org/10.22034/APJCP.2017.18.3.621

Orji, K. U., Sapari, N., Yusof, K. W., Asadpour, R., & Olisa, E. (2013). Comparative study of water quality of rivers used for raw water supply & ex-mining lakes in Perak, Malaysia. *IOP Conference Series: Earth and Environmental Science*, *16*(1). https://doi.org/10.1088/1755-1315/16/1/012072

Oros, A. (2025). Bioaccumulation and trophic transfer of heavy metals in marine fish: Ecological and ecosystem-level impacts. *Journal of Xenobiotics*, *15*(2), 59. https://doi.org/10.3390/jox15020059

Paul, D. (2017). Research on heavy metal pollution of river Ganga: A review. *Annals of Agrarian Science*, *15*(2), 278–286. https://doi.org/10.1016/j.aasci.2017.04.001

Petrović, Z., Teodorović, V., Dimitrijević, M., Borozan, S., Beuković, M., & Milićević, D. (2013). Environmental Cd and Zn concentrations in liver and kidney of european hare from different serbian regions: Age and tissue differences. *Bulletin of Environmental Contamination and Toxicology*, *90*(2), 203–207. https://doi.org/10.1007/s00128-012-0901-7

Pistelli, L., D'Angiolillo, F., Morelli, E., Basso, B., Rosellini, I., Posarelli, M., & Barbafieri, M. (2017). Response of spontaneous plants from an ex-mining site of Elba Island (Tuscany, Italy) to metal(loid) contamination. *Environmental Science and Pollution Research*, *24*(8), 7809–7820. https://doi.org/10.1007/s11356-017-8488-5

Pourfallah Koushali, H., Mastouri, R., & Khaledian, M. R. (2021). Impact of precipitation and flow rate changes on the water quality of a coastal river. *Shock and Vibration*, *2021*. https://doi.org/10.1155/2021/6557689

Rajeshkumar, S., & Li, X. (2018). Bioaccumulation of heavy metals in fish species from the Meiliang Bay, Taihu Lake, China. *Toxicology Reports*, *5*, 288–295. https://doi.org/10.1016/j.toxrep.2018.01.007

Rashid, N. N. K. A. (2014). *Effecrs of Different Values of pH and Temperatureon Survival and Growth of Fry and Juvenile Barbonymus schwanenfeldii and Oreochromis niloticus*. Rashid, A. N. N. K. (2014). Effects of different values of pH and temperature on survival and growth of fry and juvenile Barbonymus schwanenfeldii and Oreochromis niloticus. Project Report (B.Sc.), Universiti Malaysia Sarawak, Retrieved from https://ir.unimas.my/id/eprint/8260/

Saat, A., Muhd Isak, N., Hamzah, Z., & Wood, A. K. (2014). Kajian mengenai hubungan radionuklid di antara ikan, air, dan sedimen dalam tasik bekas lombong di Kampung Gajah, Perak, Malaysia [Study of radionuclides linkages between fish, water and sediment in former tin mining lake in Kampung Gajah, Perak, Malaysia]. *The Malaysian Journal of Analytical Sciences*, *18*(1), 170–177.

Seitaj, D., Sulu-Gambari, F., Burdorf, L. D. W., Romero-Ramirez, A., Maire, O., Malkin, S. Y., Slomp, C. P., & Meysman, F. J. R. (2017). Sedimentary oxygen dynamics in a seasonally hypoxic basin. *Limnology and Oceanography*, *62*(2), 452–473. https://doi.org/10.1002/lno.10434

Silbergeld, E. K., Waalkes, M., & Rice, J. M. (2000). Lead as a carcinogen: Experimental evidence and mechanisms of action. *American Journal of Industrial Medicine*, *38*(3), 316–323. https://doi.org/https://doi.org/10.1002/1097-0274(200009)38:3%3C316::AID-AJIM11%3E3.0.CO;2-P

Srivastava, N., Harit, G., & Srivastava, R. (2009). A study of physico-chemical characteristics of lakes around Jaipur, India. *Journal of Environmental Biology*, *30*(5), 889–894.

Stone, N., Shelton, J. L., Haggard, B. E., & Thomforde, H. K. (2013). *Interpretation of Water Analysis Reports for Fish Culture Southern regional aquaculture center*.

Sultana, M. S., Rana, S., Yamazaki, S., Aono, T., & Yoshida, S. (2017). Health risk assessment for carcinogenic and non-carcinogenic heavy metal exposures from vegetables and fruits of Bangladesh. *Cogent Environmental Science*, *3*(1). https://doi.org/10.1080/23311843.2017.1291107

Tacon, A. G. J., & Metian, M. (2013). Fish matters: Importance of aquatic foods in human nutrition and global food supply. *Reviews in Fisheries Science*, *21*(1), 22–38. https://doi.org/10.1080/10641262.2012.753405

United States Environmental Protection Agency (USEPA). (1989). Risk assessment guidance for Superfund. Volume I: human health evaluation manual (Part A), Interim Final. 1989. U.S. Environmental Protection Agency, Office of Emergency and Remedial Response (EPA/540/1-89/002)

United States Environmental Protection Agency (USEPA). (1991). Methods for the determination of metals in environmental samples. June 1991. U.S. Environmental Protection Agency, Office of Research and Development (EPA/600/4-91/010)

United States Environmental Protection Agency (USEPA). (2012). EPA Region III Risk-Based Concentration (RBC) Table 2008 Region III, 1650 Arch Street, Philadelphia, Pennsylvania 19103.

Wang, X., Sato, T., Xing, B., & Tao, S. (2005). Health risks of heavy metals to the general public in Tianjin, China via consumption of vegetables and fish. *Science of the Total Environment*, *350*(1–3), 28–37. https://doi.org/10.1016/j.scitotenv.2004.09.044

Wurts, W. A. (2003). Daily pH Cycle and Ammonia Toxicity. *World Aquaculture*, *34*(2), 20–121. https://www.researchgate.net/publication/307122387

Xie, Z., Jiang, Y., Zhang, H., Wang, D., Qi, S., Du, Z., & Zhang, H. (2016). Assessing heavy metal contamination and ecological risk in Poyang Lake area, China. *Environmental Earth Sciences*, *75*(7), 1–15. https://doi.org/10.1007/s12665-015-5240-7

Yang, L., Hirt, M. V., Sado, T., Arunachalam, M., Manickam, R., Tang, K. L., Simons, A. M., Wu, H.-H., Mayden, R. L., & Miya, M. (2012). Phylogenetic placements of the barbin genera Dischero dontus, Chagunius, and Hypselobarbus in the subfamily Cyprininae (Teleostei: Cypriniformes) and their relationships with other barbins. *Zootaxa*, *3586*, 26–40. www.mapress.com/zootaxa/Article

Zheng, L. P., Yang, J. X., & Chen, X. Y. (2016). Molecular phylogeny and systematics of the Barbinae (Teleostei: Cyprinidae) in China inferred from mitochondrial DNA sequences. *Biochemical Systematics and Ecology*, *68*, 250–259. https://doi.org/10.1016/j.bse.2016.07.012

Pertanika J. Trop. Agric. Sci. 48 (6): 1983 - 2005 (2025)

PERTANIKA JOURNALS

TROPICAL AGRICULTURAL SCIENCE

Journal homepage: http://www.pertanika.upm.edu.my/

Independent Effect of Water Regime and Fertilisers Treatments on GHG Emissions from Lowland Rice in West Java, Indonesia

Egi Nur Muhamad Sidiq[1], Edi Santosa[2]*, Herdhata Agusta[2], and Trikoesoemaningtyas[3]

[1]Agronomy and Horticulture Study Program, Faculty of Agriculture, IPB University, Jl. Meranti Kampus IPB Darmaga, 16680 Bogor, Indonesia

[2]Plant Ecophysiology Laboratory, Department of Agronomy and Horticulture, Faculty of Agriculture, IPB University, Jl. Meranti Kampus IPB Darmaga, 16680 Bogor, Indonesia

[3]Genetic and Plant Breeding Laboratory, Department of Agronomy and Horticulture, Faculty of Agriculture, IPB University, Jl. Meranti Kampus IPB Darmaga, 16680 Bogor, Indonesia

ABSTRACT

Lowland rice cultivation is a major contributor to agricultural greenhouse gas (GHG) emissions. Managing water and fertilizer is important GHG emissions. This paper evaluated GHG emissions of rice production under contrasting water regimes, i.e., continuous flooding (CF) versus alternate wetting and drying (AWD), with six nitrogen fertilizer combinations: no nitrogen (F1), urea 175 kg ha^{-1} (F2), urea 350 kg ha^{-1} (F3), urea 262.5 kg ha^{-1} + manure 3 tons ha^{-1} (F4), urea 525 kg ha^{-1} + rice straw 3 tons ha^{-1} (F5), and urea 175 kg ha^{-1} + manure 3 tons ha^{-1} + biochar 0.6 tons ha^{-1} (F6). The field experiments were conducted at Bogor Regency, West Java, Indonesia, using a randomized complete block design with three replications. Growth, yield components, and GHG emissions were observed in this study throughout the growing season. Results showed AWD reduced CH_4 emissions by 30% but increased N_2O by 43% compared to CF, yielding a net 23% lower global warming potential (GWP). Organic-amended treatments (F6) maintained yields equivalent to conventional fertilization while showing numerically lower GWP. The independent effect of the water regime and the nitrogen fertilizer combinations implies that the best level of biochar and manure combined with AWD has the most promising prospect of maintaining rice yield while reducing GHG emissions.

Keywords: AWD, biochar, carbon sequestration, continuous flooding, manure

ARTICLE INFO

Article history:
Received: 17 January 2025
Accepted: 08 May 2025
Published: 25 November 2025

DOI: https://doi.org/10.47836/pjtas.48.6.17

E-mail addresses:
eginurmsidiq@gmail.com (Egi Nur Muhamad Sidiq)
edisang@gmail.com (Edi Santosa)
agusta@apps.ipb.ac.id (Herdhata Agusta)
trikaditya@gmail.com (Trikoesoemaningtyas)
* Corresponding author

INTRODUCTION

Mitigating greenhouse gas (GHG) emissions across multiple sectors, including agriculture, is a global calling to reduce global warming. Agricultural ecosystems have a major contribution to global GHG

emissions, accounting for 44% and 50% of anthropogenic CH4 and N_2O emissions, respectively (Jia et al., 2019). Among agricultural practices, rice cultivation contributes to 10.1% of the total emissions from the agricultural sector and about 1.3–1.8% of the world's anthropogenic GHG emissions, primarily due to methane emissions (Wang et al., 2023). Simultaneously, global climate change is expected to negatively impact rice production under the global scenario, reducing rice yields by 0.6% to 1.2% by 2050 (Sun et al., 2023). Therefore, emission reduction in rice farming is important, while unscientific and unsustainable efforts may be increased to yield compensation (Ebrahimi et al., 2021; Souri & Hatamian, 2019).

Lowland rice farming mainly depends on saturated water management, which is called continuous flooding (CF). However, prolonged soil saturation promotes anaerobic microbial decomposition, producing methane. CF rice field stimulates complex methane emissions to the atmosphere due to the activity of methane-producing bacteria (methanogens) and methane-oxidizing bacteria (methanotrophs). Methane is produced at the final stage of anaerobic microbial organic material degradation, including materials from rice root exudates utilized by those microbes (Rajendran et al., 2023).

In Asia, CF rice cultivation uses about 80% of total irrigation water resources (Bin Rahman & Zhang, 2023). Water conservation techniques have been implemented, including alternate wetting and drying (AWD) that can reduce 38% of irrigation water usage without negatively impacting grain production (Gharsallah et al., 2023; Lampayan et al., 2015). Unlike CF, AWD implements alternating cycles of saturation (inundation) and unsaturation (drying), similar to intermittent irrigation implemented by IRRI (Mallareddy et al., 2023). AWD systems reduce percolation and seepage, thus reducing water use (Carrijo et al., 2017).

Livsey et al. (2019) and Mallareddy et al. (2023) found that AWD not only enhances water efficiency but also reduces GHG emissions. Ishfaq et al. (2020) estimated that implementing AWD reduces methane emissions by 11-95%. Thus, changing rice cultivation from CF to AWD reduces CH_4 emissions (Hoang et al., 2023). From a farmer's perspective, AWD is a simple and cheap technology for smallholders (Mallareddy et al., 2023).

While AWD is a promising mitigation strategy, nitrogen (N) fertilizer management is also important in optimizing rice production and minimizing GHG emissions. Excessive or inefficient application of N fertilizer can lead to increased N_2O emissions (Hou et al., 2024). In Indonesia, where rice farming is a crucial component of the country's agricultural sector, N fertilizer use is still suboptimal, with farmers often applying excessive or insufficient amounts (Susanti et al., 2024). Thus, combining AWD with a proper N fertilizer strategy can support sustainable rice farming by reducing CH_4 and N_2O emissions. However, there are trade-offs between CH_4 and N_2O emissions under AWD. While AWD reduces CH_4, at the same time, it increases N_2O emission (Gao et al., 2024). Therefore, discovering a suitable N fertilization strategy combined with AWD is critical to maximize its benefit.

This study compares CF and AWD water regimes with different N fertilizer applications. While AWD has been widely studied, its interaction with N fertilizer application remains an important area of research. According to the Food and Agriculture Organization of the United Nations (FAO) (2017), AWD can be considered a practical Climate-Smart Agriculture (CSA) practice that boosts agricultural productivity while lowering greenhouse GHG emissions. This study evaluates rice yields and the associated CH_4 and N_2O emissions under different water regimes and N fertilizer treatments.

MATERIALS AND METHODS

Experimental Site

This experiment was conducted from February 2024 to July 2024 at Cikarawang Experimental Field, Bogor, West Java, Indonesia (-6.5502208, 106.7290211). The yield component analysis was conducted at the Cikarawang Research Station, Department of Agronomy and Horticulture, Faculty of Agriculture, IPB. The GHG analysis was conducted at the Greenhouse Gas Laboratory of the Indonesian Agricultural Environment Standardization Institute, Central Java, Indonesia.

Experimental Design

This study used a split-plot Randomized Complete Block Design (RCBD) with two factors: irrigation treatment as the main plot and various combinations of N fertilizer doses with organic amendments as subplots. The water regime treatment consisted of continuous flooding (CF) and alternate wetting and drying (AWD), adapted from Lampayan et al. (2015). In CF, the water level was maintained at a 5–10 cm depth, except during fertilizer application and a week before harvest. In AWD, an initial 5–10 cm watering was applied and maintained until two weeks after transplanting (WAT). After this period, the water inlet was closed to stop water input, allowing the water level to decline gradually and initiating the wetting and drying cycle. The water inlet was opened when the water level dropped 15 cm below the ground surface to restore it to 5–10 cm above the surface. The re-flooding cycle lasts from about one day to more than 10 days after the water inlet is closed, depending on weather conditions, with longer periods if there is heavy rain. The water level below the soil surface was monitored by installing a perforated PVC pipe to allow water to seep into the pipe. The water inside the pipe was checked using a ruler stick.

The basic dose of N fertilizer followed the recommendation from the Regulation of Ministry of Agriculture No. 13/2022, namely the specific fertilization recommendation for the Dramaga location with a dose of urea fertilizer of 350 kg ha-1, SP-36 100 kg ha-1, and KCl 100 kg ha-1 with the content for each fertilizer: 46% N, 36% P2O5 and 60% K2O. The N fertilizer treatments consisted of six combinations, which integrated different N fertilizer doses with various organic materials, as detailed in Table 1.

Table 1
Treatments of N fertilizer combination

Code	N Fertilizer combination	Details
F1	No N fertilizer	Control
F2	Urea 175 kg ha^{-1}	50% N recommended rate
F3	Urea 350 kg ha^{-1}	100% N recommended rate
F4	Urea 262.5 kg ha^{-1} + manure 3 tons ha^{-1}	75% N recommended rate supplemented with additional N from manure
F5	Urea 525 kg ha^{-1} + rice straw 3 tons ha^{-1}	150% N recommended rate supplemented with N from rice straw decomposition
F6	Urea 175 kg ha^{-1} + manure 2.4 tons ha^{-1} + biochar 0.6 tons ha^{-1}	50% N recommended rate supplemented with N from manure and biochar

Urea was applied in three split doses: one-third at 1 day after transplanting (DAT), another third at 7 DAT, and the remaining dose at 30 DAT. During field preparation, one month before transplanting, organic amendments, including manure, chopped rice straw (10 cm pieces), and rice husk biochar (pyrolyzed at 350°C), were incorporated into the soil to ensure proper decomposition and nutrient availability. Organic amendments were incorporated based on typical nutrient compositions reported by other studies: Manure: 1.06–2.77% N, 0.74–0.95% P, 0.34–1.25% K, 28.42–37.64% C (Alghifari et al., 2023; Sudarsono et al., 2014; Zhang et al., 2020); rice straw: 0.66–1.85% N, 0.09–1.8% P, 1.2–1.8% K, 39.9–44.4% C (Ali et al., 2024; Duan et al., 2015; Yan et al., 2019); rice husk biochar (350°C): 0.23% N, 0.08 % P, 0.48 % K, 44.32 % C. While the exact nutrient composition of manure and rice straw was not directly measured in this study, the reported ranges are based on data from relevant studies that reflect typical nutrient values for these materials under comparable conditions.

The experiment used 36 plots arranged in three replications, each measuring 7.5 m × 4.5 m and separated by 50 cm buffers to prevent treatment interference. The Inpari 32 rice variety was transplanted using 21-day-old seedlings at 20 cm × 20 cm spacing. A 1-meter border zone was maintained around each plot, with 10 representative hills randomly selected for sampling inside part of the border area to avoid border effects. The fertilization regime included full doses of phosphorus (P) and potassium (K) applied with the first urea split at 1 DAT, followed by additional urea applications at 7 DAT and 30 DAT. Manual weeding was performed throughout the growing season, while pest and disease control involved using carbofuran and mancozeb when necessary. Bird nets were installed at a height of 2 m during anthesis and remained until harvest to protect the crop during the critical stage. The rice was harvested at 110 DAT, with yield and biomass measurements taken from the sampled hills to evaluate treatment effects.

Measurements

Plant observation included plant height, tiller number per hill, and productive tiller number per hill. Yield components observation included panicle length, filled grains number per panicle, unfilled grains number per panicle, grains number per panicle, filled grains percentage, index of 1000-grain weight, harvest index, and yield per hectare. The calculation of harvest index was performed according to Du et al. (2022):

Harvest index = (grain yield / aboveground dry matter accumulation)

GHG emissions of CH_4 and N_2O were measured, and Global Warming Potential (GWP) was calculated according to AR5 of IPCC. Gas sampling used a transparent closed chamber method (Setyanto et al., 2018) with some modifications. A fan-equipped chamber with dimensions of 0.5 m × 0.5 m × 1 m (L × W × H) was used for the experiment. At the top of the chamber, there is a hole covered with a septum (cover), which functions to take gas samples, and a hole to insert a thermometer sensor.

The gas sampling occurred three times per week, with additional sampling conducted for three days in a row following the N application. GHG sample was collected at 07.00-10.00 a.m. The chamber was installed on the third row of plant hills for each plot. The base chamber was installed from the first day of GHG sampling to the last day to maintain similar site until the end of the study.

Sampling was conducted simultaneously at 0, 15, and 30 minutes after the chamber was installed. The fan was turned on during sampling so that the air in the chamber became homogeneous, and the temperature was measured using a thermometer. A 20 mL syringe with a three-way stopcock is used to collect gas samples. The syringe was pumped for 2-3 injections to make the air inside homogeneous and then put into a 10 mL labeled glass vial. The vial was stored at room temperature before analysis. Gas samples were analyzed using gas chromatography (Varian 450-GC, Varian Inc., CA, USA) with a flame ionization detector and an electron capture detector for CH_4 and N_2O analysis, respectively.

Data Analysis

Statistical analysis of the data was carried out analysis of variance (ANOVA). For any treatments showing significant effects, Duncan's Multiple Range Test (DMRT) was performed at α=5% across all parameters, except for GHG, which used α=10% due to high uncertainty and variation in field GHG measurement. Pearson correlation analysis was conducted to analyze the relationships among parameters. All statistical tests were carried out using RStudio 4.4.1.

RESULTS

ANOVA Analysis

Analysis of variance did not show any significant effect of interaction between water management and N combination for all observed parameters (Table 2). Water management could significantly affect plant height at 8 WAT, panicle length, and grain weight per panicle, as well as CH_4 emission, N_2O emission, and GWP. In contrast, N combinations demonstrated broader effects, significantly affecting vegetative parameters (plant height, tiller numbers, and productive tillers), panicle length, grain development (filled/unfilled grain numbers, grain weights, and filling percentage), and GWP. In comparison, N combinations had no significant effect on CH_4 and N_2O emissions. Conversely, neither treatment significantly affected 1000-seed weight, grain yield per hectare, or the harvest index.

Table 2
Effects of water regime and N combination on agronomic and yield parameters of rice

Variable	Water regime (A)	N combination (B)	A × B
Plant height 8 WAT	*	**	ns
No. tillers 8 WAT	ns	**	ns
No. productive tillers per hill	ns	**	ns
Panicle length	*	*	ns
No. filled grains per panicle	ns	*	ns
No. unfilled grains per panicle	ns	*	ns
No. grains per panicle	ns	*	ns
Percentage of filled grains per panicle	ns	*	ns
Index 1000 seed	ns	ns	ns
Grain weight per panicle	*	*	ns
Grain weight per hill	ns	*	ns
Grain yield per ha	ns	ns	ns
Harvest index	ns	ns	ns
CH_4	*z	ns	ns
N_2O	**	ns	ns
GWP	*z	*z	ns

Note. ** = significantly different at 0.01; * = significantly different at 0.05; *z = significantly different at 0.1 according to DMRT; ns = not significant

Plant Height and Number of Tillers

The plant responded differently to water regimes and N combination treatment throughout the vegetative space (Table 3). While early growth (2-4 weeks) showed no treatment differences, plants under CF grew taller than those under AWD by 6 WAT. Among N combination treatments, the manure-reduced urea combination (F4) produced plants as tall as those receiving full N recommendation rate and high N rate with straw treatments. Unfertilized

plants (F1) remained the shortest throughout the vegetative stage. In particular, reduced N rates combined with biochar and manure (F6) resulted in intermediate plant heights but were shorter than those combined with higher N rates and manure treatments (F4).

Tiller development showed different responses to treatments during the vegetative stage at 2–8 WAT (Table 4). AWD produced more tillers than CF at 4 WAT, although this difference was not observed at 6 and 8 WAT. All treatments showed a reduction in tiller numbers after the peak growth period at 4 WAT. The combination of N treatments significantly affected tiller production at particular times of the vegetative phase. The unfertilized control (F1) had fewer tillers than the fertilized treatments throughout the vegetative stage. In particular, the reduced

Table 3
Plant height at various water regimes and N fertilizer combinations at 2-8 weeks after transplanting (WAT)

Treatment	Plant height (cm)			
	2 WAT	4 WAT	6 WAT	8 WAT
Water regime				
CF	45.02	65.97	83.56 a	103.39 a
AWD	44.70	64.58	79.70 b	99.44 b
Significance level	ns	ns	*	*
N combination ha^{-1}				
F1 (no N)	41.68	60.07	73.56 c	93.57 cd
F2 (urea 175 kg)	45.33	65.69	80.35 b	97.79 d
F3 (urea 350 kg)	44.75	64.69	80.73 ab	103.02 abc
F4 (urea 262.5 kg, manure 3 tons)	47.09	68.16	86.87 a	107.05 a
F5 (urea 525 kg, rice straw 3 tons)	45.81	68.10	85.89 ab	105.99 ab
F6 (urea 175 kg, manure 2.4 tons, biochar 0.6 tons)	44.52	64.94	82.38 ab	101.08 bc
Significance level	ns	ns	**	**

Note. Values within the same column marked with identical letters indicate no significant difference based on DMRT, ** = significantly different at 0.01, * = significantly different at 0.05, ns = not significant

Table 4
Tiller number per hill at various water regimes and N fertilizer combinations at 2-8 weeks after transplanting (WAT)

Treatment	Tiller number			
	2 WAT	4 WAT	6 WAT	8 WAT
Water regime				
CF	13.08	22.40 b	21.41	18.66
AWD	12.73	24.69 a	21.30	17.54
Significance level	ns	*	ns	ns
N combination ha^{-1}				
F1 (No N)	12.13	20.13 b	17.57 b	15.22 b
F2 (urea 175 kg)	12.75	22.69 ab	20.46 a	16.10 b

Table 4 *(continue)*

Treatment	Tiller number			
	2 WAT	4 WAT	6 WAT	8 WAT
F3 (urea 350 kg)	13.42	24.55 a	23.38 a	20.42 a
F4 (urea 262.5 kg, manure 3 tons)	13.50	25.08 a	22.77 a	18.79 a
F5 (urea 525 kg, rice straw 3 tons)	12.10	25.57 a	22.85 a	18.89 a
F6 (urea 175 kg, manure 2.4 tons, biochar 0.6 tons)	13.53	23.23 ab	21.13 a	19.18 a
Significance level	ns	*	**	**

Note. Values within the same column marked with identical letters indicate no significant difference based on DMRT, ** = significantly different at 0.01, * = significantly different at 0.05, ns = not significant

N rate treatment with manure and biochar (F6) had similar tiller numbers to the full N rate (F3) and the other organic-amended treatments (F4–F5) at 8 WAT. At 4 WAT, the treatments combining N with organic inputs (F4–F5) showed numerically higher tiller numbers than the other treatments, although statistically similar to the conventional high-N rate approach (F3) and the low-N combined with biochar and manure (F6). This suggests organic amendments can increase early tillering production without requiring full N recommended doses.

Yield Component

The water regime significantly affected panicle length but not productive tiller number, with CF producing longer panicles than AWD (Table 5). N fertilizer combinations affected both parameters, with the full N recommendation rate treatment (F3) and all that combined organic amendment treatments (F4-F6) producing more productive tillers than plots with no N or lower N rates (F1-F2), with no statistical difference among the best performing groups. For panicle length, the N-enriched treatments (F3-F6) outperformed the unfertilized control (F1), with all organic-added combinations (F4-F6) matching the performance of the conventional full N recommendation rate (F3). Particularly, the reduced N rate treatment supplemented with manure and biochar (F6) achieved an equivalent tiller number and panicle length compared to the full N rate (F3) and higher N rate fertilizer combinations (F4-F5) despite using 50% less urea than F3.

The combination of N fertilizer significantly affected all yield component parameters except 1000-seed weight, while the water regime showed no significant effect on grain characteristics (Table 6). The combination of reduced N rate with manure and biochar (F6) resulted in the number of filled grains and its percentage equivalent to the high N rate with straw treatment (F5) for filled grains and higher than the unfertilized control (F1) and some treatments with relatively lower N levels (F2, F4). In particular, all N-amended treatments except F2 and F4 matched the performance of F6 in total grain number. The 1000-seed weight remained uniform across all treatments since this study used one variety, indicating that the treatment did not affect individual grain weight.

Table 5
Number of productive tillers and panicle length at different water regimes and N fertilizer combinations

Treatment	No. productive tillers per hill	Panicle length (cm)
Water regime		
CF	12.89	20.82 a
AWD	12.89	19.98 b
Significance level	ns	*
N combination ha^{-1}		
F1 (No N)	9.61 c	19.04 b
F2 (urea 175 kg)	11.68 b	20.05 ab
F3 (urea 350 kg)	14.38 a	20.64 a
F4 (urea 262.5 kg, manure 3 tons)	13.72 a	20.88 a
F5 (urea 525 kg, rice straw 3 tons)	14.37 a	20.88 a
F6 (urea 175 kg, manure 2.4 tons, biochar 0.6 tons)	13.59 a	20.88 a
Significance level	**	*

Note. Values within the same column marked with identical letters indicate no significant difference based on DMRT, ** = significantly different at 0.01; * = significantly different at 0.05; ns = not significant

Table 6
Number of filled, unfilled, total, percentage of filled grains per panicle, and index 1000 seed at different water regimes and N fertilizer combinations

Treatment	Number of grains per panicle				Index 1000 seed (g)
	Filled	Unfilled	Total	Filled grains (%)	
Water regime					
CF	68.52	30.31	96.88	70.70	28.14
AWD	61.30	28.35	91.62	67.35	28.37
Significance level	ns	ns	ns	ns	ns
N combination ha^{-1}					
F1 (No N)	58.52 b	21.26 b	79.78 b	72.23 ab	28.07
F2 (urea 175 kg)	59.35 b	32.85 a	92.20 ab	64.29 b	27.64
F3 (urea 350 kg)	66.75 ab	34.10 a	100.84 a	66.79 ab	28.05
F4 (urea 262.5 kg, manure 3 tons)	57.52 b	33.30 a	90.82 ab	63.49 b	28.58
F5 (urea 525 kg, rice straw 3 tons)	71.82 ab	27.99 ab	99.81 a	72.26 ab	27.83
F6 (urea 175 kg, manure 2.4 tons, biochar 0.6 tons)	75.52 a	26.51 ab	102.03 a	75.13 a	29.35
Significance level	*	*	*	*	ns

Note. Values within the same column marked with identical letters indicate no significant difference based on DMRT, * = significantly different at 0.05; ns = not significant

The water regime significantly affected grain weight per panicle, with CF producing heavier grains per panicle than AWD but not grain weight per hill (Table 7). N combinations affected grain weight per panicle and hill, where treatments combining N with organic amendments (F5-F6) performed statistically equivalent to the conventional full N rate (F3) in panicle weight with higher yields compared to the unfertilized treatment (F1) and the lower N rate and manure treatments (F2, F4). In particular, F6 (lower N with manure and biochar) performed similarly to F5 (high N with straw) in both panicle and hill grain weight despite using 50% less inorganic N input. No significant differences were found in grain yield per hectare or harvest index across treatments. This result indicates that those water regimes resulting similar yields, even though AWD uses less water.

Table 7
Grain weight per panicle and hill, grain yield, and harvest index at different water regimes and N fertilizer combinations

Treatment	Grain weight (g)		Grain yield (ton ha^{-1})	Harvest index
	per panicle	per hill		
Water regime				
CF	1.84 a	13.63	4.13	0.46
AWD	1.61 b	11.70	4.11	0.45
Significance level	*	ns	ns	ns
N combination ha^{-1}				
F1 (No N)	1.56 b	9.83 b	3.54	0.43
F2 (urea 175 kg)	1.59 b	10.84 ab	4.15	0.45
F3 (urea 350 kg)	1.77 ab	14.77 ab	3.79	0.47
F4 (urea 262.5 kg, manure 3 tons)	1.53 b	10.41 ab	4.24	0.48
F5 (urea 525 kg, rice straw 3 tons)	1.89 ab	15.42 a	4.24	0.41
F6 (urea 175 kg, manure 2.4 tons, biochar 0.6 tons)	2.01 a	15.10 a	4.77	0.47
Significance level	*	*	ns	ns

Note. Values within the same column marked with identical letters indicate no significant difference based on DMRT, * = significantly different at 0.05; ns = not significant

GHG Emission

Water regime treatments significantly affected GHG emissions (Table 8). CF produced higher CH_4 emissions than AWD, while AWD produced more significant N_2O emissions than CF. Despite these opposing patterns, AWD showed a reduction in GWP relative to CF due to methane's more significant and dominant contribution to the overall GWP value.

Nitrogen management strategies showed a more limited effect on individual gas emissions. No significant differences were observed among N treatments for either CH_4 or N_2O. However, some variation in GWP was observed, with conventional high-N

Table 8
Total emissions of CH_4 and N_2O, and GWP of rice plants at different water regimes and N fertilizer combinations

Treatment	CH_4 (kg CH_4 ha^{-1})	N_2O (kg N_2O ha^{-1})	GWP (kg CO_{2eq} ha^{-1})
Water regime			
CF	148.22 a	1.62 b	4578.73 a
AWD	103.78 b	2.31 a	3518.81 b
Significance level	**	***	*z
N combination ha^{-1}			
F1 (No N)	86.04	1.6	2833.82 b
F2 (urea 175 kg)	140.94	2.0	4475.78 ab
F3 (urea 350 kg)	144.67	2.11	4609.06 a
F4 (urea 262.5 kg, manure 3 tons)	121.64	2.08	3956.72 ab
F5 (urea 525 kg, rice straw 3 tons)	145.14	2.29	4669.79 a
F6 (urea 175 kg, manure 2.4 tons, biochar 0.6 tons)	117.56	1.72	3747.82 ab
Significance level	ns	ns	*z

Note. Values within the same column marked with identical letters indicate no significant difference based on the DMRT test. *** = significantly different at 0.01; ** = significantly different at 0.05; *z = significantly different at 0.1; ns = not significant at 0.1

treatments (F3–F5) higher than the control (F1), with lower N rate treatments showing more moderate effects (F2, F4, and F6), and the unfertilized control (F1) having the lowest GWP. This trend hints at the potential to reduce GHG emissions through N fertilizer management, particularly in treatments that combine reduced inorganic N inputs with organic amendments.

Correlation Analysis

Pearson correlation analysis revealed the pattern of relationships between vegetative growth, yield components, and environmental parameters (Figure 1). Vegetative growth parameters showed time-dependent relationships with yield components. Tiller number at 8 WAT (TN8) was more strongly correlated with productive tillers (r = 0.73) and had a weak correlation with yield (r = 0.39) than earlier tiller numbers (TN2-TN6), showing that late vegetative tiller number is critical for productivity. In contrast, plant height (PH2-PH8) showed a weaker correlation with yield (r = 0.04–0.26) but a moderate correlation with panicle length (r = 0.19–0.46).

On the other hand, a significant positive relationship was observed between traits related to grain production, including filled grains (FG) along with grain weight per panicle (GPW) and grain weight per hill (GHW). These results showed that the rice's ability at the grain-filling stage substantially affected yield potential. In particular, grain weight per panicle

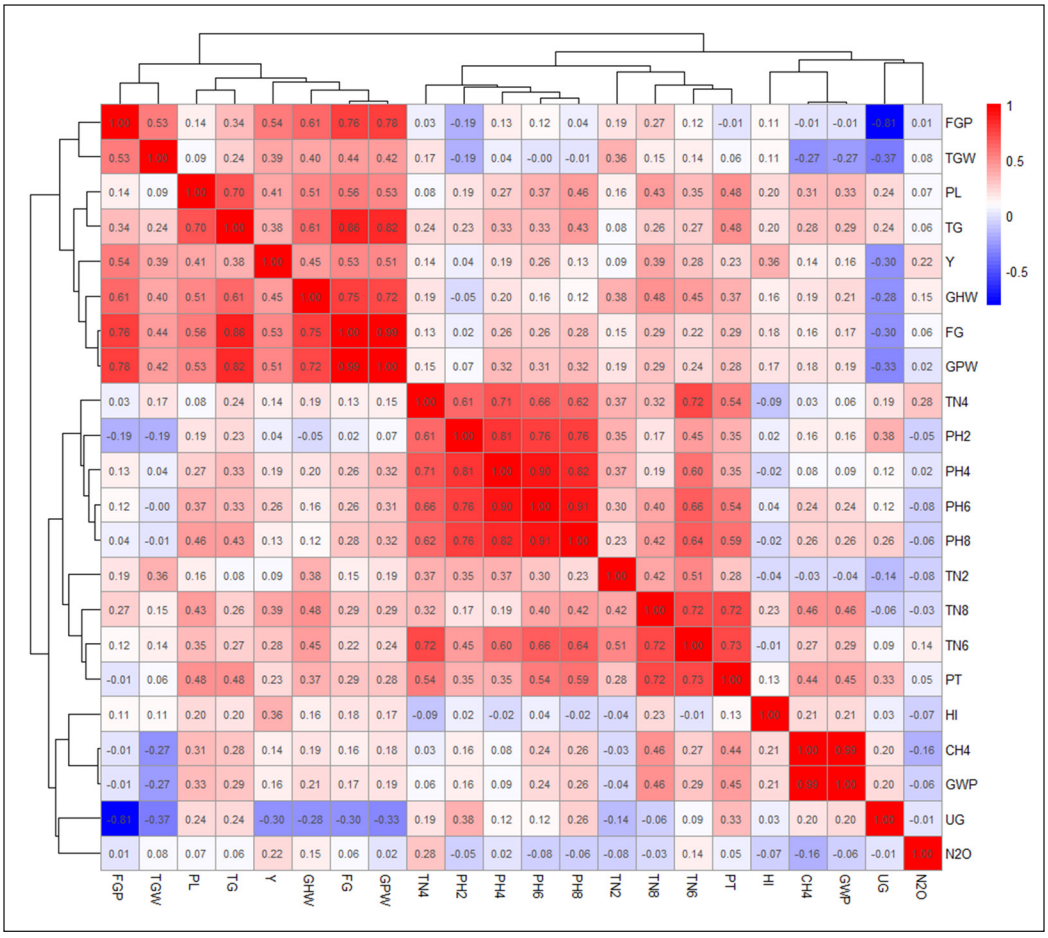

Figure 1. Correlation patterns among growth, yield, and greenhouse gas parameters of rice plants at different water regimes and N fertilizer combinations

Note. PH2 = Plant height at 2 WAT; PH4 = Plant height at 4 WAT; PH6 = Plant height at 6 WAT; PH8 = Plant height at 8 WAT; TN2 = Tiller number at 2 WAT; TN4 = Tiller number at 4 WAT: TN6 = Tiller number at 6 WAT; TN8 = Tiller number at 8 WAT; PT = Num. of productive tiller; PL = Panicle length; FG = Num of filled grain per panicle; UG = Num of unfilled grain per panicle; TG = Total num of grain per panicle; FGP = Filled grain percentage; GPW = Grain per panicle weight; GHW = Grain per hill weight; TGW = 1000 grain weight; Y = Yield per ha; HI = Harvest index; CH4 = CH_4 emission; N2O = N_2O emission; GWP = GWP

(GPW) showed a very strong correlation with FG (r = 0.99), while its relationship with yield per hectare was moderate (r = 0.51). Unfilled grain (UG) showed a slight negative correlation with grain weight (GHW/GPW; r = -0.28 to -0.33), indicating that resource allocation during grain filling is related to the source-sink balance.

GHG emissions parameter formed a separate cluster from the other clusters, showing a relatively insignificant direct relationship with morphological traits, especially in the early growth phase. However, plant height and number of tillers at 8 WAT showed an increasing

trend in the relationship with GHG emissions over time. This study also found a very strong correlation between CH_4 emissions and GWP (r = 0.99), which showed that most of the GWP contributors to lowland rice cultivation are dominated by CH_4.

DISCUSSION

Rice Growth and Yield

This study showed different responses to water regime treatments and N fertilizer combinations at different stages of growth. CF produced taller plants at 8 WAT while in the peak vegetative phase than AWD. This also happens in similar studies by Khairi et al. (2015). Other crops also show a pattern in other irrigated crops, including taro and maize (Hidayatullah et al., 2020; Ramadhani et al., 2024). However, the early tillering phase showed the opposite pattern, with AWD producing more tillers than CF at 4 WAT. This result contrasts previous reports (Khairi et al., 2015) and may indicate variability in our experimental condition in newly developed lowland land. The subsequent tillering senescence observed between 4–8 WAT, more in F3 (fully synthetic N) and F6 (organic reduced N), may indeed be related to the process of asynchronous tillering (Kariali et al., 2012) and variable of N mineralization in newly developed soils.

Water availability significantly affects panicle development through several pathways. Continuous flooding conditions in CF can increase cell elongation and nutrient uptake (Chen et al., 2024), while periodic drying in AWD may optimize resource allocation to reproductive structures. The treatment that combined a low N rate with manure and biochar (F6) resulted in comparable grain-filling performance to the increased N application rate. This led to equal filled grains and percentage of filled grains per panicle (Table 6). Organic amendments work in synergy with minimal nitrogen inputs to reduce expenses associated with inorganic nitrogen usage. Studies confirm that biochar can enhance nutrient-holding capacity (Xie et al., 2022), and manure releases nitrogen gradually for crop needs (Ebrahimi et al., 2021; Zhou et al., 2022).

The findings proved that water conservation through AWD could match conventional flooding irrigation yields and reduce water usage. Using AWD water conservation techniques helps decrease production expenses in pump irrigation systems while maintaining crop yields, leading to possible economic benefits. A study by Johnson et al. (2023) showed that AWD yield levels were sometimes lower than CF, but the results of Rahman and Bulbul (2014) showed higher yields than CF. Our study found similar yield levels between AWD and CF systems, similar to the study by Howell et al. (2015). This variation in yield is thought to be due to genotype-environment interactions, as rice exhibits plasticity in resource allocation depending on its environment (Kumar et al., 2022).

Promoting AWD Practice

Numerous studies have examined the effects of AWD on rice cultivation, but it is still an attractive area of research. The inconsistency and variability in research outcomes, mainly yield and GHG emissions under AWD, present an interesting subject for further study. Location and country-level variation in AWD performance due to differences in genetics and environment suggest further investigation. In the present research, the AWD water regime produced an insignificant difference in rice grain yield to CF (Table 7), which is in line with the findings reported by Howell et al. (2015). Nevertheless, AWD experiments often resulted in inconsistent rice yield. According to Khairi et al. (2015) and Johnson et al. (2023), AWD decreases rice yield more than conventional flooding systems, while Rahman and Bulbul (2014) reported increasing rice yield. Generally, rice yield is determined by genetic and environmental factors (Agusta et al., 2022; Dulbari et al., 2021). Kumar et al. (2022) further highlighted that rice has molecular plasticity that determines the response to environmental conditions, allowing it to adapt to environmental conditions.

In this study, AWD was recharged nine times throughout the experiment, while CF was recharged daily. In this study, AWD resulted in an estimated 62% reduction in irrigation water use compared to CF. Given that there was no significant interaction between the water regime and N treatment (Table 2), AWD presents a viable option for improving water-use efficiency in rice cultivation while maintaining yield, particularly in regions with limited water resources.

In Indonesia, lowland rice can be planted in three planting seasons in a year. However, using the continuous flooding system that farmers have widely used, the available irrigation water is usually only sufficient for two planting seasons. The transition from CF to AWD can increase water availability due to water saving, which has the potential to allow for additional planting seasons, as shown in Bangladesh (Hossain & Islam, 2022).

Moreover, AWD has shown significant potential in reducing GHG emissions from rice fields (Table 8). In the present study, GWP decreased by 23.15%, and CH_4 emissions decreased by 29.98% under AWD relative to CF. It is important to note that AWD practice increased N_2O emission by about 42.59%. Since the impact of N_2O and CH_4 relative to CO2 are 265 times and 28 times, respectively, controlling N_2O emission under AWD is important. Hassan et al. (2022) recommended many methods to mitigate N_2O emission, i.e., 1) increase soil pH by lime application, 2) reduce soil moisture by proper tillage, 3) increase soil temperature by applying bacterial population, 4) adding cereal straw with higher C:N ratio, 5) application of side banding N than broadcasting and deeper layer, 6) increase soil depth of plowing to reduce soil microorganism activity, 7) manage the proportion of sandy soil to maximize soil texture, 8) modification of irrigation system, 9) apply less tillage, 10) crop residue management, 11) use slow release N and proper amount, 12) selecting suitable fertilizers, 13) biochar application, 14) use nitrification inhibitors, 15) use organic amendments such as manure and fermented organic manure, 16) apply arbuscular

mycorrhizal fungi, 17) selecting plant genotype, 18) crop rotation, and 19) integrated nutrient management of inorganic fertilizers and organic amendment. Furthermore, Cheng et al. (2024) revealed that the selection of plowing equipment significantly decreased soil bulk density while enhancing soil redox potential and reducing GWP by 10.7-28.6%.

The significantly higher CH_4 emissions observed under CF (Table 8) can be attributed to anaerobic conditions that favor methanogenic bacteria. These bacteria do not use oxygen and produce methane as the final product. In contrast, AWD disrupts continuous anaerobic conditions, which leads to a decrease in CH_4 emission. More than 90% of CH_4 is released through plant-mediated transport via aerenchyma (Bhattacharyya et al., 2016). A recent study suggests that reducing aerenchyma formation in rice plants through genetic modification has shown potential in mitigating CH_4 emissions by limiting oxygen diffusion and altering methanotroph diversity in the rhizosphere (Iqbal et al., 2020). However, as aerenchyma is an important structure in oxygen transport to the root zone, limiting aerenchyma might affect the survival rate of rice in flooded environments.

On the other hand, AWD showed higher N_2O emissions than CF (Table 8), as alternating wet and dry conditions enhance nitrification-denitrification processes, key pathways for N_2O production. Previous studies have noted that N_2O emission increases up to 18–280% in AWD relative to CF (Liao et al., 2020; Liu et al., 2023). Nevertheless, the present research shows that AWD had 42.59% more N2O emissions but 23.15% lower GWP than CF. Other studies have reported a relatively more expansive range of GWP reductions under AWD, which ranged from 13% to 41% (Hossain & Islam, 2022; Islam et al., 2020; Pramono et al., 2022). The results show that AWD indeed can reduce GHG emissions, but the exact level of reduction cannot be ascertained.

Fertilizer Management to Mitigate GHGs

The combination of N fertilizers with organic amendments influences various effects on GHG emissions and GWP (Table 8). The GWP of the treated field (F2 to F6) was higher than the control (F1). Treatments of F3 and F5 showed the highest GWP, highlighting the substantial contribution of CH_4 emissions to the overall GWP. In contrast, F1 (control no N fertilizer) had the lowest GWP, followed by F6, which combined biochar and manure with moderate urea levels (50% of the recommended dose). Although still an early indication, biochar application can potentially reduce CH_4 and N_2O emissions.

Moreover, Hassan et al. (2022) reported that adding biochar can improve the soil's physical, biological, and chemical characteristics with a very slow decomposition process. Their study observed that biochar application was associated with lower N_2O emissions, potentially due to increased soil pH. The biochar derived from rice husks used in this research has enhanced soil carbon sequestration without significantly increasing GHG emissions (Koyama et al., 2015, 2016).

Due to high data variability (data not shown), no statistically significant differences were found between N fertilizer combination treatments for CH_4 and N_2O emissions. However, F1 tends to have a low CH_4 emission trend due to the absence of additional N and organic matter. On the other hand, a high CH_4 emission trend was found in treatments with higher N levels, such as F3 and F5 (Table 8). Li et al. (2022) also reported that increasing N fertilizer doses generally led to higher CH_4 emissions, especially at higher application rates. This increase could be attributed to the increased N input and organic matter as the substrate for methanogenesis.

Similarly, while N_2O emissions did not differ significantly among the treatments (Table 8), an increasing trend was observed from F1 to F2 to F3. At the same urea application rate (F2 vs. F6), the manure and biochar supplementation slightly reduce N_2O, though this reduction is not statistically significant. The highest N_2O emission was found in F5 (the highest level of urea application rate), indicating an increasing nitrification process. Since there is no interaction between the water regime and the N fertilizer combinations (Table 2), the F6 treatment appears promising for further evaluation due to the lower urea requirement and reduced GHG emissions. In their review, Hassan et al. (2022) emphasized that to mitigate N_2O substantially, the application of biochar at a rate larger than 5 tons ha^{-1} is common. Future studies should explore higher biochar application levels and reduced urea rates to optimize GHG mitigation.

Moreover, Table 7 shows that the F6 treatment resulted in the same grain production per hill as F5, the highest urea application rate in this study. These results suggest that reducing urea rates while combining it with organic amendments (manure and biochar) can provide the same grain production results as higher urea rates while potentially reducing GHG emissions, hence offering economic and environmental benefits. However, further long-term studies are required to confirm its effectiveness (Lee et al., 2024). Thus, incorporating biochar into fertilizer management may effectively reduce GHG emissions while reducing farmers' costs since biochar can be made from agricultural waste.

Correlation Analysis of Growth, Yield, and Emission Variables

The Pearson correlation and hierarchical clustering analysis showed the relationships between plant morphological traits, yield components, and GHG emissions (Figure 1). The dendrogram separated the variables into three main groups: (i) morphological traits, including plant height (PH) and tiller number (TN) during the vegetative stage, and (ii) yield components, such as panicle length (PL), number of productive tillers (PT), filled grains per panicle (FG), total grains per panicle (TG), grain weight per hill (GHW), and grain yield (Y). (iii) GHG emissions, including GHG emissions and GWP. Interestingly, CH_4 and N_2O emissions, as well as GWP, formed subgroups that tended to separate.

The correlation matrix showed that early plant growth variables (PH2, TN2) showed weak correlations with yield-related traits. However, the relationship between these variables and yield increased over time as the plant progressed through vegetative growth, especially for tiller number (TN) in the vegetative phase before shifting to the reproductive phase. The number of productive tillers (PT) observed before harvest showed a stronger positive correlation with filled grains per panicle (FG; r = 0.72) and grain yield (Y; r = 0.76), indicating the importance of productive tiller capacity in determining rice productivity. Previous studies have reported that the maximum tiller number is one of the main determinants of yield, with high-yielding tillers contributing significantly to yield (Martinez-Eixarch et al., 2015). In contrast, unfilled grains per panicle (UG) and grain yield (Y) had a negative correlation, indicating that fertilization failure during the anthesis phase may affect final grain yield. Thus, minimizing sterility during this phase is important to maximize the total grain yield. Therefore, ensuring optimal environmental conditions and nutrient availability minimizes sterility and maximizes yield (Raharimanana et al., 2023).

Regarding GHG emissions, CH_4 showed a strong correlation with GWP (r = 0.99), confirming its dominant role in total emissions from rice cultivation. Other studies reported that CH_4 contributes about 71.9 to 86.1% of the total GWP from the rice growing period (Naser et al., 2020). However, in this study, CH_4 had only moderate correlations with plant morphological traits, especially with late-stage vegetative phase variables such as PH8 (r = 0.42) and TN8 (r = 0.38). This suggests that methane emissions are influenced by the physiological status of rice plants at later stages, possibly due to increased aerenchyma formation that facilitates methane transport. As rice plants mature, root biomass, shoot architecture, and aerenchyma development are crucial in regulating methane production and oxidation (Rajendran et al., 2023). In contrast, N_2O emissions showed relatively weak correlations with plant growth parameters, indicating that N_2O emissions are driven more by external factors such as soil properties and N fertilization than plant traits. This underscores the importance of an integrated assessment of soil, water, and fertilization management to understand better and mitigate N_2O emissions in agricultural systems (Carbonell-Bojollo et al., 2022).

Yield-related parameters showed weak to moderate correlations with CH_4 and N_2O emissions, showing that the increase in rice yield does not necessarily result in increased emissions. This finding also showed an opportunity to optimize water and N management strategies to achieve higher yields while minimizing emissions. Strategies used in this study, such as AWD and biochar application, have a promising potential to minimize environmental impacts without yield penalties. Other studies found that practices like AWD irrigation can reduce methane emissions without yield loss (Tarlera et al., 2015), biochar enhances soil fertility and carbon sequestration (Xu et al., 2022) and optimized N

application maximizes yields while reducing yield-scaled GWP by 21% (Pittelkow et al., 2014). These findings suggest further investigation and integration with other low-emission practices to optimize sustainable rice farming.

CONCLUSION

This study found that alternate wetting and drying water regimes can reduce CH_4 emissions by 30% while at the same time increasing N_2O emissions by 43% compared to continuous flooding. However, the total GWP of alternate wetting and drying was 23% lower than that of continuous flooding, reducing the environmental impact. Most importantly, these benefits came without significantly compromising rice growth and yield and combining half the recommended urea dosage with manure 2.4 tons ha^{-1} and biochar 0.6 tons ha^{-1} produced yields comparable to conventional high-nitrogen treatments while showing the potential to reduce climate impacts. Since water regime and nitrogen fertilizer combinations had an independent effect, applying alternate wetting and drying irrigation with lower dosages of urea combined with 2.4 tons ha^{-1} and biochar 0.6 tons ha^{-1} may offer a promising approach for the sustainable reduction of GHG emissions and maintaining rice production yield. Further research on biochar's long-term benefits under local conditions needs to be investigated.

ACKNOWLEDGEMENT

We thank the Ministry of Education, Culture, Research, and Technology of the Republic of Indonesia for financial support through the PMDSU Program (Grant Numbers: 027/E5/PG.02.00.PL/2024 and 22193/IT3.D10/PT.01.03/P/B/2024). Part of this research was also supported by Rize Pte Ltd, which provided access to the GHG analysis facility and technical guidance.

REFERENCES

Agusta, H., Santosa, E., Dulbari, D., Guntoro, D., & Zaman, S. (2022). Continuous heavy rainfall and wind velocity during flowering affect rice production. *AGRIVITA Journal of Agricultural Science, 44*(2), 290-302. https://doi.org/10.17503/agrivita.v44i2.2539

Alghifari A. F., Santosa E., & Susila A. D. (2023). Growth and production of beneng taro genotypes (*Xanthosoma undipes* K. Koch) on different soil organic carbon. *Jurnal Agronomi Indonesia (Indonesian Journal of Agronomy)*, *51*(1), 17-26. https://doi.org/10.24831/ija.v51i1.44975

Ali, B. A., Hosny, M., Nassar, H. N., A. Elhakim, H. K., & El-Gendy, N. S. (2024). A study on the valorization of rice straw into different value-added products and biofuels. *International Journal of Chemical Engineering*, *2024*(1), Article 9185870. https://doi.org/10.1155/2024/9185870

Bhattacharyya, P., Roy, K. S., Das, M., Ray, S., Balachandar, D., Karthikeyan, S., Nayak, A. K., & Mohapatra, T. (2016). Elucidation of rice rhizosphere metagenome in relation to methane and nitrogen metabolism

under elevated carbon dioxide and temperature using whole genome metagenomic approach. *Science of The Total Environment, 542,* 886–898. https://doi.org/10.1016/j.scitotenv.2015.10.154

Bin Rahman, A. N. M. R., & Zhang, J. (2023). Trends in rice research: 2030 and beyond. *Food and Energy Security, 12*(2), Article e390. https://doi.org/10.1002/fes3.390

Carbonell-Bojollo, R. M., Veroz-González, Ó., González-Sánchez, E. J., Ordóñez-Fernández, R., Moreno-García, M., & Repullo-Ruibérriz de Torres, M. A. (2022). Soil management, irrigation, and fertilization strategies for N_2O emissions mitigation in Mediterranean agricultural systems. *Agronomy*, *12*(6), Article 1349. https://doi.org/10.3390/agronomy12061349

Carrijo, D. R., Lundy, M. E., & Linquist, B. A. (2017). Rice yields and water use under alternate wetting and drying irrigation: A meta-analysis. *Field Crops Research, 203,* 173–180. https://doi.org/10.1016/j.fcr.2016.12.002

Chen, R., Lu, H., Wang, Y., Tian, Q., Zhou, C., Wang, A., Feng, Q., Gong, S., Zhao, Q., & Han, B. (2024). High-throughput UAV-based rice panicle detection and genetic mapping of heading-date-related traits. *Frontiers in Plant Science, 15,* Article 1327507. https://doi.org/10.3389/fpls.2024.1327507

Cheng, S., Xing, Z., Tian, C., Liu, M., Feng, Y., & Zhang, H. (2024). Optimized tillage methods increase mechanically transplanted rice yield and reduce the greenhouse gas emissions. *Journal of Integrative Agriculture, 23*(4), 1150–1163. https://doi.org/10.1016/j.jia.2023.05.033

Du, S., Zhang, Z., Li, T., Wang, Z., Zhou, X., Gai, Z., & Qi, Z. (2022). Response of rice harvest index to different water and nitrogen management modes in the black soil region of Northeast China. *Agriculture, 12,* Article 115. https://doi.org/10.3390/agriculture12010115

Duan, F., Chyang, C.-S., Zhang, L., & Yin, S.-F. (2015). Bed agglomeration characteristics of rice straw combustion in a vortexing fluidized-bed combustor. *Bioresource Technology*, *183*, 195–202. https://doi.org/10.1016/j.biortech.2015.02.044

Dulbari, D., Santosa, E., Koesmaryono, Y., Sulistyono, E., Wahyudi, A., Agusta, H., & Guntoro, D. (2021). Local adaptation to extreme weather and its implication on sustainable rice production in Lampung, Indonesia. *AGRIVITA Journal of Agricultural Science, 43*(1), 125–136. https://doi.org/10.17503/agrivita.v43i1.2338

Ebrahimi, M., Souri, M. K., Mousavi, A., & Sahebani, N. (2021). Biochar and vermicompost improve growth and physiological traits of eggplant (*Solanum melongena* L.) under deficit irrigation. *Chemical and Biological Technologies in Agriculture*, *8*, Article 19. https://doi.org/10.1186/s40538-021-00216-9

Food and Agriculture Organization of the United Nations. (2017). *Climate-smart agriculture sourcebook: Second edition.* FAO.

Gao, R., Zhuo, L., Duan, Y., Yan, C., Yue, Z., Zhao, Z., & Wu, P. (2024). Effects of alternate wetting and drying irrigation on yield, water-saving, and emission reduction in rice fields: A global meta-analysis. *Agricultural and Forest Meteorology*, *353*, Article 110075. https://doi.org/10.1016/j.agrformet.2024.110075

Gharsallah, O., Rienzner, M., Mayer, A., Tkachenko, D., Corsi, S., Vuciterna, R., Romani, M., Ricciardelli, A., Cadei, E., Trevisan, M., Lamastra, L., Tediosi, A., Voccia, D., & Facchi, A. (2023). Economic, environmental, and social sustainability of alternate wetting and drying irrigation for rice in northern Italy. *Frontiers in Water, 5,* Article 1213047. https://doi.org/10.3389/frwa.2023.1213047

Hassan, M. U., Aamer, M., Mahmood, A., Awan, M. I., Barbanti, L., Seleiman, M. F., Bakhsh, G., Alkharabsheh, H. M., Babur, E., Shao, J., Rasheed, A., & Huang, G. (2022). Management strategies to mitigate N_2O emissions in agriculture. *Life, 12*(3), Article 439. https://doi.org/10.3390/life12030439

Hidayatullah, C. S. R., Santosa, E., Sopandie, D., & Hartono, A. (2020). Phenotypic plasticity of eddoe and dasheen taro genotypes in response to saturated water and dryland cultivations. *Biodiversitas, 21*(10)*,* 4550–4557. https://doi.org/10.13057/biodiv/d211012

Hoang, T. N., Minamikawa, K., Tokida, T., Wagai, R., Tran, T. X. P., Tran, T. H. D., & Tran, D. H. (2023). Higher rice grain yield and lower methane emission achieved by alternate wetting and drying in central Vietnam. *European Journal of Agronomy, 151,* Article 126992. https://doi.org/10.1016/j.eja.2023.126992

Hossain, M. M., & Islam, M. R. (2022). Farmers' participatory alternate wetting and drying irrigation method reduces greenhouse gas emission and improves water productivity and paddy yield in Bangladesh. *Water, 14*(7), Article 1056. https://doi.org/10.3390/w14071056

Hou, D., Meng, X., Qin, M., Zheng, E., Chen, P., Meng, F., & Zhang, C. (2024). Nitrous oxide (N_2O) emission characteristics of farmland (rice, wheat, and maize) based on different fertilization strategies. *PLOS ONE*, *19*(7), Article e0305385. https://doi.org/10.1371/journal.pone.0305385

Howell, K. R., Shrestha, P., & Dodd, I. C. (2015). Alternate wetting and drying irrigation maintained rice yields despite half the irrigation volume, but is currently unlikely to be adopted by smallholder lowland rice farmers in Nepal. *Food and Energy Security, 4*(2), 144–157. https://doi.org/10.1002/fes3.58

Iqbal, M. F., Liu, S., Zhu, J., Zhao, L., Qi, T., Liang, J., Luo, J., Xiao, X., & Fan, X. (2020). Limited aerenchyma reduces oxygen diffusion and methane emission in paddy. *Journal of Environmental Management, 279,* Article 111583. https://doi.org/10.1016/j.jenvman.2020.111583

Ishfaq, M., Farooq, M., Zulfiqar, U., Hussain, S., Akbar, N., Nawaz, A., & Anjum, S. A. (2020). Alternate wetting and drying: A water-saving and ecofriendly rice production system. *Agricultural Water Management, 241,* Article 106363. https://doi.org/10.1016/j.agwat.2020.106363

Islam, S. M. M., Gaihre, Y. K., Islam, M. R., Akter, M., Mahmud, A. A., Singh, U., & Sander, B. O. (2020). Effects of water management on greenhouse gas emissions from farmers' rice fields in Bangladesh. *Science of The Total Environment, 734,* Article 139382. https://doi.org/10.1016/j.scitotenv.2020.139382

Jia, G., Shevliakova, E., Artaxo, P., De Noblet-Ducoudré, N., Houghton, R., House, J., Kitajima, K., Lennard, C., Popp, A., Sirin, A., Sukumar, R., & Verchot, L. (2019). Land–climate interactions. In P. R. Shukla, E. Calvo Buendia, V. Masson-Delmotte, H. O. Pörtner, D. C. Roberts, & P. Zhai (Eds.), *Climate change and land: An IPCC special report on climate change, desertification, land degradation, sustainable land management, food security, and greenhouse gas fluxes in terrestrial ecosystems* (pp. 133–243). Cambridge University Press.

Johnson, K., Vo, T. T. B., Van Nha, D., & Asch, F. (2023). Genotypic responses of rice to alternate wetting and drying irrigation in the Mekong Delta. *Journal of Agronomy and Crop Science, 209*(5)*,* 593–612. https://doi.org/10.1111/jac.12649

Kariali, E., Sarangi, S., Panigrahi, R., Panda, B., & Mohapatra, P. (2012). Variation in senescence pattern of different classes of rice tillers and its effect on panicle biomass growth and grain yield. *American Journal of Plant Sciences, 3*(8)*,* 1047–1057. https://doi.org/10.4236/ajps.2012.38125

Khairi, M. Z., Nozulaidi, M., Afifah, A., Jahan, S., & Abidin, Z. U. (2015). Effect of various water regimes on rice production in lowland irrigation. *Australian Journal of Crop Science, 9*(2)*,* 153–159.

Koyama, S., Inazaki, F., Minamikawa, K., Kato, M., & Hayashi, H. (2015). Increase in soil carbon sequestration using rice husk charcoal without stimulating CH_4 and N_2O emissions in an Andosol paddy field in Japan. *Soil Science and Plant Nutrition, 61*(5), 873–884. https://doi.org/10.1080/00380768.2015.1065511

Koyama, S., Katagiri, T., Minamikawa, K., Kato, M., & Hayashi, H. (2016). Effects of rice husk charcoal application on rice yield, methane emission, and soil carbon sequestration in Andosol paddy soil. *Japan Agricultural Research Quarterly, 50*(4), 319–327. https://doi.org/10.6090/jarq.50.319

Kumar, S., Kumar, S., Krishnan, G. S., & Mohapatra, T. (2022). Molecular basis of genetic plasticity to varying environmental conditions on growing rice by dry/direct-sowing and exposure to drought stress: Insights for DSR varietal development. *Frontiers in Plant Science, 13,* Article 1013207. https://doi.org/10.3389/fpls.2022.1013207

Lampayan, R. M., Rejesus, R. M., Singleton, G. R., & Bouman, B. A. M. (2015). Adoption and economics of alternate wetting and drying water management for irrigated lowland rice. *Field Crops Research, 170,* 95–108. https://doi.org/10.1016/j.fcr.2014.10.013

Lee, H.-S., Gwon, H.-S., Lee, S.-I., Park, H.-R., Lee, J.-M., Park, D.-G., Lee, S.-R., Eom, S.-H., & Oh, T.-K. (2024). Reducing methane emissions with humic acid–iron complex in rice cultivation: Impact on greenhouse gas emissions and rice yield. *Sustainability, 16*(10)*,* Article 4059. https://doi.org/10.3390/su16104059

Li, X., Jiang, J., Guo, J., McClung, A. M., Chen, K., Velarca, M. V., Torbert, H. A., & Dou, F. (2022). Effect of nitrogen application rate under organic and conventional systems on rice (*Oryza sativa* L.) growth, grain yield, soil properties, and greenhouse gas emissions. *Journal of Plant Nutrition, 46*(8), 1627–1649. https://doi.org/10.1080/01904167.2022.2093746

Liao, B., Wu, X., Yu, Y., Luo, S., Hu, R., & Lu, G. (2020). Effects of mild alternate wetting and drying irrigation and mid-season drainage on CH_4 and N_2O emissions in rice cultivation. *Science of The Total Environment, 698,* Article 134212. https://doi.org/10.1016/j.scitotenv.2019.134212

Liu, Z., Zhang, W., Ma, R., Li, S., Song, K., Zheng, J., Wang, Y., Bian, R., Zhang, X., & Pan, G. (2023). Biochar-plant interactions enhance nonbiochar carbon sequestration in a rice paddy soil. *Communications Earth and Environment, 4,* Article 494. https://doi.org/10.1038/s43247-023-01155-z

Livsey, J., Kätterer, T., Vico, G., Lyon, S. W., Lindborg, R., Scaini, A., Da, C. T., & Manzoni, S. (2019). Do alternative irrigation strategies for rice cultivation decrease water footprints at the cost of long-term soil health? *Environmental Research Letters, 14*(7)*,* Article 074011. https://doi.org/10.1088/1748-9326/ab2108

Mallareddy, M., Thirumalaikumar, R., Balasubramanian, P., Naseeruddin, R., Nithya, N., Mariadoss, A., Eazhilkrishna, N., Choudhary, A. K., Deiveegan, M., Subramanian, E., Padmaja, B., & Vijayakumar, S. (2023). Maximizing water use efficiency in rice farming: A comprehensive review of innovative irrigation management technologies. *Water*, *15*(10), Article 1802. https://doi.org/10.3390/w15101802

Martinez-Eixarch, M., Català, M. del M., Tomàs, N., Pla, E., & Zhu, D. (2015). Tillering and yield formation of a temperate Japonica rice cultivar in a Mediterranean rice agrosystem. *Spanish Journal of Agricultural Research*, *13*(4), Article e0905. https://doi.org/10.5424/sjar/2015134-7085

Naser, H. M., Nagata, O., Sultana, S., & Hatano, R. (2020). Carbon sequestration and contribution of CO_2, CH_4 and N_2O fluxes to global warming potential from paddy-fallow fields on mineral soil beneath peat in Central Hokkaido, Japan. *Agriculture*, *10*(1), Article 6. https://doi.org/10.3390/agriculture10010006

Pittelkow, C. M., Adviento-Borbe, M. A., Hill, J. E., & Linquist, B. A. (2014). Optimizing rice yields while minimizing yield-scaled global warming potential. *Global Change Biology*, *20*(5), 1382-1393. https://doi.org/10.1111/gcb.12413

Pramono, A., Adriany, T. A., & Susilawati, H. L., Jumari, & Yunianti, I. F. (2022). Alternate wetting and drying combined farmyard manure for reducing greenhouse gas while improving rice yield. *IOP Conference Series: Earth and Environmental Science, 950,* Article 012012. https://doi.org/10.1088/1755-1315/950/1/012012

Raharimanana, V., Yamaguchi, T., Tsujimoto, Y., Oo, A. Z., Nishigaki, T., Rakotonindrina, H., & Katsura, K. (2023). A machine learning approach is effective to elucidate yield-limiting factors of irrigated lowland rice under heterogeneous growing conditions and management practices. *Field Crops Research*, *304*, Article 109170. https://doi.org/10.1016/j.fcr.2023.109170

Rahman, M. R., & Bulbul, S. H. (2014). Effect of alternate wetting and drying (AWD) irrigation for Boro rice cultivation in Bangladesh. *Agriculture, Forestry and Fisheries, 3*(2), 86–92. https://doi.org/10.11648/j.aff.20140302.16

Rajendran, S., Park, H., Kim, J., Park, S. J., Shin, D., Lee, J.-H., Song, Y. H., Paek, N., & Kim, C. M. (2023). Methane emission from rice fields: Necessity for molecular approach for mitigation. *Rice Science, 31*(2), 159–178. https://doi.org/10.1016/j.rsci.2023.10.003

Ramadhani, R. P., Santosa, E., & Purwono. (2024). Growth and water-needs analysis of sweet corn and peanuts in different cropping systems. *Jurnal Agronomi Indonesia (Indonesian Journal of Agronomy), 52*(2), 151–162. https://doi.org/10.24831/jai.v52i2.57440

Setyanto, P., Pramono, A., Adriany, T. A., Susilawati, H. L., Tokida, T., Padre, A. T., & Minamikawa, K. (2018). Alternate wetting and drying reduces methane emission from a rice paddy in Central Java, Indonesia without yield loss. *Soil Science and Plant Nutrition, 64*(1), 23–30. https://doi.org/10.1080/00380768.2017.1409600

Souri, M. K., & Hatamian, M. (2019). Aminochelates in plant nutrition: a review. *Journal of Plant Nutrition*, *42*(1), 67–78. https://doi.org/10.1080/01904167.2018.1549671

Sudarsono, W. A., Melati, M., & Aziz, S. A. (2014). Growth and yield of organic rice with cow manure application in the first cropping season. *AGRIVITA Journal of Agricultural Science, 36*(1), 19–25. https://doi.org/10.17503/agrivita.v36i1.334

Sun, J., Chen, L., Ogle, S., Cheng, K., Xu, X., Li, Y., & Pan, G. (2023). Future climate change may pose pressures on greenhouse gas emission reduction in China's rice production. *Geoderma, 440,* Article 116732. https://doi.org/10.1016/j.geoderma.2023.116732

Susanti, W. I., Cholidah, S. N., & Agus, F. (2024). Agroecological nutrient management strategy for attaining sustainable rice self-sufficiency in Indonesia. *Sustainability*, *16*(2), Article 845. https://doi.org/10.3390/su16020845

Tarlera, S., Capurro, M. C., Irisarri, P., Scavino, A. F., Cantou, G., & Roel, A. (2015). Yield-scaled global warming potential of two irrigation management systems in a highly productive rice system. *Scientia Agricola*, *73*(1), 43–50. https://doi.org/10.1590/0103-9016-2015-0050

Wang, X., Chang, X., Libang, M., Bai, J., Liang, M., & Yan, S. (2023). Global and regional trends in greenhouse gas emissions from rice production, trade, and consumption. *Environmental Impact Assessment Review, 101,* Article 107141. https://doi.org/10.1016/j.eiar.2023.107141

Xie, Z., Shah, F., & Zhou, C. (2022). Combining rice straw biochar with leguminous cover crop as green manure and mineral fertilizer enhances soil microbial biomass and rice yield in South China. *Frontiers in Plant Science, 13,* Article 778738. https://doi.org/10.3389/fpls.2022.778738

Xu, Q., Wang, J., Liu, Q., Chen, Z., Jin, P., Du, J., Fan, J., Yin, W., Xie, Z., & Wang, X. (2022). Long-term field biochar application for rice production: effects on soil nutrient supply, carbon sequestration, crop yield and grain minerals. *Agronomy*, *12*(8), Article 1924. https://doi.org/10.3390/agronomy12081924

Yan, C., Yan, S.-S., Jia, T.-Y., Dong, S.-K., Ma, C.-M., & Gong, Z.-P. (2019). Decomposition characteristics of rice straw returned to the soil in northeast China. *Nutrient Cycling in Agroecosystem*, *114*, 211–224. https://doi.org/10.1007/s10705-019-09999-8

Zhang, S., Sun, L., Wang, Y., Fan, K., Xu, Q., Li, Y., Ma, Q., Wang, J., Ren, W., & Ding, Z. (2020). Cow manure application effectively regulates the soil bacterial community in tea plantation. *BMC Microbiology*, *20*, Article 190. https://doi.org/10.1186/s12866-020-01871-y

Zhou, W., Yan, F., Chen, Y., & Ren, W. (2022). Optimized nitrogen application increases rice yield by improving the quality of tillers. *Plant Production Science*, *25*(3), 311–319. https://doi.org/10.1080/1343943X.2022.2061538

Pertanika J. Trop. Agric. Sci. 48 (6): 2007 - 2032 (2025)

PERTANIKA JOURNALS

TROPICAL AGRICULTURAL SCIENCE

Journal homepage: http://www.pertanika.upm.edu.my/

Species Composition of Bee and Non-bee Hymenoptera as Effective and Less Effective Pollinators in the Tengku Hassanal Wildlife Reserve Forest, Pahang, Malaysia, with New Insights from DNA Barcoding

Muhamad Ikhwan Idris[1,2], Suhainah Pejalis[3], Aqilah Sakinah Badrulisham[1], Fahimee Jaapar[4], and Salmah Yaakop[1]*

[1]Centre for Insect Systematics, Faculty of Science and Technology, Universiti Kebangsaan Malaysia, 43600 Bangi, Selangor, Malaysia
[2]Centre for Pre-University Studies, Universiti Malaysia Sarawak, 94300 Kota Samarahan, Sarawak, Malaysia
[3]Tengku Hassanal Wildlife Reserve, Department of Wildlife and National Parks, Bukit Rengit, 28500 Lanchang, Pahang, Malaysia
[4]Agrobiodiversity and Environment Research Centre, MARDI Headquarters, 43400 Serdang, Selangor Malaysia; Agrobiodiversity and Environment Research Centre, MARDI Headquarters, 43400 Serdang, Selangor Malaysia

ABSTRACT

The species composition of bee and non-bee Hymenoptera in the Tengku Hassanal Wildlife Reserve (THWR) Forest, Pahang, Malaysia, was studied to document their diversity and to explore their relatedness using DNA barcoding of the cytochrome c oxidase subunit I (*COI*) region inferred by Neighbour-Joining tree. DNA of 56 specimens were successfully extracted from the trapping between February 2023 and January 2024 by using 12 malaise traps. The collection represents 34 species from 33 genera across 11 families; eight families identified as an effective pollinators (Apidae, Halictidae, Liopteridae, Tenthredinidae, Crabronidae, Pompilidae, Tiphiidae and Vespidae), while three families were classified as less effective pollinators (Braconidae, Evaniidae, and Ichneumonidae). Unique DNA sequences revealed limited or no matches in global databases, highlighting Malaysia's underexplored hymenopteran diversity. This study provides essential baseline data on pollinator diversity, emphasizing the roles of effective pollinators (*Apis cerana*, *Tetrigona apicalis*) and less effective pollinators (e.g., parasitoid wasps) through flower visitation in sustaining ecosystem stability. The inclusion

ARTICLE INFO

Article history:
Received: 21 February 2025
Accepted: 24 October 2025
Published: 25 November 2025

DOI: https://doi.org/10.47836/pjtas.48.6.18

E-mail addresses:
mikhwanidris@gmail.com (Muhamad Ikhwan Idris)
suhainah@wildlife.gov.my (Suhainah Pejalis)
aqilah.sakinah01@gmail.com (Aqilah Sakinah Badrulisham)
miesre@mardi.gov.my (Fahimee Jaapar)
salmah78@ukm.edu.my (Salmah Yaakop)
*Corresponding author

of genetic tools alongside morphological approaches offers valuable insights for biodiversity conservation and highlights the global importance of preserving tropical ecosystems.

Keywords: Biodiversity conservation, DNA barcoding, Hymenoptera diversity, pollinators, tropical ecosystems

INTRODUCTION

The order Hymenoptera which includes bees, wasps, ants, and sawflies, represents one of the most diverse and ecologically significant insect groups globally (Blaimer et al., 2023). While bees are critical pollinators in natural and agricultural ecosystems, other hymenopterans such as parasitoid wasps support pest control and ecosystem stability (Khalifa et al., 2021). However, knowledge of hymenopteran biodiversity remains limited, particularly in tropical regions like Malaysia. This underscores the need for comprehensive studies on both bee and non-bee species to better understand their ecological roles and conservation needs, especially regarding their function as pollinators.

Numerous studies in Malaysia have catalogued hymenopteran pollinators species for forest trees (Idris et al., 2023; Lee et al., 2002; Nagamitsu et al., 1999; Santos et al., 2022) and from agricultural crops (Azmi et al., 2017; Fahimee et al., 2021). Most of the studies conducted in Malaysia focus on other insect groups such as moths, butterflies, beetles, flies, and also hymenopteran species, which include bees and ants as important pollinators (Momose et al., 1998; Pfeiffer et al., 2011). Some parasitoids, particularly those from the families Ichneumonidae and Braconidae, play a role as less effective pollinators. However, their function as pollinators cannot be ignored as bees and wasps have comparable pollination activities (Borchardt et al., 2024).

DNA barcoding data remain scarce for hymenopteran species, particularly in Malaysia and minimally covered in existing publications. Generally, most identifications conducted use morphological identification and field observations, which may lead to misidentification. Although morphological identification is commonly used as an initial approach, it is time-consuming compared to DNA barcoding (Chan et al., 2014; Schenk et al., 2020).

The longer approach to morphological identification persists due to the scarcity of hymenopteran taxonomists and the lack of comprehensive taxonomic keys for Malaysian species. Interestingly, molecular identification offers a rapid and precise method for taxonomic resolution (Schenk et al., 2020; Tahir et al., 2018). Additionally, it provides genetic baseline data for advanced analyses, such as diet assessment using Next-Generation Sequencing (NGS) for metabarcoding analysis of *trnL*, contributing to a better understanding of the functional role of hymenopterans as pollinators of forest trees (Bell et al., 2017; Namin et al., 2022).

Malaysia's tropical forests, including the Tengku Hassanal Wildlife Reserve (THWR) in Pahang, are home to a rich diversity of Hymenoptera species. THWR serves as a model

site for studying the natural dynamics of these pollinators and their interactions with forest trees. The underexplored hymenopteran diversity in THWR can act as a bioindicator for forest health (Catalano et al., 2024) and provide indirect insights into herbivorous wildlife populations. Documenting this diversity is crucial for understanding ecological contributions and informing conservation efforts. Therefore, this study aims to identify the species composition of hymenopteran pollinators and to barcode all species collected from THWR.

MATERIALS AND METHODS

Sampling Location

The hymenopteran samplings were conducted at the model forest, THWR, located at the east coast of Peninsular Malaysia (Figure 1). It covers approximately 60,551.608 hectares. Four locations were chosen as the sampling sites, namely Lembah Klau (LK), Bukit Rengit (BR), Kuala Lompat (KL), and Perlok (PP) (Table 1). These sites were strategically chosen to represent the northern, southern, easthern and western regions of the forest, to get the holistic view of the hymenopteran species diversity within the area.

Sample Collection and Identification

Three malaise traps were placed at each location in the THWR for hymenopteran samples collection (Table 1), making a total of 12 traps. The traps were left for 12 months, from February 2023 to January 2024. The samples were preserved in 70% ethanol for the molecular work.

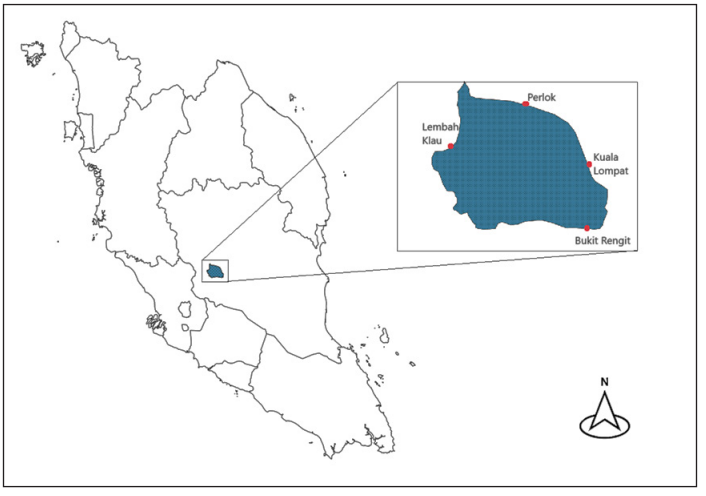

Figure 1. Map of Tengku Hassanal Wildlife Reserve (THWR), Pahang, Malaysia
Source: Author's own work

Table 1
List of locality, Global Positioning System (GPS) coordinates and the type of ecosystem for all study sites

Sample code	Location	Grid	Ecosystem
LK	Lembah Klau	03°41.354'N, 102°1.196'E	Lowland dipterocarp forest
BR	Bukit Rengit	03°35.580'N, 102°10.817' E	Lowland dipterocarp forest
KL	Kuala Lompat	03°42.957'N, 102°17.286'E	Lowland dipterocarp forest, Riverine
PP	Perlok	03°50.544'N, 102°12.234'E	Lowland dipterocarp forest

Morphological Identification

All hymenopteran samples were identified using a stereomicroscope (StemiD4, Zeiss, Germany). Identification was done based on the morphological characteristics of the hymenopteran species following species key provided by Goulet and Huber (1993), Michener (2007) and Van Noort and Broad (2024). The morphological identification was conducted prior to DNA barcoding analysis.

Digital Photograph of Specimens

A comprehensive observation was conducted on adult samples by using a StemiD4 stereomicroscope (Carl Zeiss, Germany) and a Dino-Lite digital microscope to facilitate detailed species identification. Detailed habitus images of the samples were acquired utilising a ZEISS SteREO Discovery V20 stereomicroscope with AxioCam MR ToupTek software.

Species Record and Their Pollination Detection

All identified species, based on morphological characters were listed up to species level where applicable in a table to illustrate the diversity of the sampled hymenopteran pollinator species from THWR. Their functional role as pollinators (effective and less effective) were confirmed based only on published literatures (Klein et al., 2019; Michener, 2007; Rader et al., 2020; Stavert et al., 2016; Van Noort & Broad, 2024; Wojcik, 2021; Yokota et al., 2024).

DNA Extraction and Amplification

Identification was further confirmed through DNA barcoding analysis. The samples were extracted using NucleoSpin DNA Insect Kit (Macherey-Nagel) and DNeasy Blood and Tissue Kit (Qiagen) following manufacturer's protocol with slight modification according to Mohammed et al. (2017) and Yaakop et al. (2013). The extraction was then amplified through Polymerase Chain Reaction (PCR) by targeting cytochrome c oxidase subunit I (*COI*) with universal forward primer LCO1490 (GGTCAACAAATCATAAAGATATTGG) and reverse primer HCO2198 (TAAACTTCAGGGTGACCAAAAAATCA) (Folmer et al., 1994). The amplification was performed under the following protocol: initial denaturation of 95°C for 3 min, followed by 35 cycles of denaturation at 95°C for 30 s, primer annealing

ranged from 42-55°C depending on the species for 30 s and extension at 72°C for 30 s, with final elongation at 72°C for 5 min (Fahimee et al., 2021; Idris et al., 2023).

Sequencing, Aligning and BLAST Analysis

All PCR products were sent to Apical Scientific Sdn. Bhd., Selangor, Malaysia for sequencing. The obtained sequences were edited using Sequencher 5.4.6 by Gene Codes Corporation. The resulting datasets were manually and automatically aligned using MEGA version 11 (Kumar et al., 2016). Basic Local Alignment Search Tool (BLAST) (Altschul et al., 1990) was used to compare the sequences with other sequences available in the GenBank database.

Tree Reconstruction

The species separation was visualised by implementing distance-based criteria through Neighbour-Joining (NJ) analysis using PAUP version 4.0 (Swofford, 2003). The distance-based method using the Kimura 2-parameter model with 1000 replications of the bootstrap analysis was selected.

RESULTS

Species Composition and Species Richness

A total of 56 individuals of hymenopteran pollinators were collected from THWR throughout the sampling duration, comprising eleven families. 34 species under 33 genera from families of Apidae, Crabronidae, Halictidae, Pompilidae, Tiphiidae, Vespidae, Braconidae, Evaniidae, Ichneumonidae, Liopteridae and Tenthredinidae were recorded and presented in Table 2. The largest family comprising the largest number of species belong to Ichneumonidae (22%) while Halictidae and Tenthredinidae had the lowest record, each comprising only 2% of the total. The species composition and richness are illustrated in Figure 2.

Table 2
List of species, genera and families collected from the samplings identified based on morphological characters

No.	Sample code	Family	Subfamily	Genus	Species
1	KL13	Apidae		*Apis*	*Apis cerana*
2	KL15	Apidae		*Apis*	*Apis cerana*
3	KL16	Apidae		*Apis*	*Apis cerana*
4	PP24	Apidae		*Lepidotrigona*	*Lepidotrigona terminata*
5	BR12	Apidae		*Tetragonilla*	*Tetragonilla collina*
6	BR3	Apidae		*Tetrigona*	*Tetrigona apicalis*

Table 2 *(continue)*

No.	Sample code	Family	Subfamily	Genus	Species
7	BR4	Apidae		*Tetrigona*	*Tetrigona apicalis*
8	BR5	Apidae		*Tetrigona*	*Tetrigona apicalis*
9	KL3	Crabronidae	Crabroninae	*Ectemnius*	*Ectemnius* sp.
10	BR14	Crabronidae	Crabroninae	*Liris*	*Liris* sp.
11	BR18	Crabronidae	Crabroninae	*Lyroda*	*Lyroda subita*
12	LK16	Crabronidae	Crabroninae	*Rhopalum*	*Rhopalum clavipes*
13	BR7	Halictidae	Nomiinae	*Nomia*	*Nomia strigata*
14	KL1	Pompilidae	Pepsinae	*Auplopus*	*Auplopus* sp.
15	KL2	Pompilidae	Pepsinae	*Auplopus*	*Auplopus* sp.
16	LK10	Pompilidae		*Leptodialepis*	*Leptodialepis ceylonica*
17	LK3	Tiphiidae		*Tiphia*	*Tiphia* sp. 1
18	PP10	Tiphiidae		*Tiphia*	*Tiphia* sp. 1
19	PP16	Tiphiidae		*Tiphia*	*Tiphia* sp. 2
20	PP18	Tiphiidae		*Tiphia*	*Tiphia* sp. 1
21	PP15	Vespidae	Eumeninae	*Euodynerus*	*Euodynerus* sp.
22	BR24	Vespidae	Stenogastrinae	*Liostenogaster*	*Liostenogaster flavolineata*
23	BR11	Vespidae		*Polistes*	*Polistes* sp.
24	BR15	Vespidae		*Polistes*	*Polistes* sp.
25	BR17	Vespidae		*Polistes*	*Polistes* sp.
26	BR9	Vespidae		*Polistes*	*Polistes* sp.
27	BR13	Vespidae	Polistinae	*Polybioides*	*Polybioides* sp.
28	BR21	Vespidae	Polistinae	*Polybioides*	*Polybioides* sp.
29	BR22	Vespidae	Polistinae	*Polybioides*	*Polybioides* sp.
81	KL11	Vespidae	Polistinae	*Polybioides*	*Polybioides* sp.
31	LK14	Vespidae	Polistinae	*Polybioides*	*Polybioides* sp.
32	KL12	Vespidae		*Stenodyneriellus*	*Stenodyneriellus similiguttulatus*
33	BR38	Braconidae	Rogadinae	*Aleiodes*	*Aleiodes procoronarius*
34	BR39	Braconidae	Rogadinae	*Aleiodes*	*Aleiodes procoronarius*
35	BR29	Braconidae	Microgastrinae	*Choeras*	*Choeras* sp.
36	BR30	Braconidae	Microgastrinae	*Choeras*	*Choeras* sp.
37	BR32	Braconidae	Microgastrinae	*Neoclarkinella*	*Neoclarkinella* sp.
38	BR20	Braconidae	Braconinae	*Syntomernus*	*Syntomernus* sp.
39	LK2	Evaniidae		*Prosevania*	*Prosevania* sp.
40	LK20	Evaniidae		*Prosevania*	*Prosevania* sp.
41	BR28	Evaniidae		*Zeuxevania*	*Zeuxevania* sp.
42	BR33	Ichneumonidae		*Acrolyta*	*Acrolyta* sp.
43	BR25	Ichneumonidae	Orthocentrinae	*Aperileptus*	*Aperileptus* sp.

Table 2 *(continue)*

No.	Sample code	Family	Subfamily	Genus	Species
44	BR19	Ichneumonidae	Campopleginae	*Hyposoter*	*Hyposoter* sp.
45	BR23	Ichneumonidae			Ichneumonidae sp.
46	BR26	Ichneumonidae			Ichneumonidae sp.
47	BR27	Ichneumonidae	Acaenitinae	*Jezarotes*	*Jezarotes* sp.
48	KL10	Ichneumonidae	Cryptinae	Cryptinae	Cryptinae sp.
49	BR36	Ichneumonidae	Orthocentrinae	*Orthocentrus*	*Orthocentrus* sp.
50	BR34	Ichneumonidae	Orthocentrinae	*Plectiscus*	*Plectiscus callidulus*
51	BR35	Ichneumonidae	Orthocentrinae	*Plectiscus*	*Plectiscus callidulus*
52	BR37	Ichneumonidae	Orthocentrinae	*Plectiscus*	*Plectiscus callidulus*
53	BR40	Ichneumonidae	Orthocentrinae	*Plectiscus*	*Plectiscus callidulus*
54	LK7	Liopteridae		*Paramblynotus*	*Paramblynotus* sp.
55	PP17	Liopteridae		*Paramblynotus*	*Paramblynotus* sp.
56	BR2	Tenthredinidae	Heterarthrinae	*Caliroa*	*Caliroa* sp.

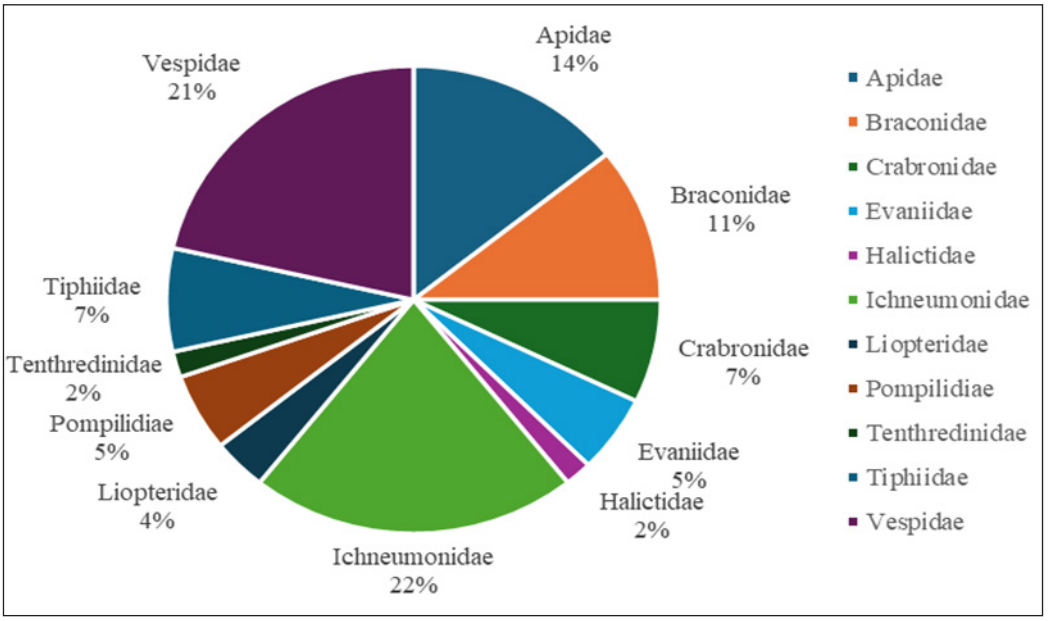

Figure 2. Family composition for the Hymenopteran pollinators collected from Tengku Hassanal Wildlife Reserve (THWR), Pahang, Malaysia

DNA Barcode Information

All 56 morphologically identified samples were barcoded using *COI* marker. The BLAST results and accession numbers obtained from GenBank are listed in Table 3.

Table 3
List of barcoded species along with their maximum score, total score, query coverage, E-value, similarity percentage, and accession number, including the additional GenBank sequences used in the phylogenetic analysis

No.	Sample code	Locality	Family	Subfamily	Maximum Score	Total Score	Query cover (%)	e-value	Similarity Percentage (%)	GenBank Accession number	Species Identified
1	KL13	Malaysia: Pahang, Kuala Lompat	Apidae		1118	1118	86	0	99.52	PQ788155	*Apis cerana*
2	KL15	Malaysia: Pahang, Kuala Lompat	Apidae		1118	1118	86	0	99.52	PQ788154	*Apis cerana*
3	KL16	Malaysia: Pahang, Kuala Lompat	Apidae		1118	1118	87	0	99.52	PQ788153	*Apis cerana*
4	PP24	Malaysia: Pahang, Perlok	Apidae		707	766	83	0	86.36	PQ815050	*Lepidotrigona terminata*
5	BR12	Malaysia: Pahang, Bukit Rengit	Apidae		789	789	72	0	93.67	PQ815047	*Tetragonilla collina*
6	BR3	Malaysia: Pahang, Bukit Rengit	Apidae		919	919	88	0	92.14	PQ788158	*Tetrigona apicalis*
7	BR4	Malaysia: Pahang, Bukit Rengit	Apidae		992	992	89	0	94.28	PQ788156	*Tetrigona apicalis*
8	BR5	Malaysia: Pahang, Bukit Rengit	Apidae		923	923	88	0	92.27	PQ788157	*Tetrigona apicalis*

Table 3 *(continue)*

No.	Sample code	Locality	Family	Subfamily	Maximum Score	Total Score	Query cover (%)	e-value	Similarity Percentage (%)	GenBank Accession number	Species Identified
9	KL3	Malaysia: Pahang, Kuala Lompat	Crabronidae	Crabroninae	748	748	84	0	87.36	OR782830.1	*Ectemnius* sp.
10	BR14	Malaysia: Pahang, Bukit Rengit	Crabronidae	Crabroninae	1183	1183	94	0	98.67	PQ827100	*Liris* sp.
11	BR18	Malaysia: Pahang, Bukit Rengit	Crabronidae	Crabroninae	820	820	87	0	89.1	PQ827101	*Lyroda subita*
12	LK16	Malaysia: Pahang, Lembah Klau	Crabronidae	Crabroninae	893	893	91	0	90.15	PQ788160	*Rhopalum clavipes*
13	BR7	Malaysia: Pahang, Bukit Rengit	Halictidae	Nomiinae	1145	1145	95	0	96.94	PQ834802	*Nomia strigata*
14	KL1	Malaysia: Pahang, Kuala Lompat	Pompilidae	Pepsinae	612	612	91	2.00E-170	81.04	PQ827097	*Auplopus* sp.
15	KL2	Malaysia: Pahang, Kuala Lompat	Pompilidae	Pepsinae	900	900	98	0	88.65	PQ800421	*Auplopus* sp.
16	LK10	Malaysia: Pahang, Lembah Klau	Pompilidae		900	900	86	0	92.37	PQ800422	*Leptodialepis ceylonica*

Table 3 *(continue)*

No.	Sample code	Locality	Family	Subfamily	Maximum Score	Total Score	Query cover (%)	e-value	Similarity Percentage (%)	GenBank Accession number	Species Identified
17	LK3	Malaysia: Pahang, Lembah Klau	Tiphiidae		820	820	92	0	87.8	PQ800426	*Tiphia* sp. 1
18	PP10	Malaysia: Pahang, Perlok	Tiphiidae		810	810	90	0	87.81	PQ800425	*Tiphia* sp. 1
19	PP16	Malaysia: Pahang, Perlok	Tiphiidae		812	812	81	0	90.77	PQ800424	*Tiphia* sp. 2
20	PP18	Malaysia: Pahang, Perlok	Tiphiidae		708	708	79	0	86.94	PQ800423	*Tiphia* sp. 1
21	PP15	Malaysia: Pahang, Perlok	Vespidae	Eumeninae	1137	1137	88	0	99.69	PQ800408	*Euodynerus* sp.
22	BR24	Malaysia: Pahang, Bukit Rengit	Vespidae	Stenogastrinae	886	886	91	0	89.97	PQ800409	*Liostenogaster flavolineata*
23	BR11	Malaysia: Pahang, Bukit Rengit	Vespidae		752	752	88	0	86.49	PQ827095	*Polistes* sp.
24	BR15	Malaysia: Pahang, Bukit Rengit	Vespidae		747	747	88	0	86.33	PQ800412	*Polistes* sp.
25	BR17	Malaysia: Pahang, Bukit Rengit	Vespidae		780	780	91	0	86.34	PQ827096	*Polistes* sp.

Table 3 *(continue)*

No.	Sample code	Locality	Family	Subfamily	Maximum Score	Total Score	Query cover (%)	e-value	Similarity Percentage (%)	GenBank Accession number	Species Identified
26	BR9	Malaysia: Pahang, Bukit Rengit	Vespidae		719	719	92	0	84.19	PQ800413	*Polistes* sp.
27	BR13	Malaysia: Pahang, Bukit Rengit	Vespidae	Polistinae	775	775	86	0	87.26	PQ819650	*Polybioides* sp.
28	BR21	Malaysia: Pahang, Bukit Rengit	Vespidae	Polistinae	765	765	86	0	87.03	PQ819651	*Polybioides* sp.
29	BR22	Malaysia: Pahang, Bukit Rengit	Vespidae	Polistinae	784	784	85	0	87.58	PQ800411	*Polybioides* sp.
81	KL11	Malaysia: Pahang, Kuala Lompat	Vespidae	Polistinae	780	780	85	0	87.42	OR782831.1	*Polybioides* sp.
31	LK14	Malaysia: Pahang, Lembah Klau	Vespidae	Polistinae	775	775	86	0	87.26	PQ800410	*Polybioides* sp.
32	KL12	Malaysia: Pahang, Kuala Lompat	Vespidae		1110	1110	88	0	98.74	OR782829.1	*Stenodyneriellus similiguttulatus*
33	BR38	Malaysia: Pahang, Bukit Rengit	Braconidae	Rogadinae	1011	1011	81	0	98.29	PQ800415	*Aleiodes procoronarius*

Table 3 *(continue)*

No.	Sample code	Locality	Family	Subfamily	Maximum Score	Total Score	Query cover (%)	e-value	Similarity Percentage (%)	GenBank Accession number	Species Identified
34	BR39	Malaysia: Pahang, Bukit Rengit	Braconidae	Rogadinae	1009	1009	81	0	98.29	PQ800414	*Aleiodes procoronarius*
35	BR29	Malaysia: Pahang, Bukit Rengit	Braconidae	Microgastrinae	1187	1187	81	0	100	PQ800417	*Choeras* sp.
36	BR30	Malaysia: Pahang, Bukit Rengit	Braconidae	Microgastrinae	1010	1010	78	0	99.82	PQ800416	*Choeras* sp.
37	BR32	Malaysia: Pahang, Bukit Rengit	Braconidae	Microgastrinae	839	839	88	0	89.32	PQ800418	*Neoclarkinella* sp.
38	BR20	Malaysia: Pahang, Bukit Rengit	Braconidae	Braconinae	878	878	83	0	89.98	PQ800419	*Syntomernus* sp.
39	LK2	Malaysia: Pahang, Lembah Klau	Evaniidae		680	680	97	0	81.6	PQ827103	*Prosevania* sp.
40	LK20	Malaysia: Pahang, Lembah Klau	Evaniidae		575	575	96	5.00E-159	78.44	PQ845697	*Prosevania* sp.
41	BR28	Malaysia: Pahang, Bukit Rengit	Evaniidae		604	604	87	1.00E-167	79.48	PQ800420	*Zeuxevania* sp.
42	BR33	Malaysia: Pahang, Bukit Rengit	Ichneumonidae	-	860	860	91	0	87.8	PQ827102	*Acrolyta* sp.

Table 3 *(continue)*

No.	Sample code	Locality	Family	Subfamily	Maximum Score	Total Score	Query cover (%)	e-value	Similarity Percentage (%)	GenBank Accession number	Species Identified
43	BR25	Malaysia: Pahang, Bukit Rengit	Ichneumonidae	Orthocentrinae	786	786	90	0	86.76	PQ800429	*Aperileptus* sp.
44	BR19	Malaysia: Pahang, Bukit Rengit	Ichneumonidae	Campopleginae	784	784	87	0	87.54	PQ827104	*Hyposoter* sp.
45	BR23	Malaysia: Pahang, Bukit Rengit	Ichneumonidae	-	781	781	90	0	86.74	PQ827106	Ichneumonidae sp.
46	BR26	Malaysia: Pahang, Bukit Rengit	Ichneumonidae	-	989	989	80	0	98.25	PQ827105	Ichneumonidae sp.
47	BR27	Malaysia: Pahang, Bukit Rengit	Ichneumonidae	Acaenitinae	800	800	79	0	90.92	PQ800428	*Jezarotes* sp.
48	KL10	Malaysia: Pahang, Kuala Lompat	Ichneumonidae	Cryptinae	753	753	89	0	85.78	PQ834819	Cryptinae sp.
49	BR36	Malaysia: Pahang, Bukit Rengit	Ichneumonidae	Orthocentrinae	882	882	86	0	91.47	PQ800427	*Orthocentrus* sp.
50	BR34	Malaysia: Pahang, Bukit Rengit	Ichneumonidae	Orthocentrinae	958	958	92	0	92.4	PQ800433	*Plectiscus callidulus*
51	BR35	Malaysia: Pahang, Bukit Rengit	Ichneumonidae	Orthocentrinae	957	957	91	0	92.25	PQ800432	*Plectiscus callidulus*

Table 3 *(continue)*

No.	Sample code	Locality	Family	Subfamily	Maximum Score	Total Score	Query cover (%)	e-value	Similarity Percentage (%)	GenBank Accession number	Species Identified
52	BR37	Malaysia: Pahang, Bukit Rengit	Ichneumonidae	Orthocentrinae	957	957	91	0	92.25	PQ800431	*Plectiscus callidulus*
53	BR40	Malaysia: Pahang, Bukit Rengit	Ichneumonidae	Orthocentrinae	953	953	91	0	92.1	PQ800430	*Plectiscus callidulus*
54	LK7	Malaysia: Pahang, Lembah Klau	Liopteridae		877	877	90	0	89.67	PQ800434	*Paramblynotus* sp.
55	PP17	Malaysia: Pahang, Perlok	Liopteridae		884	884	99	0	87.71	PQ827098	*Paramblynotus* sp.
56	BR2	Malaysia: Pahang, Bukit Rengit	Tenthredinidae	Heterarthrinae	810	810	91	0	87.6	OR782832.1	*Caliroa* sp.
57	-	Malaysia	Pyralidae	Pyralinae	-	-	-	-		JN277359.1	*Vitessa splendida*
58	-	Thailand	Apidae		-	-	-	-		PV197633.1	*Lepidotrigona terminata*

Neighbour-Joining (NJ) Tree

All sequences obtained from this study were included in the phylogenetic analysis together with several GenBank sequences that were listed in Table 3. The NJ tree showed distinct separation between species, with each species cladded together and located at a specific lineage, supported by bootstrap values ranging between 51%–100%. Furthermore, a clear separation between ingroups and outgroups visualised, supported by 91% bootstrap value. The grouping or classification of species into families, genera and species is indicated in the tree in Figure 3, with the hymenopteran families were found to be paraphyletic. Habitus image of hymenopteran representative recorded are shown in Figures 4A and 4B.

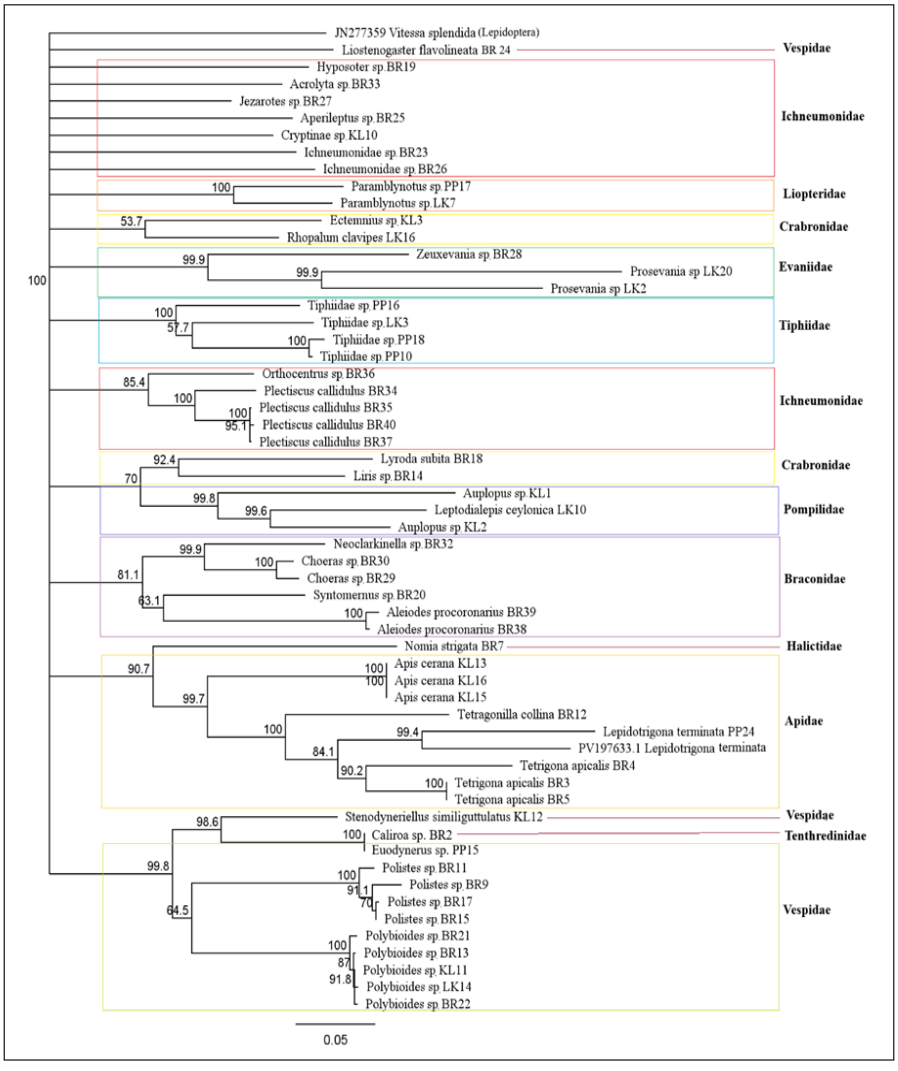

Figure 3. The NJ tree resulted from the Neighbour-Joining (NJ) analysis (distance criterion) based on *COI* sequences of hymenopteran pollinators collected from Tengku Hassanal Wildlife Reserve (THWR), Pahang, Malaysia. The bootstrap values, based on 1000 replications, are indicated above the branches

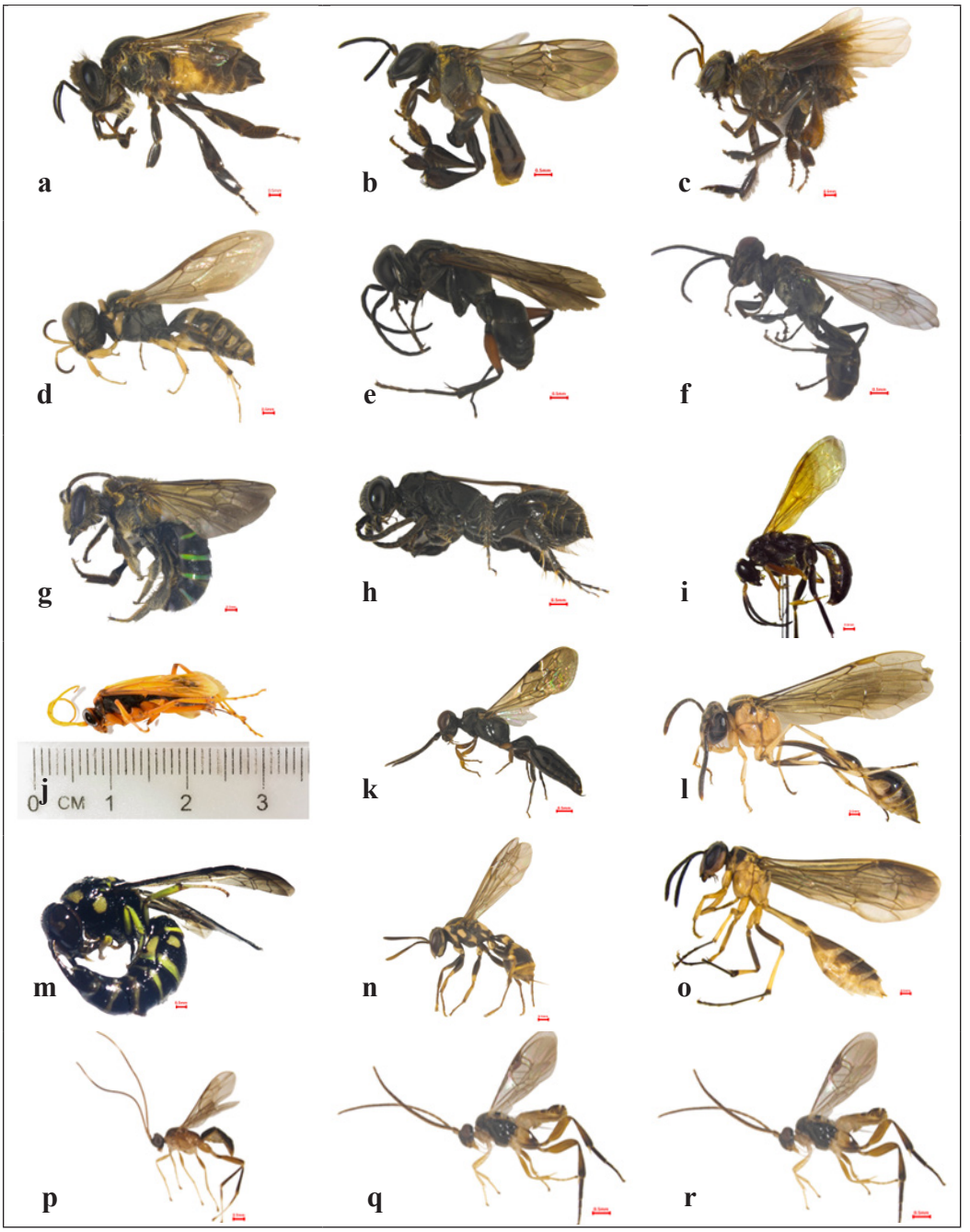

Figure 4A. a, *Apis cerana* (KL13); b, *Lepidotrigona terminata* (PP24); c, *Tetrigona apicalis* (BR4); d, *Ectemnius* sp. (KL3); e, *Liris* sp. (BR14); f, *Lyroda subita* (BR18); g, *Nomia strigata* (BR7); h, *Tiphia* sp. 1 (PP18); i, *Auplopus* sp. (KL1/KL2); j, *Leptodialepis ceylonica* (LK10); k, *Tiphia* sp. 2 (PP16); l, *Liostenogaster flavolineata* (BR24); m, *Stenodyneriellus similiguttulatus* (KL12); n, *Polistes* sp. (BR9); o, *Polybioides* sp. (LK14); p, *Aleiodes procoronarius* (BR39); q, *Choeras* sp. (BR30); r, *Neoclarkinella* sp. (BR32)

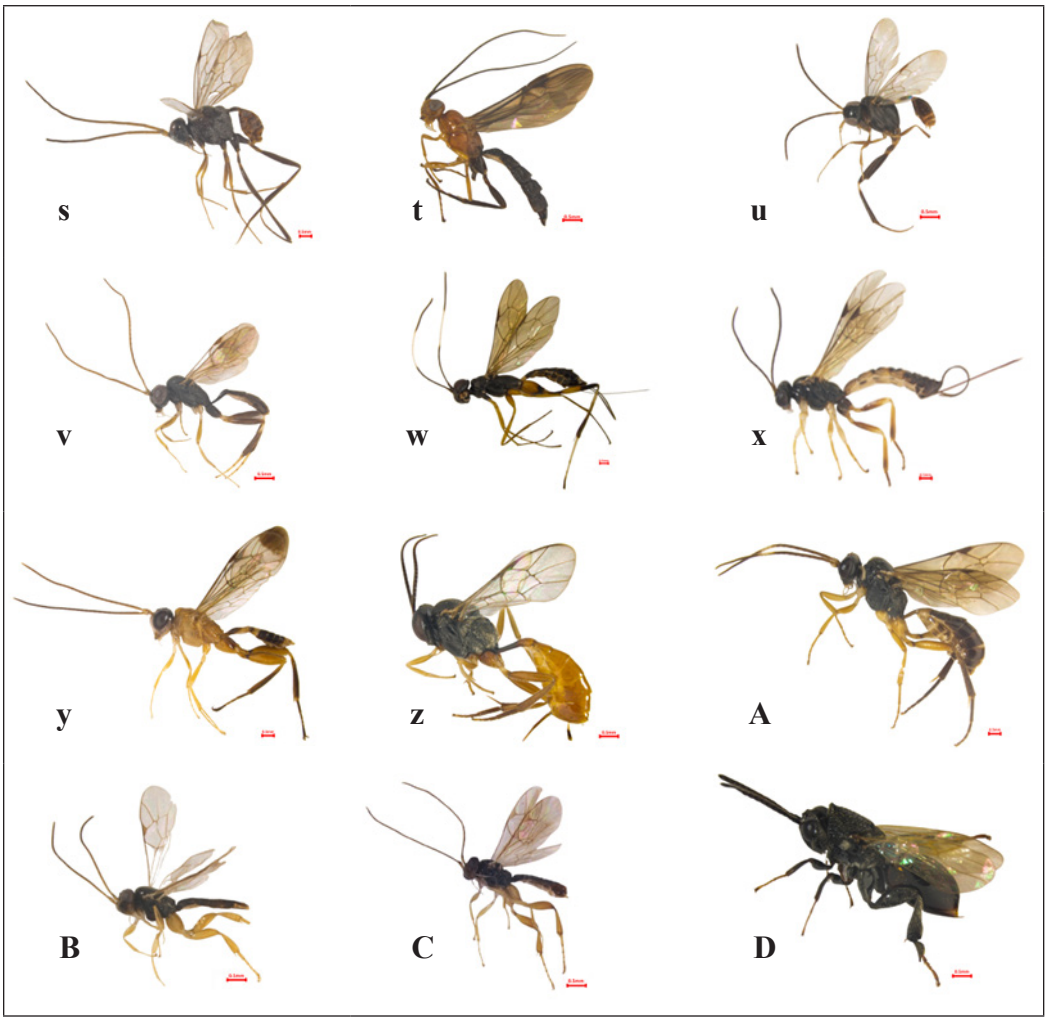

Figure 4B. s, *Zeuxevania* sp. (BR28); t, *Syntomernus* sp. (BR20); u, *Prosevania* sp. (LK20); v, *Acrolyta* sp. (BR33); w, *Aperileptus* sp. (BR25); x, Ichneumonidae sp. (BR26); y, *Jezarotes* sp. (BR27); z, *Hyposoter* sp. (BR19); A, Cryptinae sp. (KL10); B, *Orthocentrus* sp. (BR36); C, *Plectiscus callidulus* (BR34); D, *Paramblynotus* sp. (LK7)

DISCUSSION

This study focused on understanding a group of hymenopteran species composition, specifically as pollinators in THWR, Pahang, Malaysia. While many previous studies on hymenopteran species in Peninsular Malaysia have focused on species found in plantations (e.g., Aman-Zuki et al., 2019) and primarily in secondary forests (Rabibah et al., 2018), nevertheless these species rarely discussed in a wildlife reserve forest. Hymenoptera has been identified as one of the most abundant and highly diverse groups within the forest ecosystem (De Souza Amorim et al., 2022), serving both as pollinators and parasitoids

(Larsen et al., 2014). However, they have often been overlooked in previous studies due to several factors, such as the lack of comprehensive research, the unavailability of identification keys, limited resources, and high taxonomic diversity. Given their ecological roles and diversity, this study fills a critical gap by exploring hymenopteran pollinators in a protected forest using both morphological and molecular approaches.

A total of 34 species from 11 families have been successfully collected. This finding is in line with Yahaya et al. (2023) that recorded 11 hymenopteran families from Kuala Keniam National Park, Pahang. In this study, eight families were identified as an effective pollinators (Apidae, Halictidae, Liopteridae, Tenthredinidae, Crabronidae, Pompilidae, and Tiphiidae, Vespidae), while three families (Braconidae, Evaniidae, Ichneumonidae) consisted of species classified as less effective pollinators. The effective pollinators were identified based on specific criteria for effectiveness (their ability to transfer pollen efficiently, frequency of flower visitation). In contrast, the less effective pollinators are those incidentally carry pollen while foraging for nectar, without playing a direct role in pollination (Klein et al., 2019; Wojcik, 2021; Yokota et al., 2024).

In this study, bee species from Apidae and Halictidae exhibited traits associated with effective pollination such as dense body pilosity (Roquer-Beni et al., 2020). Three Apidae stingless bees collected in this study, namely *Lepidotrigona terminata*, *Tetragonilla collina*, and *Tetrigona apicalis*, are recognized as pollinators. Among them, *T. apicalis* has been particularly noted as an important pollinator in forest ecosystems (Dumesh & Sabu, 2014). In addition, collected *Apis cerana* has also been documented as a significant pollinator of native forest trees and is considered a keystone species that contributes valuable pollination and other ecosystem services (Chen et al., 2018).

In contrast, non-bee Hymenoptera, while more taxonomically diverse, varied widely in their pollination roles. Families such as Vespidae and Tenthredinidae contributed to pollination but often incidentally or opportunistic manner, while others like Braconidae and Ichneumonidae were more likely to act as parasitoids or nectar feeders with limited pollination impact (Borchardt et al., 2024). This contrast highlights the importance of bees as primary pollinators in forest ecosystems, with non-bees contributing supplementary roles in maintaining floral diversity (Katumo et al., 2022).

Two families namely Vespidae and Ichneumonidae had the highest number of species identified as observed, with nine and seven species, respectively. Vespidae are known as generalist pollinators of forest flowering plants and contribute to maintaining plant biodiversity (Rojas-Nossa et al., 2023). Although Ichneumonidae are not as efficient as bees in pollination, they do serve as pollinators. In contrast, the families Halictidae, Liopteridae, and Tenthredinidae were represented by only one or two species, belonging to a single genus, despite being recognised as very effective pollinators in forest and other ecosystem (Garibaldi et al., 2013; Michener, 2007; Müller & Kuhlmann, 2008;), except

for Evaniidae, which is not commonly associated with pollination. Several other families such as Apidae, Crabronidae, Pompilidae, Tiphiidae, and Braconidae, consisting of effective and less effective pollinators, with moderate number of species and genera (Roubik, 2023) (Tables 2 and 3).

Species-level resolution is critical in pollination ecology to accurately delineate pollinator-plant interactions (Van der Niet et al., 2014). Molecular tools, particularly DNA barcoding, significantly enhance identification reliability by resolving taxa that are morphologically cryptic or exhibit high intraspecific variation. When integrated with classical morphological diagnostics, DNA barcoding improves taxonomic precision and facilitates more accurate ecological inferences. Such integration combining molecular and morphological datasets, have become necessary in contemporary systematic and biodiversity research (Schlick-Steiner et al., 2010; Simonsen et al., 2012).

The barcoding analysis revealed that some species share over 98% similarity with reference sequences previously deposited in GenBank (NCBI). However, several other specimens could only be identified up to the genus level, with similarity scores greater than 80% to the available GenBank sequences. This highlights the need for barcoding analysis in hymenopteran species, which some are minute organisms that show high morphological variation. In this case, the species or genus-level identification based on morphological characteristics alone was difficult and impossible, leading to misidentifications which required confirmation through DNA barcoding (Chac & Thinh, 2023). Only 20 out of 56 (35.7%) specimens were successfully identified up to species level based on molecular data. However, the remaining specimens could only be identified up to genus level, both morphologically and molecularly. Although BLAST analysis yielded low sequence similarity with GenBank entries, morphological identification was consistent and accurate. This discrepancy likely reflects database limitations rather than misidentification. Many GenBank records are uncurated or lack representative sequences for closely related species, particularly in under-sampled taxa. Moreover, BLAST performs local alignments and may not capture full-sequence similarity, especially when reference sequences are incomplete or geographically divergent (Spouge & Mariño-Ramírez, 2012).

This study provides new insights into the barcode data for hymenopteran species. Even though morphological identification was conducted, barcode information was very important and informative in supporting species identification (Powell et al., 2019). The molecular approach proved to be highly effective in providing accurate species identification, especially given the close morphological similarities among hymenopteran species (Jeong et al., 2010) and their significant intraspecific variation (Rasool et al., 2018). Such challenges were particularly evident in hymenopetran parasitoids (Farrokhdazeh et al., 2014) and members of the Braconidae family (Sharanowski et al., 2011). The *COI* marker used in this study was shown to be suitable for the barcoding approach (Lv et al., 2014), as mitochondrial DNA (mtDNA) evolves rapidly, making it ideal for resolving

taxonomic relationships at the species or genus level (Guo et al., 2022) as seen in similar studies by Hussain et al. (2024).

The NJ tree provided valuable insights into distinguishing species and families relatedness (Figure 3). However, it did not account for the evolutionary process, as it did not incorporate mutation rates (Kalinowski, 2009). Nonetheless, clear separations were observed between the ingroups and outgroups, with outgroup species *Vitessa splendida* (Pyralidae: Lepidoptera) showing significant divergence, which helped differentiate the more primitive ancestors from the more derived Hymenoptera species. *Polybioides* sp. formed a well-supported cluster with high bootstrap values, indicating good confidence in this grouping. This species clustered closely with *Polistes* sp., reflecting their taxonomic relationship within the family Vespidae. Similarly, *Neoclarkinella* sp. and *Choeras* sp. from the Braconidae family and *Prosevania* sp. and *Zeuxevania* sp. of the Evaniidae family, also formed closely related cluster. *Tetrigona apicalis* samples form a distinct cluster with *Lepidotrigona terminata*. The high bootstrap value supports their grouping within the Meliponini tribe of stingless bees.

The exclusion of species within Crabronidae and Vespidae family to cluster together (Figure 3) may reflect long-branch attraction or limited resolution of the NJ method. Branch lengths nonetheless offer useful insights into evolutionary relationships (Kumar & Gadagkar, 2000). Short branch lengths among species within a family generally suggest closer relatedness, which should align with their taxonomic classification (Fernández et al., 2023). However, the NJ tree may not accurately reflect complex evolutionary relationships as it simplifies evolutionary history by relying on distance matrices. This can obscure complex evolutionary scenarios such as hybridisation, rate heterogeneity among lineages, and multiple substitutions at the same site (Zou et al., 2024). Moreover, the use of mtDNA alone may be inadequate for resolving deeper divergences or relationships influenced by introgression or incomplete lineage sorting (Toews & Brelsford, 2012). Additionally, it is recommended to integrate mtDNA with other nuclear markers to enhance resolution and provide a more comprehensive view of evolutionary history (Yoshida & Nei, 2016; Zou et al., 2024).

CONCLUSION

This study offers new insights into the taxonomic composition and relatedness of THWR's bee and non-bee hymenopterans, documenting 34 species across 11 families. By incorporating both morphological identification with DNA barcoding, it improves species-level resolution in a taxonomically challenging group while reducing the gap in current knowledge for Peninsular Malaysia. Identifying both effective and incidental pollinators has important conservation implications, supporting the needs to protect pollination services and maintaining the forest ecosystem. Future studies could explore pollinator-

plant interactions within seasonal and spatial variation to further strengthen conservation and ecological understanding.

ACKNOWLEDGEMENT

The study was funded by the National Conservation Trust Fund (NCTF) from the Malaysia Ministry of Natural Resources, Environment and Climate Change (ST-2022-028) and a study permit by the Department of Wildlife and National Parks of Peninsular Malaysia JPHL&TN (IP):600-6/1/ 4 Jld 2 (74) with extension JPHL&TN (IP):600-6/1/ 4 Jld 2 (199). Special thanks to Mr. Mohd Happy Mohd Noor and Mr. Muhammad Nizam Ahmad who managed the administration of PERHILITAN staff at THWR namely Mr. Noorhazlie Mohd Hatta, Mr. Tuan Muhd Ridzwan Tuan Hassan, Mr. Muhamad Nor Jefri and Cik Wan Suriani Wan Azlan in helping with samples collection. Not to forget, Mrs. Roberta Chaya Tawie Tingga and Mr Muhammad Afiq Senen who helped in laboratory work at UKM.

REFERENCES

Altschul, S. F., Gish, W., Miller, W., Myers, E. W., & Lipman, D. J. (1990). Basic local alignment search tool. *Journal of Molecular Biology, 215*(3), 403–410. https://doi.org/10.1016/S0022-2836(05)80360-2

Aman-Zuki, A., Mohammed, M. A., Md-Zain, B. M., & Yaakop, S. (2019). Phylogenetic relationships of five Oriental *Apanteles* species-groups (Hymenoptera: Braconidae: Microgastrinae) by concatenating four molecular markers. *Journal of Asia-Pacific Entomology, 22*(1), 341-352. https://doi.org/10.1016/j.aspen.2019.01.012

Azmi, W. A., Samsuri, N., Mohd Hatta, M. F., Ghazi, R., & Chuah, T. S. (2017). Effects of stingless bee (*Heterotrigona itama*) pollination on greenhouse cucumber (*Cucumis sativus*). *Malaysian Applied Biology*, *46*(1), 51-55.

Bell, K. L., Fowler, J., Burgess, K. S., Dobbs, E. K., Gruenewald, D., Lawley, B., Morozumi, C., & Brosi, B. J. (2017). Applying pollen DNA metabarcoding to the study of plant-pollinator interactions. *Applications in Plant Sciences, 5*(6), apps.1600124. https://doi.org/10.3732/apps.1600124

Blaimer, B. B., Santos, B. F., Cruaud, A., Gates, M. W., Kula, R. R., Mikó, I., Rasplus J. Y., Smith, D. R., Talamas, E. J., Brady, S. G., & Buffington, M. L. (2023). Key innovations and the diversification of Hymenoptera. *Nature Communications, 14*, 1212. https://doi.org/10.1038/s41467-023-36868-4

Borchardt, K. E., Holthaus, D., Soto Méndez, P. A., & Toth, A. L. (2024). Debunking wasp pollination: Wasps are comparable to bees in terms of plant interactions, body pollen and single-visit pollen deposition. *Ecological Entomology*, *49*(4), 569–584. https://doi.org/10.1111/een.13329

Catalano, P., Della Sala, F., Cavaliere, M., Caputo, C., Pecoraro, D., Crispino, G., Lettera, S., Caioni, G., Esposito, M., Verre, A., Castellone, L., Bianco, E., & Amorena, M. (2024). Use of honey bees and hive products as bioindicators to assess environmental contamination in targeted areas of the Campania Region (Italy). *Animals*, *14*(10), 1446. https://doi.org/10.3390/ani14101446

Chac, L. D., & Thinh, B. B. (2023). Species identification through DNA barcoding and its applications: A review. *Biology Bulletin of Russian Academy of Sciences, 50*, 1143–1156. https://doi.org/10.1134/S106235902360229X

Chan, A., Chiang, L. P., Hapuarachchi, H. C., Tan, C. H., Pang, S. C., Lee, R., Lee, K. S., Ng, L. C., & Phua, S. G. L. (2014). DNA barcoding: Complementing morphological identification of mosquito species in Singapore. *Parasites & Vectors, 7*, 569. https://doi.org/10.1186/s13071-014-0569-4

Chen, C., Wang, H., Liu, Z., Chen, X., Tang, J. Meng, F., & Shi, W. (2018). Population genomics provide insights into the evolution and adaptation of the eastern honey bee (*Apis cerana*). *Molecular Biology and Evolution, 35*(9), 2260–2271. https://doi.org/10.1093/molbev/msy130

De Souza Amorim, D., Brown, B. V., Boscolo, D., Ale-Rocha, R., Alvarez-Garcia, D. M., Balbi, M. I. P. A., de Marco Barbosa, A., Capellari, R. S., de Carvalho, C. J. B., Couri, M. S., de Vilhena Perez Dios, R., Fachin, D. A., Ferro, G. B., Flores, H. F., Frare, L. M., Gudin, F. M., Hauser, M., Lamas, C. J. E., Lindsay, K. G., Marinho, M. A. T., … Rafael, J. A. (2022). Vertical stratification of insect abundance and species richness in an Amazonian tropical forest. *Scientific Reports, 12*, 1734. https://doi.org/10.1038/s41598-022-05677-y

Dumesh, S., & Sabu, M. (2014). Pollination ecology of *Tetrigona apicalis* (Apidae: Meliponinae) in tropical forests. *Journal of Pollination Ecology*, *12*(1), 53-61.

Fahimee, J., Badrulisham, A. S., Zulidzham, M. S., Reward, N. F., Muzammil, N. Jajuli, R., Md-Zain, B. M., & Yaakop, S. (2021). Metabarcoding in diet assessment of *Heterotrigona itama* based on *trnL* marker toward domestication program. *Insects, 12*(3), 205. https://doi.org/10.3390/insects12030205

Farrokhzadeh, H., Moravvej, G., Awal, M. M., & Karimi, J. (2014). Molecular and morphological identification of hymenoptran parasitoids from the pomegranate aphid, *Aphis punicae* in Razavi Khorasan province, Iran. *Turkish Journal of Entomology*, *38*(3), 291-306.

Fernández, A., Segura-Alabart, N., & Serratosa, F. (2023). The multifurcating Neighbor-Joining algorithm for reconstructing polytomic phylogenetic trees. *Journal of Molecular Evolution, 91*, 773–779. https://doi.org/10.1007/s00239-023-10134-z

Folmer, O., Black, M., Hoeh, W., Lutz, R., & Vrijenhoek, R. (1994). DNA primers for amplification of mitochondrial cytochrome *c* oxidase subunit I from diverse metazoan invertebrates. *Molecular Marine Biology and Biotechnology, 3*(5), 294–299.

Garibaldi, L. A., Steffan-Dewenter, I., Winfree, R., Aizen, M. A., Bommarco, R., Cunningham, S. A., Kremen, C., Carvalheiro, L. G., Harder, L. D., Afik, O., Bartomeus, I., Benjamin, F., Boreux, V., Cariveau, D., Chacoff, N. P., Dudenhöffer, J. H., Freitas, B. M., Ghazoul, J., Greenleaf, S., Hipólito, J., … Klein, A. M. (2013). Wild pollinators enhance fruit set of crops regardless of honey bee abundance. *Science, 339*(6127), 1608–1611. https://doi.org/10.1126/science.1230200

Goulet, H., & Huber, J. T. (1993). *Hymenoptera of the world: An identification guide to families.* Canada Communications Group.

Guo, M., Yuan, C., Tao, L., Cai, Y., & Zhang, W. (2022). Life barcoded by DNA barcodes. *Conservation Genetics Resources, 14*, 351–365. https://doi.org/10.1007/s12686-022-01291-2

Hesse, M., & Waha, M. (1989). A new look at the acetolysis method. *Plant Systematics and Evolution*, *163*, 147–152. https://doi.org/10.1007/BF00936510

Hussain, A., Kakar, A., Naseem, M., Kamran, K., Ullah, Z., Obaid, M. K., Shehla, S., Ahmed, N., Khan, Q., & Liaqat, I. (2024). Molecular identification of Hymenopteran insects collected by using Malaise traps from Hazarganji Chiltan National Park Quetta, Pakistan. *PLOS One, 19*(4), e0300903. https://doi.org/10.1371/journal.pone.0300903

Idris, M. I., Fuat, S., Pejalis, S., & Yaakop, S. (2023). Kajian awalan: Hymenoptera pendebunga di Rizab Hidupan Liar Tengku Hassanal, Pahang, Malaysia [A Preliminary Study: Pollinator Hymenopterans of Tengku] Hassanal Wildlife Reserve, Pahang, Malaysia]. *Serangga, 28*(3), 321-329. https://doi.org/10.17576/serangga-2023-2803-22

Jeong, G., Kim, H., Choi, Y., Kim, W., Park, K., Bae, S., Kim, J., & Choi, J. (2010). Molecular Identification of two *Trichogramma* species (Hymenoptera: Trichogrammatidae) in Korea. *Journal of Asia-Pacific Entomology, 13*(1), 41-44. https://doi.org/10.1016/j.aspen.2009.09.004

Kalinowski, S. (2009). How well do evolutionary trees describe genetic relationships among populations? *Heredity, 102*, 506–513. https://doi.org/10.1038/hdy.2008.136

Katumo, D. M., Liang, H., Ochola, A. C., Lv, M., Wang, Q. F. & Yang, C. F. (2022). Pollinator diversity benefits natural and agricultural ecosystems, environmental health, and human welfare. *Plant Diversity*, 44(5), 429-435. https://doi.org/10.1016/j.pld.2022.01.005.

Khalifa, S. A. M., Elshafiey, E. H., Shetaia, A. A., El-Wahed, A. A. A., Algethami, A. F., Musharraf, S. G., AlAjmi, M. F., Zhao, C., Masry, S. H. D., Abdel-Daim, M. M., Halabi, M. F., Kai, G., Al Naggar, Y., Bishr, M., Diab, M. A. M., & El-Seedi, H. R. (2021). Overview of bee pollination and its economic value for crop production. *Insects*, *12*(8), 688. https://doi.org/10.3390/insects12080688

Klein, S., Pasquaretta, C., He, X. J., Perry, C., Søvik, E., Devaud, J. M., Barron, A. B., Lihoreau, M. (2019). Honey bees increase their foraging performance and frequency of pollen trips through experience. *Scientific Reports, 9*(6778). https://doi.org/10.1038/s41598-019-42677-x

Kumar, S., & Gadagkar, S. R. (2000). Efficiency of the neighbor-joining method in reconstructing deep and shallow evolutionary relationships in large phylogenies. *Journal of Molecular Evolution, 51*: 544 -553. http:// doi: 10.1007/s002390010118.

Kumar, S., Stecher, G., & Tamura, K. (2016). MEGA 7: Molecular evolutionary genetics analysis version 7.0 for bigger datasets. *Molecular Biology and Evolution, 33*(7), 1870-1874. https://doi.org/10.1093/molbev/msw054

Larsen, N. J., Minor, M. A., Cruickshank, R. H., & Robertson, A. W. (2014). Optimising methods for collecting Hymenoptera, including parasitoids and Halictidae bees, in New Zealand apple orchards. *Journal of Asia-Pacific Entomology, 17*(3), 375-381. https://doi.org/10.1016/j.aspen.2014.03.004

Lee, S. S., Yaakob, N. S., Boon, K. S., & Chua, L. S. L. (2002). The role of selected animals in pollination and dispersal of trees in the forest: Implications for conservation and management. *Journal of Tropical Forest Science, 14*(2), 234–263. http://www.jstor.org/stable/43594457

Lv, J., Wu, S., Zhang, Y., Chen, Y., Feng, C., Yuan, X., Jia, G., Deng, J., Wang, C., Wang, Q., Lin, M., & Lin, X. (2014). Assessment of four DNA fragments (*CO1*, 16S rDNA, ITS2, 12S rDNA) for species identification of the Ixodida (Acari: Ixodida). *Parasites & Vectors, 7,* 93. https://doi.org/10.1186/1756-3305-7-93

Michener, C. D. (2007). *The bees of the world.* The Johns Hopkins University Press.

Mohammed, M. A., Aman-Zuki, A., Yusof, S., Md-Zain, B. M., & Yaakop, S. (2017). Prevalence and evolutionary history of endosymbiont *Wolbachia* (Rickettsiales: Anaplasmataceae) in parasitoids (Hymenoptera: Braconidae) associated with *Bactrocera* fruit flies (Diptera: Tephritidae) Infesting carambola. *Entomological Science, 20*(1), 382-395. https://doi:10.1111/ens.12264

Momose, K., Yumoto, T., Nagamitsu, T., Kato, M., Nagamasu, H., Sakai, S., Harrison, R. D., Itioka, T., Hamid, A. A., & Inoue, T. (1998). Pollination biology in a lowland dipterocarp forest in Sarawak, Malaysia. I. Characteristics of the plant-pollinator community in a lowland dipterocarp forest. *American Journal of Botany*, *85*(10), 1477–1501.

Müller, A., & Kuhlmann, M. (2008). Pollen hosts of western palaearctic bees of the genus *Colletes* (Hymenoptera: Colletidae): The Asteraceae paradox. *Biological Journal of the Linnean Society, 95*(4), 719-733. https://doi.org/10.1111/j.1095-8312.2008.01113.x

Nagamitsu, T., Momose, K., Inoue, T., & Roubik, D. W. (1999). Preference in flower visits and partitioning in pollen diets of stingless bees in an Asian tropical rainforest. *Resource of Population Ecology*, *41*, 195–202.

Namin, S. M., Kim, M. J., Son, M., & Jung, C. (2022). Honey DNA metabarcoding revealed foraging resource partitioning between Korean native and introduced honey bees (Hymenoptera: Apidae). *Scientific Report, 12*, 14394. https://doi.org/10.1038/s41598-022-18465-5

Pfeiffer, M., Mezger, D., Hosoishi, S., Yahya, B. E., & Kohout, R. J. (2011). The Formicidae of Borneo (Insecta: Hymenoptera): a preliminary species list. *Asian Myrmecology, 4*, 9–58.

Powell, C., Caleca, V., Sinno, M., van Staden, M., van Noort, S., Rhode, C., Allsopp, E., & van Asch, B. (2019). Barcoding of parasitoid wasps (Braconidae and Chalcidoidea) associated with wild and cultivated olives in the Western Cape of South Africa. *Genome, 62*(3), 183-199. https://doi.org/10.1139/gen-2018-0068

Rabibah, R., Muhaimin, A. M. D., & Yaakop, S. (2018). Altitudinal diversity of braconid wasps (Hymenoptera: Braconidae) at Fraser's Hill, Pahang, Malaysia. *Pertanika Journal of Tropical and Agricultural Sciences, 41* (1), 463 – 476.

Rader, R., Cunningham, S. A., Howlett, B. G., & Inouye, D. W. (2020). Non-bee insects as visitors and pollinators of crops: Biology, ecology, and management. *Annual Review of Entomology, 65,* 391–407. https://doi.org/10.1146/annurev-ento-011019-025055

Rasool, A., Ahmad, T., Ganai, B. A., Shaziya (2018). An overview of molecular identification of insect fauna with special emphasis on chalcid wasps (Hymenoptera: Chalcidoidea) of India. *Acta Agriculturae Slovenica, 111*(1), 229-239. http://dx.doi.org/10.14720/aas.2018.111.1.22

Rojas-Nossa, S., O'Shea-Wheller, T., Juliette, P., Mato, S., Osborne, J., & Garrido, J. (2023). Predator and pollinator? An invasive hornet alters the pollination dynamics of a native plant. *Basic and Applied Ecology, 71*, 119-128. https://doi.org/10.1016/j.baae.2023.07.005

Roubik, D. W. (2023). Stingless bee (Apidae: Apinae: Meliponini) ecology. *Annual Review of Entomology, 68,* 231-256. https://doi.org/10.1146/annurev-ento-120120-103938

Roquer-Beni, L., Rodrigo, A., Arnan, X., Klein, A-M, Fornoff, F. Boreux, V. & Bosch, J. (2020). A novel method to measure hairiness in bees and other insect pollinators. *Ecology Evolution*, *10*(6), 2979-2990. https ://doi.org/10.1002/ece3.6112

Santos, N., de Andrade, J. F., Pereira, R. A. S., & Farache, F. H. A. (2022). Community structure and specialization in fig wasps (Hymenoptera: Chalcidoidea) in a region of Cerrado. *Revista Brasileira de Entomologia, 66*(1), 1-9. https://doi.org/10.1590/1806-9665-RBENT-2021-0101

Schenk, J., Kleinbölting, N., & Traunspurger, W. (2020). Comparison of morphological, DNA barcoding, and metabarcoding characterizations of freshwater nematode communities. *Ecology and Evolution, 10*(6), 2885-2899. https://doi.org/10.1002/ece3.6104

Schlick-Steiner, B. C., Steiner, F. M., Seifert, B., Stauffer, C., Christian, E., & Crozier, R. H. (2010). Integrative taxonomy: A multisource approach to exploring biodiversity. *Annual Review of Entomology, 55,* 421-438. https://doi.org/10.1146/annurev-ento-112408-085432

Sharanowski, B. J., Dowling, A. P., & Sharkey, M. J. (2011). Molecular phylogenetics of Braconidae (Hymenoptera: Ichneumonoidea), based on multiple nuclear genes, and implications for classification. *Systematic Entomology*, *36*(3), 549-572. https://doi.org/10.1111/j.1365-3113.2011.00580.x

Simonsen, T. J., de Jong, R., Heikkilä, M., & Kaila, L. (2012). Butterfly morphology in a molecular age – Does it still matter in butterfly systematics? *Arthropod Structure and Development*, *41*(4), 307–322. https://doi.org/10.1016/j.asd.2012.04.006

Spouge, J. L., & Mariño-Ramírez, L. (2012). The practical evaluation of DNA barcode efficacy. Methods. *Molecular Biology, 858*: 365-77. http:// doi: 10.1007/978-1-61779-591-6_17.

Stavert, J. R., Liñán-Cembrano, G., Beggs, J. R., Howlett, B. G., Pattemore, D. E., & Bartomeus, I. (2016). Hairiness: The missing link between pollinators and pollination. *PeerJ, 4*, e2779. https://doi.org/10.7717/peerj.2779

Swofford, D. L. (2003). PAUP*. *Phylogenetic analysis using Parsimony (*and other methods). Version 4*. Sinauer Associates.

Tahir, H. M., Noor, A., Mehmood, S., Sherawat, S. M., & Qazi, M. A. (2018). Evaluating the accuracy of morphological identification of insect pests of rice crops using DNA barcoding. *Mitochondrial DNA Part B Resources, 3*(2), 1220–1224. https://doi.org/10.1080/23802359.2018.1532334

Toews, D. P. L., & Brelsford, A. (2012). The biogeography of mitochondrial and nuclear discordance in animals. *Molecular Ecology, 21*(16), 3907-3930. https://doi.org/10.1111/j.1365-294X.2012.05664.x

Van der Niet, T., Peakall, R., & Johnson, S. D. (2014). Pollinator-driven ecological speciation in plants: New evidence and future perspectives. *Annals of Botany, 113*(2), 199-211. https://doi.org/10.1093/aob/mct290

Van Noort, S., & Broad, G. (2024). *Wasps of the world: A guide to every family*. Princeton University Press.

Wojcik, V. (2021). Pollinators: Their evolution, ecology, management, and conservation. In R. E. R. Ranz (Ed.), *Arthropods - Are They Beneficial for Mankind?* IntechOpen. http://dx.doi.org/10.5772/intechopen.97153

Yaakop, S., Achterberg, C. V., Idris, A. B., & Aman, A. Z. (2013). Freezing method as a new non-destructive modification of DNA extraction. *Pertanika Journal of Tropical Agricultural Science, 36(4)*, 373-391.

Yahaya, I. N. S., Khalid, N., Ibrahim, N., Nizam, N. Naser, N., Md Yusof, N. N., Kamarudin, S., Zazi, N., & Hatta, S. (2023). Diversity, distribution and abundance of Hymenopteran from different landscapes of Kuala Keniam National Park, Pahang, Malaysia. In *IOP Conference Series: Earth and Environmental Science* 1271, 012014. http://dx.doi.org/10.1088/1755-1315/1271/1/012014

Yokota, S. C., Broeckling, C., & Seshadri, A. H. S. (2024). Pollen foraging preferences in honey bees and the nutrient profiles of the pollen. *Scientific Reports, 14*, 15028. https://doi.org/10.1038/s41598-024-65569-1

Yoshida, R., & Nei, M. (2016). Efficiencies of the NJp, maximum likelihood, and Bayesian methods of phylogenetic construction for compositional and noncompositional genes. *Molecular Biology and Evolution, 33*(6), 1618–1624. https://doi.org/10.1093/molbev/msw042

Zou, Y., Zhang, Z., Zeng, Y., Hu, H., Hao, Y., Huang, S., & Li, B. (2024). Common methods for phylogenetic tree construction and their implementation in R. *Bioengineering 11*(5), 480. https://doi.org/ 10.3390/ bioengineering110504

Pertanika J. Trop. Agric. Sci. 48 (6): 2033 - 2055 (2025)

PERTANIKA JOURNALS

TROPICAL AGRICULTURAL SCIENCE

Journal homepage: http://www.pertanika.upm.edu.my/

Metabolomics Profile of *Ziziphus mauritiana* and Its Anti-*Vibrio* Activity Using ^{1}H NMR Spectroscopy Coupled with Multivariate Data Analysis

Azizul Isha[1]*, Noraznita Sharifuddin[2], Mazni Abu Zarin[3], Yaya Rukayadi[1], and Ahmad Faizal Abdull Razis[1]

[1]Natural Medicines and Products Research Laboratory, Institute of Bioscience, Universiti Putra Malaysia, 43400 UPM Serdang, Selangor, Malaysia
[2]Aquatic Animal Health and Therapeutics Laboratory, Institute of Bioscience, Universiti Putra Malaysia, 43400 UPM Serdang, Selangor, Malaysia
[3]Laboratory of Vaccine and Biomolecules, Institute of Bioscience, Universiti Putra Malaysia, 43400 UPM Serdang, Selangor, Malaysia

ABSTRACT

Ziziphus mauritiana is a medicinal plant commonly used in conventional therapies since it has health-beneficial effects, as it is rich with many biologically active compounds. However, scientific research on this plant's metabolite profile is insufficient. The goals of this study are to establish chemical profiles of *Z. mauritiana* leaves that were extracted using a variety of polarity solvents. ^{1}H NMR-metabolomics was employed to investigate the correlation between chemical markers and anti-*Vibrio* activities. A portion of the powdered sample of *Z. mauritiana* was extracted using different solvent systems (hexane, chloroform, acetone, and 70% (v/v) ethanol). The profiles of metabolites in each extract obtained were determined by NMR spectroscopy. The correlation between the identified metabolites and anti-*Vibrio* properties of *Z. mauritiana* was interpreted using the metabolomics approach. The *Z. mauritiana* extracts were successfully clustered using principal component analysis according to their metabolite profiles. Acetone and 70% (v/v) ethanol were determined to have good extraction efficiency. The anti-*Vibrio* activity was shown to be highly correlated with the polar metabolites of the 70% (v/v) ethanol extract in the partial least squares analysis. The 70% (v/v) ethanol extracts exhibit a more diverse spectrum than the other extracts, with a total of 42 metabolites that include carbohydrates, amino acids, organics, and fatty acids. The rapid examination of the

ARTICLE INFO

Article history:
Received: 19 February 2025
Accepted: 06 November 2025
Published: 25 November 2025

DOI: https://doi.org/10.47836/pjtas.48.6.19

E-mail addresses:
azizul_isha@upm.edu.my (Azizul Isha)
noraznita@upm.edu.my (Noraznita Sharifuddin)
mazniaz@upm.edu.my (Mazni Abu Zarin)
yaya_rukayadi@upm.edu.my (Yaya Rukayadi)
madfaizal@upm.edu.my (Ahmad Faizal Abdull Razis)
*Corresponding author

metabolite composition of *Z. mauritiana* in relation to its various solvent extractions with a specific anti-*Vibrio* biological activity has been facilitated by the implementation of NMR-metabolomics.

Keywords: Anti-*Vibrio* activity, ^{1}H-NMR-based metabolomics, multivariate data analysis, *Ziziphus mauritiana*

INTRODUCTION

Viral infections continue to pose a substantial public health threat due to their transmission. The *Vibrio* species are Gram-negative rods that are motile and found in freshwater and estuarine water environments (Alam et al., 2009; Ramalingam & Ramarani 2006). *V. vulnificus, V. parahaemolyticus, V. campbellii, and V. harveyi* are the most common *Vibrio* species causing infections in people. The pathogenicity of *Vibrio* strains can be harmful to humans or marine animals using a broad repertory of virulence factors encoded by virulence genes (Schroeder et al., 2017). It may present three main syndromes of clinical illness, including primary septicemia, wound infections, and gastroenteritis (Yun & Kim, 2018). According to Baker-Austin & Oliver (2018), the transmission of *Vibrio* to humans can occur by the ingestion of undercooked marine products or contamination of water.

Antibiotics and other antimicrobial agents have been extensively employed to effectively cure, manage, and avoid bacterial infections in humans as well as animals (Saga & Yamaguchi, 2009). *Vibrio* infections are treated with the following antibiotics: tetracycline, chloramphenicol, expanded-spectrum cephalosporins (ceftazidime), quinolones (doxycycline or fluoroquinolone), trimethoprim-sulphamethoxazole, gentamicin, levofloxacin, and ciprofloxacin (Elmahdi et al., 2016; Malla et al., 2014; Wong et al., 2015). Nevertheless, the environment has been contaminated with antimicrobial-resistant *Vibrio* species because of the ubiquitous application of antibiotics in aquaculture, farming, livestock fields, and pharmaceuticals (Heuer et al., 2009; Gao et al., 2017; Lulijwa et al., 2020). Antibiotic resistance is a major cause of therapeutic failures and significant morbidity and death. Consequently, urgent action is required to avert the proliferation of resistant bacteria. Natural anti-*Vibrio* agents derived from natural resources could be the subject of future research and development efforts.

Given the growing concern regarding the resistance of bacteria to commercial antibiotics in the pharmaceutical industry, it is imperative to investigate alternative plant sources and consider *Z. mauritiana* as a potential source of antimicrobial medications (Febriza et al., 2022; Jain et al., 2019. It is a plant that is indigenous to the Southeast Asia's Indo-Malaysia and commonly known as bidara in Malaysia. The genus *Ziziphus*, belonging to the family *Rhamnaceae*, comprises approximately 170 species and is widely utilized to treat of health issues (Abdallah et al., 2016). The leaves have traditionally been used to alleviate a variety of ailments, including diarrhea, nausea, vomiting, asthma, fever, and dermatitis (Abalaka et al., 2010). The roots are utilized to prevent and treat cutaneous

diseases (Adzu et al., 2001). People consume the immature foliage as a vegetable and use it to treat liver disorders, fever, and asthma (Dahiru & Obidoa, 2007).

Previous studies reported that *Z. mauritiana* leaves have phytochemical compounds, which act as anti-*Vibrio* activity. Febriza et al. (2022) found that a *Z. mauritiana* leaf inhibited the growth of *V. cholera*. Another study by Jain et al. (2019) claimed that extracts from *Z. mauritiana* leaf had anti-*Vibrio* activity against *V. parahemolyticus.* Secondary metabolites, including alkaloids, tannins, phenolic substances, and flavonoids, have been identified in *Z. mauritiana* leaves (Najafi, 2013). The fruits are abundant in vitamin C and contain 20–30% sugar, 2.5% more protein, and 12.8% carbohydrates (Priyanka et al., 2015). Furthermore, research has indicated that the bark exhibits cytotoxic activity to a range of cancer cell lines (Pisha et al., 1995). It has also been noted that *Z. mauritiana* has certain therapeutic advantages, including antioxidant, anticancer, antidiarrheal, antibacterial, anti-inflammatory and hypoglycemic activities (Butt et al., 2021; Dahiru et al., 2010; Goyal et al., 2012; Prakash et al., 2020; Ramar et al., 2022; Verma et al., 2018). There is limited scientific research on the anti-*Vibrio* potential of *Z. mauritiana*, and most of the existing studies focus on *V. cholerae* and *V. parahemolyticus*. Therefore, there is a need for further research to investigate the potential anti-*Vibrio* effects of *Z. mauritiana* leaf against different *Vibrio* spp. for a comprehensive understanding of this plant's antimicrobial properties.

By combining NMR with multivariate data analysis, the metabolomic profiles of numerous plant species and traditional phytomedicines can be determined (Choi et al., 2007). Multivariate methods, such as PCA, PLS-DA, and OPLS-DA, have been utilized to evaluate the intricate sets of NMR data. Through a combination of anti-*Vibrio* activity, ^{1}H NMR data and a metabolomics approach, the biomarkers and mechanism of action exerted by *Z. mauritiana* leaves extracted should be better understood. Hence, the purpose of this work is to identify the chemical profiles of *Z. mauritiana* leaves extracted by varying polarity solvents and to correlate the chemical markers to anti-*Vibrio* activities using the ^{1}H NMR-metabolomics approach. The findings of this investigation may offer novel prospects for the effective treatment of *Vibrio* infections.

MATERIALS AND METHODS

Materials

Extractions were conducted using solvents of analytical grade, including ethanol, n-hexane, acetone, and chloroform. NMR solvents such as deuterated methanol-d_4 (CD_3OD, 99.8%), nondeuterated potassium dihydrogen phosphate (KH_2PO_4, pH 6.0), deuterium oxide (D_2O, 99.9%), and trimethylsilylpropionic acid-d_4 sodium salt (TSP) were supplied by Merck (Darmstadt, Germany). Deionized water was obtained from a PURELAB Chorus 2 system (ELGA Lab Water, USA). The American Type Culture Collection (Manassaa, VA, USA) was the source of *V. vulnificus* (ATC.33147)*, V. parahaemolyticus* (ATC.17802), *V.*

campbellii (ATC.BAA-1116) and *V. harveyi* (ATC.35084). Mueller Hinton agar (MHA; Difco, Sparks, USA) and Mueller Hinton broth (MHB; Difco, Sparks, USA) were used as media for the antibacterial assays. Dimethyl sulfoxide (DMSO) was obtained from Sigma-Aldrich.

Leaves of *Z. mauritiana* Harvesting and Preparation

Leaves of *Z. mauritiana* were harvested at the Universiti Putra Malaysia campus. The mature leaves collected from the *Z. mauritiana* tree were taken from the uppermost branches, where they received ample sunlight. The harvested leaf samples were rinsed with flowing distilled water and delicately dried using paper towels. The samples were subsequently stored in an ultra-low temperature freezer overnight in sealed receptacles. The frozen samples were dried in a freeze-dryer (Scanvac Labogene) for 72 h and pulverised into fine powder using a grinder (Waring, 32 BL80, New Hartford, NY, USA). Until the subsequent analysis, the powder samples were stored in an ultra-low temperature freezer.

Preparation of *Z. mauritiana* Leaves Extracts

The *Z. mauritiana* freeze-dried leaves powder (10 g) was extracted using sonication in 200 mL of the respective solvents, including 70% (v/v) ethanol, acetone, chloroform and hexane (20 min, 25°C). The crude extracts were obtained by evaporating the combined filtered supernatants with a rotary evaporator after the process was re-extracted twice. A total of six replicates for each solvent were prepared.

Antibacterial Assay

To prepare a stock solution of each plant extract, 100 mg of the extract was dissolved with 1 ml of DMSO. For each stock solution, 100 µL of the stock solution was mixed with 900 µL of pure water to make a 1% test solution (10 mg/mL).

Disc Diffusion Assay

An agar diffusion assay was implemented to evaluate antibacterial activity (Rukayadi et al., 2009). *Vibrio* isolates were cultured on Mueller–Hinton agar medium that contained 1% NaCl from the culture stock. Subsequently, pure colonies were employed to generate 0.5 McFarland turbidity. To inoculate fresh Petri dishes, a cotton swab was used. The extracts of *Z. mauritiana* leaves were dissolved with DMSO to make a 10 mg/mL concentration. *Vibrio* isolates were cultured on Mueller–Hinton agar medium that contained 1% NaCl from the culture stock. Subsequently, pure colonies were employed to generate 0.5 McFarland turbidity. Inhibition zones were observed after the inoculated dishes were incubated at 37°C for 24 hours. Six replicates were utilised in each experiment, and the inhibition zone

diameter was determined in millimetres (mm) for each experiment. Tetracycline (5 µg) was used as a standard drug against the tested *Vibrio* strains.

Determination of Minimum Inhibitory Concentration (MIC) Values

The MIC for *Vibrio* isolates that are susceptible to the *Z. mauritiana* leaves extracts was determined using the broth microdilution method. To produce test concentrations ranging from 10 to 0.0195 mg/mL for each solvent extract derived from a 10 mg/mL stock of plant extracts, a series of two-fold serial dilutions were prepared using filtered sterile distilled water. Each well of the 96-well plates was filled with a 100 µL aliquot of double-strength Mueller-Hinton broth containing 1% NaCl. Subsequently, 50 µL of the extract was added in descending order, along with 50 µL of the test bacteria suspension. 50 µL of tetracycline, 50 µL of the test microorganisms, and 100 µL of Mueller-Hinton broth with 1% NaCl are present in the positive control well. The negative control well is composed of 50 µL of the test microorganisms, 50 µL of filtered sterile distilled water, and 100 µL of Mueller-Hinton broth with 1% NaCl. After the test extract was added to the inoculated plates, they were incubated aerobically at 37°C for 24 hours to evaluate the MIC. The minimal concentration of the test sample that resulted in complete inhibition of bacterial growth is denoted by the MIC value. The MICs were obtained in triplicate.

Determination of Minimum Bactericidal Concentration (MBC) Values

A 10 µL suspension sample was transferred to an MHA plate for sub-culture in order to ascertain the MBC from each of the 12 wells used in the MIC test. The MBC value of the test extract was calculated after the inoculation plates had been incubated at 37°C for 24 hours. The MBC value was the minimum concentration at which no bacterial growth was observed. The MBCs were obtained in triplicate.

NMR Measurement and Multivariate Data Analysis

The ^{1}H NMR spectra were run at 25˚C using a 500 MHz Varian INOVA NMR spectrometer. The samples were prepared as per the earlier published approach (Kim et al., 2011). A 1:1 mixture of CD_3OD and KH_2PO_4 (pH 6.0) in D_2O containing 0.1% TSP sodium salt was added to a 2.0 mL Eppendorf tube containing 50 milligrams of each extract. 0.75 mL of volume was introduced. The mixture was vortexed for one minute, ultrasonically for twenty minutes, and centrifuged for ten minutes at 10,000 rpm (7,826 G-force) at 27°C. The ^{1}H NMR measurement was conducted by promptly transferring the supernatant (0.6 mL) to a 5 mm NMR tube and employing a pre-saturation sequence.

The acquired spectra were analysed with Chenomx software (v.5.1, Alberta, Canada) with a consistent configuration used across all spectra. The spectral intensities were grouped

into bins of similar width (0.04) within the range of 0.50–10.00. The areas between 4.70 and 4.90, which correspond to water and 3.23 and 3.36, which represent residual methanol, were omitted.

The multivariate data analysis was employed to examine the variation in metabolite contents of *Z. mauritiana* leaves extracted with various solvents, including acetone, chloroform, hexane, and ethanol (70% (v/v) using SIMCA-P software (v. 13.0, Umetrics, Umeå, Sweden). Principal component analysis (PCA) was used to establish the categorization properties of the four different solvent samples, as well as the metabolites that influenced their variation. The samples were grouped according to their similarity in the score plot of PCA, while the variables' contributions to the observed differences among the samples were illustrated in the loading plot. Pareto scaling was selected in this analysis.

A Partial Least Squares (PLS) analysis, which is a kind of multivariate regression, was used to look at how the biological activities of certain metabolites relate to the responses of chosen Vibrio strains. This technique helps uncover the correlations between these two datasets, providing insights into which metabolites might be influencing the activity of the bacteria. The *X*-variables used in the PLS analysis were NMR chemical shifts, while the *Y*-variable represented the inhibition zone value as determined by the disc diffusion method. The accuracy and predictiveness of the PLS model were confirmed through the use of a model validation technique, such as a permutation test.

The identification of metabolites was conducted by comparing the distinctive signals recognized in the ^{1}H NMR spectra of the extract derived from *Z. mauritiana* leaves with those documented in the literature, the Chenomx database (Chenomx NMR Suite 7.7 library) and the human metabolome database (www.hmdb.ca; accessed on 2nd December 2024). Additionally, the 2D *J*-resolved was utilized to aid in the identification of metabolites.

RESULTS AND DISCUSSION

Antibacterial Activity of Extracts of *Z. mauritiana* Leaves

The disk diffusion susceptibility test was used to screen the *Z. mauritiana* leaves extracted with different solvents for measurement of antimicrobial activity against *Vibrio* strain. The extracts' potency was assessed by the extent of the inhibition zone that emerged as a result of the anti-*Vibrio* effect. The extract is more efficacious and has a higher anti-*Vibrio* activity when the zone of inhibition is larger. In Table 1, the inhibition zones of *Z. mauritiana* leaves against *Vibrio* strains (*V. vulnificus, V. parahaemolyticus, V. campbellii* and *V. harveyi*) are illustrated. The leaves were extracted with various solvents, including 70% (v/v) ethanol, acetone, chloroform, and hexane. The ethanol with 70% (v/v) had the best effect on all *Vibrio* strains. At a concentration of 10 mg/mL, it had inhibition zones of 15.66 mm for *V. parahaemolyticus*, 10.46 mm for *V. vulnificus*, 24.18 mm for *V. campbellii* and 19.53 mm for *V. harveyi* from the different extract solvents.

Table 1
Inhibition zones of Z. mauritiana *leaves extracted with different solvents against Vibrio strains*

***Vibrio* Strain**	**Tetracycline (5 µg)**	**Inhibition Zone Diameter (mm)**			
		70% (v/v) Ethanol	**Acetone**	**Chloroform**	**Hexane**
V. vulnificus (ATC.33147)	22.00±0.00	15.66±0.16	11.60±0.19	9.46±0.38	9.48±0.40
V. parahaemolyticus (ATC.17802)	17.00±0.00	10.46±0.17	9.55±0.30	7.53±0.16	7.46±0.33
V. campbellii (ATC.BAA-1116)	24.55±0.30	24.18±1.85	18.00±0.71	13.57±1.42	11.33±0.88
V. harveyi (ATC.35084)	16.33±0.88	19.53±0.34	12.62±0.35	10.42±0.34	9.43±0.24

Diameter of inhibition zones in mm (including disc). Values are expressed as means ± standard deviation (SD)

It can be observed that the inhibition zone increases with the polarity of the extracts as it increases from hexane to ethanol. The antibacterial activities of 70% (v/v) ethanol and acetone extract against the *Vibrio* strain were significantly enhanced. It is likely a result of the ability of high-polarity solvents to dissolve a greater number of secondary metabolites (Kebede & Shibeshi, 2022). Extraction of active metabolites and their possible antibacterial effects are affected by the solvent's polarity.

MIC and MBC Values of Extracts of *Z. mauritiana* Leaves

The anti-*Vibrio* activity of the *Z. mauritiana* leaves that were extracted using different solvents was further investigated by determining the MIC and MBC values, in addition to the total activity. Table 2 displays the MIC and MBC values for the extracts that were tested on the four *Vibrio* strains. The results show the level of growth inhibition exhibited by the various extracts against the *Vibrio* strains.

Table 2
Minimum inhibitory concentration (MIC) and minimum bactericidal concentration (MBC) values (mg/mL) of different solvent extracts of Z. mauritiana *leaves against Vibrio strains*

***Vibrio* spp.**		**70% (v/v) Ethanol**	**Acetone**	**Chloroform**	**Hexane**
V. vulnificus (ATC.33147)	MIC	0.625	2.500	2.500	2.500
	MBC	1.250	2.500	2.500	5.000
V. parahaemolyticus (ATC.17802)	MIC	0.313	1.250	1.250	2.500
	MBC	1.250	2.500	2.500	2.500
V. campbellii (ATC.BAA-1116)	MIC	0.625	2.500	2.500	2.500
	MBC	0.625	2.500	2.500	5.000
V. harveyi (ATC.35084)	MIC	1.250	2.500	2.500	2.500
	MBC	1.250	2.500	2.500	5.000

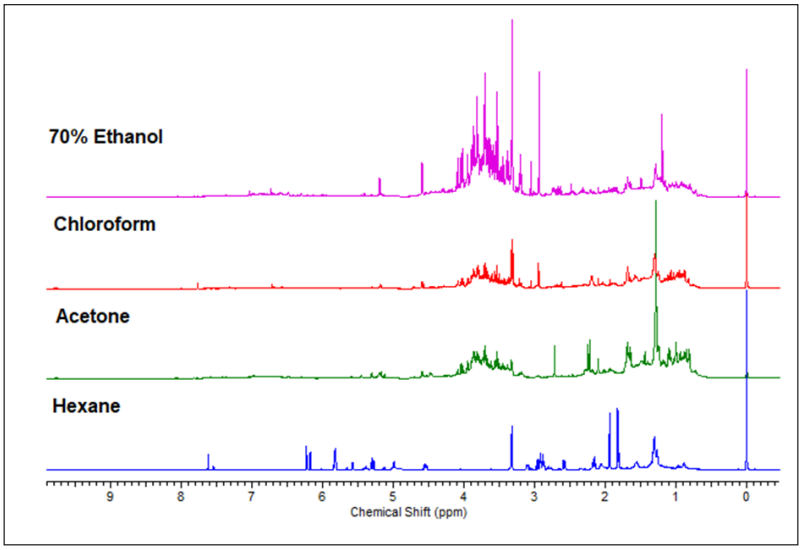

Figure 1. Representative 500 MHz ^{1}H NMR spectra of different solvent extracts of *Z. mauritiana* leaves

The MIC and MBC values of the 70% (v/v) ethanol extracts varied from 0.313 to 1.250 mg/mL, respectively. Compared to the *V. harveyi* strain, which demonstrated a MIC and MBC of 1.250 mg/mL, the 70% (v/v) ethanol extract exhibited greater efficacy against *V. parahaemolyticus* (MIC 0.313 mg/mL; MBC 1.250 mg/mL), *V. campbellii* (MIC 0.625 mg/mL; MBC 0.625 mg/mL), and *V. vulnificus* (MIC 0.625 mg/mL; MBC 1.250 mg/mL). The acetone and chloroform extracts have MICs and MBCs of 1.250–2.500 mg/mL and 2.500 mg/mL, respectively. Nevertheless, MIC and MBC of the hexane extracts were 2.500 mg/mL and 2.500–5.000 mg/mL, respectively.

Tamokou et al. (2017) reported that plant extracts or their components are considered highly potent if they exhibit MIC values below 100 µg/ml. They are considered significantly active if the MIC is from 100 to 512 µg/ml, moderately active if the MIC is between 512 and 2048 µg/ml, and inactive if the MIC exceeds 2048 µg/ml. Hence, the current findings demonstrate that the extracts from *Z. mauritiana* leaves exhibit a moderate to significant level of activity against the *Vibrio* strains that were determined. Furthermore, some polar metabolites found in the leaves' extracts have significant anti-*Vibrio* properties and could contribute strongly to the overall plant's anti-*Vibrio* activity.

^{1}H NMR Spectra of Extracts of *Z. mauritiana* Leaves and Its Metabolites Identification

The ^{1}H NMR analysis has been used to identify the metabolites of *Z. mauritiana* leaves extracted with different solvents (70% (v/v) ethanol, acetone, chloroform and hexane). Figure 1 illustrates representative ^{1}H NMR spectra of the extracts of *Z. mauritiana* leaves. A total of 42 metabolites were detectable in *Z. mauritiana,* comprising carbohydrates, fatty

acids, sesquiterpene lactones and amino acids. Table 3 and Figure 2 display the identified metabolites and their corresponding distinctive signals obtained from different extracts of *Z. mauritiana* leaves. These metabolites were identified by comparing them with those documented in the literature, the Chenomx database (Chenomx NMR Suite 7.7 library), and the human metabolome database. The 2D *J*-resolved experiment was additionally employed to support the identified metabolites (Figure S1-Supplementary data).

Table 3
NMR signal assignments for metabolites identified in the ^{1}H and 2D NMR spectra of Z. mauritiana *leaves extract, in addition with their corresponding multiplicity (s: singlet; d: doublet; t: triplet; m: multiplet) and scalar coupling constant (J(Hz)) values*

Peak No.	Metabolites	^{1}H Chemical Shifts (multiplicity, J)
1	Alanine	1.50 (d, J= 10.0 Hz), 3.16 (d, J=2.5 Hz)
2	Acetic acid	1.94 s
3	Proline	4.09 (dd, J = 1.5 Hz, 1.0 Hz)
4	Succinic acid	2.49 s
5	Asparagine	4.04 (dd, J = 1.5 Hz, 0.5 Hz), 2.98 (dd, J=3.5 Hz, J=3.5 Hz)
6	Choline	4.07 s, 3.22 s
7	Betaine	3.27 s
8	Sucrose	3.68 s, 4.06 (t, J= 3.5 Hz), 4.14 (d, J= 8.0 Hz), 5.41 (d, J= 4.5 Hz)
9	Formic acid	8.47 s
10	Valine	1.00 (d, J=6.5 Hz), 1.03 d (J=6.5 Hz)
11	Glycine	3.53 s
12	Oleic acid	2.33 (t, J=5.0 Hz)
13	Glucose	5.20 (d, J=5.0 Hz), 3.49 (dd, J=5.0 Hz, J=5.0 Hz)
14	Quercetin	6.31 (d, J=2.5 Hz), 6.48 s
15	Kaempferol	7.77 (d, J=5.0 Hz), 6.41 s
16	Myricetin	6.52 (d, J=5.0 Hz), 7.04 s
17	Catechin	4.60 (d, J=10.0 Hz), 6.99 (d, J=5.0 Hz), 3.95 (m)
18	Fructose	4.19 (d, J=10.0 Hz)
19	Malic acid	4.24 (dd, J=5.0 Hz, J=10.0 Hz), 4.31 (dd, J=5.0 Hz, J=5.0 Hz)
20	Fumaric acid	6.55 s
21	Lactic acid	1.35 (d, J=10.0 Hz)
22	Arginine	3.22 (t, J=10.0 Hz)
23	*γ*-Aminobutyric acid	3.02 (t, J=5.0 Hz)
24	Hydroxybenzoic acid	7.82 (d, J=5.0 Hz)
25	Chlorogenic acid	3.88 (dd, J=5.0 Hz, J=5.0 Hz)
26	*N,N*-Dimethylglycine	2.94 s
27	Ascorbic acid	4.54 (d, 5.0 Hz)
28	Betulin	0.96 s, 0.94 s, 0.92 s
29	(*E*)-Aconitic acid	6.72 s, 3.58 s

Table 3 *(continue)*

Peak No.	Metabolites	^{1}H Chemical Shifts (multiplicity, J)
30	(*Z*)-Aconitic acid	6.22 s, 3.55 s
31	Phosphorylcholine	3.23 s
32	4-Hydroxyisoleucine	1.88 m, 3.81 (d, J=10.0 Hz)
33	Aspartic acid	2.85 (dd, J=10.0 Hz, J=10.0 Hz)
34	Leucine	2.66 m
35	Quinic acid	3.05 s
36	Caffeoylquinic acid	2.20 (dd, J=10.0 Hz, J=10.0 Hz), 3.96 (dd, J=5.0 Hz, J=5.0 Hz)
37	Orientin	6.14 s
38	1-*O*-ethyl-β-glucoside	1.19 (t, J=10.0 Hz)
39	Rutin	1.10 (d, J=5.0 Hz)
40	*L*-Rhamnitol	1.27 (t, J=5.0Hz)
41	*β*-Pinene	2.46 m
42	Glutamic acid	3.79 (dd, J=1.5 Hz, J=2.5)

The signals observed in the aliphatic area of δ 0.50–3.00 were used to assign the following compounds: valine, acetic acid, succinic acid, oleic acid, lactic acid, *γ*-aminobutyric acid, *N*,*N*-dimethylglycine, betulin, 1-*O*-ethyl-*β*-glucoside, rutin, aspartic acid, leucine, quinic acid, *L*-rhamnitol and *β*-pinene. Alanine was detected with the doublet at δ 1.50 and δ 3.16, whereas the signals at δ 2.98 (dd) and δ 4.04 (dd) were detected as asparagine. Additionally, the signals at δ 1.88 (m) and δ 3.81 (d) were assigned to 4-hydroxyisoleucine, whereas the signals at δ 2.20 (dd) and δ 3.96 (dd) were detected as caffeoylquinic acid.

In the sugar area (δ 3.00-5.50), sucrose, glucose, and fructose were discovered. Other metabolites present in the sugar area were proline, choline, betaine, glycine, malic acid, arginine, chlorogenic acid, ascorbic acid, phosphorylcholine, quinic acid, glutamic acid and *γ*-aminobutyric acid. The signals exhibited on the singlet at δ 3.58 and δ 6.72 were used to attribute (*E*)-aconitic acid, while (*E*)-aconitic acid was detected at δ 3.55 and δ 6.22. The signals at δ 3.95 (m), δ 4.60 (d) and δ 6.99 (d) were ascribed to catechin.

In the aromatic region (δ 5.50-8.50), formic acid, fumaric acid, hydroxybenzoic acid and orientin were identified with the signals at δ 8.47 (s), δ 6.55 (s), δ 7.82 (d) and δ 6.14 (s), respectively. Quercetin was observed with the signals at δ 6.31 (d) and δ 6.48 (s), respectively. Meanwhile, the signals at δ 6.41(s) and δ 7.77 (d) were ascribed to kaempferol. The identified peaks of myricetin were detectable at δ 6.52 (d) and δ 7.04 s, respectively.

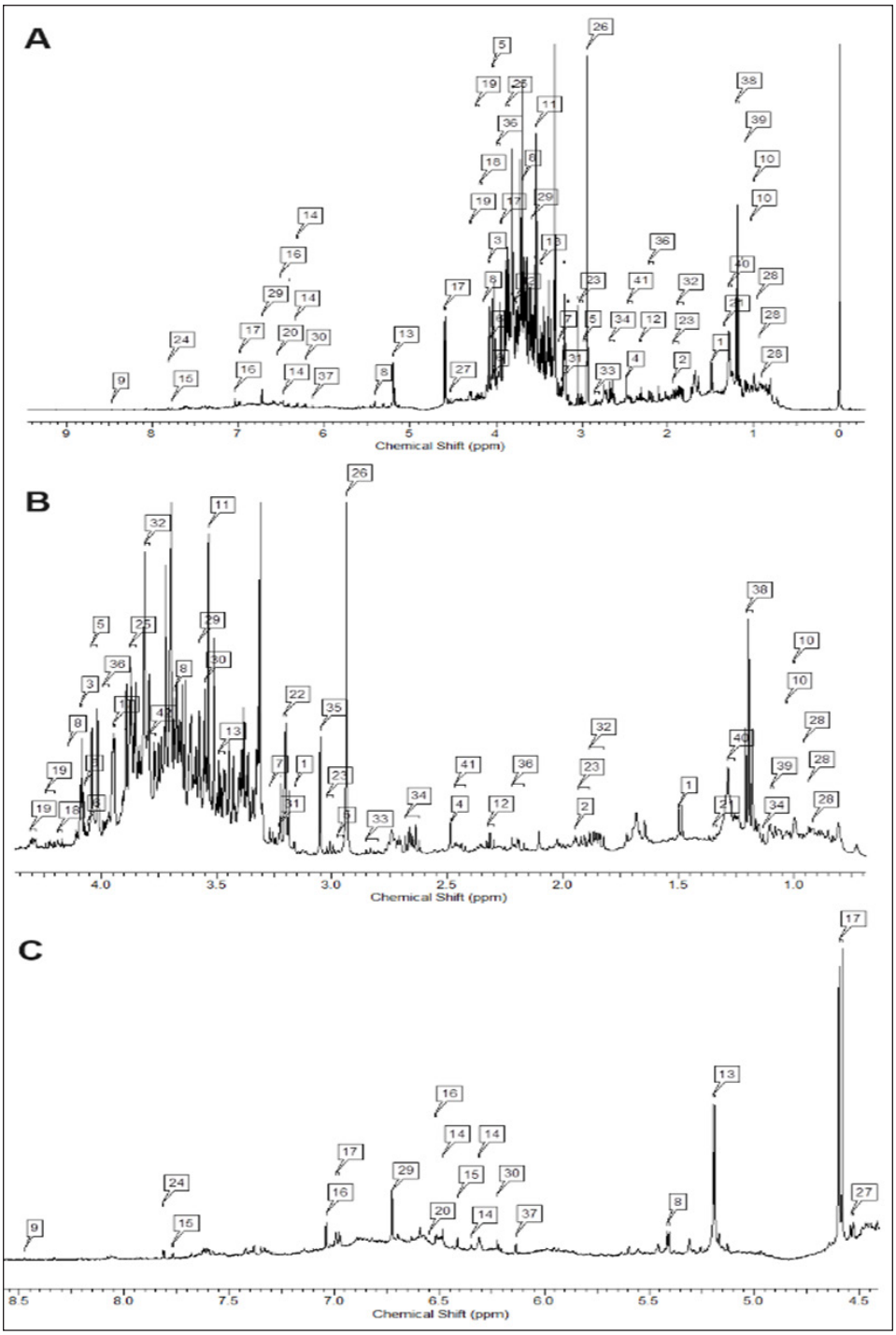

Figure 2. (A) ^{1}H NMR spectrum of *Z. mauritiana* leaves extract. (B) An expanded ^{1}H NMR spectrum between 0.50 and 4.30. (C) An expanded ^{1}H NMR spectrum between δ 4.40 and 8.51. Refer Table 1 for metabolite number interpretation

Discrimination of Extracts of *Z. mauritiana* Leaves by PCA Model from NMR Analysis

The changes of metabolite content in the four solvent extracts, i.e., hexane, chloroform, acetone, and 70% (v/v) ethanol of *Z. mauritiana* leaves were further evaluated using MVDA. PCA was applied to understand the clustering features of the four different extract samples and the metabolites contributing to the variability. PCA is an unsupervised technique that is advantageous for the identification of patterns and the fingerprinting of metabolites in data sets that lack any prior knowledge of sample information or classification (Kosmides et al., 2013). The utilization of PCA in MVDA is to recognize the pattern and cluster of the samples depending on their variance by exposing the samples to different principal components (PCs). PCA uses the PC to project original data based on a specific feature, enabling a simple evaluation of sample variability. The PCA score plot displays how samples are grouped together, while the loading plot shows how much each variable contributes and how they relate to the differences between samples (Son et al., 2008). In this study, PCA was applied to the NMR data of the four different solvent extracts of *Z. mauritiana* leaves to evaluate the differences in their metabolite contents. The score plot was created to assess the differences among the four different solvents, while the loading plot showed the metabolite signals that might help explain the differences between the clusters. Pareto scaling was selected in this analysis to reduce the influence of variables with large magnitudes while preserving the overall variance.

As shown in Figure 3A, the PCA score plot of four different solvent extracts of *Z. mauritiana* leaves obtained from ^{1}H NMR data spectra show different metabolite profiles. PC1 exhibited the greatest sample variation, followed by PC2. The PCA score plot demonstrates that PC1 accounted for 54.2% of the data's variation, while PC2 explained 30.8% of it. The different extracts of *Z. mauritiana* leaves were clustered into three groups. The chloroform and hexane extracts were combined, resulting in negative scores for PC1 and PC2, respectively. The acetone and 70% (v/v) ethanol extracts were clearly distinguished, with positive and negative PC2 scores, respectively.

Based on the PCA loading plot displayed in Figure 3B, the chloroform and hexane extracts contain higher levels of acetic acid, aspartic acid, (*Z*)-aconitic acid, lactic acid, ascorbic acid and orientin. The acetone extract was separated by having a higher content of hydroxybenzoic acid, kaempferol, (*E*)-aconitic acid, quercetin, proline, caffeoylquinic acid, alanine, succinic acid, oleic acid, *L*-rhamnitol, rutin, valine and botulin. Meanwhile, 1-*O*-ethyl-*β*-glucoside, 4-hydroxyisoleucine, arginine, asparagine, betaine, catechin, chlorogenic acid, choline, formic acid, fructose, fumaric acid, glucose, glutamic acid, glycine, leucine, malic acid, myricetin, *N,N*-dimethylglycine, phosphorylcholine, quinic acid, sucrose, *β*-pinene and *γ*-aminobutyric acid were found more abundant in 70% (v/v) ethanol extract. The metabolite distribution among these four different solvent samples extracted could be due to the polarity of these metabolites. Abdusalam et al. (2022) also

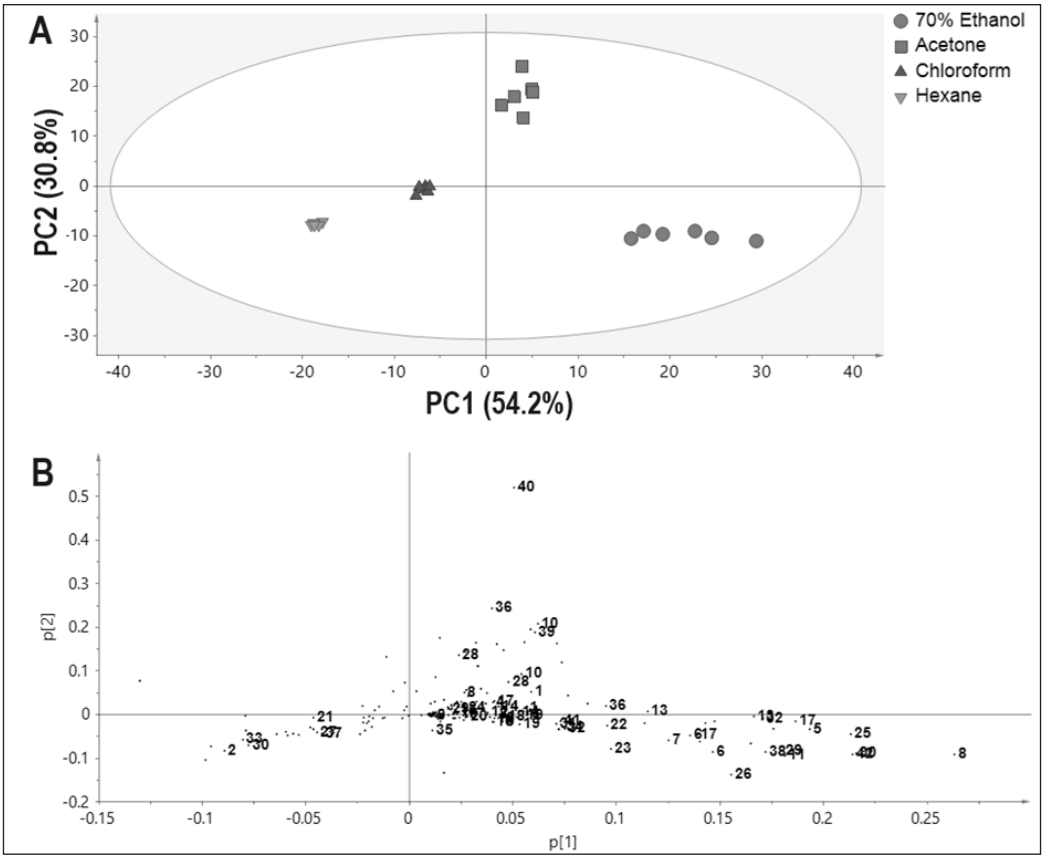

Figure 3. The PCA score (A) and loading (B) plots of different extracts of *Z. mauritiana*. Refer Table 1 for metabolite number interpretation

reported that the influence of the separation on the sample in PCA analysis is based on the polarity of the metabolites, i.e., their hydrophobic and hydrophilic characteristics.

A partial least squares (PLS) analysis was carried out to evaluate the relationship between the biological activities of the extract-identified metabolites and the selected *Vibrio* strains. *X* variables are represented by the NMR signals, while *Y* variables are represented by the inhibition zone value obtained through the disc diffusion method of anti-*Vibrio* activities against *Vibrio* species. The PLS model was validated through *R2* and *Q2* cumulative internal cross-validation. The *R2* metric quantifies the viability of a model, whereas *Q2* measures the model's prediction accuracy.

Theoretically the model's performance improves when the *R2* and *Q2* values approach 1. Indicating that the model shows a goodness-of-fit and predictive quality (Eriksson, 2006). The autofit analysis of the PLS model for *Z. mauritiana* extracts proved that the resulting model is effectively characterized by four principle components (PCs), as proven

by a cumulative goodness of fit (*R2Y*) of 0.965. Additionally, the model demonstrates strong predictive ability, as indicated by the cumulative *Q2* value of 0.936. Permutation tests were utilized to validate the PLS model. The cross-validation and permutation tests showed no PLS model overfitting (Figure S2-Supplementary data). The *Y*-intercepts of *Q2* and *R2* were below 0.5 and 0.05, respectively, signifying that the PLS model was valid and not indicative of overfitting (Maulidiani et al., 2013). Based on these results, the PLS model shows an adequate fit of the model. The PLS biplot (Figure 4) showed that the 70% (v/v) ethanol extract of *Z. mauritiana* leaves had closer anti-*Vibrio* activity against *V. parahaemolyticus, V. harveyi, V. vulnificus* and *V. campbelli.*

Among the compounds in the 70% (v/v) ethanol extract contributing to the anti-*Vibrio* activity of the *Vibrio* strains were alanine, arginine, asparagine, betaine, caffeoylquinic acid, catechin, chlorogenic acid, choline, formic acid, fructose, fumaric acid, *γ*-aminobutyric acid, glucose, glutamic acid, glycine, hydroxybenzoic acid, kaempferol, malic acid, myricetin, phosphorylcholine, proline, quercetin, quinin acid, sucrose, *N*,*N*-dimethylglycine, leucine, (*E*)-aconitic acid, (*Z*)-aconitic acid, and 4-hydroxyisoleucine. These metabolites have been

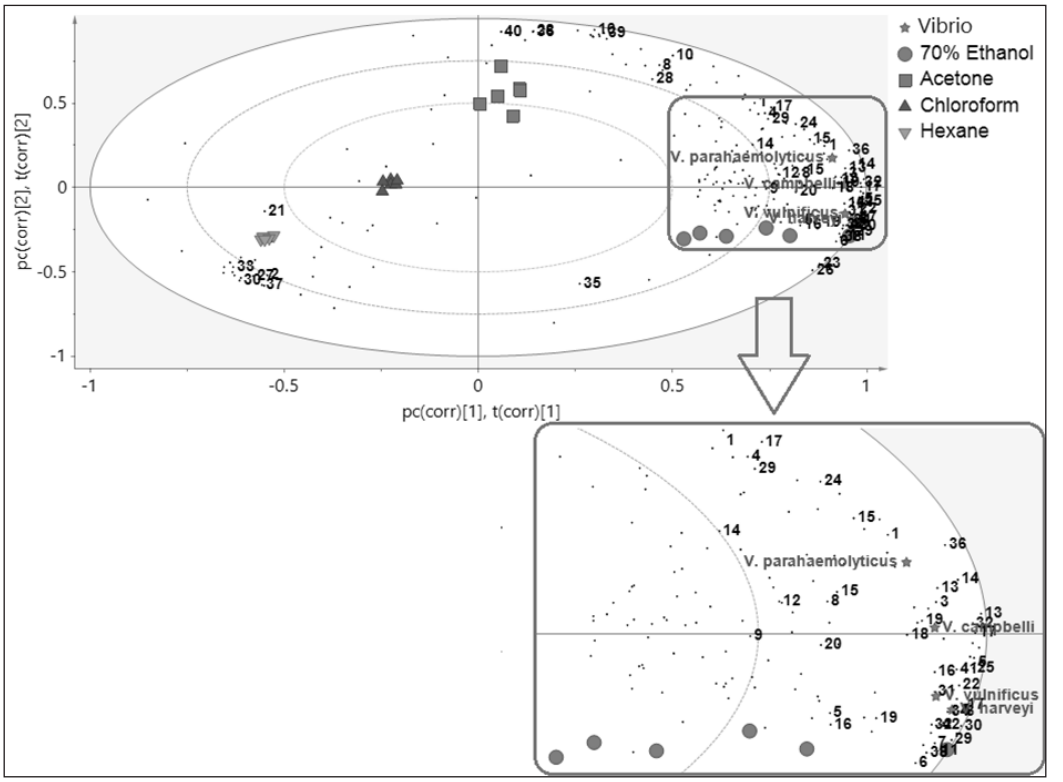

Figure 4. The PLS biplot illustrates the correlation between the metabolites found in various *Z. mauritiana* extracts and their antibacterial activity against selected *Vibrio* species. Refer Table 1 for metabolite number interpretation

shown to be antibacterial against numerous bacteria, including *Vibrio* species (Cho et al. 1998; Duranti et al., 2020; He et al., 2011; Lu et al., 2021; Mine & Boopathy, 2011; Ng et al., 2017; Otsuka et al., 2008; Roy et al., 2022; Taguri et al., 2006).

Several secondary metabolites showed significant antibacterial biological activity. Hydroxybenzoic acid has been demonstrated to be efficient against some bacteria. Cho et al. (1998) demonstrated that hydroxybenzoic acid had antibacterial properties against many types of Gram-positive and Gram-negative bacteria strains, such as *V. vulnificus*. The other metabolites of this plant, such as quercetin, catechin, myricetin, kaempferol, malic acid, formic acid and fumaric acid, were also reported to have antibacterial activity. Quercetin has been reported to exhibit high antibacterial action against *V. parahaemolyticus* (Roy et al., 2022)*, V. harveyi* (Vikram et al., 2010) and *V. campbelli* (Phuong et al., 2020). It was discovered that catechin and myricetin were responsible for inhibiting the growth of many microorganisms, including *V. parahaemolyticus, V. vulnificus* and *Aeromonas hydrophila* (Taguri et al., 2006). Kaempferol and some derivatives exhibit efficacy against *Vibrio* species, demonstrating significant antibacterial capabilities (Christopoulou et al., 2008; Habbu et al., 2009; Martini et al., 2004; Otsuka et al., 2008). Malic acid effectively inhibits infections caused by *Vibrio* species, including *V. harveyi* and *V. parahaemolyticus* (Mine & Boopathy 2011; Ng et al., 2017; Tomotake et al., 2006).

Formic acid has been shown to be a relatively effective antimicrobial. Mine & Boopathy (2011) investigated the MIC of four organic acids (formic, acetic, propionic, and butyric acids) on *V. harveyi* and discovered that formic acid was the most effective inhibitor. Fumaric acid serves as a potent antibacterial agent. Prior studies have demonstrated that fumaric acid displays potent antibacterial properties against many spoilage pathogens, such as *Campylobacter jejuni*, *Salmonella typhimurium, Escherichia coli, Listeria monocytogenes* and *Staphylococcus aureus* (Kim et al., 2001, He et al., 2011). Quinic acid has demonstrated significant antibacterial efficacy against *Staphylococcus aureus* (Bai et al., 2018) and *Pseudomonas aeruginosa* (Lu et al., 2021).

Gamma-aminobutyric acid (GABA) is found in several microbes, plants, and humans (Duranti et al., 2020). In plants, it participates in processes such as pH regulation, nitrogen storage, and growth (Shelp et al., 2012). Additionally, it serves as a plant defence mechanism against biotic stress caused by insects and necrotrophic fungi (Bown & Shelp, 2016; Seifi et al., 2013). GABA is predominantly synthesised via the irreversible α-decarboxylation of *L*-glutamic acid. The enzyme glutamic acid decarboxylase catalyses this reaction (Michaeli et al., 2011). Within the mitochondrial matrix, GABA undergoes metabolism through the GABA shunt, which is associated with various physiological processes, including the influx of carbon into the tricarboxylic acid cycle (TCAC), modulation of cytosolic pH, osmoregulation, and the generation of energy and signalling. The GABA shunt's relationship with the TCAC ultimately links carbon and nitrogen metabolism in plants (Ramos-Ruiz et

al., 2019; Shelp et al., 2017). Phong et al. (2023) determined the GABA content in lactic acid bacteria strains from seven types of Nem Chua products and tested their antibacterial efficacy against *Bacillus subtilis*. They found that the lactic acid bacteria strains contain GABA and possess antibacterial activity against *Bacillus subtilis*.

Our results suggested that the metabolites including amino acids, organic acids and fatty acid had a synergistic effect on enhancing the anti-*Vibrio* activity. It can be indicated that the combined effect of these metabolites is greater than the sum of their individual effects, leading to a more potent and effective action against *Vibrio* bacteria. This synergy can be achieved by targeting different mechanisms within the bacteria, such as disrupting cell membranes or inhibiting biofilm formation.

CONCLUSION

The study examined the phytochemical profile of *Z. mauritiana* leaf extracts, identifying various metabolites, including carbohydrates, amino acids, and both organic and fatty acids. The extract obtained using 70% ethanol exhibited elevated levels of these compounds. Additionally, it demonstrated anti-*Vibrio* activity against *V. parahaemolyticus*, *V. harveyi*, *V. vulnificus*, and *V. campbelli*, thereby supporting its traditional applications. Further investigation is required to elucidate *Z. mauritiana*'s role in antimicrobial agents, particularly regarding its effects on signalling pathways and network pharmacology. The findings highlight the potential of *Z. mauritiana* for traditional use.

ACKNOWLEDGEMENT

This work was funded by Universiti Putra Malaysia under the Geran Inisiatif Putra Muda [GP-IPM/2022/9731700].

REFERENCES

Abalaka, M.E, Daniyan, S.Y. & Mann, A. (2010). Evaluation of the antimicrobial activities of two Ziziphus species (*Ziziphus mauritiana* L. and *Ziziphus spinachristi* L.) on some microbial pathogens. *African Journal of Pharmacy and Pharmacology,* 4(4), 135-139.

Abdallah, E.M., Elsharkawy, E.R. & Ed-dra, A. (2016). Biological activities of methanolic leaves extract of *Ziziphus mauritiana*. *Bioscience Biotechnology Research Communications, 9*(4), 605-614. https://doi.org/10.21786/bbrc/9.4/6

Abdusalam, K.B., Lee, S.Y., Mediani, A., Akhtar, M.T., Buzgaia, N., Rukayadi, Y., Ismail, I.S. & Shaari, K. (2022). ^{1}H NMR-based metabolomics profiling of *Syzygium grande* and *Oenanthe javanica* and relationship between their metabolite compositions and antimicrobial activity against Bacillus species. *Records of Natural Products, 16*(2), 128-143. http://doi.org/10.25135/rnp.258.21.01.1927

Adzu, B., Amos, S., Wambebe, C. & Gamaniel, K. (2001). Antinociceptive activity of *Ziziphus* spina-christi root bark extract. *Fitoterapia, 72*(4), 344–350. https://doi.org/10.1016/S0367-326X(00)00289-6

Alam, M., Chowdhury, W.B., Bhuiyan, N.A., Islam, A., Hasan, N.A., Nair, G.B., Watanabe, H., Siddique, A.K., Huq, A., Sack, R.B., Akhter, M.Z., Grim, C.J., Kam, K.M., Luey, C.K., Endtz, H.P., Cravioto, A. & Colwell, R.R. (2009). Serogroup, virulence, and genetic traits of *Vibrio* parahaemolyticus in the estuarine ecosystem of Bangladesh. *Applied and Environmental Microbiology, 75*, 6268–6274. https://doi.org/10.1128/AEM.00266-09

Bai, J., Wu, Y., Zhong, K., Xiao, K., Liu, L., Huang, Y., Wang, Z. & Gao,0 H. (2018). A comparative study on the effects of quinic acid and shikimic acid on cellular functions of *Staphylococcus aureus*. *Journal of Food Protection, 81*(7), 1187-1192. https://doi.org/10.4315/0362-028X.JFP-18-014

Baker-Austin, C. & Oliver, J.D. (2018). *Vibrio vulnificus:* New insights into a deadly opportunistic pathogen. *Environmental Microbiology, 20*(2), 423–430. https://doi.org/10.1111/1462-2920.13955

Bown, A.W. & Shelp, B.J. (2016). Plant GABA: Not just a metabolite. *Trends in Plant Science, 21*, 811–813. https://doi.org/10.1016/j.tplants.2016.08.001

Butt, S.Z., Hussain, S., Munawar, K.S., Tajammal, A. & Muazzam, M.A. (2021). Phytochemistry of *Ziziphus mauritiana*; Its nutritional and pharmaceutical potential. *Scientific Inquiry and Review, 5*(2),1–15. https://doi.org/10.32350/sir.52.01

Cho, J.Y., Moon, J.H., Seong, K.Y. & Park, K.H. (1998). Antimicrobial activity of 4-hydroxybenzoic acid and trans 4-hydroxycinnamic acid isolated and identified from rice hull. *Bioscience, Biotechnology and Biochemistry, 62*, 2273–2276. https://doi.org/10.1271/bbb.62.2273

Choi, H.K., Yoon, J.H., Kim, Y.S. & Kwon, D.Y. (2007). Metabolomic profiling of Cheonggukjang during fermentation by ^{1}H NMR spectrometry and principal components analysis. *Process Biochemistry, 42*, 263-266. https://doi.org/10.1016/j.procbio.2006.07.014

Christopoulou, C., Graikou, K. & Chinou, I. (2008). Chemosystematic value of chemical constituents from *Scabiosa hymettia* (Dipsacaceae). *Chemistry & Biodiversity, 5,* 318-323. https://doi.org/10.1002/cbdv.200890029

Dahiru, D. & Obidoa, O. (2007). Pretreatment of albino rats with aqueous leaves extract of *Ziziphus mauritiana* protects against alcohol-induced liver damage. *Tropical Journal* of *Pharmaceutical Research, 6*(2), 705-710. https://doi.org/10.4314/tjpr.v6i2.14649

Dahiru, D., Mamman, D.N. & Wakawa H.Y. (2010). *Ziziphus mauritiana* fruit extract inhibits carbon tetrachloride-induced hepatotoxicity in male rats. *Pakistan Journal of Nutrition, 9*(10), 990–993. https://doi.org/10.3923/pjn.2010.990.993

Duranti, S., Ruiz, L., Lugli, G.A., Tames, H., Milani, C., Mancabelli, L., Mancino, W., Longhi, G., Carnevali, L., Sgoifo, A., Magolles, A., Ventura, M., Ruas-Madiedo, P. & Turroni, F. (2020). *Bifidobacterium adolescentis* as a key member of the human gut microbiota in the production of GABA. *Scientific Reports, 10,* 1–13. https://doi.org/10.1038/s41598-020-70986-z

Elmahdi, S., DaSilva, L.V. & Parveen, S. (2016). Antibiotic resistance of *Vibrio parahaemolyticus* and *Vibrio vulnificus* in various countries: A review. *Food Microbiology, 57,* 128–134. https://doi.org/10.1016/j.fm.2016.02.008

Eriksson, L. (2006). *Multi- and Megavariate Data Analysis.* 2nd ed. Umea, Sweden: Umetrics AB.

Febriza, A., Faradiana, S. & Abdullah, M.F. (2022). Antibacterial Effects of *Ziziphus mauritiana* (Lam) Leaf Extract Against *Vibrio* cholerae. *Herb-Medicine Journal, 5*(3), 9-13. https://doi.org/10.30595/hmj.v5i3.14307

Gao, H., Zhang, L., Lu, Z., He, C., Li, Q. & Na, G. (2017). Complex migration of antibiotic resistance in natural aquatic environments. *Environmental Pollution, 232*, 1–9. https://doi.org/10.1016/j.envpol.2017.08.078

Goyal, M., Nagori, B.P. & Sasmal, D. (2012). Review on ethnomedicinal uses, pharmacological activity and phytochemical constituents of *Ziziphus mauritiana* (*Z. jujuba* Lam., nonMill). *Spatula DD, 2*(2), 107-106. https://doi.org/10.5455/spatula.20120422080614

Habbu, P.V., Mahadevan, K.M., Shastry, R.A. & Manjunatha, H. (2009). Antimicrobial activity of flavanoid sulphates and other fractions of *Argyreia speciosa* (Burm.f) Boj. *Indian Journal of Experimental Biology, 47*, 121-128.

He, C.L., Fu, B.D., Shen, H.Q., Jiang, X.L. & Wei, X.B. (2011). Fumaric acid, an antibacterial component of Aloe Vera L. *African Journal of Biotechnology, 10*, 2973-2977. https://doi.org/10.5897/AJB10.1497

Heuer, O.E., Kruse, H., Grave, K., Collignon, P., Karunasagar, I. & Angulo, F.J. (2009). Human health consequences of use of antimicrobial agents in aquaculture. *Clin Infectious Diseases, 49*, 1248–1253. https://doi.org/10.1086/605667.

Jain, P., Haque, A., Islam, T., Alam, Md. A., & Reza, H. M. (2019). Comparative evaluation of *Ziziphus mauritiana* leaf extracts for phenolic content, antioxidant and antibacterial activities. *Journal of Herbs, Spices & Medicinal Plants*, *25*(3), 236–258. https://doi.org/10.1080/10496475.2019.1600627

Kebede, B. & Shibeshi, W. (2022). In vitro antibacterial and antifungal activities of extracts and fractions of leaves of *Ricinus communis* Linn against selected pathogens. *Veterinary Medicine and Science,* 8, 1802–1815. https://doi.org/10.1002/vms3.772

Kim, H.K., Choi, Y.H. &Verpoorte, R. (2011). NMR-based plant metabolomics: where do we stand, where do we go? *Trends in Biotechnology, 29*(6), 267–275. https://doi.org/10.1016/j.tibtech.2011.02.001

Kim, K.Y., Davidson, P.M. & Chung, H.J. (2001). Antibacterial activity in extracts of Camellia japonica L. petals and its application to a model food system. *Journal of Food Protection, 64*, 1255-1260. https://doi.org/10.4315/0362-028X-64.8.1255

Kosmides, A.K., Kamisoglu, K., Calvano, S.E., Corbett, S.A. & Androulakis, I.P. (2013). Metabolomic fingerprinting: Challenges and opportunities. *Critical Reviews in Biomedical Engineering*, *41*(3), 205-221. https://doi.org/10.1615/critrevbiomedeng.2013007736.

Lu, L., Zhao, Y., Yi, G., Li, M., Liao, L., Yang, C., Cho, C., Zhang, B., Zhu, J., Zou, K. & Cheng, Q. (2021). Quinic acid: A potential antibiofilm agent against clinical resistant *Pseudomonas aeruginosa*. *Chinese Medicine, 16*, Article 72. https://doi.org/10.1186/s13020-021-00481-8

Lulijwa, R., Rupia, E.J. & Alfaro, A.C. (2020). Antibiotic use in aquaculture, policies and regulation, health and environmental risks: A review of the top 15 major producers. *Reviews in Aquaculture, 12,* 640–663. https://doi.org/10.1111/raq.12344

Malla, S., Dumre, S.P., Shakya, G., Kansakar, P., Rai, B., Hossain, A., Nair, G.B., Albert, M.J., Sack, D., Baker, S. & Rahman, M. (2014). The challenges and successes of implementing a sustainable antimicrobial

resistance surveillance programme in Nepal. *BMC Public Health,* 14, 1–7. https://doi.org/10.1186/1471-2458-14-269

Martini, N.D., Katerere, D.R. & Eloff, J.N. (2004). Biological activity of five antibacterial flavonoids from *Combretum erythrophyllum* (Combretaceae). *Journal of Ethnopharmacology, 93*, 207–212. https://doi.org/10.1016/j.jep.2004.02.030

Maulidiani, M., Abas, F., Khatib, A., Shitan, M., Shaari, K. & Lajis, N.H. (2013). Comparison of partial least squares and artificial neural network for the prediction of antioxidant activity in extract of Pegaga (Centella) varieties from ^{1}H nuclear magnetic resonance spectroscopy. *Food Research International, 54*, 852-860. https://doi.org/10.1016/j.foodres.2013.08.029

Michaeli, S., Fait, A., Lagor, K., Nunes-Nesi, A., Grillich, N., Yellin, A., Bar, D., Khan, M., Fernie, A.R., Turano, F.J. & Fromm, H. (2011). A mitochondrial GABA permease connects the GABA shunt and the TCA cycle and is essential for normal carbon metabolism. *The Plant Journal, 67*(3), 485-498. https://doi.org/10.1111/j.1365-313X.2011.04612.x

Mine, S. & Boopathy, R. (2011). Effect of organic acids on shrimp pathogen, *Vibrio harveyi*. *Current Microbiology, 63*, 1–7. https://doi.org/10.1007/s00284-011-9932-2

Najafi, S. (2013). Phytochemical screening and antibacterial activity of leaves extract of *Ziziphus mauritiana* Lam. *International Research Journal* of *Applied* and *Basic Sciences, 4*(11), 3274–3276. https://doi.org/10.9734/JAMPS/2021/v23i830252

Ng, W.K., Lim, C.L., Romano, N. & Kua, B.C. (2017). Dietary short-chain organic acids enhanced resistance to bacterial infection and hepatopancreatic structural integrity of the giant freshwater prawn, *Macrobrachium rosenbergii. International Aquatic Research, 9,* 293–302. https://doi.org/10.1007/s40071-017-0177-y

Otsuka, N., Liu, M.H., Shiota, S., Ogawa, W., Kuroda, T., Hatano, T. & Tsuchiya, T. (2008). Anti-methicillin resistant Staphylococcus aureus (MRSA) compounds isolated from *Laurus nobilis*. *Biological & Pharmaceutical Bulletin, 31,* 1794-1797. https://doi.org/10.1248/bpb.31.1794

Phong, H.X., Viet, L.Q., Chau, L.M., Long, B.H.D., Thanh, N.N., Phat, D.T. & Truong, L.D. (2023). Isolation and selection of lactic acid bacteria with the capacity of producing γ-aminobutyric acid (GABA) and antimicrobial activity: Its application in fermented meat product. *Current Nutrition & Food Science, 19*, 831-37. https://doi.org/10.2174/1573401319666221115111236

Phuong, N.N.M., Le, T.T., Camp, J.V. & Raes, K. (2020). Evaluation of antimicrobial activity of rambutan (*Nephelium lappaceum* L.) peel extracts. *International Journal of Food Microbiology, 321*, Article 108539. https://doi.org/10.1016/j.ijfoodmicro.2020.108539

Pisha, E., Chai, H., Lee, I.S., Chagwedera, T.E., Farnsworth, N.R., Cordell, G.A., Beecher, C.W., Fong, H.H., Kinghorn, A.D., Brown, D.M., Wani, M.C., Wall, M.E., Hieken, T.J., Gupta, T.K.D. & Pezzuto, J.M. (1995). Discovery of betulinic acid as a selective inhibitor of human melanoma that functions by induction of apoptosis. *Nature Medicine, 1*, 1046–1051. https://doi.org/10.1038/nm1095-1046

Prakash, O., Usmani, S., Singh, R., Singh, N., Gupta, A. & Ved, A. (2020). A panoramic view on phytochemical, nutritional, and therapeutic attributes of *Ziziphus mauritiana* Lam.: a comprehensive review. *Phytotherapy Research, 35*(1), 63–77. https://doi.org/10.1002/ptr.6769

Priyanka, C., Kumar, P., Bankar, S.P. & Karthik, L. (2015). In vitro antibacterial activity and gas chromatography–mass spectroscopy analysis of *Acacia karoo* and *Ziziphus mauritiana* extracts. *Journal of Taibah University for Science, 9*(1), 13-19. https://doi.org/10.1016/j.jtusci.2014.06.007

Ramalingam, K. & Ramarani, S. (2006). Pathogenic changes due to inoculation of gram-negative bacteria *Pseudomonas aeruginosa* (MTCC 1688) on host tissue proteins and enzymes of the giant freshwater prawn, *Macrobrachium rosenbergii* (De Man). *Journal* of *Environmental Biology, 27,* 199–205.

Ramar, M.K., Henry, L.J.K., Ramachandran, S., Chidambaram, K. & Kandasamy, R. (2022). *Ziziphus mauritiana* Lam attenuates inflammation via downregulating NFκB pathway in LPS-stimulated RAW 264.7 macrophages & OVA-induced airway inflammation in mice models. *Journal of Ethnopharmacology, 295,* Article 115445. https://doi.org/10.1016/j.jep.2022.115445

Ramos-Ruiz, R., Martinez, F. & Knauf-Beiter, G. (2019). The effects of GABA in plants. *Cogent Food & Agriculture, 5*(1). https://doi.org/10.1080/23311932.2019.1670553

Roy, P.K., Song, M.G., Jeon, E.B., Kim, S.H., Park, S.Y. (2022). Antibiofilm efficacy of quercetin against *Vibrio parahaemolyticus* biofilm on food-contact surfaces in the food industry. *Microorganisms, 10*(10), Article 1902. https://doi.org/10.3390/microorganisms10101902

Rukayadi, Y., Lee, K., Han, S., Yong, D., Hwang, J.K. (2009). In vitro activities of panduratin A against clinical Staphylococcus strains. *Antimicrobial Agents and Chemotherapy, 53,* 4529–4532. https://doi.org/10.1128/AAC.00624-09

Saga, T. & Yamaguchi, K. (2009). History of antimicrobial agents and resistant bacteria. *Japan Medical Association Journal*, 52, 103–108.

Schroeder, M., Brooks, B.D. & Brooks, A.E. (2017). The complex relationship between virulence and antibiotic resistance. *Genes, 8*(1), Article 39. https://doi.org/10.3390/genes8010039

Seifi, H.S., Curvers, K., Vleesschauwer, D.D., Delaere, I., Azis, A. & Höfte, M. (2013). Concurrent overactivation of the cytosolic glutamine synthetase and the GABA shunt in the ABA-deficient sitiens mutant of tomato leads to resistance against Botrytis cinerea. *New Phytologist, 199*(2), 490–504. https://doi.org/10.1111/nph.12283

Shelp, B.J., Bown, A.W. & Zarei, A. (2017). γ-aminobutyrate (GABA): A metabolite and signal with practical significance. *Botany, 95*(11)*,* 1015–1032. https://doi.org/10.1139/cjb-2017-0135

Shelp, B.J., Bozzo, G.G., Trobacher, C.P., Zarei, A., Deyman, K.L. & Brikis, C.J. (2012). Hypothesis/review: Contribution of putrescine to 4-aminobutyrate (GABA) production in response to abiotic stress. *Plant Science, 193–194,* 130-135. https://doi.org/10.1016/j.plantsci.2012.06.001

Son, H.S., Kim, K.M., van den Berg F., Hwang, G.S., Park, W.M., Lee, C.H. & Hong, Y.S. (2008). ^{1}H nuclear magnetic resonance-based metabolomic characterization of wines by grape varieties and production areas. *Journal of Agricultural and Food Chemistry*, *56*(17), 8007-8016. https://doi.org/10.1021/jf801424u

Taguri, T., Tanaka, T. & Kouno, I. (2006). Antibacterial spectrum of plant polyphenols and extracts depending upon hydroxyphenyl structure. *Biological and Pharmaceutical Bulletin, 29*(11), 2226—2235. https://doi.org/10.1248/bpb.29.2226

Tamokou, J.D.D., Mbaveng, A.T. & Kuete, V. (2017). Antimicrobial activities of African medicinal spices and vegetables. In: Kuete, V. (eds), *Medicinal spices and vegetables from Africa: Therapeutic potential against metabolic inflammatory infectious and systemic diseases.* (pp 207-237). Cambridge: Academic Press.

Tomotake, H., Koga, T., Yamato, M., Kassu, A. & Ota, F. (2006). Antibacterial activity of citrus fruit juices against *Vibrio* species. *Journal of Nutritional Science and Vitaminology (Tokyo), 52*(2), 157-160. https://doi.org/10.3177/jnsv.52.157

Verma, S.S., Verma, R.S., Verma, S.K., Yadav, A.L. & Verma, A.K. (2018). Impact of salt stress on plant establishment, chlorophyll and total free amino acid content of ber (*Ziziphus mauritiana* Lamk.) cultivars. *Journal of Pharmacognosy and Phytochemistry, 7*(2), 556–559.

Vikram, A., Jayaprakasha, G.K., Jesudhasan, P.R., Pillai, S.D. & Patil, B.S. (2010). Suppression of bacterial cell–cell signalling, biofilm formation and type III secretion system by citrus flavonoids. *Journal of Applied Microbiology, 109*(2), 515-527. https://doi.org/10.1111/j.1365-2672.2010.04677.x

Wong, K.C., Brown, A.M., Luscombe, G.M., Wong, S.J. & Mendis, K. (2015). Antibiotic use for *Vibrio* infections: important insights from surveillance data. *BMC Infectious Diseases, 15,* Article 226. https://doi.org/10.1186/s12879-015-0959-z

Yun, N.R. & Kim, D.M. (2018). *Vibrio* vulnificus infection: a persistent threat to public health. *The Korean Journal of Internal Medicine, 33*(6), 1070-1078. https://doi.org/10.3904/kjim.2018.159

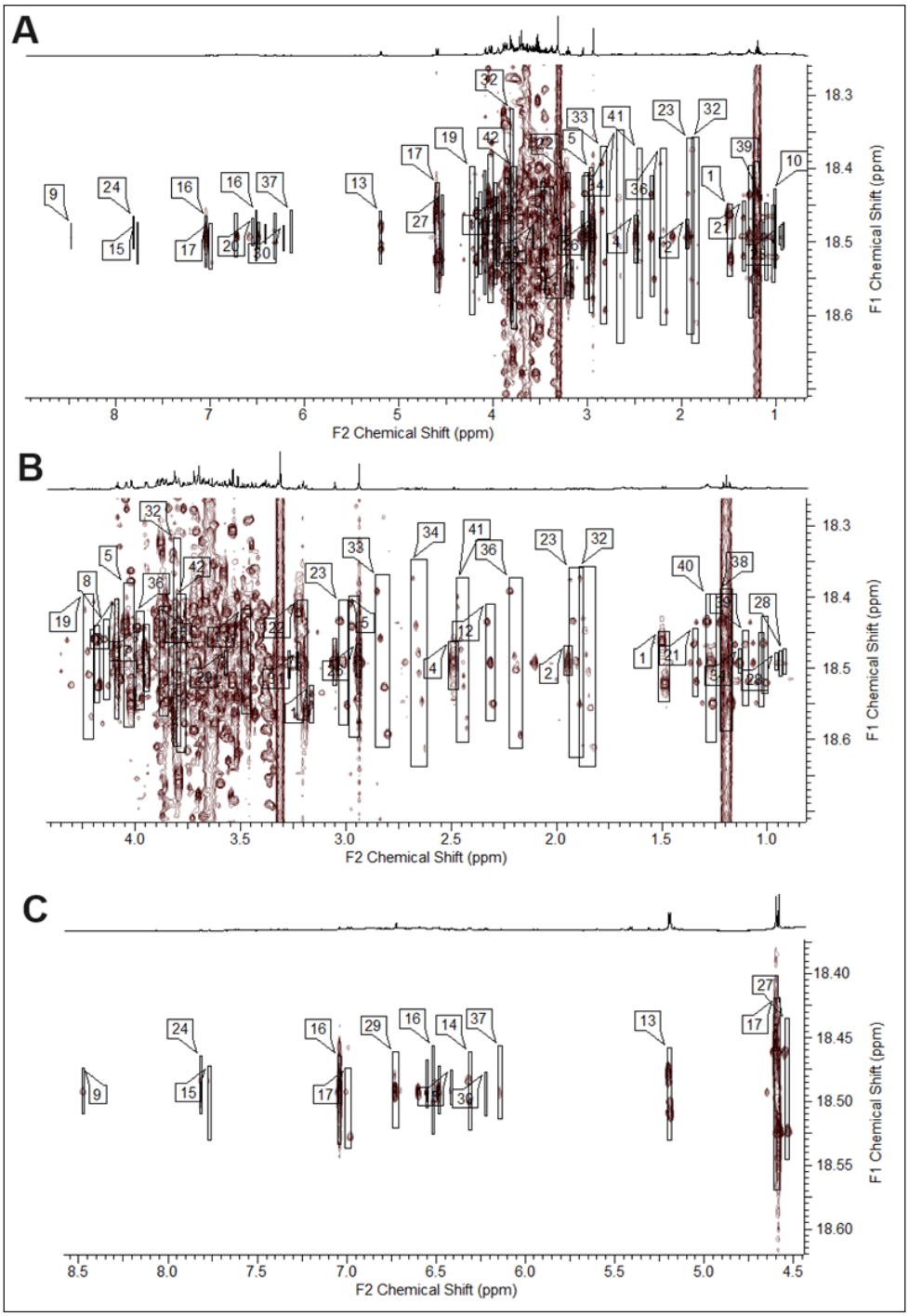

Figure S1. 2D *J*-resolved experiments of *Z. mauritiana* leaves extract: (A) in the region from *δ* 0.85 to 9.00; (B) in the region from *δ* 0.80 to 4.40; (C) in the region from *δ* 4.45 to 8.55. Refer Table 1 for metabolite number interpretation

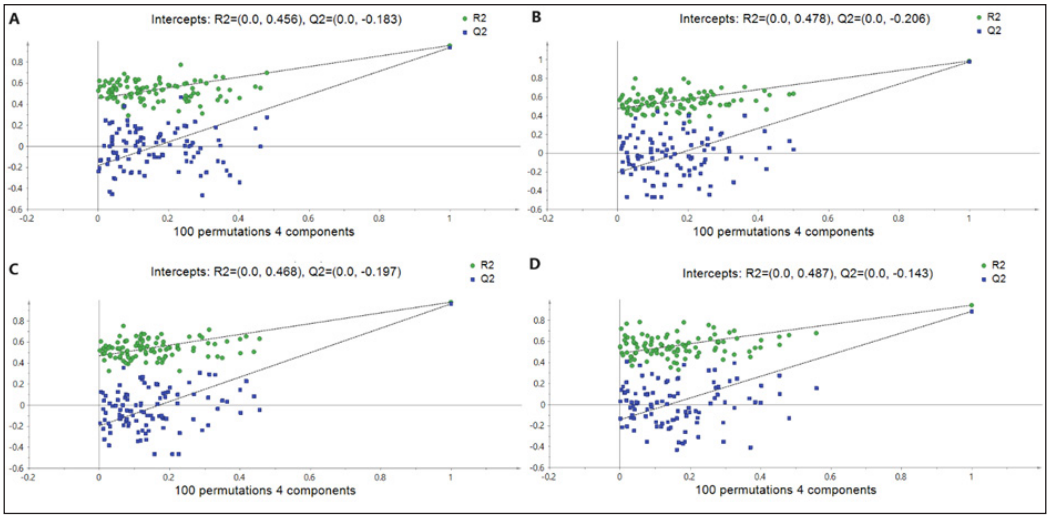

Figure S2. The permutation plots of the developed PLS model generated for the anti-*Vibrio* activity of *Z. mauritiana* extract against (A) *V. parahaemolyticus* (B) *V. harveyi* (C) *V. vulnificus* (D) *V. campbellii*

Pertanika J. Trop. Agric. Sci. 48 (6): 2057 - 2085 (2025)

PERTANIKA JOURNALS

TROPICAL AGRICULTURAL SCIENCE

Journal homepage: http://www.pertanika.upm.edu.my/

Effect of *Pennisetum purpureum* cv. Gama Umami and *Calliandra calothyrsus* Silage on Growth Performance of Thin-Tailed Sheep

Maudi Nayanda Delastra, Nafiatul Umami*, Endang Baliarti, Suci Paramitasari Syahlani, Tri Anggraeni Kusumastuti, Andriyani Astuti, and Yogi Sidik Prasojo

Faculty of Animal Science, Universitas Gadjah Mada, Jl. Fauna No. 3, Bulaksumur, 55281 Yogyakarta, Indonesia

ABSTRACT

The issue of ruminant livestock feed shortages can be addressed by utilizing innovative feed that is both nutritionally rich and available year-round. The study aimed to examine how silage influences the growth performance of thin-tailed sheep. The study was conducted in Sleman, Yogyakarta. The study involved thirty thin-tailed ewes, aged 10 to 12 months and weighing 15.03±1.09 kg. A completely randomized design (CRD) with a unidirectional arrangement was applied, involving three diet treatments and ten replications. In this study, the silage consisted of *Pennisetum purpureum* cv. Gama Umami and *Calliandra calothyrsus* in a 70:30 ratio, respectively. The diets were as follows: T0 = 60% concentrate and 40% water spinach straw, T1 = 40% concentrate and 60% silage, and T2 = 60% concentrate and 40% silage. The study focused on variables such as growth performance, apparent nutrient digestibility, and nitrogen (N) utilization. The data were examined through analysis of variance (ANOVA), followed by Duncan's new multiple range test (DMRT) for comparisons of significant differences. The performance indicators for treatments T0, T1, and T2 were as follows: dry matter intake (DMI) of 57.99, 60.12, and 65.57 g/kg $LW^{0.75}$/day, respectively; crude protein intake (CPI) of 5.98, 8.36, and 6.78 g/kg $LW^{0.75}$/day; average daily gain (ADG) of 38.96, 43.94, and 49.10 g/sheep/day; N intake of 0.90, 1.34, and 1.09 g/kg $LW^{0.75}$/day; N digestible of 0.70, 0.95, and 0.80 g/kg $LW^{0.75}$/day; and N retention of 0.56, 0.85, and 0.70 g/kg $LW^{0.75}$/day. Therefore, no single dietary treatment was universally superior, but each offered unique advantages.

Keywords: *Calliandra calothyrsus*, digestibility, nitrogen balance, *P. purpureum* cv. Gama Umami, sheep performance, silage

ARTICLE INFO

Article history:
Received: 10 March 2025
Accepted: 27 August 2025
Published: 25 November 2025

DOI: https://doi.org/10.47836/pjtas.48.6.20

E-mail addresses:
Maudi.nayanda.d@mail.ugm.ac.id (Maudi Nayanda Delastra)
nafiatul.umami@ugm.ac.id (Nafiatul Umami)
bali_arti@ugm.ac.id (Endang Baliarti)
suci.syahlani@ugm.ac.id (Suci Paramitasari Syahlani)
trianggraeni@ugm.ac.id (Tri Anggraeni Kusumastuti)
andriyaniastuti@ugm.ac.id (Andriyani Astuti)
yogi.sidik.p@ugm.ac.id (Yogi Sidik Prasojo)
*Corresponding author

e-ISSN: 2231-8542

INTRODUCTION

Indonesia is a country where small ruminants play a crucial role in the daily lives of its people. These animals not only meet the national demand for meat but also have deep cultural and religious significance (Udo & Budisatria, 2011). In the Yogyakarta region, sheep are an integral part of the local culinary tradition. However, the region faces a shortage in local sheep supply due to limited population, necessitating reliance on neighboring areas such as Central Java and Solo. According to data from the Central Bureau of Statistics Indonesia, the sheep population in Yogyakarta decreased by 36.17% between 2021 and 2023 (Badan Pusat Statistik [BPS], 2024). The rising demand for sheep, both for meat consumption and religious practices, presents a business opportunity for sheep farmers. Nevertheless, challenges persist due to limited feed availability (quality, quantity, and continuity) and high production costs.

To address the forage shortage in Indonesia, a superior grass variety, *P. purpureum* cv. Gama Umami was introduced. This variety is a mutation of the conventional Napier grass, developed through Gamma ray radiation at 100 Gy to create a new breed (Sanjaya et al., 2022). *Pennisetum purpureum* cv. Gama Umami was cultivated at the Faculty of Animal Science, Universitas Gadjah Mada, and was granted a plant variety protection certificate (889/pvhp/2020) by the Indonesian Ministry of Agriculture (Mudhita et al., 2024; Sanjata et al., 2022). It was officially recognized as a new Napier grass variety, distinguished by its longer, broader leaves compared to conventional varieties. The benefits of this grass include higher yields of fresh biomass (141.9 tons/ha), dry matter (25.85 tons/ha), and organic matter (22.96 tons/ha), all of which exceed the productivity of conventional Napier grass (104.47, 16.67, and 16.67 tons/ha, respectively) (Nurjanah et al., 2023). The high biomass potential of this grass offers an opportunity to fulfill the forage demands of ruminant livestock, though seasonal variations remain a challenge.

The grasses often lack essential nutrients and proteins necessary for optimal growth performance, leading to reduced weight gain (Marsetyo et al., 2022). Many studies have shown that supplementation of low-quality grasses with legumes not only enhances the nutritional value of animal diets but also improves growth performance. Incorporating legumes such as *C. calothyrsus* can effectively address these deficiencies due to their high protein content and favorable nutrient composition. This legume is widely cultivated in Yogyakarta and provides an affordable protein source. Therefore, as animal feed, its use must be optimized (Mudhita et al., 2024; Nurjanah et al., 2023; Roychan et al., 2023).

A strategy is needed to address the current challenges. One promising approach is to develop an innovative feed by combining *P. purpureum* cv. Gama Umami with *C. calothyrsus* and converting it into silage. This method provides an effective solution to ensure long-term feed availability while maintaining nutrient quality for ruminants. Producing silage with legume supplementation presents some challenges, as legumes can

increase silage protein content but may also lead to undesirable fermentation (Mudhita et al., 2024). However, these issues can be mitigated by carefully controlling factors such as pH levels, lactic acid bacteria (LAB) growth, moisture content, and anaerobic conditions (Dong et al., 2023; Mudhita et al., 2024). Mudhita et al. (2024) demonstrated that silage made with *P. purpureum* cv. Gama Umami and *C. calothyrsus* yielded promising results for chemical quality and *in vitro* digestibility.

In addition to forage, farmers depend on concentration, particularly when fattening thin-tailed sheep to promote rapid weight gain (Alqaisi et al., 2021; Hao et al., 2020; Huang et al., 2021). However, the heavy reliance on concentrates is problematic due to the cost of protein, which competes with human consumption and is mainly dependent on imports (Roychan et al., 2023). The synergistic effect of optimizing the forage-to-concentrate ratio in livestock is essential for maintaining nutritional balance, enhancing animal productivity, and improving cost efficiency.

Building on these findings, it hypothesized that incorporating silage (*P. purpureum* cv. Gama Umami and *C. calothyrsus*) and increasing concentrate can also improve the growth performance of thin-tailed sheep compared to water spinach straw, an alternative forage commonly used by sheep farmers in this area. However, the ratio of forage and concentration needs to be further tested. The main purpose of this study was to investigate the effect of *P. purpureum* cv. Gama Umami and *C. calothyrsus* silage affected the growth performance, nutrient digestibility, and nitrogen utilization of thin-tailed sheep.

MATERIALS AND METHODS

Animal Care

The Animal Care and Use Committee at the Faculty of Veterinary Medicine, Universitas Gadjah Mada, Yogyakarta, Indonesia, approved this study (Certification no. 32/EC-FKH/int./2024).

Description of the Study Area

The study was carried out at Savana Farm, situated in Sardonoharjo, Ngaglik, Sleman, Yogyakarta, Indonesia, with geographic coordinates 7°42'23.4"S and 110°24'02.5"E, at an altitude of 290 meters above sea level (masl). The region experienced an average temperature of 28.62±1.07°C and a humidity of 79.03±5.35%, typical of tropical climates. The area also had an average light intensity of 5.49±2.83 hr/day and a relatively low wind speed of 1.77±0.43 m/s, making it suitable for diverse ecosystems. Data from the Indonesian Agency for Meteorological, Climatological and Geophysics (2024) supports these findings. Table 1 presents the details of the agroecological zones in the study area.

Table 1
Measurement of environmental conditions during the study

Variables	Mean±Standard deviation	Minimum	Maximum
Temperature (°C)	28.62±1.07	24.19	31.74
Wind velocity (m/s)	1.77±0.43	1.00	3.94
Humidity (%)	79.03±5.35	66.00	88.00
Light intensities (h)	5.49±2.83	0.30	10.30

Source: Indonesia Agency for Meteorological, Climatological, and Geophysics (2024)

Experimental Animals

Thirty thin-tailed ewes, with an initial live weight of 15.03±1.09 kg, aged 10 to 12 months, were used in the study. Each ewe was identified with an ear tag, and a deworming treatment using Leva-200® (containing levamisole, PT Tekad Mandiri Citra, Bandung, Indonesia) was administered orally at a dose of 1 cc/20 kg of live weight to ensure proper health management and facilitate observation throughout the study. Additionally, Wormectine® (containing ivermectin, PT Medion, Bandung, Indonesia) was provided to the sheep at the study's onset (adaptation period) to prevent worm infection. Ewes were randomly placed in individual pens, each measuring 70 × 150 cm, with water available *ad libitum*. Each sheep pen was fitted with separate containers for collecting feces and urine (metabolic pens). All animals were healthy, non-pregnant, and non-lactating adults.

Silage Material

Both grass (*P. purpureum* cv. Gama Umami) and legume (*C. calothyrsus*) were planted in Turi, Sleman, Yogyakarta, Indonesia (-7.6743080°S, 110.3729523°E), and harvested at 60 and 90 days of age, respectively. After harvesting, both the grass and legume were air-dried naturally for 2 to 4 days. It was considered ready for processing into silage if only a small amount of moisture was released when the material was squeezed in the palm. The edible parts of the grass and legumes were selected for silage. They were then chopped into 3-5 cm pieces using a chopping machine. The final silage mixture consisted of grass and legumes in a 70:30 ratio, respectively, with the addition of 7.5% wheat pollard as an accelerator to stimulate LAB fermentation. All components were thoroughly mixed and then placed into the drum silos gradually. Each layer was compacted by manually stepping on it with the feet to minimize trapped air and create an anaerobic condition during the fermentation process. Finally, the drum silos were closed with an airtight seal and then placed upside down (the silo lid was at the bottom). In this study, the silo used PVC drum silos that stand 82 cm tall and had a diameter of 42 cm, with a 100 kg capacity. Each silo was fermented for 21 days with a daily temperature of 24 to 27°C and a relative humidity of 55 to 65%. The silage was composed of *P. purpureum* cv. Gama Umami (21.10% DM),

legumes (34.36% DM), and wheat pollard (86.00% DM). The chemical composition (%) of the silage is shown in Table 2.

Table 2
Chemical composition (%) of the raw materials used in the experimental diets

Composition (%)	Ingredients		
	Silage (*Pennisetum purpureum* cv. Gama Umami x *Calliandra calothyrsus*)*	**Nutrifeed® concentrate****	**Water spinach straw***
DM	28.19	86.00	88.56
OM	73.11	87.00	85.18
CP	13.58	13.00	6.28
CF	28.61	12.00	29.18
EE	5.76	7.00	2.45
NFE	25.16	45.00	42.49
TDN***	60.48	70.00	56.39

Note. *Analysis results from Forage and Pasture Laboratory, Faculty of Animal Science, Universitas Gadjah Mada; **KJUB Puspetasari; *** Calculated according to Hartadi et al. (1990); DM = Dry matter; OM = Organic matter; CP = Crude protein ; CF = Crude fiber ; EE = Extract ether ; NFE = Nitrogen-free extract; TDN = Total digestible nutrients

Diets

The diet treatments were formulated based on dry matter requirements, approximately 3.3% of the sheep's body weight, to support a daily weight gain of 25 g/day according to the National Research Council (NRC) (2007). Specifically, the diets delivered 42 g of crude protein (CP) and 240 g of total digestible nutrient (TDN) per day for sheep weighing 15 kg (Kearl, 1982). The diets were provided in equal portions, given twice a day at 8 a.m. and 4 p.m. For each treatment, the forage (either silage or water spinach straw) was mixed with a Nutrifeed® concentrate sourced from KJUB Puspetasari Klaten, Central Java, Indonesia, in different ratios. The composition included rice bran, wheat bran, molasses, palm kernel meal, cassava pulp, coconut cake, corn bran, corn gluten feed (CGF), and distiller's dried grains with soluble (DDGS). While the water spinach straw was taken from local farmers in Krasaan, Jogotirto, Berbah, Sleman Regency, Yogyakarta, with geographic coordinates 7°48′56″S and 110°27′49″E. Before it was given to the sheep, the water spinach straw had been cut into 1 to 3 cm pieces. The experimental diet treatments were as follows: T0 = 60% concentrate and 40% water spinach straw, T1 = 40% concentrate and 60% silage, and T2 = 60% concentrate and 40% silage. Table 1 presents the chemical composition (%) of the raw materials used in the experimental diets, while Table 3 presents the ingredient proportions and chemical compositions (% on DM basis) for the experimental diets for thin-tailed sheep.

Table 3
Ingredients proportion and chemical compositions in the feed ratio treatments (% on DM basis) of thin-tailed sheep

Ingredients	Treatments (%)		
	T0	T1	T2
Silage based on *Pennisetum purpureum* cv. Gama Umami x *Calliandra calothyrsus*	0	60	40
Nutrifeed® concentrate	40	40	60
Water spinach straw	60	0	0
Total	100	100	100
Chemical compositions [(%) DM]			
DM	87.02	51.31	62.88
OM	86.27	78.67	81.44
CP	10.31	13.35	13.23
CF	18.87	21.97	18.64
EE	5.18	6.26	6.50
NFE	44.00	33.10	37.06
TDN	64.56	64.29	66.19

Note. T0 = 60% concentrate and 40% water spinach straw; T1 = 40% concentrate and 60% silage; T2 = 60% concentrate and 40% silage; DM = Dry matter; OM = Organic matter; CP = Crude protein; CF = Crude fiber; EE = Extract ether; NFE = Nitrogen-free extract; TDN = Total digestible nutrients

Determination of Nutrient Intake, Growth Performance, and Feed Conversion

The *in vivo* period lasted for 56 days, including 14 days as an adaptation period (from day 1 to day 14), followed by 42 days as the actual study period (from day 15 to day 56).

During the adaptation period, all sheep were weighed before entering to determine their initial body weight as a basis for feed requirements. The purpose of this period was to acclimate the sheep to the diet treatment and to eliminate the effects of the previous feed. Feed was given twice a day at 8 a.m. and 4 p.m. Feeding and drinking water were provided *ad libitum*.

The actual study period began on day 15 (after the adaptation period was completed) and lasted until day 56 (the end of the *in vivo* period). During this period, the measurements of nutrient intake, ADG, and feed conversion were carried out. The treatment diet was administered daily at 8 a.m., while the remaining feed was collected and weighed at 7 a.m. the following day. Samples of both the provided feed and the remaining feed were collected daily for each individual sheep (g/sheep/day). The samples were weighed, placed in sample bags, and dried in an oven at 55°C for five days or until a constant weight was achieved. After drying, the samples were ground using a Willey mill with a 1 mm sieve for subsequent nutrient content analysis in the laboratory. The nutrient intake was determined based on metabolic live weight (g/kg $LW^{0.75}$). This method was adopted from Sanjaya et al. (2022):

nutrient intake was measured by subtracting the remaining feed from the provided feed and multiplying this value by the nutrient content of the feed, including dry matter (DM), organic matter (OM), crude protein (CP), crude fiber (CF), extract ether (EE); nitrogen-free extract (NFE), and total digestible nutrients (TDN). The ADG was carried out before morning feeding every two weeks (d-14, d-28, d-42, and d-56) to monitor the increase in sheep body weight during the dietary treatment period. In the ADG calculation (Suhartanto et al., 2022), the weight of each sheep was recorded before feeding, both at the initial body weight (IBW) and at the final body weight (FBW). The ADG absolute was determined by the formula: (FBW – IBW) / 14 days, while the relative ADG was determined by the formula: ADG absolute x 100%. Feed conversion was determined based on the ratio of DMI to ADG, measured by the formula: DMI/ADG (Suhartanto et al., 2022).

Determination of the Apparent Nutrient Digestibility and Nitrogen Utilization

Ten days before the end of the actual study period (from day 46 to day 56), feces and urine were collected from each sheep to analyze the apparent nutrient digestibility and nitrogen content in urine. These samples were collected every morning before the sheep were fed. The feces and urine sample collection method was adopted from Rahayu et al. (2021).

The feces excreted by each sheep over 24 hours were collected daily in a collection tray, separated from impurities such as remaining feed or foreign materials, and weighed to determine the total daily output. Subsequently, up to 50% of the total daily feces were sampled, placed into sample bags, and dried in an oven at 55°C for 5 days or until a constant weight was achieved to prevent decomposition and nitrogen loss. The dried samples were then weighed and stored in a refrigerator. At the end of the collection period (day 56), a daily sample from each sheep was ground, and as much as 10% of each was composited to produce a homogeneous composite sample. A sub-sample of the composite was then taken for chemical analysis of the feces. Apparent nutrient digestibility was calculated by the formula: (nutrient intake [NI] – a nutrient in feces) / NI × 100% (Rahayu et al., 2021).

Urine excreted by each sheep over 24 hours was collected daily in a plastic bucket, then filtered to remove contaminants. As much as 10% of the total daily volume was taken and acidified with 10% sulfuric acid (H_2SO_4 98%, Merck, Germany) to achieve an acidic pH (below 3), in order to preserve nitrogen content. The acidified samples were transferred into 50 ml bottles and stored in a freezer at -20°C. Daily urine samples collected from each sheep over a 10-day collection period were combined to obtain a homogeneous composite sample. Sub-samples from the composite were then used for nitrogen analysis in the urine. The nitrogen balance was assessed by determining the difference between input nitrogen from feed and the nitrogen excreted in feces and urine (Rahayu et al., 2021).

Chemical Analysis

The analysis of feed and feces was conducted following the Association of Official Analytical Chemists (AOAC) guidelines to determine dry matter (AOAC 934.01), crude protein (AOAC 2001.11), crude fiber (AOAC 978.10), ether extract (AOAC 920.39), and ash (AOAC 942.05) (AOAC, 2005). The nitrogen-free extract (NFE) was calculated by subtracting the sum of CP, EE, CF, and ash from the DM, as follows: NFE = [100 - (CP + EE + CF + ash)]. The total digestible nutrients (TDN) were calculated by the formula: TDN = -26.685 + 1.334(CF) + 6.598(EE) + 1.423(NFE) + 0.967(CP) – 0.002$(CF)^2$ – 0.67$(EE)^2$ – 0.024(CF)(NFE) – 0.055(EE)(CP) + 0.039(EE)(CP) (Hartadi et al., 1990). The nitrogen concentration in urine was assessed using Kjeldahl method (AOAC 2001.11) in the AOAC-recommended method (AOAC, 2005).

Study Design and Data Analysis

The data was analyzed by a CRD with a unidirectional arrangement, involving three different diet treatments and ten replications. The independent factor was the diet treatment: T0 = 60% concentrate and 40% water spinach straw, T1 = 40% concentrate and 60% silage, and T2 = 60% concentrate and 40% silage. The variables examined were nutrient intake, ADG, feed conversion, apparent nutrient digestibility, and nitrogen utilization. Statistical analysis was performed using analysis of variance (ANOVA) through SPSS software (version 26.0). A p-value < 0.05 was considered to determine significant differences between the treatment means.

RESULT AND DISCUSSION

Nutrient Intake

Nutrient intake observed in this study was expressed on a metabolic live weight (g/kg $LW^{0.75}$) basis, including DM, OM, EE, CF, CP, and NFE in each treatment. The statistical analysis results in this study show that nutrient intake (DM, OM, EE, CF, CP, and NFE) exhibited significant differences among treatments (p<0.05). Nutrient intake of thin-tailed sheep fed based on silage in different ratios (g/kg $LW^{0.75}$/day) is presented in Table 4.

According to the statistical analysis, the incorporation of *P. purpureum* cv. Gama Umami and *C. calothyrsus* silage (T1 and T2) in different ratios significantly increased DMI by 3.67 and 13.07%, respectively, compared to water spinach straw (T0) (p<0.05). Moreover, T2 exhibited a significantly higher DMI than T1, with an increase of 9.06% (p<0.05). The results of this study indicate that feed containing high CP and low CF produced higher DMI. The higher DMI in the silage (T1 and T2) than in water spinach straw (T0) resulted in higher CP content in T1 and T2. Meanwhile, the higher DMI in T2 than in T1 influenced the low CF content in T2. Several factors influenced the high DMI

Table 4
Nutrient intake of thin-tailed sheep fed based on silage in different ratios (g/kg $LW^{0.75}$/day)

Nutrient intake (g/kg $LW^{0.75}$/day)	Treatments			SEM	*p*-value
	T0	T1	T2		
DM	57.99[c]	60.12[b]	65.57[a]	0.63	0.00
OM	50.03[b]	45.66[c]	52.76[a]	0.58	0.00
EE	3.00[c]	4.14[a]	3.47[b]	0.09	0.00
CF	10.95[b]	12.23[a]	12.06[a]	0.13	0.00
CP	5.98[c]	8.36[a]	6.78[b]	0.18	0.00
NFE	25.51[b]	18.84[c]	28.76[a]	0.77	0.00

Note. Different superscripts in the same row represent significant differences ($p<0.05$); T0 = 60% concentrate and 40% water spinach straw; T1 = 40% concentrate and 60% silage; T2 = 60% concentrate and 40% silage; SEM = Standard error of the mean; DM = Dry matter; OM = Organic matter; EE = Ether extract; CF = Crude fiber; CP = Crude protein; NFE = Nitrogen-free extract

in the silage (T1 and T2) compared to water spinach straw (T0). First, the inclusion of *Calliandra* in the forage ratios increased the protein content of the silage. Legumes such as Calliandra are known for their high protein content, which enhances the overall nutritional value of the feed. This is supported by the chemical composition of silage, which contained 13.58% CP compared to 6.28% in water spinach straw, as shown in Table 2. Furthermore, CP contents in T1 (13.35%) and T2 (13.23%) were higher than in T0 (10.31%), as shown in Table 3. Second, a synergistic interaction between pollard and Calliandra in the silage may have enhanced rumen microbial activity. Such synergy can optimize fermentation, accelerate rumen emptying, and ultimately increase feed intake. Third, fermented feeds generally exhibit more desirable physical characteristics (e.g., aroma, texture, and shape), which improve palatability and acceptance by ruminants. The findings of this study align with those of Abdelraheem et al. (2023), who observed that sheep fed with higher CP levels tend to consume more feed, likely due to the improved palatability and nutritional content. A study on Assaf lambs revealed that those on high-protein diets (23% CP) had significantly higher DMI at 885 g/day than lambs fed lower-protein diets (16% CP) (Saro et al., 2020). The combination of legumes and grasses in silage not only enhances protein content but also improves its overall nutritional value (Castro-Montoya & Dickhoefer, 2018; Niderkorn et al., 2015). Previous studies have shown that increasing the proportion of legumes, such as *Calliandra*, in ruminant rations can increase the degradation of other feeds, such as grasses (Rira et al., 2022). This synergistic blending not only increases the overall digestibility of the ration but also accelerates rumen emptying. Increasing the rumen turnover rate is essential for optimizing feed intake and utilization, as faster rumen emptying allows animals to consume more feed (Knowles et al., 2017; Sriyani et al., 2018).

Fermented feeds are generally more palatable than non-fermented ones due to factors like aroma, texture, and shape, which influence sheep's feeding preferences (Ahmad et al., 2023; Berthel et al., 2022). Additionally, LAB involved in silage fermentation can contribute to a better taste and scent, thereby encouraging greater intake (Ridwan et al., 2023). Han et al. (2022) noted that LAB plays a key role in shaping the fermentation process and the microbial community within silage.

Although both silage treatments improved DMI, T2, which contained 60% concentrate, resulted in a significantly higher DMI than T1, which contained 40% concentrate ($p<0.05$). This may be due to the inverse relationship between CF content and DMI. Despite having comparable CP levels (T1: 13.35%, T2: 13.23%), T2 had a lower CF content (18.64%) than T1 (21.97%), contributing to its higher DMI, as presented in Table 3. A higher concentrate ratio reduces the structural carbohydrate content of the diet, which facilitates rumen emptying and enhances feed intake. This finding aligns with Ipharraguerre et al. (2002), who reported that diets high in neutral detergent fiber (NDF) reduce DMI due to increased gut fill and slower digestion rates. High CF content increases satiety by slowing digestion, potentially limiting overall nutrient intake. Several studies have shown that extended rumination times are associated with reduced DMI, as animals spend more time chewing fibrous feeds and less time-consuming additional feed. Parente et al. (2016) demonstrated that diets high in fiber increase chewing and rumination time, thereby reducing voluntary intake. Similarly, Sanjaya et al. (2022) reported that low-quality forages with high CF content are associated with reduced DMI. Additionally, CF content influences the metabolic energy (ME) value of the feed. According to Utama et al. (2023), CF can improve the ME value, potentially leading to higher feed consumption. In the present study, DMI was highest in T2, followed by T1 and T0, with values of 65.57, 60.12, and 57.99 g/kg $LW^{0.75}$/day, respectively. However, these values were lower than those reported by Sanjaya et al. (2022), who observed a DMI of 78.88 g/kg $LW^{0.75}$/day in thin-tailed sheep fed a diet consisting of 25% *P. purpureum* cv. Gama Umami + 8% water spinach + 68% concentrate.

Organic matter intake (OMI) in this study showed a significant effect on all treatments ($p<0.05$). Interestingly, the OMI value at T2 was significantly higher than in T0, whereas T1 exhibited a lower value than T0 ($p<0.05$). Although T0 and T2 had the same concentrate ratios (60%), OMI in T2 remained significantly higher than in T0 ($p<0.05$). This finding is consistent with the DMI, which was also highest in T2 compared to the other treatments. These results suggest a synergistic effect of the balanced combination of silage and concentrate in T2, enhancing the efficiency of both DMI and OMI. The close relationship between DMI and OMI can be attributed to the fact that the majority of dry matter consists of organic matter (Abun et al., 2022). Accordingly, an increase in DMI tends to be accompanied by a rise in OMI, provided the feed composition is of good quality. Carvalho et al. (2020) further emphasized the critical role of feed quality in determining nutrient

intake, which correlates strongly with both DMI and OMI. Interestingly, DMI in T1 was higher than in T0; OMI in T1 was the lowest among all treatments. This discrepancy is likely due to the suboptimal feed composition in T1, particularly its high CF or indigestible lignin content, which limits the proportion of OM that can be effectively utilized by livestock. As noted by Carvalho et al. (2020), feed quality is a critical factor influencing nutrient intake efficiency. Diets with poor nutritional value—characterized by high CF content—may result in high DMI but low nutrient absorption, including OMI. Specifically, elevated levels of NDF or acid detergent fiber (ADF) can lead to this paradoxical effect: DMI increases while the absorption of organic matter remains limited due to the physical constraints imposed by fibrous components on digestion (Huuskonen & Pesonen, 2017; Oliveira et al., 2020). In the present study, OMI was highest in T2, followed by T0 and T1, with values of 52.75, 50.03, and 45.66 g/kg $LW^{0.75}$/day, respectively. However, these values were lower than those reported by Sanjaya et al. (2022), who observed an OMI of 71.06 g/kg $LW^{0.75}$/day in thin-tailed sheep fed a diet consisting of 25% *P. purpureum* cv. Gama Umami, 8% water spinach, and 68% concentrate.

Ether extract intake (EEI) in this study showed a significant effect on all treatments (p<0.05). The incorporation of *P. purpureum* cv. Gama Umami and *C. calothyrsus* silage (T1 and T2) in different ratios significantly increased EEI compared to water spinach straw (T0) (p<0.05). Interestingly, although both silage treatments increased EEI, the value was significantly higher in T1 than in T2 (p<0.05). These results indicate a strong correlation between EEI and total energy intake in thin-tailed sheep, with consistent trends observed across treatments. Notably, T1 produced the highest EEI despite exhibiting the lowest OMI. This condition reflects a compensatory physiological response, where livestock increase fat consumption to meet energy needs and maintain energy balance. In contrast, at T2, energy balance has been achieved. The relationship between EEI and energy intake becomes especially critical under conditions of limited OMI availability. Tewari et al. (2022) reported that supplementation with crude lecithin derived from rice bran EE increased the digestibility of crude lecithin but reduced the digestibility of DM and OM. This supports the notion that under suboptimal feeding conditions, livestock may rely more heavily on fat as an alternative energy source, influencing overall metabolic function. Furthermore, dos Santos et al. (2011) found a significant interaction between EEI and energy intake levels in sheep fed different corn varieties, highlighting the broader relevance of EEI in ruminant energy metabolism. Overall, the interaction between EEI and energy retention is vital for maintaining energy balance, particularly in animals under nutritional constraints. In the present study, EEI was highest in T1, followed by T2 and T0, with values of 4.14, 3.47, and 3.00 g/kg $LW^{0.75}$/day, respectively. Sanjaya et al. (2022), who observed an EEI of 3.89 g/kg $LW^{0.75}$/day in thin-tailed sheep fed a diet consisting of 25% *P. purpureum* cv. Gama Umami, 8% water spinach, and 68% concentrate.

Crude fiber intake (CFI) in this study showed the incorporation of *P. purpureum* cv. Gama Umami and *C. calothyrsus* silage (T1 and T2) in different ratios significantly increased CFI compared to water spinach straw (T0) ($p<0.05$). While T1 and T2 did not show a significant difference ($p>0.05$). In this study, CFI values were closely associated with other intake parameters such as DMI and OMI. The lowest CFI observed in T0 correlated with its lowest DMI (57.99 g/kg $LW^{0.75}$/day). In contrast, T2 recorded the highest DMI (65.57 g/kg $LW^{0.75}$/day), accompanied by a proportional increase in CFI, indicating that the ration in T2 supported fiber intake without compromising overall feed consumption. While T1 also showed relatively high CFI, it was accompanied by the lowest OMI (45.66 g/kg LW0.75/day), suggesting an imbalance in organic matter composition, likely due to the ration's high fiber content (21.97%; Table 3). Therefore, T2 appears to represent a more optimal balance among DMI, OMI, and CFI, reflecting a ratio that supports both nutrient intake and utilization. Fiber plays a key role as a physical stimulant in ruminants, promoting grazing behavior, mastication, and salivation—all of which are essential for maintaining rumen health and facilitating efficient fermentation (Carvalho et al., 2020). High CFI generally reflects low energy density of feed. To meet energy needs, ruminants will increase DMI as a form of compensation (Carvalho et al., 2020). This means that when forage quality is low, animals tend to increase CFI to maximize nutrient acquisition. One reason for the increase in CFI in low OMI conditions is the decrease in forage digestibility. Forage-based diets, such as hay, typically contain high CF but low levels of digestible organic matter, prompting animals to increase fiber intake despite its limited energy yield. In the present study, CFI was highest in T1, followed by T2 and T0, with values of 12.23, 12.06, and 10.95 g/kg $LW^{0.75}$/day, respectively. However, these values were lower than those reported by Sanjaya et al. (2022), who observed a CFI of 14.75 g/kg $LW^{0.75}$/day in thin-tailed sheep fed a diet consisting of 25% *P. purpureum* cv. Gama Umami, 8% water spinach, and 68% concentrate.

Crude protein intake (CPI) in this study showed a significant effect on all treatments ($p<0.05$). The incorporation of *P. purpureum* cv. Gama Umami and *C. calothyrsus* silage (T1 and T2) in different ratios significantly increased CPI compared to water spinach straw (T0) ($p< 0.05$). Interestingly, although both silage treatments increased CPI, the value was significantly higher in T1 than in T2 ($p< 0.05$). In this study, the increase in CPI was related to the CP content in the ration and the availability of digestible protein. Higher dietary protein levels enhance the likelihood of meeting the animals' protein requirements. The CP content in the rations for T0, T1, and T2 was 10.31%, 13.35%, and 13.23%, respectively (Table 3), with CPI values reflecting this composition. These findings are consistent with those of Fajemisin et al. (2020), who reported that goats fed diets with higher-quality protein sources exhibited greater CPI. In this study, the CPI value at T1 (8.36 g/kg $LW^{0.75}$/day) was recorded as higher than that at T2 (6.78 g/kg $LW^{0.75}$/day), although the CP content in both

rations was relatively similar. This difference can be attributed to the feed composition, where T1 has a forage to concentrate ratio of 60:40, while T2 is 40:60. The higher CPI at T1 suggests that protein derived from silage may be more bioavailable, leading to greater protein utilization despite a lower total DMI than T2. These findings align with Yousefi et al. (2025) , who noted that fermentation can enhance nutritional quality by improving protein solubility and digestibility. Furthermore, the activity of rumen microbes in degrading protein plays a critical role in determining CPI, implying that silage-derived protein in T1 was more effectively utilized by rumen microorganisms, resulting in greater protein intake. In the present study, CPI was highest in T1, followed by T2 and T0, with values of 8.36, 6.78, and 5.98 g/kg $LW^{0.75}$/day, respectively. However, these values were lower than those reported by Sanjaya et al. (2022), who observed a CPI of 11.84 g/kg $LW^{0.75}$/day in thin-tailed sheep fed a diet consisting of 25% *P. purpureum* cv. Gama Umami, 8% water spinach, and 68% concentrate.

Nitrogen-free extract intake (NFEI) in this study was significantly affected by all treatments ($p<0.05$). Notably, NFEI at T2 was significantly higher than T0, while T1 showed a significantly lower value than T0 ($p<0.05$). The NFEI was found to correlate with other nutritional components, such as CP, EE, and CF. In T1, there was high CF content and CFI, and it also had the lowest TDN value at 64.29% exhibiting the lowest NFEI. In contrast, T2 recorded the highest TDN value at 66.19% resulting in the highest NFEI. The availability of energy-rich NFE in the diet is directly correlated with microbial protein synthesis in the rumen (Abdelkader., 2019; Parchami et al., 2024). When ruminants consume a diet high in NFE, the microbial population utilizes carbohydrates to synthesize microbial proteins from non-protein nitrogen sources such as urea and ammonia (Molitor et al., 2023). Microbial proteins are crucial because they pass into the small intestine, where they are absorbed and provide essential amino acids for growth and production. Thus, maintaining a balanced NFE intake is critical for maximizing microbial protein synthesis and optimizing the animal's nutritional status (Wei et al., 2024). A balanced NFEI supports optimal rumen fermentation processes, resulting in increased production of volatile fatty acids (VFAs), which serve as the primary energy source for their host ruminants (Mudgal et al., 2018). Research has demonstrated that diets with appropriate NFE levels enhance the production of key VFAs, particularly propionate and butyrate, thereby improving overall energy availability (Liu et al., 2024).

Growth Performance and Feed Conversion

Growth performance determination can be done by measuring ADG absolute, ADG relative, and feed conversion. The statistical analysis results in this study show that ADG absolute and ADG relative differed significantly among treatments ($p<0.05$). While incorporating *P. purpureum* cv. Gama Umami and *C. calothyrsus* silage (T1 and T2) exhibited lower

feed conversion (p<0.05) than water spinach straw (T0), although T1 and T2 showed no significant difference (p>0.05). The comparison of ADG absolute, ADG relative, and feed conversion of thin-tailed sheep fed based on silage in different environments is presented in Figure 1.

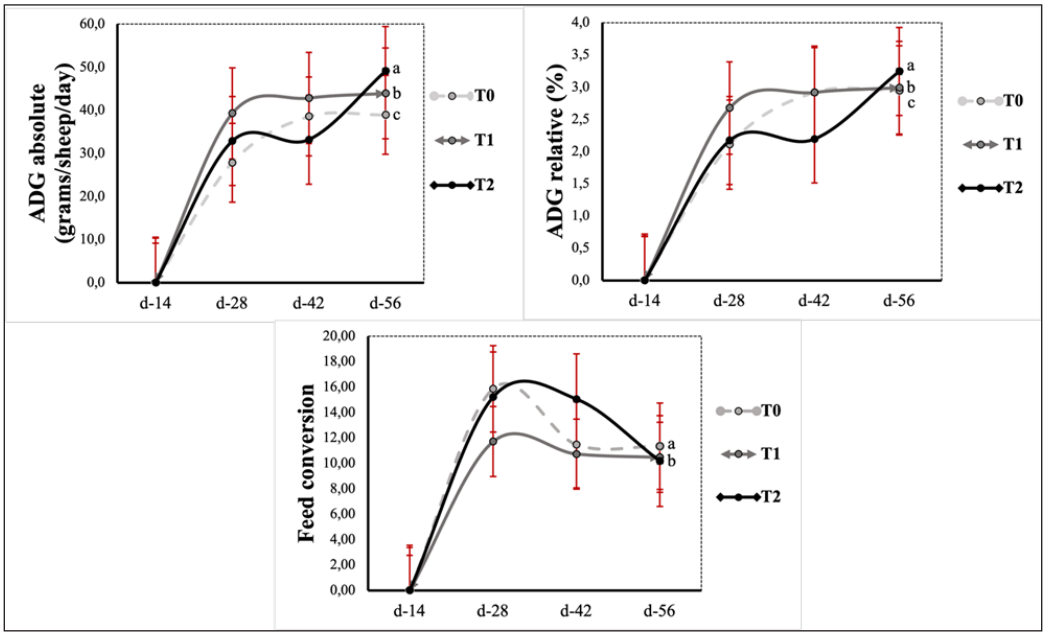

Figure 1. Comparison between the average daily gain (ADG) absolute, relative, and feed conversion of thin-tailed sheep fed based on silage in different ratios
Note. T0 = 60% concentrate and 40% water spinach straw; T1 = 40% concentrate and 60% silage; T2 = 60% concentrate and 40% silage; a, b, and c represent significant differences (p<0.05)

As shown in Figure 1, the incorporation of *P. purpureum* cv. Gama Umami and *C. calothyrsus* silage (T1 and T2), combined with different concentrate ratios, significantly increased ADG by 12.78 and 26.02%, respectively, compared to water spinach straw (T0) (p<0.05). Furthermore, T2 showed a higher ADG than T1 (p<0.05). Relative ADG is a percentage result of absolute ADG, so it will follow the results shown as absolute ADG.

In this study, ADG was positively associated with the nutrient content and the intake of nutrients, as indicated in Tables 3 and 4. The nutrient content is a key factor in determining ADG in sheep. The addition of high-protein feed improves nutrient availability, thereby enhancing growth performance. Increased feed intake typically results in higher ADG, as long as the feed is of high quality. Suhartanto et al. (2022) highlighted the strong relationship between feed intake and ADG, emphasizing the need to ensure adequate feed intake to support growth. This aligns with the findings of this study, where thin-tailed sheep fed on silage showed DMI ranked from highest to lowest were T2, T1, and T0, at 65.57, 60.12,

and 57.99 g/kg $LW^{0.75}$/day, respectively, with both absolute and relative ADG following the same pattern. The ADG was influenced by multiple factors, especially when considering the use of fermented feeds. This study incorporated silage based on *P. purpureum* cv. Gama Umami x *C. calothyrsus* (T1 and T2), which was easier to digest due to rumen activity in breaking down fiber. Silage enhances nutrient availability, increases palatability, and promotes better digestion, all of which contribute to improved ADG (Y. Xu et al., 2024). In this study, the use of silage enhanced the overall fermentation quality of the silage, as presented in Table 2. Previous research demonstrated that combining legumes with grasses can enhance the fermentation properties of silage, leading to better nutrient availability and improved growth performance (Niderkorn et al., 2015). To prevent weight loss in sheep, the minimum CP content in their diet should exceed 7.5% of DM (Yimenu & Abebe, 2023). According to the results of this study, the absolute ADG from lowest to highest were T0, T1, and T2 at 38.96, 43.94, and 49.10 grams/sheep/day, respectively. The results were lower than those reported by Sanjaya et al. (2022), who found that thin-tailed sheep fed 25% *P. purpureum* cv. Gama Umami+8% water spinach straw+68% concentrate had an ADG of 105.48 grams/sheep/day.

Thin-tailed sheep that were fed the incorporation of *P. purpureum* cv. Gama Umami and *C. calothyrsus* silage (T1 and T2), combined with different concentrate ratios, exhibited lower feed conversion ($p<0.05$) than water spinach straw (T0), although T1 and T2 showed no significant difference ($p>0.05$). Feed conversion in this study was influenced by factors such as feed quality, digestibility, and the efficiency with which sheep utilize nutrients. The higher the nutrient content, the lower the feed conversion. According to the results of this study, the nutrient content of feeds T1 and T2 was higher than that of T0, resulting in lower feed conversion. Sheep consuming higher-quality feed requires less feed to meet their nutritional needs compared to those consuming lower-quality feed. This supports the findings of Sileshi et al. (2021), who stated that livestock performance improves when they are provided with high-quality feed that has a balanced nutrient composition. Therefore, the nutrient levels in feed play an indirect role in determining the feed conversion. Feed conversion showed how much feed was needed to add 1 kg of animal body weight, and a smaller feed conversion value meant that more feed was used efficiently. The feed conversion value depends on the quality of the feed distributed. Sanjaya et al. (2020) stated that the smaller the ratio conversion values are, the less ratio is used to produce units of body weight gain. The nutrients in the feed play an essential role in determining the feed conversion value. Increasing body weight requires more building components, namely water, protein, fat, carbohydrate, and minerals. Feed conversion was closely related to production costs (Ahmed et al., 2020). The feed conversion in this study, from the lowest to the highest, was T2, T1, and T0 at 10.20, 10.47, and 11.38. For increasing 1 kg of body weight, the treatment T2 required 10.20 kg of feed, while T1 and T0 required 10.47 and

11.38 kg, respectively. The feed conversion in this study was higher than reported by Sanjaya et al. (2022), thin-tailed sheep fed a diet consisting of 25% *P. purpureum* cv. Gama Umami+8% water spinach + 68% concentrate showed feed conversion of 5.75.

Apparent Nutrient Digestibility

Apparent nutrient digestibility was measured for DM, OM, EE, CF, CP, NFE, and TDN in each treatment. The statistical analysis results in this study showed apparent digestibility of OM, NFE, and TDN exhibited significant differences among treatments ($p<0.05$). The apparent digestibility of DM, EE, CF, and CP did not show any statistical differences among treatments ($p>0.05$). The apparent nutrient digestibility of thin-tailed sheep fed based on silage in different rasios (%) is presented in Table 5.

Table 5
Apparent nutrient digestibility of thin-tailed sheep fed based on silage in different ratios (%)

Nutrient digestibility (%)	Treatments			SEM	*p*-value
	T0	T1	T2		
DM	67.97	68.60	69.76	0.55	0.42
OM	66.15[a]	62.52[b]	66.38[a]	0.71	0.04
EE	77.54	82.58	79.48	0.91	0.07
CF	65.77	61.13	61.26	1.05	0.12
CP	73.06	70.84	73.68	0.53	0.07
NFE	57.27[b]	51.10[c]	63.23[a]	1.18	0.00
TDN	54.17[a]	51.13[b]	56.10[a]	0.65	0.00

Note. Different superscripts in the same row represent significant differences ($p<0.05$); T0 = 60% concentrate and 40% water spinach straw; T1 = 40% concentrate and 60% silage; T2 = 60% concentrate and 40% silage; SEM = Standard error of the mean; DM = Dry matter; OM = Organic matter; EE = Ether extract; CF = Crude fiber; CP = Crude protein; NFE = Nitrogen-free extract; TDN = Total digestible nutrients

According to the statistical analysis, dry matter digestibility (DMD) did not differ significantly among treatments ($p>0.05$). DMD is influenced by multiple factors, including nutrient composition of the feed, processing methods, intake levels, and retention time within the rumen. When examined alongside the intake data presented in Table 4, treatment T2 exhibited the highest DMI, followed by T1 and T0. Despite these differences in DMI, DMD values remained consistent across treatments. Notably, T0 and T2 shared the same forage-to-concentrate ratio of 40:60, whereas T1 had a ratio of 60:40. These findings suggest that, under identical forage-to-concentrate ratios, silage-based feed (T2) may facilitate a faster digesta flow rate than water spinach straw (T0). The digesta flow rate in

the rumen refers to the speed at which feed passes through the rumen compartment. J. Xu et al. (2025) explained that the fermentation process can reduce the size of feed particles, thereby enabling them to exit the rumen more rapidly. In general, smaller particles have a higher passage rate than larger ones, which are typically retained longer to undergo further fermentation (Al-Mamouri & Al-Ani, 2024; F. Li et al., 2019). Moreover, increased feed intake is associated with an accelerated digesta flow rate, which may shorten retention time and potentially diminish digestive efficiency. However, ruminants that consistently consume high-quality forage tend to maintain a stable and efficient rumen microbial ecosystem, which is essential for optimal fermentation and nutrient synthesis (Husain et al., 2018). In contrast, abrupt changes in digesta flow rate, particularly those induced by high concentrate diets, can disrupt the rumen microbial population and elevate the risk of metabolic disorders such as subacute ruminal acidosis (SARA) (Franzolin & Dehority, 2010). In the present study, DMD ranged from 67.97 to 69.76%. However, these values were lower than those reported by Sanjaya et al. (2022), who observed a DMD of 71.14% in thin-tailed sheep fed a diet consisting of 25% *P. purpureum* cv. Gama Umami, 8% water spinach, and 68% concentrate.

Organic matter digestibility (OMD) in T1 was lower than in T0 and T2 ($p<0.05$). While T0 and T2 did not show a significant difference ($p>0.05$). One of the primary factors contributing to the low OMD is the high CF in the feed, particularly due to the presence of cellulose and lignin. In this study, treatment T1 included a higher proportion of forage (60%) than the other treatments, which resulted in the highest CF content of 21.97%. In contrast, treatments T0 and T2 each contained 40% forage and exhibited similar CF levels, measured at 18.87 and 18.64%, respectively. Click or tap here to enter text.When forages form a substantial part of the diet, they frequently contain higher fiber levels, which can lead to decreased digestibility if not balanced adequately with concentrates that supply rapidly fermentable carbohydrates (Manthey et al., 2016). Furthermore, as reported by J. Li et al. (2022), different types of roughages affect the digestibility of organic matter and NDF, with higher forage intake associated with improved digestive efficiencies in Holstein calves. According to Jamarun et al. (2024), feeds such as mature grasses or the stem portions of green forages contain higher levels of lignin. This lignin can inhibit the activity of rumen enzymes and microbes that break down fibrous components, thereby reducing the efficiency of nutrient utilization in ruminant livestock. In the present study, OMD ranged from 62.52 to 66.38%. However, these values were lower than those reported by Sanjaya et al. (2022), who observed an OMD of 73.08% in thin-tailed sheep fed a diet consisting of 25% *P. purpureum* cv. Gama Umami, 8% water spinach, and 68% concentrate.

Ether extract digestibility (EED) did not differ significantly among treatments ($p>0.05$), indicating a pattern similar to that observed for DMD. DMD strongly influences fat digestibility in livestock, as both parameters are closely linked in the digestive process.

Several studies have demonstrated that an increase in DMD is generally accompanied by an improvement in EEI, highlighting the interrelationship between these two variables (Mukhopadhyay, 2001). Similarly, Widiana et al. (2021) emphasized that high DMD indicates good feed quality, which, in turn, enhances the digestibility of fat and protein. In the present study, EED ranged from 77.54 to 79.48%. However, these values were lower than those reported by Sanjaya et al., (2022), who observed an EED of 86.23% in thin-tailed sheep fed a diet consisting of 25% *P. purpureum* cv. Gama Umami, 8% water spinach, and 68% concentrate.

Crude fiber digestibility (CFD) did not differ significantly among treatments (p>0.05). Interestingly, although T1 included a higher forage proportion (60%) to concentrate (40%), its CFD value was comparable to those of T0 and T2, both of which had a lower forage proportion (40%) and a higher concentrate level (60%). This finding suggests that silage, despite its high fiber content, can still be effectively degraded by rumen microbes. A key factor supporting the digestibility of CF in silage is the activity of specific rumen microorganisms that efficiently break down fibrous components. Ferreira et al. (2016) reported that the synergistic interaction between proteolytic and cellulolytic bacteria in the rumen plays a crucial role in fiber degradation, thereby enhancing digestibility. The complex interplay among diverse microbial populations increases the efficiency of fiber breakdown, allowing for high digestibility even in fiber-rich feeds. Ribas et al. (2019) also noted that silage with good fermentation quality exhibited greater dry matter loss in the rumen, indicating a positive relationship between fermentation quality and fiber digestibility. Effective fermentation promotes an environment conducive to microbial activity, which in turn improves the digestibility of CF in silage. In the present study, CFD ranged from 61.13 to 65.77%. However, these values were lower than those reported by Sanjaya et al. (2022), who observed a CFD of 57.99% in thin-tailed sheep fed a diet consisting of 25% *P. purpureum* cv. Gama Umami, 8% water spinach, and 68% concentrate.

Crude protein digestibility (CPD) did not differ significantly among treatments (p>0.05). Although T1 included a higher proportion of forage (60%) relative to concentrate (40%), its CPD was comparable to that of T0 and T2, both of which contained a lower proportion of forage (40%) and a higher proportion of concentrate (60%). It is important to note that the silage used in this study was a mixture of *P. purpureum* cv. Gama Umami and *C. calothyrsus* in a 70:30 ratio. Calliandra species, including *C. calothyrsus*, are known for their relatively high levels of condensed tannins (CT), which can influence protein utilization in ruminants. Mudhita et al. (2024) reported that a silage blend of *P. purpureum* cv. Gama Umami and *C. calothyrsus* (70:30) contained 2.10% total tannins. Tannins are known to form complexes with feed proteins, thereby protecting them from ruminal degradation and increasing the flow of amino acids to the small intestine (Yanza et al., 2021). Therefore, the potential formation of tannin-protein complexes in the T1 ration

may have conferred a protective effect, reducing excessive protein degradation in the rumen and enhancing protein utilization efficiency. This aligns with findings by Jayanegara et al. (2019), who reported that moderate tannin levels can increase the rumen undegradable protein (RUP) fraction, making more protein available for intestinal absorption and improving overall nitrogen efficiency. Similarly, Kondo et al. (2007) demonstrated that tannins can slow ruminal protein degradation and increase amino acid flow to the intestine. Controlled inclusion of tannins in ruminant diets has been shown to enhance protein utilization efficiency (Arik et al., 2024). Supporting this, Mudhita et al. (2024) found that supplementing Gama Umami silage with *Calliandra* at 10, 20, and 30% increased *in vitro* protein digestibility to 13.22, 14.68, and 16.86%, respectively. These findings reinforce the notion that moderate tannin inclusion can improve protein digestibility in ruminant feed. In the present study, CPD ranged from 70.84 to 73.68%. However, these values were lower than those reported by Sanjaya et al. (2022), who observed a CPD of 77.06% in thin-tailed sheep fed a diet consisting of 25% *P. purpureum* cv. Gama Umami, 8% water spinach, and 68% concentrate.

Nitrogen-free extract digestibility (NFED) showed significant differences among treatments ($p<0.05$), with the highest value observed in T2, followed by T0, and the lowest in T1. The elevated NFED in T2 is likely attributed to its higher energy content and greater proportion of readily digestible carbohydrates. In contrast, the low NFED in T1 suggests limitations in the availability or quality of non-fiber carbohydrates accessible to the animals. According to McDonald et al. (2011), NFE digestibility is strongly influenced by the composition of feed ingredients—particularly the proportion of rapidly fermentable energy sources such as starch and sugars—and by the presence of anti-nutritional factors that may inhibit digestion. The reduced NFED in T1 may also be associated with its high CF content (21.97%), which can hinder the utilization of non-structural carbohydrates (Van Soest, 1994). Elevated fiber levels can increase rumen emptying rate and reduce fermentation efficiency, thereby limiting substrate availability for digestive enzymes.

The results demonstrated that the Total Digestible Nutrients (TDN) values in thin-tailed sheep differed significantly among treatments ($p<0.05$), with the highest value observed in T2, followed by T0, and the lowest in T1. The TDN values represent the total utilizable energy derived from feed and are influenced by the digestibility of various nutrient fractions, including dry matter, organic matter, NFE, and fat. The elevated TDN value in T2 indicates that a higher concentrate proportion in the diet enhances energy utilization, as corroborated by the high NFE digestibility (63.23%), reflecting increased availability of readily fermentable non-structural carbohydrates. Conversely, the reduced TDN value in T1 is likely attributable to the high silage proportion (60%) with a substantial crude fiber content (21.97%). Excessive fiber may impair ruminal fermentation efficiency, accelerate rumen evacuation, and consequently limit optimal energy utilization. Additionally, the

lower NFE digestibility observed in T1 (51.10%) further contributes to the decreased TDN in this treatment. Nonetheless, the relatively high TDN value in T0 suggests that water spinach straw possesses potential as an energy source when appropriately balanced with concentrate. The critical role of energy-protein balance in the diet is underscored by Dutta et al. (2002), who reported that protein supplementation can enhance metabolizable energy and improve the efficiency of TDN utilization. Therefore, optimizing the proportional composition of feed ingredients is essential for maximizing the nutritional value and performance of livestock.

Nitrogen Utilization

Nitrogen utilization observed in this study included N intake, N fecal and urine, digestible nitrogen, N retention, and biological value in each treatment. The statistical analysis results in this study showed N intake, N fecal, N digestible, and N retention exhibited significant differences among treatments ($p<0.05$). While incorporating *P. purpureum* cv. Gama Umami and *C. calothyrsus* silage (T1 and T2) exhibited lower N urine and higher biological value than water spinach straw (T0) ($p<0.05$), although T1 and T2 showed no significant difference ($p>0.05$). Nitrogen content in feces and urine, and balance in thin-tailed sheep (g/kg $LW^{0.75}$/day) presented in Figure 2.

The elevated N intake observed in T1 was primarily due to the higher CPI. The relationship between N intake and CPI is displayed in Table 4. The feed ratio treatments in this study were ranked from highest to lowest in CPI as T1, T2, and T0, with values of 8.36±0.16, 6.78±0.13, and 5.98±0.00 g/kg $LW^{0.75}$/day, respectively, following a similar pattern for N intake. There is a positive correlation between CPI and N intake, meaning that as CPI increases, N intake also rises. Crude protein represents the total protein content in feed, which includes both true protein and non-protein nitrogen (NPN). When animals consume more protein, they are ingesting greater amounts of nitrogen, as proteins are made up of amino acids that contain nitrogen in their structure. Previous studies have shown that as the CP content in the diet increases, N intake also increases proportionally due to the nitrogen present in the protein sources (Shen et al., 2020).

The amount of nitrogen excreted in feces was influenced by microbial digestion. A reduction in N fecal leads to improved nitrogen digestibility, making nitrogen use more efficient. One key factor affecting N fecal was the protein content and feed quality. Diets with higher CP result in increased N intake, which can lead to greater N fecal as shown in this study (Figure 2). In this experiment, T1 had the highest N intake, followed by T2, and then T0, with N fecal following the same trend. Zhou et al. (2015) emphasized that the digestibility of protein sources plays a critical role, as diets with more digestible proteins typically result in lower nitrogen loss in feces due to improved absorption and utilization. Although this study utilized silage-based diets, the varying ratios of forage and

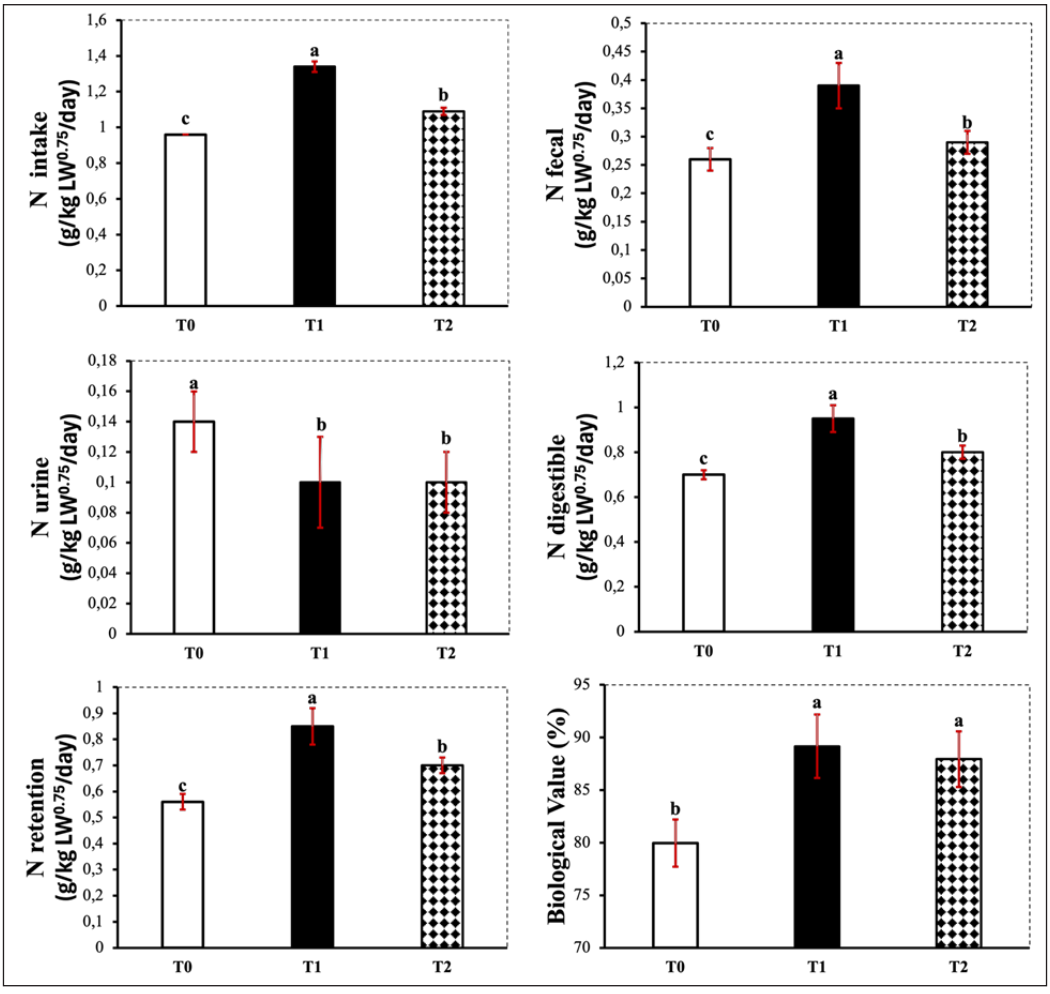

Figure 2. Nitrogen (N) content of feces and urine, and balance in thin-tailed sheep
Note. T0 = 60% concentrate and 40% water spinach straw; T1 = 40% concentrate and 60% silage; T2 = 60% concentrate and 40% silage; a, b, and c represent significant differences (p<0.05)

concentrate led to an imbalance between energy and protein content in the feed (Table 2). Diets that offer both sufficient protein and energy can optimize microbial growth and nitrogen utilization, thus reducing N fecal. Zhang et al. (2019) also reported that diets rich in fermentable carbohydrates promote the synthesis of microbial protein in the rumen, leading to better nitrogen retention and reduced N feces.

As shown in Figure 2, the silage-based diets (T1 and T2) resulted in significantly lower N urine (p<0.05) than the non-fermented diet (T0). This suggests that T1 and T2 had a higher feed solubility rate, which contributed to the reduced N urine. The fermentation characteristics of the diet, especially the balance between fiber and concentrate, play a

crucial role in nitrogen metabolism. Diets that support effective rumen fermentation can enhance microbial protein synthesis, leading to improved nitrogen retention and reduced N excretion. Previous studies have shown that diets with higher CF content tend to reduce N urine, while high-concentrate diets can lead to excess nitrogen being excreted (Chelkapally et al., 2023; Ma et al., 2014).

The inclusion of mixed silage with *C. calothyrsus* positively influenced protein utilization efficiency in livestock because of the protective effect of tannins on protein. Tannins in high-quality feed proteins help protect these proteins from degradation by rumen microbes, thereby improving their utilization (Jayanegara et al., 2019). This protection process converts some rumen-degradable proteins (RDP) into rumen-undegradable proteins (RUP), which can then be metabolized, digested, and absorbed in the small intestine. Jayanegara et al. (2019) found that silages with higher tannin content were associated with lower levels of RDP, suggesting that tannins play a significant role in improving protein utilization in livestock.

The highest N digestible in T1 compared to T0 and T2 was attributed to the higher N intake. Digestible nitrogen levels were positively correlated with CPI and CP digestibility in thin-tailed sheep. When protein digestibility increases, so does the amount of nitrogen that can be digested. This process is facilitated by rumen microbial activity and improving this activity requires providing a balanced nutrient profile in the feed. Silva et al. (2022) emphasized that maintaining a balance between energy and protein is essential for optimizing rumen microbial performance, which plays a critical role in digestion. As protein digestibility increases, fecal nitrogen decreases, leading to greater N digestibility.

N retention reflects how effectively sheep utilize nitrogen, determined by the difference between N intake and the N excreted (feces and urine). Several factors can influence the amount of retained nitrogen, such as the amount of N intake, the nutrient content, nutrient digestibility, and the efficiency of the sheep's metabolic processes. In this study, T1 and T2 resulted in higher N retention than T0. The tannins in the mixed silage protected proteins from microbial breakdown in the rumen, thus enhancing the efficiency of protein utilization by the sheep. According to Loregian et al. (2023), tannins bind with proteins, decreasing protein degradation in the rumen and enhancing the proportion of RUP. Specific microbial populations in the rumen can help break down dietary proteins and synthesize microbial proteins, which act as a vital source of nitrogen for the animal (Cui et al., 2021).

Biological value refers to the quality of protein, measured by the percentage of nitrogen that is absorbed and used by the body, rather than being excreted in urine or feces. In this study, the higher biological value observed in T1 and T2 than in T0 suggests that the combination of concentrate feed and silage enhanced nitrogen utilization efficiency, likely due to the tannin content. The lower biological value in T0 may be attributed to increased protein degradation, leading to increased ammonia production. A higher biological value

indicates more efficient protein use by livestock in the given feed treatments (Rahayu et al., 2021).

CONCLUSION

This study highlights that no single dietary treatment was universally superior, but each offered unique advantages. Feeding sheep a combination of 60% concentrate and 40% silage (*P. purpureum* cv. Gama Umami x *C. calothyrsus*), referred to as T2, has been shown to improve productivity, as reflected in better nutrient intake, higher average ADG, and improved feed conversion, positioning it as a strong alternative to water spinach straw (T0). In contrast, the T1 or feeding sheep a combination of 40% concentrate and 60% silage excelled in protein-related metrics, including crude protein and EEI, nitrogen digestibility, and retention, making it more effective for improving nitrogen utilization. These findings underline the importance of aligning dietary strategies with specific production goals. T2 may be best suited for a growth-focused system, whereas T1 offers strategic benefits for protein efficiency and nutrient retention.

ACKNOWLEDGMENT

The authors would like to express their deepest gratitude to the postgraduate program of the Faculty of Animal Science, Universitas Gadjah Mada, which has funded this research in the 2024 Postgraduate Competition Grant program with contract number 2041/UN1/PT.1.3/PT.01.00/2024.

REFERENCES

Abdelraheem, N., Li, F., Guo, P., Sun, Y., Liu, Y., Cheng, Y., Cui, X., Tan, Y., & Hou, F. (2023). Nutrient utilization of native herbage and oat forage as feed for Tibetan sheep (*Ovis aries*). *Grassland Science*, *69*(1), 12–22. https://doi.org/10.1111/GRS.12381

Abun, A., Nurhalisa., Haetami, K., & Saefulhadjar, D. (2022). Effect of additional feed supplement fermentation shrimp waste extract on digestibility in Sentul chicken growth phase. *Journal of Zoological Research*, *4*(3), 13-19.

Ahmad, M., Suhartati, F. M., & Bata, M. (2023). Energy metabolism of sheep supplemented with Complete Rumen Modifier (CRM). *Buletin Peternakan*, *47*(1), 12-17. https://doi.org/10.21059/buletinpeternak.v47i1.76964

Ahmed, S., Rakib, M. R. H., Hemayet, M. A., Roy, B. K., & Jahan, N. (2020). Effect of complete pellet feed on commercial goat production under the stall feeding system in Bangladesh. *Journal of Advanced Veterinary and Animal Research*, *7*(4), 704–709. https://doi.org/10.5455/javar.2020.g471

Al-Mamouri, T. A. M., & Al-Ani, J. A. T. (2024). Influence of feeding corn impurities on rumen bacteria and fermentation characteristics of sheep. *Iraqi Journal of Agricultural Sciences*, *55*(1), 579–586. https://doi.org/10.36103/MD4WQN86

Alqaisi, O., Ali, H., Al-Abri, M., Johnson, E. H., & Al-Marzooqi, W. (2021). Effect of dietary concentrate content on feed intake, feed efficiency, and meat quality of Holstein steers fattened in a hot environment. *Animal Science Journal*, *92*(1), e13547. https://doi.org/10.1111/asj.13547

Arik, H. D., Inanc, Z. S., Kahraman, O., Damar, S., & Akkaya, A. B. (2024). Effects of quebracho tannin supplementation in early lactation dairy cow rations on milk yield parameters, rumen fermentation, digestibility and blood parameters. *Journal of Animal and Feed Sciences*, *33*(3), 321–330. https://doi.org/10.22358/JAFS/183438/2024

Association Official Analytical Chemists. (2005). *Official Method of Analysis of the AOAC International* (18th ed.). AOAC.

Badan Pusat Statistik. (2024). *Populasi domba menurut provinsi (ekor), 2021-2023* [Sheep population by province (heads), 2021-2023]. BPS. https://www.bps.go.id/id/statistics-table/2/NDczIzI=/populasi-domba-menurut-provinsi--ekor-.html

Berthel, R., Simmler, M., Dohme-Meier, F., & Keil, N. (2022). Dairy sheep and goats prefer the single components over the mixed ration. *Frontiers in Veterinary Science*, *9*, 1017669. https://doi.org/10.3389/fvets.2022.1017669

Carvalho, D. M. G., da Silva, J. J., Santos, M. J., de Souza Teixeira, C., Brito, E. P., & Fragata, N. P. (2020). Protein supplementation for sheep fed with tropical forage. *Boletim de Indústria Animal*, *77*, 1–13. https://doi.org/10.17523/BIA.2020.V77.E1475

Castro-Montoya, J., & Dickhoefer, U. (2018). Effects of tropical legume silages on intake, digestibility and performance in large and small ruminants: A review. *Grass and Forage Science*, *73*(1), 26–39. https://doi.org/10.1111/GFS.12324

Chelkapally, S. C., Terrill, T. H., Estrada-Reyes, Z. M., Ogunade, I. M., & Pech-Cervantes, A. A. (2023). Effects of dietary inclusion of dry distillers grains with solubles on performance, carcass characteristics, and nitrogen metabolism in meat sheep: A meta-analysis. *Frontiers in Veterinary Science*, *10*, 1141068. https://doi.org/10.3389/fvets.2023.1141068

Cui, X., Wang, Z., Tan, Y., Chang, S., Zheng, H., Wang, H., Yan, T., Tsedan, G., & Hou, F. (2021). Selenium yeast dietary supplement affects rumen bacterial population dynamics and fermentation parameters of Tibetan sheep (*Ovis Aries*) in alpine meadow. *Frontiers in Microbiology*, *12*, 663945. https://doi.org/10.3389/fmicb.2021.663945

Dong, Z., Li, J., Wang, S., Dong, D., & Shao, T. (2023). Diurnal variation of epiphytic microbiota: An unignorable factor affecting the anaerobic fermentation characteristics of sorghum-sudangrass hybrid silage. *Microbiology Spectrum*, *11*(1). e03404-22. https://doi.org/10.1128/spectrum.03404-22

dos Santos, R. D., Pereira, L. G. R., Neves, A. L. A., de Araújo, G. G. L., de Aragão, A. S. L., & Chizzotti, M. L. (2011). Intake and total apparent digestibility in lambs fed six maize varieties in the Brazilian Semiarid. *Revista Brasileira de Zootecnia*, *40*(12), 2922–2928. https://doi.org/10.1590/S1516-35982011001200040

Dutta, N., Sharma, K., & Naulia, U. (2002). Use of undecorticated sunflower cake as a critical protein supplement in sheep and goats fed wheat straw. *Asian-Australasian Journal of Animal Sciences*, *15*(6), 834–837. https://doi.org/10.5713/AJAS.2002.834

Fajemisin, A. N., Ibhaze, G. A., Oluwaloyo, O. E., & Omotoso, O. B. (2020). Dietary effect of *Pleurotus pulmonaris* treated cocoa bean shell meal on fibre fractions utilisation by the West African Dwarf goats. *Nigerian Journal of Animal Production*, *45*(5), 169–175. https://doi.org/10.51791/NJAP.V45I5.251

Ferreira, A. C. H., Rodriguez, N. M., Neiva, J. N. M., Pimentel, P. G., Gomes, S. P., Campos, W. E., Lopes, F. C. F., Mizubuti, I. Y., & Moreira, G. R. (2016). *In situ* degradability of elephant grass ensiled with increasing levels of pineapple agro-industrial by-product. *Semina: Ciências Agrárias*, *37*(4), 2807–2818. https://doi.org/10.5433/1679-0359.2016V37N4SUPL1P2807

Franzolin, R., & Dehority, B. A. (2010). The role of pH on the survival of rumen protozoa in steers. *Revista Brasileira De Zootecnia*, *39*(10), 2262–2267. https://doi.org/10.1590/S1516-35982010001000023

Han, H., Wang, C., Huang, Z., Zhang, Y., Sun, L., Xue, Y., & Guo, X. (2022). Effects of lactic acid bacteria-inoculated corn silage on bacterial communities and metabolites of digestive tract of sheep. *Fermentation*, *8*(7), 320. https://doi.org/10.3390/fermentation8070320

Hao, X. Y., Yu, S. C., Mu, C. T., Wu, X. D., Zhang, C. X., Zhao, J. X., & Zhang, J. X. (2020). Replacing soybean meal with flax seed meal: Effects on nutrient digestibility, rumen microbial protein synthesis and growth performance in sheep. *Animal*, *14*(9), 1841–1848. https://doi.org/10.1017/S1751731120000397

Hartadi, H., Reksohadiprodjo, S., Tillman, A. D., & Supriyono. (1990). *Ilmu gizi ternak* [Animal nutrition science]. Gadjah Mada University Press.

Huang, Y. F., Matthew, C., Li, F., & Nan, Z. B. (2021). Common vetch varietal differences in hay nutritive value, ruminal fermentation, nutrient digestibility and performance of fattening lambs. *Animal*, *15*(7), 100244. https://doi.org/10.1016/j.animal.2021.100244

Husain, M. S. S., Syahrir, S., & Natsir, A. (2018). Substitution of complete feed with hydroponic corn fodder on rumen characteristics and nitrogen dynamics in goats. *American-Eurasian Journal of Sustainable Agriculture*, *12*(3), 28-31. https://doi.org/10.22587/AEJSA.2018.12.3.4

Huuskonen, A., & Pesonen, M. (2017). A comparison of first-, second- and third-cut timothy silages in the diets of finishing beef bulls. *Agricultural and Food Science*, *26*, 16–24. https://doi.org/10.23986/AFSCI.60413

Indonesian Agency for Meteorological, Climatological and Geophysics (2024). Indonesia Climate and Air Quality Notes. Jakarta. Accessed November 20, 2025, from https://iklim.bmkg.go.id/bmkgadmin/storage/buletin/Catatan%20Iklim%20dan%20Kualitas%20Udara%202024%20BMKG.pdf

Ipharraguerre, I. R., Ipharraguerre, R. R., & Clark, J. H. (2002). Performance of lactating dairy cows fed varying amounts of soyhulls as a replacement for corn grain. *Journal of Dairy Science*, *85*(11), 2905–2912. https://doi.org/10.3168/JDS.S0022-0302(02)74378-6

Jamarun, N., Ikhlas, Z., Zain, M., Negara, W., Pazla, R., & Yanti, G. (2024). Feed wafers from fermented sugarcane tops and *Tithonia diversifolia* with added tapioca starch: Effects on physical quality and *in-vitro* parameters for ruminant feed. *Open Veterinary Journal*, *14*(12), 3599–3613. https://doi.org/10.5455/OVJ.2024.v14.i12.41

Jayanegara, A., Sujarnoko, T. U. P., Ridla, M., Kondo, M., & Kreuzer, M. (2019). Silage quality as influenced by concentration and type of tannins present in the material ensiled: A meta-analysis. *Journal of Animal Physiology and Animal Nutrition*, *103*(2), 456–465. https://doi.org/10.1111/JPN.13050

Jayanegara, A., Yaman, A., & Khotijah, L. (2019). Reduction of proteolysis of high protein silage from Moringa and Indigofera leaves by addition of tannin extract. *Veterinary World*, *12*(2), 211–217. https://doi.org/10.14202/VETWORLD.2019.211-217

Kearl, L. C. (1982). *Nutrient requirements of ruminants in developing countries*. International Feedstuffs Institute, Utah State University.

Knowles, M. M., Pabón, M. L., Hess, H. D., & Carulla, J. E. (2017). Changes in *in vitro* ruminal and post-ruminal degradation of tropical tannin-rich legumes due to varying levels of polyethylene glycol. *Journal of Animal Physiology and Animal Nutrition*, *101*(4), 641–648. https://doi.org/10.1111/jpn.12610

Kondo, M., Kita, K., & Yokota, H. O. (2007). Ensiled or oven-dried green tea by-product as protein feedstuffs: Effects of tannin on nutritive value in goats. *Asian-Australasian Journal of Animal Sciences*, *20*(6), 880–886. https://doi.org/10.5713/AJAS.2007.880

Li, F., Hitch, T. C. A., Chen, Y., Creevey, C. J., & Guan, L. L. (2019). Comparative metagenomic and metatranscriptomic analyses reveal the breed effect on the rumen microbiome and its associations with feed efficiency in beef cattle. *Microbiome*, *7*, 6. https://doi.org/10.1186/S40168-019-0618-5

Li, J., Lian, H., Zheng, A., Zhang, J., Dai, P., Niu, Y., Gao, T., Li, M., Zhang, L., & Fu, T. (2022). Effects of different roughages on growth performance, nutrient digestibility, ruminal fermentation, and microbial community in weaned Holstein calves. *Frontiers in Veterinary Science*, *9*, 864320. https://doi.org/10.3389/FVETS.2022.864320

Liu, S., Xie, B., Ji, H., & Li, S. (2024). Effects of dietary supplementation with alkaline mineral complex on *in vitro* ruminal fermentation and bacterial composition. *Frontiers in Veterinary Science*, *11*, 1357738. https://doi.org/10.3389/FVETS.2024.1357738

Loregian, K. E., Pereira, D. A. B., Rigon, F., Magnani, E., Marcondes, M. I., Baumel, E. A., Branco, R. H., Del Bianco Benedeti, P., & Paula, E. M. (2023). Effect of tannin inclusion on the enhancement of rumen undegradable protein of different protein sources. *Ruminants*, *3*(4), 413–424. https://doi.org/10.3390/RUMINANTS3040034

Ma, T., Deng, K.-D., Tu, Y., Jiang, C.-G., Zhang, N.-F., Li, Y.-L., Si, B.-W., Lou, C., & Diao, Q.-Y. (2014). Effect of dietary concentrate: Forage ratios and undegraded dietary protein on nitrogen balance and urinary excretion of purine derivatives in Dorper×thin-tailed Han crossbred lambs. *Asian-Australasian Journal of Animal Sciences*, *27*(2), 161–168. https://doi.org/10.5713/ajas.2013.13338

Manthey, A., Kalscheur, K., Garcia, A., & Mjoun, K. (2016). Lactation performance of dairy cows fed yeast-derived microbial protein in low- and high-forage diets. *Journal Dairy Science*, *99*(4), 2775–2787. https://doi.org/10.3168/jds.2015-10014

Marsetyo., Rusiyantono, Y., & Sulendre, I. W. (2022). Liveweight gain, change in body dimension and condition score of Donggala bulls fed corn stover supplemented with different tree legume leaves. In *IOP Conference Series: Earth and Environmental Science* (Vol. 1075, No. 1, p. 012006). IOP Publishing. https://doi.org/10.1088/1755-1315/1075/1/012006

McDonald, P., Edwards, R. A., Greenhalgh, J. F. D., Morgan, C. A., Sinclair, L. A., &, & Wilkinson, R. G. (2011). *Animal nutrition* (7th ed.). Pearson Education Limited.

Molitor, R. W., Fischborn, T., Dagan, L., & Shellhammer, T. H. (2023). Examining how the fermentation medium influences thiol expression and its perceived aroma in commercial brewing yeast strains. *Journal of Agricultural and Food Chemistry*, *71*(5), 2493–2502. https://doi.org/10.1021/ACS.JAFC.2C06966

Mudgal, V., Mehta, M. K., & Rane, A. S. (2018). Lentil straw (*Lens culinaris*): An alternative and nutritious feed resource for kids. *Animal Nutrition*, *4*(4), 417–421. https://doi.org/10.1016/J.ANINU.2018.04.009

Mudhita, I. K., Putra, R. A., Rahman, M. M., Widyobroto, B. P., Agussalim, & Umami, N. (2024). The silage quality of *Pennisetum purpureum* cultivar Gamma Umami mixed with *Calliandra calothyrsus* and *Lactobacillus plantarum*. *Tropical Animal Science Journal*, *47*(1), 112–124. https://doi.org/10.5398/tasj.2024.47.1.112

Mukhopadhyay, N. (2001). Effect of fermentation on apparent total and nutrient digestibility of sesame (*Seasamum indicum*) seed meal in rohu, *Labeo rohita* (Hamilton) fingerlings. *Acta Ichthyologica Et Piscatoria*, *31*(2), 19–28. https://doi.org/10.3750/AIP2001.31.2.02

National Research Council. (2007). *Nutrient requirements of small ruminants (sheep, goats, cervids, and New World Camelids)*. The National Academic Press.

Niderkorn, V., Martin, C., Rochette, Y., Julien, S., & Baumont, R. (2015). Associative effects between orchardgrass and red clover silages on voluntary intake and digestion in sheep: Evidence of a synergy on digestible dry matter intake. *Journal of Animal Science*, *93*(10), 4967–4976. https://doi.org/10.2527/JAS.2015-9178

Nurjanah, L. L., Umami, N., Kurniawati, A., Hanim, C., Prasetyo Wb, B., Paradhipta, D. H. V., & Meidiana, T. (2023). The quality of physic and pH of Gama Umami grass silage supplemented with calliandra leaves and pollard. In *IOP Conference Series: Earth and Environmental Science* (Vol. 1183 No. 1, p. 012019). IOP Publishing. https://doi.org/10.1088/1755-1315/1183/1/012019

Oliveira, S., Costa, K. A., Severiano, E., da Silva, A., Dias, M., Oliveira, G., & Costa, J. V. (2020). Performance of grain sorghum and forage of the genus *Brachiaria* in integrated agricultural production systems. *Agronomy, 10*(11), 1714. https://doi.org/10.3390/AGRONOMY10111714

Parchami, M., Rustas, B.-O., Taherzadeh, M. J., & Mahboubi, A. (2024). Effect of agro-industrial by products derived from volatile fatty acids on ruminant feed *in vitro* digestibility. *Animals*, *14*(16), 2330. https://doi.org/10.3390/ANI14162330

Parente, H. N., de Parente, M. O. M., da Gomes, R. M. S., de dos Sodré, W. J. S., Moreira Filho, M. A., Rodrigues, R. C., dos Santos, V. L. F., & dos Araújo, J. S. (2016). Increasing levels of concentrate digestibility, performance and ingestive behavior in lambs. *Revista Brasileira de Saude e Producao Animal*, *17*(2), 186-194. https://doi.org/10.1590/S1519-99402016000200006

Rahayu, E. R. V., Suhartanto, B., Budisatria, I. G. S., & Astuti, D. (2021). The effect of sorghum varieties on digestibility and nitrogen balance of complete feed in goats. *Key Engineering Materials*, *884*(1), 184–190. https://doi.org/10.4028/www.scientific.net/KEM.884.184

Ribas, T. M. B., Neumann, M., de Souza, A. M., Dochwat, A., de Almeida, E. R., & Horst, E. H. (2019). Effect of inoculants combining *Lactobacillus buchneri* strain LN40177 in different strata of the silo. *Acta Scientiarum. Animal Sciences*, *41*(1), e44847. https://doi.org/10.4025/ACTASCIANIMSCI.V41I1.44847

Ridwan, R., Abdelbagi, M., Sofyan, A., Fidriyanto, R., Astuti, W. D., Fitri, A., Sholikin, M. M., Rohmatussolihat, Sarwono, K. A., Jayanegara, A., & Widyastuti, Y. (2023). A meta-analysis to observe silage microbiome differentiated by the use of inoculant and type of raw material. *Frontiers in Microbiology*, *14*, 1063333. https://doi.org/10.3389/FMICB.2023.1063333/BIBTEX

Rira, M., Morgavi, D. P., Popova, M., Maxin, G., & Doreau, M. (2022). Microbial colonization of tannin-rich tropical plants: Interplay between degradability, methane production and tannin disappearance in the rumen. *Animal*, *16*(8), 100589. https://doi.org/10.1016/j.animal.2022.100589

Roychan, I., Umami, N., & Noviandi, C. T. (2023). Nitrogen utility on income over feed cost in complete feed Napier grass cv Gama Umami based with different calliandra (*Calliandra calothyrsus*) substitution levels. In *IOP Conference Series: Earth and Environmental Science* (Vol. 1241, No. 1, p. 012127). IOP Publishing. https://doi.org/10.1088/1755-1315/1241/1/012127

Sanjaya, H. B., Umami, N., Astuti, A., Muhlisin, Suwignyo, B., Rahman, M. M., Umpuch, K., & Rahayu, E. R. V. (2022). Performance and *in vivo* digestibility of three varieties of Napier grass in thin-tailed sheep. *Pertanika Journal of Tropical Agricultural Science*, *45*(2), 505–517. https://doi.org/10.47836/pjtas.45.2.11

Saro, C., Mateo, J., Caro, I., Carballo, D. E., Fernández, M., Valdés, C., Bodas, R., & Giráldez, F. J. (2020). Effect of dietary crude protein on animal performance, blood biochemistry profile, ruminal fermentation parameters and carcass and meat quality of heavy fattening Assaf lambs. *Animals*, *10*(11), 2177. https://doi.org/10.3390/ANI10112177

Shen, J., Wang, H., Pi, Y., Gao, K., & Zhu, W. (2020). Casein hydrolysate supplementation in low-crude protein diets increases feed intake and nitrogen retention without affecting nitrogen utilization of growing pigs. *Journal of the Science of Food and Agriculture*, *100*(4), 1748–1756. https://doi.org/10.1002/JSFA.10196

Sileshi, G., Mitiku, E., Mengistu, U., Adugna, T., & Fekede, F. (2021). Effects of dietary energy and protein levels on nutrient intake, digestibility, and body weight change in Hararghe highland and Afar sheep breeds of Ethiopia. *Journal of Advanced Veterinary and Animal Research*, *8*(2), 185–194. https://doi.org/10.5455/JAVAR.2021.H501

Silva, C. F., Véras, A. S. C., Conceição, M. G., Macedo, A. V. M., Luna, R. E. M., de Figueiredo Monteiro, C. C., Souza, F. G., de Paula Almeida, M., Silva, J. A. B. A., & de Andrade Ferreira, M. (2022). Intake, digestibility, water balance, ruminal dynamics, and blood parameters in sheep fed diets containing extra-fat whole corn germ. *Animal Feed Science and Technology*, *285*, 115248. https://doi.org/10.1016/J.ANIFEEDSCI.2022.115248

Sriyani, N. L. P., Siti, W., Suarta, G., Partama, I. B. G., Ariana, N. T., & Yupardhi, W. S. (2018). Responses of corncob as replacement of elephant grass on performance and carcass profile of Bali cattle. *International Journal of Life Sciences*, *2*(1), 42–49. https://doi.org/10.29332/IJLS.V2N1.93

Suhartanto, B., Rahayu, E. R. V., Umami, N., & Astuti, D. (2022). Microbial protein synthesis, digestible nutrients, and gain weight of Bligon goats receiving total mixed ration based on sorghum silages (*Sorghum bicolor* L. Moench). *Journal of Advanced Veterinary and Animal Research*, *9*(2), 175–183. https://doi.org/10.5455/JAVAR.2022.I582

Tewari, D., Chaturvedi, V. B., Chaudhary, L. C., Verma, A. K., & Chaudhary, S. K. (2022). Effect of dietary supplementation of rice bran crude lecithin on nutrient metabolism, methanogenesis and metabolic profile

of crossbred calves. *Indian Journal of Animal Sciences*, *92*(5), 585–591. https://doi.org/10.56093/IJANS.V92I5.124407

Udo, H. M. J., & Budisatria, I. G. S. (2011). Fat-tailed sheep in Indonesia; An essential resource for smallholders. *Tropical Animal Health and Production*, *43*, 1411–1418. https://doi.org/10.1007/s11250-011-9872-7

Utama, C. S., Sulistiyanto, B., & Haidar, M. F. (2023). The feasibility of *Sorghum* (*Sorghum vulgare*) fodder as poultry feed ingredients seen from growth performance, nutrient content and fiber profile of *Sorghum* fodder. *Journal of Advanced Veterinary and Animal Research*, *10*(2), 222–227. https://doi.org/10.5455/javar.2023.j672

Van Soest, P. J. (1994). *Nutritional ecology of the ruminant* (2nd ed.). Cornell University Press.

Wei, H., Liu, J., Liu, M., Zhang, H., & Chen, Y. (2024). Rumen fermentation and microbial diversity of sheep fed a high-concentrate diet supplemented with hydroethanolic extract of walnut green husks. *Animal Bioscience*, *37*(4), 655–667. https://doi.org/10.5713/AB.23.0213

Widiana, A., Ukit., Kusumah, P., Hanifah, H., & Wiharyati, A. (2021). Increasing the potential of Cajuput leaf waste as cattle feed through fermentation pretreatment. *Biogenesis: Jurnal Ilmiah Biologi*, *9*(1), 81–86. https://doi.org/10.24252/BIO.V9I1.21215

Xu, J., Li, X., Fan, Q., Zhao, S., & Jiao, T. (2025). Effects of yeast culture on lamb growth performance, rumen microbiota, and metabolites. *Animals*, *15*(5), 738. https://doi.org/10.3390/ANI15050738

Xu, Y., Yi, M., Sun, S., Wang, L., Zhang, Z., Ling, Y., & Cao, H. (2024). The regulatory mechanism of garlic skin improving the growth performance of fattening sheep through metabolism and immunity. *Frontiers in Veterinary Science*, *11*, 1409518. https://doi.org/10.3389/FVETS.2024.1409518/BIBTEX

Yanza, Y. R., Fitri, A., Suwignyo, B., Elfahmi., Hidayatik, N., Kumalasari, N. R., Irawan, A., & Jayanegara, A. (2021). The utilisation of tannin extract as a dietary additive in ruminant nutrition: A meta-analysis. *Animals*, *11*(11), 3317. https://doi.org/10.3390/ANI11113317

Yimenu, S. A., & Abebe, A. (2023). Effects of traditional brewery dried residue and field pea hull mixtures supplementation on feed utilization and performance of Washera sheep fed natural pasture grass hay as basal diet. *Veterinary Medicine and Science*, *9*(5), 2238–2246. https://doi.org/10.1002/vms3.1226

Yousefi, N., Shokrollahi Yancheshmeh, B., & Gernaey, K. V. (2025). The Potential of Fermentation-Based Processing on Protein Modification: A Review. *Foods, 14*(20), 3461. https://doi.org/10.3390/FOODS14203461

Zhang, Y.-S., Xu, Y.-X., Fan, W.-L., Zhou, Z.-K., Zhang, Z.-Y., & Hou, S.-S. (2019). Relationship between residual feed intake and production traits in a population of F_2 ducks. *Journal Poultry Science*, *56*(1), 27–31. https://doi.org/10.2141/jpsa.0180008

Zhou, J. W., Mi, J. D., Degen, A. A., Guo, X. S., Wang, H. C., Ding, L. M., Qiu, Q., & Long, R. J. (2015). Apparent digestibility, rumen fermentation and nitrogen balance in Tibetan and fine-wool sheep offered forage-concentrate diets differing in nitrogen concentration. *The Journal of Agricultural Science*, *153*(6), 1135–1145. https://doi.org/10.1017/S0021859615000465

Pertanika J. Trop. Agric. Sci. 48 (6): 2087 - 2117 (2025)

PERTANIKA JOURNALS

TROPICAL AGRICULTURAL SCIENCE

Journal homepage: http://www.pertanika.upm.edu.my/

Exploring Venom-derived Peptides from *Calloselasma rhodostoma* Snake as Promising Cholinesterase Inhibitors for Alzheimer's Disease Therapy

Annisa Maghfira[1], Itsar Auliya[1], Tri Rini Nuringtyas[1,2], Fajar Sofyantoro[1], Donan Satria Yudha[1], Slamet Raharjo[3], and Yekti Asih Purwestri[1,2]*

[1]Department of Tropical Biology, Faculty of Biology, Universitas Gadjah Mada, Yogyakarta 55281, Indonesia
[2]Research Center for Biotechnology, Universitas Gadjah Mada, Yogyakarta 55281, Indonesia
[3]Department of Internal Medicine, Faculty of Veterinary Medicine, Universitas Gadjah Mada, Yogyakarta 55281, Indonesia

ABSTRACT

Alzheimer's disease (AD) is a neurodegenerative disorder that primarily affects individuals over 60 years of age, characterized by symptoms such as memory impairment and cognitive decline. The pathogenesis of AD involves multiple factors, including protein misfolding and oxidative stress. A crucial aspect of AD progression is the dysregulation of cholinesterase enzymes, particularly acetylcholinesterase (AChE) and butyrylcholinesterase (BChE), which contribute to neurotoxic amyloid plaques and neurofibrillary tangles. This study investigates the potential of proteins and peptides from the venom of *Calloselasma rhodostoma* as BChE inhibitors, aiming to explore new therapeutic avenues for AD. Venom was extracted, fractionated, and analyzed using ultrafiltration, SDS-PAGE, and LC-HRMS. In vitro assays evaluated the BChE inhibition activity, while in silico molecular docking assessed the binding affinities of the identified peptides. The study identified several venom-derived peptides with significant BChE inhibitory potential, notably CFVVQPWEGK and IDVLSDEPR, which demonstrated strong binding affinities and stability in docking studies. These findings highlight the potential of peptides derived from *C. rhodostoma* venom as natural BChE inhibitors, offering a promising basis for developing novel AD therapies. Further research is warranted to fully understand the mechanisms and therapeutic potential of these bioactive compounds.

Keywords: Alzheimer's disease, butyrylcholinesterase, molecular docking, snake venom, therapeutic peptides

ARTICLE INFO

Article history:
Received: 11 March 2025
Accepted: 10 November 2025
Published: 25 November 2025

DOI: https://doi.org/10.47836/pjtas.48.6.21

E-mail addresses:
annisamaghfira@mail.ugm.ac.id (Annisa Maghfira)
itsarauliya@mail.ugm.ac.id (Itsar Auliya)
tririni@ugm.ac.id (Tri Rini Nuringtyas)
fajar.sofyantoro@ugm.ac.id (Fajar Sofyantoro)
donan.satria@ugm.ac.id (Donan Satria Yudha)
priesta_raharjo@ugm.ac.id (Slamet Raharjo)
yekti@ugm.ac.id (Yekti Asih Purwestri)
* Corresponding author

e-ISSN: 2231-8542

INTRODUCTION

Alzheimer's disease (AD) represents a prevalent neurodegenerative disorder predominantly afflicting individuals aged 60 years and above (Abubakar et al., 2022; Breijyeh & Karaman, 2020; Monteiro et al., 2023; Panachamnong et al., 2014). Various lifestyle factors, such as smoking, alcohol consumption, high cholesterol, and high sugar intake, along with genetic predispositions, exert notable influences on AD susceptibility (P. Chen et al., 2023; Stern et al., 2022). Dementia, an outcome of AD, presents a range of symptoms, including temporal and spatial disorientation, memory impairment, mood swings, and aphasic manifestations (Duce et al., 2019; Liao et al., 2022; van der Schaar et al., 2022). The pathogenesis of AD encompasses protein misfolding, aggregation phenomena, oxidative stress, mitochondrial dysfunction, and neuronal inflammation within cerebral tissues (Bendjedid et al., 2020; Bhushan et al., 2018; Monteiro et al., 2023). Recent pharmacological studies have emphasized the importance of cholinesterase inhibition as a therapeutic strategy for AD management, with heterocyclic scaffolds and flavonoid derivatives being particularly promising (Mughal et al., 2021; Obaid, Mughal, et al., 2022; Obaid, Naeem, et al., 2022).

Central to neurotransmission, acetylcholine (ACh) orchestrates pivotal roles by interacting with cholinesterase enzymes, comprising predominantly acetylcholinesterase (AChE), and to a lesser extent, butyrylcholinesterase (BChE) (Darvesh, 2016; Greig et al., 2005; Makin, 2018; Xing et al., 2021). In physiological states, AChE predominantly facilitates ACh hydrolysis, accounting for approximately 80%, while BChE contributes to roughly 10% (R. Chen et al., 2023; Pereira et al., 2022). Conversely, in AD pathology, elevated AChE activity may lead to amyloid accumulation and neurofibrillary tangle (NFT) formation (Ferreira-Vieira et al., 2016; Ma et al., 2022), potentially diminishing ACh levels (Abubakar et al., 2022; Bhushan et al., 2018). Concurrently, escalated BChE activity may foster neuritic plaque and NFT formation, culminating in cerebral tissue degeneration and clinical dementia manifestations (Liao et al., 2022; Mushtaq et al., 2014; Stern et al., 2022). Furthermore, heightened AChE activity may trigger an escalation in ACh levels, thereby augmenting the activity of BChE in the brain (Darvesh, 2016; Mushtaq et al., 2014). This surge in activity fosters the formation of neocortical amyloid-rich neurotic plaques and NFT, thereby instigating cerebral tissue degeneration and consequent clinical manifestations of dementia (Mushtaq et al., 2014). The dual role of AChE and BChE in both neurotransmission and amyloid aggregation has been further supported by in vitro and in vivo studies of novel cholinesterase inhibitors, including chalcone derivatives and other small molecules that show neuroprotective potential (Al-ghulikah et al., 2023). Importantly, in advanced stages of AD, AChE activity diminishes while BChE activity remains stable or even increases, shifting the regulation of acetylcholine primarily to BChE (Lee et al., 2018; Wright et al., 1993). This highlights the therapeutic relevance of

targeting BChE, particularly since most current treatments such as Donepezil are highly AChE-selective, with only Rivastigmine acting as a dual inhibitor (Kandiah et al., 2017; Nordberg et al., 2009).

Snake venom serves not only as a defensive mechanism but also fulfils a pivotal role in prey immobilization (Aird et al., 2015; Fry et al., 2006; Lai & Lu, 2023). Consequently, venom constituents predominantly comprise bioactive agents, encompassing a spectrum of compounds such as carbohydrates, biogenic amines, lipids, purine nucleosides, peptides, and proteins, constituting 70-90% of its composition (Adukauskienė et al., 2011; Chan et al., 2016; Lai & Lu, 2023; Oliveira et al., 2022). The heterogeneity in venom composition is notably influenced by factors such as habitat, seasonal variations, age, gender, and dietary preferences (Durban et al., 2017; Ferreira De Oliveira et al., 2022; Neumann et al., 2020). Interestingly, snake venoms themselves have been screened for intrinsic cholinesterase-inhibiting components, highlighting their potential as natural sources of enzyme inhibitors relevant to AD research (Liesener et al., 2007). *Calloselasma rhodostoma*, commonly known as the Malayan Pit Viper, thrives in tropical climates and prevalent across Southeast Asian territories including Vietnam, Thailand, Malaysia, and the Indonesian archipelago, particularly Borneo and Java Island (Aphrodita et al., 2025; Oh et al., 2021; Tan et al., 2022; Tang et al., 2019). As a constituent of the Viperidae family, which boasts the largest venom gland and longest fangs among its serpentine counterparts, *C. rhodostoma* venom holds considerable intrigue for its potential therapeutic applications (Cerda et al., 2022; Khimmaktong et al., 2022; Kusuma et al., 2023; Tang et al., 2019). In recent years, there has been an increasing focus on researching peptides and proteins as promising candidates for new therapeutic interventions (Chan et al., 2016; Oliveira et al., 2022; Sofyantoro et al., 2022). Several studies have been conducted to identify anticholinesterase activity from snake venom, specifically for the AChE inhibitor. Snake venom proteins that have already been identified as AChE inhibitors are fasciculin-1 and fasciculin-2, which are isolated from green mamba *Dendroaspis angusticeps*. Research has also found that there is AChE inhibition activity in *Bothrops moojeni* venom using ESI/MS and Ellman assay (Karlsson et al., 1984; Liesener et al., 2007). However, the potential of snake venom as a BChE inhibitor is a promising area yet to be explored and needs further investigation. The current study aimed to identify the proteinaceous constituents within *C. rhodostoma* venom and assess their viability as inhibitors of BchE, particularly in the context of Alzheimer's disease.

MATERIALS AND METHODS

Venom Collection

The study protocol was approved by the Ethics Committee of Research and Testing Laboratory (LPPT), Universitas Gadjah Mada, Indonesia (Certificate Number: 00051/04/LPPT/X/2023). Venoms were sourced from *C. rhodostoma*, a member of the Viperidae

family from Kaliurang, Yogyakarta, Indonesia. This specimen, encompassing one adult female, was approximately 1 to 2.5 years old. Venom extraction procedures were carried out after a 2-week period of fasting to ensure repletion of the venom glands. The harvested venom was kept at -80°C for 24 hours, followed by freeze-drying to preserve the protein integrity. Upon completion, the powdered venom specimen was stored at -20°C.

Ultrafiltration

Snake venom proteins were separated using Ultrafiltration Vivaspin® Maeso (50, 30, and 10 kDa) and Amicon® Ultrafiltration (3 kDa). Each apparatus underwent a preliminary washing procedure with PBS (0.01 M; pH 7) followed by centrifugation. Five milligrams of venom were dissolved in 2 mL of PBS (0.01M; pH7), followed by centrifugation (5000 rpm; 5 minutes; 4°C). Supernatant was then transferred to the Vivaspin device (50 kDa) and subjected to centrifugation (10,000 rpm; 5 minutes; 4°C). The filtered samples were further refined through successive filtration steps using decreasing filter sizes (50 - 10 kDa). The residual content was obtained through reverse centrifugation (3000 rpm; 3 minutes; 4°C). The filtrate from the 10 kDa filtration stage was subsequently transferred to the Amicon device (3 kDa) and subjected to centrifugation (14,000 G; 30 minutes; 4°C). The resulting residue was obtained through reverse centrifugation (14,000 G; 10 minutes; 4°C). Following these procedures, the fractions, encompassing both filtrates and residues, were preserved at -20°C until subsequent analysis.

Anion Exchange Chromatography

Snake venom protein was subjected to fractionation using a HiTrap Q HP Column (5 mL) as in Tang et al., (2016). Approximately 5 mg of *C. rhodostoma* venom was dissolved in 2 mL of PBS (0.01 M, pH 7) and subsequently subjected to centrifugation at 10,000 rpm for 5 minutes. The supernatant was carefully isolated and subjected to fractionation. The column was initially pre-equilibrated with a starting buffer (Tris HCl 0.02 M, pH 8) followed by elution with NaCl 0.5 M in Tris HCl 0.02 M, pH 8, at a flow rate of 1 mL/min. Fractions were collected at 3 mL intervals over 15 cycles and subsequently stored at -20°C for subsequent analysis.

Protein Quantification

Protein quantification was performed using the Bradford Assay method with Bovine Serum Albumin (BSA) stock solution (1 mg/mL) serving as the standard reference. Samples of 5 µL were combined with 795 µL of distilled water and 200 µL of Bradford reagent. The absorbance was then measured at 595 nm wavelength employing a Spectrophotometer.

SDS-PAGE

In SDS-PAGE analysis, aliquots of 25 µL samples were dispensed into sterile microtubes, followed by the addition of 6.25 µL of 5x sample buffer (Abbkine). Subsequently, the tubes were homogenized using a vortex and sealed with parafilm. These samples underwent incubation at 100°C for 2 - 3 minutes using a water bath, followed by immediate transfer to ice for 15 - 30 minutes, thus undergoing a heat shock treatment. The SDS gel (Q-PAGE TGN Precast Gel; QP4510; SMOBio Technology) was set up within the SDS chamber containing the running buffer. Gel electrophoresis ensued at 80 V for 90 minutes. Post-electrophoresis, the gel was stained utilizing Coomassie Brilliant Blue (CBB) on a shaker overnight. Subsequent destaining involved immersion in a solution comprising 50% methanol, 40% distilled water, and 10% glacial acetic acid on a shaker for 2-3 hours. Upon complete destaining, immersion in 10% glacial acetic acid followed.

Protein Digestion

For protein digestion, a 1 mg venom sample was diluted in 200 µL of MilliQ water as in Tang et al., (2016). From this dilution, 30 µL was aliquoted into a fresh microtube. To this, 4 µL of Protease Max and 2 µL of DTT were added. The mixture underwent incubation at 55°C for 20 minutes within a water bath. Subsequent to this, 2 µL of iodoacetamide was introduced, followed by incubation at room temperature for 15 minutes in the dark. Tris-HCl (100 mM), in a volume three times that of the total mixture, was added, followed by 2 µL of Trypsin Gold (Trypsin Gold, Mass Spectrometry Grade; V5280; Promega). The sample was subjected to overnight incubation at room temperature or incubated at 37°C for 3 hours. The digested protein was subjected to Liquid Chromatography High-Resolution Mass Spectrometry (LC-HRMS) analysis and BChE inhibition assay.

LC-HRMS

Trypsin-digested crude venom and AEC fractions were subjected to LC-HRMS. LC-HRMS analysis was conducted at the Laboratory for Integrated Research and Testing (LPPT), Universitas Gadjah Mada, Indonesia. Samples were injected into the LC-HRMS system, which featured a reverse-phase separation column connected to an EASY-Spray column system (Thermo Scientific Q Exactive benchtop LC-HRMS with High-Performance Quadrupole Precursor and High-Resolution Accurate Mass Orbitrap Detection). Elution was conducted using two mobile phases: mobile phase A (0.1% formic acid in water) and mobile phase B (0.1% formic acid in acetonitrile), with a gradient applied at a flow rate of 100 µL/minute. For mass spectrometry detection, high-resolution and accurate mass mode in positive ion mode were utilized. Subsequently, data from LC-HRMS underwent processing utilizing Proteome Discoverer 3.0 software on a computer system to obtain peptide sequences present in the digested venom, alongside information regarding the

master protein, isoelectric point (pI) values, and molecular weight. For data validation, a precursor mass error tolerance of ±10 ppm and a fragment mass error tolerance of ±0.02 Da were applied. Protein identifications were filtered using a false discovery rate (FDR) of <1% at both peptide and protein levels, and only proteins with at least two unique peptides were considered confidently identified.

Inhibition Assay

The evaluation of Butyrylcholinesterase (BChE) inhibition activity was carried out using the Butyrylcholinesterase Inhibitor Screening Kit (Colorimetric; ABCAM) (Li et al., 2021; Obaid, Naeem, et al., 2022). Trypsin-digested crude venom was diluted with 0.3% DMSO. Subsequently, 1 µL of the diluted samples and 9 µL of BChE Assay buffer were dispensed into designated wells, to achieve final concentrations of 200 and 300 ppm. The enzyme control and background control wells received 10 µL of BChE Assay buffer, whereas the positive control well was loaded with 5 µL of Rivastigmine at final concentrations of 200 and 300 ppm. The negative control well was filled with 10 µL of 0.3% DMSO. Each well, excluding the background control well, was supplemented with 5 µL of BChE enzymes. The final volume in each well was adjusted to 80 µL, followed by an incubation period of 30 minutes at room temperature in the absence of light. Subsequently, 20 µL of reaction mix (10 µL of diluted BChE substrate, 5 µL of probe mix, and 5 µL of BChE assay buffer) was loaded into each well. Absorbance readings were recorded using a Microplate Reader at a wavelength of 412 nm, with measurements taken at 5-minute intervals over a total duration of 60 minutes.

Molecular Docking

Molecular docking is an effective method for predicting and aligning target binding sites, exploring potential conformations of compounds, and elucidating the interactions between a ligand and its receptor (Frimayanti et al., 2021; Hidayatullah et al., 2020). Post-acquisition of peptide sequences via LC-HRMS, a meticulous selection process ensued employing ProtParam, ToxinPred, and AllerTop algorithms to discern stable, non-toxic, and non-allergenic peptides. Three-dimensional structure of peptides were modelled using the PEPFOLD4 webserver (https://mobyle2.rpbs.univ-paris-diderot.fr/cgi-bin/portal.py#forms::PEP-FOLD4). Rivastigmine (CID 77991), as a positive control, was obtained through PubChem. BChE receptors were retrieved from Uniprot (Code: P06276) and then modelled using the Swiss Model Expasy web server. As the BChE receptor structure obtained from UniProt does not include a native ligand, Rivastigmine, a clinically established BChE inhibitor, was used as a positive control and benchmark for validating peptide interactions. Ligand and receptor preparation were meticulously executed employing Biovia Discovery, Chimera, and PyMol, followed by molecular docking using

PyRx. The result of protein-peptide docked complexes was rendered visually utilizing PyMol and Discovery Studio.

ADMET Prediction

The Simplified Molecular Input Line Entry System (SMILES) structural format of the two best peptides from the molecular docking result was acquired using a web-based tool, PepSMI (https://www.novoprolabs.com/tools/convert-peptide-to-smiles-string). The PepSMI web server will convert the peptide sequences into SMILES. The ADMET evaluation was carried out using ADMETlab 3.0 web server (https://admetlab3.scbdd.com/) by entering the peptide's SMILES (Xiong et al., 2021). Then, Absorption, Distribution, Metabolism, Excretion, and Toxicity properties, including several parameters such as Human Intestinal Absorption (HIA), Papp/Caco-2 permeability, Blood-Brain Barrier (BBB), Plasma Protein Binding (PPB), CYP1A2 inhibitor-substrate, CYP3A4 inhibitor-substrate, T½ Half-Life, hERG blockers, Drug Induced Liver Injury (DILI), Ames mutagenicity, and Human Hepatoxicity were examined using the ADMETlab 3.0 webserver.

RESULTS AND DISCUSSION

SDS-PAGE Analysis

The initial determination of the protein concentration within the crude venom revealed a concentration of 40 µg/mL. Subsequent ultrafiltration procedures were conducted, segregating the filtrate and residue across varying molecular weight cut-off (MWCO) filters (50, 30, 10, and 3 kDa). Notably, the protein concentration within the residues surpassed that of the filtrates. Specifically, the residue obtained from the 50 kDa filter exhibited a protein concentration of 13.60 µg/mL, in stark contrast to the filtrate's concentration of 5.70 µg/mL. Similarly, the filtrates from the 30 kDa and 10 kDa filters displayed protein concentrations of 7.02 µg/mL and 8.53 µg/mL, respectively. Notably, no residue was obtained from the filtrates of these two filter sizes. Conversely, the residue from the 3 kDa filter demonstrated a protein concentration of 44.38 µg/mL, while its filtrate showcased a concentration of 11.21 µg/mL. These quantifications underscored the presence of a protein-enriched fraction resulting from Anion Exchange Chromatography (AEC), with the highest observed protein concentration within one of the 15 fractions derived from the venom of *C. rhodostoma*, amounting to 11.02 µg/mL.

Figure 1A shows 11 discernible protein bands evident within the SDS gel. These identified molecules within the crude venom spanned molecular weights ranging from approximately 13.68 to 115.08 kDa. This observation highlighted distinct protein clusters visualized within the SDS gel, indicative of disparate molecular size ranges. SDS-PAGE analysis of proteins harvested from AEC revealed 9 distinct bands within the fraction

derived from *C. rhodostoma* snake venom (Figure 1B), spanning molecular weights from 14.74 to 67.49 kDa. Figure 1B illustrates that the bands observed in the residue on the SDS gel are frequently characterized by smearing. This phenomenon is attributed to the filtration process, as outlined in the device manual, wherein residue concentration typically occurs during centrifugation, consequently resulting in smearing during SDS-PAGE analysis.

Notably, discrepancies in protein banding patterns were discernible among the filtrates from each filtration step. Particularly, filtrates from filters with smaller MWCO exhibited fewer discernible bands in comparison to those from larger filters (Figure 1C). Commencing with the 50 kDa residue (R50) displaying 12 bands, the subsequent filtrate (F50) exhibited a reduced band count of approximately 5. A further decline in band count was evident in the subsequent filtrate of 30 kDa (F30), manifesting only 2 bands. These banding patterns persisted in subsequent filtrates, namely filtrate 10 kDa (F10) and filtrate 3 kDa (F3).

Snake venom, traditionally perceived as predominantly proteinaceous with concentrations ranging between 70% to 90%, exhibits variability across different snake families (Fry et al., 2006; Oliveira et al., 2022; Vejayan et al., 2010). Protein content in the Colubridae family was found to range from 49.8% to 96.4% (Hill & Mackessy, 1997). Factors such as freeze-drying and improper storage conditions can influence protein concentration, potentially leading to sample degradation (Sofyantoro et al., 2024; Vejayan et al., 2010).

The SDS-PAGE analysis of the protein content in the crude venom and its subsequent fractions reveals a complex and heterogeneous protein composition. The differential

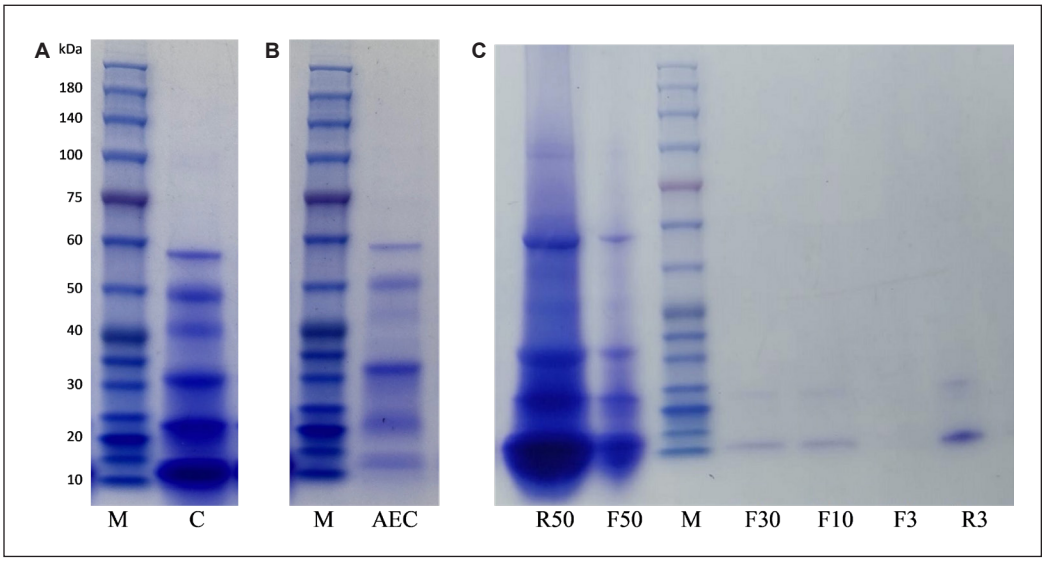

Figure 1. Electrophoretic analysis via SDS-PAGE depicting (A) crude venom, (B) Anion Exchange Chromatography (AEC) fractions, and (C) ultrafiltration fractions of *C. rhodostoma* snake venom. M: marker; C: crude venom; AEC: Anion Exchange Chromatography fractions; R50: 50 kDa residue; F50: 50 kDa filtrate; M: marker; F30: 30 kDa filtrate; F10: 10 kDa filtrate; F3: 3 kDa filtrate; R3: 3 kDa residue

protein concentrations observed across various molecular weight cut-off (MWCO) filters underscore the selective retention and passage of proteins based on size. The stark contrast in protein concentrations between residues and filtrates, especially in the 50 kDa and 3 kDa filters, indicates that larger proteins are predominantly retained, while smaller proteins pass through. The presence of multiple distinct protein bands, ranging from 13.68 to 115.08 kDa in the crude venom, highlights the diversity of protein sizes. The progressive reduction in the number of protein bands in the filtrates as the MWCO decreases suggests effective size-based separation. However, the smearing of protein bands, particularly in the residues, likely results from the concentration process during filtration, as noted in the device manual. This phenomenon could indicate potential aggregation or degradation during processing, warranting further optimization of the filtration protocol. Moreover, the identification of nine distinct bands in the fraction derived from anion exchange chromatography, spanning molecular weights from 14.78 to 67.49 kDa, suggests a selective enrichment of specific protein subsets. These findings provide a foundational understanding of the protein composition and separation dynamics in *C. rhodostoma* venom, offering valuable insights for future studies on the functional and toxicological properties of these proteins.

In vitro Inhibition Activity of BChE

The observed in vitro inhibition activities unveiled that the trypsin-digested crude venom of *C. rhodostoma*, administered at a concentration of 200 ppm, showed an estimated BChE inhibition of 43.75% (Table 1). Similarly, at a concentration of 300 ppm, the trypsin-digested venom exhibited an inhibition activity of 25%. In contrast, compared to the positive control (Rivastigmine), concentrations of 200 ppm displayed inhibition activity of 91.67%, while concentrations of 300 ppm showed inhibition activity of 93.75% (Table 1).

The observed inhibition activity of BChE by the trypsin-digested crude venom of *C. rhodostoma* demonstrates a dose-dependent response, with higher concentrations (300 ppm) not consistently leading to increased inhibition compared to lower concentrations (200 ppm). This suggests the presence of both inhibitory and potentially counteractive components within the trypsin-digested venom. The variation in inhibition percentages, ranging from 25% to 43.75%, indicates a complex interaction between the venom

Table 1
Evaluation of the inhibitory efficacy of trypsin-digested crude venom against Butyrylcholinesterase (BChE)

Samples	Concentration (ppm)	Inhibition Activity (%)
Trypsin-digested crude venom	200	43.75
	300	25
Rivastigmine	200	91.67
	300	93.75

constituents and BChE. In contrast, the positive control, Rivastigmine, exhibited significantly higher inhibition rates (91.67% to 93.75%), underscoring its potency and specificity as a BChE inhibitor. The lower efficacy of the venom might be attributed to the crude nature of the extract, which could contain a mixture of compounds with varying levels of inhibitory activity. These findings highlight the need for further fractionation and identification of active components within the venom to elucidate the specific mechanisms underlying BChE inhibition. Additionally, comparing these results with those from other snake venoms or natural sources could provide insights into unique or shared biochemical pathways. Although the observed inhibition percentages were lower than those of the positive control, the significance of these findings lies in the successful identification of novel peptides with measurable BChE inhibitory activity. This preliminary evidence provides an important foundation for future optimization and structural modification aimed at improving potency and therapeutic potential. It should also be noted that only two concentrations were tested in this preliminary screening, which was sufficient to identify promising inhibitory activity but limited in providing detailed dose–response relationships. More comprehensive concentration-dependent assays will be needed in future studies to validate and expand upon these findings.

In silico Inhibition Activity Assessment

Analysis of LC-HRMS from crude venom data revealed the presence of 15 proteins across 5 distinct protein families within the crude venom of *C. rhodostoma* (Supplementary Table 1). These families encompass L-Amino Acid Oxidase, Snake Venom Metalloproteinase Kistomin, Zinc Metalloproteinase or Disintegrin, Snaclec Rhodocytin subunit beta, Snaclec Rhodocentin subunits alpha, beta, delta, and gamma, Thrombin-like Enzyme, Acidic and Basic Phospholipase A2. Moreover, the crude venom exhibited a spectrum of 136 identified peptide sequences upon trypsin digestion (Supplementary Table 2). Conversely, samples isolated through AEC revealed 10 proteins spanning 4 protein families, including Zinc Metalloproteinase or Disintegrin, Snake Venom Metalloproteinase Kistomin, Thrombin-like Enzyme Ancrod, Snaclec Rhodocentin subunits alpha, beta, delta, and gamma, Snaclec Rhodocytin subunit alpha, and Basic Phospholipase A2 (Supplementary Table 3). Meanwhile, a total of 42 peptide sequences were discerned from the trypsin-digested venom subjected to Anion Exchange Chromatography (Supplementary Table 4).

Peptide sequences were chosen based on their physicochemical attributes, including stability, non-toxicity, and non-allergenicity. This selection process yielded 12 peptide sequences from the crude venom (Table 2) and 7 peptide sequences from AEC (Table 3). All identified peptide sequences underwent docking simulations using PyRx to assess their inherent inhibitory activity against BChE. The docking outcomes revealed diverse binding modes, characterized by varying binding affinities and RMSD values. Modes

Table 2
Evaluation of binding affinity and RMSD values for peptide components derived from trypsin digestion of C. rhodostoma crude venom against BChE

No.	Peptide Sequence	Mode	Binding Affinity (kcal/mol)	RMSD (Å)
	Rivastigmine (control)	3	-6.3	0.965
1.	NEEAGWYANLGPMR	2	-7.9	2.834
2.	DCADIVFNDLSLIHQLPK	2	-6.5	2.651
		6	-6.2	2.67
3.	DFDGNTVGLAFVGGICNEK	3	-6.3	2.231
		8	-6.1	3.203
4.	YCAGVVQDHTK	1	-7.6	2.36
		3	-7.5	2.055
		8	-6.9	2.773
5.	LEAVFVDMVMENNFENK	1	-7	1.541
6.	SNLEWSDGSSISYENLYEPYMEK	3	-6.4	2.891
		8	-6	2.525
7.	GPNPCAQPNKPALYTSIYDYR	2	-7	2.251
		4	-6.9	1.93
8.	DELADEDYVWIGLR	1	-7	1.674
9.	EQQCSSEWSDGSSVSYENLIDLHTK	1	-6.3	2.021
		4	-5.7	2.024
10.	CFVVQPWEGK	2	-7.8	2.226
11.	QAENGHLVSIGSAAEADFLDLVIVVNFDK	8	-4.7	2.042
12.	GHLVSIGSDGEADFVAQLVTNNIK	2	-7.2	2.516
		4	-7.1	2.187
		6	-7.1	2.114

meeting predefined criteria for both binding affinity and RMSD were deemed indicative of peptides' potential to inhibit BChE activity (Table 2 and Table 3).

Table 2 demonstrates the binding affinities of peptides derived from crude venom, ranging from -4.7 to -7.9 kcal/mol, while Table 3 showcases the binding affinities of peptides from AEC samples, ranging from -6.5 to -8.8 kcal/mol. A more negative binding affinity indicates a stronger interaction between the peptide and the BChE receptor (Alsedfy et al., 2024). Notably, within Table 2, the sequence CFVVQPWEGK (mode 2) exhibits the highest affinity value of -7.8 Å and a favorable RMSD value of 2.226 kcal/mol among peptides from crude venom. Conversely, from Table 3, the peptides from AEC samples highlight the sequence IDVLSDEPR (mode 2) with the highest affinity value of -8.8 Å and a commendable RMSD value of 2.228 kcal/mol. Considering the binding affinity and RMSD scores of CFVVQPWEGK and IDVLSDEPR, it can be inferred that these two sequences demonstrate the most promising interaction with the BChE receptor.

The 3D visualization of the interaction between the CFVVQPWEGK peptide and the BChE receptor is depicted in Figure 2A. Similarly, the interaction between the IDVLSDEPR peptide and the BChE receptor is illustrated in Figure 2B. As illustrated in Figure 3A, CFVVQPWEGK binds with BChE with amino acid residues Trp110, Asp98, Leu314, Gly361, Phe306, Pro309, Tyr310, Gln95, Leu301, Ala305, Asn96, Pro387, Thr312 and Phe357 engage in van der Waals interactions (Figure 3A). Meanwhile, as illustrated in Figure 3B, the active peptide ligand IDVLSDEPR binds with Ser107, Asp98, Ala356, Asn111, Gly149, His466, Gly467, Tyr468, Gly145, Val316, Leu314, Ser315, Gln95, Glu304, Thr312, Gln147, and Gly361 of receptor amino acid residues through van der Waals interactions. A comprehensive depiction of the interactions occurring between the ligand and the amino acid residues within the BChE receptor is provided in Table 4.

Table 3
Binding affinity and Root Mean Square Deviation (RMSD) analysis of peptides derived from trypsin-digested Anion Exchange Chromatography fractions of C. rhodostoma *venom against BChE*

No.	Peptide Sequence	Mode	Binding Affinity (kcal/mol)	RMSD (Å)
1.	IDVLSDEPR	2	-8.8	2.228
		4	-8.7	2.291
		6	-8.6	2.297
		7	-8.6	2.871
2.	VLCAGDLR	1	-7.5	2.618
		2	-7.5	1.857
		3	-7.3	2.182
		4	-7.1	2.418
		5	-7.1	2.307
		6	-7	3.177
		8	-7	2.725
3.	SWIGLK	1	-8.7	2.052
		2	-8.5	1.896
4.	CFVVQPWEGK	2	-8.8	2.381
		3	-8.8	2.257
		4	-8.5	2.61
5.	DFDGNTVGLAFVGGICNEK	1	-6.8	1.367
		4	-6.7	1.887
		8	-6.5	2.807
6.	LASQTLK	1	-7.5	2.496
		2	-7.3	2.903
		3	-7.2	2.781
		7	-7	2.195
7.	DELADEDYVWIGLR	2	-7.7	1.942
		4	-7.5	2.244

Table 4
Computational analysis of molecular interactions between peptides derived from trypsin digestion of C. rhodostoma *venom and the BChE receptor using the PyRx application*

Ligand	Carbon Hydrogen Bond	Conventional Hydrogen Bond	Van Der Waals	Other Types of Bond Formation
Rivastigmine (Control)	Tyr468 Gly106	-	Ser107 His466 Asp98 Thr148 Gly144 Gly467	Pi-Pi Stacked Trp110 Pi Alkyl / Alkyl Tyr360 Ala356 Trp458
CFVVQPWEGK	Pro313 Gly311	Gly311 Ile384 Val308 Asn317 Gln147 Glu304	Phe357 Gly145 Leu314 Asn111 Asp98 Trp110 Thr312 Pro387 Ala305 Gly361 Phe306 Pro309 Tyr310 Gln95 Leu301 Asn96	Amide-Pi Stacked Gly144 Pi-Alkyl / Alkyl Tyr360
IDVLSDDEPR	Trp110 Ala305 Gly144 Gln147	Pro313 Asn317 Asn96 Gly311	Ser107 Asp98 Ala356 Asn111 Gly149 His466 Gly467 Tyr468 Gly145 Val316 Leu314 Ser315 Gln95 Glu304 Thr312 Gln147 Gly361	Pi-Sigma Tyr360 Pi-Alkyl Phe357 Trp110

Previous research has shown that hydrogen bonds help to improve the binding and AChE inhibitory activity (Lu et al., 2011; Obaid, Mughal, et al., 2022; Obaid, Naeem, et al., 2022; Peitzika & Pontiki, 2023). Hydrogen bonds play an important role to stabilize the ligand inside the catalytic triad. The active peptide ligand CFVVQPWEGK is observed

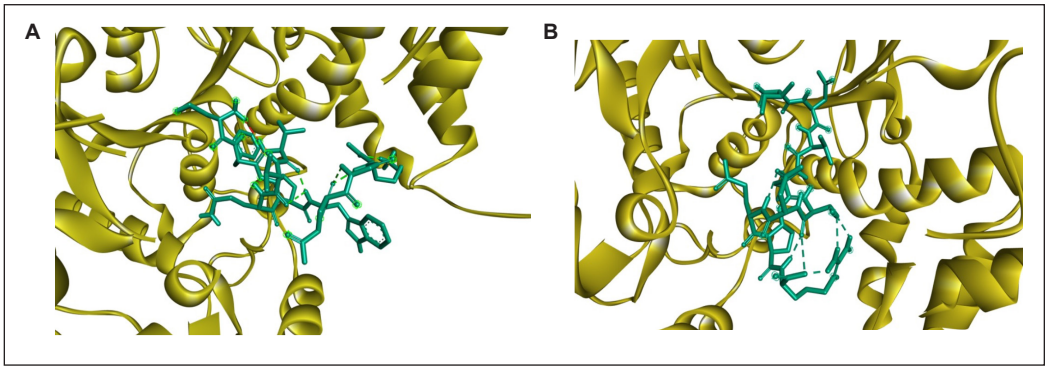

Figure 2. Three-Dimensional visualization illustrating the interactions between (A) CFVVQPWEGK and (B) IDVLSDEPR peptides with the Butyrylcholinesterase (BChE) receptor. Yellow: BChE; green: peptides

binding to Gly311, Ile384, Val308, Asn317, Gln147, and Glu304, as well as IDVLSDEPR binds to Pro313, Asn317, Asn96, and Gly311 in hydrogen bonds. Hydrogen bonds enhance the binding affinity of these peptides. The π-π interactions, hydrogen bonds, and strong hydrophobic interactions between the ligand and AChE inhibit AChE's activity by competing for the acetylcholine binding site. These interactions may also prevent amyloid fibrillogenesis by blocking the beta-amyloid recognition zone at the peripheral site. In recent studies, N-, O-, and S- based heterocyclic agents have demonstrated potential anti-cholinesterase activity. Their easy preparation, low toxicity, and high bioavailability are driving their increasing use (Lu et al., 2011; Obaid, Mughal, et al., 2022; Obaid, Naeem, et al., 2022; Peitzika & Pontiki, 2023).

In human catalytic BChE, the active site of BChE is positioned in a deep gorge with specific amino acid keys such as Ser226, His466, and Glu353 surrounded by six amino acids. At the lip of the active site, the substrate interacts with aspartic acid (Asp) and tyrosine (Tyr). Tryptophan (Trp) facilitates the creation of an anionic site (Jovičić, 2024). Molecular docking analysis shows that the CFVVQPWEGK ligands may not interact with the active site of the BChE enzyme, indicating they likely inhibit the enzyme through other sites. On the other hand, IDVLSDEPR and Rivastigmine interact with the active site of BChE with only one amino acid key residue, His666, with van der Waals interaction.

In the docking analysis of Rivastigmine (Table 2; Figure 4), it is apparent that the ligand engages with the BChE, displaying a binding affinity of -6.3 kcal/mol and an RMSD value of 0.965 Å. Comparative scrutiny between the docking outcomes of Rivastigmine as the reference and the active peptide ligand sequences CFVVQPWEGK and IDVLSDEPR derived from crude venom and AEC showcases concordant specific amino acid residues pivotal in BChE receptor interaction. As delineated in Figure 4 and Table 4, the Rivastigmine ligand forms van der Waals interactions with Thr 148, Asp 98, His 466, Ser 107, Gly 144, and Gly 467.

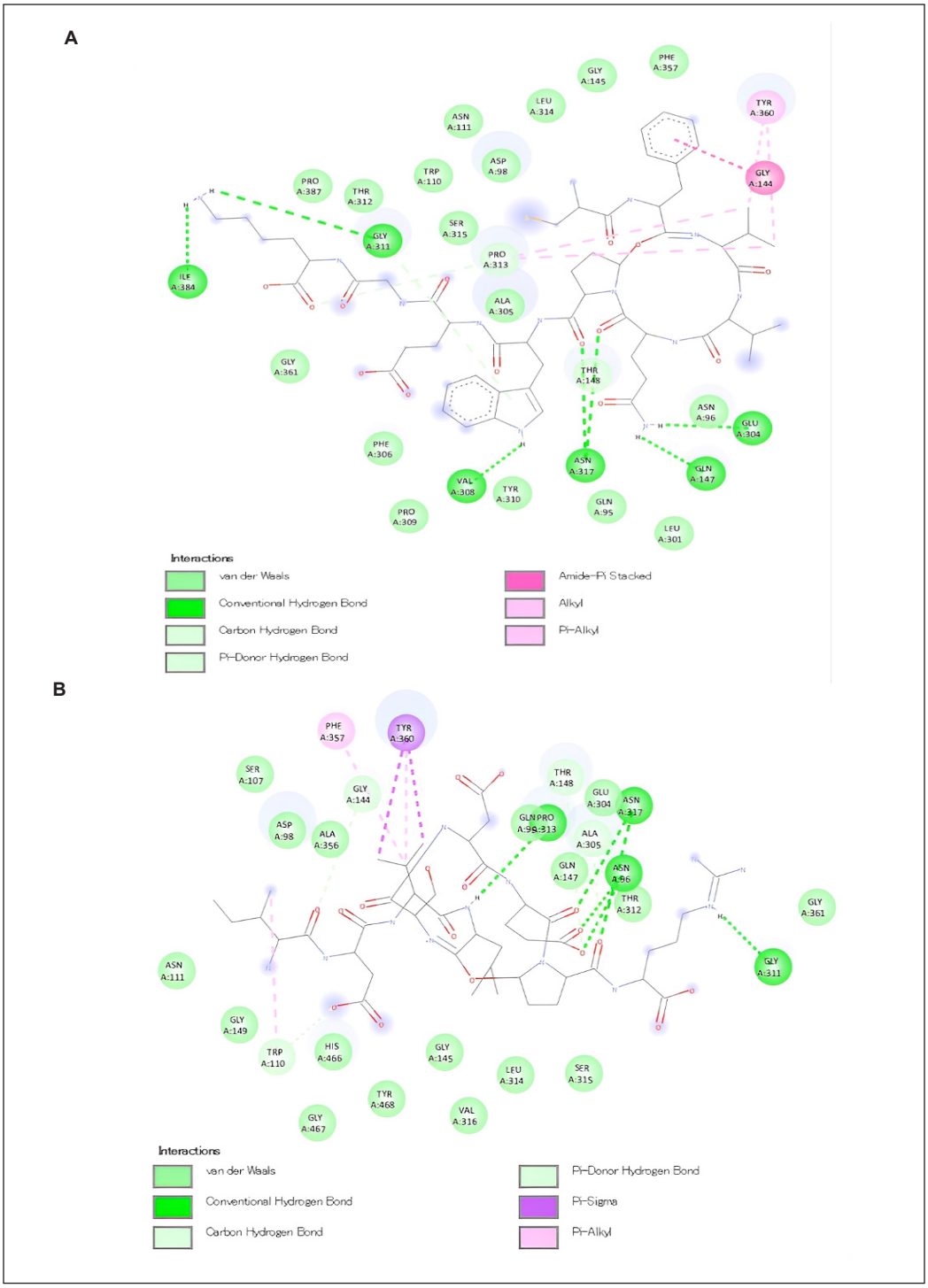

Figure 3. Two-Dimensional visualization of the molecular interaction between (A) CFVVQPWEGK and (B) IDVLSDEPR peptides with the Butyrylcholinesterase (BChE) receptor

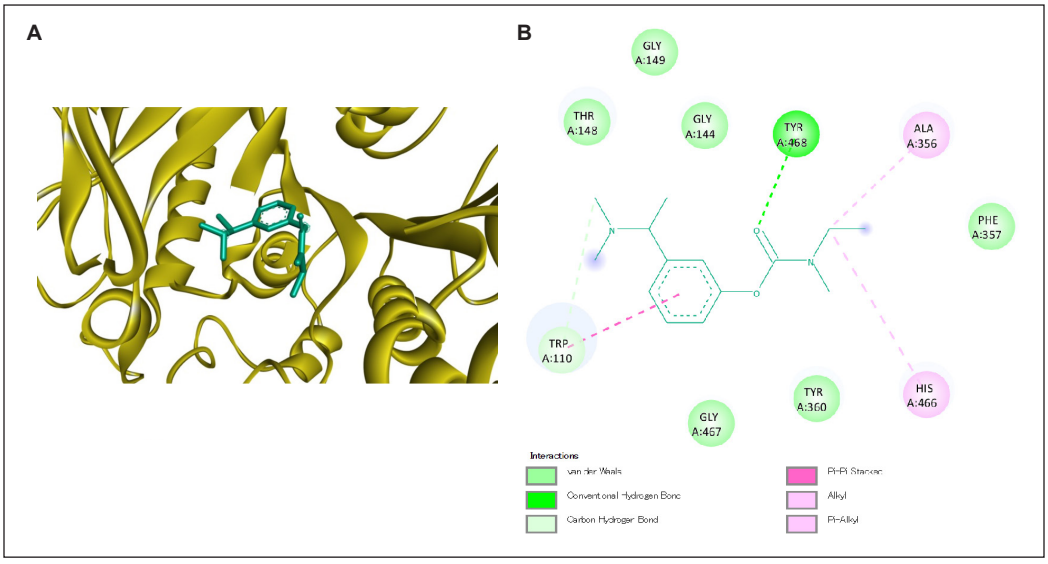

Figure 4. (A) Three-dimensional (3D) and (B) two-dimensional (2D) representations of the molecular interaction between Rivastigmine (control) and the Butyrylcholinesterase (BChE) receptor. Yellow: BChE; green: Rivastigmine

The in-silico inhibition activity assessment of trypsin-digested peptides from the crude venom and AEC samples from *C. rhodostoma* provides a comprehensive view of the venom's biochemical diversity and potential therapeutic applications. The identification of 15 proteins across five distinct families in the crude venom, including L-Amino Acid Oxidase, Snake Venom Metalloproteinases (like Kistomin), Zinc Metalloproteinases or Disintegrins, Snaclec Rhodocytin and Rhodocentin subunits, Thrombin-like Enzymes, and Acidic and Basic Phospholipase A2, underscores the complex nature of snake venoms. The detection of 136 peptide sequences further highlights the intricate peptide landscape within the venom. In contrast, the AEC samples, which revealed 10 proteins spanning four families and 42 peptide sequences, suggest that chromatographic techniques can effectively enrich specific bioactive components, potentially offering a more targeted approach to peptide isolation.

The docking simulations using PyRx revealed significant variations in binding affinities and Root Mean Square Deviation (RMSD) values among the identified peptides, suggesting a range of inhibitory activities against BChE. Notably, peptides such as CFVVQPWEGK and IDVLSDEPR demonstrated the strongest binding affinities, with values reaching -7.8 kcal/mol and -8.8 kcal/mol, respectively. These values indicate a strong interaction with the BChE receptor, surpassing the binding affinity of the control compound, Rivastigmine, which was -6.3 kcal/mol. The detailed molecular interactions, particularly van der Waals interactions and hydrogen bonds with key residues like Trp 110, Asp 98, and Gly 467, highlight the specificity of these peptides in binding to BChE.

The variations in peptide sequences and binding affinities between the crude venom and AEC samples underscore the importance of peptide diversity in modulating enzymatic activity. The results suggest that specific peptides, potentially more concentrated or isolated through AEC, may offer more potent inhibition of BChE. This finding aligns with the broader pharmacological interest in identifying and optimizing venom-derived peptides for therapeutic use, particularly as inhibitors of cholinesterases, which are relevant in the treatment of neurodegenerative diseases like Alzheimer's.

Absorption, Distribution, Metabolism, Excretion, and Toxicity (ADMET) Prediction

The two best peptides identified through virtual screening and molecular docking were analyzed for their ADMET properties. ADMET evaluation was performed to predict pharmacology and pharmacodynamic properties. By assessing the molecule's ADMET scores, drug pharmacokinetics in the human body can be predicted (Flores-Holguín et al., 2021; Sarkar et al., 2021). The result of the ADMET prediction for the lead peptides is presented in Table 5, along with a comparative analysis with Rivastigmine as a positive control. CFVVQPWEGK and IDVLSDEPR exhibit quite similar properties in ADMET evaluation. In the absorption category, human intestinal absorption (HIA) results are positive for all peptides, excluding Rivastigmine, which has a negative HIA, indicating that the absorption of peptides in the intestine is poorly absorbed compared to Rivastigmine. However, the Caco-2 permeability of the two lead peptides is poor compared to Rivastigmine, which exhibits optimal permeability. Drug bioavailability is determined by its absorption in the body after oral administration (Flores-Holguín et al., 2021). The ability of a peptide to traverse the Blood-Brain Barrier (BBB) is assessed through the BBB permeability index. BBB and Central Nervous System (CNS) permeability are important factors in designing an Alzheimer's drug candidate (Abdelazeem et al., 2024). Both CFVVQPWEGK and IDVLSDEPR peptides, as well as Rivastigmine, show BBB-positive results and optimal plasma protein binding (PPB), suggesting they can effectively penetrate the BBB. Regarding metabolism, none of the peptides or Rivastigmine inhibit the CYP1A2 and CYP3A4 enzymes, indicating that these peptides may enhance metabolism (Abdul-Hammed et al., 2021). Similar to Rivastigmine, the peptides CFVVQPWEGK and IDVLSDEPR display a short half-life. In terms of toxicity, several parameters were assessed, including hERG blockers, drug-induced liver injury (DILI), Ames mutagenicity (AMES), and human hepatotoxicity. All lead peptides and Rivastigmine were found to be non-blockers, non-toxic to the liver, and AMES-negative. Nonetheless, the human hepatotoxicity results raised the possibility of toxicity for the two peptides, including Rivastigmine. These findings indicate that the CFVVQPWEGK and IDVLSDEPR peptides from *C. rhodostoma* venom are able to cross the BBB and imply the potential safety as a new drug candidate.

Table 5
The ADMET prediction of the best two peptides along with Rivastigmine as a positive control

Category	Property (unit)	CFVVQPWEGK		IDVLSDEPR		Rivastigmine		Inference/references range
Absorption	HIA/Human Intestinal Absorption (%)	1.000	HIA Positive	1.000	HIA Positive	0.001	HIA Negative	HIA>0.3: HIA Positive, HIA<0.3: HIA Negative; or 0-0.3: excellent; 0.3-0.7: medium; 0.7-1.0: poor
	Papp/Caco-2 permeability (cm/s)	-6.223	Poor	-6.369	Poor	-4.639	Optimal	Optimal: higher than -5.15 Log unit
Distribution	BBB/Blood Brain Barrier Penetration (%)	0.000	BBB Positive	0.000	BBB Positive	0.734	BBB Positive	BBB≥0: BBB Positive, BBB<0.1: BBB Negative
	PPB/Plasma Protein Binding (%)	19.700	Optimal	20.197	Optimal	37.035	Optimal	PPB<90%: Optimal; PPB>90%: Low Therapeutic Index
Metabolism	CYP1A2-Inhibitor	0.000	Non-inhibitor	0.000	Non-inhibitor	0.477	Non-inhibitor	>0.5: An inhibitor; <0.5: Non-inhibitor
	CYP1A2-Substrate	0.000	Non-substrate	0.000	Non-substrate	0.982	Substrate	>0.5: An substrate; <0.5: Non-substrate
	CYP3A4-Inhibitor	0.000	Non-inhibitor	0.000	Non-inhibitor	0.018	Non-inhibitor	>0.5: An inhibitor; <0.5: Non-inhibitor
	CYP3A4-Substrate	0.000	Non-substrate	0.000	Non-substrate	0.965	Substrate	>0.5: An substrate; <0.5: Non-substrate
Excretion	T1/2/Half-life (H)	0.916	Short half-life	1.321	Intermediate short half-life	0.999	Short half-life	Long half-life: >3 h; Short half-life: <3 h
Toxicity	hERG blockers	0.001	Non blocker	0.000	Non blocker	0.319	Non-blocker	>0.5: Blocker; <0.5: Non blocker
	DILI/Drug Induced Liver Injury	0.267	Non-toxic to liver	0.059	Non-toxic to liver	0.312	Non-toxic to liver	>0.5: Toxic to liver; <0.5: Non toxic to liver
	AMES (Ames Mutagenicity)	0.064	Negative	0.004	Negative	0.326	Negative	>0.5: Positve; <0.5: Negative
	Human Hepatoxicity	0.544	Probability of being toxic	0.11	Probability of being toxic	0.797	Probability of being toxic	0-0.3: excellent; 0.3-0.7: medium; 0.7-1.0: poor

Taken together, the differential binding modes observed for these peptides provide valuable insights into the structure-activity relationships that govern their interactions with the BChE receptor. This knowledge is crucial for the rational design of peptide-based inhibitors, where modifications to enhance binding affinity and specificity can be guided by the docking results. The ADMET prediction also indicates that our peptides nearly met the pharmacokinetics criteria for a drug-like molecule. The study's comprehensive approach, combining LC-HRMS analysis, peptide sequencing, and in silico docking, and ADMET evaluation, provides a robust framework for exploring the therapeutic potential of venom-derived peptides. These findings pave the way for future studies focusing on the functional characterization of these peptides and their development as leads in drug discovery. While molecular dynamics (MD) simulations would provide deeper insights into peptide–BChE interactions, this study was limited to docking-based screening as an initial step, and MD analysis is planned for future validation of the most promising candidates.

CONCLUSION

This study successfully isolated and identified specific protein components from the venom of *C. rhodostoma*, revealing their potential as inhibitors of BChE. The venom's protein and peptide fractions demonstrated promising inhibitory activity against BChE, suggesting a possible application in the management of Alzheimer's disease (AD). Notably, two peptides, CFVVQPWEGK and IDVLSDEPR, exhibited the highest binding affinities and optimal interactions with BChE, positioning them as candidates for further investigation. Looking ahead, there is a compelling need for in vivo studies to evaluate the efficacy and safety of these peptides in animal models of AD. Additionally, further refinement of peptide isolation techniques could enhance the purity and yield of these bioactive compounds. Understanding the detailed mechanisms through which these peptides interact with BChE at a molecular level will be crucial for the development of new therapeutic strategies. Exploration of venom components from other snake species may also yield novel inhibitors, broadening the scope of potential treatments. Ultimately, these endeavours could lead to the development of innovative therapeutics for neurodegenerative diseases, offering hope for more effective management options for patients with AD.

ACKNOWLEDGEMENT

We extend our gratitude to Ananto Puradi and Budi Khoiri Ardiansyah for their invaluable assistance and support throughout the course of this study.

REFERENCES

Abdelazeem, N. M., Aboulthana, W. M., Hassan, A. S., Almehizia, A. A., Naglah, A. M., & Alkahtani, H. M. (2024). Synthesis, in silico ADMET prediction analysis, and pharmacological evaluation of sulfonamide

derivatives tethered with pyrazole or pyridine as anti-diabetic and anti-Alzheimer's agents. *Saudi Pharmaceutical Journal*, *32*(5), 102025. https://doi.org/10.1016/j.jsps.2024.102025

Abdul-Hammed, M., Adedotun, I. O., Falade, V. A., Adepoju, A. J., Olasupo, S. B., & Akinboade, M. W. (2021). Target-based drug discovery, ADMET profiling and bioactivity studies of antibiotics as potential inhibitors of SARS-CoV-2 main protease (Mpro). *VirusDisease*, *32*(4), 642–656. https://doi.org/10.1007/s13337-021-00717-z

Abubakar, M. B., Sanusi, K. O., Ugusman, A., Mohamed, W., Kamal, H., Ibrahim, N. H., Khoo, C. S., & Kumar, J. (2022). Alzheimer's Disease: An Update and Insights Into Pathophysiology. *Frontiers in Aging Neuroscience*, *14*, 742408. https://doi.org/10.3389/fnagi.2022.742408

Adukauskienė, D., Varanauskienė, E., & Adukauskaitė, A. (2011). Venomous Snakebites. *Medicina*, *47*(8), 461. https://doi.org/10.3390/medicina47080061

Aird, S. D., Aggarwal, S., Villar-Briones, A., Tin, M. M.-Y., Terada, K., & Mikheyev, A. S. (2015). Snake venoms are integrated systems, but abundant venom proteins evolve more rapidly. *BMC Genomics*, *16*(1), 647. https://doi.org/10.1186/s12864-015-1832-6

Al-ghulikah, H. A., Mughal, E. U., Elkaeed, E. B., Naeem, N., Nazir, Y., Alzahrani, A. Y. A., Sadiq, A., & Shah, S. W. A. (2023). Discovery of chalcone derivatives as potential α-glucosidase and cholinesterase inhibitors: Effect of hyperglycemia in paving a path to dementia. *Journal of Molecular Structure*, *1275*, 134658. https://doi.org/10.1016/j.molstruc.2022.134658

Alsedfy, M. Y., Ebnalwaled, A. A., Moustafa, M., & Said, A. H. (2024). Investigating the binding affinity, molecular dynamics, and ADMET properties of curcumin-IONPs as a mucoadhesive bioavailable oral treatment for iron deficiency anemia. *Scientific Reports*, *14*(1), 22027. https://doi.org/10.1038/s41598-024-72577-8

Aphrodita, A., Sentono, D. N., Yudha, D. S., Purwestri, Y. A., Nuringtyas, T. R., Raharjo, S., Wahid, I., Rahmi, S. N., Wahyudi, S. T., & Sofyantoro, F. (2025). Comparative analysis of hemotoxic, myotoxic, and inflammatory profiles of Calloselasma rhodostoma and Trimeresurus insularis venoms in mice. *Narra J*, *5*(2), 1–16.

Bendjedid, S., Djelloul, R., Tadjine, A., Bensouici, C., & Boukhari, A. (2020). In vitro assessment of total bioactive contents, antioxidant, anti-alzheimer and antidiabetic activities of leaves extracts and fractions of Aloe vera. *Natural and Life Sciences Communications*, *19*(3), 469–485.

Bhushan, I., Kour, M., Kour, G., Gupta, S., Sharma, S., & Yadav, A. (2018). Alzheimer's disease: Causes & treatment – A review. *Annals of Biotechnology*, *1*(1). https://doi.org/10.33582/2637-4927/1002

Breijyeh, Z., & Karaman, R. (2020). Comprehensive Review on Alzheimer's Disease: Causes and Treatment. *Molecules (Basel, Switzerland)*, *25*(24), 5789. https://doi.org/10.3390/molecules25245789

Cerda, P. A., Crowe-Riddell, J. M., Gonçalves, D. J. P., Larson, D. A., Duda, T. F., & Davis Rabosky, A. R. (2022). Divergent Specialization of Simple Venom Gene Profiles among Rear-Fanged Snake Genera (Helicops and Leptodeira, Dipsadinae, Colubridae). *Toxins*, *14*(7), 489. https://doi.org/10.3390/toxins14070489

Chan, Y. S., Cheung, R. C. F., Xia, L., Wong, J. H., Ng, T. B., & Chan, W. Y. (2016). Snake venom toxins: Toxicity and medicinal applications. *Applied Microbiology and Biotechnology*, *100*(14), 6165–6181. https://doi.org/10.1007/s00253-016-7610-9

Chen, P., Yao, H., Tijms, B. M., Wang, P., Wang, D., Song, C., Yang, H., Zhang, Z., Zhao, K., Qu, Y., Kang, X., Du, K., Fan, L., Han, T., Yu, C., Zhang, X., Jiang, T., Zhou, Y., Lu, J., … Liu, Y. (2023). Four Distinct Subtypes of Alzheimer's Disease Based on Resting-State Connectivity Biomarkers. *Biological Psychiatry*, *93*(9), 759–769. https://doi.org/10.1016/j.biopsych.2022.06.019

Chen, R., Li, X., Chen, H., Wang, K., Xue, T., Mi, J., Ban, Y., Zhu, G., Zhou, Y., Dong, W., Tang, L., & Sang, Z. (2023). Development of the "hidden" multi-target-directed ligands by AChE/BuChE for the treatment of Alzheimer's disease. *European Journal of Medicinal Chemistry*, *251*, 115253. https://doi.org/10.1016/j.ejmech.2023.115253

Darvesh, S. (2016). Butyrylcholinesterase as a Diagnostic and Therapeutic Target for Alzheimer's Disease. *Current Alzheimer Research*, *13*(10), 1173–1177. https://doi.org/10.2174/1567205013666160404120542

Duce, J. A., Zhu, X., Jacobson, L. H., & Beart, P. M. (2019). Therapeutics for dementia and Alzheimer's disease: New directions for precision medicine. *British Journal of Pharmacology*, *176*(18), 3409–3412. https://doi.org/10.1111/bph.14767

Durban, J., Sanz, L., Trevisan-Silva, D., Neri-Castro, E., Alagón, A., & Calvete, J. J. (2017). Integrated Venomics and Venom Gland Transcriptome Analysis of Juvenile and Adult Mexican Rattlesnakes *Crotalus simus*, *C. tzabcan* , and *C. culminatus* Revealed miRNA-modulated Ontogenetic Shifts. *Journal of Proteome Research*, *16*(9), 3370–3390. https://doi.org/10.1021/acs.jproteome.7b00414

Ferreira De Oliveira, N., Sachetto, A. T. A., & Santoro, M. L. (2022). Two-Dimensional Blue Native/SDS Polyacrylamide Gel Electrophoresis for Analysis of Brazilian Bothrops Snake Venoms. *Toxins*, *14*(10), 661. https://doi.org/10.3390/toxins14100661

Ferreira-Vieira, T. H., Guimaraes, I. M., Silva, F. R., & Ribeiro, F. M. (2016). Alzheimer's disease: Targeting the Cholinergic System. *Current Neuropharmacology*, *14*(1), 101–115. https://doi.org/10.2174/1570159x13666150716165726

Flores-Holguín, N., Frau, J., & Glossman-Mitnik, D. (2021). In Silico Pharmacokinetics, ADMET Study and Conceptual DFT Analysis of Two Plant Cyclopeptides Isolated From Rosaceae as a Computational Peptidology Approach. *Frontiers in Chemistry*, *9*, 708364. https://doi.org/10.3389/fchem.2021.708364

Frimayanti, N., Yaeghoobi, M., Ikhtiarudin, I., Putri, D. R. W., Namavar, H., & Bitaraf, F. S. (2021). Insight on the in silico study and biological activity assay of chalcone-based 1, 5-benzothiazepines as potential inhibitor for breast cancer MCF7. *Natural and Life Sciences Communications*, *20*(1), e2021019.

Fry, B. G., Vidal, N., Norman, J. A., Vonk, F. J., Scheib, H., Ramjan, S. F. R., Kuruppu, S., Fung, K., Blair Hedges, S., Richardson, M. K., Hodgson, Wayne. C., Ignjatovic, V., Summerhayes, R., & Kochva, E. (2006). Early evolution of the venom system in lizards and snakes. *Molecular & Cellular Proteomics*, *439*(7076), 584–588. https://doi.org/10.1038/nature04328

Greig, N. H., Utsuki, T., Ingram, D. K., Wang, Y., Pepeu, G., Scali, C., Yu, Q.-S., Mamczarz, J., Holloway, H. W., Giordano, T., Chen, D., Furukawa, K., Sambamurti, K., Brossi, A., & Lahiri, D. K. (2005). Selective butyrylcholinesterase inhibition elevates brain acetylcholine, augments learning and lowers Alzheimer β-amyloid peptide in rodent. *Proceedings of the National Academy of Sciences*, *102*(47), 17213–17218. https://doi.org/10.1073/pnas.0508575102

Hidayatullah, A., Putra, W. E., Salma, W. O., Muchtaromah, B., Permatasari, G. W., Susanto, H., Widiastuti, D., & Kismurtono, M. (2020). Discovery of Drug Candidate from Various Natural Products as Potential Novel Dengue Virus Nonstructural Protein 5 (NS5) Inhibitor. *Chiang Mai University Journal of Natural Sciences*, *20*(1). https://doi.org/10.12982/CMUJNS.2021.018

Hill, R. E., & Mackessy, S. P. (1997). Venom yields from several species of colubrid snakes and differential effects of ketamine. *Toxicon*, *35*(5), 671–678. https://doi.org/10.1016/S0041-0101(96)00174-2

Jovičić, S. M. (2024). Enzyme ChE, cholinergic therapy and molecular docking: Significant considerations and future perspectives. *International Journal of Immunopathology and Pharmacology*, *38*, 03946320241289013. https://doi.org/10.1177/03946320241289013

Kandiah, N., Pai, M.-C., Senanarong, V., Looi, I., Ampil, E., Park, K. W., Karanam, A. K., & Christopher, S. (2017). Rivastigmine: The advantages of dual inhibition of acetylcholinesterase and butyrylcholinesterase and its role in subcortical vascular dementia and Parkinson’s disease dementia. *Clinical Interventions in Aging*, *Volume 12*, 697–707. https://doi.org/10.2147/CIA.S129145

Karlsson, E., Mbugua, P. M., & Rodriguez-Ithurralde, D. (1984). Fasciculins, anticholinesterase toxins from the venom of the green mamba Dendroaspis angusticeps. *Journal De Physiologie*, *79*(4), 232–240.

Khimmaktong, W., Nuanyaem, N., Lorthong, N., Hodgson, W. C., & Chaisakul, J. (2022). Histopathological Changes in the Liver, Heart and Kidneys Following Malayan Pit Viper (Calloselasma rhodostoma) Envenoming and the Neutralising Effects of Hemato Polyvalent Snake Antivenom. *Toxins*, *14*(9), 601. https://doi.org/10.3390/toxins14090601

Kusuma, W. A., Fadli, A., Fatriani, R., Sofyantoro, F., Yudha, D. S., Lischer, K., Nuringtyas, T. R., Putri, W. A., Purwestri, Y. A., & Swasono, R. T. (2023). Prediction of the interaction between Calloselasma rhodostoma venom-derived peptides and cancer-associated hub proteins: A computational study. *Heliyon*, *9*(11), e21149. https://doi.org/10.1016/j.heliyon.2023.e21149

Lai, R., & Lu, Q. (2023). Advanced Research on Animal Venoms in China. *Toxins*, *15*(4), 272. https://doi.org/10.3390/toxins15040272

Lee, S., Youn, K., Lim, G., Lee, J., & Jun, M. (2018). In Silico Docking and In Vitro Approaches towards BACE1 and Cholinesterases Inhibitory Effect of Citrus Flavanones. *Molecules*, *23*(7), 1509. https://doi.org/10.3390/molecules23071509

Li, S., Li, A. J., Travers, J., Xu, T., Sakamuru, S., Klumpp-Thomas, C., Huang, R., & Xia, M. (2021). Identification of Compounds for Butyrylcholinesterase Inhibition. *SLAS Discovery: Advancing Life Sciences R & D*, *26*(10), 1355–1364. https://doi.org/10.1177/24725552211030897

Liao, Y., Mai, X., Wu, X., Hu, X., Luo, X., & Zhang, G. (2022). Exploring the Inhibition of Quercetin on Acetylcholinesterase by Multispectroscopic and In Silico Approaches and Evaluation of Its Neuroprotective Effects on PC12 Cells. *Molecules*, *27*(22), 7971. https://doi.org/10.3390/molecules27227971

Liesener, A., Perchuc, A.-M., Schöni, R., Schebb, N. H., Wilmer, M., & Karst, U. (2007). Screening of acetylcholinesterase inhibitors in snake venom by electrospray mass spectrometry. *Pure and Applied Chemistry*, *79*(12), 2339–2349. https://doi.org/10.1351/pac200779122339

Lu, S.-H., Wu, J. W., Liu, H.-L., Zhao, J.-H., Liu, K.-T., Chuang, C.-K., Lin, H.-Y., Tsai, W.-B., & Ho, Y. (2011). The discovery of potential acetylcholinesterase inhibitors: A combination of pharmacophore

modeling, virtual screening, and molecular docking studies. *Journal of Biomedical Science*, *18*(1), 8. https://doi.org/10.1186/1423-0127-18-8

Ma, C., Hong, F., & Yang, S. (2022). Amyloidosis in Alzheimer's Disease: Pathogeny, Etiology, and Related Therapeutic Directions. *Molecules (Basel, Switzerland)*, *27*(4), 1210. https://doi.org/10.3390/molecules27041210

Makin, S. (2018). The amyloid hypothesis on trial. *Nature*, *559*(7715), S4–S7. https://doi.org/10.1038/d41586-018-05719-4

Monteiro, A. R., Barbosa, D. J., Remião, F., & Silva, R. (2023). Alzheimer's disease: Insights and new prospects in disease pathophysiology, biomarkers and disease-modifying drugs. *Biochemical Pharmacology*, *211*, 115522. https://doi.org/10.1016/j.bcp.2023.115522

Mughal, E. U., Sadiq, A., Ayub, M., Naeem, N., Javid, A., Sumrra, S. H., Zafar, M. N., Khan, B. A., Malik, F. P., & Ahmed, I. (2021). Exploring 3-Benzyloxyflavones as new lead cholinesterase inhibitors: Synthesis, structure–activity relationship and molecular modelling simulations. *Journal of Biomolecular Structure and Dynamics*, *39*(16), 6154–6167. https://doi.org/10.1080/07391102.2020.1803136

Mushtaq, G., Greig, N., Khan, J., & Kamal, M. (2014). Status of Acetylcholinesterase and Butyrylcholinesterase in Alzheimer's Disease and Type 2 Diabetes Mellitus. *CNS & Neurological Disorders - Drug Targets*, *13*(8), 1432–1439. https://doi.org/10.2174/1871527313666141023141545

Neumann, C., Slagboom, J., Somsen, G. W., Vonk, F., Casewell, N. R., Cardoso, C. L., & Kool, J. (2020). Development of a generic high-throughput screening assay for profiling snake venom protease activity after high-resolution chromatographic fractionation. *Toxicon*, *178*, 61–68. https://doi.org/10.1016/j.toxicon.2020.02.015

Nordberg, A., Darreh-Shori, T., Peskind, E., Soininen, H., Mousavi, M., Eagle, G., & Lane, R. (2009). Different Cholinesterase Inhibitor Effects on CSF Cholinesterases in Alzheimer Patients. *Current Alzheimer Research*, *6*(1), 4–14. https://doi.org/10.2174/156720509787313961

Obaid, R. J., Mughal, E. U., Naeem, N., Al-Rooqi, M. M., Sadiq, A., Jassas, R. S., Moussa, Z., & Ahmed, S. A. (2022). Pharmacological significance of nitrogen-containing five and six-membered heterocyclic scaffolds as potent cholinesterase inhibitors for drug discovery. *Process Biochemistry*, *120*, 250–259. https://doi.org/10.1016/j.procbio.2022.06.009

Obaid, R. J., Naeem, N., Mughal, E. U., Al-Rooqi, M. M., Sadiq, A., Jassas, R. S., Moussa, Z., & Ahmed, S. A. (2022). Inhibitory potential of nitrogen, oxygen and sulfur containing heterocyclic scaffolds against acetylcholinesterase and butyrylcholinesterase. *RSC Advances*, *12*(31), 19764–19855. https://doi.org/10.1039/D2RA03081K

Oh, A. M. F., Tan, K. Y., Tan, N. H., & Tan, C. H. (2021). Proteomics and neutralization of Bungarus multicinctus (Many-banded Krait) venom: Intra-specific comparisons between specimens from China and Taiwan. *Comparative Biochemistry and Physiology Part C: Toxicology & Pharmacology*, *247*, 109063. https://doi.org/10.1016/j.cbpc.2021.109063

Oliveira, A. L., Viegas, M. F., Da Silva, S. L., Soares, A. M., Ramos, M. J., & Fernandes, P. A. (2022). The chemistry of snake venom and its medicinal potential. *Nature Reviews Chemistry*, *6*(7), 451–469. https://doi.org/10.1038/s41570-022-00393-7

Panachamnong, N., Methapatara, P., Sungkarat, S., Taneyhill, K., & Intasai, N. (2014). Clusterin as a blood biomarker for diagnosis of mild cognitive impairment and Alzheimer's disease. *Natural and Life Sciences Communications*, *13*(3), 331–344.

Peitzika, S.-C., & Pontiki, E. (2023). A Review on Recent Approaches on Molecular Docking Studies of Novel Compounds Targeting Acetylcholinesterase in Alzheimer Disease. *Molecules*, *28*(3), 1084. https://doi.org/10.3390/molecules28031084

Pereira, G. R. C., Gonçalves, L. M., Abrahim-Vieira, B. de A., & De Mesquita, J. F. (2022). In silico analyses of acetylcholinesterase (AChE) and its genetic variants in interaction with the anti-Alzheimer drug Rivastigmine. *Journal of Cellular Biochemistry*, *123*(7), 1259–1277. https://doi.org/10.1002/jcb.30277

Sarkar, B., Alam, S., Rajib, T. K., Islam, S. S., Araf, Y., & Ullah, Md. A. (2021). Identification of the most potent acetylcholinesterase inhibitors from plants for possible treatment of Alzheimer's disease: A computational approach. *Egyptian Journal of Medical Human Genetics*, *22*(1), 10. https://doi.org/10.1186/s43042-020-00127-8

Sofyantoro, F., Septriani, N. I., Yudha, D. S., Wicaksono, E. A., Priyono, D. S., Putri, W. A., Primahesa, A., Raharjeng, A. R. P., Purwestri, Y. A., & Nuringtyas, T. R. (2024). Zebrafish as Versatile Model for Assessing Animal Venoms and Toxins: Current Applications and Future Prospects. *Zebrafish*, zeb.2023.0088. https://doi.org/10.1089/zeb.2023.0088

Sofyantoro, F., Yudha, D. S., Lischer, K., Nuringtyas, T. R., Putri, W. A., Kusuma, W. A., Purwestri, Y. A., & Swasono, R. T. (2022). Bibliometric analysis of literature in snake venom-related research worldwide (1933–2022). *Animals*, *12*(16), 2058. https://doi.org/10.3390/ani12162058

Stern, N., Gacs, A., Tátrai, E., Flachner, B., Hajdú, I., Dobi, K., Bágyi, I., Dormán, G., Lőrincz, Z., Cseh, S., Kígyós, A., Tóvári, J., & Goldblum, A. (2022). Dual Inhibitors of AChE and BACE-1 for Reducing Aβ in Alzheimer's Disease: From In Silico to In Vivo. *International Journal of Molecular Sciences*, *23*(21), 13098. https://doi.org/10.3390/ijms232113098

Tan, K. Y., Shamsuddin, N. N., & Tan, C. H. (2022). Sharp-nosed Pit Viper (Deinagkistrodon acutus) from Taiwan and China: A comparative study on venom toxicity and neutralization by two specific antivenoms across the Strait. *Acta Tropica*, *232*, 106495. https://doi.org/10.1016/j.actatropica.2022.106495

Tang, E. L. H., Tan, C. H., Fung, S. Y., & Tan, N. H. (2016). Venomics of Calloselasma rhodostoma , the Malayan pit viper: A complex toxin arsenal unraveled. *Journal of Proteomics*, *148*, 44–56. https://doi.org/10.1016/j.jprot.2016.07.006

Tang, E. L. H., Tan, N. H., Fung, S. Y., & Tan, C. H. (2019). Comparative proteomes, immunoreactivities and neutralization of procoagulant activities of Calloselasma rhodostoma (Malayan pit viper) venoms from four regions in Southeast Asia. *Toxicon*, *169*, 91–102. https://doi.org/10.1016/j.toxicon.2019.08.004

van der Schaar, J., Visser, L. N. C., Bouwman, F. H., Ket, J. C. F., Scheltens, P., Bredenoord, A. L., & van der Flier, W. M. (2022). Considerations regarding a diagnosis of Alzheimer's disease before dementia: A systematic review. *Alzheimer's Research & Therapy*, *14*(1), 31. https://doi.org/10.1186/s13195-022-00971-3

Vejayan, J., Shin Yee, L., Ponnudurai, G., Ambu, S., & Ibrahim, I. (2010). Protein profile analysis of Malaysian snake venoms by two-dimensional gel electrophoresis. *Journal of Venomous Animals and Toxins Including Tropical Diseases*, *16*(4), 623–630. https://doi.org/10.1590/S1678-91992010000400013

Wright, C. I., Geula, C., & Mesulam, M. -Marsel. (1993). Neuroglial cholinesterases in the normal brain and in Alzheimer's disease: Relationship to plaques, tangles, and patterns of selective vulnerability. *Annals of Neurology*, *34*(3), 373–384. https://doi.org/10.1002/ana.410340312

Xing, S., Li, Q., Xiong, B., Chen, Y., Feng, F., Liu, W., & Sun, H. (2021). Structure and therapeutic uses of butyrylcholinesterase: Application in detoxification, Alzheimer's disease, and fat metabolism. *Medicinal Research Reviews*, *41*(2), 858–901. https://doi.org/10.1002/med.21745

Xiong, G., Wu, Z., Yi, J., Fu, L., Yang, Z., Hsieh, C., Yin, M., Zeng, X., Wu, C., Lu, A., Chen, X., Hou, T., & Cao, D. (2021). ADMETlab 2.0: An integrated online platform for accurate and comprehensive predictions of ADMET properties. *Nucleic Acids Research*, *49*(W1), W5–W14. https://doi.org/10.1093/nar/gkab255

APPENDIX

Supplementary Table 1

Composition of proteins within crude C. rhodostoma venom following trypsin-mediated digestion elucidated via LC-HRMS analysis

Protein Family	Protein	Accession Protein	Total Peptide Sequences	Molecular Weight (kDa)
LAAO	L-amino-acid oxidase OS=*Calloselasma rhodostoma*	P81382	31	58,2
	L-amino-acid oxidase OS=*Bungarus fasciatus*	A8QL52	3	58,7
PLA-2	Basic phospholipase A2 homolog W6D49 OS=*Calloselasma rhodostoma*	Q9PVF4	10	15,4
	Acidic phospholipase A2 S1E6-c OS=*Calloselasma rhodostoma*	Q9PVE9	7	15,8
	Phospholipase A2 OS=*Calloselasma rhodostoma*	A0A0H3U266	6	15,5
SVMP	Snake venom metalloproteinase kistomin OS=*Calloselasma rhodostoma*	P0CB14	18	47,4
	Zinc metalloproteinase/disintegrin OS=*Calloselasma rhodostoma*	P30403	11	54
Thrombin like Enzyme ancrod	Thrombin-like enzyme ancrod OS=*Calloselasma rhodostoma*	P26324	10	26,6
	Thrombin-like enzyme ancrod-2 OS=*Calloselasma rhodostoma*	P47797	4	29,1
Snaclec/ CTL	Snaclec rhodocetin subunit alpha OS=*Calloselasma rhodostoma*	P81397	12	16
	Snaclec rhodocetin subunit beta OS=*Calloselasma rhodostoma*	P81398	6	15,2
	Snaclec rhodocetin subunit delta OS=*Calloselasma rhodostoma*	D2YW40	5	14,8
	Snaclec rhodocetin subunit gamma (Fragment) OS=*Calloselasma rhodostoma*	D2YW39	5	15,7
	Snaclec rhodocytin subunit alpha OS=*Calloselasma rhodostoma*	Q9I841	5	15,8
	Snaclec rhodocytin subunit beta OS=*Calloselasma rhodostoma*	Q9I840	3	16,8

Supplementary Table 2
Peptide sequences identified in the crude venom of C. rhodostoma following trypsin digestion, analyzed via Liquid Chromatography-High Resolution Mass Spectrometry (LC-HRMS)

No	Master Protein	Sequence
1.	L-amino-acid oxidase	NEEAGWYANLGPMR
		RFDEIVDGMDKLPTAMYR
		KDIQSFCYPSVIQK
		VTVVYETLSK
		SAGQLYEESLGK
		RFDEIVDGMDK
		FDEIVDGMDKLPTAMYR
		ETPSVTADYVIVCTTSR
		EGDLSPGAVDMIGDLLNEDSGYYVSFIESLKHDDIFAYEK
		NPLAECFQENDYEEFLEIAR
		DCADIVFNDLSLIHQLPK
		HVVIVGAGMAGLSAAYVLAGAGHQVTVLEASERPGGR
		EGDLSPGAVDMIGDLLNEDSGYYVSFIESLK
		NEEAGWYANLGPMRLPEK
		DIQSFCYPSVIQK
		LNEFSQENDNAWYFIK
		HDDIFAYEK
		EGDLSPGAVDMIGDLLNEDSGYYVSFIESLK
		IFLTCTTK
		KDPGLLK
		YDTYSTK
		STTDLPSR
		FDEIVDGMDK
		FWEDDGIHGGK
		KVGEVK
		VHFNAQVIK
		DPGLLK
		VVEELK
		FNPPLLPK
		LPTAMYR
		LIKFNPPLLPK
2.	Snake venom metalloproteinase kistomin	VYLVIVADKSMVDK
		ETLYSFAK
		SSAKETLYSFAK
		WRVEDLSK
		IEEQGHQMVNTMNECYRPMGIIIIMAGIECWTTNDFFEVK
		DFDGNTVGLAFVGGICNEK
		DFDGNTVGLAFVGGICNEKYCAGVVQDHTK
		VPLLMAITMGHEIGHNLGMEHDEANCK

Supplementary Table 2 *(continue)*

No	Master Protein	Sequence
		ACVMAPEVNNNPTKK
		DRKPECLFK
		KPECLFK
		KPHNDAQFLTNK
		ACVMAPEVNNNPTK
		YCAGVVQDHTK
		SMVDKHNGNIK
		VEDLSK
		ACVMAPEVNNNPTK
		VYLVIVADK
3.	Zinc metalloproteinase/ disintegrin	AYLDSICDPER
		YIENQNPQCILNKPLR
		HVDIVVVVDSR
		HDGEYCTCYGSSECIMSSHISDPPSK
		SVGIVQNYHGITLNVAAIMAHEMGHNLGVR
		HSNDLEVIR
		ESDLIK
		LRPGAQCGEGLCCEQCK
		GDMPDDR
		CTGQSADCPR
		ECDCSSPENPCCDAATCK
4.	Snaclec rhodocetin subunit alpha	CFLMDHQSGLPK
		SWIGLK
		LEAVFVDMVMENNFENK
		SNLEWSDGSSISYENLYEPYMEK
		TWEEAER
		DCPDGWSSTK
		EAHLVSMENR
		FCTEQEKEAHLVSMENR
		WHTADCEEK
		CFLMDHQSGLPK
		NVFMCK
		FCTEQEK
5.	Thrombin-like enzyme ancrod	GPNPCAQPNKPALYTSIYDYR
		IDVLSDEPR
		DSCNSDSGGPLICNEELHGIVAR
		TSWDEDIMLIR
		FDDEQERYPK
		VIGGDECNINEHR
		FDDEQER

Supplementary Table 2 *(continue)*

No	Master Protein	Sequence
		RIDVLSDEPR
		SEKFDDEQERYPK
		VLCAGDLR
6.	Basic phospholipase A2 homolog	QQFNTGIFCSK
		GEILCGETNPCLNQACECDK
		FEKGEILCGETNPCLNQACECDK
		DNLDTYNKK
		DATDQCCADHDCCYK
		NYGMYGCNCGPMK
		MIMVMTGK
		KLTDCDPK
		ESYSYK
		DNLDTYNK
7.	Acidic phospholipase A2	TATYSYTEENDGIVCGGDDPCK
		TATYSYTEENDGIVCGGDDPCKK
		SGFFWYSFYGCYCGWGGHGLPQDPTDR
		RSGFFWYSFYGCYCGWGGHGLPQDPTDR
		CCFVHDCCYGK
		QVCECDR
		CQEDPEPC
8.	Phospholipase A2	FNTGIFCSK
		GEILCGETNPCLNQACECDK
		FEKGEILCGETNPCLNQACECDK
		NYGMYGCNCGPMK
		MIMVMTGK
		ESYSYK
9.	Snaclec rhodocytin subunit alpha	AQENGAHLASIESNGEADFVSWLISQK
		DELADEDYVWIGLR
		GLEDCDFGWSPYDQHCYQAFNEQK
		EQQCSSEWSDGSSVSYENLIDLHTK
		TWDEAEK
10.	Thrombin-like enzyme ancrod-2	LDSCHCDSGGPLICSEEFHGIVYR
		YIDVLPDEPR
		FDDEQER
		FDDEQERFPK
11.	Snaclec rhodocetin subunit beta	CFVVQPWEGK
		QAENGHLVSIGSAAEADFLDLVIVVNFDK
		NAFLCK
		CPTTWSASK
		TWIEAER
		AWTGLTER

Supplementary Table 2 *(continue)*

No	Master Protein	Sequence
12.	Snaclec rhodocetin subunit delta	TWEDAESFCYAQHK
		EEEAFVGK
		TVSFVCK
		RPYCAVMVVK
		WEWSDDAK
13.	Snaclec rhodocetin subunit gamma (Fragment)	GHLVSIGSDGEADFVAQLVTNNIK
		DFNCLPGWSAYDQHCYQAFNEPK
		TWDEAER
		WDYSDCQAK
		NPFVCK
14.	Snaclec rhodocytin subunit beta	DWQEQSECLAFR
		GVHTEWLNMDCSSTCSFVCK
		NWADAER
15.	L-amino-acid oxidase	YPVKPSEEGK
		YDTYSTK
		STTDLPSR

Supplementary Table 3
Characterization of proteins elicited from Anion Exchange Chromatography fractionation of C. rhodostoma venom via trypsin digestion and analyzed by LC-HRMS

Protein Family	Protein	Accession Protein	Total Peptide Sequences	Molecular Weight (kDa)
SVMP	Snake venom metalloproteinase kistomin	P0CB14	2	47,4
	Zinc metalloproteinase atau disintegrin	P30403	8	54
PLA-2	Basic phospholipase A2 homolog	Q9PVF4	2	15,4
Thrombin-like Enzyme Ancrod	Thrombin-like enzyme ancrod	P26324	10	26,6
	Thrombin-like enzyme ancrod-2	P47797	3	29,1
Snaclec atau CTL	Snaclec rhodocetin subunit alpha	P81397	6	16
	Snaclec rhodocetin subunit beta	P81398	6	15,2
	Snaclec rhodocetin subunit delta	D2YW40	3	14,8
	Snaclec rhodocytin subunit alpha	Q9I841	1	15,8
	Snaclec rhodocetin subunit gamma	D2YW39	1	15,7

Supplementary Table 4
Peptide sequences identified from the Anion Exchange Chromatography fraction of C. rhodostoma following trypsin digestion analyzed by LC-HRMS

No	Master Protein	Sequence
1	Zinc metalloproteinase/ disintegrin	LRPGAQCGEGLCCEQCK
		HDGEYCTCYGSSECIMSSHISDPPSK

Supplementary Table 4 *(continue)*

No	Master Protein	Sequence
		ECDCSSPENPCCDAATCK
		HVDIVVVVDSR
		HSNDLEVIR
		CTGQSADCPR
		YIENQNPQCILNKPLR
		AYLDSICDPER
2	Thrombin-like enzyme ancrod	DSCNSDSGGPLICNEELHGIVAR
		VIGGDECNINEHR
		RIDVLSDEPR
		TSWDEDIMLIR
		IDVLSDEPR
		MNLVFGMHR
		FDDEQERYPK
		FDDEQER
		VLCAGDLR
		VMGWGSINR
3	Snaclec rhodocetin subunit alpha	LEAVFVDMVMENNFENK
		CFLMDHQSGLPK
		EAHLVSMENR
		DCPDGWSSTK
		TWEEAER
		SWIGLK
4	Snaclec rhodocetin subunit beta	CFVVQPWEGK
		CPTTWSASK
		KCFVVQPWEGK
		TWIEAER
		AWTGLTER
		KTWIEAER
5	Snake venom metalloproteinase kistomin	IEEQGHQMVNTMNECYRPMGIIIIMAGIECWTTNDFFEVK
		DFDGNTVGLAFVGGICNEK
6	Basic phospholipase A2 homolog W6D49	GEILCGETNPCLNQACECDK
		QQFNTGIFCSK
7	Snaclec rhodocetin subunit delta	TWEDAESFCYAQHK
		WEWSDDAK
		LASQTLK
8	Thrombin-like enzyme ancrod-2	ILCAGDLQGR
		FDDEQER
		YIDVLPDEPR
9	Snaclec rhodocytin subunit alpha	DELADEDYVWIGLR
10	Snaclec rhodocetin subunit gamma (Fragment)	WDYSDCQAK

Pertanika J. Trop. Agric. Sci. 48 (6): 2119 - 2136 (2025)

PERTANIKA JOURNALS

TROPICAL AGRICULTURAL SCIENCE

Journal homepage: http://www.pertanika.upm.edu.my/

Effect of *Trichanthera gigantea* (Humb & Bonpl.) Nees Leaf Harvested at Different Stages of Maturity on Its Nutrient and Secondary Metabolites Compounds

Rohaida Abdul Rashid[1,3], Lokman Hakim Idris[1,2]*, Hasliza Abu Hassim[1,2], and Mohd Hezmee Mohd Noor[1]

[1]*Department of Veterinary Preclinical Sciences, Faculty of Veterinary Medicine, Universiti Putra Malaysia, 43400 Serdang, Selangor, Malaysia*
[2]*Institute of Tropical Agriculture and Food Security (ITAFoS), Universiti Putra Malaysia, 43400 Serdang, Selangor, Malaysia*
[3]*Faculty of Sustainable Agriculture, Universiti Malaysia Sabah, 90509 Sandakan, Sabah, Malaysia*

ABSTRACT

Trichanthera gigantea (*ketum ayam*) is a species of flowering plant in the acanthus family, Acathaceae. Younger *T. gigantea* leaf was reported to contain good protein content with positive effect on livestock. This study aimed to determine the harvesting effect of *T. gigantea* leaves at 2 different stages of maturity (young: less than 2 months old, mature: 3 to 4 months old) on the nutrient and secondary metabolites compounds. The significant differences were determined at $p<0.05$. Young leaves showed significantly 5.44% higher protein, 4.04% ash, 3.19% fibre contents and 2.7% lower fat and 0.57% energy compared to mature leaves. Phenol and saponin were detected in both young and mature leaves, with the younger leaves contained 0.011% higher percentage in phenol and 3.22% in saponin. However, there is no significant difference in Ca (4.62%, 4.91%) and (0.31%, 0.19%) for both stages of leaf maturity. In conclusion, the young leaves showed higher nutritional value, suggesting potential as a partial protein source in broiler diets. However, feeding trials are needed to confirm its suitability.

Keywords: Broiler, *ketum ayam*, protein, secondary metabolite, *Trichanthera gigantea*

ARTICLE INFO

Article history:
Received: 09 October 2025
Accepted: 11 November 2025
Published: 25 November 2025

DOI: https://doi.org/10.47836/pjtas.48.6.22

E-mail addresses:
GS59717@upm.student.upm.edu.my (Rohaida Abdul Rashid)
hakim_idris@upm.edu.my (Lokman Hakim Idris)
haslizaabu@upm.edu.my (Hasliza Abu Hassim)
hezmee@upm.edu.my (Mohd Hezmee Mohd Noor)
* Corresponding author

INTRODUCTION

Ketum ayam or its scientific name, *Trichanthera gigantea* (Humb & Bonpl.) Nees is a flowering shrub plant species belonging to the Acanthaceae family and is commonly known by the names; Madre de Agua (Latin America), Nacedero, Suiban, Cenicero, Tuno, Naranjilo, and Palo de

e-ISSN: 2231-8542

Agua. This plant is native to America and was introduced to Malaysia in 2012 by a local farmer. It grows wild and thrives in tropical regions such as the Philippines, Vietnam, Cambodia, including Malaysia, especially in most parts of Peninsular Malaysia. In fact, it is easy to be grown at high environmental temperatures, poor quality soil, and under minimal management (Tran, 2003), with a short harvesting period, as early as two months after planting. In Malaysia, it is locally known as *ketum ayam* because of its physical appearance which looks like *ketum* or kratom or *biak* (*Mitragyna speciosa*) leaf which belongs to the Rubiaceae family and is mostly used as chicken feed. *Kratom* leaf is listed under the Malaysian Poison Act of 1952 because it contains the psychoactive prohibited compounds mitragynine which has a stimulating, sedative, and euphoric effect that can cause addiction. To date, there has been no discovery of that prohibited compound in the leaf of *ketum ayam*.

The consumption of meat in Malaysia in 2019 was reported to be above the average values stated by the Organization for Economic Cooperation and Development (OECD) for that particular year. The poultry meat per capita consumption in Malaysia was 49.3 kg in the year 2020 and increased to 49.7kg by 2021. Malaysia was listed amongst the top global consumers of poultry meat worldwide, and the intake is expected to increase to 51.28 kilograms per capita in 2025 (Hirschmann, 2022).

The increase in the import price of animal feed ingredients such as corns and soybeans in the international market can inadvertently cause an increase in the price of chicken. In 2016, Malaysia spent RM5.6 billion to import corns and soybeans for their use in livestocks such as poultry, goats, and cattle to meet its protein and energy sources, with RM2.2 billion alone is for soybeans. In the year 2020, the price of soybeans increased almost 1.5 times within 1.5 years which is RM 1480/metric ton in June 2020 to RM 2210/metric ton in January 2022 (New Straits Times, 2022). Various efforts were made by the Government to reduce the dependency on imported ingredients, finding sources by looking into other potential locally available and cheaper sources such as cassava meal, palm kernel cake, and so on.

One of the most important aspects is that the leaves can be considered safe to be used in animal feed. It can be offered directly (fresh) or in dried form. Having an acceptable proximal composition as well as the content of secondary metabolites and the presence of low concentrations of anti-nutrients make it possible for this leaf to be used in livestock production systems in tropical areas (Garcia et al., 2006). However, the nutritive value of *T.* gigantea leaf may vary depending on the ages of leaves (Tran, 2003) and cutting intervals (Kien et al., 2020). *T. gigantea* are usually harvested at the age of 3 to 4 months. Tran (2003) noted that the livestock should have better performance traits when they are fed younger leaves rather than the older leaves. For example, the young leaves contained higher crude protein than the old leaves. A 50 to 60-day cutting interval of the *T. gigantea* tree was recommended by Kien et al. (2020).

Thus, this study aimed to investigate the effect of *T. gigantea* (ketum ayam) leaf harvested at two different stages of maturity (young, mature) on its nutrient and secondary metabolite contents.

MATERIALS AND METHODS

Collection and Sample Preparation

About 2 kilograms of each group of leaves were collected randomly in the morning at a local farm located in Bentong, Pahang, Malaysia. The young leaves were taken from the top, whereas the matured leaves were taken from the bottom of the *T. gigantea* trees. The part of the leaves harvested only includes the leaf (from the basal leaf to the tip) and the stipule. The leaf was plucked manually using plant-cutting scissors, weighed immediately, and sealed in plastic bags. The leaf samples were then transferred to the Nutrition Laboratory, Faculty of Veterinary Medicine, Universiti Putra Malaysia for chemical analysis. The identification and authentication were done by the Biodiversity Unit, Institute of Bioscience, Universiti Putra Malaysia with voucher no. MFI 0236/21.

Chemical Analysis

Upon arrival at the laboratory, all leaves were washed quickly under running tap water to remove any bruised, soiled, or imperfect leaves before the drying process. The leaves were dried in an oven at a temperature of 50±1°C until a constant weight was obtained. Later, the leaves were ground using a laboratory grinder to obtain a fine meal measuring approximately 2 mm in diameter. These leaves were then placed in a separate airtight bottle and stored in a cool and dry place for further analysis.

Proximate Analysis, Van Soest and Gross Energy

The proximate analysis including dry matter (DM), ash, organic matter (OM), crude fibre (CF), crude protein (CP), ether extract (EE), nitrogen free extract (NFE), acid detergent fibre (ADF), acid detergent lignin (ADL), neutral detergent fibre (NDF), and also gross energy were conducted according to the methods of Association of Official Analytical Collaboration (AOAC), 1984.

Determination of M, DM, Ash and OM

About 1 g of each sample was weighed and placed in a pre-weighed crucible. Then, these crucibles containing the samples were dried in an oven at 105°C for 24 hours, cooled in a desiccator for 30 minutes, and was weighed. Next, the crucibles containing the dried sample were burned in a muffle furnace at 550°C for 3 hours, cooled in a desiccator and then weighed. The M, DM, ash and OM contents were determined based on calculation as stated in the method.

Determination of Crude Protein (CP)

Approximately 1 g of each sample was placed in a digestion tube. The digestion tube was then added with a Kjeldahl tablet, followed by 12 mL of concentrated sulfuric acid (H_2SO_4) and 3 mL of 30% hydrogen peroxide (H_2O_2). The samples were digested, distilled and titrated using the AOAC (1984) methods. The protein percentage was calculated by the stated formula in this method.

Determination of Crude Fibre (CF)

Briefly, 1 g of each dried sample was weighed and loaded in a fiber bag (Gerhardt®) and inserted with a glass spacer. Then, each fibre bag was loaded onto the carousel and inserted into a 600 mL beaker. Three hundred sixty (360) mL 0.13 mol/L sulfuric acid (H_2SO_4) was poured into the beaker and mixed it by rotating the carousel for about 1 min. Next, the beaker was placed on the hot plate that had been preheated for about 5 minutes. The hotplate was set up to full before boiling (about 3-5 min) before reducing it to obtain a gentle simmer for about 30 minutes. The beaker was removed from the hotplate, and the carousel was taken out. The solution and soluble within the beaker were discarded, and the carousel was rinsed with hot water several times. The previous steps were repeated with 360 mL 0.313 mol/L natrium hydroxide (NaOH). After boiling with NaOH, the fibrebags were rinsed with hot water and dried with fibre-free tissue before putting into pre-ashed crucible and dried in an oven at a temperature of 105°C for 4 hrs. Next, the crucible contained fibrebags were taken out from the oven, cooled in desiccator, weighed, incinerated at 600°C for 4 hours, cooled at 105°C for 30 min in an oven, and finally cooled in desiccator before weighing. The calculation for crude fibre determination followed the formula described by Gerhardt®.

Determination of Ether Extract (EE)

The ether extract determination was conducted using a manual system, Soxhlet apparatus Gerhardt®. Approximately 1 g of each sample was weighed into an extraction thimble (33x80mm)‑and then inserted into the Soxhlet chamber. A 250 mL pre-weighed round bottom flask was loaded with 200 mL of petroleum ether boiling range of 40-60°C before being fitted into the Soxhlet apparatus. The extraction process was conducted for about 6 hours before removing the round bottom flask containing the ether extract residue. Next, the round bottom flask was dried in an oven at 105°C overnight, cooled in a desiccator and weighed. The ether extract content was calculated using the difference between the weight of the sample and the residue, as stated in the methods.

Nitrogen free extract of each sample was calculated using the stated formula.

NFE (%) = 100 - % CP - % EE - % CF - % Ash

Determination of Neutral Detergent Fibre (NDF)

About 1 g of each sample was weighed and placed in a pre-weighed Gerhardt® fibrebags inserted with a glass spacer. Next, the fibrebag containing the sample was attached to the carousel prior to boiling with the NDF solution. After a gentle simmer for about an hour, the solution was discarded, and the fibrebag was rinsed with hot water before wiping it with fibre-free tissue. Later, the fibrebag was put into a pre-weighed crucible and dried in an oven at 105°C for 4 hours prior to ash in a muffle furnace at 600°C for 4 hours. To cool the sample after ashing, the sample was placed in an oven at 105°C for 30 min, followed by cooling in desiccator for 30 min. The NDF was calculated by a formula.

Determination of Acid Detergent Fibre (ADF)

One gram of each sample was weighed and loaded in a pre-weighed Gerhardt® fibrebag that was already inserted with glass spacer. The fibrebag then was loaded into carousel in a beaker prior to boiling with ADF solution in a hotplate. The fibrebags were drained to free from detergent after one hour boiling, rinsed with hot water, wipped with fibre-free tissue and placed into a pre-weighed crucible before drying in an oven at 105° for 4 hours. After 4 hours, the fibrebag was allowed to cool in an oven at 105°C for 30 min before cooling in desiccator for 30 minutes, then weighed before incinerating in a muffle furnace at 600°C for 4 hrs. Next, the fibrebag was taken out from the muffle furnace and allowed to cool in an oven at 105°C for 30 minutes followed by cooling in desiccator about 30 min. The calculation for determining the percentage of ADF was calculated by a formula.

Determination of Acid Detergent Lignin (ADL)

To determine the ADL content, some steps used in ADF are required before soaking the sample with 72% H_2SO_4 solution. Briefly, approximately 1 g of each sample was weighed and loaded into a pre-weighed Gerhardt® fibrebags containing a glass spacer. Then, the fibrebag was inserted into the carousel in a beaker prior to an hour of gentle simmering with ADF solution. Next, the fibrebags was free from the detergent solution by rinsing with hot water. The rinsed fibrebag was later inserted again into the carousel in a beaker. A 360 mL of ADL solution was poured slowly into the beaker containing the sample, and mixed by rotating the carousel carefully for about 1 min. The fibrebag was allowed to soak in the solution for 3 hours before rinsing it with hot water. After being free from detergent, the fibrebag was wiped with fibre-free tissue and loaded in a pre-ashed crucible. Then, it was placed in an oven at 105°C for 4 hours to dry the fibre bag, cooled in a desiccator for 30 minutes, and weighed. To ash the sample, the fibrebag was incinerated in a muffle furnace at 600° for 4 hours. The fibrebag was allowed to cool in the furnace overnight before

transferring it in an oven at 105°C for 30 minutes and further cooled in a desiccator for about 30 minutes. The cooled pre-ashed sample was weighed and recorded. The calculation for ADL was determined using a formula.

Gross Energy

The gross energy in the samples was determined using an automated bomb calorimeter IKA® C5000 that had been calibrated with benzoic acid prior to analysis.

Minerals

Calcium and phosphorus were determined using the In-house Method, SGS-SOP-LAB-028, based on AOAC 986.15, 975.03, and 922.02, APHA 3120B and APHA 3125B (ICP-OES).

Qualitative Analysis of Secondary Metabolites

The presence of secondary metabolite compounds such as phenols, saponins, tannins, flavonoids, cardiac glycosides, anthocyanides and terpenoids was conducted according to the methods as reported by Raipuria et al. (2018), steroids (Aliyu et al., 2017), alkaloids and antraquinones (Abdullahi et al., 2020); Perveen and Zaid, 2013), Phlobatannins (Ezeonu and Ejikeme, 2016) and oxalates (Kgosana, 2019).

Extraction of Leaves Meal

Approximately 100 mg of each dried sample was kept overnight in 25 ml of ethanol. The extracts were filtered using Whatman filter paper no. 1 and used for phytochemical screening as follows:

Phenol

Two ml of the above filtrate was taken into a 15 ml glass test tube and 1 ml of 1% Ferric Chloride ($FeCI_3$) was added to it. Brown haziness indicated the presence of phenols.

Saponins

One ml of the filtrate was mixed with 5 ml of H_2O, and then shaken vigorously using IKA vortex mixer. The persistence of frothing showed the presence of saponins.

Tannins

Two ml of the filtrate was taken into a 15 ml glass test tube followed by 2 ml of 0.1% $FeCI_3$. Brownish color indicated the presence of tannins.

Flavanoids

The test for flavonoid adopted is as stated by Ezeonu and Ejikeme (2016). Briefly, 300 mg of each sample was mixed with 30 ml of H_2O for 2 hours. The solutions were filtered with Whatman filter paper no. 42 (90 mm). Each 5 ml of extract was added with 2.5 ml of 1.0M ammonia (NH_3) solution followed by 2.5 ml of concentrated H_2SO_4. Yellow color indicated the presence of flavonoid.

Cardiac Glycosides

One mL glacial acetic acid was added into each 2 ml filtrate followed by addition of 1 ml glacial acetic acid (CH_3COOH), 1 ml of 1% $FeCI_3$ and 1 ml concentrated H_2SO_4. The presence of cardiac glycosides was indicated by a brown ring.

Anthocyanides

Five ml of 10-12% hydrochloric acid (HCI) was added to 1 ml of each above filtrate. The presence of pale pink color, indicating the presence of anthocyanides.

Terpenoids

Five mL of each extract was added by 2 ml of chloroform ($CHCI_3$) followed by 3 mL of concentrated H_2SO_4. The terpenoids were shown by the presence of a reddish-brown coloration at interface formed.

Steroids

Three mL of $CHCI_3$ was added into 0.5 mL of each extract followed by 3 ml of concentrated H_2SO_4. With green fluorescence, the presence of steroids was indicated when the upper layer turned red whereas the H_2SO_4 layer turned yellow.

Alkaloids

Two grams of dried *T. gigantea* leaves was extracted by boiling it for 2 minutes in a solution contained 20 ml 5% H_2SO_4 in 50% ethanol. The sample was filtered using Whatman Filter paper no. 42, and the filtrate was made alkaline using 5 ml of 28% NH_3 in a separating funnel. The filtrate then was extracted again with 5 ml chloroform and 5 ml of 1M H_2SO_4. The final filtrate (2 ml) was added with 1 ml of Mayer's reagent and shaken. No emergence of whitish precipitate confirmed the presence of alkaloids (Ezeonu and Ejikeme, 2016; Abdullahi et al., 2020).

Quantitative Analysis of Secondary Metabolites

The total phenol was determined according to the methods used by Singleton and Rossi (1965) and Sreeramulu and Raghunath (2011) while saponins (Nwosu et al., 2010) with slight modification.

Total Phenols

The phenol content was determined based on the methods used by Singleton and Rossi (1965) and Sreeramulu and Raghunath (2011). One g of the sample was placed in a 50 mL centrifuge tube, followed by 20 mL of 70% methanol (MeOH) containing 0.1% hydrochloric acid (HCI) for sample extraction. The tube was shaken vigorously for 4 hours at room temperature using an IKA® vortex mixer. The sample suspension was centrifuged at 10000 g for 15 minutes at 10°C. The supernatant was collected using a Pasteur pipette and then filtered it with a Whatman filter paper no. 1. The resultant filtrate was kept at -20°C for phenol determination. Gallic acid was used as a standard and it was prepared in a 100 mL volumetric flask by dissolving 500 mg of dry gallic acid (Merck®) in 10 mL of 99.9% MeOH and was topped up to the volume with distilled water (H_2O). A gallic acid calibration curve was prepared by adding 0, 5, 10, 15, 20, and 25 mL of the above phenol stock solution into 100 mL volumetric flasks, and then diluting to the mark with H_2O (Figure 1). The resulting solutions will have phenol concentrations of 0, 0.25, 0.50, 0.75, 1.0 and 1.25 mg/mL. To prepare 20% sodium carbonate (Na_2CO_3) solution, 100 g of anhydrous Na_2CO_3 was dissolved in 400 mL H_2O by heating it to boiling. After cooling, a few crystals of Na_2CO_3 were added into the solution. Twenty-four hours later, it was filtered into a 500 mL volumetric flask using a Whatman filter paper no. 1. The filtrate was made up to the mark with H_2O. Next, 20 µL of each calibration solution, sample and blank were pipette into separate cuvettes, followed by 1.58 mL H_2O and 100 µL Folin-Ciocalteu

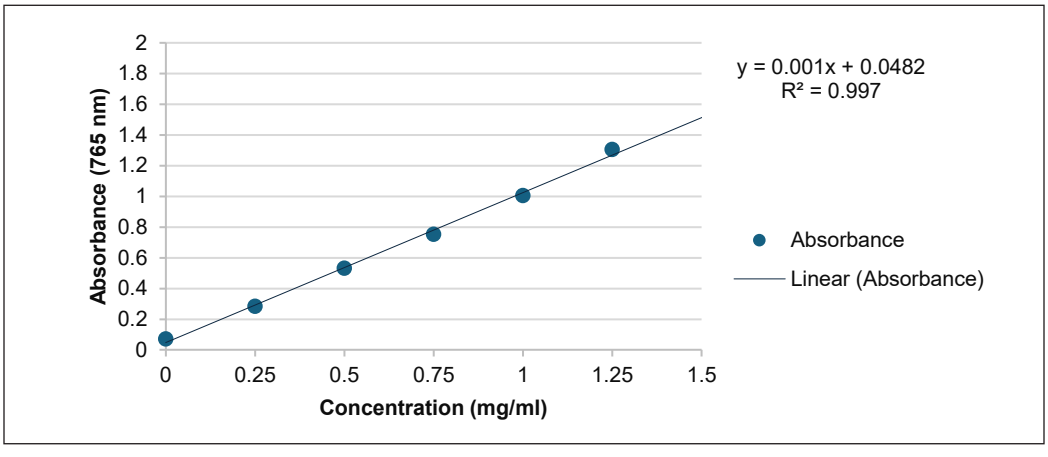

Figure 1. Standard calibration curve of gallic acid for the quantitation of phenols

reagent (Merck®). The solutions in the cuvettes were mixed well. After 4 minutes, 300 µL of the Na_2CO_3 was added to each cuvette and shaken vigorously. The solution in the cuvettes was incubated at 40°C for 30 minutes before reading the absorbance at 765 nm against the blank (the '0 mL' solution) using the TECAN Multimode Microplate Reader Infinite M200 PRO instrument. The phenol concentration of the T. *gigantea* dried leaves meal was determined from the graph plotted absorbance versus concentration of gallic acid. Gallic acid was used in the phenol determination because it is the most used standard, more stable, provide consistent and reproducible results, a pharmacologically active antioxidant, and quantitatively equivalent to other phenolics (Claudine et al., 2005).

Total Saponins

The saponin content in the samples were analyzed based on the methods stated by Nwosu et al. (2010). Briefly, 1 g of the fried sample was weighed and placed into a cellulose thimble and covered with cotton wool. The thimble bearing the sample was inserted into Soxhlet extractor chamber before pouring 200 mL of petroleum benzine (boiling point 40-60°C into a pre-weighed 250 mL round bottom flask. The extraction was conducted for around 3 hours and the defatted material in the thimble was used for second extraction. The extraction was repeated using the same procedure with a new pre-weighed round bottom flask containing 150 mL 99.9% MeOH. Later, the flask was removed from the apparatus when the saponin content was almost dried. The flask was then dried in an oven at 70±1°C for 2 hours, cooled in a desiccator, and weighed. The calculation of saponin was as follows:

Saponin (%) = (Mass of saponin (g) / Mass of sample) x 100

Statistical Analysis

All data were analyzed using T-test in R to compare the means between two groups. The statistical significance was determined at $p<0.05$.

RESULTS AND DISCUSSION

Table 1 below shows the proximate analysis and gross energy content in young and matured dried *T. gigantea* leaves meal. The dry matter, organic matter, crude fat, nitrogen free extract, neutral detergent fibre and gross energy content of the leaves increased with age whereas the remaining components were vice versa. Tran (2003) indicated that the dry matter and nitrogen content of *dried T. gigantea* leaves meal in Vietnam were higher in younger than older leaves. In that experiment, the DM content of young and old leaves were 17.1% and 18.5% respectively, while the N content were 4.32% and 2.48%. In this current experiment, the dry matter of young and mature leaves was 12.15% and 17.72% (Table 1).

Table 1
Proximate analysis of Trichanthera gigantea *meal at different stages of leaves*

No.	Components	Stages of Maturity		SEM	*P* value
	Proximate analysis	**Young Leaves**	**Mature Leaves**		
1	[x]Moisture (%)	87.85[a]	82.28[b]	0.45	<0.001
2	[x]Dry matter$_{fw}$ (%)	12.15[b]	17.72[a]	0.45	<0.001
3	Moisture (%)	6.32	6.20	0.42	0.791
4	Dry matter (%)	93.68	93.80	0.42	0.791
3	Ash (%)	24.34[a]	20.30[b]	0.26	<0.001
4	Organic matter (%)	82.40[b]	86.31[a]	0.29	<0.001
5	Crude Protein (%)	21.24[a]	15.80[b]	0.58	<0.001
6	Crude Fat (%)	1.35[b]	4.05[a]	0.03	<0.001
7	Crude Fibre (%)	17.64[a]	14.45[b]	0.44	<0.001
8	Nitrogen free extract (%)	42.38[b]	51.30[a]	0.90	0.001
9	Neutral detergent fibre (%)	44.82[b]	59.72[a]	0.41	<0.001
10	Acid detergent fibre (%)	46.63[a]	39.55[b]	0.36	0.002
11	Acid detergent lignin (%)	19.53[a]	18.95[b]	0.12	0.040
12	Gross energy (MJ/kg)	15.57[b]	16.14[a]	0.06	<0.001

Note. Mean within the same rows with different superscript letters indicate statistical significance (p<0.05). Based on dry matter, SEM: Standard error of mean, *P*: Probability, [x]: fresh weight

Previous findings noted that the minimum and maximum values of *T. gigantea* leaves ranges were as follows; Berdos et al. (2019) stated that on dry matter basis, the leaves presented 93.3% DM, 19.59 % CP, 11.89% CF, 2.33 % EE, 20.15% ash, 39.34% NFE, 3665 kcal/kg gross GE and 2310 kcal/kg ME while Balraj et al. (2018) reported that based on dry matter, the OM, CP, CF, EE, NDF and ADF of dried *T. gigantea* leaf were 80.3%, 18.1%, 18.4%, 2.97%, 28.8% and 21.4% respectively. Heuze et al. (2016) showed DM, 13 to 26.3%, CP, 12 to 21.7%, CF, 13 to 25.1%, NDF, 28.2 to 65.5%, ADF, 24.5 to 56.3%, ADL, 2.7 to 9.5%, EE, 1.5 to 5.8%, Ash, 9.3 to 32.3% and gross energy, 15.2 to 18.4 MJ/kg. When expressed on fed basis, proximate analysis showed that the leaves contained 15.80% CP, 15.42% CF, 1.15% EE, 18.07% ash and 35.86 NFE (Saguidan, 2015). The *T. gigantea* leaves dried in an oven at 60°C for 72 hours contained 94.1% residual DM, 72% OM, 20.3% CP and 49.9% NDF (Rodriquez et al., 2014). Edwards et al. (2012) demonstrated that the cutting interval from 6 to 12 weeks had no effect on the content of OM, ADF, NDF, ADL, soluble condensed tannins (SCT) and insoluble condensed tannins (ICT) of *T. gigantea* leaves at three different locations except on DM, CP and acid detergent insoluble nitrogen (ADIN). The minimum and maximum chemical composition values for the locations were DM, 85.6 to 87.7%, OM, 72.2 to 74.9%, CP, 18.5 to 22.6%, ADIN, 28 to 38%, ADF, 30 to 53.8%, NDF, 62.2 to 65.5%, ADL, 24 to 28%, SCT, 0 to 0.01% and ICT, 0 to 0.01%. The fresh leaves contained 13.7% dry matter, 15.1% ash, 21.6% crude protein, 4.3% crude fat,

and 39% crude fibre (Leterme et al., 2005) while the dried ones were reported to contain 78.9% dry matter, 23.9% crude protein, 23.8 crude fibre, 2.5% crude fat, 24.3% ash, and 25.5% nitrogen free extract (Sarwatt et al., 2003). It also contained macro elements and microelements of minerals mainly calcium. Ly et al. (2001) found that fresh *T. gigantea* leaf contained 26.30% dry matter while on a dry matter basis, the content of ash, organic matter, NDF and N were 14.6%, 85.4%, 30.8% and 2.72% respectively.

The plant varieties, season of the year (dry or raining season), irrigation, plantation, fertilizer application and harvesting techniques, etc. could contribute to varying in results obtained. The harvesting techniques can influence the production and quality of green fodders. For example, the long cutting interval will increase the proportion of mature leaves, leading to increasing fibre contents in leaves and decreasing of crude protein in leaves, hence declines the quality of feed (Kien et al., 2010; Nouman, 2012; Hien et al., 2013; Hien et al., 2019; Kien et al., 2020). Its special characteristic is that it contains high amounts of crude protein (about 23%) which consists of 17 amino acid components including 10 essential and 7 non-essential amino acids which are required by poultry. Some researchers also reported that the leaves can be incorporated up to 25% in broiler diet. For instance, in 2015, it has widely used in Venezuela, Peru, Equador and Philippines livestock feed, such as in pig, rabbit and poultry as a replacement for the conventional protein sources in the diet.

Bageel and Borthakur (2022) reported that the contents of moisture and CP of giant Leucaena fodder were decreased with maturity while DM and NDF increased as the leaves gets older. Hut et al. (2012) also noted that the nutritional content of cassava leaves was affected by the age of leaves except for ash. DM, NDF and ADF increased with the maturity of the leaves while CP was vice versa. Crude protein reduced significantly ($p<0.05$) with the maturity age of the *Celosia argentea* L. plant leaves (Adediran et al., 2015). This decline can contribute to the accumulation of cell wall material as leaves mature (Edwards et al., 2012). The uppermost eleven leaves of cassava tress were considered very young, young and mature leaves (Ravindran and Ravindran, 1988). Leaves that are one month old were considered young leaves while mature leaves are 3 to 4 months old (Leterme et al., 2005).

No significant ($p>0.05$) difference was seen in Ca and P of young and matured *T. gigantea* leaves as presented in Table 2. The minimum and maximum of Ca and P values of this plant's leaves were 2.45 to 3.80% and 0.25 to 0.47% respectively (Hueze et al., 2016). Berdos et al. (2019) stated that on dry matter basis, the leaves presented 4.47% calcium and 0.25% total P while Saguidan (2015) found it contained 4.7% Ca and 0.32% available P.

In general, the differences in plant nutrient contents may be due to the age, parts, and the development stage of the plant itself. Phosphorus (P) is higher at the beginning and decreases with age while calcium (Ca) is on the opposite. P is a mobile element, and the deficiencies occur in older tissues, whereas Ca is an immobile element, and the deficiencies occur in newer tissues. The Ca and P contents in plants typically range from 0.005 to 5%

Table 2
Macrominerals content of dried Trichanthera gigantea *leaves meal*

No.	Components (%)	Stages of Maturity		SEM	*P* value
		Young Leaves	Mature Leaves		
1	Calcium, Ca	4.62	4.92	0.166	0.411
2	Phosphorus, P	0.31	0.19	0.028	>0.05

Note. Mean within the same rows with different superscript letters indicate statistical significance ($p<0.05$). Based on dry matter, SEM: Standard error of mean, *P*: Probability

and 0.05 to 0.5% of dry weight respectively. However, a similar pattern was observed in *Moringa oleifera* leaves which there was no difference in P content between young and old leaves of Moringa (Andi et al., 2018).

The presence of phenol (450 ppm), saponin and steroid (0.62%) were detected by Leterme et al. (2005). Garcia et al. (2006) revealed that *T. gigantea* leaf contained alkaloids, bitter compounds (B. compounds), condensed tannins, coumarins, cyanogen, flavonoids, phenols, precipitants of proteins, saponins, slimes, steroids, tannins and terpens. Riascos Vallejos et al. (2020) reported that the leaf contains total alkaloids (0.3%), condensed tannnis (0.24%) and phenols (1.15%). Eighteen chemical compounds in *T. gigantea* have been identified by Quan et al. (2022) in their phytochemical screening study consisting of amino acids, betalains, carbohydrates, organic acids, coumarins, flavonoids, carotenoids, mucilages, gum-resins, phlobatannin, xanthoprotein, phenol and essential oil.

However, in this study (Table 3), only phenol and saponin were detected in both cutting intervals of *T. gigantea* leaves meal while the remaining component was unavailable. Edwards et al. (2012) and Hueze et al. (2016) also noted that no tannin was detected in T. *gigantea* leaves. The presence of secondary metabolites compound in those leaves may be vary due to many factors such as temperature, humidity, light intensity, the supply of water, soil fertility, minerals and CO_2 (Akula and Gokare, 2011; Li Yang et al., 2018). For example, deficiencies in potassium, sulfur and magnesium increases phenolic concentration. Genetic, environmental conditions and physiological factors may modify or influence the composition of the secondary metabolites in plants (Hongyan et al., 2012).

In this current study, it was also noted that phenol and saponin compounds in younger leaves were higher than in older leaves which are 0.023% and 0.012 and 9.67% and 6.45% respectively (Table 4). In a study of cassava leaves by Ravindran and Ravindran (1987) found that the levels of some anti-nutritive compounds like tannin and hydrocyanic acid were decreased as the maturity of those leaves increased. The saponin and steroid (0.62%) were low (Leterme et al. 2005) while phenol was 450 ppm. Riascos Vallejos et al. (2020) reported that the leaf contained total alkaloids (0.3%), condensed tannnis (0.24%) and phenols (1.15%). The tannin concentration of giant Leucaena fodder also reduced with maturity (Bageel and Borthakur, 2022). Similar trend was observed for HCN content in

Table 3
Qualitative determination of secondary metabolites in Trichanthera gigantea *leaves meal at different cutting intervals*

No.	Constituents	Test	Stages of Maturity	
			Young Leaves	Mature Leaves
1	Phenols		+	+
2	Saponins	Foam Test	+	+
3	Steroids	Lieberman Burchard's Test	-	-
4	Alkaloids	Mayer's Test	-	-
5	Tannins	Ferric Chloride Test	-	-
6	Flavanoids	Shinoda's Test	-	-
7	Anthraquinones	Bontrager Test	-	-
8	Cardiac Glycosides	Keller Killiani's Test	-	-
9	Oxalates	Oxalates Test	-	-
10	Anthocyanides		-	-
11	Terpenoids	Salkowski Test	-	-
12	Phlobatannins		-	-

Note. + Detected, - Not detected

Table 4
Quantitative determination of secondary metabolites in Trichanthera gigantea *meal at different cutting intervals*

No.	Components	Stages of Maturity		SEM	*P* value
		Young Leaves	Mature Leaves		
1	Total phenols (%)	0.023^{a}	0.012^{b}	0.002	0.012
2	Total saponins (%)	9.67^{a}	6.45^{b}	0.264	0.005

Note. Mean within the same rows with different superscript letters indicate statistical significance ($p<0.05$). Based on dry matter, SEM: Standard error of mean, *P*: Probability

the local variety of cassava which also declined with foliage maturity, but tannin was vice versa (Hue et al., 2012).

Generally, the colour, rigidity and location of the leaves are factors that influence the selection of leaves based on age. The leaves at the top of a tree or shrub are young leaves while the old leaves are at the bottom (Tran, 2003). According to Bageel and Borthakur (2022), young leaves are light green, while mature and old leaves are green and dark green respectively. The position of young leaves is in the middle of the tip of the twig, while mature and old leaves are at the middle of the branch and at the base of the stem, respectively. Young leaves are hairy, smaller, and softer than mature and young leaves.

CONCLUSION

The results indicate that leaf maturity significantly influences nutrient composition and metabolite content, with younger leaves showing higher protein and saponin levels.

ACKNOWLEDGEMENT

The research was fully funded by the *Inisiatif Putra Siswazah* (IPS) Putra Grant (No. 9718400) from Universiti Putra Malaysia. The authors would like to express their gratitude to Mr. Badrul Hisyam bin Hanafiah for providing the research material, *T. gigantea* leaves.

REFERENCES

Abbood, A. A., Azhar, K., Jawab, H. S. A., Abdul Manap, Y., and Sazili, A. Q. (2017). Effects of feeding the herb Borreria latifolia on the meat quality of village chickens in Malaysia. *Poultry Science*. 96 (6), 1767-1782.

Abdullahi, R. A., Ibrahim, H. S., Sani, M. and Abdullahi, H. Y. (2020). Quantititave determination of secondary metabolites of fractions obtained from *Solanum aethiopicum* (L.) fruit. *Dutse Jurnal of Pure and Applied Science* (DUJOPAS). 6(3).

Akula, R. and Gokare, A. R. (2011). Influence of abiotic stress signals on secondary metabolites in plants. *Plant Signalling and Behavior*. 6(11), 1720-1731.

Aliyu, M. Y., Ismail, S. and Mansur, A. I. (2017). Phytochemical analysis and determination of antioxidant activity in methanol and chloroform etxracts of Moringa oleifera leaves.

Andi, S., Muh, H. and Adriyani, A. 2018. Nutrient contents of Moringa leaves based on leaf age. *Indian Journal of Public Health Research and Development*. 9(1), 397. DOI:10.5958/0976-5506.2018.00073.6

AOAC (1984) Official Methods of Analysis. Association of Official Analytical Chemists. 14th Edition, AOAC, Arlington.

Awad, W. A., Bohm, J., Razzazi-Fazeli, E., and Zentek, J. (2006). Effects of feeding dexynivalenol contamined wheat on growth performance, organ weights and histological parameters of the intestine of broiler chickens. Journal of Animal Physiology and Animal Nutrition. 90 (1-2), 32-37.

Bageel, A. M. and Borthakur, D. (2022). The effects of pH, salinity, age of leaves, post-harvest storage duration, and psyllid infestation on nutritional qualities of giant Leucaena fodder. *Journal of Crop Science and Biotechnology*. 25, 381-392. https://doi. Org/10.1007/s12892-021-00139-9

Balraj, D., Krisnamoorty, U., Nayak, S. and Paul, A. (2018). Effect of partial replacement of commercial sheep ration with Trichanthera gigantea (Nacedero) leaves on feed intake and carcass yield of Barbados blackvalley lambs. *Indian Journal of Small Ruminants*. 24(2), 264-268. DOI: 10.5958/0973-9718.2018.00062.4.

Banerjee, G. C. (1998). Poultry. 3rd edition. Bombay: Oxford and IBH Publishing Co. Pvt. Ldt. p. 104.

Bansal, G. R., Singh vp. And Sachan, N. (2011). Carcass quality characteristics of broilers as affected by dried poultry excreta supplementation. *Asian Journal of Poultry Science*. 5(3):116-123. doi: 10.3923/ajpsaj.2011.116.123.

Basit, M. A., Arifah, A. K., Loh, T. C., Saleha, A. A., Annas, S., Kaka, A. and Banke, I. S. (2020). Effects of graded dose dietary supplementation of Piper bettle leaf meal and Persicaria odorata leaf meal on growth performance, apparent ileal digestibility, and gut morphology in broilers. *Saudi Journal of Biological Sciences*. 27(6). Doi: 10.1016/j.sjbs.2020.04.017.

Berdos, J. I., Martin, E. A., Celestino, O. F. and Paragas, E. J. S. 2019. Egg production performance of improved Philippine Mallard ducks (Anas platyrhynchos) fed diets supplemented with fresh Trichanthera (*Trichanthera gigantea*) leaves. *Philippines Journal of Veterinary Animal Science*. 45(1), 48-57.

Bryan, D. D. S. L. and Classen, H. L. (2020). In vitro methods of assessing protein quality for poultry.

Edwards, A., Mlambo, V., Lallo, C. H. O. and Garcia, G. W. (2012). Yield, chemical composition and In Vitro Ruminal Fermentation of the Leaves of *Leucaena Leucocephala*, *Gliricidia Sepium* and *Trichanthera Gigantea* as influenced by harvesting frequency. Journal of Animal Science Adv. 2(3.2), 321-331. ISSN: 2251-7219.

Elbayoumi, Z. H., Shawish R. R., Hamada, M., and Esmail, H. R. (2018). Molecular characterization of Escherichia coli isolated from poultry meat and its products. *Alexandria Journal of Veterinary Science*, 56(2), 39-47.

Ezeonu, C. S. and Ejikeme, C. M. 2016. Qualitative and quantitative determination of phytochemicals contents of indigenous Nigerian softwoods. *New Journal of Science*. http://dx.doi.org/10.1155/2016/5601327

Francisco, F. Buctot, Jr. (2018). Growth response and carcass evaluation of broilers fed with varying levels of *Trichanthera gigantea* leaf. *Journal of Science Technology*, 4, 17-22.

Garcia, D. E., Medina, M. G., Dominquez, C., Baldizan, A. and Luis Cova, J. H. y. (2006). Chemical evaluation of non-leguminous species with fodder potential in Trujillo state, Venezuela. Zootecnia Tropical. Instituto Nacional De Investigaciones Aricolas Venezuela. [online]. 24(4), 401-415. ISSN 0798-7269.

Gehrt, A. J., Caldwell, M. J. and Elmslie, W. P. (1955). Feed digestibility, chemical method for measuring relative digestibility of animal protein feedstuffs. *Journal of Agric. Food Chemistry*. 3, 159-162.

Hien, T. Q., Hoan, T. T., Khoa mai Anh, Kien, T. T., huong, P. T., Nhung, H. T. H. (2017). Nutrient digestibility determination of cassava, Leucaena, Stylosanthes, Moringa and Trichantera gigantea leaf meals in chickens. Bulgarian Jpournal of Agricultural Science. 23(3), 476-480. Hien, Q. T., Kien, T. T. and Hoan, T. T. 2013. "Determination of the appropriate cutting intervals for *Brachiria decumhens* basilisk grown in Thai Nguyen". TNU Journal of Science and Technology. 104(4), 23-27.

Hien, Q. T., Hoang, T. H. N. and Trung, T. Q. (2019). "Determination of optimum harvesting interval for *Moringa oleifera* in first year production". *Vietnam Journal of Science and Technology. Ministry of Science and Technology*. 61(5), 42-47.

Hirschmann, R. (2022). Per capita poultry consumption in Malaysia 2006-2025. Published April 14. Online. https://www.statista.com/statistics/757983/malaysia-poultry-consumption-per-capita/

Hongyan, L., Rong, T. and Zeyuan, D. (2012). Factors affecting the antioxidant potential and health benefits of plant foods. *Canadian Journal of Plant Science*. https://doi.org/10.4141/cjps2011-239.

Hue, K. T., Van, D. T. T., Ledin, I., Wredle, E. and Sporndly, E. (2012). Effect of harvesting frequency, variety and leaf maturity on nutrient composition, hydrogen cyanide content and Cassava foliage yield. *Asian-Aust Journal of Animal Sciece.* 25(12), 1691-1700. http://dx.doi.org/10.5713/ajas.2012.12052

Hueze, V., Tran, G., Boudon, A. and Bastianelli, D. (2016). Nacedero (Trichanthera gigantea). Feedipedia, a program by INRA, CIRAD, AFZ and FAO. http://www.feedipedia.org/node/7270 Last updated on February 25, 2016, 4.53 pm.

Jaya, A. F., Soriano, M. L. and Carpentaro, B. B. (2009). Utilization of Madre de Agua (*Trichantera gigantea* var guianensis) leaf meal as feed for growing-finishing pigs. *Philipines Journal of Veterinary and Animal Science.*

Kgosana, K. G. (2019). The effects of extraction techniques and quantitative determination of oxalates in Nerium oleander and feeds. *Onderstepoot Journal of Veterinary Research*. 86(1), 1-9. https://doi.org/10.4102/ojvr.v86i1.1611.

Kien, T.T., Hien, T. Q., Huan, T. T. and Nhung, T. T. (2010). "Study the effect of different cutting intervals on the ability to receive, the grate of grass used and the digestibility of some imported grass species (*P. atranum, B. brizantha, B. decumhens*) on beef cattle". *TNU Journal of Science and Technology*. 67(5), 109-112.

Kien, T. T., Khoa, M. A., Han, T. T. and Hien, T. Q. (2020). Effect of cutting intervals on yield and quality of the green fodder *Trichantera gigantea*. *AGROFOR International Journal*. 5(1), 22-29.

Law, F. L. (2018). Effects of supplementing protease in low protein and low energy diets on growth performance and physiological responses of broiler chicken under different environmental conditions. PhD Thesis, Universiti Putra Malaysia.

Laudadio, V., Passantino, L., Perillo, A., Lopresti, A., Passantino, A., Khan, R. U. and Tufarelli, V. (2012). Productive performance and histological features of intestinal mucosa of broiler chickens fed different dietary protein levels. Production, modelling and education. *Poultry Science*. 91, 265-270.doi:10.3382/ps.2011-01675.

Leterme, P., Angela, M. L, Fernando, E., Wolfgang B. S, and Andre Buldgen (2005). Chemical composition, nutritive value and voluntary intake of tropical free foliage and cocoyam in pigs. Journal of Science Food Agriculture 85, 1725-1732.

Lisnahan, C. V., Wihandoyo, Zuprizal, and Sri Harimurti (2017). Growth performance of native chickens in the grower phase fed methionine and lysine-supplemented cafeteria standard feed. Pak. J Anim Nutr. 16, 940-944.

Li, Y., Kui-Shan, W., Xioa, R., Ying-Xian, Z., Feng, W. and Qiang, W. (2018). Response of plant secondary metabolites to environmental stress. *Molecules.* 23, 762; doi. 10.3390/molecules23040762.

Ly, J., Chhay, Ty., Phiny, C. and Preston, T. R. (2001). Some aspects of the nutritive value of leaf meals of Trichanthera gigantea and Morus alba for Mong Cai Pigs. *Livestock Research for Rural Development*.

Mohanty, S., Mohapatra, S. and Acharya, G. (2020). Comparative haematology and biochemical parameters of indigenous and broiler chicken. *International Journal of Scientific & Technology Research.* 9(4), 972-979.

Morbos, C. E., Espina, D. M., and Bestil, M. E. (2016). Growth performance of Philippine native chicken fed diet supplemented with varying levels of Madre de agua (Trichanthera gigantea Nees) leaf meal. *Annals of Tropical Research* 38(1), 174-182.

Morgan, N. K., Scholey, D. V. and Burton, E. J. (2014). A comparison of two methods for determining titanium dioxide marker content in broiler digestibility studies. *Animal.* 8(4), 529-533. doi:10.1017/S1751731114000068.

New Straits Times (2022). https://www.nst.com.my/opinion/letters/2022/03/776759/ketum-ayam-can-be-new-source-protein-poultry. Published online March 4, 2022.

Nouman, W. (2012). Biomass production and nutritional quality of Moringa oleifera as field crop. Turk Agric Forestry. 37, 410-419.

NRC (1994). Nutrient Requirements of poultry. Ninth Revised Edition, 1994, National Academy Press, Washington D. C.

New Straits Times (2022). https://www.nst.com.my/opinion/letters/2022/03/776759/ketum-ayam-can-be-new-source-protein-poultry. Published online March 4, 2022.

Nouman, W. (2012). Biomass production and nutritional quality of Moringa oleifera as field crop. Turk Agric Forestry. 37, 410-419.

NRC (1994). Nutrient Requirements of poultry. Ninth Revised Edition, 1994, National Academy Press, Washington D. C.

Nwosu, J. N., Ubaonu, C. N., Banigo, E. O. I. and Uzomah, A. (2010). The effects on processing on the anti-nutritional properties of 'oze' (Bosqueia angolensis) seeds. *New York Science Journal* 3(9), 106-111.

Perveen, F. and Zaib, S. (2013). Phytochemical and spectrophotometric analyses of the Hill Toon, Cedrela Serrata Royle methanolic leaves extract and its fraction. International Journal of Agriculture Innovations and Research, 1(5), ISSN (Online) 2319-1473.

Pesti, G. M. (2009). Impact of dietary amino acid and crude protein levels in broiler feeds on biological performance. Journal of Applied Poultry Research 18(3), 477-486.

Pietras, M., Orczewska-Dudek, S., Szczurek, W. and Pieszka, M. (2021). Effect of dietary lupine seeds (Lupinus luteus L.) and different insect larvae meals as protein sources in broiler chicken diet on growth performance, carcass, and meat quality. Livestock Science. 250, 104537. https://doi.org/10.1016/j.livsci.2021.104537

Preston, T. R. (1995). Tropical animal feeding. A manual for research workers. *FAO Animal Production and Health Paper* No. 126. p. 305.

Raipuria, N., Kori, D., Saxena, H. O., Pawar, G., and Choubey, S. K. (2018). Qualitative and guantitative evaluation of secondary metabolites in leaves, roots, and stem of *Cleome viscosa L. International Journal of Green Pharmacy*, 12(4), 285-290.

Ravidran, G. and Ravindran, V. (1988). Changes in the nutritional composition of cassava (*Manihot esculenta* Crantz) leaves during maturity. *Food Chemistry*, 27, 299-309.

Rodriquez, R., Gonzalec, N., Alonso, J., Dominquez, M. and Sarduy, L. (2014). Nutritional value of foliage meal from four species of tropical trees for feeding ruminants. *Cuban Journal Of Agricultural Science.* 48(4), 371-378.

Rosales, M. (1997). *Trichantera gigantea* (Humboldt & Bonpland.) *Nees*: A review Livest. Res. Rural Dev., 9(4).

Riascos-Vallejos, A. R., Reyes-Gonzalez, J. J. and Aquirre-Mendoza, L. A. (2020). Nutritional characterization of trees from amazonian piedmont Putumayo department, Colombia. Cuban Journal of. Agricultural Science 54, 257-265.

Saguidan, J. A. (2015). Growth performance of pigs fed grower diets with madre de agua (Trichanthera gigantea) leaf meal. Thesis/ Dissertation. https://www.ukdr.uplb.edu.ph/etd-undergrad/1431. Retrieved 30 August 2022. 2.01 am.

Sarwatt, S. V., Laswai, G. H., and Ubwe, R. (2003). Evaluation of potential of Trichanthera gigantea as a source of nutrients for rabbit diets under small-holder production system in Tanzania.

Singleton, V. L. and Rossi, J. A. (1965). Calorimetry of total phenols with Phosphomolydic. Phosphotungstic acid reagents. American Journal of Enology and Viticulture. 16(3), 144-158.Sreeramulu, D. and Raghunath, M. 2011. Antioxidant and phenolic content of nuts, oil seeds, milk and milk products commonly consumed in India. *Food and Nutrition Science*. 2, 422-427.

Tran, N. T. B. (2003). Effect of age of leaves from forage trees on nutritive value. MEKARN_Miniprojects_2003.

Wang, F., Zuo, Z., Chen, K., Gao, C., Yang, Z., Zhoa, S., Li, J., Song, H., Fang, J., Cui, H., Ouyang, P., Zhou, Y., Shu, G. and Jing, B. (2018). Histological injuries, ultrastructural changes, and depressed TLR expression in the small intestine of broiler chickens with Aflatoxin B1. *Toxins*. 10, 131. doi:10.3390/toxins10040131

Pertanika J. Trop. Agric. Sci. 48 (6): 2137 - 2151 (2025)

PERTANIKA JOURNALS

TROPICAL AGRICULTURAL SCIENCE

Journal homepage: http://www.pertanika.upm.edu.my/

Tree Age Affects the Physicochemical, Antioxidant, and Minerals Composition of Musang King Durian Fruits

Eliwanzita Sospeter[1,2], Phebe Ding[1]*, Teh Huey Fang[3], Azizah Misran[1], Faridah Abas[4], Wei Yingying[5], Jiang Shu[5], and Shao Xingfeng[5]

[1]Department of Crop Science, Faculty of Agriculture, Universiti Putra Malaysia, 43400 Serdang, Selangor, Malaysia

[2]Department of Food Science and Technology, Mbeya University of Science and Technology, P.O Box 131, Mbeya, Tanzania

[3]Department of Industrial Biotechnology and Chemistry, SD Guthrie Technology Centre Sdn. Bhd., UPM-MTDC Technology Centre III, Lebuh Silikon,43400, UPM Serdang, Selangor, Malaysia

[4]Department of Food Science, Faculty of Food Science and Technology, Universiti Putra Malaysia, 43400 Serdang, Selangor, Malaysia

[5]College of Food Science and Engineering, Ningbo University, Ningbo 315800, China

ABSTRACT

The quality of fruits, including durian, can be significantly affected by the age of the tree. The impact of tree age on the physicochemical, antioxidant, and mineral compositions of Musang King durian (MKD) fruit was investigated using physicochemical and biochemical approaches. The results revealed that firmness, pH, reducing sugar, polyphenol, and antioxidant activity were affected by tree age. Durian fruits from old trees exhibited higher firmness and reduced sugar compared to young and middle-aged trees. Fruits from old and middle-aged trees had higher polyphenol and antioxidant activity compared to young trees durian fruits. Calcium and nitrogen were significantly higher in durian fruits from young trees, while potassium and zinc were higher in fruits from old trees. The finding demonstrated that tree age impacts the physicochemical, antioxidant content, and mineral composition of MKD fruits, and these changes may respond to the sensory perception of MKD fruits.

Keywords: Durian, macro-minerals, micro-minerals, postharvest quality, tree age

ARTICLE INFO

Article history:
Received: 20 January 2025
Accepted: 05 May 2025
Published: 25 November 2025

DOI: https://doi.org/10.47836/pjtas.48.6.23

E-mail addresses:
ellynyeura@gmail.com/eliwanzita.sospeter@must.ac.tz (Eliwanzita Sospeter)
phebe@upm.edu.my (Phebe Ding)
teh.huey.fang@sdguthrie.com (Teh Huey Fang)
azizahm@upm.edu.my (Azizah Misran)
faridah_abas@upm.edu.my (Faridah Abas)
weiyingying@nbu.edu.cn (Wei Yingying)
jiangshu@nbu.edu.cn (Jiang Shu)
shaoxingfeng@nbu.edu.cn (Shao Xingfeng)
*Corresponding author

INTRODUCTION

Malaysia is known for growing varieties of durian species and boasts a great variety

of durian cultivars (Siew et al., 2018). Among these, the Musang King durian (MKD), registered as D197, is well-known for its buttery, golden yellow flesh and intense flavor with a hint of bitterness aftertaste (Specialtyproduce, 2024). After Malaysian durians were introduced to China, demand increased tremendously, particularly for the MKD variety, resulting in a price premium over other varieties (MalaysiaSun, 2024). As a result, durians are now cultivated on a large scale in Malaysia. It was reported that the planting acreage and production of durian increased by 22.71% and 33.11%, respectively, between 2018 and 2022 (Department of Agriculture Malaysia, 2023).

Malaysian durians are categorized as harvested from young or old trees. Fruits from old trees are considered superior in flavor, and consumers are willing to pay more for them. MKD has been receiving positive reviews and now cultivated on a large scale. However, most of the MKD in the market comes from young trees, as durian begins to bear fruit from 4-5 years after grafting (Ketsa et al., 2020).

The eating quality of fruit is determined by sensory characteristics (e.g., flavor, aroma, firmness) and nutritional profile (e.g., antioxidant content) (Brasil & Siddiqui, 2018). Physicochemical properties, such as pH, titratable acidity (TA), and soluble solids content (SSC), define the fruit's eating quality (Athmaselvi et al., 2014). Antioxidants, such as phenolic compounds and ascorbic acid, enhance the nutritional and sensory appeal, influencing their acceptability and sensory perception of a fruit (Pott et al., 2019). These characteristics can be influenced by various preharvest factors, including tree age (Meena & Asrey, 2018), environmental conditions, and genetic variations (Brasil & Siddiqui, 2018).

Tree age was observed to significantly impact the quality characteristics of fruits, including the physicochemical and biochemical composition of fruits (Asrey et al., 2007; Khalid et al., 2012; Meena & Asrey, 2018a; Yaacob, 1983). The physiological changes that occur as a tree ages and grows significantly influence fruit composition and result in quality changes (Yaacob, 1983). These changes often involve differences in minerals allocation (Estravis-Barcala et al., 2020; Zhou & Melgar, 2020). For instance, compared to young trees, older trees allocate more dry matter and minerals to flowers and fruits (Karmacharya & Singh, 1992). Young guava trees produced fruits with higher iron content and low magnesium content (Asrey et al., 2007). Similarly, Kinnow mandarin harvested from young age trees (3 years old) contained higher Mn and Fe contents than old age trees (Khalid et al., 2012). Besides, the difference in tree ages has been associated with the change in the physicochemical and antioxidant characteristics of fruits. Meena and Asrey (2018a) revealed that Amrapali mango fruits from 18-year-old trees have the highest SSC and total sugars, while 30-year-old trees have lower TA. In addition, the antioxidant content of 6-year-old mango trees had higher total phenols, antioxidant capacity, and ascorbic acid than fruits from 18 and 30 years (Meena & Asrey, 2018b).

Despite the well-documented impacts of the development and ripening (Husin et al., 2022; Wiangsamut & Wiangsamut, 2023) and postharvest processing (Razali et al., 2022;

Tagubase & Ueno, 2016; Tan et al., 2020) on durian fruit quality, the influence of tree age on MKD fruit physicochemical properties, antioxidant content, and minerals composition remains uninvestigated. However, many durian lovers believe that older trees produce fruits with superior flavor. This claim is critical, but there is no scientific evidence to explain the influence of tree age on the eating quality of MKD fruit. Thus, this study aims to explore the impact of tree age on the eating quality attributes of MKD fruit.

MATERIALS AND METHODS

Plant Materials

Fresh and fully ripe MKD fruits from three tree age groups (5-9 years [young], 10-15 years [middle], and >16 years [old]) were harvested from commercial orchards in Raub (latitude 3° 03′ N, longitude 101° 51′ E), Pahang, Malaysia, during the peak season in November 2022. Fruits with similar size (1.3 ± 0.2 kg), well-formed shape, and no visual defects were selected for this study. Six fruits from each tree age group were used. After harvest, the pulp was removed from the locules for physicochemical analysis, while a separate set of pulp was extracted for mineral composition and antioxidant content analysis. The remaining pulp from each locule was lyophilized for 48 hours using a freeze drier (LaboGene Scanvac CoolSafe 4L, United Kingdom). The freeze-dried powder was then stored at -80 °C until the mineral's composition analysis.

Determination of Physicochemical Characteristics

Color

L*, a*, and b* were measured using a chroma meter CR- 400 (Konica Minolta, Inc., Japan) at three different spots on the surface of each durian fruit pulp sample. The L* (lightness), a* (+a* = redness, −a* = greenness), b* (+b* = yellowness, − b* = blueness), and total color change (ΔE*). Given that MKD fruits are predominantly yellow, only the b* value was reported. ΔE* was determined using Equation [1];

$$\Delta E^* = \sqrt{\Delta L^2 + \Delta a^2 + \Delta b^2} \quad [1]$$

Firmness

The firmness of the durian pulp was analyzed using an Instron texture analyzer (Model TA-XT2 Stable Micro Systems, UK). A 250-N load and a cylindrical probe (P/0.25) with a 5-mm diameter were used. The probe was pressed downwards to a depth of 3 mm at a speed of 20 mm/min, and the force (N) was recorded. Firmness measurements were taken at three different locations on the pulp (top, middle, and bottom) of each locule, and the

average values were calculated. The readings were recorded using the Instron Merlin Software version M12-13664-EN.

pH and titratable acidity (TA)

Durian pulp (7 g) was homogenized with 70 ml of distilled water, and the pH was measured using a pH meter (Professional Bench Top, Bp 3001, Singapore). The diluted durian homogenate was titrated against 0.1 N NaOH to pH 8.1 using phenolphthalein as an indicator according to Sospeter et al. (2025). TA (% citric acid) was calculated using Equation [2]:

$$\% \text{ citric acid} = \frac{\textit{Volume of titre (ml)} \times 0.1 \times \textit{volume made (ml)} \times \textit{equivalent of citric acid} \times 100}{\textit{Weight of the sample (g)} \times \textit{volume of sample used for titration (ml)} \times 1000} \quad [2]$$

Equivalent of citric acid = 64.04g/equivalent

Soluble Solids Content

Soluble solid content (SSC) was measured using a method by Sospeter et al. (2025). 20 µl of the same homogenate of durian pulp used for pH analysis was applied onto the prism surface of the digital handheld refractometer (Atago Co., Tokyo, Japan) to obtain SSC readings. These readings were then multiplied by the dilution factor (10) to obtain the % SSC at 25 °C.

Determination of Antioxidant Content

Ascorbic acid content (AA)

The ascorbic acid content of the durian pulp in all treatment groups was estimated using the dye titration method (Nor et al., 2023). A total of 5 g of durian sample was blended with 20 ml of 3% metaphosphoric acid (HPO_3). Subsequently, 5 ml of the resulting extract was titrated with a standardized dye solution until the solution turned pink. The titration readings were recorded, and the ascorbic acid content was calculated using Equations [3] and [4].

$$\text{Ascorbic acid contents (mg/100 g)} = \frac{\text{Titre volume(ml)} \times \text{dye factor} \times \text{volume made up (ml)} \times 100}{\text{Weight of the sample (g)} \times \text{volume used for titration (ml)}} \quad [3]$$

$$\text{Dye factor} = \frac{0.5}{\text{Volume of the dye}} \quad [4]$$

Total Polyphenols (TP)

Extraction. Polyphenols were extracted according to the method described by Sospeter et al. (2025), with some modifications. One gram of freeze-dried powdered durian pulp samples was extracted using 15 ml of a binary mixture containing 0.2 M HCl and methanol (1:1, v/v). The sample mixture was then sonicated for 60 min at 50 °C and centrifuged for 7 min at 9000×g. This process was repeated three times, and thereafter, the extracts were concentrated at 40 °C by a centrifugal evaporator (Genevac EZ-2 Elite, Sysmex Belgium N.V). Subsequently, the extract was examined for total polyphenol content.

Polyphenol Content Analysis. The Folin-Ciocalteu technique was used according to Singleton & Rossi (1965) with modification. A 100 µl aliquot of the extract was placed in a 15 ml test tube and diluted with Milli-Q water to achieve a total volume of 1 ml. Subsequently, 0.5 ml of Folin-Ciocalteu reagent and 2.5 ml of 20% (w/v) sodium carbonate solution were added to each test tube. The mixture was vortexed thoroughly and then left to react in the dark for 40 minutes. The absorbance measurements were taken at 765 nm using ultraviolet-visible spectroscopy (UV-VIS- Infinite M200) and gallic acid as the standard. The results were represented as milligrams of gallic acid equivalents (mg GAE) per 100 g of dry weight (DW) based on a calibration curve ($R^2 = 0.99$). Refer to the additional document (S1).

2,2-Diphenyl-1-picrylhydrazyl (DPPH) Radical-Scavenging Activity

DPPH radical-scavenging activity (AA) of durian pulp extract was assessed using the stable radical DPPH, as described by Saminathan & Doraiswamy (2000) with modification. 200 µg/ml of the diluted durian pulp extracts was adjusted to 1ml using methanol. The sample aliquots were well mixed with approximately 3 ml of a 0.1 mM DPPH solution. 1 ml of methanol was added to 3 ml of a 0.1 mM DPPH solution to generate a control sample. Then, the mixture was allowed to stand in the dark for 20 minutes at room temperature. The absorbances of the samples were measured at 517 nm using UV-VIS (Infinite M200) against the control. Next, the DPPH radical scavenging activity was calculated using Equation [5].

$$\text{DPPH radical scavenging activity (\%)} = \frac{\text{Absorbance (Control)} - \text{Absorbance (Sample)}}{\text{Absorbance (Control)}} \times 100 \quad [5]$$

Determination of Macro and Microminerals

Sample Digestion

The sample was digested according to Uresti-Porras et al. (2021) with modification. A 0.25 g portion of the freeze-dried sample was mixed with 5 ml of concentrated sulfuric acid

in a test tube. The mixture was allowed to stand overnight. Following this, 2 ml of 50% hydrogen peroxide was added slowly to the mixture, and the test tube was then rotated gently to thoroughly mix the mixture. Subsequently, the test was placed in a digestion block operating at 285°C for 45 minutes until the solution became clear.

Atomic Absorption Spectroscopy (AAS) Measurements

The freeze-dried pulp samples were analyzed for the target elements using an Atomic Absorption Spectrometer (Shimadzu AA-670, Japan) equipped with appropriate hollow cathode lamps for each element. The concentrations of various elements were quantified by generating standard calibration curves using analytical reagent (AR) grade standard solutions of the respective elements. The elements analyzed included potassium (K), magnesium (Mg), calcium (Ca), nitrogen (N), iron (Fe), and zinc (Zn). The calibration and analysis followed standard AAS protocols to ensure accuracy and reliability.

Statistical Analysis

An experimental study was designed to investigate the null hypothesis that the tree age has no effects on the physicochemical quality parameters, antioxidant content and mineral composition of the whole MKD fruits. The collected physicochemical, antioxidant content and mineral composition data were analyzed using ANOVA with the JMP software version 17 pro (SAS Institute, Inc., Cary, NC, USA). Means were compared using Tukey's HSD ($p = 0.05$). In correlation analysis, Pearson correlation coefficients (r) as a measure for distance was used.

RESULTS

Physicochemical Characteristics of MKD Fruit

It was revealed that tree age significantly affected the firmness of MKD fruit; fruits from older trees exhibited higher firmness (1.35 N) compared to fruits from young (0.62 N) and middle-aged trees (0.81 N) ($p < 0.05$) (Figure 1a). While color parameters (b* and E* values), SSC and TA did not show any significant differences across the three tree age groups ($p < 0.05$) (Figures 1b, 1c and 1e). The pH of the MKD fruit from younger trees was higher (7.25) than that of durian from older trees (6.56). However, fruits from young- and middle-aged trees showed no significant differences. Furthermore, no significant differences were observed in the pH levels of fruit from middle- and old-aged trees ($p < 0.05$) (Figure 1d). Along with the aforementioned results, fruits from old trees exhibited significantly higher reducing sugars compared to those from young- and middle-aged trees (Figure 1f).

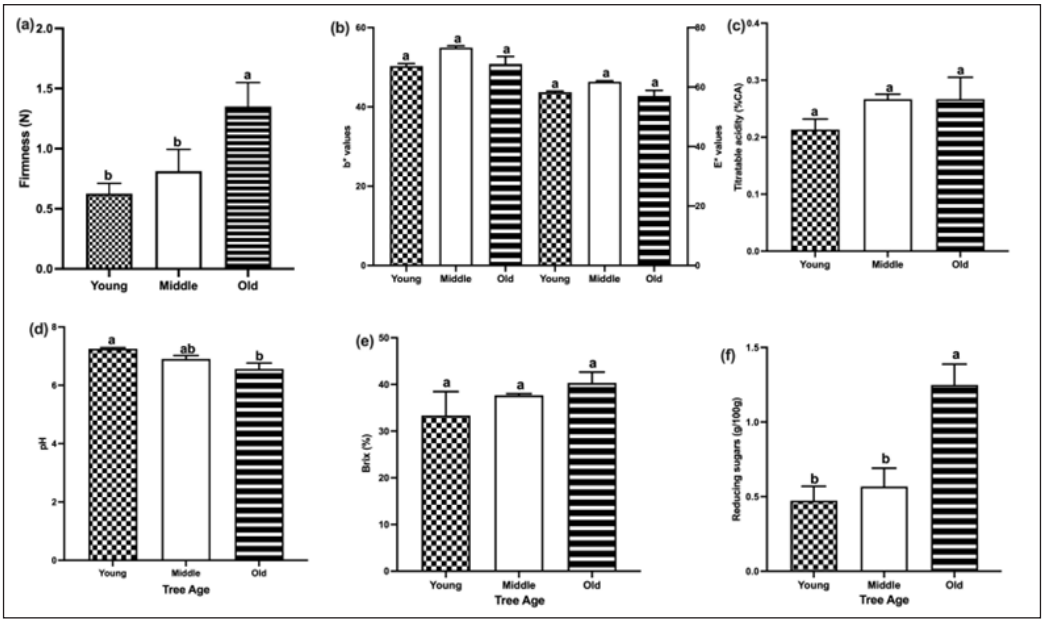

Figure 1. Means (n=6) of physicochemical parameters of Musang King durian fruits harvested from different tree ages (young, middle and old). Same letters indicate no significant differences between groups based on Tukey's HSD test ($p < 0.05$). Parameters include b* = yellowness/ blueness, ΔE = change of color and CA = Citric acid. Error bars represent standard error

Antioxidant Content of MKD Fruit

The findings revealed that tree age did not affect the ascorbic acid content of MKD (Figure 2a). However, it affected the polyphenol content and antioxidant activity of MKD fruits ($p < 0.05$) (Figure 2b and 2c). Fruits from middle-aged trees displayed higher levels of polyphenol content and DPPH scavenging activity (antioxidant activity) as compared to those from young- and old-aged trees (Figure 2b and 2c).

Mineral Contents of MKD Fruit

The findings from the minerals analysis of MKD fruit reveal that an old-aged tree has significantly lower N than middle-aged and young trees (Figure 3a). Unlike N, K in old-aged trees was significantly higher than both young- and middle-aged trees (Figure 3b). For Ca, young-aged trees were significantly higher than middle- and old-aged trees (Figure 3c). However, there were no significant differences in Mg among the three tree ages (Figure 3d). For Zn content, just like the K, the old-aged tree has a significantly higher concentration of Zn than young- and middle-aged trees (Figure 3e). Unlike other minerals, the Fe concentration of middle-aged trees was significantly higher than young- and old-aged trees (Figure 3f). However, there was no significant difference between young- and old-aged trees.

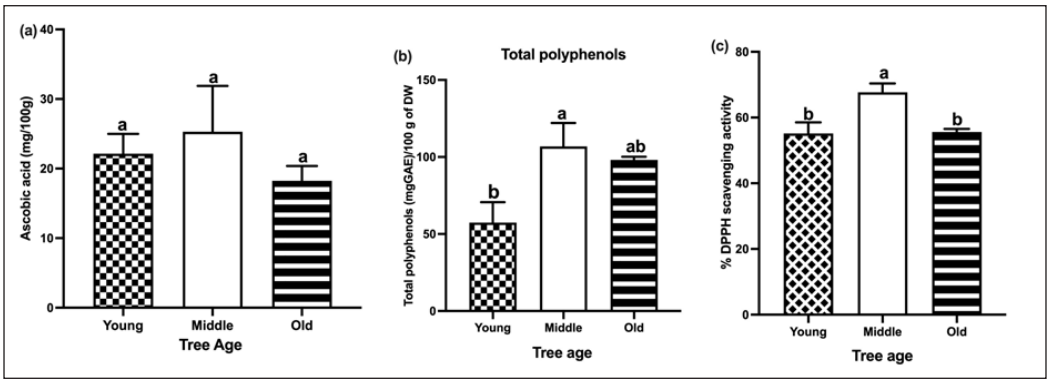

Figure 2. Means (n=6) of (a) ascorbic acid, (b) total polyphenol and % DPPH scavenging activity of Musang King durian fruits harvested from different tree ages (young, middle and old). Same letters indicate no significant differences between groups based on Tukey's HSD test ($p < 0.05$). DW = Dry weight and GAE = Gallic acid equivalent. Error bars represent standard error

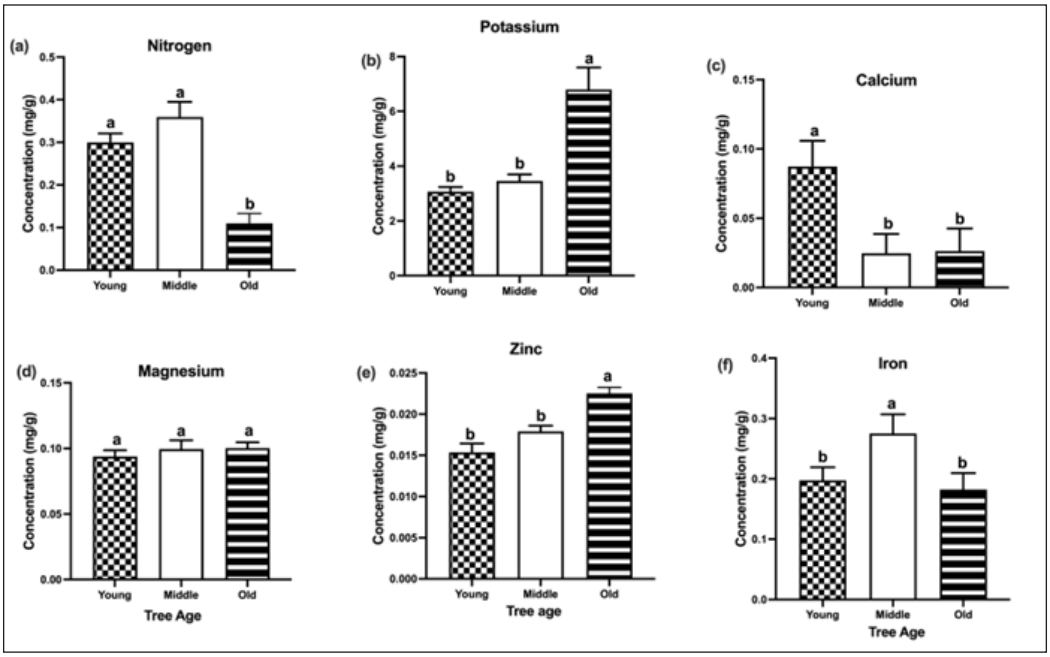

Figure 3. Means (n = 6) of macro- and microminerals concentrations in Musang King durian fruits harvested from trees of different age groups (young, middle, and old). The same letters indicate no significant differences between groups based on Tukey's HSD test ($p < 0.05$). Error bars represent standard error

Correlation between Minerals, Physicochemical, and Antioxidant Characteristics of Musang King Durian Fruit

In this study, Zn demonstrated significant positive correlations with the firmness and reducing sugar content of MK durian fruit ($r = 0.6$, $p < 0.05$) and negatively correlated with pH ($r = -0.7$, $p < 0.05$). Similarly, Fe showed a positive correlation with ascorbic acid content ($r = 0.6$, $p < 0.05$). K was positively associated with TA, firmness, and reducing sugar content ($r = 0.6$, $p < 0.05$). Additionally, N exhibited positive correlations with SSC, ΔE*, and antioxidant activity. However, a negative correlation was observed between reducing sugar content and N content ($r = 0.5$, $p < 0.05$) (Figure 4: and Additional document (S2))

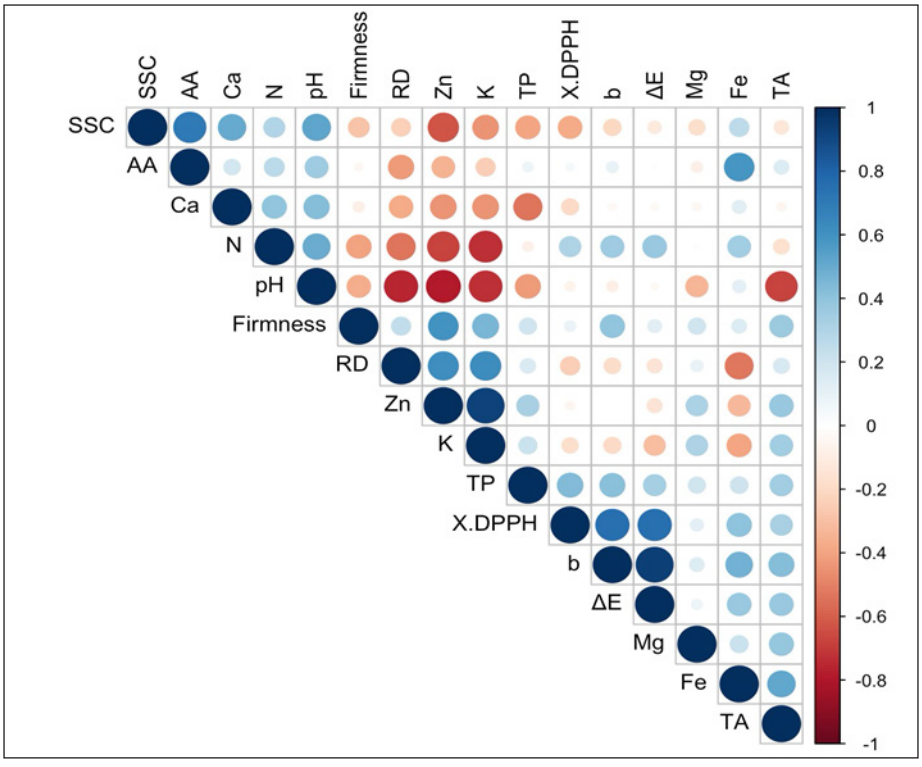

Figure 4. Correlation matrix between physico-chemical attributes, antioxidant content, and mineral content of Musang King durian across different tree ages. Correlation coefficients are represented by colors as indicated in the color key. Significant correlations are highlighted by .Abbreviations: TP = Total polyphenol; AA = Ascorbic acid; X.DPPH = 2,2-diphenyl-1-picrylhydrazyl; RD = Reducing sugar; SSC = Soluble solid content; TA = Titratable acidity; N = Nitrogen; K = Potassium; Mg = Magnesium; Fe = Iron; Ca = Calcium; Zn = Zinc

DISCUSSION

The study investigated the impact of tree age on physicochemical characteristics, antioxidant content, and mineral composition of MKD fruits. The findings reveal that tree age significantly affected the firmness of the MKD fruit. Fruit firmness is a complex

attribute perceived through the senses of touch, hearing, vision, and kinesthesia, which plays a crucial role in determining consumer acceptability (Feng et al., 2024). These results are inconsistent with the results obtained by Meena and Asrey (2018a), who observed that Amparali mango fruits from young-aged trees (6 years old) exhibit higher firmness. The authors suggested that firmness differences between fruits from different age groups could be attributed to the content of Ca and cell wall degrading enzymes. However, in our study the Ca content in old tree age fruits was lower compared to younger trees, suggesting a different mechanism influences durian fruit firmness. Furthermore, since cell wall-degrading enzyme activity, such as pectin methylesterase (PME) and polygalacturonase (PG) activities, was not measured in this study, we suspect that PG could contribute to firmness variations observed among tree ages. This enzyme has been shown to influence fruit softening (Lazan et al., 1995) and may exhibit species-specific activity patterns as observed in tomato and strawberry fruits (García-Gago et al., 2009). Additionally, firmness in this study was correlated with Zn content (Figure 4). Zn affects auxins, gibberellins, and abscisic acid hormones, which regulate cell wall enzymes and, hence, influence fruit firmness (Zhang et al., 2016). This may explain why durian from old trees has higher firmness compared to durian from younger trees.

Contrary to firmness, the current study also reveals that the pH value of MKD fruit was lower in fruits from old-aged trees, whereas reducing sugar content was higher in these fruits. The lower pH in durian from old-aged trees reflects their higher acidity. These results align with the study by Aregay et al. (2021) who reported that Gunda Gundo Orange (*Citrus* spp.) fruit from old-aged trees contained higher acidity than young-aged trees. These researchers reported that the high acidity was attributed by N content accumulation in the older trees. As it was hypothesized that N content is considered a phloem-mobile nutrient, and as trees mature, the transport of these mobile nutrients tends to be more pronounced (Khalid et al., 2018), N content influences the biosynthesis of organic acids, hence increasing fruit acidity (Zheng et al., 2023). However, our study observed lower N content in durian fruits from older trees, suggesting an alternative mechanism for the observed acidity. The lower pH and higher reducing sugar content in fruits from old-aged durian trees are speculated to result from the accumulation of K, as observed in the correlation analysis in this study. The high K content has been associated with increased acidity and sugar content in Cara Cara navel orange (*Citrus sinensis* L. Osbeck) (Wu et al., 2021). The K content enhanced sucrose metabolism and citrate synthesis in Cara Cara orange by increasing the activity of citrate-synthesizing enzymes, thereby contributing to higher acidity and reducing sugar levels (Wu et al., 2021). Further, K content was shown to up-regulate sugar and minerals transport genes, increasing sugar concentration in fruit and thereby increasing its quality (Shen et al., 2019). Additionally, Zn was also higher in durian from older trees. Zn content regulates enzymatic activities and the expression of

genes associated with sugar and acid metabolism, as observed in loquats (Ali et al., 2023). These mechanisms likely explain the observed low pH and increased reducing sugar content in MKD fruits in this study.

MKD fruits of middle-aged trees had higher polyphenols and DPPH antioxidant activity than fruits from young- and old-aged trees. This is inconsistent with Meena and Asrey (2018a), who found that phenolic content of Amrapali mangoes decreased with tree age. The inconsistencies in these findings may be attributed to variations between species. Different fruit species exhibit distinct gene expression profiles, which can influence the production of secondary metabolites, such as polyphenols (Xu et al., 2012). Additionally, the higher antioxidant content might be as a result of higher N content in fruits from middle-aged trees. N content was positively correlated with the antioxidant activity in this study (Figure 4). N content modulated the biosynthesis of carotenoids and phenolic acids hence improving the antioxidant content of the fruits (Narvekar & Tharayil, 2021; Zhang et al., 2024). A reduction in polyphenol content may indicate a loss of the nutritional value of durian fruit, as in apples, pears, durian, and peaches (Leontowicz et al., 2002, 2008).

Moreover, the MKD from young trees contained high concentrations of N and Ca. Previous studies showed that peach young trees allocated more of N, P, K, and Ca in fruits and pruned woods (Zhou & Melgar, 2020). The authors suggested a more efficient utilization of these nutrients for vegetative growth and fruit production (Zhou & Melgar, 2020). However, in our study, K content was higher in fruits from old trees. This could be due to the large size of the tree and reduced vegetative growth in old trees as compared with young trees (Khalid et al., 2018). This aligns with observations in forest canopy trees, where younger trees prioritize vegetative growth over older trees (Gavin & Peart, 1999).

Interestingly, the concentration of Zn and Fe was observed higher in fruit from old trees compared to young trees. This observation has not been reported previously in the literature. The higher content of these minerals could be due to age-related root patterns and the distribution of root hairs across soil strata (Mohsin et al., 2000), or efficiency in minerals uptake (Zhou & Melgar, 2020). Future research is needed to understand the mechanism behind this minerals variation across tree ages.

CONCLUSION

The impact of tree age on physicochemical characteristics, antioxidant content, and nutrient composition was investigated in this study. The findings reveal that MKD tree age significantly impacted fruit firmness and pH, reducing sugar content, antioxidant content, and mineral composition. Fruits from older trees exhibited greater firmness, higher reducing sugar levels, and a lower pH compared to those from middle-aged and young trees. In contrast, durians from middle-aged trees had the highest antioxidant content. Mineral composition analysis showed significantly higher concentrations of K,

Zn, and Fe in fruits from older trees, while fruits from younger trees had increased levels of N and Ca. These findings highlight tree age as a critical factor influencing both the physicochemical properties and nutritional value of MKD fruit. Moreover, Correlations between physicochemical, antioxidant, and mineral content were observed, suggesting associations. Future studies should focus on mechanistic research to confirm these links and better understand how tree age affects MKD fruit quality.

ACKNOWLEDGEMENT

We acknowledge Green Mile Gain Limited (Vote: 6380067), Hong Kong; the Higher Education for Economic Transformation (HEET) Project under the Tanzania Ministry of Education, Science and Technology (Project no. TZ.960); and the Ningbo Agricultural Research Project (2024Z275) for funding this research.

REFERENCES

Ali, M. M., Gull, S., Hu, X., Hou, Y., & Chen, F. (2023). Exogenously applied zinc improves sugar-acid profile of loquat (*Eriobotrya japonica* lindl.) by regulating enzymatic activities and expression of their metabolism-related genes. *Plant Physiology and Biochemistry*, *201*, Article 107829. https://doi.org/10.1016/j.plaphy.2023.107829

Athmaselvi, K. A., Jenney, P., Pavithra, C., & Roy, I. (2014). Physical and biochemical properties of selected tropical fruits. *International Agrophysics*, *28*(3), 383–388. https://doi.org/10.2478/intag-2014-0028

Aregay, N., Belew, D., Zenebe, A., Haile, M., Gebresamuel, G., & Girma, A. (2021). Tree age and harvesting season affected physico-chemical and bioactive compounds of elite type of Gunda Gundo Orange (*Citrus* spp) in the Northern Ethiopia. *International Journal of Fruit Science*, *21*(1), 26–39. https://doi.org/10.1080/15538362.2020.1852150

Asrey, R., Pal, R. K., Sagar, V. R., & Patel, V. B. (2007). Impact of tree age and canopy position on fruit quality of guava. *Acta Horticulturae*, *735*, 259–262. https://doi.org/10.17660/ActaHortic.2007.735.34

Brasil, I. M., & Siddiqui, M. W. (2018). Postharvest quality of fruits and vegetables: an overview. In *Preharvest Modulation of Postharvest Fruit and Vegetable Quality* (pp.1–40). Elsevier. Academic Press. https://doi.org/10.1016/B978-0-12-809807-3.00001-9

Department of Agriculture Malaysia. (2023). *Hectareage, production and value of production of fruit crops by type, Malaysia, 2023 in fruit crops statistic*s. Department of Agriculture Malaysia. http://pvpbkkt.doa.gov.my/NationalList/Search.php

Doraiswamy, R., & Saminathan, V. (2020). Phytochemical analysis, antioxidant and anticancer activities of durian (*Durio zibethinus* Murr.) fruit extract. *Journal of Research in Pharmacy*, *24*(6), 882–892. https://doi.org/10.35333/JRP.2020.247

Feng, S., Bi, J., Laaksonen, T., Laurén, P., & Yi, J. (2024). Texture of freeze-dried intact and restructured fruits: Formation mechanisms and control technologies. *Trends in Food Science & Technology*, *143*, Article 104267. https://doi.org/10.1016/j.tifs.2023.104267

García-Gago, J. A., Posé, S., Muñoz-Blanco, J., Quesada, M. A., & Mercado, J. A. (2009). The polygalacturonase: *FaPG1* gene plays a key role in strawberry fruit softening. *Plant Signaling & Behavior*, *4*(8), 766–768. https://doi.org/10.4161/psb.4.8.9167

Gavin, D. G., & Peart, D. R. (1999). Vegetative life history of a dominant rain forest canopy tree[1]. *Biotropica*, *31*(2), 288–294. https://doi.org/10.1111/j.1744-7429.1999.tb00140.x

Husin, N. A., Rahman, S., Karunakaran, R., & Bhore, S. J. (2022). Transcriptome analysis during fruit developmental stages in durian (*Durio zibethinus* Murr.*)* var. *D24*. *Genetics and Molecular Biology*, *45*(4), Article e20210379. https://doi.org/10.1101/2022.10.08.511399

Karmacharya, S. B., & Singh, K. P. (1992). Production and nutrient dynamics of reproductive components of teak trees in the dry tropics. *Tree Physiology*, *11*(4), 357–368. https://doi.org/10.1093/treephys/11.4.357

Ketsa, S., Wisutiamonkul, A., Palapol, Y., & Paull, R. E. (2020). The durian: Botany, horticulture, and utilization. In I. Warrington (Ed.) *Horticultural reviews* (1st ed., pp. 125–211). Wiley. https://doi.org/10.1002/9781119625407.ch4

Khalid, S., Malik, A. U., Saleem, B. A., Khan, A. S., Khalid, M. S., & Amin, M. (2012). Tree age and canopy position affect rind quality, fruit quality and rind nutrient content of "Kinnow" mandarin (*Citrus nobilis Lour*×*Citrus deliciosa Tenora*). *Scientia Horticulturae*, *135*, 137–144. https://doi.org/10.1016/j.scienta.2011.12.010

Khalid, S., Malik, A. U., Singh, Z., Ullah, S., Saleem, B. A., & Malik, O. H. (2018). Tree age influences nutritional, pectin, and anatomical changes in developing 'Kinnow' mandarin (*Citrus nobilis Lour* × *Citrus deliciosa Tenora*) fruit. *Journal of Plant Nutrition*, *41*(14), 1786–1797. https://doi.org/10.1080/01904167.2018.1462378

Lazan, H., Selamat, M. K., & Ali, Z. M. (1995). β-Galactosidase, polygalacturonase and pectinesterase in differential softening and cell wall modification during papaya fruit ripening. *Physiologia Plantarum*, *95*(1), 106–112. https://doi.org/10.1111/j.1399-3054.1995.tb00815.x

Leontowicz, H., Gorinstein, S., Lojek, A., Leontowicz, M., Číž, M., Soliva-Fortuny, R., Park, Y. S., Jung, S. T., Trakhtenberg, S., & Martin-Belloso, O. (2002). Comparative content of some bioactive compounds in apples, peaches and pears and their influence on lipids and antioxidant capacity in rats. *The Journal of Nutritional Biochemistry*, *13*(10), 603–610. https://doi.org/10.1016/S0955-2863(02)00206-1

Leontowicz, H., Leontowicz, M., Haruenkit, R., Poovarodom, S., Jastrzebski, Z., Drzewiecki, J., Ayala, A. L. M., Jesion, I., Trakhtenberg, S., & Gorinstein, S. (2008). Durian (*Durio zibethinus* Murr.) cultivars as nutritional supplementation to rat's diets. *Food and Chemical Toxicology*, *46*(2), 581–589. https://doi.org/10.1016/j.fct.2007.08.042

MalaysiaSun. (2024). *Economic watch: Fresh Malaysian durians debut in China, set to spike in popularity.* MalaysiaSun. https://www.malaysiasun.com/news/274551464/economic-watch-fresh-malaysian-durians-debut-in-china-set-to-spike-in-popularity.

Meena, N. K., & Asrey, R. (2018a). Tree age affects physicochemical, functional quality and storability of Amrapali mango (*Mangifera indica* L.) fruits. *Journal of the Science of Food and Agriculture*, *98*(9), 3255–3262. https://doi.org/10.1002/jsfa.8828

Meena, N. K., & Asrey, R. (2018b). Tree age affects postharvest attributes and mineral content in Amrapali mango (*Mangifera indica*) Fruits. *Horticultural Plant Journal*, *4*(2), 55–61. https://doi.org/10.1016/j.hpj.2018.01.005

Mohsin, F., Singh, R., Jattan, S. S., & Singh, K. (2000). Root studies in a Eucalyptus hybrid plantation at various ages. *The Indian Forester, 126*(11), 1165-1174

Narvekar, A. S., & Tharayil, N. (2021). Nitrogen fertilization influences the quantity, composition, and tissue association of foliar phenolics in strawberries. *Frontiers in Plant Science*, *12*, Article 613839. https://doi.org/10.3389/fpls.2021.613839

Nor, S. M., Ding, P., & Chun, T. J. (2023). Locule position and thawing duration affect postharvest quality of freshly cryo-frozen musang king durian fruit. *Pertanika Journal of Tropical Agricultural Science*, *46*(2), 517–528. https://doi.org/10.47836/pjtas.46.2.09

Pott, D. M., Osorio, S., & Vallarino, J. G. (2019). From central to specialized metabolism: an overview of some secondary compounds derived from the primary metabolism for their role in conferring nutritional and organoleptic characteristics to fruit. *Frontiers in Plant Science*, *10*, Article 835. https://doi.org/10.3389/fpls.2019.00835

Razali, N. A., Ibrahim, W. M. W., Safari, S., Rosly, N. K., Hamzah, F. A., & Husin, W. M. R. I. W. (2022). Cryogenic freezing preserves the quality of whole durian fruit for the export market. *Food Research*, *6*(3), 360–364. https://doi.org/10.26656/fr.2017.6(3).428

Saminathan, V., & Doraiswamy, R. (2000). Phytochemical analysis, antioxidant and anticancer activities of durian (*Durio zibethinus* Murr.) fruit extract. *Journal of Research in Pharmacy*, *24*(6). https://doi.org/10.35333/jrp.2020.247

Shen, C., Shi, X., Xie, C., Li, Y., Yang, H., Mei, X., Xu, Y., & Dong, C. (2019). The change in microstructure of petioles and peduncles and transporter gene expression by potassium influences the distribution of nutrients and sugars in pear leaves and fruit. *Journal of Plant Physiology*, *232*, 320–333. https://doi.org/10.1016/j.jplph.2018.11.025

Siew, G. Y., Ng, W. L., Tan, S. W., Alitheen, N. B., Tan, S. G., & Yeap, S. K. (2018). Genetic variation and DNA fingerprinting of durian types in Malaysia using simple sequence repeat (SSR) markers. *PeerJ*, *6*, Article e4266. https://doi.org/10.7717/peerj.4266

Singleton, V. L., & Rossi, J. A. (1965). Colorimetry of total phenolics with phosphomolybdic-phosphotungstic acid reagents. *American Journal of Enology and Viticulture*, *16*(3), 144–158. https://doi.org/10.5344/ajev.1965.16.3.144

Sospeter, E., Ding, P., Fang, T. H., Misran, A., & Abas, F. (2025). Long-term frozen storage affects the volatile compound profile, physicochemical and antioxidant content of vacuum-packed Musang King durian fruit. *Journal of Food Science*, *90*(3), Article e70118. https://doi.org/10.1111/1750-3841.70118

Specialtyproduce. (2024). *Musang King Durian*. Specialtyproduce. https://specialtyproduce.com/produce/Musang_King_Durian_6241.php

Tagubase, J. L., & Ueno, S. (2016). Effect of freezing and thawing on the quality of durian (*Durio zibethinus* Murr) Pulp. *Transactions of the Japan Society of Refrigerating and Air Conditioning Engineers*, *33*(3), 267–272. https://doi.org/10.11322/tjsrae.16-17NR

Tan, X. Y., Misran, A., Daim, L. D. J., Ding, P., & Dek, M. S. P. (2020). Effect of freezing on minimally processed durian for long term storage. *Scientia Horticulturae*, *264*, Article 109170. https://doi.org/10.1016/j.scienta.2019.109170

Uresti-Porras, J. G., Cabrera-De-La Fuente, M., Benavides-Mendoza, A., Olivares-Sáenz, E., Cabrera, R. I., & Juárez-Maldonado, A. (2021). Effect of graft and Nano ZnO on nutraceutical and mineral content in bell pepper. *Plants*, *10*(12), Article 12. https://doi.org/10.3390/plants10122793

Wiangsamut, B., & Wiangsamut, M. E. L. (2023). Assessment of natural fruit ripening and fruit quality of three elite durian cultivars for overland export. *Trends in Sciences*, *20*(5), Article 4647. https://doi.org/10.48048/tis.2023.4647

Wu, S., Zhang, C., Li, M., Tan, Q., Sun, X., Pan, Z., Deng, X., & Hu, C. (2021). Effects of potassium on fruit soluble sugar and citrate accumulations in Cara Cara navel orange (*Citrus sinensis* L. Osbeck). *Scientia Horticulturae*, *283*, Article 110057. https://doi.org/10.1016/j.scienta.2021.110057

Xu, K., Wang, A., & Brown, S. (2012). Genetic characterization of the Ma locus with pH and titratable acidity in apple. *Molecular Breeding*, *30*(2), 899–912. https://doi.org/10.1007/s11032-011-9674-7

Yaacob, O. (1983). The growth pattern and nutrient uptake of durian *(Durio zibethinus* Murr.) on an oxisol. *Communications in Soil Science and Plant Analysis*, *14*(8), 689–698. https://doi.org/10.1080/00103628309367400

Zhang, L., Zhang, F., He, X., Dong, Y., Sun, K., Liu, S., Wang, X., Yang, H., Zhang, W., Lakshmanan, P., Chen, X., & Deng, Y. (2024). Comparative metabolomics reveals complex metabolic shifts associated with nitrogen-induced color development in mature pepper fruit. *Frontiers in Plant Science*, *15*, Article 1319680. https://doi.org/10.3389/fpls.2024.1319680

Zhang, Y., Yan, Y., Fu, C., Li, M., & Wang, Y. (2016). Zinc sulfate spray increases activity of carbohydrate metabolic enzymes and regulates endogenous hormone levels in apple fruit. *Scientia Horticulturae*, *211*, 363–368. https://doi.org/10.1016/j.scienta.2016.09.024

Zheng, Y., Yang, Z., Luo, J., Zhang, Y., Jiang, N., & Khattak, W. A. (2023). Transcriptome analysis of sugar and acid metabolism in young tomato fruits under high temperature and nitrogen fertilizer influence. *Frontiers in Plant Science*, *14*, Article 1197553. https://doi.org/10.3389/fpls.2023.1197553

Zhou, Q., & Melgar, J. C. (2020). Tree age influences nutrient partitioning among annually removed aboveground organs of peach. *HortScience*, *55*(4), 560–564. https://doi.org/10.21273/HORTSCI14731-19

Pertanika J. Trop. Agric. Sci. 48 (6): 2153 - 2176 (2025)

PERTANIKA JOURNALS

TROPICAL AGRICULTURAL SCIENCE

Journal homepage: http://www.pertanika.upm.edu.my/

Antagonistic Potential and Plant Growth Enhancement by Endophytic *Bacillus* Isolated from Citrus Plants

Erika Ananda Putri, Elvi Yuningsih, Siti Subandiyah, and Tri Joko*

Department of Plant Protection, Faculty of Agriculture, Universitas Gadjah Mada, Flora Street No. 1, Bulaksumur, 55281 Yogyakarta, Indonesia

ABSTRACT

Citrus is a horticultural commodity with high economic value. However, citrus production is constrained by various plant diseases caused by infectious pathogens. Endophytic bacteria that live in plant tissues can function as plant growth promoters and biological control agents by producing growth hormones and encoding antibacterial and antifungal genes. This study aimed to isolate endophytic *Bacillus* from citrus plants as plant growth-promoting bacteria. Endophytic bacteria were initially isolated from citrus leaf tissue, followed by morphological characterization and KOH tests and the detection of growth-encoding (*ipdC*, *acdS*, *pqqE*, and *nifH*), antibacterial (*aiiA* and *sfp*), and antifungal (*fenD*, *bamC*, and *ituA*) genes with specific primers. Thereafter, antagonistic tests against *Colletotrichum* sp. were performed, and the *Bacillus* isolates were applied to citrus seedlings. Ten *Bacillus* isolates were obtained from different locations. Detection of the plant-beneficial traits encoding genes showed that the isolate BYL-4 had all the genes encoding for growth, antibacterial, and antifungal properties. Antagonist testing was performed using the dual culture and coculture methods, which revealed that the SH-1, SH-2, SH-3, BYL-1, BYL-2, BYL-3, B2B, M2, and P4 isolates were able to inhibit the growth of *Colletotrichum* sp. Based on the application of the *Bacillus* isolates to seedlings, the *Bacillus* BYL-3 isolate significantly increased the height, fresh weight, dry weight, and root weight of the citrus plant seedlings. Molecular identification using conventional PCR was performed with a pair of universal 16S rRNA primers, 27F/1492R, with an amplification target of ±1500 bp, followed by Sanger sequencing. This showed that the isolated endophytic bacteria were closely related to two *Bacillus* species, namely *Bacillus subtilis* subsp. *subtilis* and *Bacillus tropicus*.

Keywords: Antibacterial, antifungal, plant-beneficial traits, PCR, 16S rDNA

ARTICLE INFO

Article history:
Received: 27 December 2024
Accepted: 27 August 2025
Published: 25 November 2025

DOI: https://doi.org/10.47836/pjtas.48.6.24

E-mail addresses:
erikaananda02@mail.ugm.ac.id (Erika Ananda Putri)
elviyuningsih@mail.ugm.ac.id (Elvi Yuningsih)
sitisubandiyah@ugm.ac.id (Siti Subandiyah)
tjoko@ugm.ac.id (Tri Joko)
*Corresponding author

e-ISSN: 2231-8542

INTRODUCTION

Citrus is a horticultural commodity that has been extensively developed worldwide. Brazil is the largest citrus producer in the world, with an estimated annual citrus production of 17.3 million tons (Dala-Paula et al., 2019). In 2016, global citrus production reached approximately 131 million tons of fresh fruit, comprising 52% oranges, 29% mandarins, 12% limes and lemons, and 7% grapefruits. Meanwhile, in the Asian region, China is one of the largest citrus producers, with fruit production reaching 7.3 million tons per year, followed by countries in the European region, which is the third largest citrus producer, with total production reaching 11,497 million tons per year (Sariasih et al., 2024). Moreover, in the Middle East region, as well as in countries such as India, Pakistan, Brazil, Argentina, and Mexico, citrus fruit production contributes to approximately 5% of the country's total agricultural economic income (Donkersley et al., 2018). As a tropical and subtropical crop, citrus is host to numerous pests and diseases. This plant is highly vulnerable to various destructive diseases that continue to emerge, thus potentially hindering or even completely wiping out production. Various bacterial, fungal, and viral diseases pose an ongoing threat to citrus cultivation, which leads to a substantial reduction in yield across all growing regions worldwide (Poveda et al., 2021). Fungi account for 25%-75% of citrus leaf disease (Asharo et al., 2024). One of the fungal pathogens that infects citrus plants is *Colletotrichum*. This fungus causes anthracnose disease in citrus plants and is characterized by leaf and flower necrosis as well as premature fruit fall (Munoz-Guerrero et al., 2021; Silva et al., 2014).

Colletotrichum was recently recognized as a major plant pathogen causing anthracnose, a plant disease that affects various hosts from trees to grasses (Gautam, 2014). *Colletotrichum* species can infect over 30 plant genera, which leads to anthracnose disease and postharvest decay in a diverse range of crops, including tropical, subtropical, and temperate fruits, grasses, vegetables, and ornamental plants. The agricultural losses caused by *Colletotrichum* infection are particularly severe in staple food crops cultivated in developing regions across the tropics and subtropics. Moreover, many *Colletotrichum* species function as latent pathogens, endophytes, epiphytes, or saprobes and shift to a pathogenic state when the host plants experience stress or are stored postharvest. Several *Colletotrichum* species have been associated with citrus, belonging to four species complexes: the *C. boninense* species complex (including *C. boninense*, *C. citricola*, *C. constrictum*, *C. karstii*, and *C. novae-zelandiae)*; the *C. acutatum* species complex (including *C. abscissum*, *C. acutatum*, *C. citri*, *C. godetiae*, *C. johnstonii*, *C. limetticola,* and *C. simmondsii*); and the *C. gloeosporioides* species complex (including *C. fructicola*, *C. gloeosporioides*, *C. kahawae* subsp. *ciggaro,* and *C. siamense*) (Guarnaccia et al., 2017).

In general, pest and disease control techniques in citrus plants are performed by managing pests and diseases in an integrated manner, namely using disease-free citrus seeds, utilizing biological agents, conducting environmental sanitation and good cultivation

practices, maintaining plants optimally, and monitoring them regularly (Paudyal, 2016; Widyaningsih et al., 2017). One effort that is currently being considered for development is using biological agents to induce plant resistance, one of which is endophytic antagonistic bacteria (Navitasari et al., 2020). Endophytic *Bacillus* are often used as biological control agents in agriculture for plant diseases (Chen et al., 2018). These bacteria have high antibiosis capabilities and can inhibit competitors with parasitism. *Bacillus* species are reported to form endospores and produce various beneficial metabolites, such as antibiotics and enzymes, and secondary metabolites that are antimicrobial and plant growth promoters.

Munir et al. (2022) reported that endophytic *B. subtilis* L1-21 isolated from healthy citrus plants presented an innovative approach to disease management in citrus plants. Furthermore, research by Nan et al. (2021) showed that *B. velezensis* was able to produce antimicrobial compounds, such as surfactin, fengycin, iturin A, macrolactin, difficidin, bacillaene, bacilysin, and bacillibactin. In addition, the application of *B. amyloliquefaciens* to two-year-old citrus plants infected with *Candidatus* Liberibacter asiaticus via root irrigation resulted in higher photosynthesis parameters, chlorophyll content, resistance-related enzyme content, and defense-related gene expression compared with those of the control plants (Lestiyani et al., 2024). Moreover, research using the antagonism test on endophytic bacteria against the anthracnose disease-causing pathogenic fungus *C. scovillei* in large chilies showed that the endophytic bacteria tested had excellent potential growth inhibitory activity against *C. scovillei* with an inhibition value of up to 80% (Wei et al., 2023). Other research related to the testing of the inhibitory effect of endophytic bacteria on the fungus *Colletotrichum*, which also causes anthracnose disease in strawberries, showed that the endophytic bacteria tested had a growth inhibitory activity of 60%–75% (Murtado et al., 2020). Based on the results of previous studies about the abilities of endophytic bacteria, this study aimed to isolate and identify endophytic bacteria from citrus plants and assess their potential as biological control agents.

MATERIALS AND METHODS

The research was performed at the Laboratory of Plant Pathology, Department of Plant Protection, Faculty of Agriculture, Universitas Gadjah Mada, Yogyakarta, Indonesia.

Isolation of Endophytic *Bacillus*

Healthy Citrus Siamese cultivar leaf samples, approximately two weeks old on stages V5 (Ribeiro et al., 2021), were collected from four locations: Purworejo, Yogyakarta, Magelang, and Boyolali. The leaf samples were disinfected with 70% alcohol for 1 min, 2% NaOCl for 3 min, absolute alcohol for 30 s, and sterile distilled water for 5 min, with three repetitions of rinsing with sterile distilled water. The leaf veins were taken and cut into small pieces until the sample weight reached 2 g. The sample was then ground using a

mortar and pestle with a mixture of 1 g of fresh leaf vein sample per 3 mL of 0.85% NaCl until smooth. The resulting suspension was then diluted to a 10^{-10} dilution series with 0.85% NaCl, and each dilution series was homogenized. The suspension was then heated at 60°C for 15 min using a water bath. Heat treatment was specifically applied for the isolation of *Bacillus* from leaf tissues to minimize the growth of non-*Bacillus* bacteria because *Bacillus* is classified as a thermophilic bacterium capable of surviving at temperatures up to 70°C (Abdollahi et al., 2021). This approach is based on the fact that most vegetative bacterial cells cannot withstand prolonged exposure to high temperatures, whereas *Bacillus* spores can remain viable. The endospores produced by *Bacillus* are formed in response to high cell density or nutritional stress, typically under carbon and nitrogen starvation conditions. Mature *Bacillus* and related genera endospores exhibit resistance to heat, UV radiation, and γ-radiation (Logan & Vos, 2015). The appropriate dilution was then spread on yeast peptone agar (YPA) media containing 0.5% yeast extract, 1% polypeptone, and 1.5% agar and incubated under aerobic conditions at 37°C for 24 h (Unban et al., 2020). YPA medium was used to culture *Bacillus* because of its rich nutrient content that supports both aerobic and facultative anaerobic metabolism, as well as spore germination. Yeast extract provides essential vitamins and amino acids, while peptone serves as a nitrogen source for protein synthesis and cellular functions (Davami et al., 2015). YPA has proven effective for promoting *Bacillus* growth and enzyme production, as shown in studies using similar media (Ismail et al., 2018), and is suitable for culturing various *Bacillus* species. Endophytic bacterial isolates were then purified by taking bacterial colonies with different characteristics from each Petri dish. The selected colonies were streaked on YPA media and incubated at 37°C for 24–48 h.

Morphological Observation and the KOH Test

The morphological characteristics of the endophytic bacterial colonies were observed based on their shape, edges, elevation, size, gloss, and texture (Lata et al., 2024). The bacterial isolate was first placed on a glass surface, and then 3% KOH was dripped onto it to perform the Gram test. The bacterial isolate and 3% KOH were mixed until smooth and then observed. The bacterial isolate being tested was determined to be a gram-negative bacterial group if mucus forms (sticky) or a gram-positive bacterial group if no mucus forms (not sticky) (Afriani et al., 2018).

Identification Based on 16S rRNA Gene Fragments

A total of 10 endophytic *Bacillus* isolates were subjected to PCR analysis using a pair of universal 16S rRNA primers, namely 27F (5′ AGA GTT TGA TCC TGG CTC AG 3′) and 1492 R (5′ GGT TAC CTT GTT ACG ACTT 3′), with an amplification target of ±1500 bp. PCR was performed on a standard thermocycler (Bio-Rad T100, Germany) using 25

µL of master mix (GoTaq, Promega), 4 µL each of the forward and reverse primers, 8 µL of DNA template, and 9 µL of nuclease-free water to a total volume of 50 µL. Next, amplification was performed according to the following PCR protocol, with an initial denaturation program of 94°C for 2 min followed by 34 cycles of denaturation at 94°C for 15 s, annealing at 55°C for 30 s, and extension at 68°C for 30 s, followed by a final extension at 72°C for 5 min. PCR products were analyzed using electrophoresis on a 1.5% agarose gel in 1× TBE buffer, with 2 µL of RedSafe added (Intron Biotechnology, Korea). DNA-size comparison was made using a 100-bp DNA ladder marker (Promega). Electrophoresis was performed using an electrophoresis machine (Bio-Rad) at 50 V for 50 min. Gel visualization was performed under a UV transilluminator (Trianom et al., 2019).

The PCR products were then purified and sent to a sequencing service company (1st Base, Malaysia). The sequencing results were analyzed using the basic local alignment search tool (BLAST), which is available on the National Center for Biotechnology Information website (www.ncbi.nlm.nih.gov/Blast.cgi), to determine the homology percentage. The nucleotide sequence of the endophytic *Bacillus* isolates was checked using the BLAST-N program, and phylogenetic analysis was performed using the Maximum Likelihood method with 1,000 bootstrap iterations and the Kimura-2 model.

Detection of Plant-Beneficial Trait (PBT) Encoding Genes

PBT-encoding gene detection was performed on the 10 identified endophytic *Bacillus*. The isolates were grown on YPA media and incubated for 48 h. Bacterial DNA was extracted using the G-spin™ Genomic DNA Extraction Kit (for Bacteria) (Intron Biotechnology, Korea) using a previously reported protocol (Kim et al., 2022). The identified PBT-encoding genes included growth promotion, antibacterial, and antifungal encoding genes, which were detected using the standard PCR method. The PCR reagents used for each reaction were 5 µL of master mix (GoTaq, Promega), 1 µL of each forward and reverse primer, 1 µL of bacterial DNA, and 2 µL of nuclease-free water to a total volume of 10 µL. The specific gene primers used are presented in Table 1. Furthermore, amplification was performed on a thermocycler (Bio-Rad T100 Thermal Cyclers) with a PCR protocol of an initial denaturation program of 95°C for 3 min, followed by 35 cycles of denaturation at 95°C for 1 min, annealing for 30 s (see Table 1 for specific annealing temperatures), extension at 72°C for 1 min, followed by a final extension at 72°C for 10 min and a final hold at 12°C for 1 min (Handiyanti et al., 2018).

The amplified DNA products were visualized using electrophoresis on a 1% agarose gel and 3 µL RedSafe (Intron Biotechnology, Korea) in 1× TBE buffer with a 100-bp and 1-kb DNA ladder (Promega) for size comparison. Electrophoresis was performed using an electrophoresis machine (Bio-Rad DNA Electrophoresis Cell) at 50 V for 50 min. The gel was then observed under a UV transilluminator.

Table 1
List of primers for genes encoding plant-beneficial traits in Bacillus *species*

Gene Expression	Gene	Primer name	Primer Sequence (5'-3')	Annealing (^{0}C)	Reference
Indolepyruvate	*ipdC*	F-ipdC	CAYTTGAAAACKCAMTATACTG	50	Raddadi et al., 2008
decarboxylase		R-ipdC	AAGAATTTGYWKGCCGAATCT		
ACC deaminase	*acdS*	105F-adS	TGCCAAGCGTGAAGACTGC	58	Jaya et al., 2019
		224R-acdS	GGGTCTGGTTCGACTGGAT		
Phosphatase solubilization	*pqqE*	pqqE-F	GARCTGACYTAYCGCTGYCC	55	Ding et al., 2005
		pqqE-R	TSAGSAKRARSGCCTGR		
Nitrogenase	*nifH*	nifH-F	GGCTGCGATCCVAAGGCCGAYTCVACCCG	55	Suleman et al., 2018
		nifH-R	CTGVGCCTTGTTYTCGCGGATSGGCATGGC		
Surfactin	*sfp*	P17	ATGAAGATTTACGGAATTTA	46	Lahlali et al., 2020
		P18	TTATAAAAGCTCTTCGTACG		
Anti quorum- sensing	*aiiA*	aiiA240B1	ATGGGATCCATGACGTAAAGAAGCTTTAT	55	Dong et al., 2002
		aiiACOT1	GTCGAATTCCTCAACAAGATACTCCTAATG		
Fengycin	*fenD*	FENDF	GGCCCGTTCTCTAAATCCAT	62	Mora et al., 2011
		FENDR	GTCATGCTGACGAGAGCAAA		
Bacillomycin	*bamC*	BACC1F	GAAGGACACGGCAGAGAGTC	60	Ramarathnam et al., 2007
		BACC1R	CGCTGATGACTGTTCATGCT		
iturinA	*ituA*	ITUD1F	GATGCGATCTCCTTGGATGT	60	Athukorala et al., 2009
		ITUD1R	ATCGTCATGTGCTGCTTGAG		

In Vitro Antagonistic Test of Endophytic *Bacillus* against *Colletotrichum* sp.

An antagonistic test of endophytic *Bacillus* against *Colletotrichum* sp. isolated from citrus plants was conducted *in vitro* using the dual culture (Wisanggeni et al., 2023) and coculture (Jayanti & Joko, 2020) methods. The dual culture method was performed by growing *Colletotrichum* sp. in the middle of potato dextrose agar (PDA) medium. Furthermore, the endophytic bacterial isolate was scratched approximately 4 cm long on the edge of the Petri dish, which was 2 cm from the pathogenic fungus. Observations were made by measuring the diameter of the fungal colony for 7 days at 25°C-28°C. The ability of the antagonistic bacteria to inhibit fungal growth was calculated using the following formula (Abdullah et al., 2024):

$$P = \frac{(R1 - R2)}{R1} x\ 100$$

Remarks:
P = Percentage of Inhibition of Radial Growth (PIRG) (%)
R1 = Average radius of plant pathogenic fungal colonies without bacteria (cm)
R2 = Average radius of fungal colonies approaching the bacteria (cm)

Meanwhile, the coculture method was conducted by adding 10 mL of 0.7% water agar (WA) at 50°C with 100 µL of bacterial suspension at a density of 10^8 CFU/mL onto PDA medium in a Petri dish. Furthermore, the *Colletotrichum* isolate was placed in the middle of the WA medium. The culture was incubated for 7 days at room temperature. The inhibitory ability of the endophytic bacterial isolates was measured by calculating the mycelium growth of *Colletotrichum* sp. for 7 days using the following formula:

$$P = \frac{C - T}{C} x\ 100$$

Remarks:
P = Percentage of Inhibition of Radial Growth (PIRG) (%)
C = Diameter of pathogenic fungal growth in the control treatment (cm)
T = Diameter of pathogenic fungal growth in the antagonistic bacteria treatment (cm)

Application of Endophytic *Bacillus* to Citrus Seedlings

Endophytic *Bacillus* was applied to Citrus Siamese cultivar seedlings by preparing the plants and suspensions of all 10 endophytic *Bacillus* isolates. A total of 55 citrus seedlings were used, with five replicates of each endophytic *Bacillus* isolate application and five control seedlings. The application was performed by watering the roots of the seedlings

once a week with a *Bacillus* isolate at a density of 10^8 CFU/mL (Marisna et al., 2024; Riera et al., 2017) and an application volume of 20 mL per tray hole.

Observation of the Effects of Endophytic *Bacillus* on the Growth of Citrus Seedlings

Observation of the citrus seedlings growth was performed for 60 days after planting. Plant height was measured using a meter ruler in centimeters (cm) from the ground surface to the tip of the last growing point once a week for 8 weeks. The fresh weight of the plant was measured using an analytical scale, while the dry weight was measured using an analytical scale after being oven-dried at 60°C for 72 h. The roots were cleaned and then measured with a ruler from the base to the tip in cm to determine the length. The root volume was determined by measuring the difference between the water volume after the roots were put into the measuring beaker and the initial water volume.

Statistical Analysis

Statistical analysis was performed using an analysis of variance with Tukey's test and a 95% confidence level in SPSS software.

RESULTS

Isolation and Characterization of Endophytic *Bacillus* Isolates

The bacterial isolates were characterized morphologically based on color, size, shape, edge, and elevation (Figure 1). A total of 10 isolates with different morphologies were successfully isolated from four regions: Boyolali (isolates BYL-1, BYL-2, BYL-3, and BYL-4), Yogyakarta (isolates SH-1, SH-2, SH-3, and P4), Purworejo (isolate B2B), and Magelang (isolate M2). All of the isolates collected were gram-positive bacteria based on the Gram test, which was indicated by the absence of mucus formation after 3% KOH dripping.

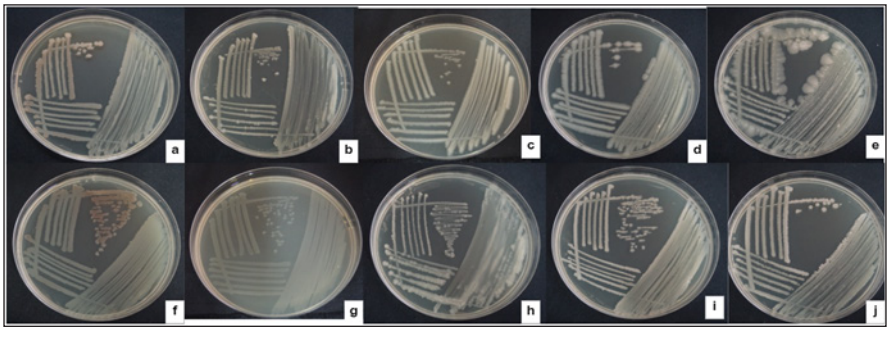

Figure 1. Bacterial growth on YPA media after 48 h. a: isolate BYL-1; b: isolate BYL-2; c: isolate BYL-3; d: isolate BYL-4; e: isolate SH-1; f: isolate SH-2; g: isolate SH-3; h: isolate P4; i: isolate M2; and j: isolate B2B

The BYL-1 isolate (Figure 1a) exhibited morphological characteristics on YPA medium, forming a reddish-white colony with a circular shape, irregular edges, convex elevation, and a shiny appearance. This aligns with the report by Flori et al. (2020), which mentions that *Bacillus* colonies are generally white to yellow, although some exhibit black, brown, orange, or pink pigments, with a convex to raised elevation. Similarly, the SH-2 isolate (Figure 1f) displayed a reddish-white colony with a circular shape, irregular edges, and a flat elevation. The BYL-2 and SH-3 isolates (Figures 1b and g) exhibited morphological similarities, characterized by cream-white colonies with a circular shape, irregular edges, and a non-shiny surface. The BYL-3 and BYL-4 isolates (Figures 1c and d) also shared similar morphological characteristics, exhibiting cream-white, non-shiny colonies with a convex elevation. Meanwhile, the SH-1, P4, M2, and B2B isolates (Figures 1e, h, i, and j) displayed comparable morphologies, forming cream-white, non-shiny, and powdery colonies with a circular shape, irregular edges, and flat elevation.

Molecular Detection of PBT-Encoding Genes

In this study, specific primer pairs were used to detect growth-promoting (indole pyruvate decarboxylase, ACC deaminase, phosphatase solubilization, and nitrogenase), antibacterial (antiquorum sensing and surfactin), and antifungal (fengycin, bacillomycin D, and iturin A) encoding genes. The results showed that among the 10 *Bacillus* isolates, six isolates (SH-2, BYL-1, BYL-3, BYL-4, B2B, and M2) had the growth promotion-encoding gene indole pyruvate decarboxylase (*ipdC*), with an amplicon size of 1850 bp (Figure 2a). Six isolates (BYL-1, SH-1, SH-2, SH-3, BYL-4, and B2B) had the ACC deaminase (*acdS*) encoding gene, with an amplicon size of 1,017 bp (Figure 2b). Six isolates (SH-2, SH-3, BYL-2, BYL-4, B2B, and M2) had the phosphatase solubilization (*pqqE*) encoding gene, as evidenced by a 451 bp amplicon size (Figure 2c). Five isolates (SH-2, SH-3, BYL-4, B2B, and M2) had the nitrogenase (*nifH*) encoding gene, with an amplicon size of 323 bp (Figure 2d). Two isolates (BYL-3 and BYL-4) had the antiquorum sensing (*aiiA*) encoding gene (antibacterial), with an amplicon size of 900 bp (Figure 2e). All isolates had the surfactin (*sfp*) encoding gene with an amplicon size of 675 bp (Figure 2f), fengycin (f*enD*) encoding gene with an amplicon size of 269 bp (Figure 2g), bacillomycin D (*bamC*) encoding gene with an amplicon size of 875 bp (Figure 2h), and iturin A (*ituA*) encoding gene with an amplicon size of 647 bp (Figure 2i).

Antagonistic Test of Endophytic *Bacillus* Against *Colletotrichum* sp.

The antagonist test using the dual culture method revealed that 70% of the endophytic *Bacillus* isolates could inhibit *Colletotrichum* grown on the same media. Of the 10 endophytic bacterial isolates tested using the dual culture method against the pathogenic fungus *Colletotrichum* sp., the endophytic bacterial isolate SH-1 exhibited the smallest mycelial diameter of *Colletotrichum* sp. compared with the control (Figure 3), with an

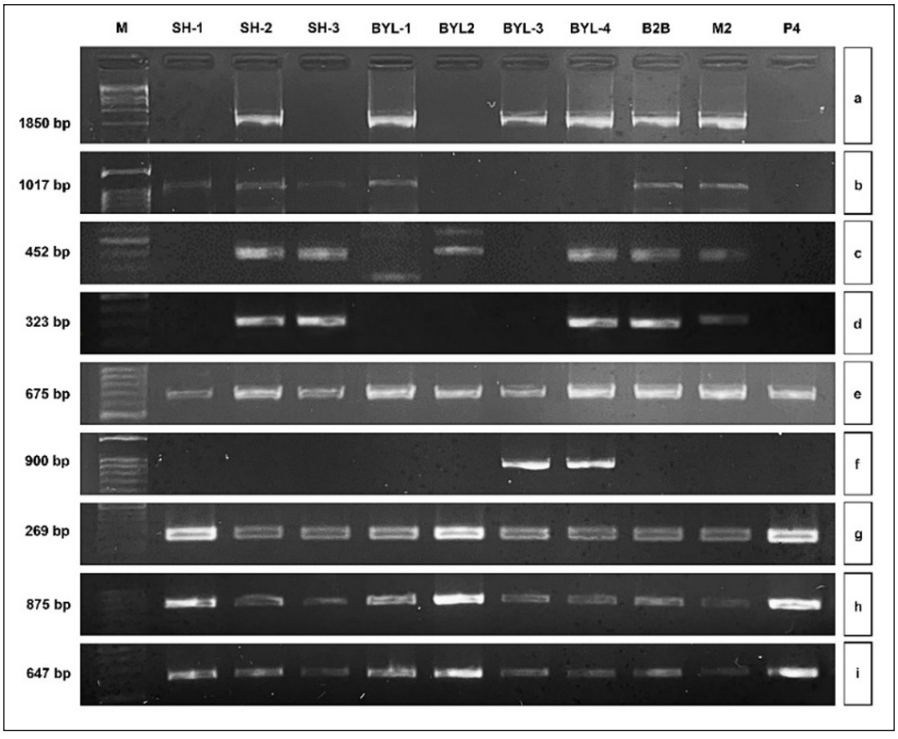

Figure 2. Amplification of plant growth-promoting bacteria (PGPB) coding genes in endophytic *Bacillu*s on a 1% agarose gel. (a) *ipdC*; (b) *acdS*; (c) *pqqE*; (d) *nifH*; (e) *sfp*; (f) *aiiA*; (g) *fenD*; (h) *bamC*; and (i) i*tuA*. The formation of a DNA band indicates a positive result

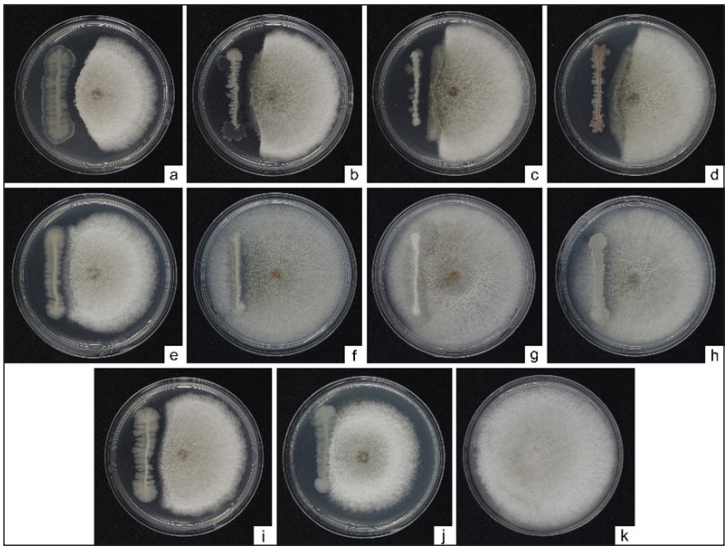

Figure 3. Antagonistic test of endophytic *Bacillus* isolates against *Colletotrichum* sp. on day 7 using the dual culture method. (A) SH-1; (B) SH-2; (C) SH-3; (D) BYL-1; (E) BYL-2; (F) BYL-3; (G) BYL-4; (H) B2B; (I) M2; (J) P4; and (K) Control

inhibitory rate of 64.81%. Seven out of the ten isolates showed significantly different results from the control, namely isolates SH-1, SH-2, SH-3, BYL-1, BYL-2, M2, and P4, while isolates BYL-3, BYL-4, and B2B did not differ significantly from the control (Table 2).

Table 2
Endophytic Bacillus *isolates' ability to inhibit the growth of* Colletotrichum *sp. on day 7 using the dual culture method*

Isolate	Mycelial diameter (cm)	Percentage of Inhibition of Radial Growth (PIRG) (%)
SH-1	5.27	64.81 a
SH-2	5.60	59.93 ab
SH-3	5.40	63.81 a
BYL-1	5.67	54.37 ab
BYL-2	5.73	46.37 b
BYL-3	7.47	5.36 d
BYL-4	7.50	9.43 d
B2B	7.87	3.33 d
M2	5.47	60.96 ab
P4	6.07	28.95 c
Control	8.13	0 d

The antagonistic tests using the coculture method on 10 endophytic *Bacillus* isolates grown on the same media, namely PDA and WA media, showed that all isolates could inhibit the growth of *Colletotrichum* sp., but had different inhibition rates. The endophytic bacterial isolates SH-1, SH-2, SH-3, and BYL-1 had the smallest mycelial diameter of *Colletotrichum* sp. compared to the control (Figure 4), with an inhibitory rate of 100% (Table 3).

Table 3
Endophytic Bacillus *isolates' ability to inhibit the growth of* Colletotrichum *sp. on day 7 using the coculture method*

Isolate	Mycelial diameter (cm)	Percentage of Inhibition of Radial Growth (PIRG) (%)
SH-1	0	100 a
SH-2	0	100 a
SH-3	0	100 a
BYL-1	0	100 a
BYL-2	3.6	55 c
BYL-3	5.42	32.25 d
BYL-4	6.9	13.75 e
B2B	4.48	44 cd
M2	3.74	78.25 c
P4	1.74	53.25 b
Control	8	0 e

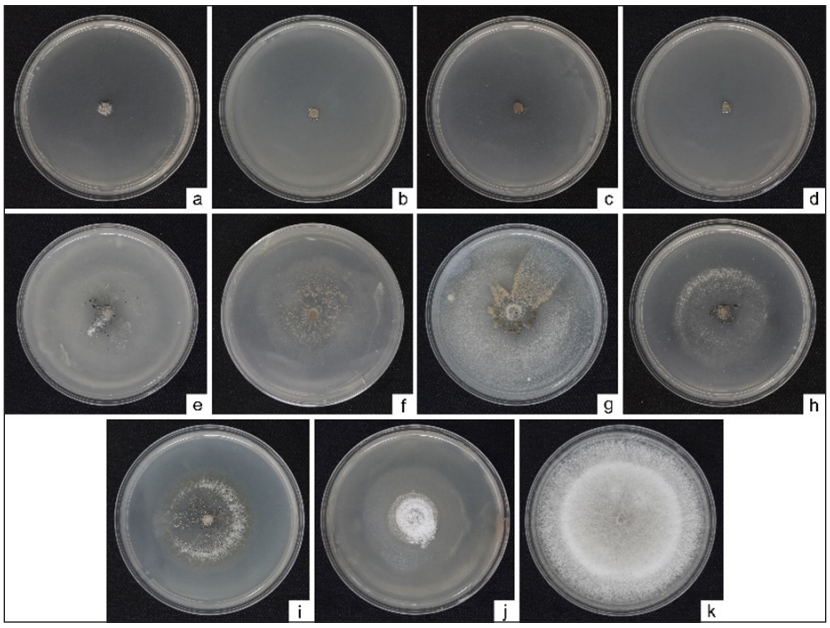

Figure 4. Antagonistic test of endophytic bacterial isolates with *Colletotrichum* sp. on day 7 using the coculture method; (A) SH-1; (B) SH-2; (C) SH-3; (D) BYL-1; (E) BYL-2; (F) BYL-3; (G) BYL-4; (H) B2B; (I) M2; (J) P4; and (K) Control

Effects of Endophytic *Bacillus* on the Growth of Citrus Seedlings

The efficiency of endophytic *Bacillus* in improving the citrus seedlings' growth was assessed in a greenhouse experiment. Citrus seedlings that were treated with endophytic *Bacillus* exhibited better agronomic characteristics compared with the control plants (Figure 5). Treatment with the BYL-3 isolate provided the best results and was significantly different from the control in terms of fresh weight, dry weight, and root weight. All treatments, except for isolate BYL-1, significantly affected the fresh weight. Meanwhile, all treatments, except for isolate BYL-2, did not significantly affect seedling height (Table 4).

Table 4
Effects of endophytic Bacillus *isolate treatment on citrus seedling height, fresh weight, dry weight, root weight, and root volume at 8 weeks after planting (mean ± standard error (SE)*

Isolate	SH (cm)	FW (gram)	DW (gram)	RW (gram)	RV (mL)
BYL-1	6.42 ± 0.92 ab	0.37 ± 0.02 cd	0.12 ± 0.01 c	0.15 ± 0.02 d	0.83 ± 0.17 a
BYL-2	4.21 ± 1.10 b	0.66 ± 0.05 abc	0.13 ± 0.04 c	0.17 ± 0.04 cd	0.63 ± 0.19 a
BYL-3	7.65 ± 0.53 a	0.98 ± 0.07 a	0.27 ± 0.04 a	0.42 ± 0.03 a	1.33 ± 0.33 a
BYL-4	7.45 ± 0. 36 a	0.76 ± 0.06 ab	0.23 ± 0.02 abc	0.30 ± 0.05 abcd	1.33 ± 0.33 a
SH-1	5.80 ± 0,68 ab	0.71 ± 0.03 ab	0.20 ± 0.01 abc	0.32 ± 0.01 abc	1.33 ± 0.33 a
SH-2	5.35 ± 0.59 ab	0.77 ± 0.04 ab	0.23 ± 0,02 abc	0.30 ± 0.02 abcd	1.00 ± 0.00 a

Table 4 *(continue)*

Isolate	SH (cm)	FW (gram)	DW (gram)	RW (gram)	RV (mL)
SH-3	6.85 ± 0.50 ab	0.61 ± 0.04 bc	0.16 ± 0.02 abc	0.26 ± 0.02 bcd	0.83 ± 0.17 a
P4	5.67 ± 0.50 ab	0.69 ± 0.06 abc	0.19 ± 0.02 abc	0.34 ± 0.03 ab	0.83 ± 0.17 a
M2	6.48 ± 0.59 ab	0.83 ± 0.12 ab	0.24 ± 0.03 ab	0.31 ± 0.04 abc	1.33 ± 0.35 a
B2B	6.82 ± 0.71 ab	0.75 ± 0.01 ab	0.18 ± 0.03 abc	0.28 ± 0.03 abcd	1.17 ± 0.44 a
Control	6.07 ± 0.87 ab	0.26 ± 0.11 d	0.13 ± 0.02 bc	0.22 ± 0.03 bcd	0.67 ± 0.17 a

Note. SH: seedling height; FW: fresh weight; DW: dry weight; RW: root weight; RV: root volume. Means followed by the same letters in the same column are not significantly different based on the Tukey test with a 95% confidence level

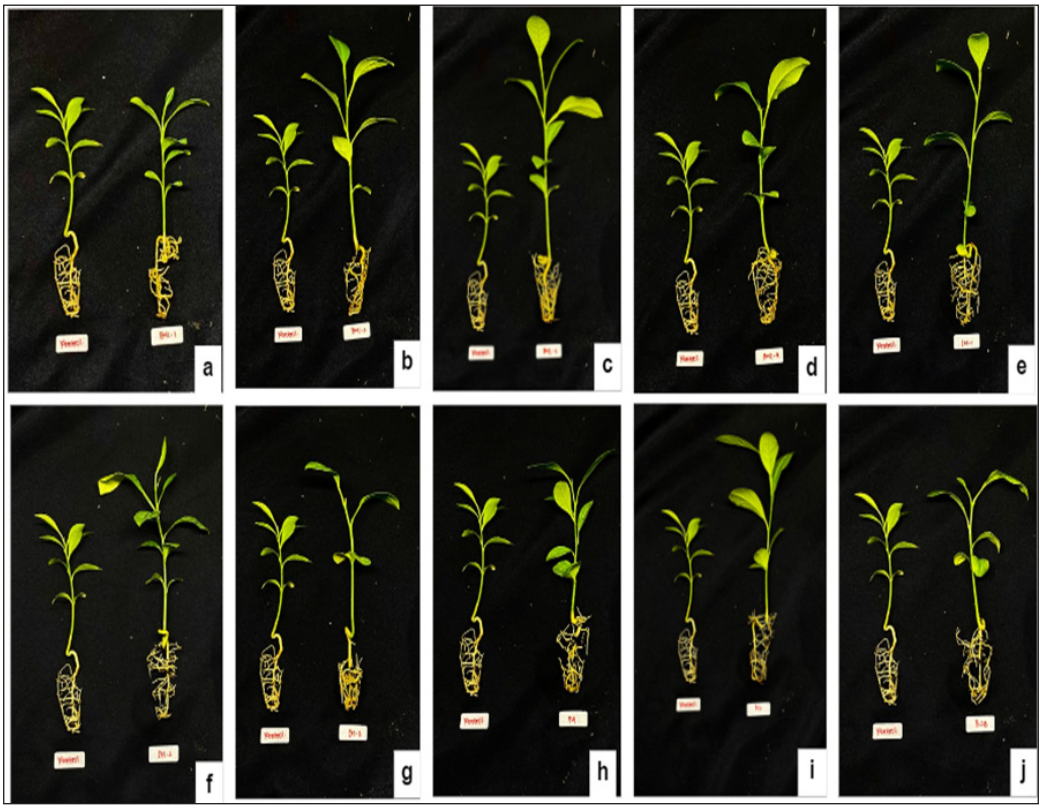

Figure 5. Comparison between citrus seedlings treated with endophytic *Bacillus* isolate and the control. (a) control vs. BYL-1; (b) control vs. BYL-2; (c) control vs. BYL-3; (d) control vs. BYL-4; (e) control vs. SH-1; (f) control vs. SH-2; (g) control vs. SH-3; (h) control vs. P4; (i) control vs. M2; and (j) control vs. B2B

Note. Right side: citrus seedlings with isolate treatment; Left side: control

Identification Based on 16S rRNA Gene Fragments

Molecular identification of the endophytic *Bacillus* isolates was performed using a pair of 16S universal primers. The amplicons of all endophytic bacterial isolates using PCR with a pair of primers 27F/1492R were ±1500 bp in size and observed using a UV transilluminator (Figure 6). Furthermore, Sanger sequencing was performed to determine the nucleotide sequences of the DNA amplicon. Phylogenetic analysis (Figure 7) revealed that isolates SH-1, SH-2, B2B, M2, BYL-1, SH-3, P4, and BYL-2 were most closely related to *B. subtilis* subsp. *subtilis*, whereas isolates BYL-3 and BYL-4 were most closely related to *B. tropicus*.

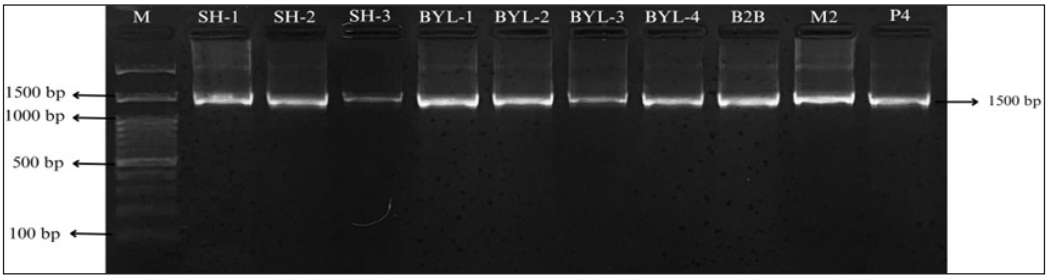

Figure 6. PCR amplification products of the 16S rRNA gene markers from 10 endophytic *Bacillus* isolates were verified on a 1.5% agarose gel
Note. M = 1 kb DNA ladder marker

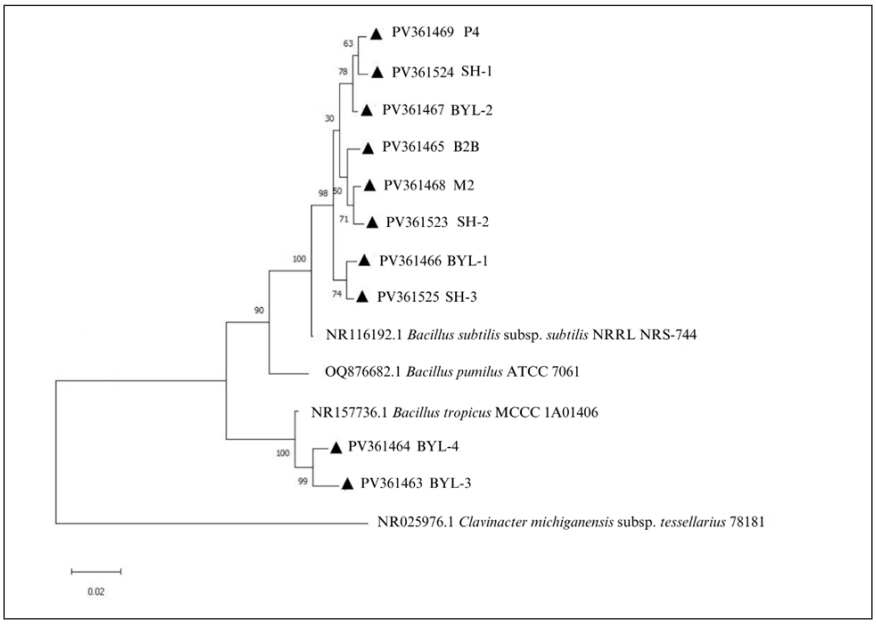

Figure 7. Phylogenetic analysis of 16S rRNA sequences of 10 endophytic *Bacillus* isolates with reference sequences from NCBI using the MEGA Maximum Likelihood method based on the Kimura-2 model with 1,000 bootstrap iterations. *Clavibacter michiganensis* subsp. *tessellarius* 78181 was used as an outgroup

DISCUSSION

This study examined the potential of endophytic *Bacillus* as a beneficial bacterium that can increase plant growth and encode several genes related to antifungal and antibacterial activities. The morphological characteristics of the 10 successfully isolated endophytic bacteria isolates revealed that they had a similar morphology to that of *Bacillus*, namely cream-colored colonies with uneven, non-slimy edges, convex or flat elevations, dry and powdery surfaces, and shiny or non-shiny appearance. This finding is supported by Astuti et al. (2017), who mentioned that *Bacillus* has round colonies with wavy edges, is white in color, and has flat or raised elevations. The collected bacterial isolates did not form mucus when reacted with 3% KOH, indicating that the bacteria were gram-positive. Gram-positive bacteria have a simpler and thicker cell wall structure (approximately 30–100 nm) compared with that of gram-negative bacteria (approximately < 10 nm), which is composed of peptidoglycan (Rohde, 2019).

The systemic induction of plant growth and antibacterial and antifungal genes by beneficial bacteria has the potential to contribute to pathogen control and plant growth enhancement. This study detected genes encoding beneficial traits in endophytic *Bacillus* isolates using PCR. Most endophytic *Bacillus* isolates used in this study demonstrated the ability to synthesize growth-promoting, antibacterial, and antifungal encoding genes. Most isolates were able to encode plant growth-encoding genes, such as indole pyruvate decarboxylase (*ipdC*), ACC deaminase (*acdS*), phosphatase solubilization (*pqqE*), and nitrogenase (*nifH*), and all isolates contained genes that are potentially involved in the synthesis of surfactin, bacillomycin D, iturin A, and fengycin. Indole pyruvate decarboxylase is an enzyme involved in the biosynthesis of indole-3-acetic acid (IAA) from tryptophan via the indole pyruvate (IpyA) pathway, which is then converted into indole 3-acetaldehyde (IAAId) (Shah et al., 2022). Batista et al. (2021) reported the presence of the *ipdC* gene in *B. thuringiensis* RZ2MS9, which encodes indole pyruvate decarboxylase. However, the presence of the *ipdC* gene in other *Bacillus* sp. strains is rare, especially in the *B. amyloliquefaciens* strain, which is known as the best auxin stimulator. ACC deaminase produced by endophytic bacteria in plants protects plants from abiotic stresses, such as salinity, drought, and heavy metal stress (Naing et al., 2021). *B. amyloliquefaciens* and *B. cereus* have been reported as being able to encode the ACC deaminase (*acdS*) gene (Shahid et al., 2023; Tian et al., 2022). Most *Bacillus* species have been reported to be able to dissolve phosphate in the environment, thereby making it available to plants. The phosphorus content in plants is important for the process of cell division and development of new tissues. In general, the availability of phosphate in the soil is abundant, but only 0.1% of the total phosphate is available to plants (Mei et al., 2021). Yahya et al. (2022) reported that *Bacillus* species, such as *B. subtilis*, *B. cereus*, *B. polymyxa*, *B. circulans*, and *B. megaterium*, can dissolve organic phosphate hydrolyzed by acid phosphatase,

alkaline phosphatase, and phytase encoded by the phosphatase gene. *B. cereus* is reported to play a role as a strong phosphate solubilizer and is resistant to soil salinity (Kulkova et al., 2023). In addition, *B. megaterium* MJ1212 plays a role in dissolving phosphate and regulating the plants' carbohydrate and amino acid content to support plant growth (Mohamed et al., 2018). Yao and Xiaomei (2020) also reported that *B. mycoides* Gnyt1 could encode phosphatase solubilization encoding genes, such as *pqqA*, *pqqB*, *pqqC*, and *pqqE*. Nitrogenase is an enzyme that catalyzes nitrogen fixation. Several genes are involved in the nitrogen fixation process, including the *nif* gene, which codes for the primary nitrogenase components (Fernandes et al., 2014). The nitrogenase gene in plant growth-promoting bacteria increases N_2 fixation from the atmosphere, thus making it available to plants. Several species of *Bacillus*, such as *B. cereus*, *B. subtilis*, and *B. licheniformis,* can encode nitrogenase-encoding genes.

Bacillus species can produce three types of antibiotics (Ramarathnam et al., 2007; Ye et al., 2012). Surfactin, bacillomycin, and iturin are the most common lipopeptide antibiotics produced by *Bacillus* species. Several antibiotic genes reported to be produced by *B. subtilis* and *B. amyloliquefaciens* include bacillomycin D (*bamC*), fengycin (*fenD*), iturin (*ituA*), surfactin (*sfp*), and zwittermicin (*zmaR*) (Olanrewaju et al., 2017). Surfactin, iturin, and bacillomycin exhibit high antifungal activity. In addition, surfactin has the highest biosurfactant ability (Arthukorala et al., 2009) and is known to induce the formation of biofilms in bacteria. Meanwhile, the mechanism of fengycin as an antifungal agent against pathogens occurs via the destruction of the plasma membrane, cell wall, hyphae, and fungal conidia. According to Hanif et al. (2019), this can result in reduced virulence, cell death, damage to cell membranes and organs, and the inhibition of pathogen DNA synthesis. Bacillomycin D causes morphological changes in the plasma membrane and cell walls of hyphae and conidia, which ultimately cause pathogenic cell death (Gu et al., 2017). Iturin has limited antibacterial activity but has a wide range of antifungal activity (Ye et al., 2012). In addition to having a high antibiotic activity, iturin can increase swarming motility in bacteria (Joko et al., 2007). This is in agreement with the findings of this study, which showed that several endophytic *Bacillus* isolates demonstrated strong inhibitory effects against *Colletotrichum* sp., with some achieving up to 100% inhibition in the coculture method. Meanwhile, the results of the dual culture method did not reveal better outcomes compared to the coculture method. This is because the dual culture method involves positioning the bacterial isolate and fungal pathogen on opposite sides of the growth medium to observe the inhibition zones. In contrast, the coculture method allows bacterial and fungal cultures to grow together within the same medium, thus enabling their direct interactions. This method closely mimics natural conditions, which facilitates the expression of antagonistic mechanisms such as competition for nutrients and space, production of lytic enzymes, and secretion of antimicrobial compounds (Selegato & Castro-Gamboa, 2023).

In addition, the antiquorum sensing gene (*aiiA*) in some isolates exhibited inhibitory activity against quorum-sensing formation in pathogenic bacteria. In general, the *aiiA* gene can deactivate N-acyl-homoserine lactones (AHLs) or quorum sensing from gram-negative bacteria. Disruption of the pathogen quorum-sensing system with quorum quenching is an effective control strategy, where there are three enzymatic mechanisms of quorum quenching in inhibiting the formation of quorum sensing in pathogens, namely AHL lactonase, AHL acylase, and AHL oxidase and reductase. Among these mechanisms, AHL lactonase encoded by the *aiiA* gene is widely found in *Bacillus* (Rafaat et al., 2019).

Bacillus is known to be able to improve plant growth, especially during the seedling phase. This occurs because *Bacillus* produces phytohormones, such as IAA, cytokinins, gibberellins, ethylene, and abscisic acid. In general, IAA is an active form of the auxin hormone found in plants, where the hormone plays a role in improving the plant quality and yield. In addition, IAA functions in increasing cell development, stimulating new roots, accelerating flowering, increasing enzyme activity, and even being able to stimulate gene expression signals of several antagonistic bacteria with plants; thus, the direct application of *Bacillus* can increase the fresh weight of plants (Ilmiah et al., 2021; Oleńska et al., 2020). However, in this study, not all endophytic *Bacillus* isolate treatments significantly affected plant growth compared with the control treatment. This depends on the plant's response to the hormones that *Bacillus* can produce, where the plant's response to these hormones usually does not depend on the absolute quantity of hormones but rather on their relative concentration compared to that of other hormones. This influences the hormonal effects that *Bacillus* produces, meaning that even if the application of *Bacillus* concentration is increased to a certain point, the hormonal effects may not be significant. This is supported by the research of Giassi et al. (2016), who reported that the application of endophytic *Bacillus* can increase the height, fresh weight, dry weight, and root weight of citrus plants because endophytic *Bacillus* can produce IAA and fix nitrogen. However, this ability depends on the concentration of bacteria during the application. In general, low application concentrations can stimulate root growth, whereas applying bacteria at high concentrations will inhibit plant growth. In addition, another report from Giassi et al. (2016) mentioned that the application of *Bacillus* to citrus seedlings did not affect the development of the stem diameter but could increase the root weight.

In this study, the application of *Bacillus tropicus* BYL-3 to citrus plants was associated with an increase in the height, fresh weight, dry weight, and root weight of the citrus seedlings under controlled conditions. Meng et al. (2016) reported that *Bacillus* increases plant growth via root colonization. *B. velezensis* has been reported to be able to produce IAA, and *B. megaterium* produces cytokinin hormones during the root colonization process (Dunlap et al., 2015). In this process, *Bacillus* plays a role in increasing plant growth directly through the secretion of cytokinins and other volatile compounds, which later

affect the plant hormone tissues (Tsotetsi et al., 2022). Although this experiment was only conducted *in vitro*, the effect of *Bacillus* on plants supports the idea that citrus plants can develop disease resistance through the application of endophytic *Bacillus*. Marisna et al. (2024) reported the potential of *B. cereus* RC76 and *B. velezensis* B-27 in suppressing the feeding behavior of *Diaphorina citri*, the vector of *Candidatus* Liberibacter asiaticus. The study found that *D. citri* feeding on citrus seedlings treated with *B. cereus* RC76 exhibited a prolonged total duration of Np and C waveform activity, which indicates a possible disruption in feeding efficiency. In addition, citrus seedlings treated with *B. velezensis* B-27 revealed an extended total duration of the Np waveform in *D. citri* compared with the control, with the longest total duration observed for waveform G. These findings suggest that the application of *Bacillus* can interfere with *D. citri* feeding behavior, thereby potentially reducing pathogen transmission.

The molecular identification of the endophytic *Bacillus* isolates was conducted based on 16S rRNA gene analysis. The phylogenetic analysis results revealed that the isolates SH-1 (PV361524), SH-2 (PV361523), SH-3 (PV361525), BYL-1 (PV361466), BYL-2 (PV361467), B2B (PV361465), M2 (PV361468), and P4 (PV361469) were closely related to *B. subtilis* subsp. *subtilis*. Meanwhile, isolates BYL-3 (PV361463) and BYL-4 (PV361464) were closely related to *B. tropicus*. The type strain of *B. subtilis* subsp. *subtilis* NRL NRS-744 has a similarity with isolate SH-1 of 96.315%, SH-2 of 96.897%, SH-3 of 93.572%, BYL-1 of 96.983%, BYL-2 of 96.034%, B2B of 97.672%, M2 of 97.432%, and P4 of 96.466%. Meanwhile, the *B. tropicus* MCCC 1A01406 type strain has a similarity with isolate BYL-3 of 93.309% and BYL-4 of 94.989%.

CONCLUSION

Ten endophytic *Bacillus* isolates were isolated from citrus plants, with four of the isolates having the best ability as PGPB, namely isolates BYL-3, SH-1, SH-2, and SH-3. The detection of PBT genes showed that isolate BYL-3 encodes the *ipdC*, *nifH*, *aiiA*, *Sfp*, *ituA*, *bamC*, and *fenD* genes. Meanwhile, isolates SH-1, SH-2, and SH-3 encode the *acdS*, *sfp*, *ituA*, *bamC*, and *fenD* genes. Isolate BYL-3, which is closely related to *B. tropicus*, can significantly improve the growth of citrus seedlings, whereas isolates SH-1, SH-2, and SH-3, which are closely associated with *B. subtilis* subsp. *subtilis*, significantly suppresses the mycelium growth of *Colletotrichum* sp.

ACKNOWLEDGMENT

This study was supported in part by the Australian Center for International Agricultural Research (grant number ACIAR HORT 2019/164) and the Universitas Gadjah Mada under the RTA Program (grant number 5286/UN1.P1/PT.01.03/2024).

REFERENCES

Abdollahi, P., Ghane, M., & Babaeekhou, L. (2021). Isolation and characterization of thermophilic bacteria from Gavmesh Goli hot spring in Sabalan geothermal field, Iran: Thermomonas hydrothermalis and Bacillus altitudinis isolates as a potential source of thermostable protease. *Geomicrobiology Journal*. *38*(1), 87-95. https://doi.org/10.1080/01490451.2020.1812774

Abdullah, J. T., Suryanti, & Joko, T. (2024). Application of silica nanoparticles in combination with *Bacillus velezensis* and *Bacillus thuringiensis* for anthracnose disease control in shallot. *Pakistan Journal of Biological Sciences*, *27*(2), 80–89. https://doi.org/10.3923/pjbs.2024.80.89

Afriani, S. R., Pujiastuti, Y., Irsan, C., Damiri, N., Nugraha, S., & Sembiring, E. R. (2018). Isolation and toxicity test of *Bacillus thuringiensis* from Sekayu region soil, South Sumatra on *Spodoptera litura*. *IOP Conference Series: Earth and Environmental Science, 102*(1), Article 012066. https://doi.org/10.1088/1755-1315/102/1/012066

Asharo, R. K., Destiyana, N., Azzahrah, R. A., Syahbani, N., Azzahra, R., Nurza, I. M. A., Pasaribu, P. O., & Indrayanti, R. (2024). Isolation of pathogenic bacteria and initial resistance assay with detached fruit assay method on orange fruits (*Citrus* sp.). *AIP Conference Proceedings, 2982*(1), Article 050039. https://doi.org/10.1063/5.0183723

Astuti, D. T., Pujiastuti, Y., Suparman, S. H. K., Damiri, N., Nugraha, S., Sembiring, E. R., & Mulawarman. (2017). Exploration of *Bacillus thuringiensis* Berl. from soil and screening test its toxicity on insects of *Lepidoptera* order. *IOP Conference Series: Earth and Environmental Science*, *102*(1), Article 012063. https://10.1088/1755-1315/102/1/012063

Athukorala, S. N. P., Fernando, W. G. D., & Rashid, K. Y. R. (2009). Identification of antifungal antibiotics of *Bacillus* species isolated from different microhabitats using polymerase chain reaction and MALDI-TOF mass spectrometry. *Canadian Journal Microbiology, 55*(9), 1021–1032. https://doi.org/10.1139/W09-067

Batista, B. D., Dourado, M. N., Figueredo, E. F., Hortencio, R. O., Marques, J. P. R., Piotto, F. A., Bonatelli, M. L., Settles, M. L., Azevedo, J. L., & Quecine, M. C. (2021). The auxin-producing *Bacillus thuringiensis* RZ2MS9 promotes the growth and modifies the root architecture of tomato (*Solanum lycopersicum* cv. Micro-Tom). *Archives of Microbiology, 203*(7), 3869–3882. https://doi.org/10.1007/s00203-021-02361-z

Chen, K., Tian, Z., Luo, Y., Cheng, Y., & Long, C. (2018). Antagonistic activity and the mechanism of *Bacillus amyloliquefaciens* DH-4 against citrus green mold. *Phytopathology, 108*(11), 1253-1262. https://doi.org/10.1094/PHYTO-01-17-0032-R

Dala-Paula, B. M., Plotto, A., Bai, J., Manthey, J. A., Baldwin, E. A., Ferrarezi, R. S., & Gloria, M. B. A. (2019). Effect of huanglongbing or greening disease on orange juice quality, a review. *Frontiers in Plant Science, 9*, Article 1976. https://10.3389/fpls.2018.01976

Davami, F., Eghbalpour, F., Nematollahi, L., Barkhordari, F., & Mahboudi, F. (2015). Effects of peptone supplementation in different culture media on growth, metabolic pathway and productivity of cho dg44 cells; A new insight into amino acid profiles. *Iranian Biomedical Journal, 19*(4), 194-205. https://doi.org/10.7508/ibj.2015.04.002

Ding, Y., Wang, J., Liu, Y., & Chen, S. (2005). Isolation and identification of nitrogen-fixing bacilli from plant rhizospheres in Beijing region. *Journal of Applied Microbiology, 99*(5), 1271–1281. https://doi.org/10.1111/j.1365-2672.2005.02738.x

Dong, Y. H., Gusti, A. R., Zhang, Q., Xu, J. L., & Zhang, L. H. (2002). Identification of quorum quenching N-acyl homoserine lactonases from *Bacillus* species. *Applied and Enivronmental Microbiology, 68*(4), 1754–1759. https://doi.org/10.1128/AEM.68.4.1754-1759.2002

Donkersley, P., Silva, F. W. S., Carvalho, C. M., Al-Sadi, A. M., & Elliot, S. L. (2018). Biological, environmental and socioeconomic threats to citrus lime production. *Journal of Plant Disease and Protection, 125*, 339–356. https://doi.org/10.1007/s41348-018-0160-x

Dunlap, C. A., Kim, S. J., Kwon, S. W., & Rooney, A. P. (2015). Phylogenomic analysis shows that *Bacillus amyloliquefaciens* subsp. Plantarum is a later heterotypic synonym of *Bacillus methylotrophicus*. *International Journal of Systematic and Evolutionary Microbiology, 65*(7), 2104–2109. https://10.1099/ijs.0.000226

Fernandes, G. D. C., Trarbach, L. J., Campos, S. B. D., Beneduzi, A., & Passaglia, L. M. P. (2014). Alternative nitrogenase and pseudogenes: Unique features of the *Paenibacillus riograndensis* nitrogen fixation system. *Research in Microbiology, 165*(7), 571–580. https://doi.org/10.1016/j.resmic.2014.06.002

Flori, F., Mukarlina, M, & Rahmawati, R. (2020). Potensi antagonis isolat bakteri *Bacillus* spp. asal rizosfer tanaman lada (*Piper nigrum* L.) sebagai agen pengendali jamur *Fusarium* sp. Jdf. *Bioma: Jurnal Biologi Makassar*, *5*(1), 111–120. http://journal.unhas.ac.id/index. php/bioma/article/view/9923

Gautam, A. K. (2014). *Colletotrichum gloeosporioides*: Biology, pathogenicity and management in India. *Journal of Plant Physiology & Pathology*, *2*(2), 2-11. http://dx.doi.org/10.4172/2329-955X.1000125

Giassi, V., Kiritani, C., & Kupper, K. C. (2016). Bacteria as growth-promoting agents for citrus rootstocks. *Microbiological Research. 190*, 46–54. https://doi.org/10.1016/j.micres.2015.12.006

Gu, Q., Yang, Y., Yuan, Q., Shi, G., Wu, L., Lou, Z., Huo, R., Wu, H., Borriss, R., & Gao, X. (2017). Bacillomycin D produced by *Bacillus amyloliquefaciens* is involved in 2 the antagonistic interaction with the plant pathogenic fungus *Fusarium graminearum*. *Applied and Environmental Microbiology, 83*(19), Article e01075-17. https://doi.org/10.1128/AEM.01075-17

Guarnaccia, V., Groenewald, J. Z., Polizzi, G., Crous, P. W. (2017). High species diversity in Colletotrichum associated with citrus diseases in Europe. *Persoonia-Molecular Phylogeny and Evolution of Fungi, 39*(1), 32-50. https://doi.org/10.3767/persoonia.2017.39.02

Handiyanti, M., Subandiyah, S., & Joko, T. (2018). Molecular detection of *Burkholderia glumae*, a causal agent of bacterial panicle blight disease. *Jurnal Perlindungan Tanaman Indonesia*, *22*(1), 98–107. https://doi.org/10.22146/jpti.30259

Hanif, A., Zhang, F., Li, P., Li, C., Xu, Y., Zubair, M., Zhang, M., Jia, D., Zhao, X., Liang, J., Majid, T., Yan, J., Farzand, A., Wu, H., Gu, Q., & Gao, X. (2019). Fengycin produced by *Bacillus amyloliquefaciens* FZB42 inhibits *Fusarium graminearum* growth and mycotoxins biosynthesis. *Toxins, 11*(5), Article 295. https://doi.org/10.3390/toxins11050295

Ilmiah, H. H., Sulistyaningsih, E., & Joko, T. (2021). Fruit morphology, antioxidant activity, total phenolic and flavonoid contents of *Salacca zalacca* (Gaertner) voss by applications of goat manures and *Bacillus velezensis* B-27. *Caraka Tani: Journal of Sustainable Agriculture*, *36*(2), 270–282. https://doi.org/10.20961/carakatani.v36i2.43798

Ismail, A. R., El-Henawy, S. B., Younis, S. A., Betiha, M. A., El-Gendy, N. S., Azab, M. S., & Sedky, N. M. (2018). Statistical enhancement of lipase extracellular production by Bacillus stratosphericus PSP8 in a batch submerged fermentation process. *Journal of Applied Microbiology*, *125*(4), 1076-1093. https://doi.org/10.1111/jam.14023

Jaya, D. K., Giyanto, G., Nurhidayat, N., & Antonius, S. (2019). Isolation, identification, and detection of ACC deaminase gene-encoding rhizobacteria from rhizosphere of stressed pineapple. *Indonesian Journal of Biotechnology, 24*(1), 17–25. https://doi.org/10.22146/ijbiotech.39018

Jayanti, R. M., & Joko, T. (2020). Plant growth promoting and antagonistic potential of endophytic bacteria isolated from melon in Indonesia. *Plant Pathology Journal*, *19*(3), 200–210. https://doi.org/10.3923/ppj.2020.200.210

Joko, T., Hirata, H., & Tsuyumu, S. (2007). Sugar transporter (MfsX) of the major facilitator superfamily is required for flagella-mediated pathogenesis in *Dickeya dadantii* 3937. *Journal of General Plant Pathology*, *73*, 266–273. https://doi.org/10.1007/s10327-007-0018-8

Kim, Y. M., Lee., K. S., Kim, W. M., Kim, M., Park, H. O., Choi, C. W., Han, J. S., Park, S. Y., & Lee, K. S. (2022). Hydrochloric acid-treated *Bacillus subtilis* ghosts induce IL-1 beta, IL-6, and TNF-alpha in murine macrophage. *Molecular & Cellular Toxicology*, *18*(2), 267–276. https://doi.org/10.1007/s13273-022-00221-5

Kulkova, I., Dobrzynski, J., Kowalczyk, P., Belzecki, G., & Kramkowski, K. (2023). Plant growth promotion using *Bacillus cereus*. *International Journal of Molecular Sciences, 24*(11), Article 9759. https://doi.org/10.3390/ijms24119759

Lahlali, R., Mchachti, O., Radouane, N., Ezrari, S., Belabess, Z., Khayi, S., Mentag, R., Tahiri, A., & Barka, E. A. (2020). The potential of novel bacterial isolates from natural soil for the control of brown rot disease (*Monilinia fructigena*) on apple fruits. *Agronomy, 10*(11), Article 1814. https://doi.org/10.3390/agronomy10111814

Lata, R., Chowdhury, S., & Gond, S. K. (2024). Functional characterization of endophytic bacteria isolated from feather grass (*Chloris virgata* Sw.). *Grass Research*, *4*(1), Article e006. https://doi.org/10.48130/grares-0024-0005

Lestiyani, A., Joko, T., Holford, P., Charles Beattie, G. A., Donovan, N., Mo, J., Subandiyah, S., & Iwanami, T. (2024). Natural infection of *Murraya paniculata* and *Murraya sumatrana* with '*Candidatus* Liberibacter asiaticus' in Java. *Plant disease*, *108*(9), 2760–2770. https://doi.org/10.1094/PDIS-12-23-2593-RE

Logan, N., & Vos, P. D. (2015). *Bacillus*: *Bergey's manual of systematics of archaea and bacteria*. John Wiley & Sons, Inc. https://doi.org/10.1002/9781118960608.gbm00530

Marisna, I., Soffan, A., Subandiyah, S., Cen, Y., & Joko, T. (2024). The feeding behavior of *Diaphorina citri* monitored by using an electrical penetration graph (DC-EPG) on citrus plants treated with *Bacillus cereus* and *Bacillus velezensis*. *Journal of Plant Protection Research, 64*(3), 234–241. https://10.24425/jppr.2024.151815

Mei, C., Chretien, R. L., Amaradasa, B. S., He, Y., Turner, A., & Lowman, S. (2021). Characterization of phosphate solubilizing bacterial endophytes and plant growth promotion in vitro and in greenhouse. *Microorganisms, 9*(9), Article 1935. https://doi.org/10.3390/microorganisms9091935

Meng, Q., Jiang, H., & Hao, J. J. (2016). Effects of *Bacillus velezensis* strain BAC03 in promoting plant growth. *Biological Control, 98*, 18–26. https://doi.org/10.1016/j.biocontrol.2016.03.010

Mohamed, E. A. H., Farag, A. G., & Youssef, S. A. (2018). Phosphate solubilization by *Bacillus subtili*s and *Serratia marcescens* isolated from tomato plant rhizosphere. *Journal of Environmental Protection, 9*(3), 266–277. https://doi.org/10.4236/jep.2018.93018

Mora, I., Cabrefiga, J., & Montesinos, E. (2011). Antimicrobial peptide genes in *Bacillus* strains from plant environments. *International Microbiology, 14*, 213–223. https://doi.org/10.2436/20.1501.01.151

Munir, S., Li, Y., He, P., He, P., He, P., Cui, W., Wu, Y., Li, X., Li, Q., Zhang, S., & Xiong, Y. (2022). Defeating Huanglongbing pathogen *Candidatus* Liberibacter asiaticus with indigenous citrus endophyte *Bacillus subtilis* L1-21. *Frontiers in Plant Science. 12*, Article 789065. https://doi.org/10.3389/fpls.2021.789065

Munoz-Guerrero, J., Guerra-Sierra, B. E., & Alvares, J. C. (2021). Fungal endophytes of tahiti lime (*Citrus citrus* × *latifolia*) and their potential for control of *Colletotrichum acutatum* J. H. simmonds causing anthracnose. *Frontiers in Bioengineering and Biotechnology*, *9*, Article 650351. https://doi.org/10.3389/fbioe.2021.650351.

Murtado, A., Mubarik, N. R., & Tjahjaleksono, A. (2020). Isolation and characterization endophytic bacteria as biological control of fungus *Colletotrichum* sp. on onion plants (*Allium cepa* L.). *IOP Conference Series: Earth and Environmental Science, 457*(1), 012043. https://10.1088/1755-1315/457/1/012043

Naing, A. H., Maung, T. T., & Kim, C. K. (2021). The ACC deaminase-producing plant growth-promoting bacteria: Influences of bacterial strains and ACC deaminase activities in plant tolerance to abiotic stress. *Physiologia Plantarum*, *173*(4), 1992–2012. https://doi.org/10.1111/ppl.13545

Nan, J., Zhang, S., & Jiang, L. (2021). Antibacterial potential of *Bacillus amyloliquefaciens* GJ1 against citrus huanglongbing. *Plants, 10*(2), Article 261. https://doi.org/10.3390/plants10020261

Navitasari, L., Joko, T., Murti, R. H., & Arwiyanto, T. (2020). Rhizobacterial community structure in grafted tomato plants infected by *Ralstonia solanacearum*. *Biodiversitas, 21*, 4888–4895. https://doi.org/10.13057/biodiv/d211055

Olanrewaju, O. S., Glick, B. R., & Babalola, O. O. (2017). Mechanisms of action of plant growth promoting bacteria. *World Journal of Microbiology and Biotechnology, 33*(11), Article 197. https://doi.org/10.1007/s11274-017-2364-9

Oleńska, E., Malek, W., Wójcik, M., Swiecicka, I., Thjis, S., & Vangronsveld, J. (2020). Beneficial features of plant growth-promoting rhizobacteria for improving plant growth and health in challenging conditions: A methodical review. *Science of The Environment, 743*, Article 140682. https://doi.org/10.1016/j.scitotenv.2020.140682

Paudyal, K. P. (2016). Technological advances in Huanglongbing (HLB) or citrus greening disease management. *Journal of Nepal Agricultural Research Council, 1*, 41–50. https://doi.org/10.3126/jnarc. v1i0.15735.

Poveda, J., Roeschlin, R. A., Marano, M. R., & Favaro, M. A. (2021). Microorganisms as biocontrol agents against bacterial citrus diseases. *Biological Control*, *158*, Article 104602. https://doi.org/10.1016/j.biocontrol.2021.104602.

Raddadi, N., Cherif, A., Boudabous, A., & Daffonchio, D. (2008). Screening of plant growth promoting traits of *Bacillus thuringiensis*. *Annals of Microbiology, 58*, 47–52. https://doi.org/10.1007/BF03179444

Rafaat, M. M., Ali-Tammam, M., & Ali, A. E. (2019). Quorum quenching activity of *Bacillus cereus* isolate 30b confers antipathogenic effects in *Pseudomonas aeruginosa*. *Infection and Drug Resistance*, *12*, 1583–1596. https://doi.org/10.2147/IDR.S182889.

Ramarathnam, R., Bo, S., Chen, Y., Fernando, W. D., Xuewen, G., & De Kievit, T. (2007). Molecular and biochemical detection of fengycin-and bacillomycin D-producing *Bacillus* spp., antagonistic to fungal pathogens of canola and wheat. *Canadian Journal of Microbiology, 53*(7), 901–911. https://doi.org/10.1139/W07-049

Ribeiro, C., Xu, J., Teper, D., Lee, D., & Wang, N. (2021). The transcriptome landscapes of citrus leaf in different developmental stages. *Plant Molecular Biology, 106*, 349-366. https://doi.org/10.1007/s11103-021-01154-8

Riera, N., Handique, U., Zhang. Y., Megan, M., Dewdney, M. M., & Wang. N. (2017). Characterization of antimicrobial-producing beneficial bacteria isolated from huanglongbing escape citrus trees. *Frontiers in Microbiology, 8*, Article 2415. https://doi.org/10.3389/fmicb.2017.02415

Rohde, M. (2019). The Gram-positive bacterial cell wall. *Microbiology Spectrum*, *7*(3), Article 10.1128. https://doi.org/10.1128/microbiolspec.gpp3-0044-2018

Sariasih, Y., Subandiyah, S., Widyaningsih, S., Khurshid, T., Mo, J., & Donovan, N. (2024). Comparison of two huanglongbing detection methods in samples with different symptom severity. *Jurnal Fitopatologi Indonesia, 20*(4), 174–186. https://doi.org/10.14692/jfi.20.4.174-186

Selegato, D. M., & Castro-Gamboa, I. (2023). Enhancing chemical and biological diversity by co-cultivation. *Frontiers in Microbiology*, *14,* Article 1117559. https://doi.org/10.3389/fmicb.2023.1117559

Shah, G., Fiaz, S., Attia, K. A., Khan, N., Jamil, M., Abbas, A., Yang, S. H., & Jumin, T. (2022). Indole pyruvate decarboxylase gene regulates the auxin synthesis pathway in rice by interacting with the indole-3-acetic acid–amido synthetase gene, promoting root hair development under cadmium stress. *Frontiers in Plant Science, 13*, Article 1023723. https://doi.org/10.3389/fpls.2022.1023723

Shahid, M., Singh, U. B., Khan, M. S., Singh, P., Kumar, R., Singh, R. N., Kumar, A., & Singh, H. V. (2023). Bacterial ACC deaminase: Insights into enzymology, biochemistry, genetics, and potential role in amelioration of environmental stress in crop plants. *In Frontiers in Microbiology, 14*, Article 1132770. https://doi.org/10.3389/fmicb.2023.1132770

Silva, F., Queiroz, R., Souza, A., Al-Sadi, A., Siqueira, D., Elliot, S., & Carvalho, C. (2014). First report of a 16SrII-C phytoplasma associated with asymptomatic acid lime (*Citrus aurantifolia*) in Brazil. *Plant Disease, 98*(11), 1577-1577. https://doi.org/10.1094/PDIS-04-14-0431-PDN.

Suleman, M., Yasmin, S., Rasul, M., Atta, B. M., & Mirza, M. S. (2018). Phosphate solubilizing bacteria with glucose dehydrogenase gene for phosphorus uptake and beneficial effects on wheat. *PLoS ONE, 13*(9), Article e0204408. https://doi.org/10.1371/journal.pone.0204408

Tian, Z., Chen, Y., Chen, S., Yan, D., Wang, X., & Guo, Y. (2022). AcdS gene of *Bacillus cereus* enhances salt tolerance of seedlings in tobacco (*Nicotiana tabacum* L.). *Biotechnology and Biotechnological Equipmen, 36*(1), 902–913. https://doi.org/10.1080/13102818.2022.2144450

Trianom, B., Arwiyanto, T., & Joko, T. (2019). Morphological and molecular characterization of Sumatra disease of clove in Central Java, Indonesia. *Tropical Life Sciences Research, 30*(2), 107–118. https://doi.org/10.21315/tlsr2019.30.2.8

Tsotetsi, T., Nephali, L., Malebe, M., & Tugizimana, F. (2022). *Bacillus* for plant growth promotion and stress resilience: what have we learned?. *Plants, 11*(9), Article 2482. https://doi.org/10.3390/plants11192482

Unban, K., Kodchasee, P., Shetty, K., & Khanongnuch, C. (2020). Tannin-tolerant and extracellular tannase producing *Bacillus* isolated from traditional fermented tea leaves and their probiotic functional properties. *Foods, 9*(4), Article 490. https://doi.org/10.3390/foods9040490

Wei, L., Yang, C., Cui, L., Jin, M., & Osei, R. (2023). *Bacillus* spp. isolated from pepper leaves and their function and inhibition of the fungal plant pathogen *Colletotrichum scovillei*. *Egyptian Journal of Biological Pest Control*, *33*(1), Article 46. https://doi.org/10.1186/s41938-023-00686-z

Widyaningsih, S., Utami, S. N. H., Joko, T., & Subandiyah, S. (2017). Development of disease and growth on six scion/rootstock combinations of citrus seedlings under huanglongbing pressure. *Journal of Agricultural Science, 9*(6), 229–238. https://doi.org/10.5539/jas.v9n6p229

Wisanggeni, G. A., Suryanti, & Joko, T. (2023). The potential of *Bacillus subtilis* subsp. *subtilis* RJ09 as a biological control agent against leaf spot diseases on clove. *Jurnal Fitopatologi Indonesia, 19*(3), 118−126. https://doi.org/10.14692/jfi.19.3.118-126

Yahya, M., Rasul, M., Sarwar, Y., Suleman, M., Tariq, M., Hussain, S. Z., Sajid, Z. I., Imran, A., Amin, I., Reitz, T., Tarkka, M. T., & Yasmin, S. (2022). Designing synergistic biostimulants formulation containing autochthonous phosphate solubilizing bacteria for sustainable wheat production. *Frontiers in Microbiology, 13*, Article 889073. https://doi.org/10.3389/fmicb.2022.889073

Yao, T., & Xiaomei, Y. (2020). Cloning and functional analysis of *pqq* genes phosphorus solubilizing from *Bacillus mycoides* Gnyt1. *Research Square*, 2−19. https://doi.org/10.21203/rs.3.rs-41467/v1

Ye, Y., Li, Q., Fu, G., Yuan, G., Miao, J., & Lin, W. (2012). Identification of antifungal substance (iturin A2) produced by *Bacillus subtilis* b47 and its effect on southern corn leaf blight. *Journal of Intergrative Agriculture, 11*(1), 90−99. https://doi.org/10.1016/S1671-2927(12)60786-X

Pertanika J. Trop. Agric. Sci. 48 (6): 2177 - 2197 (2025)

PERTANIKA JOURNALS

TROPICAL AGRICULTURAL SCIENCE

Journal homepage: http://www.pertanika.upm.edu.my/

The Effects of Sweet Corn and Groundnut Intercropping on the Growth of Durian Seedlings (Musang King Variety) and Soil Physico-chemical Properties in a Durian Orchard

Borhan Abdul Haya[1,2*], Zulkefly Sulaiman[1], Mohd Fauzi Ramlan[3], Mohd Rizal Ariffin[4], Martini Mohammad Yusoff[1], Tsan Fui Ying[5], Ismail Rakibe[5], Annur Mohd Razıb[4], Sharif Azmi Abdurahman[6], and Sanjeev Ramarao[1]

[1]Department of Crop Science, Faculty of Agriculture, Universiti Putra Malaysia, 43400 Serdang, Selangor, Malaysia

[2]Department of Crop Production, Faculty of Sustainable Agriculture, Universiti Malaysia Sabah, 90509 Sandakan, Sabah, Malaysia

[3]UPM Holdings Sdn Bhd, Universiti Putra Malaysia, UPM-MTDC Technology Centre, 43400 Serdang, Selangor, Malaysia

[4]Department of Land Management, Faculty of Agriculture, Universiti Putra Malaysia, 43400 Serdang, Selangor, Malaysia

[5]Faculty of Plantation and Agrotechnology, Universiti Teknologi MARA, Jasin Campus, 77300 Merlimau, Melaka, Malaysia

[6]Department of Horticulture and Landscaping, Faculty of Sustainable Agriculture, Universiti Malaysia Sabah, 90509 Sandakan, Sabah, Malaysia

ABSTRACT

Between 2016 and 2021, the area under durian (*Durio zibethinus* Murr.) cultivation expanded by 29% in Malaysia, with farmers increasingly preferring high-value varieties such as Musang King. During the durian tree's five-year vegetative stage, intercropping with crops like sweet corn and groundnut offers farmers an additional income stream and supports durian growth. From January 2020 to April 2021, a two-season study at Pusat Pertanian Putra Puchong, Universiti Putra Malaysia, employed a between-subjects design, comparing durian plots with and without intercropping. Crop growth variables and soil physical and chemical properties were measured, and differences were analyzed using independent t-tests. Results showed that intercropping had minimal effects on durian seedling height, canopy diameter, and stem girth. However, the intercropping practices significantly increased chlorophyll a (by 17.80%), chlorophyll b

ARTICLE INFO

Article history:
Received: 01 May 2025
Accepted: 22 October 2025
Published: 25 November 2025

DOI: https://doi.org/10.47836/pjtas.48.6.25

E-mail addresses:
borhanyahya@ums.edu.my (Borhan bin Abdul Haya @ Yahya)
zulkefly@upm.edu.my (Zulkefly Sulaiman)
fauzi@upm.edu.my (Mohd Fauzi Ramlan)
ra_rizal@upm.edu.my (Mohd Rizal Ariffin)
martinimy@upm.edu.my (Martini Mohammad Yusoff)
tsanfuiying@uitm.edu.my (Tsan Fui Ying)
ismailrakibe@uitm.edu.my (Ismail Rakibe)
annur@upm.edu.my (Annur Mohd Razıb)
sh.azmi@ums.edu.my (Sharif Azmi Abdurahman)
sanjeevgep@gmail.com (Sanjeev Ramarao)
* Corresponding author

e-ISSN: 2231-8542

(11.57%), total chlorophyll (15.46%), and carotenoid content (28.57%) in durian leaves. Soil quality also improved in the intercropped plots, with pH rising from 4.35 to 5.38 and calcium concentration increasing from 0.07 to 0.30%, representing 1.89% and 109.46% increases compared to the control plot after the second season. Soil compaction was reduced, as penetration resistance dropped from 1.59 MPa in the control to 0.70–0.78 MPa in the intercropped plots. These findings indicate that intercropping sweet corn and groundnut in young durian orchards can be considered a sustainable practice, enhancing soil health and diversifying farmers' income without compromising durian growth. Farmers are encouraged to adopt intercropping during the non-fruiting stage to maximize both economic and agronomic benefits.

Keywords: Agroforestry, durian, groundnut, intercropping, smallholders, sweet corn

INTRODUCTION

Durian, scientifically known as *Durio zibethinus* Murr., is the most popular species in the Durio genus, has been cultivated for centuries and known as the king of tropical fruits (Salma et al., 2018). In Malaysia, the planted area for this crop increased by approximately 29% from 66,000 hectares in 2016 to 85,000 hectares in 2021, as reported by the Ministry of Agriculture (2019) and Department of Agriculture (DoA, 2021). In 2021, the production value of durian reached 4.5 million tons, equivalent to 8.5 billion in value, the highest among other types of fruit (DoA, 2021). One of the factors contributing to the increase in the planted area for durian was the involvement of small farmers who were changing their existing crops to durian. Additionally, there were farmers who were converting their existing durian plants to commercial and high-value varieties such as Musang King (D197) and Black Thorn (D200). This trend was in line with government encouragement (DoA, 2016).

During the vegetative stage of durian cultivation, smallholders need to find additional income for their livelihoods. Practicing intercropping is one way to help farmers earn an income before profiting from the durian crop. This is because durian only bears fruit five years after planting (Rushidah et al., 2006). In durian orchards, two types of intercropping systems can be implemented. Firstly, durian can be intercropped with permanent crops such as cocoa (Mohd Jelani et al., 1992), coconut (Pamplona & Garcia, 1997), and mangosteen, rambutan, longkong, and petai (Issarakraisila et al., 2014). Secondly, durian can be intercropped during its vegetative or uneconomical stage with options like banana (DoA, 2000; Pamplona & Garcia, 1997), or cereals such as corn and legumes like groundnut (Ratanarat et al., 1997; Susiloadi et al., 1994).

Banana is a popular crop often intercropped with durian, a practice commonly adopted by many durian growers to provide temporary shading before durian trees begin to bear fruit (Pamplona & Garcia, 1997; DoA, 2000). Durian seedlings intercropped with banana exhibit greater height, larger stem diameter, and higher survival rates compared

to those grown in open areas. Nonetheless, the incidence of phytophthora disease increases under this system (Pamplona & Garcia, 1997). Additionally, researchers have noted that durian trees grown in proximity to coconut trees tend to be slender, tall, and frequently afflicted by phytophthora. Phytophthora canker have been reported when durian is intercropped with cocoa (Solpot, 2022).

To overcome this problem, intercropping durian with short term cash crops such as sweet corn and groundnut between the wide rows of durian plants can be a solution. Additionally, smallholders often possess limited land size that may not be economically viable for monoculture durian planting. This necessitates reducing the number of planted durian trees to allow for larger spacing between them, facilitating intercropping with other plants. This preference for monoculture durian planting is driven by the desire to maximize the number of durian trees per area, thereby increasing revenue potential compared to intercropping with jungle fruit trees or other cultivation systems such as durian with forestry or durian with para rubber (Radchanui & Keawvongsri, 2017).

The produce from sweet corn and groundnuts can be sold to enable smallholders to earn a profit. However, the effects of intercropping activities on durian seedlings and soil conditions in the orchard need to be studied. This is because durians are susceptible to root disease infection. Additionally, the cost of establishing durian orchards is very high, and improper management will increase production costs. A study conducted by Susiloadi et al. (1994) concluded in general terms that the growth of durian seedlings is not adversely affected by intercropping with sweet corn and several types of legumes, including groundnuts, in young durian orchards. Therefore, this study was conducted to investigate the effects of intercropping sweet corn and groundnuts in a young durian orchard on the (i) growth of durian seedlings and (ii) soil physical and chemical characteristics.

MATERIALS AND METHODS

Experimental Site Description and Duration of Study

The experiment was conducted in a one-year-old durian orchard at Pusat Pertanian Putra – Putra Agricultural Center (PPP), Universiti Putra Malaysia (UPM), Puchong, Selangor (N 2º 98’ 61.9’’, E 101º 64’ 65.6’’), from January 2020 to April 2021. During this period, a study on intercropping sweet corn and groundnut was carried out over two cropping seasons. The soil at the experimental site belongs to the Bungor Series, which is classified as a Typic Paleudult (Radziah et al., 2006). The monthly mean temperatures ranged from 24.40 to 34.70 °C, monthly rainfall varied between 3.70 and 17.40 mm, and the monthly mean relative humidity ranged from 49.20% to 74.60% (Table 1) (Malaysian Meteorological Department, 2022).

Table 1
Selected climatic factors during the experimental period from January to April 2020, and from January to April 2021

Year/month	Temperature (°C)		Rainfall (mm)	Mean relative humidity (%)
	Minimum	Maximum		
2020				
January	25.70	33.7	8.3	70.0
February	25.70	33.8	7.0	66.5
March	26.00	34.6	12.5	71.2
April	25.70	34.7	17.4	74.6
2021				
January	25.00	31.7	4.9	70.4
February	23.40	31.6	3.7	49.2
March	25.20	33.9	13.1	71.9
April	24.40	32.6	11.1	73.0

Source: Malaysian Meteorological Department (2022)

Experimental Design and Treatments

The experimental design employed in this study was a between-subjects design comparing two treatments, consisting of durian area where, (1) without intercropping (control) and (2) with intercropping of sweet corn and groundnut. Each treatment was replicated using six durian seedlings. The size of the experimental area for both treatments (with and without intercropping) was 7,200 m² (120 m × 60 m) (Figure 1). The intercropped sweet corn and groundnut plots were established within the durian planting rows, approximately 2.00 m

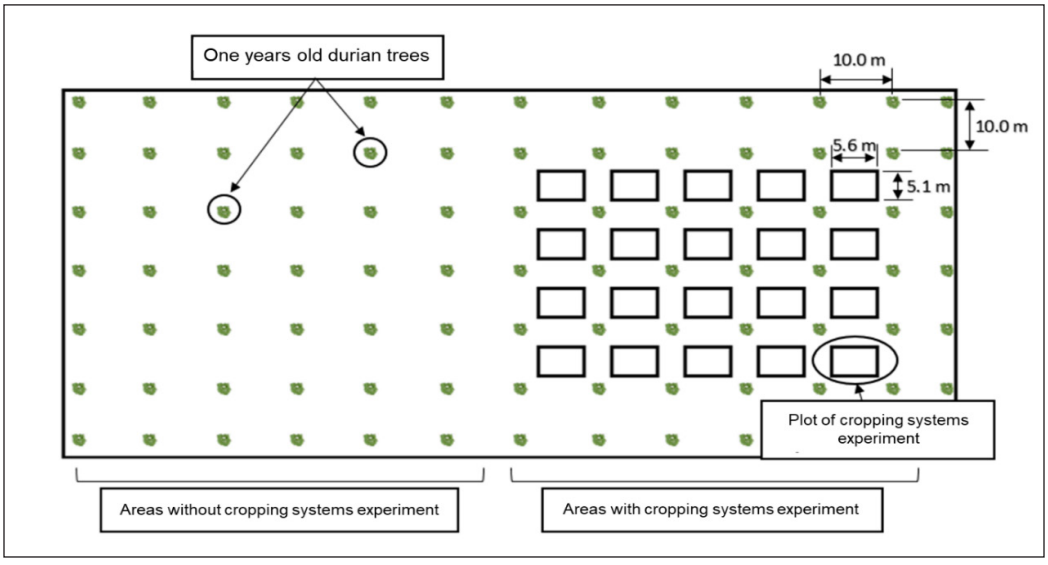

Figure 1. General plot layout

away from each durian seedling. The durian seedlings in this orchard were not planted specifically for this experiment but had been planted one year earlier. All routine activities and general field maintenance, such as weeding, manuring and liming were managed by PPP, UPM Puchong, and carried out on a scheduled basis.

Durian Seedlings Growth Parameters

Plant Height, Canopy Diameter, Main Stem Diameter and Girth

The growth parameters of durian, such as plant height, canopy diameter, main stem diameter, and main stem girth, were measured both before the commencement of the cropping systems experiment in season 1 and after the conclusion of season 2 was based on the works of Yaacob et al. (1978) and, Hoe and Palaniappan (2013). Plant height, canopy diameter, and main stem diameter were measured using a measuring tape, while the main stem girth was measured using a vernier calliper. A permanent marker was used to denote the base of the trunk at ground level. Plant height was measured from this mark to the top of the canopy, while main stem diameter and girth were measured 10 cm from the mark. The canopy diameter was determined by measuring the longest spread of the canopy from left to right. The values obtained were expressed in cm plant^{-1}.

Root Weight

Root weight measurements were done based on the method outlined by Masri (1991). Two soil core samples were extracted for each selected durian seedling using an aluminium tube with a diameter of 3 cm. To ensure unbiased sampling, the samples were taken at 50 cm (approximately half of the canopy radius) from the base of the main stem. The aluminium tubes were gently hammered into the soil until a depth of 50 cm was reached. The soil and root-containing samples were then washed through a 2 mm sieve to separate the roots from the soil. Smaller roots that passed through the sieve were collected and suspended on a fine nylon mesh. The collected roots were subsequently dried in the oven at 72ºC for 2 days before being weighed using an analytical digital balance (Radwag AS 220-R2, Torunska, Poland). The values obtained were expressed in g plant^{-1}.

Leaf Parameters

Five fully mature leaves per plant (leaves number 6 – 7 from the plant apex) were selected for the measurement of several leaf parameters, including SPAD data, chlorophyll ‘a’, ‘b’, and total chlorophyll content, as well as nitrogen concentration. SPAD values were assessed using the SPAD meter (502Plus Chlorophyll Meter, Minolta Camera Co., Osaka, Japan) in the field. Subsequently, the leaves were punched using a paper hole puncher to obtain approximately 200 mg of small leaf cuts for chlorophyll determination, following

the method described by Srivastava (2009). Similar leaves were harvested, dried in the oven at 72ºC for 2 days, ground into powder using a pulverizer and passed through a 0.7 mm sieve. The ground leaf samples were then used for the determination of total nitrogen concentration, following the method outlined by Horneck and Miller (1998).

Chlorophyll Content

Chlorophyll content measurements were done based on the method outlined by Srivastava (2009). The small pieces of leaves, approximately 200 mg per sample per plant, were ground together with 10 ml of 80% acetone in a pestle and mortar. The homogenate was then transferred into a 25 ml volumetric flask through a filter funnel covered with filter paper (Whatman Filter Paper No. 1). The pestle was washed with 5 ml of 80% acetone before transferring the remaining homogenate into the same volumetric flask. This process was repeated 2 to 3 times. The final volume of homogenate in the volumetric flask was adjusted with 80% acetone. The filtrate was then filled into the cuvette up to three-quarters of its total volume, and its absorbance was measured by a spectrophotometer (UV-3101PC UV-VIS-NIR, Shimadzu, Japan) at wavelengths of 645 and 663 nm against the solvent. Acetone with 80% concentration served as a blank. The amount of chlorophyll was calculated based on the formula below:

- Chlorophyll 'a' = [(12.7 × A663) – (2.69 × A645)] × V / 1000 x W
- Chlorophyll 'b' = [(22.9 × A645) – (4.68 × A663)] × V / 1000 x W
- Total Chlorophyll = [(8.02 × A663) + (20.2 × A645)] × V / 1000 x W

Where A is the absorbance at the given wavelength (663 or 645 nm), V is the total volume of the extract (ml), and W is the weight of the sample (g). The value obtained is expressed as mg of chlorophyll per gram of fresh weight sample (mg g^{-1}).

Leaf Total Nitrogen Concentration

The leaf samples, approximately 0.25 g were weighed. They were then mixed with 5 ml of 98% sulfuric acid (H_2SO_4) and one Kjeldahl tablet in a 100 ml digestion tube. The mixture was mixed using a vortex mixer for 15 seconds to thoroughly wet the sample with acid. The digestion tube was heated in a block digester at 150ºC for one and a half hours before further heating at 400ºC until the digestion became clear or colourless. After cooling down, the mixture was transferred into a 100 ml volumetric flask through a filter funnel covered with filter paper (Whatman Filter Paper No. 1). The digestion tube was rinsed with 10 ml of distilled water to collect the remaining sample solution, which was also transferred into the same volumetric flask. This rinsing process was repeated 2 to 3 times. The solution was then adjusted to a volume of 100 ml using distilled water before being transferred into a 100 ml plastic vial. The sample solution was pipetted into the distillation flask, mixed with 10 ml of 30% NaOH solution, and attached to the distillation unit. The condensate

from the solution was collected in a 10 ml trap containing 2% boric acid mixed with an indicator dye (bromocresol green + methyl red) in a conical flask. The conical flask was removed from the distillation unit when the solution turned from purplish red to green, and the volume increased to approximately 50 ml. It was then slowly titrated with 0.01N hydrochloric acid (HCl) from a 100 ml glass burette attached to a stand until the colour returned to purplish red. The initial and final volumes of HCl in the burette were recorded and used for the determination of total nitrogen using the formula below:

$$\text{Tot. N concentration} = \frac{(Y_{HCl} - Z_{HCl}) \times HCl_{concentration} \times 14}{1000} \times \frac{V_{sam.}}{W_{sam.}} \times \frac{1}{10} \times 100\%$$

Where Tot. N concentration is total nitrogen concentration, Y_{HCl} and Z_{HCl} is final and initial volume of HCl (ml) respectively, $HCl_{concentration}$ is concentration of hydrochloric acid used (0.01N), $V_{sam.}$ is volume of sample solution (ml) and $W_{sam.}$ is weight of sample (g). The value obtained was expressed in %.

The values of nutrient concentrations obtained from the instrument were based on the sample weight. All samples used were standardized to a common or constant weight before being statistically analysed using the formula below:

$$N_{concentration(0.25)} = (N_{concentration\ (sam.)} \times W_{0.25} / W_x$$

Where, $N_{concentration(0.25)}$ is nitrogen concentration in % per 0.25 g, $N_{concentration(sam.)}$ is value of leaf nitrogen concentrations based on the sample weight, $W_{0.25}$ is sample weight of 0.25 g and W_x is sample weight (g) of measured for N concentration analysis. The same method of calculation was applied to all analysis to standardize all samples to a constant weight.

Soil Parameters

Soil Penetration Resistance

Soil penetration resistance data were obtained using Penetrologger 6.0, a portable electronic penetrometer equipped with a built-in data logger (Royal Eijkelkamp, Nijverheidsstraat, Giesbeek, The Netherlands). Two data points were measured for each selected durian seedling area at 50 cm from the base of the main stem. This measurement was conducted using a load cell connected to a cone screwed onto the bottom end of a bipartite probing rod. The cone utilized in this study has a 60° angle and a base area of 1 cm^2. The penetration speed was set at 2 cm s^{-1}. By exerting equal pressure on both electrically insulated grips, the cone is vertically pushed into the soil. An internal ultrasonic sensor accurately records the vertical distance above the soil surface, while the load cell calculates the readings at each depth. The device stores data up to a depth of 80 cm in the profile. However, to ensure consistent measurement points at each location, only resistance readings at every 10 cm up

to a maximum soil penetration depth of 70 cm were utilized. Pressure measurements were expressed in MPa, and the measurement method was based on Royal Eijkelkamp (2022).

Soil pH, Cation Exchange Capacity and Organic Matter

Soil Sample Collection and Preparation

The soil sample collection and preparation were based on Van Reeuwijk (2002). Soil samples were collected from the orchard at four points around the durian seedlings, within a depth of 15.00 to 30.00 cm and at 1.00 m from the base of the main stem, using a soil probe. The soil probe ensured uniform soil volume throughout the sample depth (Sullivan et al., 2019). These samples were placed in plastic bags before being transferred to plastic trays for air-drying. Each plastic tray was labelled according to the area where the samples were collected. Large soil clods were broken up to expedite drying, and plant residue was removed. Once dried, the soil was sieved through a 2 mm sieve. Any remaining clods that did not pass through the sieve were crushed using a pestle and mortar and sieved again. The fine soil samples were then stored in Ziploc bags before analysis.

Soil pH

The soil pH was measured potentiometrically in the supernatant suspension of a 1:2.5 liquid (soil: liquid mixture). Distilled water was used as the liquid. Approximately 20 g of soil sample was weighed and placed into a 100 ml plastic vial and mixed with 50 ml of distilled water. The plastic vial was then sealed with a bottle cap and shaken for 2 hours using an orbital shaker at a speed of 180 rpm. The vial was manually shaken once or twice before taking the pH reading using a pH Benchtop meter (HI-2211, Hanna Instruments SRL, Romania), which had been calibrated beforehand. The reading was considered stable when it did not change by more than 0.1 unit per 30 seconds. The pH meter electrode was rinsed with distilled water and cleaned with a soft tissue before taking readings from another sample (Van Reeuwijk, 2002).

Cation Exchange Capacity

Cation exchange capacity determination was performed according to Ross & Ketterings (1995) and Purnamasari et al. (2021). The 10 g soil sample was weighed using an analytical digital balance (Radwag AS 220-R2, Torunska, Poland) and placed in a 150 ml leaching tube clipped to the rack after ashless floc and 3 cm diameter filter paper were placed at the bottom of the leaching tube. The soil sample was then levelled, and a 5 cm diameter filter paper was placed on top of the sample and levelled as well. Subsequently, 100 ml of 1N ammonium acetate (NH_4OAc) buffered at pH 7 was added into the funnel to leach out the exchangeable cations (K^+, $Ca2^+$, Mg^{2+}, and Na^+) and to saturate the exchange material with

ammonium. Following this, 100 ml of 95% ethyl alcohol was added to the leaching tube to remove excess or non-adsorbed ammonium ions and prevent the hydrolysis process from taking place. The soil, saturated with NH_4^+ ions, was then leached with 100 ml of 0.1N K_2SO_4 to remove the adsorbed NH_4^+ ions. The collected leachates containing NH_4^+ were determined by distillation and titration techniques. The CEC was determined using calculations based on the formula below:

$$CEC = \frac{(Y_{HCl} - Z_{HCl}) \times HCl_{concentration}}{W_{sam.}} \times \frac{100\ ml}{10\ ml} \times \frac{1000\ g}{1\ kg} \times \frac{1 cmol}{10\ mmol}$$

Where, CEC is cation exchange capacity, Y_{HCl} and Z_{HCl} are final and initial volume of hydrochloric acid (ml) respectively, $HCl_{concentration}$ is concentration of hydrochloric acid (0.01N), $W_{sam.}$ is the weight of sample (g). The value obtained was expressed in cmol (+)/kg of soil.

Soil Organic Matter

Soil organic matter determination followed the method outlined by Konaré et al. (2010). The porcelain crucible was heated for 1 hour at 400ºC in a muffle furnace, then cooled down in the open to about 150ºC before being further cooled in a desiccator for 30 minutes before being weighed. Thereafter, the soil sample was oven-dried at 105ºC for 24 hours and placed in the desiccator. Ten grams of the soil sample were then placed in the crucible. The weight of the crucible plus the weight of the soil sample is considered the pre-ignition weight. The crucible containing samples was placed in the muffle furnace at 400ºC for at least 16 hours or overnight. The furnace temperature was then adjusted to 150ºC to cool down the sample for approximately 3 hours. The crucible was then placed in the desiccator using tongs for 30 minutes and weighed to obtain the post-ignition weight. Soil organic matter was calculated using the following formula:

$$SOM = \frac{Wpre. - Wpost.}{W_{pre.}} \times 100\%$$

Where, SOM is soil organic matter, $W_{pre.}$ is pre-ignition weight, W_{post}. is post-ignition weight of soil sample + crucible before and after heated at 400ºC respectively. The value obtained was expressed in %.

Soil Nutrient Concentrations

Nitrogen (N) Concentration

Soil nitrogen concentration was prepared and determined following the method outlined by Horneck and Miller (1998). The same method was used for leaf samples; however, the weight of the soil sample used was 1.0 g.

Phosphorus, Potassium, Calcium, and Magnesium Concentrations (P, K, Ca, Mg)

Soil phosphorus, potassium, calcium, and magnesium concentration determination were based on Campbell and Plank (1998). A 1.0 g soil sample was placed in a 100 mL digestion tube, to which 5 mL of concentrated sulfuric acid (H_2SO_4) was added. The mixture was vortexed until all plant material was fully moistened and then allowed to stand overnight, or for at least 2 hours. The digestion tube was subsequently heated using a block digester at 285°C in a fume chamber for approximately 45 minutes. After heating, the tube was removed from the block digester, allowed to cool, and 2 mL of 50% hydrogen peroxide (H_2O_2) was added. This process, involving heating and the addition of H_2O_2, was repeated until the digestate became clear or colourless. The resulting solution was then transferred into a volumetric flask before being stored in a plastic vial. Nutrient concentrations were determined using Inductively Coupled Plasma Optical Emission Spectrometry (ICP-OES), Optima 7300 DV (PerkinElmer, Massachusetts, United States). The nutrient values obtained from the instrument were subsequently converted into percentages using appropriate calculations. Typically, the values measured by ICP-OES are expressed in units of µg/mL, mg/kg, or ppm, where 1 µg/mL is equivalent to 1 mg/kg, 1 ppm, or 0.0001%.

Statistical Analysis

Statistical analysis was conducted using Minitab version 16 (Minitab Inc., State College, PA, USA). An independent t-test was used to compare the means between treatments. A significance level of $p \leq 0.05$ was considered statistically significant.

RESULTS

Growth of Durian Seedlings

Plant Height, Canopy Diameter, Main Stem Diameter and Girth

Generally, no significant differences were observed in above-ground durian growth parameters such as plant height, canopy diameter, main stem diameter, and main stem girth for the two cropping systems at the end as affected by the intercropping experiments from pre-season 1 to post-season 2 (Figure 2).

Root Weight

The root weight of durian seedlings was not significantly affected by the intercropping with sweet corn and groundnut after two seasons (Figure 3).

Durian Leaf Chlorophyll Content

Chlorophyll a and b contents, total chlorophyll, and carotenoid contents of durian seedlings leaves in the intercropping plot were significantly higher compared to the monocropping

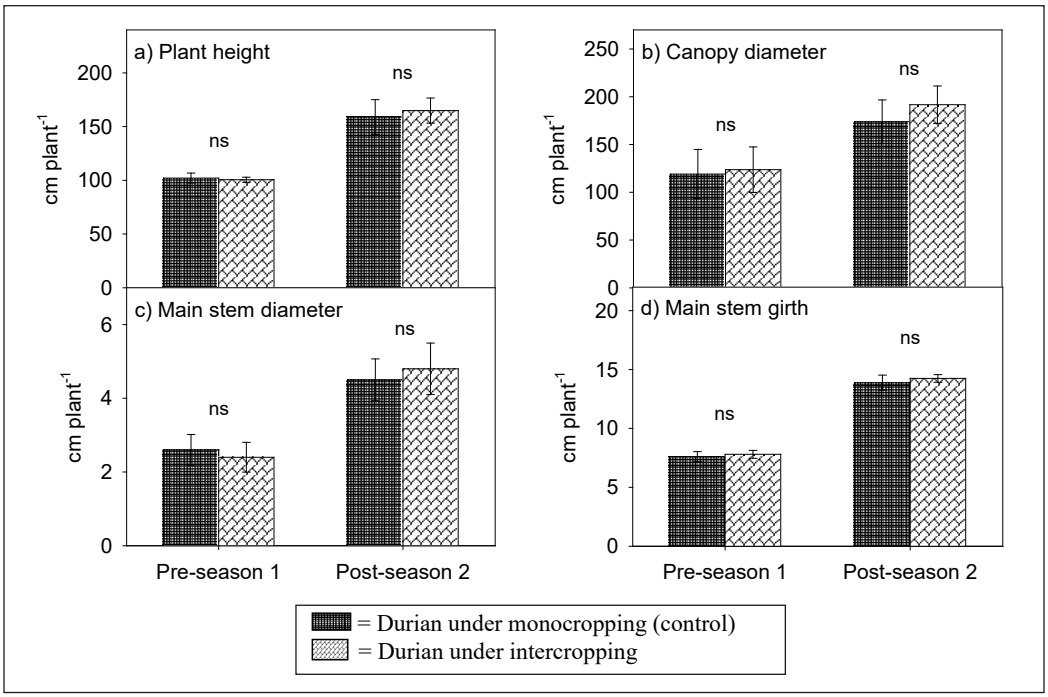

Figure 2. Plant height, canopy diameter, main stem diameter, and main stem girth of durian seedlings as affected by intercropping with sweet corn and groundnut from pre-season 1 to post-season 2. Different letters assigned to various treatments indicate a significant difference at $P \leq 0.05$, while 'ns' denotes no significance. The values represent the means of six replicates

plot. However, SPAD values and N concentration were not significantly affected by the intercropping experiments (Table 2). The values of leaf chlorophyll a, chlorophyll b, total chlorophyll, and carotenoid content of durian under intercropping were 1.04, 0.64, 2.09, and 0.08 mg/g fresh weight (FW), respectively. In contrast, the values for similar parameters for durian under monocropping were 0.87, 0.57, 1.79, and 0.06 mg/g FW, respectively.

Soil Nutrient Content

Soil Strength

At soil depths of 0, 10, 20, and 30 cm, soil strength in the monocropping plot was significantly higher than in the intercropping plot during post-season 2. In contrast, intercropping had no significant effect on soil strength at depths of 40 to 70 cm (Figure 4).

Soil pH, Cation Exchange Capacity and Organic Matter

Soil pH, cation exchange capacity (CEC), and organic matter (OM) increased from pre-season 1 to post-season 2, except for OM in the intercropping plot, where it remained constant (Table 3). In pre-season 1, soil pH in the monocropping plot was significantly higher

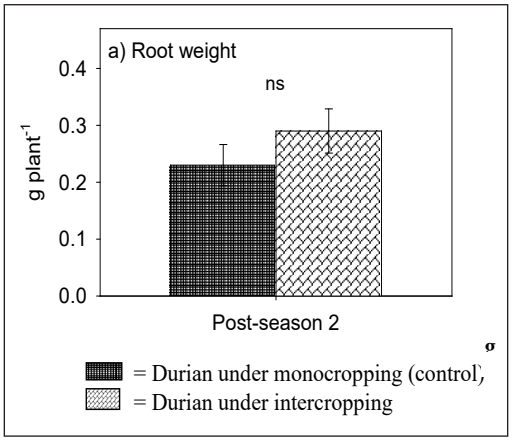

Figure 3. Illustrates the root weight of durian seedlings as affected by intercropping with sweet corn and groundnut post-season 2. Different letters assigned to various treatments indicate a significant difference at P ≤ 0.05, while 'ns' indicates no significance. The values represent the means of six replicates

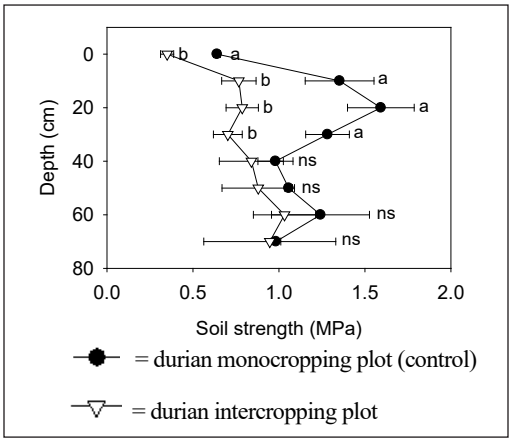

Figure 4. Soil strength in durian cultivation plots at the durian planting points as affected by intercropping with sweet corn and groundnut post-season 2. Different letters assigned to various treatments indicate a significant difference at P ≤ 0.05, while 'ns' indicates no significance. The values represent the means of six replicates

Table 2
Leaf parameters of durian seedlings as affected by intercropping with sweet corn and groundnut post-season 2

Parameters	Plot		P value
	Durian under monocropping	Durian under intercropping	
Nitrogen concentration (N conc.) (%)	2.66a±0.02	2.72a±0.08	0.48
SPAD (SPAD unit)	47.00a±1.30	50.48a±2.49	0.24
Chlorophyll a content (mg/g FW)	0.87b±0.02	1.04a±0.03	0.002
Chlorophyll b content (mg/g FW)	0.57b±0.01	0.64a±0.01	0.04
Total chlorophyll content (mg/g FW)	1.79b±0.04	2.09a±0.05	0.01
Carotenoid content (mg/g FW)	0.06b±0.001	0.08a±0.002	0.01

Note. FW = fresh weight. Different letters assigned to various treatments indicate a significant difference at P ≤ 0.05, while 'ns' denotes no significance. The values represent the means of six replicates

than in the intercropping plot. However, by post-season 2, soil pH in the intercropping plot had increased significantly and became higher than in the monocropping plot. Meanwhile, CEC and OM in the intercropping plot were significantly higher than in the monocropping plot throughout the study period, from pre-season 1 to post-season 2.

Soil Nutrient Concentrations

Soil nutrient concentrations are presented in Figure 5. The soil N and Fe concentrations decrease, while P concentration remains consistently low from pre-season 1 to post-season

Table 3
Soil pH, cation exchange capacity, and organic matter in durian cultivation plots as affected by intercropping with sweet corn and groundnut

Parameters	Plot		P value
	Durian under monocropping	Durian under intercropping	
pH			
Pre-season 1	4.61a ± 0.01	4.35b ± 0.03	0.02
Post-season 2	5.28b ± 0.003	5.38a ± 0.003	0.003
Cation exchange capacity (CEC)			
Pre-season 1	10.60a ± 0.87	11.60a ± 0.35	0.17
Post-season 2	11.60a ± 0.12	12.15a ± 0.55	0.25
Organic matter (OM)			
Pre-season 1	0.94a ± 0.10	1.18a ± 0.04	0.11
Post-season 2	0.95b ± 0.02	1.18a ± 0.05	0.01

Note. Different letters assigned to various treatments indicate a significant difference at $P \leq 0.05$, while 'ns' denotes no significance. The values represent the means of six replicates

2. The K concentration decreases in the monocropping plot but increases in the intercropping plot. Soil Ca, Mg, Zn, and Cu concentrations increase in both plots. The soil N and P concentrations in the intercropping plot are significantly higher than in the monocropping plot during pre-season 1, but no significant differences are observed thereafter. The concentrations of K, Mg, Fe, Zn, and Cu were not significantly affected by the intercropping treatments throughout the study. The soil Ca concentration did not differ significantly between plots before the start of season 1 however, Ca concentration in the intercropping plot is significantly higher than in the monocropping plot by post-season 2.

DISCUSSION

Growth of Durian Seedlings

The intercropping activities of corn and groundnut did not significantly affect the plant height, canopy diameter, main stem diameter, main stem girth, or root weight of young durian seedlings. However, the trend indicated that the growth of durian seedlings in intercropping plot showed improvement compared to those in monocropping plot after the experiment concluded, with increases of 3.65% in plant height, 9.74% in canopy diameter, 6.45% in main stem diameter, 2.56% in main stem girth, and 23.08% in root weight. This suggests that intercropping activities with annual or cash crops can be beneficial in young durian orchards without negatively affecting the growth of durian seedlings, as also observed by Susiloadi et al. (1994). A similar trend was observed in rubber (Paisan, 1996) plantations and young oil palm (Putra et al., 2012). Growing annual crops alongside perennial crops, which typically take 4-5 years to bear fruit, offers various benefits. It can help meet household food needs while generating income through sales to ready markets.

Consequently, it can narrow the income gap between planting and the first oil palm harvest (typically 3-5 years), enabling farmers to sell produce while waiting for palms to mature (Ecological Trends Alliance and Tropenbos International, 2021).

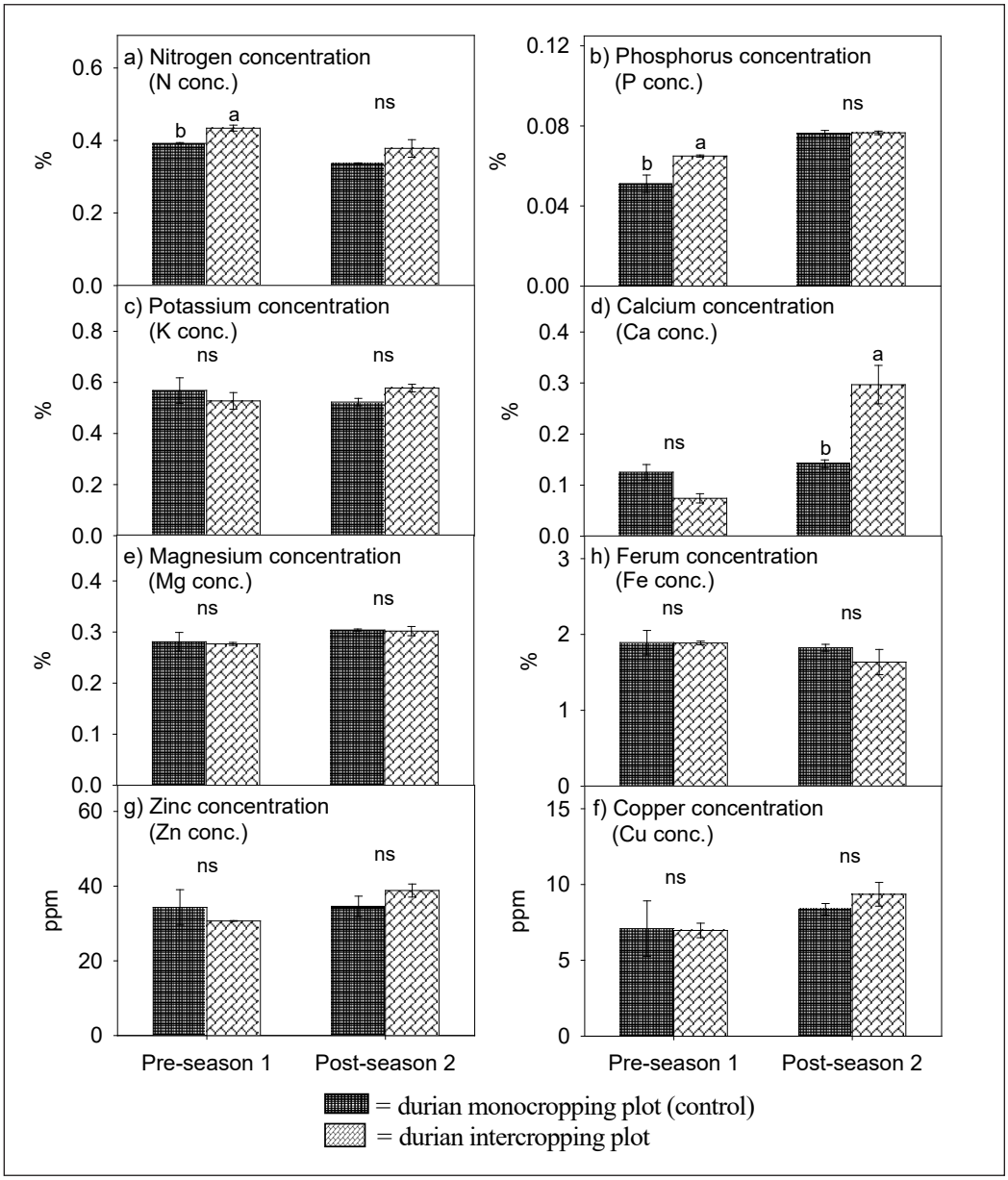

Figure 5. Soil nutrient concentrations in durian cultivation plots as affected by intercropping with sweet corn and groundnut from pre-season 1 to post-season 2. Different letters assigned to various treatments indicate a significant difference at $P \leq 0.05$, while 'ns' indicates no significance. The values represent the means of six replicates

Leaf Chlorophyll Content

Among durian leaf parameters, chlorophyll a, b, total chlorophyll, and carotenoid content exhibited a positive response in intercropping compared to monocropping plots. Leaf N concentration and SPAD value also showed a similar trend, although no significant difference was observed. Durian seedlings in the intercropping plot have chlorophyll a, b, total chlorophyll, and carotenoid content significantly higher by 17.80%, 11.57%, 15.46%, and 28.57% respectively, than those in the monocropping plot. Chlorophyll, a green pigment in leaves, absorbs light energy and converts it into chemical energy during photosynthesis (Rabinowitch, 1965; Kurniawan et al., 2021). The chlorophyll content in leaves reflects photosynthetic function and capacity, thus indicating plant growth and health (Li et al., 2018; Shi, 2019; Kurniawan et al., 2021). The growth of perennial crops within intercropping activities tends to improve compared to those grown in monoculture (Paisan, 1996; Putra et al., 2012).

Soil Strength

The soil strength from 0 to 30 cm depth exhibited a positive response in the monocropping plot. In contrast, no significant difference was observed for soil strength from 40 to 70 cm, although the trend was similar. The greatest differences in soil strength between monocropping and intercropping plots occurred at soil depths of 10 to 30 cm. This area is within the durian root zone, especially during the vegetative stage of durian seeding (Masri, 1991; DoA, 2012). However, the high soil strength in the monocropping plot was probably not a result of greater durian root. It could be due to the nature of the soil in the monocropping plot being harder than in the intercropping plot. In the monocropping plot, at a depth of 20 cm, the penetration resistance was 1.59 MPa, as indicated in Figure 4. The growth rates of roots in numerous crops decrease by around 50% when the penetration resistance reaches 1.5 MPa (Van den Akker et al., 2023). Soil strength restricts root growth and may slow down root system development (Correa et al., 2019).

Intercropping activities seemed to contribute to the improved growth of durian, not only above ground with stems and leaves but also below ground with roots. Supporting this observation is the higher root weight of durian in the intercropping plot compared to the monocropping plot, even though no significant difference was observed (Figure 3). The lower soil strength in the intercropping plot may be attributed to root penetration, which reduces soil hardness. The penetration resistance in the intercropping plot ranges from 0.70 to 0.78 MPa at depths of 10 to 30 cm, falling within the maximum axial root growth pressure range of 0.4 to 1.4 MPa (Misera et al., 1986). Mechanical energy investment per unit length increases with larger plant root diameters, while mechanical energy per unit of displaced soil volume decreases with larger diameters (Ruiz et al., 2015). The factors contributing to the weaker soil strength in the intercropping plot may also be due to watering activities in the intercropping

plot for corn and groundnut between the rows of durian seedlings, leading to increased soil water content. Soil strength decreases with higher soil water content, resulting in reduced soil-root bond strength and facilitating root growth (Fan et al., 2021). Root penetration was observed to be 80% of the maximum or greater when the average soil strength was 0.75 MPa or less and when the average matric potential was 0.77 MPa or greater (Yapa et al., 1988).

Soil pH and Nutrient Concentration

The intercropping activities resulted in significant differences in soil pH and Ca concentration. In terms of soil pH, it responded positively to the intercropping plot, increasing from 4.35 to 5.38, approximately a 21.17% increment. In contrast, in a monocropping plot, it increased from 4.61 to 5.28, with approximately a 13.55% increment. After the intercropping experiment ended, soil pH in the intercropping plot was significantly higher than in the monocropping plot by 1.88%. Soil in durian cultivation areas is generally strongly acidic. Liming is a common practice to mitigate soil acidification, enhance soil quality, and improve crop productivity on many agricultural soils (Daba et al., 2021; Kalkhoran et al., 2019). However, the amount of lime used may not be adequate to increase the soil pH, as demonstrated in the monocropping plot. Additionally, the use of nitrogen-based fertilizers applied together with lime can slow down the process of increasing soil pH. Nitrogen fertilizers themselves can lower soil pH through the nitrification process (Nasedjanov, 2012; Hart et al., 2013). In the intercropping plot, the rapid increase in soil pH is probably due to increased liming activity performed before planting sweet corn and groundnut in the intercropping experiment. This suggests that a high amount of lime application can accelerate the increment of soil pH, as demonstrated in experiments conducted by Nasedjanov (2012), Bossolani et al. (2023) and Ejigu et al. (2023).

The Ca concentration responded positively in the intercropping plot following the completion of the intercropping experiment. The Ca concentration in the intercropping plot was significantly higher at 70.74% compared to the monocropping plot. This rapid increase in Ca concentration could be attributed to the substantial quantity of lime utilized in the intercropping plot. Moreover, the type of lime employed is dolomite, a double salt comprising calcium carbonate ($CaCO_3$) and magnesium carbonate ($MgCO_3$), with the chemical composition $CaMg(CO_3)_2$ (Sholicha et al., 2019; Sanz et al., 2022). Dolomite is added to the growing medium to elevate pH to the range of 5.5 to 6.5 and to provide plants with calcium and magnesium essential for healthy growth (Conover et al., 1995). However, the significant effect observed was on calcium, as calcium is the primary element contained in this type of lime, as described by Peters et al. (1996). Although no significant differences were observed, the plant height, canopy diameter, main stem diameter, main stem girth, and root weight of young durian seedlings in the intercropping plot were enhanced compared to the monocropping plot, possibly due to the high soil calcium content. In oil palm, growth

parameters such as total, shoot, and root dry mass, as well as plant height of oil palm seedlings, were improved by calcium amendment treatment (Husain et al., 2021). However, calcium-deficient crops exhibited significant reductions in shoot length, shoot and trunk fresh weights, leaf area, and chlorophyll, eventually leading to drooping, yellowing, and chlorosis of leaves. Roots were less dense and primarily dark and necrotic, as shown in grapevines (Duan et al., 2022).

CONCLUSION

In conclusion, intercropping with annual or cash crops in young durian orchards does not negatively affect the growth of durian seedlings. It offers benefits such as reducing soil compaction and increasing soil pH, likely due to irrigation and liming activities. The increase in calcium concentration in the soil, resulting from liming, positively contributes to the improvement of physical growth parameters of durian seedlings.

ACKNOWLEDGEMENT

The authors would like to express their sincere gratitude to the Putra Agricultural Centre Puchong, Universiti Putra Malaysia, for granting access to their durian plantation plot as the site for this study on the intercropping of sweet corn and groundnuts. The authors also extend their deepest appreciation to Mr. Norhaimanshah bin Ismail for his invaluable assistance and guidance throughout the research.

REFERENCES

Bossolani, J. W., Crusciol, C. A. C., Mariano, E., Moretti, L. G., Portugal, J. R., Fonseca, M., & Cantarella, H. (2023). Higher lime rates for greater nitrogen recovery: A long-term no-till experiment labeled with 15N. *Field Crops Research, 299*, Article 108971. https://doi.org/10.1016/j.fcr.2023.108971

Campbell, C. R., & Plank, C. (1998). Preparation of plant tissue for laboratory analysis. In Y. P. Kalra (Ed.), *Handbook of reference methods for plant analysis* (pp. 37–49). CRC Press Taylor & Francis Group.

Conover, C. A., Steinkamp, R. J., & Steinkamp, K. (1995). *Effects of dolomite source, dolomite rate, and fertilizer rate on change in pH of growing medium leachate* (Research Report RH-95-4). University of Florida, IFAS, CFREC-Apopka.

Correa, J., Postma, J. A., Watt, M., & Wojciechowski, T. (2019). Soil compaction and the architectural plasticity of root systems. *Journal of Experimental Botany, 70*(21), 6019–6034. https://doi.org/10.1093/jxb/erz383

Daba, N. A., Li, D., Huang, J., Han, T., Zhang, L., Ali, S., Numan Khan, M., Du, J., Liu, S., Legesse, T. G., Liu, L., Xu, Y., Zhang, H., & Wang, B. (2021). Long-term fertilization and lime-induced soil pH changes affect nitrogen use efficiency and grain yields in acidic soil under wheat–maize rotation. *Agronomy, 11*(10), 2069. https://doi.org/10.3390/agronomy11102069

Department of Agriculture. (2000). *Pakej teknologi tanaman pisang (Banana crop technology package).* Department of Agriculture Peninsular of Malaysia.

Department of Agriculture. (2012). *Pakej teknologi durian (Durian crop technology package).* Ministry of Agriculture and Agro-based Industries.

Department of Agriculture. (2016). *Pelan strategik Jabatan Pertanian 2016–2020 (Strategic plan of the Department of Agriculture).* Department of Agriculture Malaysia.

Department of Agriculture. (2021). *Fruit crops statistic in Malaysia, 2021.* Department of Agriculture Malaysia.

Duan, S., Zhang, C., Song, S., Ma, C., Zhang, C., Xu, W., … Wang, S. (2022). Understanding calcium functionality by examining growth characteristics and structural aspects in calcium-deficient grapevine. *Scientific Reports, 12*(1), Article 3233. https://doi.org/10.1038/s41598-022-06867-4

Ejigu, W., Selassie, Y. G., Elias, E., & Molla, E. (2023). Effect of lime rates and method of application on soil properties of acidic Luvisols and wheat (*Triticum aestivum* L.) yields in northwest Ethiopia. *Heliyon, 9*(3), Article e14783. https://doi.org/10.1016/j.heliyon.2023.e14783

Ecological Trends Alliance, & Tropenbos International. (2021). *Intercropping in oil palm plantations: A technical guide.* Ecological Trends Alliance (Kampala, Uganda) and Tropenbos International (Ede, the Netherlands).

Fan, C. C., Lu, J. Z., & Chen, H. H. (2021). The pullout resistance of plant roots in the field at different soil water conditions and root geometries. *Catena, 207*, 105593. https://doi.org/10.1016/j.catena.2021.105593

Hart, J. M., Sullivan, D. M., Anderson, N. P., Hulting, A. G., Horneck, D. A., & Christensen, N. W. (2013). *Soil acidity in Oregon: Understanding and using concepts for crop production.* Oregon State University Extension Service.

Hoe, T. K., & Palaniappan, S. (2013). Performance of a durian germplasm collection in a Peninsular Malaysian fruit orchard. *Acta Horticulturae, 975*, 127–137. https://doi.org/10.17660/ActaHortic.2013.975.13

Horneck, D. A., & Miller, R. O. (1998). Determination of total nitrogen in plant tissue. In Y. P. Kalra (Ed.), *Handbook of reference methods for plant analysis* (pp. 75–83). CRC Press.

Husain, S. H., Mohammed, A., Ch'ng, H. Y., & Khalivulla, S. I. (2021). Residual effects of calcium amendments on oil palm growth and soil properties. In *IOP Conference Series: Earth and Environmental Science, 756*(1), Article 012060. IOP Publishing. https://doi.org/10.1088/1755-1315/756/1/012060

Issarakraisila, M., Lamers, H., Yoovatana, M. C., & Somsri, S. (2014). Empowering a community to conserve tropical fruit trees by the utilization of their products and agro-tourism. In *XXIX International Horticultural Congress on Horticulture: Sustaining Lives, Livelihoods and Landscapes (IHC2014): 1128* (pp. 323–326). International Society for Horticultural Science. https://doi.org/10.17660/ActaHortic.2016.1128.48

Kalkhoran, S. S., Pannell, D. J., Thamo, T., White, B., & Polyakov, M. (2019). Soil acidity, lime application, nitrogen fertility, and greenhouse gas emissions: Optimizing their joint economic management. *Agricultural Systems, 176*, Article 102684. https://doi.org/10.1016/j.agsy.2019.102684

Konaré, H., Yost, R. S., Doumbia, M., McCarty, G. W., Jarju, A., & Kablan, R. (2010). Loss on ignition: Measuring soil organic carbon in soils of the Sahel, West Africa. *African Journal of Agricultural Research, 5*(22), 3088–3095.

Kurniawan, N. S. H., Kirana, I. A. P., Abidin, A. S., Jupri, A., Widyastuti, S., Hernawan, A., Nikmatullah, A., Sunarpi, H., Prasedya, E. S. (2021). Analysis of leaf chlorophyll content of paddy plants during vegetative

stage grown in soil media containing macroalgae organic fertilizer. In *IOP Conference Series: Earth and Environmental Science, 913*(1), Article 012025. IOP. https://doi.org/10.1088/1755-1315/913/1/012025

Li, Y., He, N., Hou, J., Xu, L., Liu, C., Zhang, J., Wang, Q., Zhang, X., & Wu, X. (2018). Factors influencing leaf chlorophyll content in natural forests at the biome scale. *Frontiers in Ecology and Evolution, 6*, Article 64. https://doi.org/10.3389/fevo.2018.00064

Malaysian Meteorological Department. (2022). Unpublished meteorological data. F.R.I. Petaling Jaya Station.

Masri, M. (1991). Root distribution of durian, Durio zibethinus Murr. cv D24. *MARDI Research Journal, 19*(2), 183–189.

Misera, R. K., Dexter, A. R., & Alson, A. M. (1986). Maximum axial and radial growth pressures of plant roots. *Plant and Soil, 95*, 315–388. https://doi.org/10.1007/bf02374612

Ministry of Agriculture. (2019). *Agrofood statistics book.* http://www.moa.gov.my/penerbitan

Mohd Jelani, B., Jamadon, B., Nik Aziz, N. M., Abdullah, O., & Denamany, G. (1992, August 13). The integration of cocoa with other plants to increase the income of small scale cocoa growers. Paper presented at the *Seminar Perdagangan Koko*, Ipoh, Perak Darul Ridzuan, Malaysia. Universiti Putra Malaysia.

Nasedjanov, M. (2012). *The effects of lime on pH values of soil at different pH levels* [Final project report]. United Nations University Land Restoration Training Programme. https://www.grocentre.is/static/gro/publication/403/document/nasedjanov-2012.pdf

Paisan, L. (1996). Intercropping of young rubber. *Suranaree Journal of Science & Technology, 3*, 171–179.

Pamplona, P. P., & Garcia, M. E. (1997). Intercropping durian with 'Lakatan' banana and/or in coconut. In *PCARRD Highlights 1996* (pp. 51–52). Philippine Council for Agriculture, Forestry and Natural Resources Research and Development (PCARRD).

Peters, J. B., Schulte, E. E., & Kelling, K. A. (1996). *Choosing between liming materials* (A3671). University of Wisconsin—Extension.

Purnamasari, L., Rostaman, T., Widowati, L. R., & Anggria, L. (2021). Comparison of appropriate cation exchange capacity (CEC) extraction methods for soils from several regions of Indonesia. *IOP Conference Series: Earth and Environmental Science, 648*(1), 012209. IOP Publishing. https://doi.org/10.1088/1755-1315/648/1/012209

Putra, E. T. S., Simatupang, A. F., Waluyo, S., & Indradewa, D. (2012). The growth of one-year-old oil palms intercropped with soybean and groundnut. *Journal of Agricultural Science, 4*(5), 169. https://doi.org/10.5539/jas.v4n5p169

Rabinowitch, E. I. (1965). The role of chlorophyll in photosynthesis. *Scientific American, 213*(1), 74–83. https://doi.org/10.1038/scientificamerican0765-74

Radchanui, C., & Keawvongsri, P. (2017). Pattern and potential production of durian in Saikhao Community, Kokpho district, Pattani province. *International Journal of Agricultural Technology, 13*(6), 791–812.

Radziah, O., Lusi, M., & Anuar, A. R. (2006). Isolation of IAA producing rhizobacteria for enhanced growth of sweetpotato. *Malaysian Journal of Soil Science, 10*(April), 1–11.

Ratanarat, S., Pimsarn, S., & Ratanapratoom, K. (1997). Soil improvement for peanut intercropping in durian orchard. In *12th Thailand National Peanut Meeting*, Udon Thani.

Ross, D. S., & Ketterings, Q. M. (1995). Recommended methods for determining soil cation exchange capacity. In *Recommended soil testing procedures for the northeastern United States* (pp. 62–69). Northeastern Regional Publication No. 493.

Royal Eijkelkamp. (2022). *Penetrologger: User manual.* https://www.royaleijkelkamp.com/media/nrwjyah3/m-0615saepenet%20rologger.pdf

Ruiz, S., Or, D., & Schymanski, S. J. (2015). Soil penetration by earthworms and plant root mechanical energetics of bioturbation of compacted soils. *PLOS ONE, 10*(6), Article e0128914. https://doi.org/10.1371/journal.pone.0128914

Rushidah, W. Z., Jamil, Z. A., & Zaki, M. M. (2006). Effects of different sizes of planting material on the establishment and precocity of durian. *Journal of Tropical Agriculture and Food Science*, *34*(1), 7–14.

Salma, I., Masrom, H., & Mohd. Nor, A. (2018). *Durian clones.* Malaysian Agricultural Research and Development Institute (MARDI).

Sanz, J., Tomasa, O., Jimenez-Franco, A., & Sidki-Rius, N. (2022). Dolomite. In *Elements and mineral resources* (pp. 987–999). Springer Textbooks in Earth Sciences, Geography, and Environment. Springer.

Shi, L. (2019). Changes of chlorophyll value and plant height in leaves of different soil materials. In *IOP Conference Series: Earth and Environmental Science, 300*(5), Article 052010. IOP Publishing. https://doi.org/10.1088/1755-1315/300/5/052010

Sholicha, S. P., Setyarsih, W., Sabrina, G. J., & Rohmawati, L. (2019). Preparation of CaCO3/MgO from Bangkalan's dolomite for raw biomaterial. In *Journal of Physics: Conference Series*, 1171(1), Article 012034. IOP Publishing. https://doi.org/10.1088/1742-6596/1171/1/012034

Solpot, T. C., & Cumagun, C. J. R. (2022). Phylogenetic analyses and cross-infection studies of *Phytophthora* species infecting cacao and durian in South-Central Mindanao, Philippines. *Journal of Phytopathology*, *170*(1), 41–56.

Srivastava, G. C. (2009). *Modern methods in plant physiology*. New India Publishing.

Sullivan, D. M., Moore, A. D., & Brewer, L. J. (2019). *Soil organic matter as a soil health indicator: Sampling, testing, and interpretation* (EM 9251). Oregon State University Extension Service. https://extension.oregonstate.edu/sites/extd8/files/ documents/em9251.pdf

Susiloadi, A. P., Budiwibowo, Soegito, & Wahyudi, T. (1994). Pengaruh tata tanam durian dengan tanaman sela palawija terhadap pertumbuhan dan produktivitas lahan. *Penelitian Hortikultura*, *1*(6), 71–78.

Van den Akker, J. J. H., ten Damme, L., Lamandé, M., & Keller, T. (2023). Compaction. In M. J. Goss & M. Oliver (Eds.), *Encyclopedia of soils in the environment* (2nd ed., Vol. 5, pp. 85–99). Elsevier. https://doi.org/10.1016/B978-0-12-822974-3.00225-1

Van Reeuwijk, L. P. (2002). *Procedures for soil analysis* (6th ed.). International Soil Reference and Information Centre (ISRIC)

Yaacob, O., Ismail, M. N., & Talib, A. H. (1978). Observations on growth and early production of some durian (*Durio zibethinus* Murr) clones at Universiti Pertanian Malaysia orchard. *Pertanika*, *1*(1), 47–52.

Yapa, L. G. G., Fritton, D. D., & Willatt, S. T. (1988). Effect of soil strength on root growth under different water conditions. *Plant and Soil*, *109*(1), 9–16. https://doi.org/10.1007/BF02197574

REFEREES FOR THE PERTANIKA
JOURNAL OF TROPICAL AGRICULTURAL SCIENCE

Vol. 48 (6) NOV. 2025

The Editorial Board of the Pertanika Journal of Tropical Agricultural Science wishes to thank the following:

A. Haitami
(UIKS, Indonesia)

Abdul Hafiz Ab Majid
(USM, Malaysia)

Adeleyda Lumingkewas
(UNSRAT, Indonesia)

Alek Ibrahim
(BRIN, Indonesia)

Alimon Abd. Razak
(UGM, Indonesia)

Ameyra Aman Zuki
(UPM, Malaysia)

Amirul Ridzuan Abu Bakar
(UniMAP, Malaysia)

Aweng Eh Rak
(UMK, Malaysia)

Azalea Hani Othman
(UPM, Malaysia)

Azlinda Abu Bakar
(USM, Malaysia)

Ehsan Ahmadifar
(UOZ, Iran)

Ehsan Ullah Mughal
(UOG, Pakistan)

Erny Ishartati
(UMM, Indonesia)

Faez Firdaus Jesse Abdullah
(UPM, Malaysia)

Farah Farhanah Haron
(MARDI, Malaysia)

Fui Ying Tsan
(UiTM, Malaysia)

Geok Hun Tan
(UPM, Malaysia)

Gyan Prakash Mishra
(IARI, India)

H. Abozaid
(NRC, Egypt)

Hafandi Ahmad
(UPM, Malaysia)

Hafiz Muhammad Ali
(IUB, Pakistan)

Indra Purnama
(ULK, Indonesia)

Lia Diniz
(USP, Brazil)

Lotanna Micah Nneji
(Howard, United States of America)

Luqman Aini
(UB, Indonesia)

Mohamadu Boyie Jalloh
(UMS, Malaysia)

Mohammad Hossein Khanjani
(UJI, Iran)

Mohammad Kazem Souri
(TMU, Iran)

BRIN	*– Badan Riset dan Inovasi Nasional (National Research and Innovation Agency)*
Howard	*– Howard University, Washington*
IARI	*– ICAR/Indian Agricultural Research Institute*
IUB	*– The Islamia University of Bahawalpur*
MARDI	*– Malaysian Agricultural Research and Development Institute*
NRC	*– National Research Centre (NRC)*
PSU	*– Prince of Songkla University*
TMU	*– Tarbiat Modarres University*
UAS	*– Universitas Airlangga Surabaya*
UB	*– Universitas Brawijaya*
UdM	*– Universidad del Magdalena / The University of Magdalena*
UGM	*– Universitas Gadjah Mada*
UIKS	*– Universitas Islam Kuantan Singingi*
UiTM	*– Universiti Teknologi Mara*
UJI	*– University of Jiroft*
ULK	*– Universitas Lancang Kuning*
UMK	*– UniversitI Malaysia Kelantan*
UMK	*– UniversitI Malaysia Kelantan*
UMM	*– Universitas Muhammadiyah Malang*
UMS	*– Universiti Malaysia Sabah*
UMY	*– Universitas Muhammadiyah Yogyakarta*
UniMAP	*– University Malaysia Perlis*
UniSZA	*– Universiti Sultan Zainal Abidin*
UNSRAT	*– Universitas Sam Ratulangi*
UOG	*– University of Gujrat Hafiz Hayat Campus*
UOZ	*– University of Zabol*
UPM	*– Universiti Putra Malaysia*
USM	*– Universiti Sains Malaysia*
USP	*– Universidade de São Paulo, Instituto de Química/*
UWI	*– The University of the West Indies*

While every effort has been made to include a complete list of referees for the period stated above, however if any name(s) have been omitted unintentionally or spelt incorrectly, please notify the Chief Executive Editor, *Pertanika* Journals at executive_editor.pertanika@upm.edu.my

Any inclusion or exclusion of name(s) on this page does not commit the *Pertanika* Editorial Office, nor the UPM Press or the university to provide any liability for whatsoever reason.

Pertanika Journal of Tropical Agricultural Science
Vol. 48 (6) Nov. 2025

Content

Pertanika Journal Section, UPM Press
Putra Science Park,
1st Floor, IDEA Tower II,
UPM-MTDC Center,
Universiti Putra Malaysia,
43400 UPM Serdang,
Selangor Darul Ehsan
Malaysia

http://www.pertanika.upm.edu.my
Email: executive_editor.pertanika@upm.edu.my
Tel. No.: +603- 9769 1622

PENERBIT UPM PRESS
http://penerbit.upm.edu.my
Email: penerbit@upm.edu.my
Tel. No.: +603- 9769 8855

e-ISSN 2231-8542